

Discovery of novel glycomimetic ligands for Siglec-8

Inauguraldissertation

zur

Erlangung der Würde eines Doktors der Philosophie

vorgelegt der

Philosophisch-Naturwissenschaftlichen Fakultät

der Universität Basel

und der Universität Ljubljana

von

Benedetta Maria Girardi

Basel, 2023

Originaldokument gespeichert auf dem Dokumentenserver der Universität

Basel <https://edoc.unibas.ch>

Genehmigt von der Philosophisch-Naturwissenschaftlichen Fakultät auf Antrag von

First Supervisor: Prof. Dr. Daniel Ricklin, Departement Pharmazeutische Wissenschaften,
Universität Basel

First Supervisor: PD Dr. Oliver Schwardt, Departement Pharmazeutische Wissenschaften,
Universität Basel

First Supervisor: Prof. Dr. Marko Anderluh, Faculty of Pharmacy, University of Ljubljana

Second Supervisor: PD Dr. Martin Smiesko, Departement Pharmazeutische Wissenschaften,
Universität Basel

External expert: Prof. Dr. Antonio Molinaro, Dipartimento di Scienze Chimiche, Università degli
studi di Napoli Federico II

Basel, 19.10.21

Prof. Dr. Marcel Mayor
Dean of Faculty

Acknowledgments

It is incredible how fast these years have passed. It was a period full of up and downs, challenges, professional and personal growth, but especially a period that I had the chance and luck to share with many amazing people. First of all, I would like to thank all my supervisors and professors who guided me and contributed to this project.

First, a big thanks to **PD Dr. Oliver Schwardt** for letting me be part of this amazing project. Thank you for all the support shown during these years and from day one, for your availability as soon as I needed something and for all the advice, especially on the many synthetical problems that I had!

Thanks to **Prof. Dr. Daniel Ricklin**, my “second first” supervisor. It was a pleasure joining your group, I immediately felt welcomed and at ease and this was for sure also thanks to your positive vibes. Thank you for your encouragement and willingness to help whenever I needed.

A special thanks to **Prof. Dr. Beat Ernst**, it has always been so inspiring talking to you, it is incredible how much passion for science you transmit. Thank you for the help, for the chance to continue one of your projects and for the interesting scientific discussions that we had.

Finally, thanks to my second supervisor **PD Dr. Martin Smiesko**, it has always been a pleasure talking to you, you have always had great suggestions for my project and every time it was a chance to learn something.

Being part of a cotutelle de thèse, I also had the opportunity to have a supervisor at the University of Ljubljana, **Assoc. Prof. Dr. Janez Mravljak**. You have always been very kind, I really appreciated when you were often coming to the lab just to make sure that everything was fine and helping me when I was struggling with some reactions, thank you a lot!

Special thanks to **Prof. Dr. Marko Anderluh**, who is the glue of the entire PhD4Glycodrug consortium. When I was in Ljubljana, I really appreciated how much you cared to make everybody feel part of a family and, in spite of your many duties, to follow as much as possible the work of all of us. Thank you for cheering me up in the bad moments, for the inspiring scientific discussions and for all the nice moments, lunches and drinks we shared with the rest of the group.

Thanks to **Prof. Dr. Antonio Molinaro** for accepting to be my co-referee for my dissertation and to the members of the commission in Ljubljana, **Prof. Dr. Lucija Peterlin Mašič**, **Assoc. Prof. Dr. Žiga Jakopin** and **Prof. Dr. Dušan Turk**, who already had the chance to follow my project and gave me important advice and constructive critiques that helped me to improve my work.

I would also like to thank **Prof. Dr. Ulf Nilsson** and **Prof. Dr. Hakon Leffler**, from the University of Lund, for being so available and collaborative for the Galectin-8 project, and **Sjors Van Klaveren** and **Barbro Kahl Knutson** for testing the Galectin-8 ligands.

Thanks to **Prof. Serge Perez**, with whom I collaborated for the publication of an online chapter on Glycopedia.

Thanks to **Dr. Christoph Sager**, for giving me the opportunity to spend 3 weeks at Idorsia in the CADD group, I have learned a lot and I really enjoyed my time in such a positive atmosphere.

Furthermore, I would like to thank **Prof. Dr. Chris Cairo** from University of Alberta, to be so willing to help with the neuraminidase project and for providing the enzyme for our assays.

Going back to the university of Basel, I would really like to thank my labmates. First of all, **Rachel**, you were always ready to help, not only for lab issues. I learned so much from you and I am super grateful I had the chance to share nice moments in the lab with you! I would also like to thank **Mergim**, for all the laughs we had together, **Sateesh, Niklas, Debbie, Priska, Gisèle, and Giulietta**, I had a great time working with you, you definitely helped a lot to get through this PhD. A special thanks to all the other members of the Molecular Pharmacy group: in particular to **PD Dr. Said Rabbani**, for all the help in the protein production, **Clement**, for all your advice with the LC-MS but especially for sharing with me late lunches and uncountable evenings in the lab, **Christina**, for all the nice moments we had in Basel and your contagious cheerfulness, but also to **Adem, Aleksandra, Butrint, Carla, Edvin, Elisa, Horst, Ivan, Katia, Kevin, Lijuan, Maja, Nicole, Richard, Riccardo, Philip**, the **Computational Pharmacy group** and all the other people and master students I had the pleasure to meet during these years. Special thanks to **Jonathan**, your contribution and support in our Siglec-8 project, especially in the bioassays, was essential, to **Xiaohua**, for sharing all your knowledge about sialic acid, and finally to **Bea** and **Claudia** for always being extremely nice and helpful in any technical and administrative issue.

At the university of Ljubljana, I would like to thank **Assoc. Prof. Dr. Tihomir Tomašič**, who introduced me to molecular modeling and provided important suggestions and contributions to the project and **Dr. Žan Toplak**. A special thanks to **Martina**, the first and only master student that I supervised. Unfortunately, you didn't deal with the easiest chemical reactions, but in spite of this, you fought until the end and the hard moments finally paid out with a paper! I know how much effort you put into this work and I am very grateful for this. A big thanks to my Sardinian family in Ljubljana, **Daniela, Federica** and **Luca**, to my roomies **Tecla** and **Ana**, to my lab mates **Maša** and **Stefan**, to **Mateja** for her incredible support in any bureaucratic issues, and to all the people I met at the Faculty of Pharmacy.

As mentioned, I was part of this amazing consortium, the **PhD4Glycodrug**. I am extremely grateful to all the members, it was an honor having meetings with the more expert people in our field, I have learned a lot from all of you, not only scientifically but also on a personal level. Thanks to you, 12 random PhD students became a family. I still can't explain how easily we bond, right from the first

meeting! We shared so much and we are always looking for opportunities to meet again and spend time together. A big thanks to **Cyril, Kanhaya, Nives, Mujtaba, Rafael** and some special ones to the people I had the chance to spend more time with: to **Tiago**, you are such an inspiring and true person, thank you for sharing your passions, for the singing in the lab, for listening to me in my bad moments, I feel very lucky to have met you. To **Elena**, I feel that you and I understood each other from the very first moment, especially about the complaints, which apparently we like a lot! Thank you for all the nice moments we had in Ljubljana and especially the ones in Sardinia! To **Dania**, I don't think I know any person as passionate as you, you are an inspiration for everyone (special thanks for adding **Rodrigo** to our family!). To **Sjors**, I could always count on you and your crazy music in our evenings in the lab! To **Margherita**, you can hide it as much as you want but you are definitively a "terrona" inside! I had such a nice time with you, I wish we could have some secondments in common! Last but not least to **Gabriele**, not only a member of this network but also a colleague who worked on my same project. We started our journey together, do you remember how different we were the first year? You were definitely the "cold" person from the north! But slowly, the colleague turned to be a true good friend, who obsesses me with food and many other things (!), but it's still nothing compared to all my complaints you've had to stand over all this time! Making fun of me, you have always been able to make me smile even in the worst moments, to help me for every personal and scientific issue, if I didn't completely lose my mind is especially thanks to you.

Infine vorrei ringraziare i miei amici di una vita, è sempre bello sapere di poter tornare e trovarvi sempre lì, ogni volta riesco ad apprezzare sempre di più le piccole cose del nostro caro paesello!

Un grazie speciale ad **Ester**, anche se ormai tra tutti gli impegni siamo diventate "amiche di penna" è bello sapere che nulla sia cambiato in tutto questo tempo e che continui ad essere sempre presente.

Silvia, ancora una volta e ormai come sempre, sei stata fondamentale in questo percorso. Grazie per avermi sempre ascoltata e incoraggiata, nonostante la distanza, nonostante non sapessi nemmeno di cosa o chi stessi parlando, grazie per avermi tirato su il morale, grazie per esserci sempre.

Eugenio, senza il tempo trascorso insieme tutto sarebbe stato più difficile durante questo dottorato, mi bastava scappare da te per poter staccare completamente la spina quando non ne potevo più. Grazie per i weekend passati a vedermi lavorare senza mai lamentarti, se ce l'ho fatta ad arrivare alla fine di questi tre anni è anche grazie a te!

Infine vorrei ringraziare i miei **genitori**, per sopportare lunghe e interminabili chiacchierate su tutto ciò che non andava in laboratorio, per cercare di incoraggiarmi nei momenti più difficili e per non farmi mai pesare la distanza, anche se, sarò sincera, andare via di casa sta diventando ogni volta più difficile!

Abstract

This thesis principally focuses on the development of glycomimetic ligands with improved affinity to Siglec-8. Siglec-8 is a member of the Siglec family, I-type lectins that contain a sialic acid-binding domain and that play different roles in cell-cell interactions and cell signaling. Siglec-8 is a CD33-related protein expressed exclusively on mast cells and eosinophils, and weakly on basophils. Cross-linking of Siglec-8 with antibodies leads to apoptosis of eosinophils and inhibition of degranulation of mast cells. Apoptosis has also been induced when eosinophils were treated with a glycopolymer (6'-sulfo-sLe^x-polyacrylamide polymer). Therefore, Siglec-8 represents a very interesting new pharmacological target for the treatment of eosinophil- or mast cell-associated diseases, such as asthma, chronic rhinosinusitis, chronic urticaria, hypereosinophilic syndromes, mast cell and eosinophil malignancies, and eosinophilic gastrointestinal disorders. Recently, the NMR solution structure of the Siglec-8 lectin domain was solved in complex with its preferred ligand, the tetrasaccharide 6'-sulfo sialyl Lewis^x (Neu5Aca2-3[6S]Galβ1-4[Fuca1-3]GlcNAc). The main interactions involve a salt bridge between Arg109 and the carboxylate of sialic acid and a second salt bridge between Arg56 and Gln59 and the sulfate at the 6-position of the galactose moiety. Interestingly, the sulfate plays a key role in both binding and specificity to Siglec-8. In addition, hydrogen bonds exist between hydroxyl groups 7, 8 and 9 of sialic acid and Tyr7, Ser118 and Gln122. In contrast, the fucose and glucosamine subunits show only minor interactions. This led to the suggestion that the disaccharide substructure 6-sulfo-Sia-Gal might represent the minimal binding epitope for Siglec-8.

We first synthesized and tested this disaccharide, which showed a 2-fold lower affinity compared to the parent tetrasaccharide, but considering the simplified structure and the much easier synthetic approach, 6-sulfo-Sia-Gal can be considered as the minimal binding epitope for Siglec-8 and represents a very good starting point for further optimization processes. Bioisosters and a deoxygenation strategy were employed to improve its affinity to Siglec-8. By replacing the galactose unit with a sulfo-substituted hydroxymethyl-cyclohexane, we obtained a new lead compound with 2-fold higher affinity compared to the minimal binding epitope, mainly caused by the reduced desolvation costs due to the decreased polarity. Finally, the introduction of a sulfonamide substituent in position 9 of the sialic acid led to the identification of a potent ligand with a further 17-fold improvement in binding affinity. Homology modeling was used to get more structural information about Siglec-8 and about the binding mode of our ligands (Chapter 2).

In a previous unpublished work, a molecule where the sialic acid of the minimal binding epitope was replaced by a lactic acid derivative showed interesting affinity to Siglec-8. Since it would be the first molecule to bind a Siglec without containing sialic acid, we decided to resynthesize and test it with different assays, together with a small library of derivatives. However, we could not confirm the activity of the reference compound and one of our derivatives showed questionable results in the applied assays. We think that the compound probably interacts with Siglec-8, but with different site(s) of the protein. Further experiments, such as ^1H - ^{15}N HSQC NMR analysis, might be useful in the future to further investigate this hypothesis (Chapter 2).

In Chapter 3, we present two different virtual screening approaches. In the first case, by looking at the docking pose of our lead compound, we could observe an empty pocket close to position 5 of the sialic acid. We therefore decided to explore this cavity by virtually combining different fragments with the core structure of the lead compound, docking the obtained molecules into the Siglec-8 NMR solution structure and evaluating their poses. The most promising ones, where fragments were attached via amine or triazole linkers, were synthesized and tested. However, none of them showed any affinity to the target protein, probably because the absence of an amide could be detrimental for the binding. In the second approach, we performed a virtual screening of commercially available molecules to identify new possible hits with no carbohydrate moieties. Also in this case, none of them showed affinity to our target protein. However, the introduction of substituents via amide linker by rational design, modifying the ligand in the binding pocket, was more successful. In particular, the introduction of a methoxypropionamide in position 5 showed an almost 2-fold enhanced affinity compared to the parent compound, revealing that modifications in this position indeed are beneficial to improve the binding potency.

In Chapter 4, we tested the stability of our most important Siglec-8 ligands towards neuraminidase 2 (NEU2), a human enzyme able to hydrolyze sialic acids connected via α 2-3 linkages. An LCMS method was developed to follow the possible hydrolysis, by checking the consumption of the substrate and the formation of the product. Our observations indicated that glycomimetic ligands show higher stability compared to the more natural minimal binding epitope. However, the positive control used is quite labile, therefore to definitively confirm our results the use of an additional control compound should be considered. The assay is anyway validated and transferable to other compounds and enzymes.

Finally, as a small side project, we synthesized and tested some ligands towards Galectin-8, which has gained attention as a potential new pharmacological target for the treatment of various diseases, including cancer, inflammation, and disorders associated with bone mass reduction. The structure of our lactic acid derivatives described in Chapter 2 is very similar to a recently published Galectin-8 ligand, the 3-*O*-[1-carboxyethyl]- β -D-galactopyranoside. Therefore, we decided to test the corresponding non-sulfated derivatives and to optimize them for binding to Galectin-8. Affinity data measured by fluorescence polarization showed that the most potent compound reached a K_D of 12 μ M. Furthermore, reasonable selectivity versus other galectins was achieved, making the highlighted compound a promising lead for the development of new selective and potent ligands for Galectin-8 as molecular probes to examine the protein's role in cell-based and *in vivo* studies (Chapter 5).

Abbreviations

4MU-NANA	4-Methylumbelliferyl N-acetyl- α -D-neuraminic acid sodium salt
6'-Sulfo-sLe ^x	6'-Sulfo-sialyl Lewis ^x
$[\alpha]_D^{20}$	Optical rotary power
Ab	Antibody
ABTS	2,2'-Azino-bis-[3-ethylbenzothiazoline-6-sulfonic acid]-diammonium salt
Ac	Acetyl
AD	Alzheimer's disease
ADC	Antibody-conjugated drugs
ADCC	Antibody-dependent cell-cytotoxicity
ADME-T	Absorption, Distribution, Metabolism, Excretion, Toxicity
AEC	Absolute eosinophil count
Ala	Alanine
ALL	Acute lymphoblastic leukemia
AML	Acute myeloid leukemia
APCs	Antigen presenting cells
aq.	Aqueous
Arg	Arginine
Asn	Asparagine
Bn	Benzyl
Bz	Benzoyl
<i>c</i>	Concentration
CADD	Computer-aided drug design
Calcd	Calculated
CAR-T	Chimeric antigen receptor T
CBA	Competitive binding assay
CD22	Cluster of differentiation-22
CD33rSiglecs	CD33 related siglecs
CNS	Central nervous system
CRDs	Carbohydrate recognition domains
CuAAC	Cu(I)-catalyzed azide-alkyne 1,3-dipolar cycloaddition
δ	Chemical shift
d (NMR)	Doublet
dd (NMR)	Doublet of doublets
ddd (NMR)	Doublet of doublets of doublets
DANA	2,3-didehydro-2-deoxy- <i>N</i> -acetylneuraminic acid
DAP12	DNAX activation protein of 12 kDa
DC	Dendritic cell
DCC	<i>N,N'</i> -Dicyclohexylcarbodiimide
DCM	Dichloromethane
DC-SIGN	Dendritic Cell-Specific Intercellular adhesion molecule-3-Grabbing non-integrin
DCU	Dicyclohexylurea

DIBAL-H	Diisobutylaluminium hydride
DIPEA	<i>N,N</i> -Diisopropylethylamine
DMAP	4-Dimethylaminopyridine
DME	Dimethoxyethane
DMF	Dimethylformamide
DMSO	Dimethyl sulfoxide
DNA	Deoxyribonucleic acid
DRESS	Drug reaction with eosinophilia and systemic symptoms
Δ	Difference
ΔG	Gibbs free energy
ΔH	Enthalpy
ΔS	Entropy
Emab	Epratuzamab
ESI	Electrospray ionization
EtOAc	Ethyl acetate
Fab	Antigen-binding fragments
FBDD	Fragment-based drug design
Fc ϵ RI	Type I high affinity IgE receptor
FP	Fluorescence polarization
Fuc	Fucose
Gal	Galactose
GBPs	Glycan binding proteins
GlcNAc	<i>N</i> -Acetylglucosamine
Gln	Glutamine
Gly	Glycine
HATU	Hexafluorophosphate azabenzotriazole tetramethyl uronium
HBA	Hydrogen bond acceptor
HBD	Hydrogen bond donor
HE	Hypereosinophilia
HEP	Human epithelial
HEPES	4-(2-Hydroxyethyl)piperazine-1-ethanesulfonic acid
HES	Hypereosinophilic syndrome
His	Histidine
HIV	Human immunodeficiency virus
HPLC	High-performance liquid chromatography
HSQC	Heteronuclear single quantum correlation
HTS	High-throughput screening
IC ₅₀	Half maximal inhibitory concentration
Ig	Immunoglobulin
Il	Interleukin
ISM	Indolent systemic mastocytosis
ITAM	Immunoreceptor tyrosine-based activation motif
ITC	Isothermal titration calorimetry
ITIM	Immunoreceptor tyrosine-based inhibitory motif

K_D	Dissociation constant
KS	Keratan sulfate
LBDD	Ligand-based drug design
LCMS	Liquid chromatography-mass spectrometry
Lys	Lysine
m (NMR)	Multiplet
mAb	Monoclonal antibody
MAG	Myelin-associated glycoprotein
MC	Mast cells
MD	Molecular dynamic
MeCN	Acetonitrile
MeOH	Methanol
Met	Methionine
Mo	Monocytes
MRM	Multiple reaction monitoring
MS	Mass spectrometry
MsOH	Methanesulfonic acid
MST	Microscale thermophoresis
MW	Molecular weight
m/z	Mass-to-charge ratio
NADPH	Nicotinamide adenine dinucleotide phosphate
nanoDSF	Nano differential scanning fluorimetry
Neu	Neuraminic acid
NEU	Neuraminidase
Neu5Ac	<i>N</i> -Acetylneuraminic acid
Neu5Gc	<i>N</i> -Glycolylneuraminic acid
NHS	<i>N</i> -Hydroxysuccinimide
NIS	<i>N</i> -Iodosuccinimide
NK	Natural killer
NMR	Nuclear magnetic resonance
NOE	Nuclear Overhauser effect
PAA	Polyacrylamide
PD	Pharmacodynamics
PDB	Protein Data Bank
Ph	Phenyl
PK	Pharmacokinetics
Pyr	Pyridine
Pro	Proline
PSA	Polar surface area
PSA	Passive systemic anaphylaxis
QC	Quality control
QQQ-MS	Triple quadrupole MS
Quant.	Quantitative
ROS	Reactive oxygen species

rt	Room temperature
s (NMR)	Singlet
Satd	Saturated
SBDD	Structure-based drug design
Ser	Serine
SH2	Src Homology 2 domain
SHP	Src Homology 2 domain-containing phosphatase
Siglec	Sialic acid immunoglobuline-like lectin
SLE	Systemic lupus erythematosus
Sn	Sialoadhesin
SPR	Surface plasmon resonance
STALs	Siglec-engaging tolerance-inducing antigenic liposomes
STD	Saturation-transfer difference
t (NMR)	Triplet
TBDPSCI	<i>tert</i> -Butyl(chloro)diphenylsilane
Tf	Triflyl
TfOH	Trifluoroacetic acid
THF	Tetrahydrofuran
TLC	Thin-layer chromatography
TLRs	Toll-like receptors
T _m	Thermal shift
Trp	Tryptophan
Tyr	Tyrosine
VEFG	Vascular endothelial growth factor

Table of contents.

1. Introduction.....	15
1.1 The world of carbohydrates.....	15
1.2 Glycomedicine: from carbohydrates to glycomimetics.....	17
1.3 Strategies for rational design of glycomimetics.....	18
1.4 Glycan-binding proteins.....	19
1.5 Sialic acids and the Siglec family.....	21
1.6 How to target Siglecs?.....	26
1.7 Siglec-8.....	27
1.8 Eosinophil and mast cell-related disorders.....	28
1.9 Siglec-8 as a druggable target.....	30
1.10 Siglec-8 structure.....	31
1.11 Objectives of the thesis.....	33
1.12 References.....	35
2. From the natural carbohydrate to glycomimetics.....	49
2.1 Introduction.....	50
2.2 Results and Discussion.....	51
2.3 Conclusions.....	65
2.4 Experimental Part.....	65
2.5 References.....	102
3. Virtual screening for the optimization of the Siglec-8 lead compound.....	109
3.1 Introduction.....	110
3.2 Results and discussion.....	112
3.3 Conclusions.....	123
3.4 Experimental part.....	123
3.5 References.....	147

4. Development of an LC-MS method for the quantification of NEU2-mediated hydrolysis of Siglec-8 ligands	151
4.1 Introduction.....	152
4.2 Results and discussion.	154
4.3 Conclusions.....	156
4.4 Experimental part.....	157
4.5 References.....	159
5. Selective monovalent Galectin-8 ligands based on 3-lactoylgalactoside	162
5.1 Introduction.....	163
5.2 Results and discussion.	167
5.3 Conclusions.....	173
5.4 Experimental part.....	173
5.5 References.....	182
6. Discussion of the hypotheses	189
7. Summary and outlook	193
8. Appendix.....	196

1. Introduction.

* Part of the introduction related to Siglecs has been published as a Glycopedia chapter (<https://www.glycopedia.eu/e-chapters/the-fascinating-world-of-siglec-proteins-a-primer/article/introduction>).

1.1 The world of carbohydrates.

Carbohydrates are one of the major classes of biomolecules found in nature. Best known as source of energy and for their role in metabolism, the growing interest and understanding of glycobiology in the last years highlighted their essential role in many physiological and pathological processes, being important mediators of signal transduction, cell-cell interaction and adhesion.

Carbohydrates form a dense coating on every type of cell, called glycocalix, where they are either free or linked to the membrane via proteins or lipids (Figure 1).

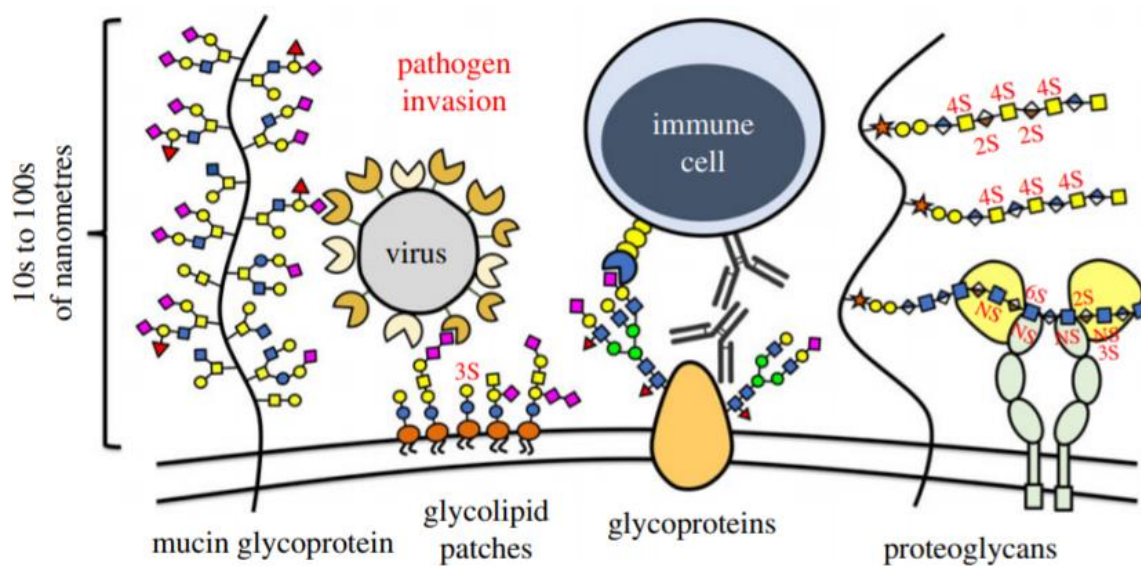


Figure 1. Simplified glycocalix structure. Figure adapted from Purcell *et al.*¹

The glycocalix has an enormous structural complexity: in fact, compared to other biopolymers, glycostructures contain several points of variability. Every monosaccharide can bind another one at various positions (creating α - or β - isomers at the anomeric center), it can establish further linkages creating branched structures, can vary in ring size (furanoside or pyranoside) and can get further modified (acetylation, sulfation, etc.).² This grade of variability is higher than the one obtained with combinations of amino acids or nucleic acids, suggesting that sugars may have a great coding capacity.^{3,4} Only lately with technological advances it has become possible to better understand the

structure and the functions of the glycocalyx, and how its glycans composition is dynamic, cell-dependent and reflects the status of the cells.^{5,6} The glycocalyx is involved in determining cell-morphology, membrane organization, and cell protection.⁷ The endothelial glycocalyx is fundamental: its constant interaction with the bloodstream leads to intracellular responses and its changes have been linked to several pathological conditions.⁸ Besides, aberrant expression of cell surface carbohydrates has been linked to various diseases as a result of different activity and expression of glycosyltransferases and glycosidases, two of the main class of enzymes involved in sugars synthesis. For example, different studies have shown how tumor cells remodel their glycocalyx, having an effect on tumor progression and metastasis, increasing and changing adhesion processes and survival.⁹⁻¹¹ Being at the cell-surface, carbohydrates serve as a first contact between cells and represent a sort of their fingerprints: in this way, our immune system can discriminate self from non-self or even between healthy and non-healthy cells.

For a long time, carbohydrates were not believed to induce an adaptive immune response: lately, several evidences have shown that also sugars can play a crucial role in immune recognition.¹² Glycan immunogenicity was discovered for the first time studying the well-known reaction that our body has during transfusion with red blood cells from individuals with different blood type. In fact, the blood types A, B and 0 correspond to three different glycan structures present on the surface of the blood cells: the recognition of “foreign” glycan epitopes causes the immune response.¹³

The same mechanism involves some carbohydrate-containing structures associated with pathogens, as for example lipopolysaccharides on the surface of Gram-negative bacteria or fungal mannans etc. For this reason, glycans conjugated to proteins have been used as vaccines to stimulate the production of antibodies.^{14,15}

On the other hand, the sugar coating can also be exploited by pathogens or cancer cells, either by miming our sugars and not being recognized by our immune system or by using them to enter the cells (e.g. *Escherichia Coli* strains which use carbohydrate-binding proteins to stay attached to the bladder’s wall or viruses that bind sugars on the cell-surface to enter).¹⁶⁻¹⁸ For example, the glycosylated spike protein of SARS-CoV-2 is recognized by this class of proteins, thus binding and promoting virus trans-infection.¹⁹

All these aspects and new insights into the carbohydrates’ world underline how the development of a “glycomedicine” is a promising and exciting new approach to understand and modulate the behavior of the cells both in physiological and pathological conditions.

1.2 Glycomedicine: from carbohydrates to glycomimetics.

Considering the several roles that carbohydrates have in our organism and the increasing understanding of their functions and structures, in the last years sugars have been recognized as an interesting class of potential drug candidates.

The first used carbohydrate-containing drug is the streptomycin, discovered in 1944, an antibiotic with two sugar rings. Since then, a growing number of small molecules have been approved as drugs (Figure 2).²⁰ Some important examples are low molecular weight heparins and Fondaparinux as anticoagulants, glycosidase inhibitors for the treatment of diabetes (e.g. miglitol), or viral neuraminidase inhibitors for the treatment of influenza.²¹

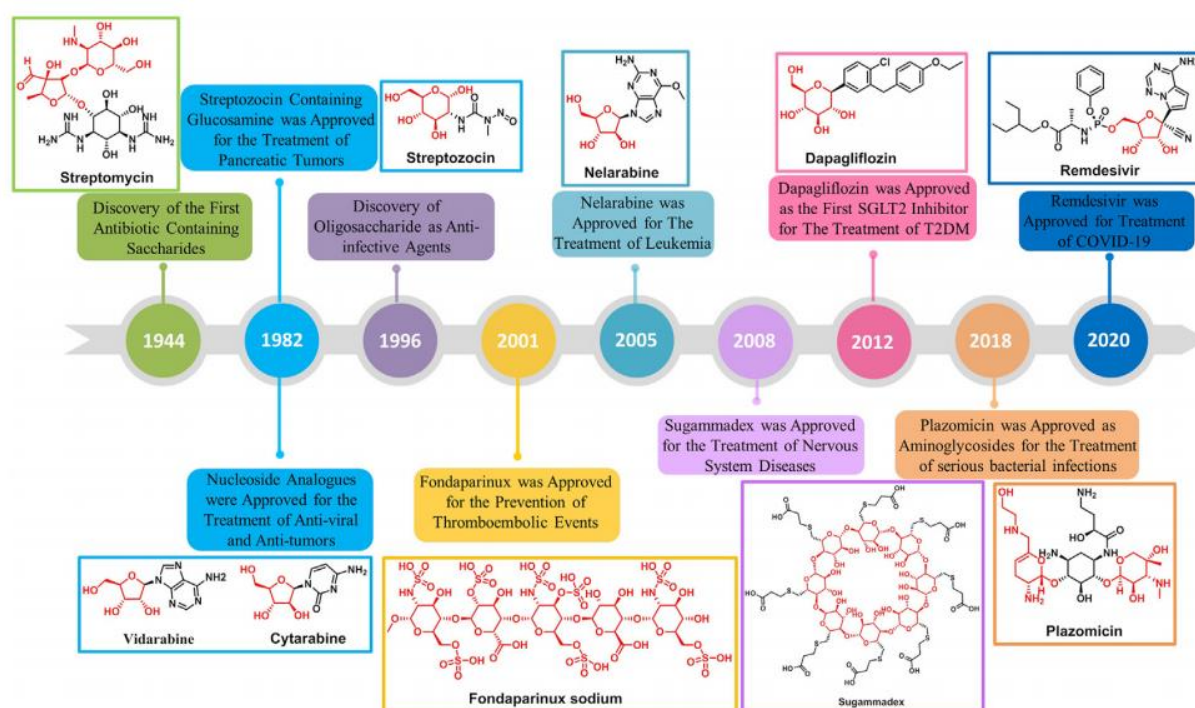


Figure 2. Examples of approved carbohydrate-containing small molecules. Figure from Jiang *et al.*²⁰

In spite of the big potential of native carbohydrates for the treatment of various diseases, they have several drawbacks, which limit their development and use as drugs. Therefore, carbohydrate-based molecules still represent a very small percentage of the drugs in clinical use. First of all, they don't have the "standard" drug-like properties which follow Lipinski's rule of five ($MW < 500$ Da, $\log P < 5$, H-bond donor < 5 , H-bond acceptor < 10), especially due to their high polarity.²² Consequently, they also have very poor pharmacokinetic properties, like low oral bioavailability (impossibility of passively cross the enterocyte layer in the small intestine) or, when administered parenterally, low half-life because of fast renal excretion.

Besides, they have very weak interactions with their targets (μM - mM range), where they usually bind in shallow binding sites with short residence times, being quickly displaced by the solvent. Nature overcomes this limit with multivalent sugar presentation, which increases a lot their affinity and avidity. Last but not least, cumbersome syntheses also limit their production.

Considering their importance and limitations, alternative ways have been explored to address the drawbacks of carbohydrate lead compounds. For example, focusing on small molecules led to the development of glycomimetics, molecules able to mimic the structure and functions of sugars while improving their drug-likeness and affinity to the target.^{23,24}

1.3 Strategies for rational design of glycomimetics.

For efficient development of glycomimetics, it is very important to understand the binding mode of the natural structures and the main interactions with the target: crystal or NMR structures are essential to facilitate the rational design. In this way, it becomes obvious which groups might be eliminated or substituted, or how the molecule might be pre-organized in the bioactive conformation, reducing the entropic cost caused by the loss of flexibility upon binding.^{24,25} Actually, the thermodynamics of binding is a key factor to be considered during a drug optimization process, especially with such polar entities like sugars (Figure 3).

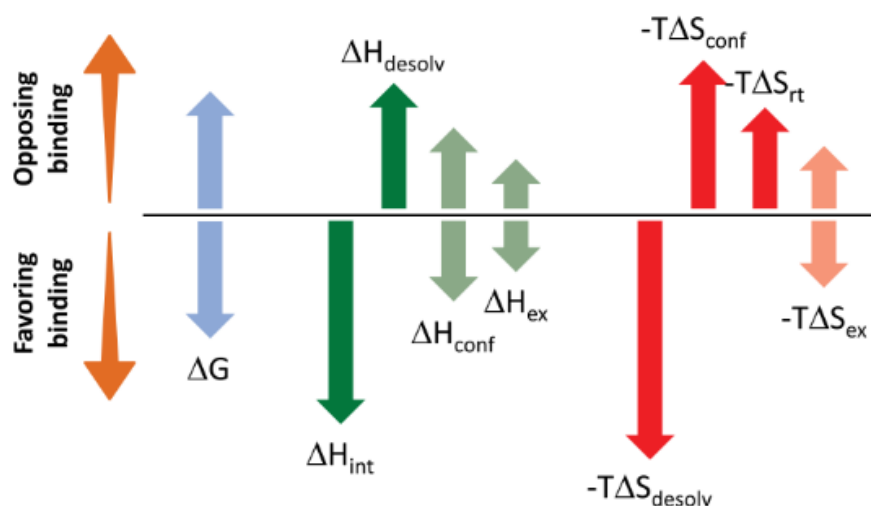


Figure 3. Thermodynamics of binding: enthalpy and entropy contributions. Main enthalpic (green) and entropic (red) contributions to the Gibbs energy of binding (blue). The intrinsic enthalpy and the desolvation enthalpy are always favorable and unfavorable, respectively, while conformational enthalpy and the ligand-exchange enthalpy may favor or oppose binding (light green). The desolvation entropy is always favorable, the conformational entropy and the rotational-entropic are always unfavorable and ligand-exchange entropy may favor or oppose binding (lighter red). The sum of all contributions gives rise to the Gibbs energy of binding. Figure from Claveria-Gimeno *et al.*²⁶

In general, upon binding there are three main events to be considered: first, solvated ligand and protein binding pocket break the interactions with the surrounding water molecules (enthalpically unfavorable), and water molecules are released (entropically favorable). Then, the ligand and the protein change their conformation to adapt to each other and finally they establish new interactions forming the complex. If the molecules are trapped between the protein surface and the ligand, then favorable enthalpy and unfavorable entropy will occur. For this reason, more information on the water molecules network in and around the binding site is important. The change of conformation and the loss of rotational and translational freedom cause an enthalpic penalty (Figure 3).²⁶⁻²⁸

Optimizing the binding from a thermodynamic aspect may be quite challenging and several factors should be considered. One of the strategies used to design glycomimetics is the deoxygenation: higher affinities can be achieved by just reducing the desolvation penalty by removing polar groups not involved in important interactions. Indeed, every hydroxyl group that does not contribute to the binding causes a desolvation penalty of approx. 26 kJ/mol (ΔG). At the same time, if the hydroxyl groups share the water molecules, the desolvation cost is reduced to 17 kJ/mol per hydroxyl.²⁹ This free energy is not always compensated by the formation of one H-bond with the protein, therefore, one OH should be at least involved in two H-bonds with the protein to be energetically favorable.

Another strategy for the design of glycomimetics involves the classical replacement with bioisosteric groups, which are substituents with similar physico-chemical properties able to preserve the same biological effect.^{30,31} Fluorine, for example, can replace OH groups, preserving polar interactions but with reduced polarity, or even a hydrogen atom thanks to its small size.³² Modifications can be also introduced to improve the pharmacokinetic properties, as for example adding groups that can bind active transporters in the intestine enabling oral absorption (e.g. valacyclovir) or to proteins in the serum in order to increase the half-life.³³

All together, these strategies demonstrate how glycomimetics can limit the drawbacks of carbohydrates and allow for the exploration of their target and functions, making them a more and more interesting class of therapeutics agents.

1.4 Glycan-binding proteins.

Given the enormous role that carbohydrates have in many physiological and pathological processes, it is also intuitively clear how important it is to read the glycan's encoded information and to translate it in cellular effects.^{34,35} The interpreters of this code are the lectins, a subgroup of the large family of

glycan-binding proteins (GBPs), which also include carbohydrate processing enzymes and glycosamino-glycan-binding proteins.^{2,36}

Lectins (from the Latin word “legere”, which means to read) are non-enzymatic proteins with specificity for carbohydrates, ubiquitously found in nature and with different roles, from cell development, to host recognition, mediation of cell-cell interactions, immune response, etc. In general, lectins can be found as integral part of the membrane or as soluble proteins.³⁷

Vertebrate lectins can be differentiated in subgroups, based on amino acids sequence homology in the carbohydrate binding domains (CRDs) and structural characteristics³⁸:

- C-type lectins, which need calcium to bind sugars (e.g. Selectins, DC-SIGN)³⁹
- I-type lectins, part of the immunoglobulin superfamily (e.g. Siglecs)⁴⁰
- S-type lectins, which need thiol groups for their activity; later renamed to Galectins, as not all members are thiol-dependent
- Pentranxins, characterized by different subunits forming pentamers
- P-type lectins, mostly specific for mannose-6-phosphate proteins.

It may be questionable how the message that lectins decode from sugars can be so specific, starting from a limited number of monosaccharides and from the fact that different lectins can recognize the same mono- or oligosaccharides. The answer resides in the extremely complex nature of lectin-carbohydrate interactions, not only for the structural complexity of the glycans but also from the flexibility, the density on the membrane, different conformations and possible multivalent presentations.^{41,42}

Multivalency is a very common mechanism that nature uses to improve binding affinities between lectins and carbohydrates. Multivalent interactions can happen in different ways: homomultimeric lectins interact with several glycans at the same time giving raise to the so-called avidity effect, monovalent lectins can form a cluster to interact with multivalent ligands, heterobivalent ligands interact with a lectin with two different binding sites, and, finally, in case of multivalent ligands, the statistical rebinding effect (Figure 4). The nature of the interactions can trigger different biological responses.⁴³⁻⁴⁵

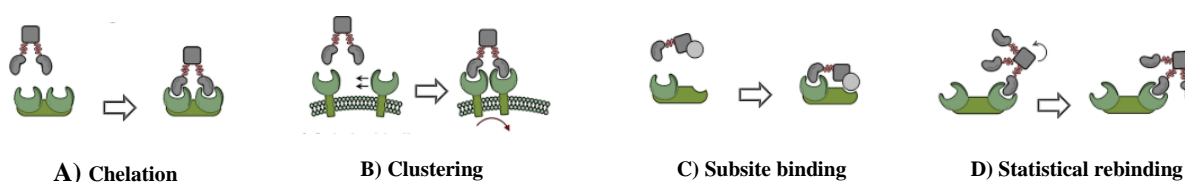


Figure 4. Mechanisms of multivalent interactions. Figure adapted from Cecioni *et al.*⁴¹

Different types of lectins have been fully characterized and validated as targets for potential pharmacological treatment. We will now focus on a subgroup of the I-type lectin family, the **Sialic-acid-binding-ImmunoGlobuline-like-Lectins (Siglecs)**.^{46,47}

1.5 Sialic acids and the Siglec family.

Sialic acids represent the major sugar component of the glyocalix. They are usually located at the terminal positions of oligosaccharides and glycoconjugates and can act as ligands for receptor recognition (trans-interactions) and for masking recognition sites (cis-interactions). Sialic acids can be found in differently substituted forms, all derived from the neuraminic acid (Neu) parent molecule, like for example the *N*-acetylated variant (Neu5Ac), which is the most abundant, or the *N*-glycolylated derivative (Neu5Gc), which cannot be synthesized by humans (Figure 5).

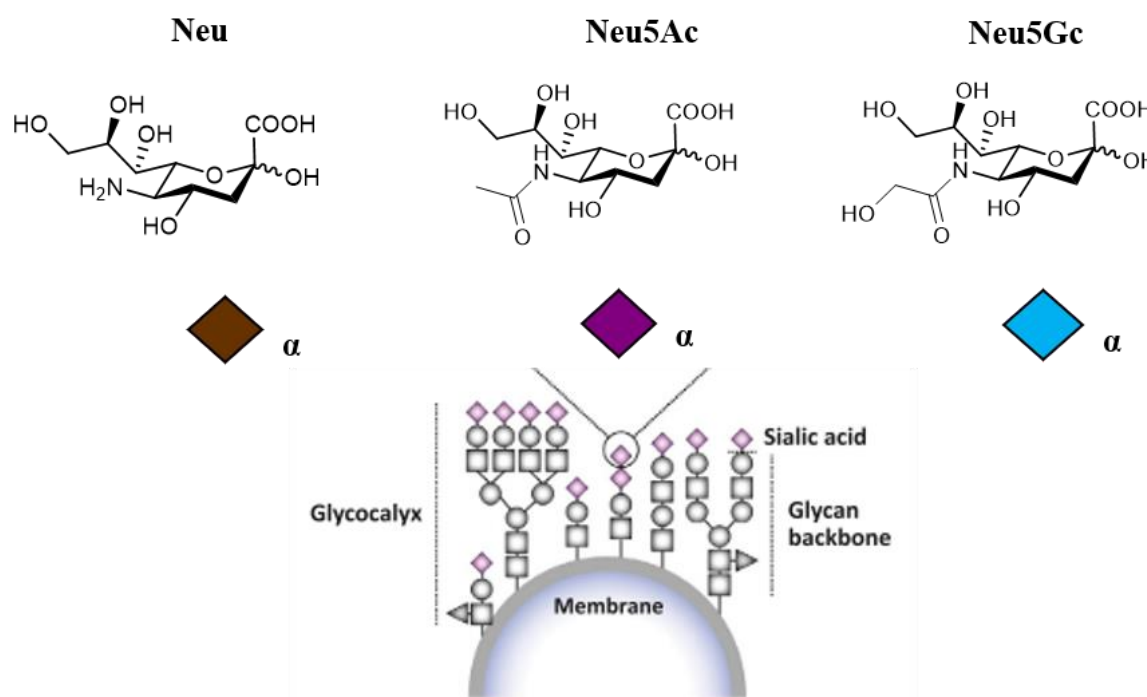


Figure 5. The most abundant sialic acids: the neuraminic acid and its *N*-acetyl and *N*-glycolyl derivatives (Neu5Ac and Neu5Gc, respectively). They are shown in their α -configuration, as if they were in bound states. The colored squares represent their standard graphic symbols.⁴⁸ Figure adapted from Bull *et al.*⁴⁹

Free sialic acids engage in the energetically preferred β -form but when bound they adopt the α -anomeric configuration.^{50,51} Because of their position on the surface of the membranes, sialic acids are particularly available for protein-ligand interactions, mediating several physiological and

pathological processes.^{52–57} As just mentioned above, Siglecs are one family of proteins that mediate these interactions.

Human Siglecs are numbered following the order in which they were discovered, same for murine Siglecs, but the representatives that are not homologous to the human ones are named by a letter (e.g. Siglec-F).⁵⁸ Human Siglecs are divided into two groups depending on their homology and evolutionary conservation (Figure 6). CD22-related Siglecs show only 25-30% of sequence identity and they have true orthologs in other mammalian species: Sialoadhesin (Siglec-1), Siglec-2 (CD22), Siglec-4 (myelin-associated glycoprotein, MAG) and Siglec-15 belong to this group. The second group consists of CD33-related Siglecs (CD33rSiglecs). Among these, Siglec-12 lost its ability to recognize sialic acid, so it was renamed Siglec-XII, and the Siglec-13 gene is not present in humans.⁵⁹ CD33rSiglecs are characterized by high sequence homology and minor conservation between species.^{60–62} CD33rSiglecs are also expressed in mice but they represent paralogs and not true orthologs of the human counterparts: Siglec-F and Siglec-G correspond to Siglec-8 and Siglec-10, respectively.⁶³ The high evolutionary differentiation might be a response to different mechanisms of evasion of the immune system by pathogens or cancer cells, like mimicking our self-glycans.^{47,64,65}

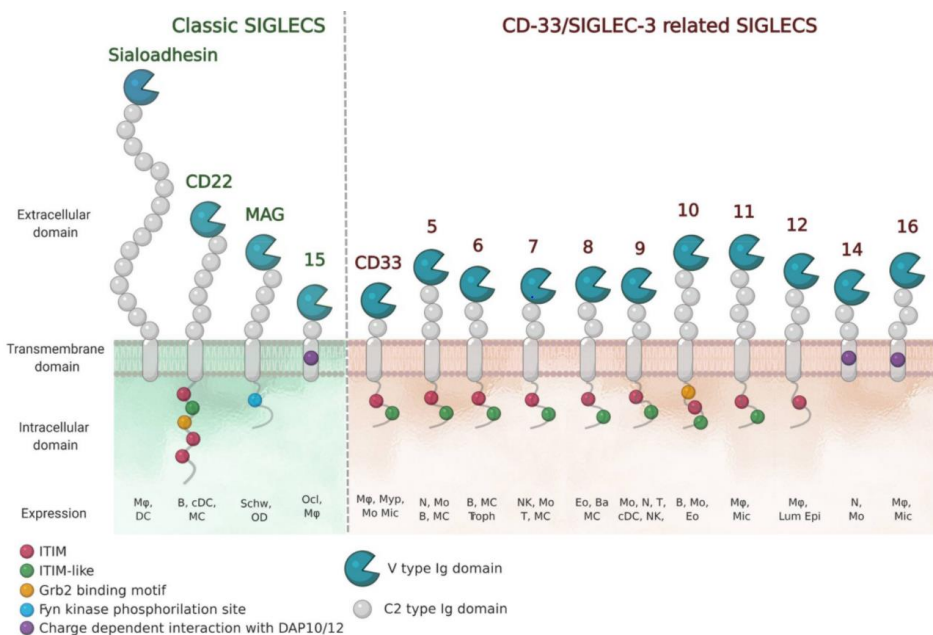


Figure 6. Structural features of human Siglecs and their expression. M ϕ , macrophages; DC, dendritic cell; B, B cells; MC, mast cells; Schw, Schwann cells; OD, oligodendrocytes; Ocl, osteoclasts; Myp, myeloid progenitor; Mo, monocytes; Mic, microglia; N, neutrophils; Troph, trophoblasts; NK, natural-killer cells; T, T cells; Eo, eosinophils; Ba, basophils; Lum epi, lumen epithelia cells). Figure from Lenza *et al.*⁶⁶

Structurally, Siglecs present on their extracellular N-terminal part a V-set domain, containing the sialic acid binding pocket, and a variable number of C-2 set domains (from 1 to 15), both Ig-like domains. Normally, in their resting state, Siglecs are engaged in cis-interactions with sialic acid

ligands expressed on the same cell-surface. Sn (Siglec-1) is an exception: because of its length (15 C-2 set domains), it is mainly involved in trans-interactions.^{61,67,68} High-affinity ligands can compete with cis-ligands and bind to Siglecs, as it has already been demonstrated with CD22 (Siglec-2).⁶⁹

The signaling is initiated by the intracellular regulatory motifs, except for Sialoadhesin that does not contain any domain in this region: most of the Siglecs present an immunoreceptor tyrosine-based inhibitory motif (ITIM). These domains are first phosphorylated by Src kinases, then the recruitment of Src-homology 2 domain (SH2)-containing phosphatases SHP-1 and SHP-2 de-phosphorylate important signaling molecules and initiate the inhibitory cascade.⁷⁰ Only Siglecs-14, -15 and -16 have an activating activity. They contain positively charged amino acid residues that bind to the coreceptor DAP12, which in turn contains an immunoreceptor tyrosine activation motif (ITAM) in its cytoplasmic domain. Once the binding to Siglecs takes place, DAP12 initiates the activating signaling.^{71,72} Generally, activating Siglecs are coupled with inhibitory counterparts: Siglec-5 vs Siglec-14 and Siglec-11 vs Siglec-16, usually expressed on the same cells.⁷³

As previously mentioned, all Siglecs bind sugars containing sialic acid, but each with its own specificities. They have evolved to recognize all the different ways in which the sialic acids are displayed on glycoproteins and glycolipids so they can be specific for the type of linkages (α 2-3, α 2-6, and/or α 2-8), or the type of sugars to which the sialic acid is bound to. Usually, Siglecs bind to their natural sialoside ligands with low affinities (0.1-1 mM).⁷⁴ The interactions (monovalent or multivalent) are very specific and can regulate the physiology of the cells where they are expressed.⁷⁵ The N-terminal V-set domain mediates the binding and it is composed of antiparallel β -sheets with a shallow binding pocket for the sugar and an additional loop in the proximity, which provides more specificity for carbohydrates. One of the most conserved amino acids in this region is an arginine which interacts with a salt bridge with the carboxylate of the sialic acid.⁷⁶

Siglecs are mostly expressed on immune cells, except for Siglec-4 which is present on myelinating cells of the nervous system. Depending on the roles and sites of expression Siglecs are involved in many physiological and pathological processes, especially as immuno-modulators. In the following sections, the involvement of Siglecs in autoimmunity, infection, inflammation, aging, and cancer will be presented in more detail.⁴⁹

Siglecs and host protection. Being at the interface between cells, some Siglecs play a key role in recognizing pathogens, such as bacteria or viruses.⁷⁷

Siglec-1, for example, is mainly expressed on macrophages (described as CD169⁺ macrophages). Upon recognition of sialic acid epitopes expressed on the cell surface of bacteria or viruses, Siglec-1 promotes phagocytic activity of macrophages, optimization of antigen presentation and subsequent

activation of the adaptive immune response.⁷⁷⁻⁷⁹ It has the same role on other antigen-presenting cells (APCs) like dendritic cells (DC), where it triggers antiviral immunity. Unfortunately, enveloped viruses such as Ebola or human immunodeficiency virus (HIV)-1 have exploited this mechanism to enhance the auto dissemination in tissues and escape the immune system.⁸⁰⁻⁸² HIV's capture by DC, for example, facilitates virus dissemination and release in sites of cell contact with the CD4⁺ T cell. Therefore, the virus can easily reach these sites and trans-infect T-cells.^{83,84} Another way to escape the immunity is to mimic self-sialic acid-containing sugars, like the group B *Streptococcus* (GBP). GBP binds to Siglec-9, expressed on neutrophils. Being an inhibitory receptor, this leads to deactivation of the immune response and the bactericidal activity. Next to sialic acid mimicry, GBP also uses a membrane-anchored protein to bind Siglec-5, expressed on macrophages and neutrophils, with again the same effect of blocking these cells.

Siglecs in neurological disorders. Even if not directly expressed in the brain, some Siglecs may have some implications in the central nervous system (CNS).⁸⁵

A recent study demonstrates that CD22, a negative regulator of B cells, can be involved in reducing the phagocytic activity of macroglia cells, which is important to maintain homeostasis in the CNS activity and it is usually reduced in aged brains or in neurodegenerative diseases. The inhibition of CD22 with an antibody or by genetic ablation increased microglia phagocytosis of debris or protein aggregates, improving cognitive performance in mouse models.⁸⁶

Dysregulation of microglia phagocytic activity is also connected to Alzheimer's disease (AD), with reduced ability to remove amyloid beta (A β) plaques in the brain. Some evidences show that polymorphisms in the CD33 gene may represent a risk for AD and that would also affect microglia phagocytic activity. However, these studies have been conducted on mice, which present a different form of CD33. Therefore, these conclusions remain to be confirmed. A recently presented human CD33 knock-in mouse model might provide answers to these open questions.⁸⁷

Finally, MAG (Siglec-4) is expressed on oligodendrocytes and Schwann cells, both in the central and peripheral nervous systems. Controversial results have been obtained regarding MAG's function but different evidences support the theory that it is involved in the inhibition of axonal regeneration. Upon myelin disruption, MAG can also diffuse as a soluble form to other sites and have a major inhibitory activity on the axon growth. This explains why in the early phases of multiple sclerosis neurons degenerate even if the myelin has not been disrupted yet. An anti-MAG humanized monoclonal antibody (mAb) from Glaxo (GSK24932) is currently on clinical trials for promoting neuronal regenerations in strokes, blocking MAG inhibitory activity.^{88,89}

Siglecs and tumor. Malignant cells usually have a different glycosylation pattern, resulting in hypersialylated glycans or higher display of Neu5Gc (which can be assimilated with the diet, then metabolized and expressed on the cells), therefore providing a high number of ligands for Siglecs.^{11,90} T-cells and natural killer (NK) cells are both tumor-infiltrating cells, participating in the recognition and killing of cancer cells. They both express Siglec-7 and Siglec-9, which are actually upregulated in some tumor-infiltrating CD8⁺ and CD4⁺ T-cells in various cancers. Evidences show that the binding of these Siglecs with antigen-binding fragments (Fab) of Siglec-7 and -9 blocking antibodies increased immune cell activity, reducing the interactions of Siglecs with their ligands. The same effect was reached by treating target cancer cells with neuraminidases, which decrease the availability of sialic acid on the surface and, consequently, the interactions with Siglecs, thus contributing to enhance the immune mediate response. However, the treatment with full-length anti-Siglec antibodies inhibits cell cytotoxicity, suggesting the induction of inhibitory signals.⁹¹⁻⁹⁵ A better comprehension of Siglec-7 and -9 signal regulation is needed to understand whether they can represent potential targets for cancer immunotherapy.

Other Siglecs identified as potential targets for cancer treatment, in particular for chronic lymphocytic leukemia, non-Hodgkin lymphoma and acute myeloid leukemia (AML) are CD22 and CD33.⁹⁶⁻¹⁰⁰

Siglecs in allergies and autoimmune diseases. Considering that Siglecs are important regulators of immune response and immune cell homeostasis, they also have important roles in allergies and in the development of autoimmune diseases. Most allergies are connected to hyperactivation of eosinophils and mast cells, therefore targeting Siglec-8, exclusively expressed on these cells, might be a promising therapeutic approach, as it will be discussed in detail in the next chapters.

Regarding autoimmune diseases, polymorphism of CD22 in humans has been associated with rheumatoid arthritis or systemic lupus erythematosus (SLE). Binding of CD22 to liposomal nanoparticles covered by both antigen and glycan ligands for CD22 causes the apoptosis of B-cells in mice and humans. These Siglec-engaging tolerance-inducing antigenic liposomes (STALs) can be exploited to tolerize B-cells to specific antigens, in order to prevent unwanted immune response.¹⁰¹

This small summary reveals how important Siglecs are and how a better understanding of their biology and functions may be a turning point in the treatment of various diseases. To reach this goal, different strategies have been explored to target Siglecs, in particular the use of antibodies, monovalent and multivalent ligands.

1.6 How to target Siglecs?

One of the first examples of targeting Siglecs is the use of antibodies. The first fully humanized anti-CD22 IgG1 antibody is Epratuzamab (Emab). It does not kill malignant B cells as a single agent but it showed positive results when associated with Rituximab.^{96,102} Clinical trials have also been conducted on the use of Emab for the treatment of autoimmune diseases like SLE.^{103,104} Since CD22 is internalized upon Ab binding, another approach is the use of Ab-conjugated drugs (ADC), such as inotuzumab ozogamicin, where the Ab is conjugated with a drug able to disrupt the DNA. This ADC has been approved for the treatment of acute lymphoblastic leukemia (ALL).¹⁰⁵ Recently, CD22 has also been a target for CAR T cell therapies, in order to redirect T cells effectors towards malignant B cells. Positive results were obtained in the treatment of B-cell ALL.¹⁰⁶ Another ADC (Mylotarg) was approved to target CD33 for the treatment of refractory AML.¹⁰⁷ Antibodies can also be used to block Siglecs and prevent their interaction and activation with endogenous ligands. For example, blocking Siglec-15 on tumor cells prevents its ability to suppress T cell activity and therefore limits tumor growth.¹⁰⁸

Considering the limitations of antibodies, such as low bioavailability and high immunogenicity, traditional approaches like the use of small molecules are still widely used (Figure 7).¹⁰⁹

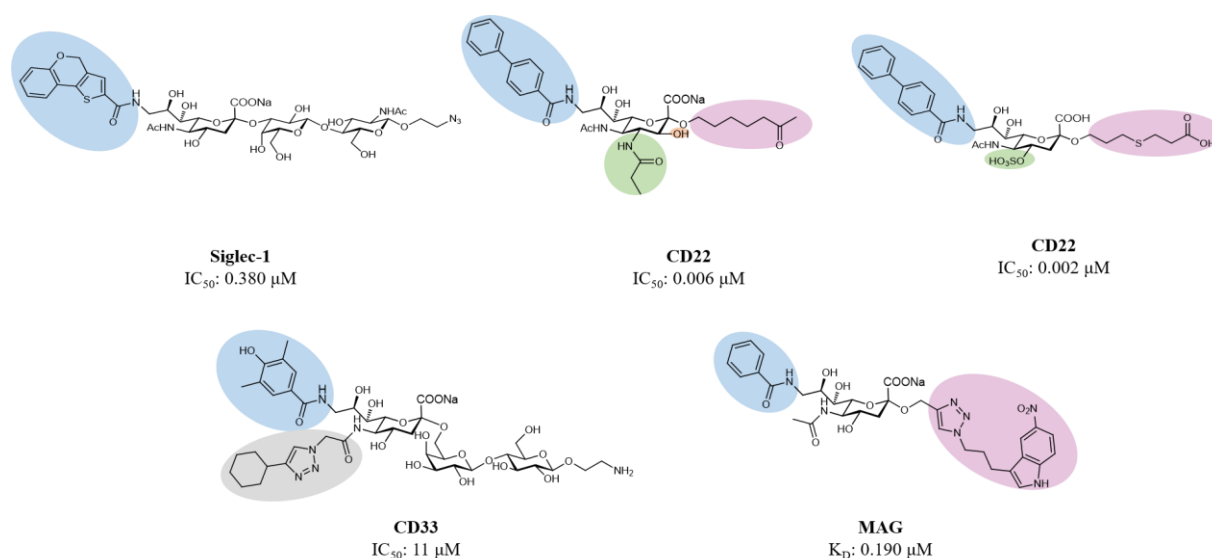


Figure 7. High affinity/selective ligands for Siglec proteins. Modifications on positions 2 (pink), 3 (orange), 4 (green), 5 (grey) and 9 (blue) have been applied.¹¹⁰

As previously discussed, different strategies can be employed to modify the neuraminic acid in different positions to improve not only its affinity towards Siglecs but also the pharmacokinetic properties. Some of the most successful examples of high affinity ligands for various Siglecs are

presented in Figure 7. Once a potent and selective monovalent ligand has been optimized, it can be presented with a multivalent approach. In the last decade, different examples of multivalent presentation of glycans have been reported. For example, liposomes or nanoparticles decorated with Sn or CD22 ligands have been used to selectively deliver cargo to B-cells or Sn⁺ macrophages.^{111–114}

1.7 Siglec-8.

Siglec-8 has been discovered around 2000 by two groups independently and was identified as a Siglec protein exclusively expressed on eosinophils and mast cells, and weakly on basophils.^{115,116} Lately, a long-form was identified, bearing the usual ITIM, common to other Siglecs. The short form was the result of a premature stop codon and since then, the term Siglec-8 refers to the predominant long form.¹¹⁷ Siglec-8 consists of a V-set domain, two C-2 set domains, one ITIM and one ITIM-like domain in the intracellular region, involved in the negative cell signaling. Siglec-8 cross-linking induces apoptosis in eosinophils, in a caspase-dependent manner on normal cells, and through production of reactive oxygen species (ROS) in eosinophils interleukin-5 (IL-5) primed.^{118,119} On mast cells, Siglec-8 inhibits their degranulation but it doesn't affect their survival.¹²⁰ The intracellular pathway is not fully characterized but lately, it was found that Siglec-8 engagement on IL-5 primed eosinophils leads to β_2 -integrin-mediated adhesion of eosinophils, necessary for the activation of nicotinamide adenine dinucleotide phosphate (NADPH) oxidase, with consequent production of ROS and eosinophil apoptosis (Figure 8).¹²¹

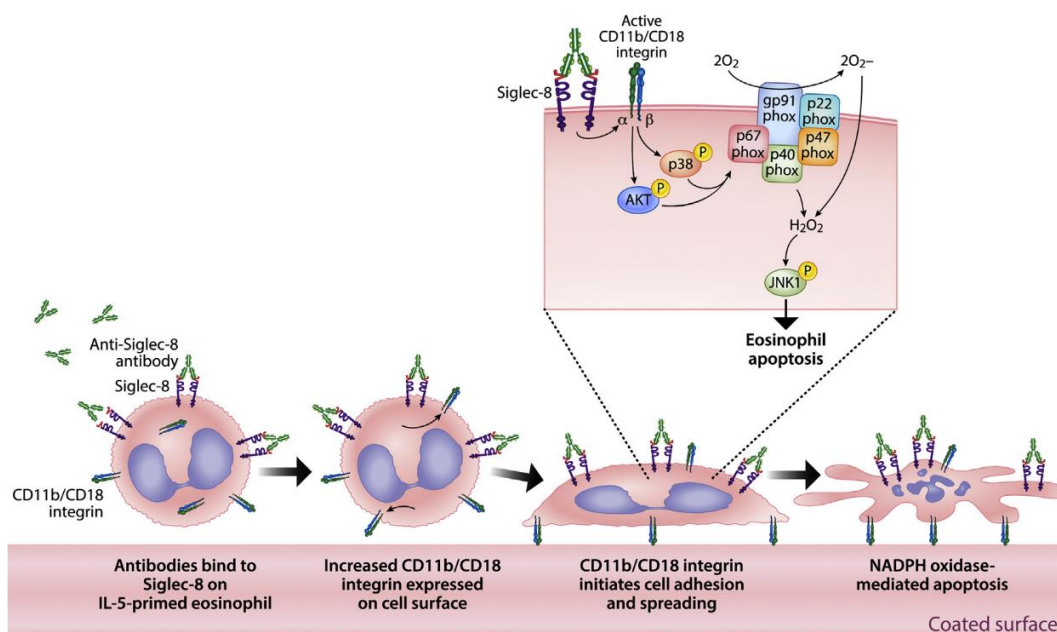


Figure 8. Siglec-8 signaling mechanism in IL-5 primed eosinophils. Figure from Carroll *et al.*¹²¹

Regarding the levels of Siglec-8 expression, different studies showed that they are quite stable on eosinophils and mast cells independently of the disease state and tissue of origin and that the protein appears quite late in the maturation process of these cells.^{122,123}

Siglec-8 is not expressed and does not have a true ortholog in mice but its closest paralog is Siglec-F. The major differences are that Siglec-F also recognizes non-sulfated ligands and that it is only expressed on eosinophils. Besides, the use of anti-Siglec-F antibodies also reduces eosinophilic inflammation in models of disease but its mechanism is pure caspase-dependent.^{124,125} These differences limit the preclinical studies and its therapeutic targeting *in vivo*. To solve these problems and to facilitate Siglec-8 biology investigation, novel mouse strains were generated, where Siglec-8 was selectively expressed on eosinophils and on mast cells.^{126,127}

Due to the selectivity of expression, the inhibition activity that Siglec-8 has on eosinophils and mast cells, and the constant levels of expression on cells both in healthy and non-healthy conditions, in the last years a lot of interest has emerged to target this protein for the treatment of many allergic and inflammatory diseases associated with eosinophils and mast cells.

1.8 Eosinophil and mast cell-related disorders.

Eosinophils and mast cells (MCs) are some of the major cells involved in allergic and inflammatory reactions. They derive from pluripotent precursor cells of the myeloid lineage and, in presence of stem cell factors or various cytokines, they mature and migrate into tissues.

MCs can be activated in immunoglobulin-E (IgE) dependent manner, by cross-linking of antigen-specific IgE to the high affinity Fc epsilon receptor 1 (FcεRI), or in an IgE independent way, which involves other mast cell receptors such as toll-like receptors (TLRs) or receptors that bind cytokines, chemokines, etc. Once activated, MCs release proinflammatory and vasoactive mediators.^{128,129}

The differentiation and activation of eosinophils are particularly guided by IL-5: once mature in the bone marrow, the cells migrate and, under homeostatic conditions, reside into the gastrointestinal tract. Additional activation forms recruit them in other affected tissues where they release their products promoting local inflammation, tissue remodeling, and sometimes tissue damage.¹³⁰ Next to the physiological roles of regulating vasodilation, angiogenesis, innate and adaptative immune response, both eosinophils and MCs, can be linked to the pathophysiology of different diseases.^{131,132}

Eosinophilic disorders are a group of diseases characterized by high absolute eosinophil count (AEC) in the peripheral blood for at least one month. Hypereosinophilia (HE) is characterized by different types of symptoms, from mild to severe, which can affect organ function because of eosinophil infiltration, and in rare cases being fatal. We can mainly distinguish primary eosinophilia (also

referred to as neoplastic, like acute and chronic eosinophilic leukemia, a result of stem cells mutation), and secondary HE, usually caused by infections (especially in third world countries) or allergies. Besides, there is also idiopathic HE, where the cause has not been identified yet. When HE is associated with tissue or organ damage it is commonly called hypereosinophilic syndrome (HES). However, there are still a lot of gaps in classification, diagnosis criteria and molecular understanding of these diseases.¹³³⁻¹³⁶

Regarding the primary neoplastic HE, they can be distinguished in myeloproliferative and lymphocytic malignancies that can have very bad or even fatal outcomes if not diagnosed or treated properly.^{137,138} Severe symptoms or a reduced quality of life also characterize the secondary HE, potentially associated with different allergic diseases such as chronic rhinosinusitis or conjunctivitis, asthma, eosinophilic gastrointestinal disorders, chronic idiopathic urticaria, and the two most severe forms, chronic eosinophilic pneumonia and delayed reactions associated with drugs, known as drug reaction with eosinophilia and systemic symptoms (DRESS).¹³³

MCs-related disorders are also characterized by local or systemic infiltration and accumulation of mast cells. MC disorders are mainly divided in mastocytosis and MC activation syndrome. Mastocytosis is a quite rare condition that can be cutaneous (skin lesion, urticaria), more common in children and with a good prognosis, or systemic with quite diffused symptoms, usually with bone marrow involvement.^{129,139,140} Rare cases can develop a more serious form of systemic mastocytosis, with end-organ damage due to infiltration of neoplastic MCs.¹⁴¹

MC activation syndrome is instead characterized by episodic symptoms of mast cell activation. It can be triggered by IgE-mediated allergy responses or it can be idiopathic, which in some rare cases reaches the severity of anaphylaxis. However, the disease is usually successfully treated with antimediation therapy.^{142,143}

Available treatment. At the moment, no cure is available for most of these diseases but there are different treatment options to control the symptoms. The priority in any of the mentioned cases should be the identification, whenever possible, of likely secondary causes, and to prevent organ damage and loss of function. HE or mastocytosis can rapidly evolve to very severe conditions, prompt diagnosis and treatment are therefore essential.

The drugs commonly used are glucocorticoids, histamine receptor antagonists, anti-leukotriene antagonists such as montelukast, and epinephrine, especially in higher risks of anaphylaxis like in systemic mastocytosis. In some cases of mastocytosis and malignant cells, as eosinophil or mast cells leukemia, cytoreductive drugs are needed, in particular interferon-alpha and imatinib.¹⁴⁴⁻¹⁴⁷ However,

all these drugs are characterized by a lot of side effects, and by very variable efficacy and toxicity profiles, especially for the common long-term use for chronic conditions.^{144,148}

Therefore, new targeted therapies with minor side effects are urgently needed. In this perspective, in the last years Siglec-8 has emerged as a new potential therapeutic target for eosinophil and mast cell-related disorders, because of its specific expression on these cells and its role in inducing eosinophils apoptosis and inhibition of mast cells degranulation. Furthermore, it would also be possible to have a synergic effect, since both of these cell types are hyperactivated in common diseases and some preliminary studies suggest that they do not act as separate identities but have an influence on each other.¹⁴⁹

1.9 Siglec-8 as a druggable target.

Different reports already support and confirm the idea that Siglec-8 can be a relevant target for the treatment of eosinophil and mast cell-related disorders.

AK002 (lirentelimab), for example, is a humanized non-fucosylated IgG1 anti-Siglec-8 antibody already in clinical trials for the treatment of different allergic and inflammatory diseases linked to eosinophils and mast cells.¹⁵⁰ It has been proven that AK002 selectively binds to mast cells, eosinophils and weakly to basophils in human blood and tissue, it reduces eosinophils inducing apoptosis and NK cell-mediated antibody-dependent cell-cytotoxicity (ADCC) against blood eosinophils. Furthermore, a murine precursor of AK002 (mAK002) was tested in a passive systemic anaphylaxis (PSA) humanized mouse model where it showed mast cell inhibition and PSA prevention.¹⁵⁰

AK002 showed positive results in phase I clinical trials for indolent systemic mastocytosis (ISM) and allergic conjunctivitis. The drug improved the general quality of life of patients and also relieved comorbidities like asthma, dermatitis and rhinitis.^{151,152} Encouraging results were reported for phase II trials for the treatment of refractory chronic urticaria (on patients not responding to antihistamines or omalizumab) and eosinophilic gastritis and duodenitis. In the last case, long-term use was well tolerated and showed histological improvements.^{153,154}

Anti-Siglec-8 monoclonal antibodies showed a reduction of non-allergic inflammation by inhibiting IgE independent mast cell activation.¹⁵⁵

As listed before, another disease that is associated with infiltration of airway eosinophils and pronounced degranulation of mast cells is asthma.^{156,157} Several findings support the idea that Siglec-8 may be involved in the treatment of this disease. For example, Siglec-8 ligands are upregulated in inflamed human airway tissues compared to healthy tissues, and eosinophils obtained from allergy

patients showed increased Siglec-8-mediated apoptosis.^{158,159} In addition, polymorphisms in the Siglec-8 gene are associated with increased susceptibility to asthma.¹⁶⁰

Lastly, it seems that eosinophils and mast cells are also quite active during SARS-CoV-2 infections, and that treatment with anti-Siglec-8 antibodies reduces the general inflammation. Hence, when this would be confirmed by further studies, Siglec-8 may represent a possible target to fight this viral infection causing the actual global pandemic.¹⁶¹

The selective expression of Siglec-8 and its endocytic property can also be exploited for selective delivery of therapeutic agents to mast cells and eosinophils, for example to treat malignancies associated with these cells.¹⁶² Next to antibodies, Siglec-8 has also been targeted with nanoparticles displaying its ligands. Liposomes decorated with Siglec-8 ligands were selectively taken up in cells expressing Siglec-8 or -F. Furthermore, when additionally decorated with allergens, these liposomes were able to suppress IgE-mediated mast cells degranulation.^{163,164}

As discussed before, the development of small molecules able to bind Siglec-8 represents a valid alternative and approach to the use of antibodies, to tackle eosinophils and mast cells diseases and to better understand the protein's biological role and function.

1.10 Siglec-8 structure.

Siglec-8 has high sequence homology with Siglec-7 (68%), CD33 (49%) and with Siglec-5 (42%).¹¹⁶ The main differences are within the loop containing Arg56: this loop presents 11 residues instead of the more common 5 residues. This confers specificity for a particular ligand, as explained in more details below.

The exact natural ligand of Siglec-8 has not been discovered yet, but recent findings identified keratan sulfate (KS) as primary carrier of endogenous human airway ligands. Once isolated and purified from trachea extracts, it increased eosinophil apoptosis *in vitro*.¹⁶⁵

In a glycan array screening the tetrasaccharide 6'-sulfo-sLe^x (NeuAc α 2-3[6-*O*-sulfo]Gal β 1-4[Fuc α 1-3]GlcNAc) was identified as the preferred Siglec-8 ligand. From this screening, it became obvious that Siglec-8 is very selective for α 2-3 linkages of neuraminic acid, and that the sulfate in position 6 of the galactose seems to be detrimental for binding (28-fold loss of affinity when removed).^{166,167} Later, an NMR solution structure of the Siglec-8 CRD was obtained in complex with this tetrasaccharide (Figure 9).¹⁶⁷

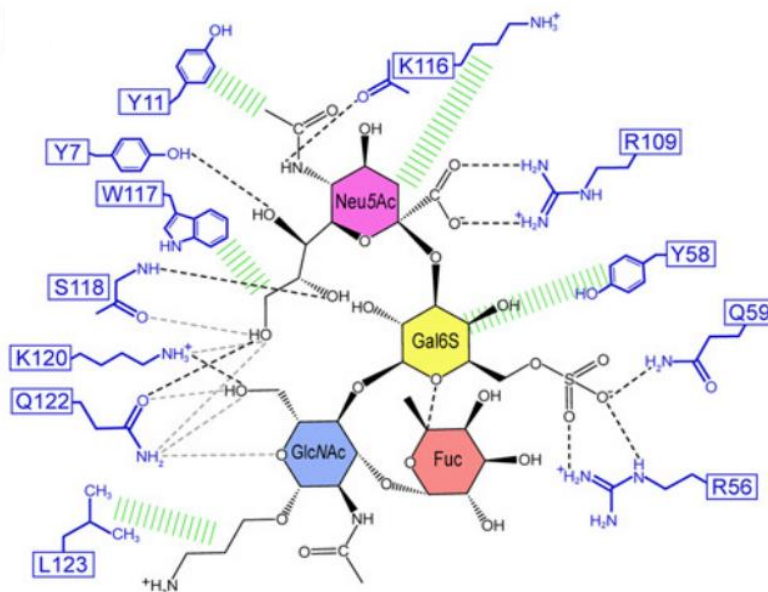


Figure 9. Main interactions between Siglec-8 and 6'-sulfo-sLe^x. Black dashed lines indicate hydrogen bonds in the depicted structure; gray dashed lines indicate hydrogen bonds abundantly observed in other structures of the ensemble. Hydrophobic contacts are shown in green. Figure from Pröpster *et al.*¹⁶⁷

The main interaction, as for the other Siglecs, involves a salt bridge between the carboxylate of the sialic acid and the conserved arginine residue (Arg109). The important sulfate in position 6 of the galactose moiety is involved in a second salt bridge with Arg56 and Gln59. As mentioned above, Arg56 is in a larger loop compared to the one present in other Siglecs, which may confer the unique binding specificity for this ligand. In addition, hydrogen bonds exist between hydroxyl groups 7, 8 and 9 of sialic acid and Tyr7, Ser118 and Gln122. In contrast, the fucose and glucosamine subunits show only minor interactions with the protein. The affinity of 6'-sulfo-sLe^x was evaluated with three different techniques: Isothermal titration calorimetry (ITC), a polyacrylamide-based competitive binding assay (CBA), and solution NMR, which all confirmed a K_D of approximately 300 μM .¹⁶⁷

The ability of this tetrasaccharide to bind Siglec-8 was also confirmed by testing a polyacrylamide polymer decorated with 6'-sulfo-sLe^x. It selectively bound to eosinophils in human blood and also induced apoptosis of IL-5-primed eosinophils in a Siglec-8-dependent manner (the binding was abrogated by the use of an anti-Siglec-8 antibody).¹⁶⁸

The Siglec-8 structural data and the binding mode of its preferred glycan ligand represent an optimal starting point for the development of high affinity ligands as molecular probes to further study Siglec-8 function and as potential therapeutic agents for the treatment of eosinophil and mast cell-related disorders.

1.11 Objectives of the thesis.

The general aim of this thesis was the development of glycomimetic ligands with improved affinity to Siglec-8. To reach this goal different approaches have been employed.

First, starting from the natural ligand, the tetrasaccharide 6'-sulfo-sialyl Lewis^x, the minimal binding epitope of the molecule was identified. Further strategies, such as the use of bioisosters, a deoxygenation process to reduce the polarity of the molecule and the introduction of substituents on the sialic acid core were carried out to improve affinity and drug-like properties of the ligands (Chapter 2).

For Siglec-8, the only structure available is an NMR solution structure of its lectin domain, which provides limited use for structure-based design due to its poor resolution. Therefore, in order to get more structural information and to better understand the binding mode of our most potent ligand, we built a homology model of Siglec-8 based on the crystal structure of homologous Siglec-7 (Chapter 2).

Looking at the docking pose of our ligands, we also aimed to explore an empty binding pocket close to position 5 of the sialic acid core. Rational design and virtual fragments screening were exploited to identify suitable fragments for this cavity. They were virtually attached to the core structure of our lead compound and docked into the Siglec-8 NMR solution structure. Virtual screening of commercially available libraries was also performed to identify non-sugar-containing hit molecules. The best compounds identified were synthesized and biologically evaluated (Chapter 3).

In addition, we developed an LCMS method to check the stability of our ligands to neuraminidases, enzymes able to hydrolyze terminal sialic acids, in order to obtain important pharmacokinetic information already in the first stages of this project (Chapter 4).

Finally, the structure of some Siglec-8 ligands resembles those of known ligands for Galectin-8. Therefore, we also synthesized and evaluated non-sulfated derivatives to target this important lectin involved in many physiological and pathological processes, such as cancer, inflammation and bone remodeling (Chapter 5).

These goals have been condensed in six hypotheses:

Hypothesis 1. Low molecular weight and monovalent glycomimetic ligands with high affinity for Siglec-8 can be designed and synthesized by replacing galactose in 6-sulfo-Sia-Gal with a sulfo-substituted cyclohexane or aromatic ring (Chapter 2).

Hypothesis 2. The sialic acid moiety is not essential for the binding to Siglec-8 (Chapter 2).

Hypothesis 3. Precise and reliable insights into the binding mode of our high affinity ligands can be provided by using homology modelling of Siglec-8 (Chapter 2).

Hypothesis 4. New fragments and virtual hit molecules that fit into the binding pocket of Siglec-8 can be predicted and their binding affinity can be scored by using fragment-based and structure-based virtual screening (Chapter 3).

Hypothesis 5. Siglec-8 ligands are stable to hydrolysis by neuraminidase-2 (Chapter 4).

Hypothesis 6. High affinity and selective ligands towards Galectin-8 can be obtained by introducing modifications in position 1 and 3 of the 3-*O*-[1-carboxyethyl]- β -D-galactopyranoside (Chapter 5).

The studies supporting every hypothesis will be discussed in the mentioned chapters.

1.12 References.

- (1) Purcell, S. C.; Godula, K. Synthetic Glycoscapes: Addressing the Structural and Functional Complexity of the Glycocalyx. *Interface Focus* **2019**, *9* (2), 20180080. <https://doi.org/10.1098/rsfs.2018.0080>.
- (2) Varki, A.; Cummings, R.; Esko, J.; Stanley, P.; Hart, G.; Aebi, M.; Darvill, I. A.; Kinoshita, T.; Packer, N.; Prestegard, J.; Schnaar, R.; Seeberger, P. *Essentials of Glycobiology*. 3rd ed.; Cold Spring Harbor (NY): Cold Spring Harbor Laboratory Press, 2015-2017.
- (3) Gabius, H. J. The Sugar Code: Why Glycans Are so Important. *BioSystems* **2018**, *164*, 102–111. <https://doi.org/10.1016/j.biosystems.2017.07.003>.
- (4) Gabius, H. J.; André, S.; Jiménez-Barbero, J.; Romero, A.; Solís, D. From Lectin Structure to Functional Glycomics: Principles of the Sugar Code. *Trends Biochem. Sci.* **2011**, *36* (6), 298–313. <https://doi.org/10.1016/j.tibs.2011.01.005>.
- (5) Reily, C.; Stewart, T. J.; Renfrow, M. B.; Novak, J. Glycosylation in Health and Disease. *Nat. Rev. Nephrol.* **2019**, *15* (6), 346–366. <https://doi.org/10.1038/s41581-019-0129-4>.
- (6) Gabius, H.; Kayser, K. Introduction to Glycopathology: The Concept, the Tools and the Perspectives. *Diagn. Pathol.* **2014**, *9*, 4. <https://doi.org/10.1186/1746-1596-9-4>.
- (7) Möckl, L. The Emerging Role of the Mammalian Glycocalyx in Functional Membrane Organization and Immune System Regulation. *Front. Cell Dev. Biol.* **2020**, *8*, 253. <https://doi.org/10.3389/fcell.2020.00253>.
- (8) Yilmaz, O.; Afsar, B.; Ortiz, A.; Kanbay, M. The Role of Endothelial Glycocalyx in Health and Disease. *Clin. Kidney J.* **2019**, *12* (5), 611–619. <https://doi.org/10.1093/ckj/sfz042>.
- (9) Paszek, M. J.; Dufort, C. C.; Rossier, O.; Bainer, R.; Mouw, J. K.; Godula, K.; Hudak, J. E.; Lakins, J. N.; Wijekoon, A. C.; Cassereau, L.; Rubashkin, M. G.; Magbanua, M. J.; Thorn, K. S.; Davidson, M. W.; Rugo, H. S.; Park, J. W.; Hammer, D. A.; Giannone, G.; Bertozzi, C. R.; Weaver, V. M. The Cancer Glycocalyx Mechanically Primes Integrin-Mediated Growth and Survival. *Nature* **2014**, *511* (7509), 319–325. <https://doi.org/10.1038/nature13535>.
- (10) Woods, E. C.; Kai, F.; Barnes, J. M.; Pedram, K.; Pickup, M. W.; Hollander, M. J.; Weaver, V. M.; Bertozzi, C. R. A Bulky Glycocalyx Fosters Metastasis Formation by Promoting G1 Cell Cycle Progression. *Elife* **2017**, *6*, e25752. <https://doi.org/10.7554/eLife.25752>.
- (11) Fuster, M. M.; Esko, J. D. The Sweet and Sour of Cancer: Glycans as Novel Therapeutic Targets. *Nat. Rev. Cancer* **2005**, *5* (7), 526–542. <https://doi.org/10.1038/nrc1649>.
- (12) Cobb, B. A.; Kasper, D. L. Coming of Age: Carbohydrates and Immunity. *Eur. J. Immunol.* **2005**, *35* (2), 352–356. <https://doi.org/10.1002/eji.200425889>.
- (13) Yamamoto, F. Review: ABO Blood Group System - ABH Oligosaccharide Antigens, Anti-A and Anti-B, A and B Glycosyltransferases, and ABO Genes. *Immunohematology* **2004**, *20* (1), 3–22. <https://doi.org/10.21307/immunohematology-2019-418>.
- (14) Vella, M.; Pace, D. Glycoconjugate Vaccines: An Update. *Expert Opin. Biol. Ther.* **2015**, *15* (4), 529–

554. <https://doi.org/10.1517/14712598.2015.993375>.
- (15) Avci, F. Y.; Kasper, D. L. How Bacterial Carbohydrates Influence the Adaptive Immune System. *Annu. Rev. Immunol.* **2010**, *28*, 107–130. <https://doi.org/10.1146/annurev-immunol-030409-101159>.
- (16) Gamblin, S. J.; Skehel, J. J. Influenza Hemagglutinin and Neuraminidase Membrane Glycoproteins. *J. Biol. Chem.* **2010**, *285* (37), 28403–28409. <https://doi.org/10.1074/jbc.R110.129809>.
- (17) Anderson, G.; Palermo, J.; Schilling, J.; Roth, R.; Heuser, J.; Hultgren, S. Intracellular Bacterial Biofilm-like Pods in Urinary Tract Infections. *Science* **2003**, *301* (5629), 105–107. <https://doi.org/10.1126/science.1084550>.
- (18) Taylor, S. L.; McGuckin, M. A.; Wesselingh, S.; Rogers, G. . Infection’s Sweet Tooth: How Glycans Mediate Infection and Disease Susceptibility. 2018, *26*, 92–101. *Trends Microbiol.* **2018**, *26* (2), 92–101. <https://doi.org/10.1016/j.tim.2017.09.011>.
- (19) Thépaut, M.; Luczkowiak, J.; Vivès, C.; Labiod, N.; Bally, I.; Lasala, F.; Grimoire, Y.; Fenel, D.; Sattin, S.; Thielens, N.; Schoehn, G.; Bernardi, A.; Delgado, R.; Fieschi, F. DC/L-SIGN Recognition of Spike Glycoprotein Promotes SARS-CoV-2 Trans-Infection and Can Be Inhibited by a Glycomimetic Antagonist. *PLoS Pathog.* **2021**, *17* (5), 1–27. <https://doi.org/10.1371/journal.ppat.1009576>.
- (20) Jiang, H.; Qin, X.; Wang, Q.; Xu, Q.; Wang, J.; Wu, Y.; Chen, W.; Wang, C.; Zhang, T.; Xing, D.; Zhang, R. Application of Carbohydrates in Approved Small Molecule Drugs: A Review. *Eur. J. Med. Chem.* **2021**, *223*, 113633. <https://doi.org/10.1016/j.ejmech.2021.113633>.
- (21) Zhang, Y.; Wang, F. Carbohydrate Drugs: Current Status and Development Prospect. *Drug Discov. Ther.* **2015**, *9* (2), 79–87. <https://doi.org/10.5582/ddt.2015.01028>.
- (22) Lipinski, C. A.; Lombardo, F.; Dominy, B. W.; Feeney, P. J. Experimental and Computational Approaches to Estimate Solubility and Permeability in Drug Discovery and Development Settings. *Adv. Drug Deliv. Rev.* **1997**, *23* (1-3), 3–25. [https://doi.org/10.1016/S0169-409X\(96\)00423-1](https://doi.org/10.1016/S0169-409X(96)00423-1).
- (23) Hevey, R. Strategies for the Development of Glycomimetic Drug Candidates. *Pharm.* **2019**, *12* (2), 55. <https://doi.org/10.3390/ph12020055>.
- (24) Ernst, B.; Magnani, J. L. From Carbohydrate Leads to Glycomimetic Drugs. *Nat. Rev. Drug Discov.* **2009**, *8* (8), 661–677. <https://doi.org/10.1038/nrd2852>.
- (25) Thoma, G.; Magnani, J. L.; Patton, J. T.; Ernst, B.; Jahnke, W. Preorganization of the Bioactive Conformation of Sialyl Lewis^x Analogues Correlates with Their Affinity to E-selectin. *Angew. Chemie - Int. Ed. English* **2001**, *40* (10), 1941–1945. [https://doi.org/10.1002/1521-3773\(20010518\)40:10<1941::AID-ANIE1941>3.0.CO;2-T](https://doi.org/10.1002/1521-3773(20010518)40:10<1941::AID-ANIE1941>3.0.CO;2-T)
- (26) Claveria-Gimeno, R.; Vega, S.; Abian, O.; Velazquez-Campoy, A. A Look at Ligand Binding Thermodynamics in Drug Discovery. *Expert Opin. Drug Discov.* **2017**, *12* (4), 363–377. <https://doi.org/10.1080/17460441.2017.1297418>.
- (27) Garbett, N. C.; Chaires, J. B. Thermodynamic Studies for Drug Design and Screening. *Expert Opin. Drug Discov.* **2012**, *7* (4), 299–314. <https://doi.org/10.1517/17460441.2012.666235>.
- (28) Ferenczy, G. G.; Keseru, G. M. Thermodynamics Guided Lead Discovery and Optimization. *Drug*

- Discov. Today* **2010**, *15* (21-22), 919–932. <https://doi.org/10.1016/j.drudis.2010.08.013>.
- (29) Cabani, S.; Gianni, P.; Mollica, V.; Lepori, L. Group Contributions to the Thermodynamic Properties of Non-Ionic Organic Solutes in Dilute Aqueous Solution. *J. Solution Chem.* **1981**, *10* (8), 563–595.
- (30) Lima, L. M.; Barreiro, E. J. Bioisosterism: A Useful Strategy for Molecular Modification and Drug Design. *Curr. Med. Chemistry* **2005**, *12* (1), 23–49. <https://doi.org/10.2174/0929867053363540>.
- (31) Hevey, R. Bioisosteres of Carbohydrate Functional Groups in Glycomimetic Design. *Biomimetics* **2019**, *4* (3), 53. <https://doi.org/10.3390/biomimetics4030053>.
- (32) Hevey, R. The Role of Fluorine in Glycomimetic Drug Design. *Chemistry*. *Chemistry* **2021**, *27* (7), 2240–2253. <https://doi.org/10.1002/chem.202003135>.
- (33) Inui, K.; Terada, T.; Masuda, S.; Saito, H. Physiological and Pharmacological Implications of Peptide Transporters, PEPT1 and PEPT2. *Nephrol. Dial. Transplant.* **2000**, *15*, 11–13. https://doi.org/10.1093/ndt/15.suppl_6.11.
- (34) Gabius, H. J.; Manning, J. C.; Kopitz, J.; Kaltner, H. Sweet Complementarity: The Functional Pairing of Glycans with Lectins. *Cell. Mol. Life Sci.* **2016**, *73* (10), 1989–2016. <https://doi.org/10.1007/s00018-016-2163-8>.
- (35) Gabius, H.; Roth, J. An Introduction to the Sugar Code. *Histochem. Cell Biol.* **2017**, *147* (2), 111–117. <https://doi.org/10.1007/s00418-016-1521-9>.
- (36) Lombard, V.; Ramulu, H. G.; Drula, E.; Coutinho, P. M.; Henrissat, B. The Carbohydrate-Active Enzymes Database (CAZy) in 2013. *Nucleic Acids Res.* **2014**, *42* (D1), D490–D495. <https://doi.org/10.1093/nar/gkt1178>.
- (37) André, S.; Kaltner, H.; Manning, J.; Murphy, P.; Gabius, H. Lectins: Getting Familiar with Translators of the Sugar Code. *Molecules* **2015**, *20* (2), 1788–1823. <https://doi.org/10.3390/molecules20021788>.
- (38) Gabius, H. J. Animal Lectins. *Eur. J. Biochem.* **1997**, *243* (3), 543–576. <https://doi.org/10.1111/j.1432-1033.1997.t01-1-00543.x>.
- (39) Brown, G.; Willment, J.; Whitehead, L. C-Type Lectins in Immunity and Homeostasis. *Nat. Rev. Immunol.* **2018**, *18* (6), 374–389. <https://doi.org/10.1038/s41577-018-0004-8>.
- (40) Varki, A.; Schnaar, R.; Crocker, P. I-Type Lectins. In *Essentials of Glycobiology [Internet]. 3rd ed.*; 2017.
- (41) Cecioni, S.; Imberty, A.; Vidal, S. Glycomimetics versus Multivalent Glycoconjugates for the Design of High Affinity Lectin Ligands. *Chem. Rev.* **2015**, *115* (1), 525–561. <https://doi.org/10.1021/cr500303t>.
- (42) Lis, H.; Sharon, N. Lectins: Carbohydrate-Specific Proteins That Mediate Cellular Recognition. *Chem. Rev.* **1998**, *98* (2), 637–674. <https://doi.org/10.1021/cr940413g>.
- (43) Heldin, C. Dimerization of Cell Surface Receptors in Signal Transduction. *Cell* **1995**, *80* (2), 213–223. [https://doi.org/10.1016/0092-8674\(95\)90404-2](https://doi.org/10.1016/0092-8674(95)90404-2).
- (44) Kiessling, L. L.; Gestwicki, J. E.; Strong, L. E. Synthetic Multivalent Ligands as Probes of Signal Transduction. *Angew. Chemie - Int. Ed. English* **2006**, *45* (15), 2348–2368.

- <https://doi.org/10.1002/anie.200502794>.
- (45) Guiard, J.; Fiege, B.; Kitov, P. I.; Peters, T.; Bundle, D. R. “Double-Click” Protocol for Synthesis of Heterobifunctional Multivalent Ligands: Toward a Focused Library of Specific Norovirus Inhibitors. *Chem. - A Eur. J.* **2011**, *17* (27), 7438–7441. <https://doi.org/10.1002/chem.201003414>.
- (46) Crocker, P. R.; Clark, E. A.; Filbin, M.; Gordon, S.; Jones, Y.; Kehrl, J. H.; Kelm, S.; Le Douarin, N.; Powell, L.; Roder, J.; Schnaar, R. L.; Sgroi, D. C.; Stamenkovic, K.; Schauer, R.; Schachner, M.; van den Berg, T. K.; van der Merwe, P. A.; Watt, S. M.; Varki, A. Siglecs: A Family of Sialic-Acid Binding Lectins. *Glycobiology* **1998**, *8* (2). <https://doi.org/10.1093/oxfordjournals.glycob.a018832>.
- (47) Varki, A.; Angata, T. Siglecs - the Major Subfamily of I-Type Lectins. *Glycobiology* **2006**, *16* (1), 1–27. <https://doi.org/10.1093/glycob/cwj008>.
- (48) Varki, A.; Cummings, R. D.; Aebi, M.; Parker, N. H.; Seeberger, P. H.; Esko, J. D.; Stanley, P.; Hart, G.; Darvill, A.; Kinoshita, T.; Prestegard, J. J.; Schnaar, R. L.; Freeze, H. H.; Marta, J. D.; Bertozzi, C. R.; Etzler, M. E.; Frank, M.; Vligenthart, J. F. G.; Lutteke, T.; Perez, S.; Bolton, E.; Rudd, P.; Paulson, J.; Kanehisa, M.; Toukach, P.; Aoki-Kinoshita, K. F.; Dell, A.; Narimatsu, H.; Yor, W.; Taniguchi, N.; Korfeld, S. Symbol Nomenclature for Graphical Representation of Glycans. *Glycobiology* **2016**, *25* (12), 1323–1324. <https://doi.org/10.1093/glycob/cwv091>.
- (49) Büll, C.; Heise, T.; Adema, G. J.; Boltje, T. J. Sialic Acid Mimetics to Target the Sialic Acid - Siglec Axis. *Trends Biochem. Sci.* **2016**, *41* (6), 519–531. <https://doi.org/10.1016/j.tibs.2016.03.007>.
- (50) Schauer, R.; Kamerling, J. P. Exploration of the Sialic Acid World. *Adv. Carbohydr. Chem. Biochem.* **2018**, *75*, 1–213. <https://doi.org/10.1016/bs.accb.2018.09.001>.
- (51) Varki, A. Loss of N-Glycolylneuraminic Acid in Humans: Mechanisms, Consequences, and Implications for Hominid Evolution. *Am. J. Phys. Anthropol.* **2001**, *Suppl.33* (S33), 54–69. <https://doi.org/10.1002/ajpa.10018>.
- (52) Wang, B. Molecular Mechanism Underlying Sialic Acid as an Essential Nutrient for Brain Development and Cognition. *Adv. Nutr.* **2012**, *3* (3), 465–472S. <https://doi.org/10.3945/an.112.001875>.
- (53) Varki, A. Sialic Acids in Human Health and Disease. *Trends Mol. Med.* **2008**, *14* (8), 351–360. <https://doi.org/10.1016/j.molmed.2008.06.002>.
- (54) Heida, R.; Bhide, Y.; Gasbarri, M.; Kocabiyik, Ö.; Stellacci, F.; Huckriede, A.; Hinrichs, W.; Frijlink, H. Advances in the Development of Entry Inhibitors for Sialic-Acid-Targeting Viruses. *Drug Discov. Today* **2021**, *26* (1), 122–137. <https://doi.org/10.1016/j.drudis.2020.10.009>.
- (55) Läubli, H.; Kawanishi, K.; George Vazhappilly, C.; Matar, R.; Merheb, M.; Sarwar Siddiqui, S. Tools to Study and Target the Siglec-Sialic Acid Axis in Cancer. *FEBS J.* **2020**. <https://doi.org/10.1111/febs.15647>.
- (56) Giancchetti, E.; Arena, A.; Fierabracci, A. Sialic Acid-Siglec Axis in Human Immune Regulation, Involvement in Autoimmunity and Cancer and Potential Therapeutic Treatments. *Int. J. Mol. Sci.* **2021**, *22* (11), 5774. <https://doi.org/10.3390/ijms22115774>.
- (57) Engin, A. B.; Engin, E. D.; Engin, A. Dual Function of Sialic Acid in Gastrointestinal SARS-CoV-2

- Infection. *Environ. Toxicol. Pharmacol.* **2020**, *79*, 103436. <https://doi.org/10.1016/j.etap.2020.103436>.
- (58) Varki, A.; Schnaar, R. L.; Crocker, P. R. I-Type Lectins. In *Essentials of Glycobiology*; 2015.
- (59) Gunten, S. Von; Bochner, B. S. Basic and Clinical Immunology of Siglecs. *Ann. N. Y. Acad. Sci.* **2008**, *1143* (1), 61–82. <https://doi.org/10.1196/annals.1443.011>.
- (60) Angata, T.; Margulies, E. H.; Green, E. D.; Varki, A. Large-Scale Sequencing of the CD33-Related Siglec Gene Cluster in Five Mammalian Species Reveals Rapid Evolution by Multiple Mechanisms. *Proc. Natl. Acad. Sci.* **2004**, *101* (36), 13251–13256. <https://doi.org/10.1073/pnas.0404833101>.
- (61) Crocker, P. R.; Paulson, J. C.; Varki, A. Siglecs and Their Roles in the Immune System. *Nat. Rev. Immunol.* **2007**, *7* (4), 255–266. <https://doi.org/10.1038/nri2056>.
- (62) Bornhöfft, K. F.; Goldammer, T.; Rebl, A.; Galuska, S. P. Siglecs: A Journey through the Evolution of Sialic Acid-Binding Immunoglobulin-Type Lectins. *Dev. Comp. Immunol.* **2018**, *86*, 219–231. <https://doi.org/10.1016/j.dci.2018.05.008>.
- (63) Jandus, C.; Simon, H.; von Gunten, S. Targeting Siglecs — A Novel Pharmacological Strategy for Immuno- and Glycotherapy. *Biochem. Pharmacol.* **2011**, *82* (4), 323–332. <https://doi.org/10.1016/j.bcp.2011.05.018>.
- (64) Angata, T. Molecular Diversity and Evolution of the Siglec Family of Cell-Surface Lectins. *Mol. Divers.* **2006**, *10* (4), 555–566. <https://doi.org/10.1007/s11030-006-9029-1>.
- (65) Macauley, M. S.; Paulson, J. C. Glyco-Engineering ‘ Super-Self .’ *Nat. Chem. Biol.* **2014**, *10* (1), 7–8. <https://doi.org/10.1038/nchembio.1415>.
- (66) Lenza, M. P.; Atxabal, U.; Oyenarte, I.; Jimenez-Barbero, J.; Ereño-Orbea, J. Current Status on Therapeutic Molecules Targeting Siglec Receptors. *Cells* **2020**, *9* (2691), 1–19. <https://doi.org/10.3390/cells9122691>.
- (67) Hartnell, A.; Steel, J.; Turley, H.; Jones, M.; Jackson, D. G.; Crocker, P. R. Characterization of Human Sialoadhesin, a Sialic Acid Binding Receptor Expressed by Resident and Inflammatory Macrophage Populations. *Blood* **2001**, *97* (1), 288–296. <https://doi.org/10.1182/blood.v97.1.288>.
- (68) Nakamura, K.; Yamaji, T.; Crocker, P. R.; Suzuki, A.; Hashimoto, Y. Lymph Node Macrophages , but Not Spleen Macrophages , Express High Levels of Unmasked Sialoadhesin : Implication for the Adhesive Properties of Macrophages in Vivo. **2002**, *12* (3), 209–216. <https://doi.org/10.1093/glycob/12.3.209>.
- (69) Collins, B. E.; Blixt, O.; Han, S.; Duong, B.; Li, H.; Nathan, J. K.; Bovin, N.; Paulson, J. C. High-Affinity Ligand Probes of CD22 Overcome the Threshold Set by Cis Ligands to Allow for Binding, Endocytosis, and Killing of B Cells. *J. Immunol.* **2006**, *177* (5), 2994–3003. <https://doi.org/10.4049/jimmunol.177.5.2994>.
- (70) Pillai, S.; Netravali, I. A.; Cariappa, A.; Mattoo, H. Siglecs and Immune Regulation. *Annu. Rev.* **2012**, *30*, 357–392. <https://doi.org/10.1146/annurev-immunol-020711-075018>.
- (71) Cao, H.; Lakner, U.; de Bono, B.; Traherne, J.; Trowsdale, J.; Barrow, A. SIGLEC16 Encodes a DAP12-Associated Receptor Expressed in Macrophages That Evolved from Its Inhibitory Counter-

- Part SIGLEC11 and Has Functional and Non-Functional Alleles in Humans. *Eur. J. Immunol.* **2008**, 38 (8), 2303–2315. <https://doi.org/10.1002/eji.200738078>.
- (72) Takamiya, R.; Ohtsubo, K.; Takamatsu, S.; Taniguchi, N.; Angata, T. The Interaction between Siglec-15 and Tumor-Associated Sialyl-Tn Antigen Enhances TGF- β Secretion from Monocytes/Macrophages through the DAP12-Syk Pathway. *2013 23* (2), 178–187. <https://doi.org/10.1093/glycob/cws139>.
- (73) Macauley, M. S.; Crocker, P. R.; Paulson, J. C. Siglec-Mediated Regulation of Immune Cell Function in Disease. *Nat. Rev. Immunol.* **2014**, 14 (10), 653–666. <https://doi.org/10.1038/nri3737>.
- (74) Blixt, O.; Collins, B. E.; van den Nieuwenhof, I. M.; Crocker, P. R.; Paulson, J. C. Sialoside Specificity of the Siglec Family Assessed Using Novel Multivalent Probes. *J. Biol. Chem.* **2003**, 278 (33), 31007–31019. <https://doi.org/10.1074/jbc.M304331200>.
- (75) Gonzalez-Gil, A.; Schnaar, R. L. Siglec Ligands. *Cells* **2021**, 10 (5), 1–21. <https://doi.org/10.3390/cells10051260>.
- (76) Movsisyan, L. D.; Macauley, M. S. Structural Advances of Siglecs : Insight into Synthetic Glycan Ligands for Immunomodulation. *Org. Biomol. Chem.* **2020**, 18 (30), 5784–5797. <https://doi.org/10.1039/d0ob01116a>.
- (77) Chang, Y.; Nizet, V. Siglecs at the Host–Pathogen Interface. In *Lectin in Host Defense Against Microbial Infections. Advances in Experimental Medicine and Biology*; Springer, Singapore, 2020.
- (78) Chang, Y.; Olson, J.; Louie, A.; Crocker, P. R.; Varki, A.; Nizet, V. Role of Macrophage Sialoadhesin in Host Defense against the Sialylated Pathogen Group B Streptococcus. *J. Mol. Med.* **2014**, 92 (9), 951–959. <https://doi.org/10.1007/s00109-014-1157-y>.
- (79) Klaas, M.; Oetke, C.; Lewis, L. E.; Lars, P.; Heikema, A. P.; Easton, A.; Willison, H. J.; Crocker, P. R. Sialoadhesin Promotes Rapid Proinflammatory and Type I IFN Responses to a Sialylated Pathogen, *Campylobacter* *Jejuni*. *J. Immunol.* **2012**, 189 (5), 2414–2422. <https://doi.org/10.4049/jimmunol.1200776>.
- (80) Gummuluru, S.; Pina Ramirez, N. G.; Akiyama, H. CD169-Dependent Cell-Associated HIV-1 Transmission: A Driver of Virus Dissemination. *J. Infect. Dis.* **2014**, 210 (Suppl 3), S641–S647. <https://doi.org/10.1093/infdis/jiu442>.
- (81) Perez-Zsolt, D.; Erkizia, I.; Pino, M.; García-Gallo, M.; Martin, M.; Benet, S.; Chojnacki, J.; Fernández-Figueras, M. T.; Guerrero, D.; Urrea, V.; Muñoz-Trabudua, X.; Kremer, L.; Martínez-Picado, J.; Izquierdo-Useros, N. Anti-Siglec-1 Antibodies Block Ebola Viral Uptake and Decrease Cytoplasmic Viral Entry. *Nat. Microbiol.* **2019**, 4 (9), 1558–1570. <https://doi.org/10.1038/s41564-019-0453-2>
- (82) Perez-zsolt, D.; Martínez-Picado, J.; Izquierdo-Useros, N. When Dendritic Cells Go Viral : The Role of Siglec-1 in Host Defense and Dissemination of Enveloped Viruses. *Viruses* **2020**, 12 (8), 1–19. <https://doi.org/10.3390/v12010008>.
- (83) McDonald, D.; Wu, L.; Bohks, S.; KewalRamani, V.; Unutmaz, D.; Hope, T. J. Recruitment of HIV

- and Its Receptors to Dendritic Cell-T Cell Junctions. *Science* **2003**, *300* (5623), 1295–1297. <https://doi.org/10.1126/science.1084238>.
- (84) Sewald, X.; Ladinsky, M.; Uchil, P.; Bloor, J.; Pi, R.; Herrmann, C.; Motamedi, N.; Murooka, T.; Brehm, M.; Greiner, D.; Shultz, L.; Mempel, T.; Bjorkman, P.; Kumar, P.; Mothes, W. Retroviruses Use CD169-Mediated Trans-Infection of Permissive Lymphocytes to Establish Infection. *Science* **2015**, *350* (6260), 563–567. <https://doi.org/10.1126/science.aab2749>.
- (85) Siddiqui, S. S.; Matar, R.; Merheb, M.; Hodeify, R.; Vazhappilly, C. G.; Marton, J.; Shamsuddin, S. A.; Al Zouabi, H. Siglecs in Brain Function and Neurological Disorders. *Cells* **2019**, *8* (10), 1125. <https://doi.org/10.3390/cells8101125>.
- (86) Pluvinae, J. V.; Haney, M. S.; Smith, B. A. H.; Sun, J.; Iram, T.; Bonanno, L.; Li, L.; Lee, D. P.; Morgens, D. W.; Yang, A. C.; Shuken, S. R.; Gate, D.; Scott, M.; Khatri, P.; Luo, J.; Bertozzi, C. R.; Bassik, M. C.; Wyss-Coray, T. CD22 Blockade Restores Homeostatic Microglial Phagocytosis in Ageing Brains. *Nature* **2019**, *568* (7751), 187–192. <https://doi.org/10.1038/s41586-019-1088-4>.
- (87) Griciuc, A.; Serrano-Pozo, A.; Parrado, A. R.; Lesinski, A. N.; Asselin, C. N.; Mullin, K.; Hooli, B.; Choi, S. H.; Hyman, B. T.; Tanzi, R. E. Alzheimer's Disease Risk Gene CD33 Inhibits Microglial Uptake of Amyloid Beta. *Neuron* **2013**, *78* (4), 631–643. <https://doi.org/10.1016/j.neuron.2013.04.014>.
- (88) McKerracher, L.; Rosen, K. M. MAG, Myelin and Overcoming Growth Inhibition in the CNS. *Front. Mol. Neurosci.* **2015**, *8*, 51. <https://doi.org/10.3389/fnmol.2015.00051>.
- (89) Barbay, S.; Plautz, E. J.; Zoubina, E.; Frost, S. B.; Cramer, S. C.; Nudo, R. J. Effects of Postinfarct Myelin-Associated Glycoprotein Antibody Treatment on Motor Recovery and Motor Map Plasticity in Squirrel Monkeys. *Stroke* **2015**, *46* (6), 1620–1625. <https://doi.org/10.1161/STROKEAHA.114.008088>.
- (90) Büll, C.; den Brok, M. H.; Adema, G. J. Sweet Escape: Sialic Acids in Tumor Immune Evasion. *Biochim. Biophys. Acta* **2014**, *1846* (1), 238–246. <https://doi.org/10.1016/j.bbcan.2014.07.005>.
- (91) Stanczak, M. A.; Siddiqui, S. S.; Trefny, M. P.; Thommen, D. S.; Boligan, K. F.; Von Gunten, S.; Tzankov, A.; Tietze, L.; Lardinois, D.; Heinzelmann-Schwarz, V.; Von Bergwelt-Baildon, M.; Zhang, W.; Lenz, H. J.; Han, Y.; Amos, C. I.; Syedbasha, M.; Egli, A.; Stenner, F.; Speiser, D. E.; Varki, A.; Zippelius, A.; Lübbli, H. Self-Associated Molecular Patterns Mediate Cancer Immune Evasion by Engaging Siglecs on T Cells. *J. Clin. Invest.* **2018**, *128* (11), 4912–4923. <https://doi.org/10.1172/JCI120612>.
- (92) Haas, Q.; Boligan, K. F.; Jandus, C.; Schneider, C.; Simillion, C.; Stanczak, M. A.; Haubitz, M.; Jafari, S. M. S.; Zippelius, A.; Baerlocher, G. M.; Laubli, H.; Hunger, R. E.; Romero, P.; Simon, H. U.; von Gunten, S. Siglec-9 Regulates an Effector Memory CD8+ T-Cell Subset That Congregates in the Melanoma Tumor Microenvironment. *Cancer Immunol. Res.* **2019**, *7* (5), 707–718. <https://doi.org/10.1158/2326-6066.CIR-18-0505>.
- (93) Jandus, C.; Boligan, K. F.; Chijioke, O.; Liu, H.; Dahlhaus, M.; Démoulin, T.; Schneider, C.; Wehrli, M.; Hunger, R. E.; Baerlocher, G. M.; Simon, H. U.; Romero, P.; Münz, C.; Von Gunten, S. Interactions

- between Siglec-7/9 Receptors and Ligands Influence NK Cell-Dependent Tumor Immunosurveillance. *J. Clin. Invest.* **2014**, *124* (4), 1810–1820. <https://doi.org/10.1172/JCI65899>.
- (94) Hudak, J. E.; Canham, S. M.; Bertozzi, C. R. Glycocalyx Engineering Reveals a Siglec-Based Mechanism for NK Cell Immuno-evasion. *Nat. Chem. Biol.* **2014**, *10* (1), 69–75. <https://doi.org/10.1038/nchembio.1388>.
- (95) Nicoll, G.; Avril, T.; Lock, K.; Furukawa, K.; Bovin, N.; Crocker, P. R. Ganglioside GD3 Expression on Target Cells Can Modulate NK Cell Cytotoxicity via Siglec-7-Dependent and -Independent Mechanisms. *Eur. J. Immunol.* **2003**, *33* (6), 1642–1648. <https://doi.org/10.1002/eji.200323693>.
- (96) Sullivan-Chang, L.; O'Donnell, R. T.; Tuscano, J. M. Targeting CD22 in B-Cell Malignancies: Current Status and Clinical Outlook. *BioDrugs* **2013**, *27* (4), 293–304. <https://doi.org/10.1007/s40259-013-0016-7>.
- (97) Dörner, T.; Shock, A.; Smith, K. G. C. CD22 and Autoimmune Disease. *Int. Rev. Immunol.* **2012**, *31* (5), 363–378. <https://doi.org/10.3109/08830185.2012.709890>.
- (98) Clark, E. A.; Giltiay, N. V. CD22: A Regulator of Innate and Adaptive B Cell Responses and Autoimmunity. *Front. Immunol.* **2018**, *9*, 1–13. <https://doi.org/10.3389/fimmu.2018.02235>.
- (99) Robertson, M. J.; Soiffer, R. J.; Freedman, A. S.; Rabinowe, S. L.; Anderson, K. C.; Ervin, T. J.; Murray, C.; Dear, K.; Griffin, J. D.; Nadler, L. M.; Ritz, J. Human Bone Marrow Depleted of CD33-Positive Cells Mediates Delayed but Durable Reconstitution of Hematopoiesis: Clinical Trial of MY9 Monoclonal Antibody-Purged Autografts for the Treatment of Acute Myeloid Leukemia. *Blood* **1992**, *79* (9), 2229–2236. <https://doi.org/10.1182/blood.v79.9.2229.2229>.
- (100) Ehninger, A.; Kramer, M.; Röllig, C.; Thiede, C.; Bornhäuser, M.; von Bonin, M.; Wermke, M.; Feldmann, A.; Bachmann, M.; Ehninger, G.; Oelschlägel, U. Distribution and Levels of Cell Surface Expression of CD33 and CD123 in Acute Myeloid Leukemia. *Blood Cancer J.* **2014**, *4* (6), e218. <https://doi.org/10.1038/bcj.2014.39>.
- (101) Macauley, M. S.; Pfrengle, F.; Rademacher, C.; Nycholat, C. M.; Gale, A. J.; Von Drygalski, A.; Paulson, J. C. Antigenic Liposomes Displaying CD22 Ligands Induce Antigen-Specific B Cell Apoptosis. *J. Clin. Invest.* **2013**, *123* (7), 3074–3083. <https://doi.org/10.1172/JCI69187>.
- (102) Leonard, J. P.; Goldenberg, D. M. Preclinical and Clinical Evaluation of Epratuzumab (Anti-CD22 IgG) in B-Cell Malignancies. *Oncogene* **2007**, *26* (25), 3704–3713. <https://doi.org/10.1038/sj.onc.1210370>.
- (103) Geh, D.; Gordon, C. Epratuzumab for the Treatment of Systemic Lupus Erythematosus. *Expert Rev. Clin. Immunol.* **2018**, *14* (4), 245–258. <https://doi.org/10.1080/1744666X.2018.1450141>.
- (104) Gottenberg, J. E.; Dörner, T.; Bootsma, H.; Devauchelle-Pensec, V.; Bowman, S. J.; Mariette, X.; Bartz, H.; Oortgiesen, M.; Shock, A.; Koetse, W.; Galateanu, C.; Bongardt, S.; Wegener, W. A.; Goldenberg, D. M.; Meno-Tetang, G.; Kosutic, G.; Gordon, C. Efficacy of Epratuzumab, an Anti-CD22 Monoclonal IgG Antibody, in Systemic Lupus Erythematosus Patients with Associated Sjogren's Syndrome: Post Hoc Analyses from the EMBODY Trials. *Arthritis Rheum.* **2018**, *70* (5), 763–773.

<https://doi.org/10.1002/art.40425>.

- (105) Kantarjian, H.; DeAngelo, D.; Stelljes, M.; Martinelli, G.; Liedtke, M.; Stock, W.; Gökbuget, N.; O'Brien, S.; Wang, K.; Wang, T.; Paccagnella, M. L.; Sleight, B.; Vandendries, E.; Advani, A. S. Inotuzumab Ozogamicin versus Standard Therapy for Acute Lymphoblastic Leukemia. *N. Engl. J. Med.* **2016**, *375* (8), 740–753. <https://doi.org/10.1056/NEJMoa1509277>.
- (106) Adeel, K.; Fergusson, N. J.; Shorr, R.; Atkins, H.; Hay, K. A. Efficacy and Safety of CD22 Chimeric Antigen Receptor (CAR) T Cell Therapy in Patients with B Cell Malignancies: A Protocol for a Systematic Review and Meta-Analysis. *Syst. Rev.* **2021**, *10* (1), 1–8. <https://doi.org/10.1186/s13643-021-01588-7>.
- (107) Baron, J.; Wang, E. S. Gemtuzumab Ozogamicin for the Treatment of Acute Myeloid Leukemia. *Expert Rev. Clin. Pharmacol.* **2018**, *11* (6), 549–559. <https://doi.org/10.1080/17512433.2018.1478725>.
- (108) Wang, J.; Sun, J.; Liu, L. N.; Flies, D. B.; Nie, X.; Toki, M.; Zhang, J.; Song, C.; Zarr, M.; Zhou, X.; Han, X.; Archer, K. A.; O'Neill, T.; Herbst, R. S.; Boto, A. N.; Sanmamed, M F Langermann, S.; Rimm, D. L.; Chen, L. Siglec-15 as an Immune Suppressor and Potential Target for Normalization Cancer Immunotherapy. *Nat. Med.* **2019**, *25* (4), 656–666. <https://doi.org/10.1038/s41591-019-0374-x>.
- (109) Chames, P.; Van Regenmortel, M.; Weiss, E.; Baty, D. Therapeutic Antibodies: Successes, Limitations and Hopes for the Future. *Br. J. Pharmacol.* **2009**, *157* (2), 220–233. <https://doi.org/10.1111/j.1476-5381.2009.00190.x>.
- (110) Rillahan, C. D.; Schwartz, E.; McBride, R.; Fokin, V. V.; Paulson, J. C. Click and Pick: Identification of Sialoside Analogues for Siglec-Based Cell Targeting. *Angew. Chemie - Int. Ed. English* **2012**, *51* (44), 11014–11018. <https://doi.org/10.1002/anie.201205831>.
- (111) Chen, W.; Completo, G.; Sigal, D.; Crocker, P.; Saven, A.; Paulson, J. In Vivo Targeting of B-Cell Lymphoma with Glycan Ligands of CD22. *Blood* **2010**, *115* (23), 4778–4786. <https://doi.org/10.1182/blood-2009-12-257386>.
- (112) Schweizer, A.; Wöhner, M.; Prescher, H.; Brossmer, R.; Nitschke, L. Targeting of CD22-Positive B-Cell Lymphoma Cells by Synthetic Divalent Sialic Acid Analogues. *Eur. J. Immunol.* **2012**, *42* (10), 2792–2802. <https://doi.org/10.1002/eji.201242574>.
- (113) O'Reilly, M. K.; Tian, H.; Paulson, J. C. CD22 Is a Recycling Receptor That Can Shuttle Cargo between the Cell Surface and Endosomal Compartments of B Cells. *J. Immunol.* **2011**, *186* (3), 1554–1563. <https://doi.org/10.4049/jimmunol.1003005>.
- (114) Nycholat, C. M.; Rademacher, C.; Kawasaki, N.; Paulson, J. C. In Silico-Aided Design of a Glycan Ligand of Sialoadhesin for in Vivo Targeting of Macrophages. *J. Am. Chem. Soc.* **2012**, *134* (38), 15696–15699. <https://doi.org/10.1021/ja307501e>.
- (115) Floyd, H.; Ni, J.; Cornish, A. L.; Zeng, Z.; Liu, D.; Carter, K. C.; Steel, J.; Crocker, P. R. Siglec-8 - A Novel Eosinophil-Specific Member of the Immunoglobulin Superfamily. *J. Biol. Chem.* **2000**, *275* (2), 861–866. <https://doi.org/10.1074/jbc.275.2.861>.

- (116) Kikly, K. K.; Bochner, B. S.; Freeman, S. D.; Tan, K. B.; Gallagher, K. T.; D'alessio, K. J.; Holmes, S. D.; Abrahamson, J. A.; Erickson-Miller, C. L.; Murdock, P. R.; Tachimoto, H.; Schleimer, R. P.; White, J. R. Identification of SAF-2, a Novel Siglec Expressed on Eosinophils, Mast Cells, and Basophils. *J. Allergy Clin. Immunol.* **2000**, *105* (6 Pt 1), 1093–1100. <https://doi.org/10.1067/mai.2000.107127>.
- (117) Aizawa, H.; Plitt, J.; Bochner, B. S. Human Eosinophils Express Two Siglec-8 Splice Variants. *J. Allergy Clin. Immunol.* **2002**, *109* (1), 176. <https://doi.org/10.1067/mai.2002.120550>.
- (118) Nutku-bilir, E.; Hudson, S. A.; Bochner, B. S. Interleukin-5 Priming of Human Eosinophils Alters Siglec-8 Mediated Apoptosis Pathways. **2008**, *38* (1), 121–124. <https://doi.org/10.1165/rcmb.2007-0154OC>.
- (119) Nutku, E.; Aizawa, H.; Hudson, S. A.; Bochner, B. S. Ligation of Siglec-8 : A Selective Mechanism for Induction of Human Eosinophil Apoptosis. *Blood* **2003**, *101* (12), 5014–5020. <https://doi.org/10.1182/blood-2002-10-3058>.
- (120) Yokoi, H.; Choi, O. H.; Hubbard, W.; Lee, H.; Canning, B. J.; Lee, H. H.; Ryu, S.; von Gunten, S.; Bickel, C. A.; Hudson, S. A.; Macglashan, D. W.; Bochner, B. S. Inhibition of FcεRI-Dependent Mediator Release and Calcium Flux from Human Mast Cells by Sialic Acid-Binding Immunoglobulin-like Lectin 8 Engagement. *J. Allergy Clin. Immunol.* **2008**, *121* (2), 499–506. <https://doi.org/10.1016/j.jaci.2007.10.004>.
- (121) Carroll, D. J.; O'Sullivan, J. A.; Nix, D. B.; Cao, Y.; Tiemeyer, M.; Bochner, B. S. Sialic Acid-Binding Immunoglobulin-like Lectin 8 (Siglec-8) Is an Activating Receptor Mediating β2-Integrin-Dependent Function in Human Eosinophils. *J. Allergy Clin. Immunol.* **2018**, *141* (6), 2196–2207. <https://doi.org/10.1016/j.jaci.2017.08.013>.
- (122) Youngblood, B. A.; Leung, J.; Falahati, R.; Williams, J.; Schanin, J.; Brock, E. C.; Singh, B.; Chang, A. T.; O'Sullivan, J. A.; Schleimer, R. P.; Tomasevic, N.; Bebbington, C. R.; Bochner, B. S. Discovery , Function , and Therapeutic Targeting of Siglec-8. *Cells* **2020**, *10* (1), 19. <https://doi.org/10.3390/cells10010019>.
- (123) Legrand, F.; Cao, Y.; Wechsler, J.; Zhu, X.; Zimmermann, N.; Rampertaap, S.; Monsale, J.; Romito, K.; Youngblood, B. A.; Brock, E. C.; Makiya, M.; Tomasevic, N.; Bebbington, C.; Maric, I.; Metcalfe, D. D.; Bochner, B. S.; Klion, A. D. Siglec-8 in Eosinophilic Disorders: Receptor Expression and Targeting Using Chimeric Antibodies. *J. Allergy Clin. Immunol.* **2019**, *143* (6), 2227–2237. <https://doi.org/10.1016/j.jaci.2018.10.066>.
- (124) Song, D. J.; Cho, J. Y.; Lee, S. Y.; Miller, M.; Rosenthal, P.; Soroosh, P.; Croft, M.; Zhang, M.; Varki, A.; Broide, D. H. Anti-Siglec-F Antibody Reduces Allergen-Induced Eosinophilic Inflammation and Airway Remodeling. *J. Immunol.* **2009**, *183* (8), 5333–5341. <https://doi.org/10.4049/jimmunol.0801421>.
- (125) Mao, H.; Kano, G.; Hudson, S. A.; Brummet, M.; Zimmermann, N.; Zhu, Z.; Bochner, B. S. Mechanisms of Siglec-F-Induced Eosinophil Apoptosis: A Role for Caspases but Not for SHP-1, Src

- Kinases, NADPH Oxidase or Reactive Oxygen. *PLoS One* **2013**, *8* (6), e68143. <https://doi.org/10.1371/journal.pone.0068143>.
- (126) O’Sullivan, J. A.; Wei, Y.; Carroll, D. J.; Moreno-Vinasco, L.; Cao, Y.; Zhang, F.; Lee, J. J.; Zhu, Z.; Bochner, B. S. Frontline Science: Characterization of a Novel Mouse Strain Expressing Human Siglec-8 Only on Eosinophils. *J. Leukoc. Biol.* **2018**, *104* (1), 11–19. <https://doi.org/10.1002/JLB.2HI0917-391R>.
- (127) Wei, Y.; Chhiba, K. D.; Zhang, F.; Ye, X.; Wang, L.; Zhang, L.; Robida, P. A.; Moreno-Vinasco, L.; Schnaar, R. L.; Roers, A.; Hartmann, K.; Lee, C. M.; Demers, D.; Zheng, T.; Bochner, B. S.; Zhu, Z. Mast Cell-Specific Expression of Human Siglec-8 in Conditional Knock-in Mice. *Int. J. Mol. Sci.* **2018**, *20* (1), 19. <https://doi.org/10.3390/ijms20010019>.
- (128) Zhang, Z.; Kurashima, Y. Two Sides of the Coin: Mast Cells as a Key Regulator of Allergy and Acute / Chronic Inflammation. *Cells* **2021**, *10* (7), 1615. <https://doi.org/10.3390/cells10071615>.
- (129) Theoharides, T. C.; Valent, P.; Akin, C. Mast Cells, Mastocytosis, and Related Disorders. *N. Engl. J. Med.* **2015**, *373* (2), 163–172. <https://doi.org/10.1056/nejmra1409760>.
- (130) Klion, A. D.; Ackerman, S. J.; Bochner, B. S. Contributions of Eosinophils to Human Health and Disease. *Annu. Rev. Pathol. Mech. Dis.* **2020**, *15*, 179–209. <https://doi.org/10.1146/annurev-pathmechdis-012419-032756>.
- (131) Krystel-Whittemore, M.; Dileepan, K. N.; Wood, J. G. Mast Cell: A Multi-Functional Master Cell. *Front. Immunol.* **2016**, *6*, 620. <https://doi.org/10.3389/fimmu.2015.00620>.
- (132) Valent, P.; Degenfeld-Schonburg, L.; Sadovnik, I.; Horny, H. P.; Arock, M.; Simon, H. U.; Reiter, A.; Bochner, B. S. Eosinophils and Eosinophil-Associated Disorders: Immunological, Clinical, and Molecular Complexity. *Semin. Immunopathol.* **2021**, *43* (3), 423–438. <https://doi.org/10.1007/s00281-021-00863-y>.
- (133) Leru, P. M. Eosinophilic Disorders: Evaluation of Current Classification and Diagnostic Criteria, Proposal of a Practical Diagnostic Algorithm. *Clin. Transl. Allergy* **2019**, *9*, 36. <https://doi.org/10.1186/s13601-019-0277-4>.
- (134) Shomali, W.; Gotlib, J. World Health Organization-Defined Eosinophilic Disorders: 2019 Update on Diagnosis, Risk Stratification, and Management. *Am. J. Hematol.* **2019**, *94* (10), 1149–1166. <https://doi.org/10.1002/ajh.25617>.
- (135) Stella, S.; Massimino, M.; Manzella, L.; Pennisi, M. S.; Tirrò, E.; Romano, C.; Vitale, S. R.; Puma, A.; Tomarchio, C.; Gregorio, S. D.; Palumbo, G. A.; Vigneri, P. Molecular Pathogenesis and Treatment Perspectives for Hypereosinophilia and Hypereosinophilic Syndromes. *Int. J. Mol. Sci.* **2021**, *22* (2), 486. <https://doi.org/10.3390/ijms22020486>.
- (136) Klion, A. D. Eosinophilic Myeloproliferative Disorders. *Hematol. Am. Soc. Hematol. Educ. program.* **2011**, *2011*, 257–263. <https://doi.org/10.1182/asheducation-2011.1.257>.
- (137) Pardanani, A.; D’Souza, A.; Knudson, R. A.; Hanson, C. A.; Ketterling, R. P.; Tefferi, A. Long-Term Follow-up of FIP1L1-PDGFR α -Mutated Patients with Eosinophilia: Survival and Clinical Outcome.

- Leukemia* **2012**, 26 (11), 2439–2441. <https://doi.org/10.1038/leu.2012.162>.
- (138) Ogbogu, P.; Rosing, D. R.; Horne, M. K. Cardiovascular Manifestations of Hyper- Eosinophilic Syndromes. *Immunol. Allergy Clin. North Am.* **2007**, 27 (3), 457–475. <https://doi.org/10.1016/j.iac.2007.07.001>.
- (139) Akin, C. Mast Cell Activation Disorders. *J. Allergy Clin. Immunol. Pract.* **2014**, 2 (3), 252–257.e1. <https://doi.org/10.1016/j.jaip.2014.03.007>.
- (140) Akin, C.; Valent, P. Diagnostic Criteria and Classification of Mastocytosis in 2014. *Immunol. Allergy Clin. North Am.* **2014**, 34 (2), 207–218. <https://doi.org/10.1016/j.iac.2014.02.003>.
- (141) Valent, P.; Sperr, W. R.; Akin, C. How I Treat Patients with Advanced Systemic Mastocytosis. *Blood* **2010**, 116 (26), 5812–5817. <https://doi.org/10.1182/blood-2010-08-292144>.
- (142) Akin, C. Mast Cell Activation Syndromes Presenting as Anaphylaxis. *Immunol. Allergy Clin. North Am.* **2015**, 35 (2), 277–285. <https://doi.org/10.1016/j.iac.2015.01.010>.
- (143) Frieri, M. Mast Cell Activation Syndrome. *Clin. Rev. Allergy Immunol.* **2018**, 54 (3), 353–365. <https://doi.org/10.1007/s12016-015-8487-6>.
- (144) Gülen, T.; Akin, C. Pharmacotherapy of Mast Cell Disorders. *Curr. Opin. Allergy Clin. Immunol.* **2017**, 17 (4), 295–303. <https://doi.org/10.1097/ACI.0000000000000377>.
- (145) Rached, A. A.; El Hajj, W. Eosinophilic Gastroenteritis: Approach to Diagnosis and Management. *World J. Gastrointest. Pharmacol. Ther.* **2016**, 7 (4), 513–523. <https://doi.org/10.4292/wjgpt.v7.i4.513>.
- (146) Khan, D. A. Alternative Agents in Refractory Chronic Urticaria: Evidence and Considerations on Their Selection and Use. *J. Allergy Clin. Immunol. Pract.* **2013**, 1 (5), 433–440. <https://doi.org/10.1016/j.jaip.2013.06.003>.
- (147) Lakhanpal, S.; Ginsburg, W. W.; Michet, C. J.; Doyle, J. A.; Moore, S. B. Eosinophilic Fasciitis: Clinical Spectrum and Therapeutic Response in 52 Cases. *Semin. Arthritis Rheum.* **1988**, 17 (4), 221–231. [https://doi.org/10.1016/0049-0172\(88\)90008-x](https://doi.org/10.1016/0049-0172(88)90008-x).
- (148) Klion, A. Hypereosinophilic Syndrome: Approach to Treatment in the Era of Precision Medicine. *Hematol. Am. Soc. Hematol. Educ. program.* **2018**, 2018 (1), 326–331. <https://doi.org/10.1182/asheducation-2018.1.326>.
- (149) Kovalszki, A.; Weller, P. F. Eosinophilia in Mast Cell Disease. *Immunol. Allergy Clin. North Am.* **2014**, 34 (2), 357–364. <https://doi.org/10.1016/j.iac.2014.01.013>.
- (150) Youngblood, B. A.; Brock, E. C.; Leung, J.; Falahati, R.; Bryce, P. J.; Bright, J.; Williams, J.; Shultz, L. D.; Greiner, D. L.; Brehm, M. A.; Bebbington, C.; Tomasevic, N. AK002, a Humanized Sialic Acid-Binding Immunoglobulin-Like Lectin-8 Antibody That Induces Antibody-Dependent Cell-Mediated Cytotoxicity against Human Eosinophils and Inhibits Mast Cell-Mediated Anaphylaxis in Mice. *Int. Arch. Allergy Immunol.* **2019**, 180 (2), 91–102. <https://doi.org/10.1159/000501637>.
- (151) Levine, H. T.; Tauber, J.; Nguyen, Q.; Anesi, S. D. Phase 1b Study of AK002, an Anti-Siglec-8 Monoclonal Antibody, in Patients with Severe Allergic Conjunctivitis (KRONOS Study). *J. Allergy Clin. Immunol.* **2020**, 145 (2), AB185. <https://doi.org/https://doi.org/10.1016/j.jaci.2019.12.323>.

- (152) Siebenhaar, F.; Bonnekoh, H.; Hawro, T.; Hawro, M.; Michaelis, E.; Rasmussen, H.; Singh, B.; Kantor, A.; Chang, A.; Maurer, M. Safety and Efficacy Data of AK002, an Anti-Siglec-8 Monoclonal Antibody, in Patients with Indolent Systemic Mastocytosis (ISM): Results from a First-in-Human, Open-Label Phase 1 Study. *Allergy* **2019**, *74*, 854–915. <https://doi.org/10.1111/all.13962>.
- (153) Dellon, E. S.; Peterson, K. A.; Murray, J. A.; Falk, G. W.; Gonsalves, N.; Chehade, M.; Genta, R. M.; Leung, J.; Khoury, P.; Klion, A. D.; Hazan, S.; Vaezi, M.; Bledsoe, A. C.; Durrani, S. R.; Wang, C.; Shaw, C.; Chang, A. T.; Singh, B.; Kamboj, A. P.; Rasmussen, H. S.; Rothenberg, M. E.; Hirano, I. Anti-Siglec-8 Antibody for Eosinophilic Gastritis and Duodenitis. *N. Engl. J. Med.* **2020**, *383* (17), 1624–1634. <https://doi.org/10.1056/NEJMoa2012047>.
- (154) Altrichter, S.; Staubach, P.; Pasha, M.; Rasmussen, H.; Singh, B.; Chang, A.; Bernstein, J.; Siebenhaar, F.; Maurer, M. Efficacy and Safety Data of AK002, an Anti-Siglec-8 Monoclonal Antibody, in Patients with Multiple Forms of Uncontrolled Chronic Urticaria (CU): Results from an Open-Label Phase 2a Study. *Allergy* **2019**, *74* (11), 117–129. <https://doi.org/10.1111/all.13958>.
- (155) Schanin, J.; Gebremeskel, S.; Korver, W.; Falahati, R.; Butuci, M.; Haw, T. J.; Nair, P. M.; Liu, G.; Hansbro, N. G.; Hansbro, P. M.; Evensen, E.; Brock, E. C.; Xu, A.; Wong, A.; Leung, J.; Bebbington, C.; Tomasevic, N.; Youngblood, B. A. A Monoclonal Antibody to Siglec-8 Suppresses Non-Allergic Airway Inflammation and Inhibits IgE-Independent Mast Cell Activation. *Mucosal Immunol.* **2021**, *14* (2), 366–376. <https://doi.org/10.1038/s41385-020-00336-9>.
- (156) Barnes, P. J. Immunology of Asthma and Chronic Obstructive Pulmonary Disease. *Nat. Rev. Immunol.* **2008**, *8* (3), 183–192. <https://doi.org/10.1038/nri2254>.
- (157) Fahy, J. V. Type 2 Inflammation in Asthma—Present in Most, Absent in Many. *Nat. Rev. Immunol.* **2015**, *15* (1), 57–65. <https://doi.org/10.1038/nri3786>.
- (158) von Gunten, S.; Vogel, M.; Schaub, A.; Stadler, B. M.; Miescher, S.; Crocker, P. R. Intravenous Immunoglobulin Preparations Contain Anti-Siglec-8 Autoantibodies. *J. Allergy Clin. Immunol.* **2007**, *119* (4), 1005–1011. <https://doi.org/10.1016/j.jaci.2007.01.023>.
- (159) Jia, Y.; Yu, H.; Fernandes, S. M.; Wei, Y.; Gonzalez-gil, A.; Bochner, B. S.; Kern, R. C.; Schleimer, R. P.; Schnaar, R. L. Expression of Ligands for Siglec-8 and Siglec-9 in Human Airways and Airway Cells. *J. Allergy Clin. Immunol.* **2015**, *135* (3), 799–810. <https://doi.org/10.1016/j.jaci.2015.01.004>.
- (160) Gao, P.; Shimizu, K.; Grant, A. V.; Rafaels, N.; Zhou, L.; Hudson, S. A.; Konno, S.; Zimmermann, N.; Araujo, M. I.; Ponte, E. V.; Cruz, A. A.; Nishimura, M.; Su, S.; Hizawa, N.; Beaty, T. H.; Mathias, R. A.; Rothenberg, M. E.; Barnes, K. C.; Bochner, B. S. Polymorphisms in the Sialic Acid-Binding immunoglobulin-like lectin-8 (Siglec-8) are Associated with Susceptibility to Asthma. *Eur. J. Hum. Genet.* **2010**, *18* (6), 713–719. <https://doi.org/10.1038/ejhg.2009.239>.
- (161) Gebremeskel, S.; Schanin, J.; Coyle, K. M.; Butuci, M.; Luu, T.; Brock, E. C.; Xu, A.; Wong, A.; Leung, J.; Korver, W.; Morin, R. D.; Schleimer, R. P.; Bochner, B. S.; Youngblood, B. A. Mast Cell and Eosinophil Activation Are Associated With COVID-19 and TLR-Mediated Viral Inflammation: Implications for an Anti-Siglec-8 Antibody. *Front. Immunol.* **2021**, *12*, 650331.

- <https://doi.org/10.3389/fimmu.2021.650331>.
- (162) O’Sullivan, J. A.; Carroll, D. J.; Cao, Y.; Salicru, A. N.; Bochner, B. S. Leveraging Siglec-8 Endocytic Mechanisms to Kill Human Eosinophils and Malignant Mast Cells. *J. Allergy Clin. Immunol.* **2018**, *141* (5), 1774–1785.e7. <https://doi.org/10.1016/j.jaci.2017.06.028>.
- (163) Duan, S.; Arlian, B. M.; Nycholat, C. M.; Wei, Y.; Tateno, H.; Smith, S. A.; Macauley, M. S.; Zhu, Z.; Bochner, B. S.; Paulson, J. C. Nanoparticles Displaying Allergen and Siglec-8 Ligands Suppress IgE-FcεRI-Mediated Anaphylaxis and Desensitize Mast Cells to Subsequent Antigen Challenge. *J. Immunol.* **2021**, *206* (10), 2290–2300. <https://doi.org/10.4049/jimmunol.1901212>.
- (164) Nycholat, C. M.; Duan, S.; Knuplez, E.; Worth, C.; Elich, M.; Yao, A.; O’Sullivan, J.; McBride, R.; Wei, Y.; Fernandes, S. M.; Zhu, Z.; Schnaar, R. L.; Bochner, B. S.; Paulson, J. C. A Sulfonamide Sialoside Analogue for Targeting Siglec-8 and-F on Immune Cells. *J. Am. Chem. Soc.* **2019**, *141* (36), 14032–14037. <https://doi.org/10.1021/jacs.9b05769>.
- (165) Gonzalez-Gil, A.; Porell, R. N.; Fernandes, S. M.; Wei, Y.; Yu, H.; Carroll, D. J.; McBride, R.; Paulson, J. C.; Tiemeyer, M.; Aoki, K.; Bochner, B. S.; Schnaar, R. L. Sialylated Keratan Sulfate Proteoglycans Are Siglec-8 Ligands in Human Airways. *Glycobiology* **2018**, *28* (10), 786–801. <https://doi.org/10.1093/glycob/cwy057>.
- (166) Bochner, B. S.; Alvarez, R. A.; Mehta, P.; Bovin, N. V.; Blixt, O.; White, J. R.; Schnaar, R. L. Glycan Array Screening Reveals a Candidate Ligand for Siglec-8. *J. Biol. Chem.* **2005**, *280* (6), 4307–4312. <https://doi.org/10.1074/jbc.M412378200>.
- (167) Pröpster, J. M.; Yang, F.; Rabbani, S.; Ernst, B.; Allain, F. H.; Schubert, M. Structural Basis for Sulfation-Dependent Self-Glycan Recognition by the Human Immune-Inhibitory Receptor Siglec-8. *Proc. Natl. Acad. Sci.* **2016**, *113* (29), E4170–E4179. <https://doi.org/10.1073/pnas.1602214113>.
- (168) Hudson, S. A.; Bovin, N. V.; Schnaar, R. L.; Crocker, P. R.; Bochner, B. S. Eosinophil-Selective Binding and Proapoptotic Effect in Vitro of a Synthetic Siglec-8 Ligand , Polymeric 6'-Sulfated Sialyl Lewis^x. *J. Pharmacol. Exp. Ther.* **2009**, *330* (2), 608–612. <https://doi.org/10.1124/jpet.109.152439.2007>.

2. From the natural carbohydrate to glycomimetics

In this chapter, we describe the successful development of a high-affinity glycomimetic ligand for Siglec-8, starting from the natural tetrasaccharide 6'-sulfo-sialyl Lewis^x. The identification of the minimal binding epitope, the disaccharide 6-sulfo-Sia-Gal, a deoxygenation strategy and the introduction of a sulfonamide substituent in position 9 of the sialic acid led to the identification of a potent ligand with 20-fold improvement in binding affinity. Homology modeling was used to get more structural information about Siglec-8.

Parts of this chapter have been published in *ChemMedChem*:

Kroezen, B. S.; Conti, G.; Girardi, B.; Cramer, J.; Jiang, X.; Rabbani, S.; Müller, J.; Kokot, M.; Luisoni, E.; Ricklin, D.; Schwardt, O.; Ernst, E. A Potent Mimetic of the Siglec-8 Ligand 6'-Sulfo-Sialyl Lewis^x, *ChemMedChem* **2020**, *15* (18), 1706-1719.¹

© 2020 Wiley-VCH GmbH

The entire article can be found in the appendix (p. 199).

Contributions to the project

Benedetta Girardi contributed with the total synthesis of the minimal binding epitope **2** and its bioisosters (**24-28**), and with completing the library of deoxygenated compounds with the total synthesis and biological evaluation of compounds **33** and **36**. She designed, synthesized and tested the lactic acid derivatives **39**, **53** and **54** (part of this work was done at the university of Ljubljana, and was part of the master thesis project of Martina Manna). She built the homology model of Siglec-8 with the help of Prof. Assoc. Tihomir Tomašič, who also contributed to the design of the lactic acid derivatives. She also contributed to the writing of the above-mentioned published paper.

2.1 Introduction.

Siglecs (sialic acid-binding immunoglobulin-type lectins) are cell surface proteins representing a subset of the I-type lectins located primarily on the surface of immune cells. They exhibit a sialic acid binding N-terminal domain, one or more C2-set immunoglobulin domains and a cytoplasmic tail.²⁻⁴ The cytoplasmic tail of most Siglecs contains an immunoreceptor tyrosine-based inhibitory motif (ITIM), which participates in immunosuppressive cell signaling. Thus, ligand-binding induces phosphorylation of the tyrosine motif by an Src family kinase, resulting in the recruitment of the SH2 domain-containing phosphatases SH1, SH2 or SHIP-1.⁵ These phosphatases inhibit cellular processes through the inactivation of essential kinases. Therefore, most of Siglecs are inhibitory receptors, which can modulate crucial immune responses.^{6,7} In their resting state, most Siglecs are engaged in *cis*-interactions with sialylated glycans expressed on the surface of the same cell.⁸ As a result, Siglecs are essentially masked and can only interact with *trans*-ligands that display sufficient affinity or avidity to outcompete the *cis*-interactions.⁹

Siglec-8 is a member of the CD33-related Siglec family and is predominantly expressed on the cell-surface of eosinophils and mast cells and weakly on basophils.^{10,11} These cell types play a crucial role in the pathophysiology of asthma, a chronic inflammatory disease characterized by a massive infiltration of eosinophils into the airways followed by degranulation of mast cells and the release of bronchoconstrictors.^{12,13} When Siglec-8 was cross-linked with antibodies, apoptosis of eosinophils¹⁴ and inhibition of the release of mediators from mast cells were observed.¹⁵ A promising alternative to target Siglec-8 with antibodies involves the multivalent display of Siglecs ligands on polymers and nanoparticles.¹⁶ Thus, it was shown that apoptosis can be initiated by treating eosinophils with a synthetic polyvalent Siglec-8 ligand¹⁷ and immunohistochemical analyses exhibited an up-regulation of Siglec-8 ligands in inflamed compared to healthy tissue.¹⁸ In addition, isolated eosinophils from the airways of allergen-challenged patients showed elevated susceptibility to Siglec-8-mediated apoptosis.¹⁹ Finally, variants in the Siglec-8 gene were associated with an increased susceptibility for asthma.²⁰ In summary, Siglec-8 has been identified as a therapeutic target for the treatment of eosinophil and mast cell disorders.²¹⁻²⁵

Natural sialylated glycans generally exhibit only low monovalent affinities (0.5 to 3 mM), which, however, can be substantially improved by a multivalent presentation.^{26,27} The development of potent monovalent Siglec ligands started from natural glycan ligands and successfully yielded high-affinity ligands for numerous Siglecs. High-affinity ligands for Siglec-1,²⁸ Siglec-2,^{9,29-31} Siglec-4,^{32,33}

Siglec-7³⁴ and Siglec-8³⁵ have been reported. The trisaccharide Neu5Ac α 2-3(6-*O*-sulfo)Gal β 1-4GlcNAc and the tetrasaccharide Neu5Ac α 2-3(6-*O*-sulfo)Gal β 1-4[Fuc α 1-3]GlcNAc [6'-sulfo-sLe^x (**1a**)] were identified in a glycan array screening as Siglec-8 ligands (Figure 2-1A).³⁶⁻³⁸ In this work, we describe the development of high-affinity Siglec-8 mimetics based on 6'-sulfo-sLe^x (**1a**).

2.2 Results and Discussion.

Our group recently published the NMR solution structures of the Siglec-8 lectin domain (PDB code: 2N7A) and its complex with 3-aminopropyl 6'-sulfo-sLe^x, **1b** (PDB code: 2N7B).³⁹ Using ¹H-¹⁵N HSQC titration and NOE experiments, both the affinity (295 μ M), and the binding mode of Siglec-8 with **1b** have been determined (Figure 1B).

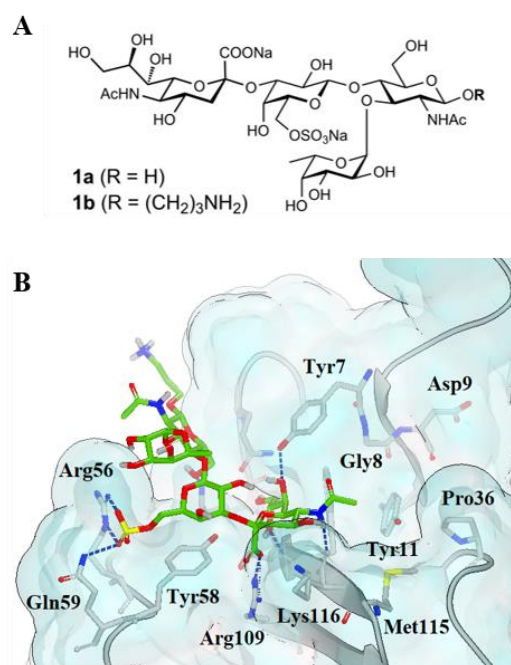
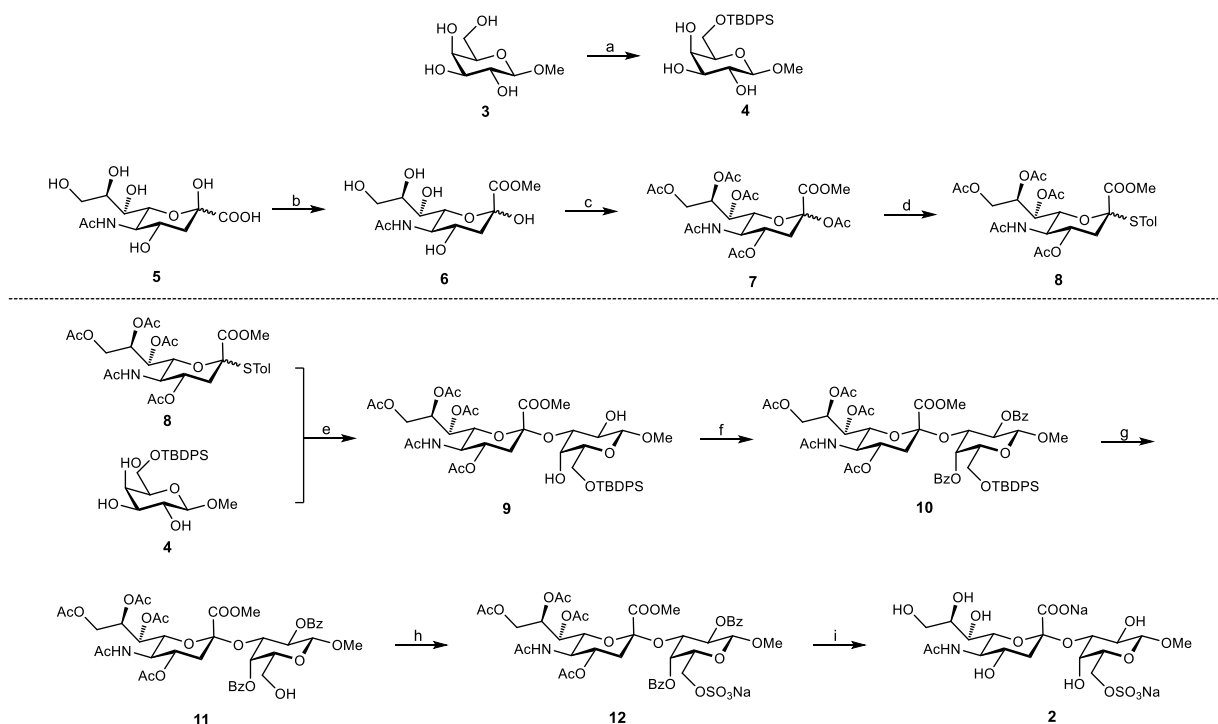


Figure 1. A: 6'-Sulfo-sLe^x (**1a**) and 3-aminopropyl 6'-sulfo-sLe^x (**1b**); B: Binding mode of 3-aminopropyl 6'-sulfo-sLe^x (**1b**) in the carbohydrate-recognition domain (CRD) of Siglec-8 (PDB ID: 2N7B).³⁹ The figure was generated using the software VIDA.⁴⁰ Color code: N: blue, O: red, S: yellow, protein backbone: grey, ligand C: green. Contacts with the protein are depicted as blue dashed lines.

Arg109, which is conserved in most siglecs,³⁹ forms an essential salt bridge with the carboxylate of Neu5Ac. Moreover, the sulfate group in the 6'-position of the Gal moiety is engaged in another salt bridge with Arg56 and Gln59. This interaction proved to be crucial, as the binding affinity dropped drastically when the sulfate group in 3-aminopropyl 6'-sulfo-sLe^x (**1b**) was removed (28-fold loss of affinity) or moved to the D-GlcNAc moiety (9-fold loss in affinity).³⁹ Essential hydrogen bonds are formed by the three hydroxyls of the glycerol side chain with Tyr7, Ser118 and Gln122, as well as

by the *N*-acetyl group with the backbone of Lys116. Furthermore, various hydrophobic interactions, including *van der Waals* and sigma- π interactions with Tyr58 contribute to the binding affinity of tetrasaccharide **1b**. Surprisingly, the L-Fuc and D-GlcNAc moieties do not form any contact with the protein surface. Glycan arrays additionally showed that the fucose moiety does not significantly contribute to affinity.⁴¹ We therefore assumed, that the disaccharide Neu5Ac α 2-3(6-*O*-sulfo)Gal (**2**, Scheme 1) represents the minimal binding epitope.

Synthesis and affinity of the minimal binding epitope. Sialic acid donor **8**⁴² was synthesized in large scale by first protecting free Neu5Ac **5** and then introducing a 4-methylbenzenethiol as a good leaving group. Sialidation of the protected galactose acceptor **4**⁴³ with sialic acid donor **8** yielded disaccharide **9**. The highest yield and the best α -selectivity were obtained using NIS/TfOH as promoter and a mix of MeCN/DCM in a 5 to 3 ratio. To avoid acetyl migration, the 2- and 4-OH of the Gal moiety were benzoylated (\rightarrow **10**) before the silyl protection was selectively cleaved using HF·pyr to afford **11**. Next, the sulfate group was introduced using an excess of SO₃·pyr in DMF (\rightarrow **12**). Finally, acetate deprotection under Zemplén conditions and hydrolysis of the methyl ester with aq. NaOH yielded the test compound Neu5Ac α 2-3(6-*O*-sulfo)Gal (**2**, Scheme 1).



Scheme 1. a) TBDPSCl, imidazole, DMF, rt, 16 h, 97%; b) Amberlyst-15, MeOH, rt, 16 h, 99%; c) Ac₂O, DMAP, pyr, 0 °C to rt, 16 h, 85%; d) *p*-thiocresol, BF₃·Et₂O, DCM, rt, 16 h, 90%; e) NIS, TfOH, MeCN/DCM, -40 °C, 16 h, 34%; f) Bz₂O, DMAP, pyr, rt, 16 h, 84%; g) HF·pyr, pyr, rt, 4 h, 93%; h) SO₃·pyr, DMF, 0 °C to rt, 4 h, 93%; i) i. MeONa/MeOH, rt to 50 °C, 24 h; ii. NaOH (aq), rt, 1 h, 81% over two steps.

3-Aminopropyl 6'-sulfo-sLe^x (**1b**) has an affinity of 295 $\mu\text{M} \pm 26 \mu\text{M}$ (K_D by NMR) or 303 $\mu\text{M} \pm 11 \mu\text{M}$ (IC_{50} in a competitive binding assay).³⁹ Surprisingly, the IC_{50} of the disaccharide Neu5Ac α 2-3(6-*O*-sulfo)Gal (**2**) is only by a factor 2 lower (733 μM , Table 1) than the IC_{50} of lead tetrasaccharide **1b**, which was quite encouraging, as the complexity of the epitope and the number of synthetic steps were significantly reduced, whilst the affinity was only modestly affected. For the determination of the IC_{50} 's, we applied a competitive binding assay⁴⁴ with Siglec-8-Fc and streptavidin-peroxidase coupled to the biotinylated polyacrylamide glycopolymer 6'-sulfo-sLe^x-PAA as competitor. After incubation of the protein and the glycopolymer with different concentrations of the tested ligand, the colorimetric reaction with the horseradish peroxidase substrate ABTS was measured to determine IC_{50} values.

Table 1. Binding affinity of 3-aminopropyl 6'-sulfo-sLe^x (**1b**)³⁹ and derivatives thereof. IC_{50} values were determined in a competitive binding assay.⁴⁴ ¹⁾ Average value over six measurements; n.a.: not active up to 10 mM.

Compound	Structure	IC_{50} [μM]
1b ³⁹		303 \pm 11
2		733 \pm 163 ¹⁾
13		n.a.
14 ⁴⁵		n.a.
15		n.a.
16		n.a.
17		n.a.

The individual fragments, the galactose derivative **13** and the neuraminic acid derivative **14**,⁴⁵ as well as the disaccharides **15-17** with modified glycerol side chains did not show any affinity. The hydrogen bond network the glycerol side chain is involved in (Figure 1B), obviously plays an important role in the binding process. Moreover, a ReLiBase⁴⁶ search shows that the 8-OH stabilizes the bioactive

conformation of sialic acid in the bound conformation via an intramolecular hydrogen bond with the carboxylate. Overall, these results confirmed that the sulfated disaccharide **2** indeed represents the minimal carbohydrate epitope necessary for Siglec-8 binding.

Bioisosteres of the carboxylate and the sulfate group. To further improve the PK/PD profile of disaccharide **2**, the possibility of bioisosteric replacements of the carboxylate and the sulfate were explored, not only to improve the affinity, but also to enhance selectivity and alter physical properties.^{47,48} The IC₅₀ measurements for the derivatives **18-28** were conducted in the competitive binding assay (Table 2). For the reference compound **2**, an additional K_D value of 561 μM was obtained in the microscale thermophoresis (MST) assay, which is in good agreement with the competitive binding assay (733 μM) (entry 1).

MST is a quick and reliable assay performed in capillaries, with serial dilution of the ligand and constant amount of protein labeled with a fluorescent dye. The fluorescence change is caused by a laser which induces a microscopic temperature gradient and the movement of the particles outside the heated area. The detection of the change of fluorescence is expressed as a function of the concentration of the ligand (Figure 2).^{49,50}

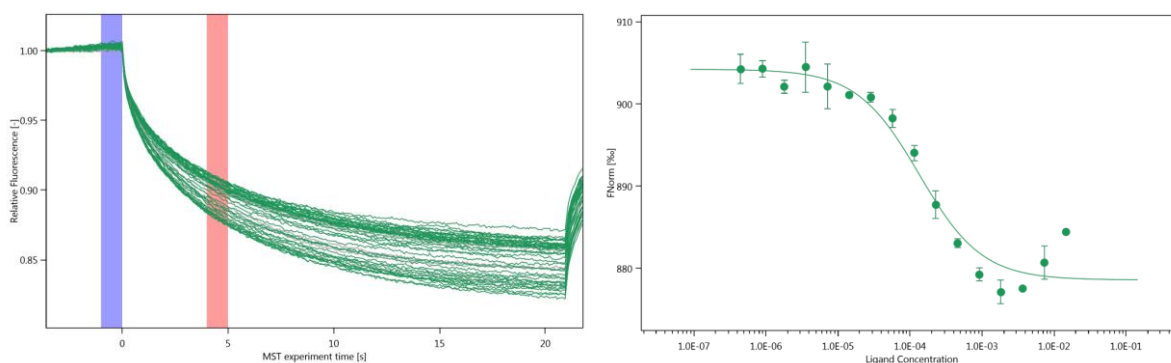
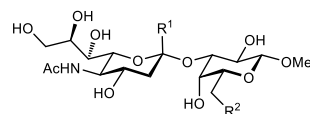
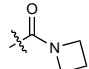


Figure 2. Exemplative figure of an MST experiment.

When the sulfate was modified while the carboxylate substituent was maintained (entries 2-8), reduced affinity was observed in three cases (entries 2, 3 & 4) while all other modifications resulted in inactive compounds. The carboxylate turned out to be the best replacement of the sulfate leading only to a moderate loss of affinity (733 μM vs. 1026 μM). Replacement of the carboxylate (entries 9-12) led to inactive or only moderately active ligands.

Table 2. Binding affinities for derivatives of lead structure **2**, bearing replacements for the sulfate and carboxylic acid functional groups. IC_{50} values were determined in a competitive binding assay,⁴⁴ while dissociation constants (K_D) were measured with MST. ¹⁾ Average value over six measurements; n.a. not active up to 10 mM; n.d. not detected.



Entry	Compound	R ¹	R ²	IC ₅₀ (μM)	K _D (μM)
Reference compound					
1	2	COONa	CH ₂ OSO ₃ Na	733 ¹⁾	561
Sulfate bioisosteres					
2	18	COONa	COONa	1026	n.d.
3	19	COONa	CH ₂ CH ₂ COONa	2199	n.d.
4	20	COONa	CH ₂ NH ₂	1393	n.d.
5	21	COONa	CH ₂ CH ₂ Ph	n.a.	n.d.
6	22	COONa	CH ₂ N ₃	n.a.	n.d.
7	23	COONa	CH ₂ NHAc	n.a.	n.d.
8	24	COONa	CH ₂ OPO ₃ Na ₂	n.d.	2830
Carboxylic acid bioisosteres					
9	25	CONH ₂	CH ₂ OSO ₃ Na	1613	1011
10	26	CONHMe	CH ₂ OSO ₃ Na	n.d.	2850
11	27	CONHOH	CH ₂ OSO ₃ Na	n.d.	n.a.
12	28		CH ₂ OSO ₃ Na	n.d.	2836

Modification of the galactose moiety. According to the structure of the complex of 3-aminopropyl 6'-sulfo-sLe^x (**1b**)/Siglec-8 obtained by NMR (Figure 1B) the 2- and the 4-OH do not significantly contribute to binding. In addition, the anomeric substituent points away from the protein surface and, when substituted with an OMe aglycone, cannot establish a contact with the protein surface. Therefore, a set of derivatives **29-34** where these three substituents were consecutively removed, was synthesized and evaluated regarding their binding to Siglec-8 with the competitive binding assay (Table 3). The affinity of compounds **2**, **34** and **38** was also evaluated by Isothermal Titration Calorimetry (ITC), a technique which measures the heat changes upon molecular interactions, it uses free ligand and protein in solution and it's able to determine not only the affinity but also the thermodynamic properties of the binding.⁵¹⁻⁵³

Table 3. Biological evaluation of deoxygenated derivatives of lead structure **2**. IC₅₀ values were determined in a competitive binding assay,⁴⁴ while dissociation constants (K_D) were measured with ITC or MST. ¹⁾ Average value over six measurements; n.a.: not active up to 10 mM; n.d.: not determined. [a] K_D measured with MST.

Entries	Compound	Structure	IC ₅₀ [μM]	K _D [μM]
1	2		733 ¹⁾	574
2	29		381	n.d.
3	30		674	n.d.
4	31		204	n.d.
5	32		271	n.d.
6	33		n.d.	784 ^[a]
7	34		117	259
8	35		1246	n.d.
9	36		n.d.	3476 ^[a]
10	37		n.a.	n.a.
11	38		n.d.	15

Almost the whole 3-fold affinity gain originated from deoxygenation at the anomeric center (→ **29**, Table 3, entry 2), rather than removal of the 2-OH group (→ **30**, entry 3). Noteworthy, these two

modifications, i.e. removal of 1-OMe and 2-OH (\rightarrow **31**, entry 4), are positively cooperative, since the affinity for **31** (IC_{50} 207 μ M) is more increased compared to the two individually deoxygenated compounds **29** (IC_{50} 381 μ M) and **30** (IC_{50} 674 μ M). Furthermore, deoxygenation in the 4-position of the galactose moiety (\rightarrow **32**, entry 5) resulted in a 3-fold improvement of affinity compared to the parent compound **2** (entry 1), while only keeping the ring oxygen (\rightarrow **33**, entry 6) surprisingly led to a decrease in affinity (K_D 784 μ M). However, by completely replacing the galactose moiety with a cyclohexane in derivative **34**, bearing only the CH_2OSO_3Na at the 5-position, a further affinity enhancement could be realized, resulting in a 6-fold higher potency for **34** (IC_{50} 117 μ M) compared to **2**. Finally, we thought about replacing the cyclohexane moiety of **29** with aromatic moieties (\rightarrow **35-36**, entries 8 and 9), in order to get possible π - π stacking interaction with the underlying Tyr58. However, binding affinity was substantially reduced, probably because the directionality of the salt bridge formed by the sulfate is disturbed.

Modification of the 9-position of the Neu5Ac moiety. Amide formation in the 9-position of neuraminic acid is generally a successful approach to increase the affinity of Siglec antagonists.^{9,28-34,54} In accordance with a recent publication of Paulson *et al.*³⁵ emphasizing that amide-linked substituents at C-9 of the neuraminic acid moiety do not yield hits, **37** did not show any activity neither in the competitive binding assay nor in ITC experiments (Table 3). When we, based on Paulson's findings, formed sulfonamide **38**, a Siglec-8 antagonist with a K_D of 15 μ M affinity was obtained.

Thermodynamics of Siglec-8 antagonist/Siglec-8 interaction. Based on the thermodynamic fingerprints of the interaction of **1b**, **2**, **34** and **38** with Siglec-8, a deeper insight into the binding process was intended. For this purpose, ITC data of the mimetics **2**, **34** and **38** were compared with the previous data for the parent tetrasaccharide 3-aminopropyl 6'-sulfo-sLe^x (**1b**).³⁹ The K_D values determined by ITC (Table 4, Figure 3) correspond well with the data obtained from the competitive binding assay and by MST (Tables 1-3).

Table 4. Thermodynamic parameters from ITC for selected Siglec-8 ligands. ¹⁾ Data reproduced from Ref.³⁹. Error estimates for thermodynamic data correspond to the 68% confidence interval from global fitting of two independent experiments. Errors in binding kinetic data represent the standard error of a single measurement.

Compound	K_D [μM]	ΔG° [kJ mol ⁻¹]	ΔH° [kJ mol ⁻¹]	$-T\Delta S^\circ$ [kJ mol ⁻¹]	k_{on} [M ⁻¹ s ⁻¹]	k_{off} [s ⁻¹]	Residence time τ [s]
1b ¹⁾	279 (273 – 285)	-20.3 (-20.3 – -20.2)	-32.6 (-33.5 – -31.8)	12.4 (11.5 – 13.2)	N/A	N/A	N/A
2	574 (505 – 650)	-18.5 (-18.8 – -18.2)	-16.3 (-17.2 – -15.3)	-2.3 (-3.5 – -1.0)	$1.2 \cdot 10^3$ ($\pm 5.1 \cdot 10^2$)	$8.2 \cdot 10^{-1}$ ($\pm 3.5 \cdot 10^{-1}$)	1.2
34	259 (222 – 303)	-20.5 (-20.9 – -20.1)	-15.0 (-16.2 – -13.9)	-5.5 (-6.9 – -3.9)	$6.6 \cdot 10^2$ ($\pm 7.5 \cdot 10^1$)	$1.6 \cdot 10^{-1}$ ($\pm 1.8 \cdot 10^{-2}$)	6.2
38	15 (13 – 18)	-27.5 (-27.1 – -27.9)	-11.6 (-11.0 – -12.2)	-16.0 (-15.0 – -16.9)	$4.7 \cdot 10^3$ ($\pm 7.1 \cdot 10^2$)	$8.7 \cdot 10^{-2}$ ($\pm 1.2 \cdot 10^{-2}$)	11.5

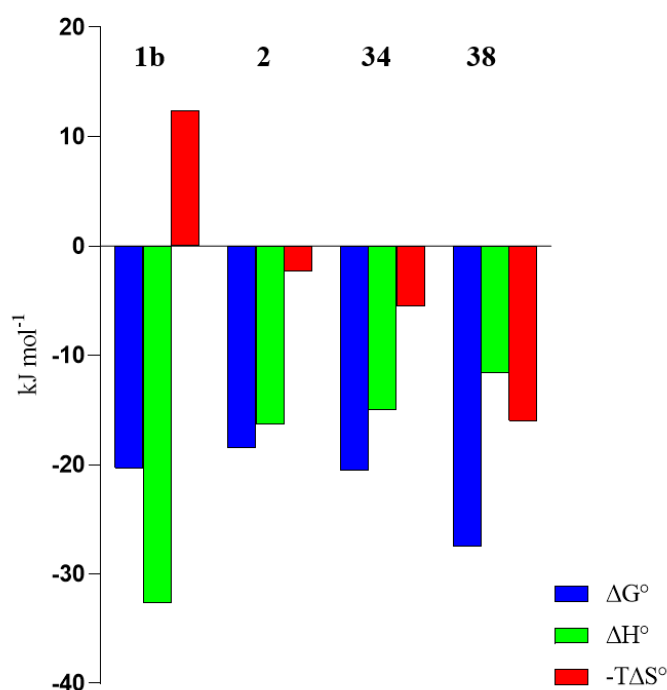


Figure 3. Thermodynamic signature (ΔG° , ΔH° and $-T\Delta S^\circ$) for 3-aminopropyl 6'-sulfo-sLe^x (**1b**) and the disaccharides **2**, **34** & **38**. Kinetic rate constants for **1b** have not been published in the cited reference (N/A).

The binding of 3-aminopropyl 6'-sulfo-sLe^x (**1b**) to Siglec-8 is driven by a strong binding enthalpy ($\Delta H^\circ = -32.6 \text{ kJ mol}^{-1}$), which is partly offset by a large unfavorable entropic term ($-T\Delta S^\circ = +12.4 \text{ kJ mol}^{-1}$). Because the protein structure of apo-Siglec-8 and the complex of 6'-sulfo-sLe^x (**1b**) with Siglec-8 are identical to a large extent,³⁹ a large entropy penalty resulting from induced fit can be excluded. A potential reason for the entropy penalty could be related to a loss of conformational flexibility, especially of the Fuc and GlcNAc moiety as well as of the glycerol side chain. On the other hand, an extended network of perfect hydrogen bonds is the main cause for the large beneficial

enthalpy term.⁵⁵ For disaccharide **2** the enthalpic contribution is much less pronounced ($\Delta\Delta H^\circ = 16.3$ kJ mol⁻¹), probably as a result of a slightly modified binding mode, aggravating a perfect alignment of the hydrophobic α -face of the Gal moiety and Tyr58. As a second consequence of the modified binding mode, the geometry of the hydrogen bond interactions is slightly altered, further reducing the enthalpy term. Overall, the complex exhibits higher flexibility, leading to a substantial improvement of the entropy term ($-T\Delta\Delta S^\circ = -14.7$ kJ mol⁻¹). Cyclohexane derivative **34** shows a slightly reduced binding enthalpy ($\Delta\Delta H^\circ = 1.3$ kJ mol⁻¹) compared to disaccharide **2**, which is overcompensated by a beneficial entropy term ($-T\Delta\Delta S^\circ = -3.2$ kJ mol⁻¹), resulting in a 2-fold higher binding affinity. Finally, the introduction of a benzamide in the 9-position of the Neu5Ac moiety (\rightarrow **37**, Table 3) yielded an inactive compound in the competitive binding assay as well as in ITC experiments. This was surprising because in a number of other Siglecs a substantial improvement of affinity could be realized by the introduction of aromatic amides.^{9,28–34,54} It is, however, in accordance with a recent publication of Paulson *et al.* emphasizing that amide-linked substituents at C-9 of the Neu5Ac moiety did not yield Siglec-8 hits.³⁵ Possible reasons could be the exit vector of the amide bond, causing the aromatic substituent to point into the water environment. In contrast, the exit vector of a sulfonamide substituent positions an aromatic group much closer to the protein surface. Sulfonamide **38** proved to be the best Siglec-8 antagonist in the series with a K_D of 15 μ M. Surprisingly, this became possible by a substantial improvement of the entropy term ($-T\Delta\Delta S^\circ = -10.5$ kJ/mol) compared to **34**, which overcompensates a marked enthalpy penalty ($\Delta\Delta H^\circ = 3.4$ kJ/mol).

The residence times $\tau = 1/k_{\text{off}}$ ⁵⁶ for carbohydrate/lectin interactions are regularly very short and represent one of the challenges to be addressed for therapeutic applications. We determined binding kinetic data for the interactions of **2**, **34**, and **38** to Siglec-8 from ITC data using the kinITC technology.^{57,58} This method analyses the equilibration time of each injection during titration and fits this information to a kinetic model to derive rate constants. The binding kinetics of disaccharide **2** are characterized by a very short residence time of 1.2 s. For the mimetic **34**, the residence time is increased by a factor of 5, probably mainly based on the reduced polarity. The residence time of the complex with sulfonamide derivative **38** is even longer, *i.e.* 10-fold increased. Thus, structural modifications leading to improved affinities go in parallel with prolonged lifetimes of the protein–ligand complex, which is often correlated with beneficial pharmacological properties. In the association rate, the simplification of the carbohydrate core from **2** to **34** is associated with a reduction of the rate constant by a factor of 2. However, through the introduction of the sulfonamide substituent in **38**, an improvement of the association rate by a factor of 4 compared to **2** was observed. Thus, the additional interactions of the hydrophobic naphthyl substituent influence both, association and dissociation kinetics towards a higher binding affinity of **38**. The prolonged residence time of **38** is

an indication that glycomimetic ligands have the potential to overcome one of the main drawbacks of carbohydrate ligands in the context of medicinal chemistry.

When we investigated the binding mode of compound **38**, we realized that the available NMR solution structure was not fitting our molecule. Therefore, to get more structural information, which can also be useful for future structure-based drug design, we built a homology model.

Homology model of Siglec-8. Many examples show how homology modeling has been extremely useful and successful to support drug discovery processes. There are many protein sequences available but not as many protein 3D structures. In the absence of structural information, this computational prediction method can be very helpful in lead identification as well as lead optimization with respect to potency and selectivity.^{59–61} Template search and sequence alignment are crucial steps to determine the precision of the model. As template, we chose Siglec-7, as the proteins share 71% sequence homology. From the several high-resolution crystal structures for Siglec-7 available in the Protein Data Bank (PDB) we chose 1O7S due to its high resolution of 1.75 Å.⁶² Sequence alignment with T-Coffee server and the Siglec-7 crystal structure were used for homology model building. Ten models were generated and validated, and the best one was chosen based on its capacity to accommodate compound **38** (Figure 4).

Looking at the binding site of the homology model of Siglec-8, it reveals that upon docking of compound **38** the Arg46 loop region has a very different conformation compared to the NMR structure. This allows for a very good accommodation of the sulfate in a small positively charged pocket that would not exist otherwise. Interestingly, in the homology model the naphthalene binds to a second aromatic cluster near the loop region. This region is not accessible in the NMR structure, because it is blocked by the N-terminus, which we did not include in our model because it is not well

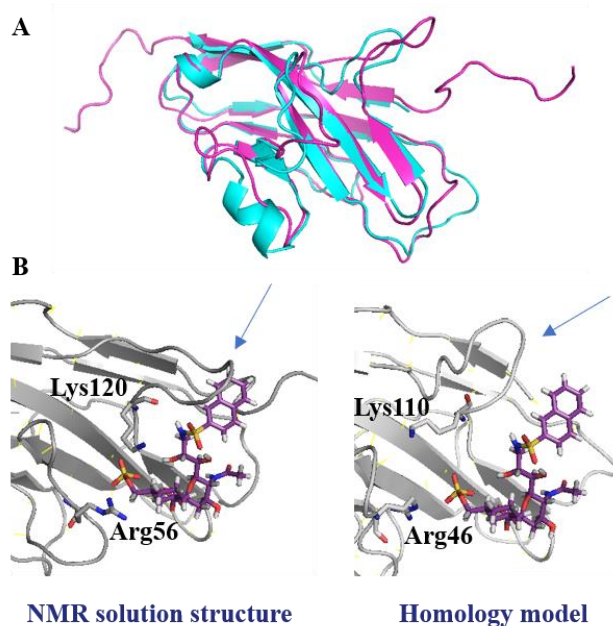


Figure 4. A: Overlay of the Siglec-8 NMR solution structure (2N7B, in magenta) and the homology model (in cyan) built on Siglec-7. B: Main structural difference between the Siglec-8 NMR solution structure and the homology model, both in complex with compound **38**. Figures were generated using the software Pymol.⁷²

resolved in the Siglec-7 crystal structure. However, in a future work it would be important to include this region as well and to determine its position because of its closeness to the binding site.

Another approach to understand the binding mode of **38** was to use an *in silico* mutation of Lys120 to Ala for docking. After visual inspection of the generated docking poses, Ala120 was mutated back to Lys and minimized. In the docking solution, the naphthyl substituent of sulfonamide **38** binds to a hydrophobic pocket generated by the displacement of Lys120. Presumably, the angular geometry of the sulfonamide bond is required for access to this region (for details see the paper attached in the appendix).

Modification of the Neu5Ac moiety. As previously illustrated, a deoxygenation strategy of the galactose moiety served to reduce the polarity of the molecule and consequently improve the general properties and the affinity by reducing the desolvation penalty. In a previous work in Prof. Ernst's group, the sialic acid of the lead compound **2** was replaced by a lactic acid derivative,⁶³ which was already successfully used as a sialic acid mimetic in Selectin ligands (Figure 5).⁶⁴ Looking at the docking pose of this compound **39**, we can see how the most important interactions with Arg56 and Arg109 are preserved.

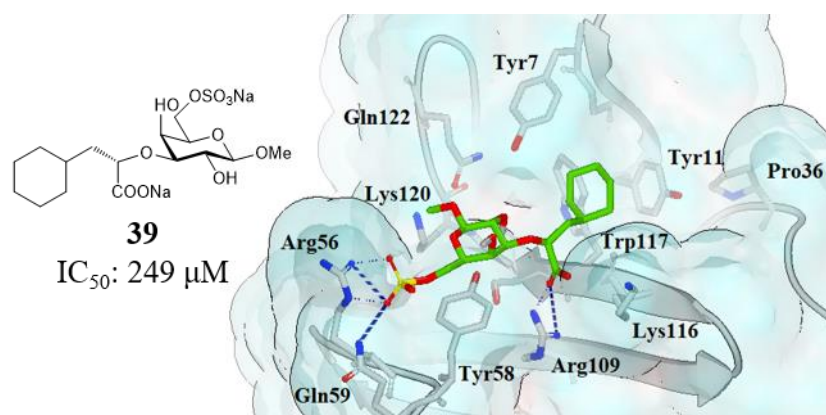
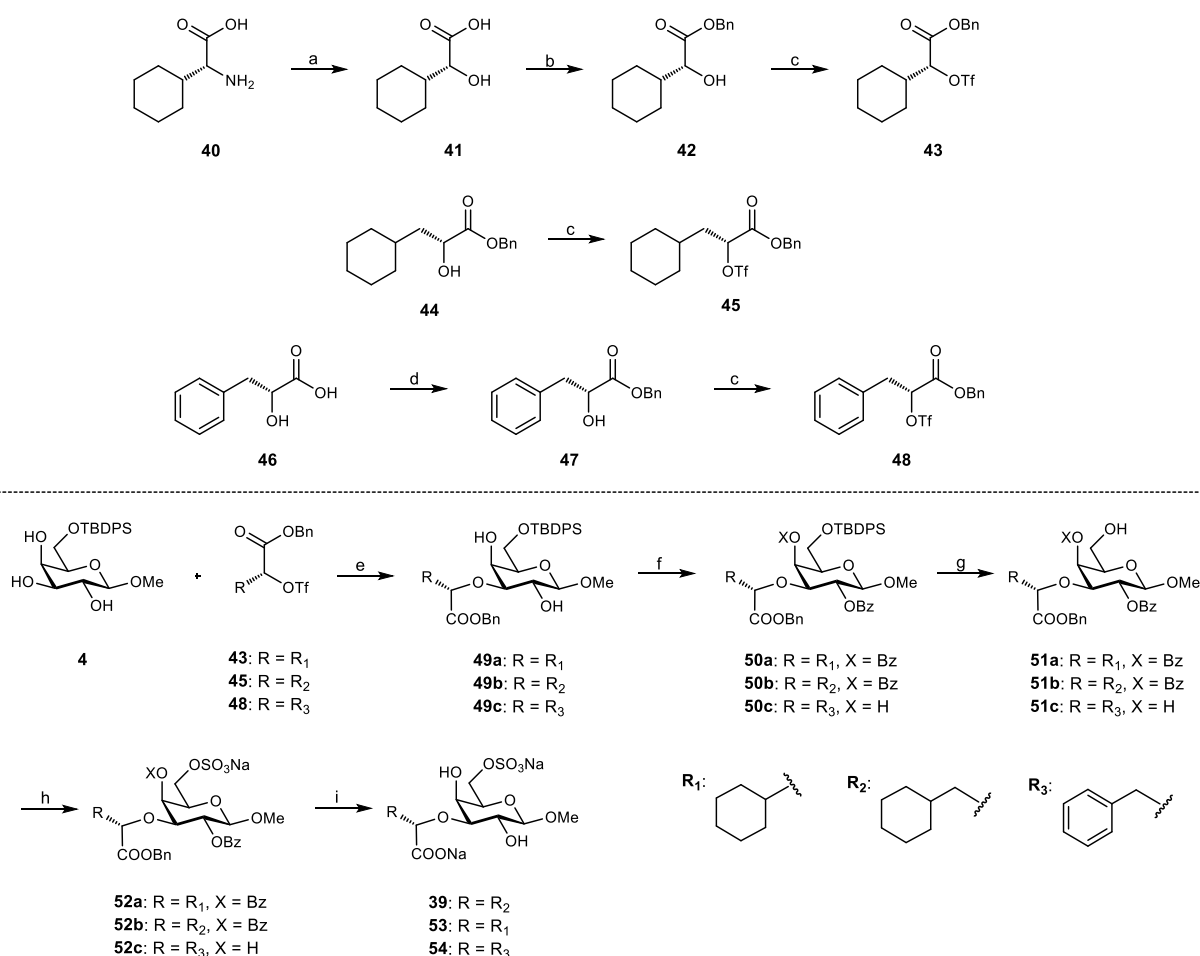


Figure 5. Docking of compound **39** into the binding site of the Siglec-8 NMR solution structure (PDB ID: 2N7B). Docking was performed using FRED algorithm on OEDocking software (OEDOCKING 3.3.0.2: OpenEye Scientific Software).⁶⁵ The figure was generated using the software VIDA.⁴⁰ Color code: N: blue, O: red, S: yellow, protein backbone: grey, ligand C: green. Contacts with the protein are depicted as blue dashed lines.

Compound **39** was tested with the above-mentioned competitive binding assay showing an IC_{50} of 249 μM , thus improving the binding affinity of 3-fold compared to parent compound **2**. Considering that this compound may be the first example of a ligand binding to a Siglec protein without containing a sialic acid and that the competitive binding assay used was not really reliable, we decided to synthesize and test it again, together with a small library of derivatives (Scheme 2).



Scheme 2. a) NaNO₂, H₂SO₄, H₂O, 0 °C to rt, 24 h, 86%; b) BnBr, Cs₂CO₃, DMF, rt, 16 h, 72%; c) Tf₂O, 2,6-lutidine, DCM, rt, 16 h, **43**: 77%, **45**: 59%, **48**: 84%; d) BnBr, Cs₂CO₃, DMF, rt, 16 h, 33%; e) i. Bu₂SnO, dry MeOH, reflux, 3 h; ii. CsF, DME, rt, 16 h, **49a**: 38%, **49b**: 54%, **49c**: 23%; f) Bz₂O, DMAP, pyr, rt, 16 h, **50a**: 62%, **50b**: 63%; g) HF/pyr, pyr, rt, 4 h, **51a**: 92%, **51b**: 69%, **51c**: 40%; h) SO₃-pyr, DMF, 0 °C to rt, 4 h, **52a**: 81%, **52b**: 60%; i) i. MeONa/MeOH, rt to 50 °C, 24 h; ii. NaOH (aq), rt, 1 h, **39**: 44%, **53**: 35%, **54**: 3% over two steps.

The synthesis of the envisaged compounds was accomplished as shown in Scheme 2. Intermediate **43** was obtained starting from α-D-cyclohexylglycine (**40**), via diazotization–hydrolysis reaction⁶⁶ (→ **41**) and subsequent esterification of the carboxylic group with benzyl bromide (→ **42**). The hydroxyl group of **42** was transformed into a good leaving group by reacting it with triflic anhydride to give donor **43**. The same sequence was employed to prepare intermediates **45** and **48**, starting from benzyl ester **44**,⁶⁷ available in-house, and commercially available D-(R)-3-phenyllactic acid **46**, respectively. The reaction steps involving the phenyllactic acid derivatives were characterized by low yields, due to the preferential formation of the elimination product, affording a conjugate system between the aromatic ring and the carbonyl group. The galactoside acceptor **4**,⁴³ protected in position 6 with a *tert*-butyldiphenylsilyl group (TBDPS), was then alkylated with the triflates **43**, **45** and **48**. The alkylation reactions were performed by first activating the galactose with dibutyltin oxide

(Bu₂SnO), followed by the treatment of the resulting stannylidene acetal with triflates **43**, **45**, and **48**, employing CsF, to afford intermediates **49a-c**. Following a similar procedure as the one previously shown, the free hydroxyl groups of the galactose were protected with benzoates (\rightarrow **50a-c**), the TBDPS group was removed (\rightarrow **51a-c**), sulfate introduced in position 6 (\rightarrow **52a-c**), and final deprotection afforded the test compounds **39**, **53** and **54**.

The steps involving the molecules containing the aromatic moiety were characterized by very low yields. First, the alkylation step (\rightarrow **49c**) yielded only 23% because of the instability of compound **48** and purification problems due to the presence of a diastereoisomer, indicating that either building block **48** was enantiomerically impure or that partial racemization occurred in the course of the reaction. Then, benzylation occurred only in position 2 of the galactose (\rightarrow **50c**). Since position 4 was not reactive, we assumed that it might not react in the subsequent sulfonation so we proceeded with the next steps. However, the sulfate partially attached in position 4 as well, making the purification of the final product **54** even more cumbersome.

Table 5. Biological evaluation of lactic acid derivatives **39**, **53** and **54**. IC₅₀ values were determined in a competitive binding assay,⁴⁴ while dissociation constants (*K_D*) were measured by MST and ITC. n.a.: not active up to 15 mM; n.d.: not determined.

Compound	Structure	IC ₅₀ [μM]	<i>K_D</i> [MST, μM]	<i>K_D</i> [ITC, μM]
39		249	1430	n.a.
53		n.d.	265	n.a.
54		n.d.	n.a.	n.d.

The obtained final compounds were first screened with the MST assay (Table 5). As it can be seen from the table, we could not confirm the affinity of compound **39** previously obtained with the competitive binding assay, neither with MST nor with ITC. Compound **54**, with the phenyl ring as lateral substituent, did not show any binding. However, results for compound **53**, missing the methylene linker, are worth to be discussed in more detail. First, we observed an affinity of 265 μM by MST, but the compound clearly interacted with the dye (Figure 6A): high ligand concentrations are quenching the fluorescence of the dye while the fluorescence intensity should always be the same

because of constant protein concentration. To assess if the affinity was a result of the binding or of the interaction with the dye, we tested the same compound on nano differential scan fluorimetry (nanoDSF) and on ITC (Figure 6B & 6C). nanoDSF is a technique which monitors intrinsic fluorescence changes of a protein during thermal unfolding. The interaction of a ligand usually stabilizes the protein and therefore causes a shift of the transition temperature from a folded to an unfolded state to higher values.⁶⁸

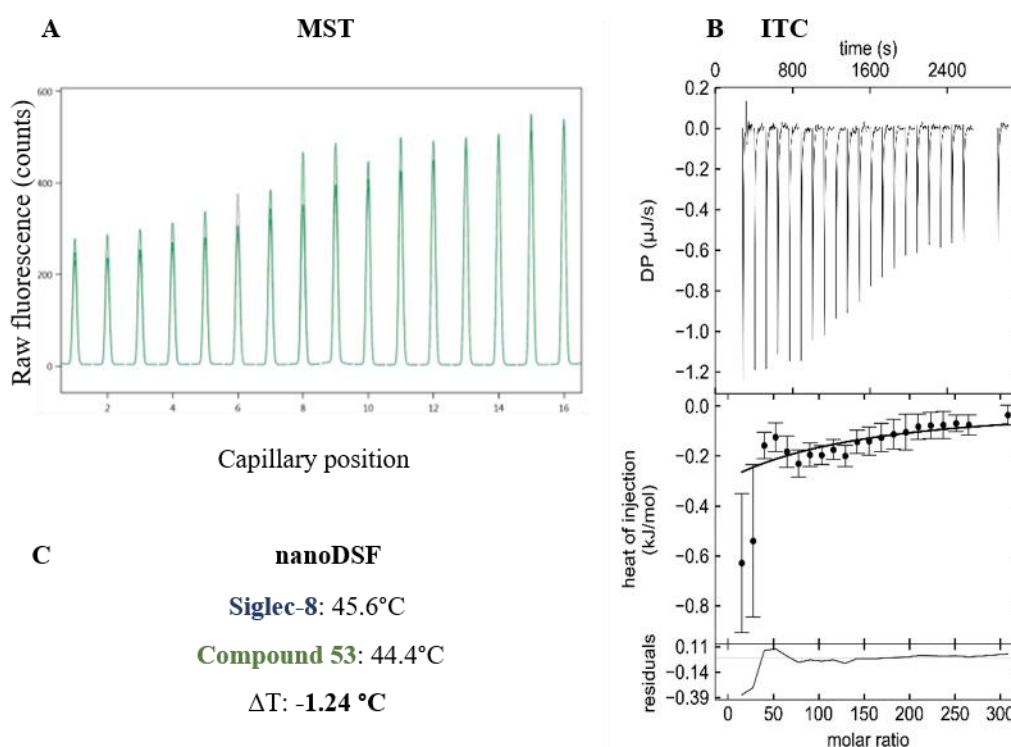


Figure 6. Binding affinity measurement of compound **53** to Siglec-8. A: MST graph showing how the fluorescence is quenched at higher ligand concentration (capillary 1). B: ITC graph after subtraction of heat of dilution. C: nanoDSF temperature values of protein transition point between folded and unfolded state with and without ligand.

The ITC graph of compound **53** shows a lot of power applied in the last injections where there should only be heat of dilution. Therefore, we measured an ITC with only the ligand and without the protein in order to be able to subtract the heat of dilution, but even after doing so we still could see a lot of heat in the last injections (Figure 6B). Regarding the nanoDSF assay, there was a negative temperature shift compared to the one of the protein alone, which generally indicates that the ligand stabilizes an unfolded state of the protein.

To conclude, the results of the different assays did not provide a clear picture and are hard to explain. Disturbances due to pH shifts can be excluded, considering that a concentrated buffer (100 mM HEPES) was used and that these conditions never caused problems with other Siglec-8 ligands, which always have two ionizable groups. Therefore, we assume that there could be some interaction between

the ligand and the protein but perhaps in a different binding site. Additional experiments, such as ^1H - ^{15}N HSQC NMR, might be useful in the future to further investigate this hypothesis.

2.3 Conclusions.

In this chapter, we identified the pharmacophores of 6'-sulfo-Lewis^x (**1a**) and successfully developed the high-affinity mimetic **38**. Its core is still neuraminic acid, however bearing a carbocyclic mimetic of the Gal moiety in the 2-position and a sulfonamide substituent in the 9-position. Compared to the lead structure 3-aminopropyl 6'-sulfo-Lewis^x (**1b**), the affinity could be improved 20-fold. We postulate a hypothetical binding mode with a homology model, which, however, requires more work because of the absence of important information regarding the N-terminus of the protein.

In addition, we synthesized and evaluated a small focused library of compounds where the sialic acid of lead compound **2** was replaced by lactic acid derivatives. Questionable results were obtained for compound **53** with the assays employed. We assume that the compound indeed might interact with Siglec-8, but with different site(s) of the protein. Additional investigations, for example by ^1H - ^{15}N HSQC NMR analysis, could probably be useful to determine the possibility of binding. However, the structure of these ligands was very similar to a recently published Galectin-8 ligand, the 3-*O*-[1-carboxyethyl]- β -D-galactopyranoside, a galactose bearing a lactic acid in position 3. Therefore, we decided to test the corresponding non-sulfated derivatives of compounds **39**, **53** and **54** and to optimize them for binding to galectin-8. Details of this project are shown in Chapter 5.

2.4 Experimental Part.

Ligand preparation. The structures of molecules were built with ChemDraw Professional 16.0 (PerkinElmer Informatics, Inc.). Conformers for each ligand, required by the docking software FRED, were generated with OMEGA (OMEGA version 2.5.1.4. OpenEye Scientific Software, Santa Fe, NM. <http://www.eyesopen.com>), with a maximum number of 200 conformations set as default.

Receptor preparation & docking protocol. The docking was performed using the Siglec-8 lectin domain NMR solution structure (PDB code: 2N7B). Docking was done inside a grid box surrounding the ligand with the volume of 8350 Å³, dimensions: 25.67 Å × 16.00 Å × 20.33 Å, and outer contour of 2766 Å² using Make Receptor 3.0.1. The docking software FRED (OEDocking version 3.0.1. OpenEye Scientific Software, Santa Fe, NM. <http://www.eyesopen.com>) was used for docking studies with the default settings, and number of poses, which was set to 10. The proposed ten binding

poses with the highest rank of the docked ligands were evaluated using final score and relative position to the native ligand. The graphical representations of the calculated binding poses were obtained using VIDA (VIDA version 4.2.1. OpenEye Scientific Software, Santa Fe, NM. <http://www.eyesopen.com>).

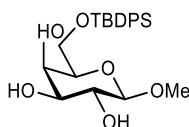
Homology model. Sequence alignment to identify the suitable protein to be used to build the homology model of Siglec-8 we performed using T-Coffee web server.⁶⁹ Siglec-7 was chosen, since they share 70.8% sequence identity. For homology modeling, we used 1O7S.pdb crystal structure of siglec-7 due to its high resolution of 1.75 Å.⁶² The obtained sequence alignment and siglec-7 crystal structure were then used for homology model building using MODELLER.⁷⁰ Ten models were generated and the obtained structures were validated using ProSA-web⁷¹ and SAVES v5.0 servers. Models were visually analyzed with Pymol⁷² and the best model was chosen based on its capacity to accommodate our ligand of reference **38**, which was finally docked using Maestro Schrodinger software.⁷³

Synthesis. Unless otherwise stated, the starting materials, reagents, and solvents were purchased as high-grade commercial products from Sigma-Aldrich, Alfa-Aesar, Apollo Scientific, Fluka and TCI, and used without further purification. MeCN and MeOH were dried over activated molecular sieves (4 Å and 3 Å, respectively) and stored under argon atmosphere. Dry DME and DCM were prepared by filtration through Al₂O₃ and stored over activated molecular sieves (4 Å) under argon atmosphere. Dry DMF, pyridine and THF were purchased from Sigma-Aldrich and TCI. Molecular sieves were activated under vacuum at 500 °C for 30 min immediately before use. Analytical TLC was performed on silica gel Merck 60 F254 plates (0.25 mm), using visualization with UV light and/or by charring with a phosphomolybdic acid solution (10 g in 100 mL of ethanol) or molybdate solution (a 0.02 M solution of ammonium cerium sulfate dihydrate and ammonium molybdate tetrahydrate in 10% aq. H₂SO₄). Acidic ion-exchange resin (Amberlyst[®] IR-120 hydrogen form) was washed with MeOH prior to use. Column chromatography was carried out on silica gel 60 (particle size 240–400 mesh). Medium pressure chromatography (MPLC) separations were carried out on a CombiFlash R_f from Teledyne Isco equipped with RediSep normal-phase or RP-18 reversed-phase flash columns. Reversed-phase chromatography was also performed on a Biotage Isolera[™] One using C-18 cartridges. Size exclusion chromatography was performed on Biogel P-2 media (Bio-Rad Laboratories, Inc.). ¹H and ¹³C NMR spectra were recorded at 400 MHz and 100 MHz, respectively, on an AVANCE III 400 spectrometer (Bruker Corporation, Billerica, MA, USA) or at 500 MHz and 126 MHz on a Bruker Avance DMX-500 spectrometer, in chloroform-*d* (CDCl₃), methanol-*d*₄

(CD₃OD) or deuterium oxide (D₂O), with TMS as internal standard. Chemical shifts (δ) are expressed in parts per million (ppm) relative to the residual solvent peaks for the ¹H and ¹³C nuclei (CDCl₃: $\delta_{\text{H}} = 7.26$, $\delta_{\text{C}} = 77.16$; CD₃OD: $\delta_{\text{H}} = 3.31$, $\delta_{\text{C}} = 49.00$; D₂O: $\delta_{\text{H}} = 4.79$); coupling constants (J) are given in hertz (Hz). The following abbreviations are used to describe peak patterns when appropriate: s (singlet), d (doublet), dd (doublets of doublet), ddd (doublets of doublets of doublet), t (triplet), m (multiplet). 2D NMR experiments (COSY and HSQC) of representative compounds were carried out to assign protons and carbons of the new structures. Mass spectra were obtained using a single quadrupole mass spectrometer Advion Expression CMS^L coupled with an Agilent 1290 liquid chromatograph or on a Waters Micromass ZQ instrument. High resolution mass spectrometry (HRMS) was performed on a Q ExactiveTM Plus Hybrid Quadrupole-OrbitrapTM Mass Spectrometer (Thermo ScientificTM; ion source: Electrospray Ionization (ESI)). MS spectra were acquired in Fourier transform-mass spectrometry (FT-MS) scan mode with a target mass resolution of 100 000 at m/z 400. Recorded spectra were analysed with Thermo Xcalibur Qual Browser (Xcalibur 4.2 SP1, Thermo Fisher Scientific Inc.). HRMS analysis was also performed on an Agilent 1100 LC, equipped with a photodiode array detector and a Micromass QTOF I, equipped with a 4 GHz digital-time converter. Optical rotations were measured with a PerkinElmer polarimeter 341. HPLC analysis for all the other compounds was performed on a Thermo Scientific Dionex Ultimate 3000 Binary Rapid Separation LC System (Thermo Fisher Scientific, Waltham, MA, USA) equipped with an autosampler, a binary pump system and a photodiode array detector. A Waters Atlantis T3 dC18 column (3 μm , 2.1 x 100 mm) was used with a flow rate of 0.3 mL/min. The eluent consisted of H₂O + 0.1% trifluoroacetic acid (TFA) as solvent A and MeCN + 0.1% TFA as solvent B (Table 6: Methods A and B).

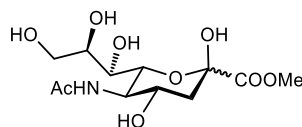
Method A		Method B	
T (min)	%B	T (min)	%B
0	0	0	5
2	0	2	5
16	70	10	20
18	70	16	80
20	0	18	80
21	0	20	0
-	-	21	0

Table 6. Methods for HPLC analysis.

Methyl 6-*O*-*tert*-butyldiphenylsilyl- β -D-galactopyranoside (4).

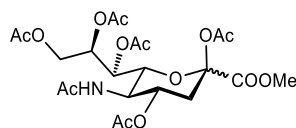
To a solution of methyl β -D-galactopyranoside (5.00 g, 0.026 mol) in dry DMF (60 mL) were added imidazole (3.90 g, 0.057 mmol) and TBDPSCl (7.40 mL, 0.280 mmol). The reaction mixture was stirred at rt for 16 h and then diluted with Et₂O. The organic layer was washed with H₂O (3 \times 60 mL) and NH₄Cl (aq. satd., 3 \times 30 mL), dried over Na₂SO₄, concentrated under reduced pressure and purified by flash chromatography (DCM/MeOH, 30:1) to give **4** (9.00 g, 80%) as a glassy white solid. $[\alpha]_D^{20}$ -14.2 (*c* 1.0, CHCl₃); ¹H NMR (400 MHz, CDCl₃): δ = 1.06 (s, 9H, C(CH₃)₃), 2.43 (d, *J* = 2.1 Hz, 1H, OH-2), 2.59 (d, *J* = 6.4 Hz, 1H, OH-3), 2.62 (d, *J* = 4.0 Hz, 1H, OH-4), 3.53 (s, 3H, OMe), 3.53-3.59 (m, 2H, H-3, H-5), 3.63 (m, 1H, H-2), 3.92 (dd, *J* = 5.1, 10.5 Hz, 1H, H-6a), 3.96 (d, *J* = 6.3, 10.5 Hz, 1H, H-6b), 4.10 (m, 1H, H-4), 4.14 (d, *J* = 7.5 Hz, 1H, H-1), 7.37-7.47 (m, 6H, Ar-H), 7.67-7.71 (m, 4H, Ar-H); ¹³C-NMR (100 MHz, CDCl₃): δ = 19.1 (C(CH₃)₃), 26.9 (3C, C(CH₃)₃), 57.1 (OMe), 63.2 (C-6), 69.0 (C-4), 72.5 (C-2), 73.9 (C-3), 74.4 (C-5), 104.0 (C-1), 127.97, 127.98, 130.1, 135.1, 135.8 (12C, Ar-C); ESI-MS: *m/z*: Calcd for C₂₃H₃₂O₆Si [M+Na]⁺: 455.2, found: 455.2.

The analytical data of **4** were in accordance with reported values.⁴³

Methyl 5-acetamido-3,5-dideoxy-D-glycero- β -D-galacto-2-nonulopyranosylonate (6).

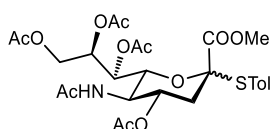
To a suspension of *N*-acetyl neuraminic acid (4.0 g, 13.0 mmol) in MeOH (200 mL), was added Amberlyst-15 (3.0 g) at rt. The mixture was stirred at rt for 16 h. The suspension was filtered over cotton and the residue was washed thoroughly with MeOH. The organic fractions were combined and the solvent was evaporated to afford **6** (4.16 g, 99%) as a white solid that was used in the next step without further purification. $[\alpha]_D^{20}$ -22.4 (*c* 2.0, H₂O); ¹H NMR (500 MHz, CD₃OD): δ = 1.92 (dd, *J* = 11.4, 12.9 Hz, 1H, H-3a), 2.04 (s, 3H, NHAc), 2.24 (dd, *J* = 4.9, 12.9 Hz, 1H, H-3e), 3.50 (dd, *J* = 1.5, 9.2 Hz, 1H, H-7), 3.64 (dd, *J* = 5.7, 11.3 Hz, 1H, H-9a), 3.70 (ddd, *J* = 2.8, 5.6, 8.9 Hz, 1H, H-8), 3.80 (s, 3H, OMe), 3.81-3.85 (m, 2H, H-7, H-9b), 4.02 (dd, *J* = 1.5, 10.6 Hz, 1H, H-6), 4.06 (m, 1H, H-4); ¹³C NMR (126 MHz, CD₃OD): δ = 21.1 (NHAc), 39.3 (C-3), 51.7 (OMe), 53.0 (C-5), 63.5 (C-9), 66.5 (C-4), 68.8 (C-7), 70.3 (C-8), 70.7 (C-6), 95.3 (C-2), 170.4, 173.7 (2C, C=O); ESI-MS: *m/z*: Calcd for C₁₂H₂₁NO₉ [M+Na]⁺: 346.1, found 346.0.

Acetyl (methyl 5-acetamido-4,7,8,9-tetra-*O*-acetyl-3,5-dideoxy-*D*-glycero- β -*D*-galacto-2-nonulopyranosylonate) (7).



To a solution of **6** (4.00 g, 12.4 mmol) and DMAP (0.30 g, 2.48 mmol) in pyridine (70 mL) was added Ac₂O (47 mL, 495 mmol) dropwise at 0 °C. The reaction mixture was stirred for 16 h, then the solvents were evaporated. The residue was taken up in EtOAc (80 mL) and washed with H₂O (4 × 20 mL), CuSO₄ (10% aq., 3 × 20 mL), H₂O (3 × 20 mL) and brine (3 × 20 mL), dried over Na₂SO₄, filtered and evaporated. The crude material was purified by flash column chromatography (DCM/MeOH, 1:0 → 95:5) to afford **7** (3.2 g, 85%) as a fluffy white solid. $[\alpha]_{\text{D}}^{20} -57.1$ (*c* 1.8, CHCl₃); ¹H NMR (500 MHz, CDCl₃): $\delta = 1.90$ (s, 3H, NHAc), 2.03, 2.04, 2.06 (3 s, 9H, OAc), 2.09 (dd, *J* = 11.8, 13.3 Hz, 1H, H-3a), 2.14, 2.15 (2 s, 6H, OAc), 2.55 (dd, *J* = 5.0, 13.5 Hz, 1H, H-3e), 3.79 (s, 3H, OMe), 4.10-4.14 (m, 3H, H-5, H-6, H-9a), 4.49 (dd, *J* = 2.6, 12.4 Hz, 1H, H-9b), 5.08 (ddd, *J* = 2.6, 5.2, 6.7 Hz, 1H, H-8), 5.18-5.30 (m, 2H, H-4, NH), 5.37 (dd, *J* = 1.8, 5.2 Hz 1H, H-7); ¹³C NMR (126 MHz, CDCl₃): $\delta = 20.76, 20.77, 20.8, 20.9$ (4C, OAc), 23.2 (NHAc), 35.9 (C-3), 49.4 (C-5), 53.2 (OMe), 62.1 (C-9), 67.8 (C-7), 68.3 (C-4), 71.3 (C-8), 72.9 (C-6), 97.5 (C-2), 166.3, 168.2, 170.2, 170.3, 170.6, 171.0 (6C, C=O); ESI-MS: *m/z*: Calcd for C₃₂H₄₁NO₁₄[M+Na]⁺: 556.2, found 556.2.

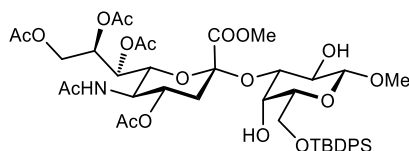
Tolyl (methyl 5-acetamido-4,7,8,9-tetra-*O*-acetyl-2,3,5-trideoxy-2-thio-*D*-glycero- α -*D*-galacto-2-nonulopyranosylonate) (8).



To a solution of **7** (4.8 g, 8 mmol) in dry DCM (50.0 mL) was added BF₃·Et₂O (1.48 mL, 12 mmol) dropwise, followed by *p*-thiocresol (1.39 g, 11.2 mmol) at rt under argon atmosphere. The reaction mixture was stirred for 16 h at rt, then it was neutralized with NEt₃ and Ac₂O (0.9 mL, 9.6 mmol) was added at 0 °C. The mixture was warmed to rt and the solvent was evaporated. The residue was dissolved in EtOAc (100 mL), washed with NaHCO₃ (aq. sat, 3 × 100 mL), NaCl (aq. sat, 3 × 100 mL), dried over Na₂SO₄, filtered and concentrated under reduced pressure. The residue was dissolved in a mixture of petroleum ether/toluene (2:1) and stirred at rt for 3 h. The mixture was then filtered under vacuum to afford **8** as a fluffy white solid (4.33 g, 90%). $[\alpha]_{\text{D}}^{20} -67.7$ (*c* 1.0, CHCl₃); ¹H NMR (500 MHz, CDCl₃): $\delta = 1.90$ (s, 3H, NHAc), 1.96 (s, 3H, OAc), 2.03 (s, 3H, CH₃-tol), 2.06 (m, 1H, H-3a), 2.08, 2.11 (2 s, 6H, OAc), 2.65 (dd, *J* = 4.9, 13.9 Hz, 1H, H-3e), 3.61 (s, 3H, OMe), 4.03 (dd,

$J = 8.4, 12.3$ Hz, 1H, H-9a), 4.12 (q, $J = 10.5$ Hz, 1H, H-5), 4.49 (dd, $J = 2.3, 12.3$ Hz, 1H, H-9b), 4.60 (dd, $J = 2.5, 10.5$ Hz, 1H, H-6), 4.97 (ddd, $J = 2.3, 2.3, 8.4$ Hz, 1H, H-8), 5.30 (d, $J = 10.4$ Hz, 1H, NH), 5.38 (ddd, $J = 4.8, 10.5, 11.7$ Hz, 1H, H-4), 5.45 (t, $J = 2.5$ Hz, 1H, H-7), 7.14 (d, $J = 7.9$ Hz, 2H, Ar-H), 7.33 (d, $J = 8.1$ Hz, 2H, Ar-H); ^{13}C NMR (126 MHz, CDCl_3): $\delta = 20.8, 20.9, 21.0, 21.2$ (4C, OAc), 21.4 (CH_3), 23.3 (NHAc), 37.5 (C-3), 49.6 (C-5), 52.7 (OMe), 62.8 (C-9), 69.0 (C-7), 69.2 (C-4), 73.21 (C-8) 73.22 (C-6), 89.0 (C-2), 125.4, 130.0, 136.3, 140.3 (6C, Ar-C), 168.4, 170.3, 170.4, 171.1, 171.3 (6C, C=O); ESI-MS: m/z : Calcd for $\text{C}_{27}\text{H}_{35}\text{NO}_{12}\text{S}$ $[\text{M}+\text{Na}]^+$: 620.2, found 620.2.

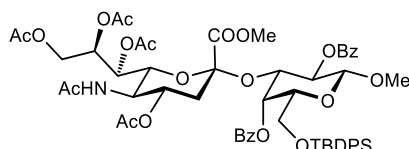
Methyl (methyl 5-acetamido-4,7,8,9-tetra-*O*-acetyl-3,5-dideoxy- α -D-galacto-2-nonulopyranosylonate)-(2 \rightarrow 3)-6-*O*-tert-butylidiphenylsilyl- β -D-galactopyranoside (9).



To a suspension of **8**⁴² (3.65 g, 6.10 mmol), **4**⁴¹ (1.20 g, 2.77 mmol) and 3Å molecular sieves in MeCN/DCM (5:3, 70 mL) at -40 °C, was added *N*-iodosuccinimide (2.74 g, 12.1 mmol), followed by dropwise addition of TfOH (98 μL , 1.1 mmol). The reaction mixture was stirred at -40 °C for 16 h under argon and then was neutralized with NEt_3 . The suspension was warmed up to rt, filtered over celite and the solvents were evaporated. The residue was dissolved in DCM (60 mL), washed with 1 M $\text{Na}_2\text{S}_2\text{O}_3$ (30 mL) and H_2O (3×30 mL), dried over Na_2SO_4 , filtered and evaporated. The crude product was purified by flash column chromatography (toluene/acetone, 1:0 \rightarrow 1:1) to afford **9** (853 mg, 34%). $[\alpha]_{\text{D}}^{20} -11.8$ (c 1.0, CHCl_3); ^1H NMR (500 MHz, CDCl_3): $\delta = 1.13$ (s, 9H, $\text{C}(\text{CH}_3)_3$), 1.98 (s, 3H, NHAc), 2.12 (s, 3H, OAc), 2.13 (m, 1H, H-3'a) 2.13, 2.20, 2.24 (3 s, 9H, OAc), 2.59 (d, $J = 4.0$ Hz, 1H, OH-2), 2.86 (dd, $J = 4.6, 12.9$ Hz, 1H, H-3'e), 2.89 (s, 1H, OH-4), 3.63 (s, 3H, OMe), 3.68 (m, 1H, H-5), 3.78 (ddd, $J = 1.1, 7.7, 9.2$ Hz, 1H, H-2), 3.85 (s, 3H, COOMe), 3.88 (d, $J = 3.6$ Hz, 1H, H-4), 3.91 (dd, $J = 5.0, 10.2$ Hz, 1H, H-6a), 4.03 (dd, $J = 7.1, 10.1$ Hz, 1H, H-6b), 4.08 (q, $J = 10.2$ Hz, 1H, H-5'), 4.16-4.22 (m, 3H, H-3, H-6', H-9'a), 4.36 (dd, $J = 2.8, 12.6$ Hz, 1H, H-9'b), 4.44 (d, $J = 7.7$ Hz, 1H, H-1), 5.04 (ddd, $J = 4.6, 10.2, 12.2$ Hz, 1H, H-4'), 5.30 (d, $J = 9.8$ Hz, 1H, NH), 5.43 (dd, $J = 2.0, 9.2$ Hz, 1H, H-7'), 5.45 (ddd, $J = 2.7, 4.9, 9.3$ Hz, 1H, H-8'), 7.44-7.53 (m, 6H, Ar-H), 7.75-7.79 (m, 4H, Ar-H); ^{13}C NMR (126 MHz, CDCl_3): $\delta = 19.4$ ($\text{C}(\text{CH}_3)_3$), 20.90, 20.91, 21.0, 21.4 (4C, OAc), 23.3 (NHAc), 26.9 (3C, $\text{C}(\text{CH}_3)_3$), 38.2 (C-3'), 49.8 (C-5'), 53.2 (COOMe), 56.8 (OMe), 62.4 (C-9'), 62.6 (C-6), 66.9 (C-7'), 67.9 (C-4), 68.0 (C-8'), 68.6 (C-4'), 69.5 (C-2), 72.7 (C-6'), 73.7 (C-5), 77.4 (C-3), 97.4 (C-2'), 104.0 (C-1), 127.88, 127.92, 129.95, 129.99, 133.1, 133.2, 135.67, 135.73 (12C, Ar-C), 168.4, 170.2, 170.4, 170.7, 171.0 (6C, C=O); ESI-MS: m/z : Calcd

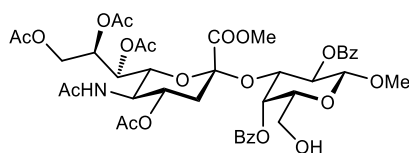
for $C_{43}H_{59}NO_{18}Si$ $[M+Na]^+$: 928.4, found: 928.4.

Methyl (methyl 5-acetamido-4,7,8,9-tetra-*O*-acetyl-3,5-dideoxy-*D*-glycero- α -*D*-galacto-2-nonulopyranosylonate)-(2 \rightarrow 3)-2,4-di-*O*-benzoyl-6-*O*-*tert*-butyldiphenylsilyl- β -*D*-galactopyranoside (10).



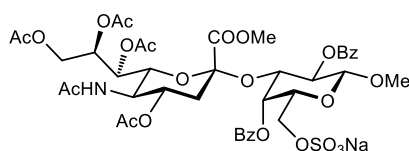
To a solution of **9** (974 mg, 1.08 mmol) in pyridine (30 mL) was added DMAP (47 mg, 0.38 mmol) followed by portion-wise addition of Bz_2O (3.18 g, 14.0 mmol) at 0 °C. The mixture was warmed up to rt and stirred for 16 h. Then, the solvent was removed by co-evaporation with toluene. The residue was dissolved in EtOAc (30 mL), washed with H_2O (3×10 mL), satd aq. $CuSO_4$ (3×10 mL), H_2O (10 mL) and brine (10 mL), dried over Na_2SO_4 , filtered and evaporated. The crude product was purified by flash column chromatography (petroleum ether/acetone, 1:0 \rightarrow 1:1) to afford **10** (1.10 g, 92%) as a brown vitreous solid. $[\alpha]_D^{20} +61.7$ (c 1.00, $CHCl_3$); 1H NMR (500 MHz, $CDCl_3$): δ = 1.03 (s, 9H, $C(CH_3)_3$), 1.46 (s, 3H, NHAc), 1.67 (t, J = 12.4 Hz, 1H, H-3'a), 1.79, 1.93, 2.10, 2.24 (4 s, 12H, OAc), 2.51 (dd, J = 4.7, 12.6 Hz, 1H, H-3'e), 3.47 (s, 3H, OMe), 3.58 (dd, J = 2.8, 10.7 Hz, 1H, H-6'), 3.64-3.74 (m, 2H, H-6), 3.81 (q, J = 10.4 Hz, 1H, H-5'), 3.93-4.02 (m, 2H, H-5, H-9'a), 3.97 (s, 3H, COOMe), 4.36 (dd, J = 2.3, 12.5 Hz, 1H, H-9'b), 4.73 (d, J = 7.9 Hz, 1H, H-1), 4.86-4.96 (m, 2H, H-3, H-4'), 5.00 (d, J = 10.2 Hz, 1H, NH), 5.25 (dd, J = 2.8, 9.7 Hz, 1H, H-7), 5.36 (dd, J = 7.9, 10.1 Hz, 1H, H-2), 5.62 (d, J = 3.2 Hz, 1H, H-4), 5.66 (ddd, J = 2.4, 5.4, 9.5 Hz, 1H, H-8'), 7.12 (t, J = 7.6 Hz, 1H, Ar-H), 7.24-7.29 (m, 6H, Ar-H), 7.34-7.52 (m, 4H, Ar-H), 7.52-7.62 (m, 2H, Ar-H), 7.62-7.70 (m, 6H, Ar-H), 8.02-8.13 (m, 2H, Ar-H), 8.14-8.23 (m, 2H, Ar-H); ^{13}C NMR (126 MHz, $CDCl_3$): δ = 19.0 ($C(CH_3)_3$), 20.3, 20.7, 20.8, 21.5 (4C, OAc), 23.1 (NHAc), 26.6 (3C, $C(CH_3)_3$), 37.3 (C-3'), 48.9 (C-5'), 53.2 (COOMe), 57.1 (OMe), 60.9 (C-6), 62.3 (C-9'), 66.4 (C-7'), 67.5 (C-8'), 67.9 (C-4), 69.6 (C-4'), 71.4 (C-2), 71.6 (C-6'), 71.9 (C-3), 73.2 (C-5), 96.9 (C-2'), 102.4 (C-1), 127.5, 127.7, 128.3, 129.6, 129.7, 129.9, 130.0, 130.2, 130.4, 132.89, 132.91, 135.4, 135.6 (24C, Ar-C), 165.4, 165.5, 168.1, 170.1, 170.2, 170.6, 170.7, 170.8 (8C, C=O); ESI-MS: m/z : Calcd for $C_{57}H_{67}NO_{20}Si$ $[M+Na]^+$: 1136.4, found: 1136.4.

Methyl (methyl 5-acetamido-4,7,8,9-tetra-*O*-acetyl-3,5-dideoxy-D-glycero- α -D-galacto-2-nonulopyranosylonate)-(2 \rightarrow 3)-2,4-di-*O*-benzoyl- β -D-galactopyranoside (11).



To a solution of **10** (485 mg, 0.44 mmol) in pyridine (10 mL) in a Teflon container was added HF·pyr (3.0 mL) dropwise and the reaction mixture was stirred at rt for 2.5 h. The reaction was neutralized with satd aq. NaHCO₃ and the aqueous phase was extracted with DCM. The crude product was purified by flash chromatography (DCM/MeOH, 1:0 \rightarrow 19:1) to afford **11** (360 mg, 93%) as a white solid. $[\alpha]_D^{20} +58.2$ (*c* 0.8, MeOH); ¹H NMR (500 MHz, CDCl₃): δ = 1.51 (s, 3H, NHAc), 1.72 (t, 1H, *J* = 12.5 Hz, H-3'a), 1.79, 1.91, 2.09, 2.24 (4 s, 12H, OAc), 2.45 (dd, *J* = 4.5, 12.7, 1H, H-3'e), 2.77 (dd, *J* = 6.5, 8.4 Hz, 1H, OH-6), 3.52 (m, 1H, H-6a), 3.53 (s, 3H, OMe), 3.70-3.76 (m, 2H, H-6b, H-6'), 3.80 (s, 3H, COOMe), 3.84 (m, 1H, H-5'), 3.88 (m, 1H, H-5), 3.98 (dd, *J* = 5.8, 12.4 Hz, 1H, H-9'a), 4.33 (dd, *J* = 2.4, 12.4 Hz, 1H, H-9'b), 4.66-4.82 (m, 3H, H-1, H-3, H-4'), 4.90 (d, *J* = 10.1 Hz, 1H, NH), 5.13 (d, *J* = 3.3 Hz, 1H, H-4), 5.21 (dd, *J* = 2.6, 9.6 Hz, 1H, H-7'), 5.47 (dd, *J* = 8.0, 10.1 Hz, 1H, H-2), 5.65 (m, 1H, H-8'), 7.47-7.50 (m, 4H, Ar-H), 7.56-7.63 (m, 2H, Ar-H), 8.04-8.14 (m, 2H, Ar-H), 8.15-8.24 (m, 2H, Ar-H); ¹³C NMR (126 MHz, CDCl₃): δ = 20.3, 20.7, 20.8, 21.5 (4C, OAc), 23.1 (NHAc), 37.5 (C-3'), 48.8 (C-5'), 53.2 (COOMe), 57.2 (OMe), 60.3 (C-6), 62.4 (C-9'), 67.5 (C-7'), 69.1 (C-8'), 69.1 (2C, C-4, C-4'), 71.0 (C-2), 71.4 (C-3), 72.0 (C-6'), 73.2 (C-5'), 96.8 (C-2), 102.4 (C-2'), 128.4 (C-1), 128.6, 128.8, 130.1, 130.18, 120.2, 133.0, 133.7 (12C, Ar-C), 165.4, 167.7, 168.3, 170.0, 170.2, 170.6, 170.70, 170.72 (8C, C=O); ESI-MS: *m/z*: Calcd for C₄₁H₄₉NO₂₀ [M+Na]⁺: 898.3, found: 898.5.

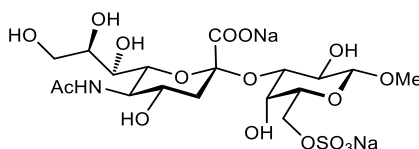
Methyl (methyl 5-acetamido-4,7,8,9-tetra-*O*-acetyl-3,5-dideoxy-D-glycero- α -D-galacto-2-nonulopyranosylonate)-(2 \rightarrow 3)-2,4-di-*O*-benzoyl-6-*O*-sulfonato- β -D-galactopyranoside (12).



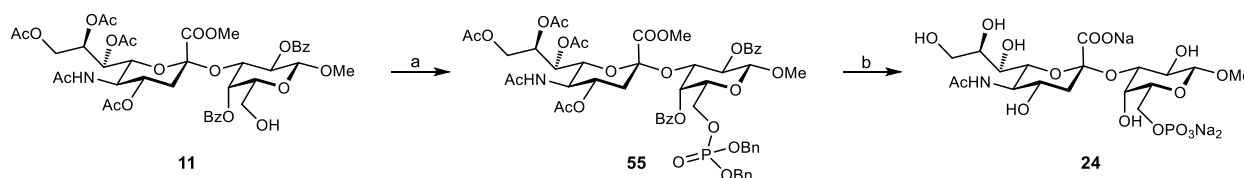
To a solution of **11** (280 mg, 0.32 mmol) in dry DMF (7 mL) was added SO₃·pyr (508 mg, 3.20 mmol) at 0 °C under argon atmosphere. The reaction mixture was warmed up to rt and stirred for 2.5 h. Then, powdered NaHCO₃ was added and the suspension was stirred for 2 h. The suspension was filtered over celite, and the solvent removed by co-evaporation with xylenes. The crude product was purified by flash column chromatography (DCM/MeOH, 1:0 \rightarrow 8:2) to afford **12** (290 mg, 93%) as a white solid. $[\alpha]_D^{20} +48.2$ (*c* 1.1, MeOH); ¹H NMR (500 MHz, CD₃OD): δ = 1.45 (s, 3H, NHAc),

1.48 (m, 1H, H-3'a), 1.73, 1.88, 2.05, 2.24 (4 s, 12H, OAc), 2.42 (dd, $J = 4.7, 12.5$ Hz, 1H, H-3'e), 3.55 (s, 3H, OMe), 3.67 (m, 1H, H-5'), 3.74 (dd, $J = 2.6, 10.7$ Hz, 1H, H-6'), 3.94 (m, 1H, H-9'a), 3.94 (s, 3H, COOMe), 4.05-4.06 (m, 2H, H-6), 4.21 (m, 1H, H-5), 4.34 (dd, $J = 2.5, 12.4$ Hz, 1H, H-9'b), 4.79-4.85 (m, 2H, H-1, H-4'), 4.93 (dd, $J = 3.3, 10.1$ Hz, 1H, H-3), 5.19 (dd, 1H, $J = 2.7, 9.7$ Hz, H-7'), 5.32 (dd, $J = 7.9, 10.1$ Hz, 1H, H-2), 5.40 (m, 1H, H-4), 5.66 (ddd, $J = 2.5, 5.9, 9.7$ Hz, 1H, H-8'), 7.51-7.57 (m, 4H, Ar-H), 7.65 (m, 2H, Ar-H), 8.05-8.14 (m, 2H, Ar-H), 8.15-8.21 (m, 2H, Ar-H); ^{13}C NMR (126 MHz, CD_3OD): $\delta = 20.6, 20.7, 21.7$ (4C, OAc), 22.7 (NHAc), 38.4 (C-3'), 49.3 (C-5'), 53.9 (COOMe), 57.5 (OMe), 63.6 (C-9'), 67.3 (C-6), 68.7 (C-7'), 68.8 (C-8'), 70.5 (C-4), 71.0 (C-4'), 72.7 (C-2), 72.8 (2C, C-6', C-3), 73.1 (C-5), 98.3 (C-2'), 103.4 (C-1), 124.6 129.7, 129.8, 130.9, 131.2, 131.5, (12C, Ar-C), 167.0, 167.2, 169.4, 171.4, 171.7, 172.4, 173.4 (8C, C=O); ESI-MS: m/z : Calcd for $\text{C}_{41}\text{H}_{48}\text{NNaO}_{23}\text{S}$ $[\text{M}+\text{Na}]^+$: 1000.2, found: 1000.3.

Methyl (sodium 5-acetamido-3,5-dideoxy-D-glycero- α -D-galacto-2-nonulopyranosylonate)-(2 \rightarrow 3)-6-O-sulfonato- β -D-galactopyranoside (2).

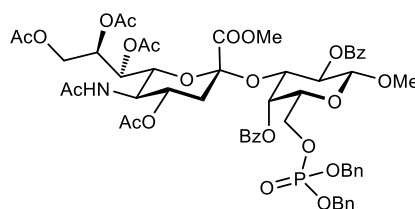


To a solution of **12** (70 mg, 0.07 mmol) in dry MeOH (2 mL) was added a freshly prepared solution of MeONa in MeOH (1.5 M, to pH 10). The reaction mixture was stirred for 5 h at 50 °C and then neutralized with Dowex50X8 (H^+ form) to pH 5. The suspension was filtered, concentrated and the crude product dissolved in 0.1 M NaOH. The reaction mixture was stirred for 1 h, then neutralized and concentrated. The crude product was purified by reversed-phase column chromatography (C_{18} , H_2O) and size-exclusion column chromatography (P-2 gel, H_2O) to afford **2** (40 mg, 84%) as a white solid. $[\alpha]_{\text{D}}^{20} +5.8$ (c 0.7, H_2O); ^1H NMR (500 MHz, D_2O): $\delta = 1.83$ (m, 1H, H-3'a), 2.06 (s, 3H, NHAc), 2.78 (dd, $J = 4.6, 12.4$ Hz, 1H, H-3'e), 3.57 (dd, $J = 8.0, 9.8$ Hz, 1H, H-2), 3.60 (s, 3H, OMe), 3.62 (dd, $J = 1.8, 8.9$ Hz, 1H, H-7'), 3.64-3.74 (m, 3H, H-4', H-6', H-9'a), 3.85-3.91 (m, 3H, H-5', H-8', H-9'b), 3.95 (m, 1H, H-5), 4.02 (m, 1H, H-4), 4.13 (dd, $J = 3.2, 9.8$ Hz, 1H, H-3), 4.20-4.22 (m, 2H, H-6), 4.44 (d, $J = 8.0$ Hz, 1H, H-1); ^{13}C NMR (126 MHz, D_2O): $\delta = 22.7$ (NHAc), 40.2 (C-3'), 52.3 (C-5'), 57.8 (OMe), 63.2 (C-9'), 68.0 (C-6), 68.1 (C-4), 68.8 (C-7'), 69.0 (C-4'), 69.7 (C-2), 72.4 (C-8'), 73.2 (C-5), 73.5 (C-6'), 76.3 (C-3), 100.6 (C-2'), 104.1 (C-1), 174.5, 175.7 (2C, C=O); HR-MS: m/z : Calcd for $\text{C}_{18}\text{H}_{29}\text{NNa}_2\text{O}_{17}\text{S}$ $[\text{M}+\text{Na}]^+$: 632.0849, found: 632.0849; HPLC purity: > 99.5%.



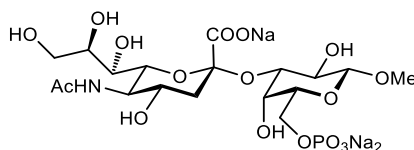
Scheme 3. a) 1,2,4-Triazole, *N,N*-diisopropylphosphoramidite, MeCN, rt, 16 h, 66%; b) i. H₂, Pd(OH)₂/C, AcOH, EtOAc, rt, 24 h; ii. MeONa/MeOH, 50 °C, 24 h; iii. NaOH (aq), rt, 24 h, 43% over 3 steps.

Methyl (methyl 5-acetamido-4,7,8,9-tetra-*O*-acetyl-3,5-dideoxy- α -D-glycero- α -D-galacto-2-nonulopyranosylonate)-(2 \rightarrow 3)-2,4-di-*O*-benzoyl-6-*O*-dibenzylphosphono- β -D-galactopyranoside (55**).**

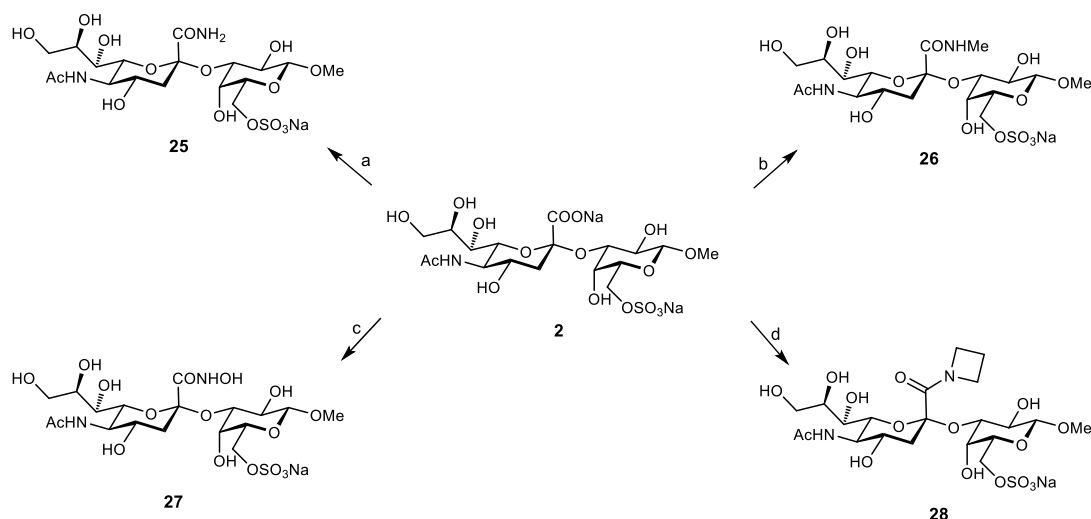


To an ice-cooled solution of **11** (200 mg, 0.23 mmol) and 1,2,4- triazole (94.6 mg, 1.37 mmol) in dry MeCN (4 mL) was added dibenzyl *N,N*-diisopropylphosphoramidite (386 μ L, 1.15 mmol), and the mixture was stirred for 30 min at 0 °C and then for 2 d at rt. Then, 70% aq. *tert*-butylhydroperoxide (188 μ L, 1.38 mmol) was added and the solution was stirred for 5 h. The reaction was quenched with 1 M aq. Na₂S₂O₃ and 1 M aq. NaHCO₃, and the mixture was extracted with DCM (3 \times 30 mL), dried over Na₂SO₄, and filtered. The solvents were removed in vacuo and the crude product was purified by flash column chromatography (toluene/acetone, 1:0 \rightarrow 6:4) to afford **55** (172 mg, 66%) as a white solid. $[\alpha]_D^{20} +36.0$ (*c* 1.0, CHCl₃); ¹H NMR (500 MHz, CDCl₃): δ = 1.45 (s, 3H, NHAc), 1.66 (m, 1H, H-3'a), 1.77, 1.91, 2.08, 2.22 (4 s, 12H, OAc), 2.44 (dd, *J* = 4.6, 12.7 Hz, 1H, H-3'e), 3.49 (s, 3H, OMe), 3.60 (dd, *J* = 2.8, 10.8 Hz, 1H, H-6'), 3.81 (m, 1H, H-5'), 3.84 (s, 3H, COOMe), 3.96 (dd, *J* = 5.6, 12.4 Hz, 1H, H-9'a), 4.00-4.09 (m, 3H, H-5, H-6), 4.33 (dd, *J* = 2.5, 12.5 Hz, 1H, H-9'b), 4.72 (d, *J* = 8.0 Hz, 1H, H-1), 4.78-4.84 (m, 2H, H-3, H-4'), 4.95-5.03 (m, 5H, NH, 2 CH₂Ph), 5.21 (dd, *J* = 2.8, 9.6 Hz, 1H, H-7'), 5.27 (d, *J* = 3.4 Hz, 1H, H-4), 5.38 (dd, *J* = 8.0, 10.1 Hz, 1H, H-2), 5.63 (ddd, *J* = 2.5, 5.6, 9.8 Hz, 1H, H-8'), 7.27-7.31 (m, 10H, Ar-H), 7.56-7.61 (m, 2H, Ar-H), 8.05-8.07 (m, 2H, Ar-H), 8.15-8.17 (m, 2H, Ar-H); ¹³C NMR (126 MHz, CDCl₃): δ = 20.4, 20.9, 21.0, 21.7 (4C, OAc), 23.3 (NHAc), 37.4 (C-3'), 48.8 (C-5'), 53.5 (COOMe), 57.5 (OMe), 62.4 (C-9'), 65.4 (m, C-6), 66.6 (C-7'), 67.4 (C-8'), 68.3 (C-4), 69.4 (2C, 2 CH₂Ph) 69.5 (C-4'), 71.1 (C-2), 71.4 (C-3), 71.7 (C-5), 71.8 (C-6'), 96.9 (C-2'), 102.4 (C-1), 125.4, 128.0, 128.1, 128.4, 128.5, 128.6, 128.7, 129.2, 130.2, 130.3, 133.2, 133.5 (24C, Ar-C), 165.5, 165.8, 168.3, 170.3, 170.4, 170.8, 170.9, 171.0 (8C, C=O); ESI-MS: *m/z*: Calcd for C₅₅H₆₂NO₂₃P [M+Na]⁺: 1158.3, found: 1158.4

Methyl (sodium 5-acetamido-3,5-dideoxy-D-glycero- α -D-galacto-2-nonulopyranosylonate)-(2 \rightarrow 3)-6-O-(disodium phosphono)- β -D-galactopyranoside (24**).**

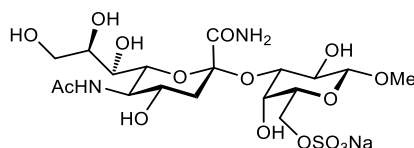


To a solution of **55** (172 mg, 0.15 mmol) in EtOAc (9 mL) were added a catalytic amount of AcOH and Pd(OH)₂/C (10% Pd, 14.7 mg). The reaction was stirred under H₂ atmosphere for 24 h. Then, the suspension was filtered and concentrated in vacuo. The residue was dissolved in dry MeOH (10 mL) and a freshly prepared MeONa/MeOH solution was added (to pH 10). The reaction was stirred overnight at 50 °C. Then, the mixture was neutralized with Dowex50X8 (H⁺ form) and concentrated under reduced pressure. The residue was dissolved in 0.1 M NaOH and stirred for 24 h. Then, the reaction mixture was neutralized and concentrated in vacuo. The crude product was purified by reversed-phase column chromatography (C₁₈, H₂O) and size-exclusion chromatography (P-2 gel, H₂O) to afford **24** (41 mg, 43%) as a white solid. $[\alpha]_{\text{D}}^{20} +0.99$ (*c* 1.0, H₂O); ¹H NMR (500 MHz, D₂O): δ = 1.81 (t, *J* = 12.1 Hz, 1H, H-3'a), 2.05 (s, 3H, NHAc), 2.78 (dd, *J* = 4.6, 12.4 Hz, 1H, H-3'e), 3.55 (dd, *J* = 7.9, 9.9 Hz, 1H, H-2), 3.59 (s, 3H, OMe), 3.61-3.67 (m, 3H, H-6', H-7', H-9'a), 3.70 (ddd, *J* = 4.6, 9.9, 11.8 Hz, 1H, H-4'), 3.81 (m, 1H, H-5), 3.84-3.93 (m, 5H, H-6, H-5', H-8', H-9'b), 4.03 (m, 1H, H-4), 4.12 (dd, *J* = 3.3, 9.8 Hz, 1H, H-3), 4.43 (d, *J* = 7.9 Hz, 1H, H-1); ¹³C NMR (126 MHz, D₂O): δ = 19.6 (NHAc), 37.3 (C-3'), 49.2 (C-5'), 54.7 (OMe), 60.2 (C-9'), 60.4 (d, *J* = 4.4 Hz, C-6), 64.8 (C-4), 65.7 (C-7'), 65.9 (C-4'), 66.7 (C-2), 69.3 (C-8'), 70.4 (C-6'), 71.3 (d, *J* = 8.1 Hz, C-5), 73.2 (C-3), 97.5 (C-2'), 101.5 (C-1), 171.3 (C-1'), 172.6 (C=O); HR-MS: *m/z*: Calcd for C₁₈H₂₉NNa₃O₁₇P [M+Na]⁺: 654.0764, found: 654.0776; HPLC purity: > 99.5%.



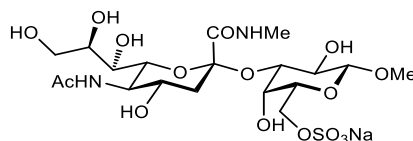
Scheme 4. a) i. Ac_2O , pyr, rt, overnight; ii. NH_3 , MeOH, rt, 48 h; iii. MeONa/MeOH, rt, 5 h, 33% over 3 steps). b) i. BnBr, KF, DMF, rt, 2 d; ii. MeNH_2/THF , $\text{MeNH}_2/\text{EtOH}$, rt, 16 h, 25% over 2 steps). c) i. NHOBn , EDC, DMF, rt, 16 h, 22%; d) H_2 , $\text{Pd}(\text{OH})_2/\text{C}$, MeOH, rt, 3 h, 90%; e) azetidine, HATU, DIPEA, DMF, rt, 16 h, 51%.

Methyl (5-acetamido-3,5-dideoxy-D-glycero- α -D-galacto-2-nonulopyranosylonamide)-(2 \rightarrow 3)-6-O-sulfonato- β -D-galactopyranoside (25).



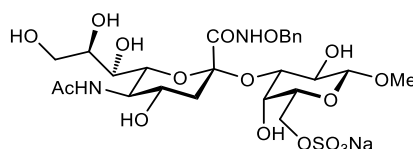
A solution of **2** (32 mg, 0.053 mmol) in Ac_2O /pyridine (1:1, 4 mL) was stirred at rt under argon for 16 h. Then, the solvents were removed via co-evaporation with toluene. The residue was dissolved in NH_3 (0.5 M in dioxane, 3 mL) and stirred at rt for 16 h under argon. Then, additional NH_3 (7 N in MeOH, 3 mL) was added, and the reaction was stirred for another 24 h. The solvents were removed via co-evaporation with toluene, the residue was dissolved in dry MeOH (3 mL) and a freshly prepared MeONa/MeOH solution was added (to pH 10). After 2 h the mixture was neutralized, concentrated under reduced pressure and purified by size-exclusion column chromatography (P-2 gel, H_2O) and reversed-phase column chromatography (C_{18} , H_2O) to afford **25** (8 mg, 27%) as a white solid. ^1H NMR (500 MHz, D_2O): δ = 1.93 (m, 1H, H-3'a), 2.06 (s, 3H, NHAc), 2.76 (dd, J = 4.6, 13.0 Hz, 1H, H-3'e), 3.57 (m, 1H, H-2), 3.59 (s, 3H, OMe), 3.66-3.69 (m, 2H, H-7', H-9'a), 3.76-3.81 (m, 2H, H-4', H-6'), 3.84 (m, 1H, H-8'), 3.88 (dd, J = 2.6, 12.0 Hz, 1H, H-9'b), 3.93 (m, 1H, H-5'), 3.98 (m, 1H, H-5), 4.06 (m, 1H, H-4), 4.14 (dd, J = 3.4, 9.7 Hz, 1H, H-3), 4.20 (d, J = 6.3 Hz, 2H, H-6), 4.44 (d, J = 8.0 Hz, 1H, H-1); ^{13}C NMR (126 MHz, D_2O): δ = 22.0 (NHAc), 37.5 (C-3'), 51.5 (C-5'), 57.2 (OMe), 63.1 (C-9'), 66.8 (C-6), 67.3 (C-4'), 67.6 (C-7'), 68.0 (C-4), 69.0 (C-2), 71.0 (C-8'), 72.3 (C-5), 73.7 (C-6'), 75.4 (C-3), 99.8 (C-2'), 103.4 (C-1), 172.1, 175.1 (2C, C=O); HR-MS: m/z : Calcd for $\text{C}_{18}\text{H}_{31}\text{N}_2\text{NaO}_{16}\text{S}$ [$\text{M}+\text{Na}$] $^+$: 609.1190, found: 609.1190; HPLC purity: >99.5%.

Methyl (5-acetamido-3,5-dideoxy-*N*-methyl-*D*-glycero- α -*D*-galacto-2-nonulopyranosylonamide)-(2 \rightarrow 3)-6-*O*-sulfonato- β -*D*-galactopyranoside (26).



A solution of **2** (50 mg, 0.08 mmol), KF (12.4 mg, 0.21 mmol) and BnBr (0.029 mL, 0.21 mmol) was stirred in anhydrous DMF (7 mL) for 3 d. Then, H₂O (7 mL) was added and the mixture was lyophilized to yield the crude benzyl ester, which was directly used in the next step. The crude ester was dissolved in MeNH₂ in EtOH (8 M, 5 mL) and MeNH₂ in THF (2 M, 3 mL) and stirred at rt under argon for 16 h. Then, the volatiles were removed under reduced pressure and the crude product was purified by flash chromatography [DCM/(MeOH/H₂O, 10:1), 1:0 \rightarrow 1:1] to afford **26** (12.2 mg, 25%) as a white solid. $[\alpha]_D^{20} +0.0$ (*c* 0.3, H₂O); ¹H NMR (500 MHz, D₂O): δ = 1.93 (m, 1H, H-3'a), 2.05 (s, 3H, NHAc), 2.78 (dd, 1H, *J* = 4.6, 13.0 Hz, H-3'e), 2.83 (s, 3H, NHMe), 3.59 (s, 3H, OMe), 3.66-3.71 (m, 3H, H-6', H-7', H-9'a), 3.75 (m, 1H, H-4'), 3.84 (ddd, *J* = 2.6, 5.4, 9.4 Hz, 1H, H-8'), 3.87-3.92 (m, 2H, H-5', H-9'b), 3.94 (m, 1H, H-4), 3.97 (t, *J* = 6.5 Hz, 1H, H-5), 4.09 (dd, *J* = 3.3, 9.8 Hz, 1H, H-3), 4.19 (dd, *J* = 6.4 Hz, 2H, H-6), 4.43 (d, *J* = 7.9 Hz, 1H, H-1); ¹³C NMR (126 MHz, D₂O): δ = 23.7 (NHAc), 27.3 (NHMe), 39.1 (C-3'), 53.1 (C-5'), 58.8 (OMe), 64.7 (C-9'), 68.3 (C-6), 68.8 (C-4'), 69.2 (C-7'), 69.5 (C-4), 70.7 (C-2), 72.7 (C-8'), 73.8 (C-5), 75.3 (C-6'), 76.9 (C-3), 101.5 (C-2'), 105.0 (C-1), 171.3 (C-38 1'), 176.7 (C=O); HR-MS: *m/z*: Calcd for C₁₉H₃₃N₂NaO₁₆S [M+Na]⁺: 623.1346, found: 623.1348; HPLC purity: > 99.5%.

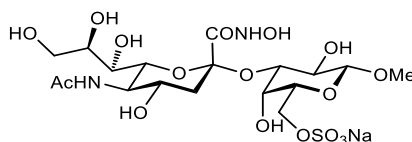
Methyl (5-acetamido-*N*-benzyloxy-3,5-dideoxy-*D*-glycero- α -*D*-galacto-2-nonulopyranosylonamide)-(2 \rightarrow 3)-6-*O*-sulfonato- β -*D*-galactopyranoside (56).



To a solution of **2** (21 mg, 0.034 mmol) in DMF (3 mL) were added *O*-benzylhydroxylamine (16 mg, 0.102 mmol) at rt and EDC (7 μ L, 0.041 mmol) at 0 °C. The reaction was warmed up to rt and stirred for 24 h. Then, the mixture was co-evaporated with toluene and the residue was purified by flash column chromatography [DCM/(MeOH/H₂O, 10:1), 1:0 \rightarrow 6:4] to afford **56** (5 mg, 22%) as a white vitreous solid. ¹H NMR (500 MHz, D₂O): δ = 1.92 (m, 1H, H-3'a), 2.07 (s, 1H, NHAc), 2.61 (dd, *J* = 4.4, 13.1 Hz, 1H, H-3'e), 3.54 (dd, *J* = 8.1, 9.7 Hz, 1H, H-2), 3.57-3.59 (m, 5H, H-4', H-7', OMe), 3.65-3.68 (m, 2H, H-6', H-9'a), 3.77 (ddd, *J* = 2.5, 5.5, 8.6 Hz, 1H, H-8'), 3.84-3.90 (m, 4H, H-4, H-5, H-5', H-9'b), 4.01 (dd, *J* = 3.3, 9.7 Hz, 1H, H-3), 4.17 (m, 2H, H-6), 4.37 (d, *J* = 8.0 Hz, 1H, H-

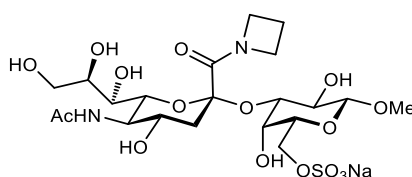
1), 5.05 (s, 2H, CH₂Ph), 7.51-7.52 (m, 3H, Ar-H), 7.54-7.56 (m, 2H, Ar-H); ESI-MS: *m/z*: Calcd for C₂₅H₃₇N₂Na₂O₁₇S [M+Na]⁺: 715.2, found: 715.2.

Methyl (5-acetamido-3,5-dideoxy-*N*-hydroxy-*D*-glycero- α -*D*-galacto-2-nonulopyranosylonamide)-(2 \rightarrow 3)-6-*O*-sulfonato- β -*D*-galactopyranoside (27).



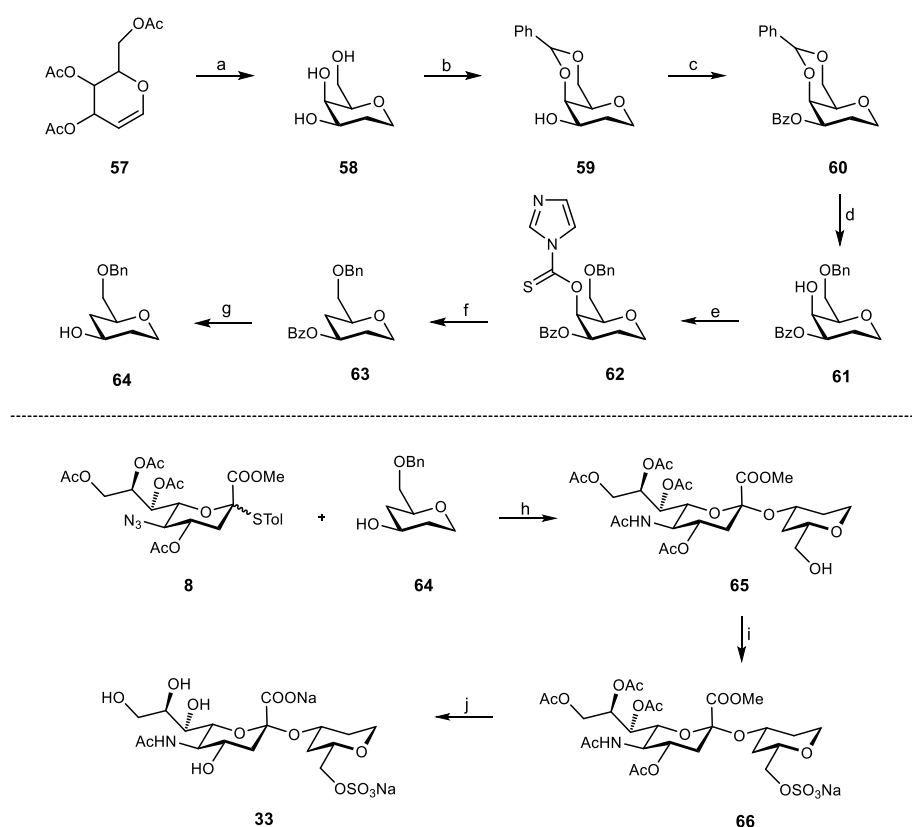
Compound **56** (5 mg, 0.008 mmol) was dissolved in MeOH (2 mL) and Pd(OH)₂/C (10% Pd, 10 mg) was added. The mixture was stirred at rt for 3 h under hydrogen atmosphere. Then, the suspension was filtrated and concentrated under reduced pressure. The crude product was purified by reversed-phase column chromatography (C₁₈, H₂O) to afford **27** (4 mg, 90%) as a white solid. $[\alpha]_{\text{D}}^{20} -1.5$ (c 0.2, H₂O); ¹H NMR (500 MHz, D₂O): δ = 1.93 (m, 1H, H-3'a), 2.06 (s, 3H, NHAc), 2.77 (dd, *J* = 4.6, 13.1 Hz, 1H, H-3'e), 3.57 (dd, *J* = 8.1, 9.7 Hz, 1H, H-2), 3.60 (s, 3H, OMe), 3.65-3.70 (m, 2H, H-7', H-9'a), 3.75 (m, 1H, H-6'), 3.79 (m, 1H, H-4'), 3.84 (ddd, *J* = 2.5, 5.5, 8.6 Hz, 1H, H-8'), 3.88-3.94 (m, 2H, H-5', H-9'b), 3.96-3.99 (m, 2H, H-4, H-5), 4.11 (dd, *J* = 3.2, 9.7 Hz, 1H, H-3), 4.19-4.21 (m, 2H, H-6), 4.44 (d, *J* = 8.0 Hz, 1H, H-1); ¹³C NMR (125 MHz, D₂O): δ = 22.7 (NHAc), 38.8 (C-3'), 52.1 (C-5'), 57.8 (OMe), 63.5 (C-9'), 67.7 (C-6), 68.1 (C-4'), 68.3 (C-7'), 68.6 (C-4), 69.6 (C-2), 71.9 (C-8'), 73.1 (C-5), 74.4 (C-6'), 76.0 (C-3), 100.5 (C-2'), 104.0 (C-1'), 175.7 (C=O); HR-MS: *m/z*: Calcd for C₁₈H₃₁N₂NaO₁₇S [M+Na]⁺: 625.1139, found: 625.1139; HPLC purity: > 99.5%.

Methyl (5-acetamido-*N*-azetidino-3,5-dideoxy-*D*-glycero- α -*D*-galacto-2-nonulopyranosylonamide)-(2 \rightarrow 3)-6-*O*-sulfonato- β -*D*-galactopyranoside (28).



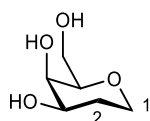
To a solution of **2** (55 mg, 0.09 mmol) in anhydrous DMF (1.8 mL) were added HATU (51 mg, 0.135 mmol), DIPEA (47 μ L, 0.27 mmol) and azetidine (61 μ L, 0.9 mmol). The solution was stirred under argon at rt for 16 h. Then, the mixture was concentrated under reduced pressure and the crude product purified by flash chromatography [DCM/(MeOH/H₂O, 10:1), 1:0 \rightarrow 1:1] and reversed-phase column chromatography (C₁₈, H₂O) to afford **28** (29 mg, 51%) as a white solid. $[\alpha]_{\text{D}}^{20} 0.0$ (c 0.2, H₂O); ¹H NMR (500 MHz, D₂O): δ = 1.97 (m, 1H, H-3'a), 2.06 (s, 3H, NHAc), 2.32-2.40 (m, 2H, H-azet), 2.58 (m, 1H, H-3'e), 3.59 (m, 1H, H-2), 3.60 (s, 3H, OMe), 3.61 (m, 1H, H-7'), 3.68-3.74 (m, 2H, H-6', H-9'a), 3.83 (ddd, *J* = 2.6, 5.3, 9.4 Hz, 1H, H-8'), 3.88 (dd, *J* = 2.6, 11.9 Hz, 1H, H-9'b), 3.91-

3.94 (m, 2H, H-4', H-5'), 3.98 (m, 1H, H-5), 4.06 (d, $J = 3.3$ Hz, 1H, H-4), 4.09-4.17 (m, 3H, H-3, H-azet), 4.19-4.20 (m, 2H, H-6), 4.44 (d, $J = 8.0$ Hz, 1H, H-1), 4.61 (m, 1H, H-azet), 4.70 (m, 1H, H-azet); ^{13}C NMR (125 MHz, D_2O): $\delta = 16.7$ ($\text{CH}_2\text{-azet}$), 23.0 (NHAc), 38.4 (C-3'), 50.4 ($\text{CH}_2\text{-azet}$), 52.6 (C-5'), 54.3 ($\text{CH}_2\text{-azet}$), 58.2 (OMe), 64.0 (C-9'), 67.6 (C-6), 68.6 (C-4'), 68.9 (C-7'), 69.5 (C-4), 69.8 (C-2), 71.5 (C-8'), 73.3 (C-5), 74.0 (C-6'), 75.7 (C-3), 101.4 (C-2'), 104.5 (C-1), 168.9, 175.9 (2C, C=O); HR-MS: m/z : Calcd for $\text{C}_{21}\text{H}_{35}\text{N}_2\text{NaO}_{16}\text{S}$ [$\text{M}+\text{Na}$] $^+$: 649.1503, found: 649.1502; HPLC purity: 95%.



Scheme 5. a) i. H_2 Pd/C, MeOH, rt, 3 h; ii. MeONa/MeOH, rt, 1 h, 60% over two steps; b) $\text{PhCH}(\text{OMe})_2$, TsOH, MeCN, rt, 16 h, 85%; c) BzO, DMAP, pyr, rt, 16 h, 84%; d) Me_3NBH_3 , AlCl_3 , H_2O , THF, 0 °C to rt, 6 h, 78%; e) 1,1'-thiocarbonyldiimidazole, toluene, 90 °C, 5 h, quant.; f) Bu_3SnH , AIBN, toluene, 105 °C, 1.5 h, 66%; g) MeONa, MeOH, rt, 6 h, 80%; h) i. NIS, TfOH, MeCN/DCM, -40 °C, 16 h; ii. H_2 Pd/C rt, MeOH, rt, 3 h, 54% over two steps; i) SO_3 pyr, DMF, 0 °C to rt, 5 h, 24%; j) NaOH ($\text{H}_2\text{O}/\text{dioxane}$, 0.1 M), rt, 24 h, 93%.

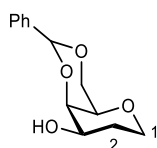
1,5-Anhydro-2-deoxy-D-lyxo-hexitol (58).



To a solution of D-galactal (420 mg, 2.87 mmol) in MeOH (3.0 mL) was added portionwise Pd/C (70.0 mg) under H_2 atmosphere. The reaction was stirred for 16 h. Then, the mixture was filtered and

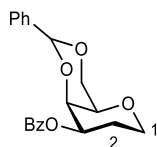
concentrated under reduced pressure. The residue was purified by flash column chromatography (DCM/MeOH, 1:0 \rightarrow 4:1) to afford **58** (0.256 g, 60%) as a white solid. $[\alpha]_D^{20} +36.8$ (c 1.05, MeOH); ^1H NMR (500 MHz, CD_3OD): δ = 1.62 (m, 1H, H-2a), 1.94 (qd, J = 5.0, 12.6 Hz, 1H, H-2e), 3.35 (m, 1H, H-5), 3.46 (ddd, J = 2.3, 11.6, 12.6 Hz, 1H, H-1a), 3.64-3.69 (m, 2H, H-3, H-6a), 3.73 (m, 1H, H-6b), 3.76 (m, 1H, H-4), 3.98 (ddd, J = 1.7, 5.0, 11.6 Hz, 1H, H-1e); ^{13}C NMR (126 MHz, CD_3OD): δ = 30.1 (C-2), 63.4 (C-6), 67.0 (C-1), 69.8 (C-4), 70.8 (C-3), 80.9 (C-5); ESI-MS: m/z : Calcd for $\text{C}_6\text{H}_{12}\text{NaO}_4$ $[\text{M}+\text{Na}]^+$: 171.1, found: 170.9.

1,5-Anhydro-4,6-*O*-benzylidene-2-deoxy-D-lyxo-hexitol (**59**).



To a solution of **58** (905 mg, 6.11 mmol) in dry MeCN (30.0 mL) were added TsOH (345 mg, 1.83 mmol) at once and benzaldehyde dimethyl acetal (1.38 mL, 9.17 mmol) dropwise. The solution became clear and was stirred for 16 h at rt under argon atmosphere. Then, it was neutralized with NEt_3 and concentrated under reduced pressure. The residue was purified by flash chromatography (petroleum ether/acetone, 9:1 \rightarrow 3:2) to afford **59** (1.23 g, 85%) as a white solid. $[\alpha]_D^{20} +43.8$ (c 1.0, CHCl_3); ^1H NMR (500 MHz, CDCl_3): δ = 1.78 (m, 1H, H-2a), 2.02 (qd, J = 4.7, 12.6 Hz, 1H, H-2e), 2.35 (d, J = 11.0 Hz, 1H, OH-3), 3.34 (m, 1H, H-5), 3.47 (dd, J = 1.8, 12.1 Hz, 1H, H-1a), 3.78 (m, 1H, H-3), 4.04 (dd, J = 1.8, 12.5 Hz, 1H, H-6a), 4.11-4.14 (m, 2H, H-1e, H-4), 4.29 (dd, J = 1.5, 12.4 Hz, 1H, H-6b), 5.61 (s, 1H, CHPh), 7.36-7.40 (m, 3H, Ar-H), 7.52-7.53 (m, 2H, Ar-H); ^{13}C NMR (126 MHz, CDCl_3): δ = 30.2 (C-2), 65.8 (C-1), 68.8 (C-3), 70.1 (C-5), 70.3 (C-6), 75.2 (C-4), 101.1 (CHPh), 126.3, 128.2, 137.8 (6C, Ar-C); ESI-MS: m/z : Calcd for $\text{C}_{13}\text{H}_{16}\text{O}_4$ $[\text{M}+\text{Na}]^+$: 259.1, found: 259.0.

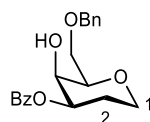
1,5-Anhydro-3-*O*-benzoyl-4,6-*O*-benzylidene-2-deoxy-D-lyxo-hexitol (**60**).



To a solution of **59** (1.10 g, 4.70 mmol) in pyridine (10.0 mL) were added benzoic anhydride (3.16 g, 14.0 mmol) and DMAP (0.345 g, 2.80 mmol) at 0 °C. The reaction was stirred for 16 h under argon atmosphere. Then, the mixture was co-evaporated with toluene under reduced pressure. The residue was dissolved in DCM (40 mL) and washed with H_2O (3 \times 20 mL) and brine (3 \times 30 mL), dried over Na_2SO_4 , filtered and concentrated under reduced pressure. The crude was purified by flash

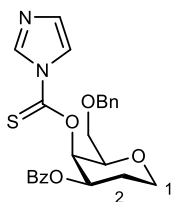
chromatography (petroleum ether/acetone, 1:0 → 4:1) to afford **60** (1.35 g, 84%) as a white solid. $[\alpha]_{\text{D}}^{20} +133.5$ (*c* 1.0, CHCl_3); $^1\text{H NMR}$ (500 MHz, CDCl_3): $\delta = 1.83$ (m, 1H, H-2a), 2.46 (qd, $J = 4.7$, 12.5 Hz, 1H, H-2e), 3.44 (m, 1H, H-5), 3.67 (dd, $J = 2.0$, 12.4 Hz, 1H, H-1a), 4.06 (dd, $J = 1.8$, 12.4 Hz, 1H, H-6a), 4.23 (ddd, $J = 1.7$, 4.7, 11.8 Hz, 1H, H-1e), 4.32 (dd, $J = 1.6$, 12.4 Hz, 1H, H-6b), 4.38 (d, $J = 3.3$ Hz, 1H, H-4), 5.21 (ddd, $J = 3.3$, 4.9, 12.2 Hz, 1H, H-3), 5.61 (s, 1H, *CHPh*), 7.32-7.38 (m, 3H, Ar-H), 7.43-7.46 (m, 2H, Ar-H), 7.54-7.59 (m, 3H, Ar-H), 8.08-8.10 (m, 2H, Ar-H); $^{13}\text{C NMR}$ (126 MHz, CDCl_3): $\delta = 26.4$ (C-2), 65.8 (C-1), 70.1 (C-5), 70.4 (C-6), 71.8 (C-4), 73.4 (C-3), 100.6 (*CHPh*), 126.3, 128.1, 128.5, 128.8, 129.9, 130.2, 133.3, 138.1 (12C, Ar-C), 166.2 (C=O); ESI-MS: *m/z*: Calcd for $\text{C}_{20}\text{H}_{20}\text{O}_5$ $[\text{M}+\text{Na}]^+$: 363.1, found: 363.1.

1,5-Anhydro-3-*O*-benzoyl-6-*O*-benzyl-2-deoxy-*D*-lyxo-hexitol (**61**).



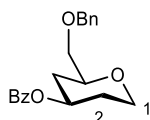
To a solution of **60** (212 mg, 0.62 mmol) in THF (5.0 mL) were added $\text{Me}_3\text{NH}\cdot\text{BH}_3$ (271 g, 3.72 mmol) and AlCl_3 (496 mg, 3.72 mmol) at 0 °C. When the reaction became clear (after 15 minutes) H_2O was added (22.0 μL , 1.24 mmol) at 0 °C. The reaction was warmed up to rt and stirred for 6 h. After that, the mixture was poured into cold water and the aqueous phase was extracted with EtOAc (3 \times 20 mL). The organic phases were then washed with NaHCO_3 (aq. sat. 3 \times 20 mL) and brine (3 \times 20 mL), dried over Na_2SO_4 , filtered and concentrated under reduced pressure. The residue was purified by flash chromatography (petroleum ether/acetone, 1:0 → 7:3) to afford **61** (165 mg, 78%) as a white solid. $[\alpha]_{\text{D}}^{20} +2.27$ (*c* 1.0, CHCl_3); $^1\text{H NMR}$ (500 MHz, CDCl_3): $\delta = 1.86$ (m, 1H, H-2a), 2.28 (qd, $J = 5.1$, 12.6 Hz, 1H, H-2e), 2.63 (d, $J = 4.8$ Hz, 1H, OH-4), 3.58-3.63 (m, 2H, H-1a, H-5), 3.72-3.75 (m, 2H, H-6), 4.12-4.16 (m, 2H, H-1e, H-4), 4.59 (s, 2H, OCH_2Ph), 5.11 (ddd, $J = 2.8$, 5.0, 12.0 Hz, 1H, H-3), 7.29 (m, 1H, Ar-H), 7.33-7.35 (m, 4H, Ar-H), 7.43-7.46 (m, 2H, Ar-H), 7.57 (m, 1H, Ar-H), 8.07 (m, 1H, Ar-H); $^{13}\text{C NMR}$ (126 MHz, CDCl_3): $\delta = 26.0$ (C-2), 66.2 (C-1), 67.8 (C-4), 70.8 (C-6), 73.0 (C-3), 74.0 (OCH_2Ph), 77.6 (C-5), 128.0, 128.55, 128.61, 129.9, 130.1, 133.3, 137.8 (12C, Ar-C), 166.0 (C=O); ESI-MS: *m/z*: Calcd for $\text{C}_{20}\text{H}_{22}\text{O}_5$ $[\text{M}+\text{Na}]^+$: 365.1, found: 365.0.

1,5-Anhydro-3-*O*-benzoyl-6-*O*-benzyl-4-*O*-(1*H*-imidazole-1-carbonothioyl)-2-deoxy-*D*-lyxo-hexitol (**62**).



To a solution of **61** (0.832 g, 2.44 mmol) in dry toluene (20.0 mL) was added 1,1'-thiocarbonyldiimidazole (3.70 g, 20.8 mmol) and the mixture was stirred at 90 °C for 5 h. Then, it was concentrated under reduced pressure and the residue was purified by flash column chromatography (petroleum ether/acetone, 1:0 to → 4:1) to afford **62** (1.29 mg, quant.) as a yellow oil. $[\alpha]_{\text{D}}^{20} + 6.99$ (*c* 1.0, CHCl_3); $^1\text{H NMR}$ (500 MHz, CDCl_3): $\delta = 2.03$ (m, 1H, H-2a), 2.19 (qd, $J = 5.0, 14.5$ Hz, 1H, H-2e), 3.49 (dd, $J = 6.3, 9.7$ Hz, 1H, H-6a), 3.60 (dd, $J = 6.1, 9.7$ Hz, 1H, H-6b), 3.74 (td, $J = 2.2, 12.3$ Hz, 1H, H-1a), 3.94 (dd, $J = 6.2, 6.9$ Hz, 1H, H-5), 4.24 (ddd, $J = 1.4, 4.9, 11.9$ Hz, 1H, H-1e), 4.42 (d, $J = 11.8$ Hz, 1H, OCH_2Ph), 4.51 (d, $J = 11.8$ Hz, 1H, OCH_2Ph), 5.41 (ddd, $J = 3.0, 5.1, 12.1$ Hz, 1H, H-3), 6.31 (d, $J = 2.9$ Hz, 1H, H-4), 7.07 (dd, $J = 0.9, 1.8$ Hz, 1H, H-imidazole), 7.22-7.30 (m, 5H, Ar-H), 7.35-7.39 (m, 2H, Ar-H), 7.53 (m, 1H, Ar-H), 7.70 (t, $J = 1.5$ Hz, 1H, H-imidazole), 7.84-7.86 (m, 2H, Ar-H), 8.38 (t, $J = 1.1$ Hz, 1H, H-imidazole); $^{13}\text{C NMR}$ (126 MHz, CDCl_3): $\delta = 27.6$ (C-2), 66.2 (C-1), 68.7 (C-6), 70.6 (C-3), 73.9 (OCH_2Ph), 76.8 (C-4), 128.0, 128.1, 128.5, 128.6, 129.9, 131.1, 133.5 (13C, Ar-C); ESI-MS: m/z : Calcd for $\text{C}_{24}\text{H}_{24}\text{N}_2\text{O}_5\text{S}$ $[\text{M}+\text{Na}]^+$: 475.1, found: 475.1.

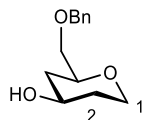
1,5-Anhydro-3-*O*-benzoyl-6-*O*-benzyl-2,4-dideoxy-*D*-erythro-hexitol (**63**).



To a solution of tributyltin hydride (1.65 mL, 6.15 mmol) and AIBN (67.3 mg, 0.41 mmol) in dry toluene (15.0 mL) was added a solution of **62** (187 mg, 0.41 mmol) in dry toluene (3.00 mL). The reaction was heated to reflux for 1.5 h. Then, the mixture was concentrated under reduced pressure and purified by flash column chromatography (petroleum ether/EtOAc, 1:0 → 4:1) to afford **63** (88 mg, 66%) as a colorless oil. $[\alpha]_{\text{D}}^{20} -12.2$ (*c* 1, CHCl_3); $^1\text{H NMR}$ (500 MHz, CDCl_3): $\delta = 1.60$ (m, 1H, H-4a), 1.79 (tdd, $J = 4.9, 11.2, 12.5$ Hz, 1H, H-2a), 2.08 (m, 2H, H-2e, H-4e), 3.49 (dd, $J = 3.7, 10.2$ Hz, 1H, H-6a), 3.54 (dd, $J = 6.0, 10.2$ Hz, 1H, H-6b), 3.59 (dd, $J = 2.1, 12.3$ Hz, 1H, H-1a), 3.69 (dddd, $J = 2.0, 3.8, 5.9, 11.7$ Hz, 1H, H-5), 4.14 (ddd, $J = 1.8, 4.9, 11.9$ Hz, 1H, H-1e), 4.57 (d, $J = 12.2$ Hz, 1H, OCH_2Ph), 4.61 (d, $J = 12.2$ Hz, 1H, OCH_2Ph), 5.16 (tt, $J = 4.7, 11.2$ Hz, 1H, H-3), 7.29 (m, 1H, Ar-H), 7.34 (d, $J = 4.4$ Hz, 4H, Ar-H), 7.41-7.47 (m, 2H, Ar-H), 7.56 (m, 1H, Ar-H), 8.03 (m, 1H, Ar-H); $^{13}\text{C NMR}$ (126 MHz, CDCl_3): $\delta = 32.1$ (C-2), 34.3 (C-4), 66.1 (C-1), 70.9 (C-3), 73.1

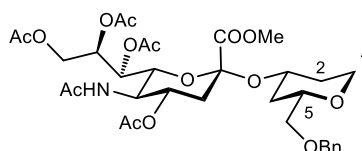
(C-6), 73.7 (OCH₂Ph), 75.5 (C-5), 127.8, 127.9, 128.5, 128.6, 129.7, 133.1 (12C, Ar-C); ESI-MS: *m/z*: Calcd for C₂₀H₂₂O₄ [M+Na]⁺: 349.1, found: 349.0.

1,5-Anhydro-6-*O*-benzyl-2,4-dideoxy-D-erythro-hexitol (64).



To a solution of **63** (88.0 mg, 0.27 mmol) in dry MeOH (3.0 mL) was added a freshly prepared solution of MeONa in MeOH (to pH 10). The reaction was stirred at rt for 6 h. Then, it was neutralized with Amberlyst-15 resin, filtered and concentrated under reduced pressure. The crude product was purified by flash column chromatography (petroleum ether/acetone, 1:0 to → 7:3) to afford **64** (48.0 mg, 80%) as a colorless oil. $[\alpha]_D^{20} -3.97$ (*c* 1, CHCl₃); ¹H NMR (500 MHz, CDCl₃): δ = 1.30 (m, 1H, H-4a), 1.53 (tdd, *J* = 4.9, 11.0, 12.5 Hz, 1H, H-2a), 1.60 (d, *J* = 4.1 Hz, 1H, OH-3), 1.87-1.95 (m, 2H, H-2e, H-4e), 3.41-3.57 (m, 4H, H-1a, H-5, 2 H-6), 3.80 (m, 1H, H-3), 4.07 (ddd, *J* = 1.8, 4.9, 11.9 Hz, 1H, H-1e), 4.55 (d, *J* = 12.2 Hz, 1H, OCH₂Ph), 4.60 (d, *J* = 12.2 Hz, 1H, OCH₂Ph), 7.29 (m, 1H, Ar-H), 7.32-7.36 (m, 4H, Ar-H); ¹³C NMR (126 MHz, CDCl₃): δ = 35.7 (C-2), 38.0 (C-4), 66.2 (C-1), 68.1 (C-3), 73.3 (C-6), 73.6 (OCH₂Ph), 75.5 (C-5), 127.8, 127.9, 128.5, 138.2 (6C, Ar-C); ESI-MS: *m/z*: Calcd for C₁₃H₁₈O₃ [M+Na]⁺: 245.1, found: 244.9.

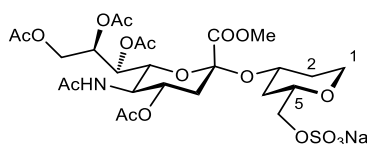
(Methyl 5-acetamido-4,7,8,9-tetra-*O*-acetyl-3,5-dideoxy-D-glycero- α -D-galacto-2-nonulopyranosylonate)-(2→3)-1,5-anhydro-2,4-dideoxy-D-erythro-hexitol (65).



Compounds **64** (44.0 mg, 0.20 mmol) and **8** (260 mg, 0.44 mmol) were dissolved in a solution of dry MeCN/DCM (5:3, 6 mL) with 3Å molecular sieves (100 mg) and the mixture was stirred under argon for 30 min. Then, the mixture was cooled down to -40 °C and NIS (198 mg, 0.880 mmol) and TfOH (7.00 μ L, 0.080 mmol) were added. The reaction was stirred at -40 °C under argon for 16 h. Then, it was neutralized with NEt₃, filtered over celite and evaporated under reduced pressure. The residue was dissolved in DCM (20 mL) and washed with 1 M aq. Na₂S₂O₃ (3 \times 20 mL) and H₂O (3 \times 20 mL), dried over Na₂SO₄ and concentrated under reduced pressure. The crude product was purified by flash chromatography (toluene/acetone, 1:0 → 7:3) to give an inseparable α/β mixture (10:1, 139 mg) which was directly used in the next step. $[\alpha]_D^{20} + 0.88$ (*c* 1, CHCl₃); ¹H NMR (500 MHz, CDCl₃): δ = 1.33 (q, *J* = 11.5 Hz, 1H, H-2a), 1.56-1.60 (m, 2H, H-2e, H-4a), 1.87 (s, 3H, NHAc), 1.90-1.98 (m,

2H, H-4e, H-3'a), 2.020, 2.023, 2.136, 2.138 (4 s, 12H, OAc), 2.57 (dd, $J = 4.6, 12.8$ Hz, 1H, H-3'e), 3.40 (dd, $J = 3.9, 10.0$ Hz, 1H, H-6a), 3.47 (dd, $J = 6.0, 10.0$ Hz, 1H, H-6b), 3.50-3.56 (m, 2H, H-1a, H-5), 3.76 (s, 3H, OMe), 3.91 (tt, $J = 4.8, 11.0$ Hz, 1H, H-3), 3.99-4.09 (m, 4H, H-5', H-9'a, H-6', H-1e), 4.28 (dd, $J = 2.6, 12.4$ Hz, 1H, H-9'b), 4.53 (d, $J = 12.2$ Hz, 1H, OCH₂Ph), 4.58 (d, $J = 12.2$ Hz, 1H, OCH₂Ph), 4.82 (ddt, $J = 5.7, 11.4, 12.6$ Hz, 1H, H-4'), 5.29 (dd, $J = 1.6, 8.8$ Hz, 1H, H-7'), 5.36 (m, 1H, H-8'), 7.28 (m, 1H, Ar-H), 7.32-7.34 (m, 4H, Ar-H); ¹³C NMR (126 MHz, CDCl₃): $\delta = 20.9, 21.0, 21.3$ (4C, OAc), 23.3 (NHAc), 35.3 (C-4), 35.6 (C-2), 38.6 (C-3'), 49.6 (C-5'), 52.8 (OMe), 62.7 (C-9'), 66.2 (C-1), 67.4 (C-7'), 68.3 (C-8'), 69.2 (C-4'), 71.7 (C-3), 72.6 (C-6'), 73.4 (C-6), 73.6 (OCH₂Ph), 75.4 (C-5), 98.8 (C-2'), 127.7, 127.9, 128.5 (6C, Ar-C), 169.1, 170.0, 170.3, 170.4, 170.8, 171.2 (6C, C=O); ESI-MS: m/z : Calcd for C₃₃H₄₅NO₁₅ [M+Na]⁺: 718.3, found: 718.2.

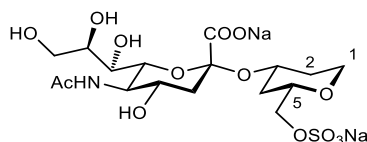
(Methyl 5-acetamido-4,7,8,9-tetra-*O*-acetyl-3,5-dideoxy-D-glycero- α -D-galacto-2-nonulopyranosylonate)-(2 \rightarrow 3)-1,5-anhydro-2,4-dideoxy-6-*O*-sulfonato-D-erythro-hexitol (66).



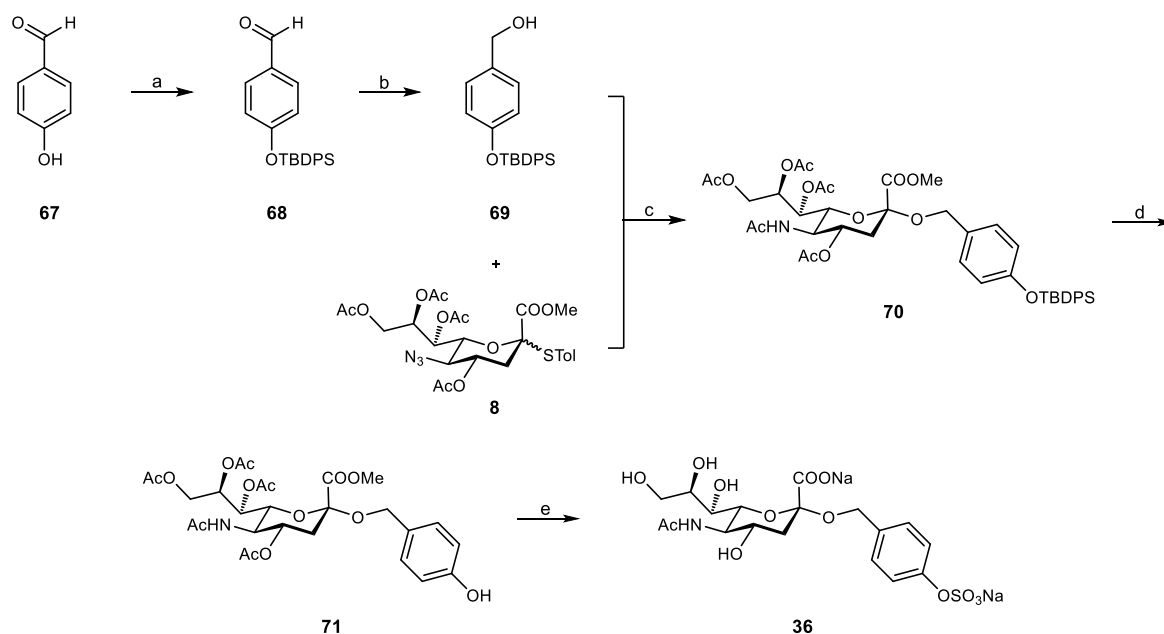
The previous mixture was dissolved in MeOH (3 mL) and stirred with Pd/C (100 mg) under H₂ (1 bar) for 3 h. The reaction was then filtered and concentrated under reduced pressure. The crude was purified by flash chromatography (toluene/acetone, 1:0 \rightarrow 1:1) to afford the deprotected product as a mix of α/β 9:1 (72 mg, 54% over two steps) and used in the next step without further purification. The mixture (72.0 mg, 0.12 mmol) was dissolved in DMF (4.0 mL) and SO₃·pyr (189 mg, 1.20 mmol) was added. The reaction was stirred at rt for 4 h under argon. Then, NaHCO₃ (500 mg) was added and stirring continued for 1 h. After that, the mixture was filtered and concentrated. The crude product was purified first by flash chromatography (DCM/MeOH, 1:0 \rightarrow 9:1) and then by reversed phase chromatography (C₁₈, H₂O/MeCN, 1:0 \rightarrow 7:3) to afford **66** (20.0 mg, 24%) as a white solid. $[\alpha]_D^{20} +3.2$ (c 1, MeOH); ¹H NMR (500 MHz, CD₃OD): $\delta = 1.26$ (m, 1H, H-4a), 1.52 (dddd, $J = 5.3, 7.3, 10.9, 12.6$ Hz, 1H, H-2a), 1.70 (ddt, $J = 2.0, 4.5, 12.5$ Hz, 1H, H-4e), 1.78 (t, $J = 12.5$ Hz, 1H, H-3'a), 1.83 (s, 3H, NHAc), 1.95 (m, 1H, H-2e), 1.98, 2.00, 2.11, 2.16 (4 s, 12H, OAc), 2.63 (dd, $J = 4.6, 12.7$ Hz, 1H, H-3'e), 3.51-3.59 (m, 2H, H-5, H-1a), 3.86-4.05 (m, 6H, H-5', H-9'a, 2 H-6, H-3, H-1e), 4.17 (dd, $J = 2.3, 10.8$ Hz, 1H, H-6'), 4.28 (dd, $J = 2.7, 12.4$ Hz, 1H, H-9'b), 4.78 (ddd, $J = 4.6, 10.2, 12.2$ Hz, 1H, H-4'), 5.31 (dd, $J = 2.3, 9.4$ Hz, 1H, H-7'), 5.40 (ddd, $J = 2.7, 5.8, 9.5$ Hz, 1H, H-8'); ¹³C NMR (126 MHz, CD₃OD): $\delta = 20.7, 20.7, 20.9, 21.3$ (4C, OAc), 22.7 (NHAc), 36.2 (C-4), 36.4 (C-2), 39.5 (C-3'), 50.0 (C-5'), 53.3 (OMe), 63.7 (C-9'), 66.8 (C-1), 68.6 (C-7'), 69.1 (C-8'),

70.7 (C-4'), 71.2 (C-6), 72.3 (C-3), 73.2 (C-6'), 75.7 (C-5), 100.0 (C-2'), 170.2, 171.7, 171.8, 172.4, 173.5 (6C, C=O); ESI-MS: m/z : Calcd for $C_{26}H_{38}NNaO_{18}$ $[M+Na]^+$: 730.2, found: 730.2.

5-Acetamido-3,5-dideoxy-D-glycero- α -D-galacto-2-nonulopyranosylonate-(2 \rightarrow 3)-1,5-anhydro-2,4-dideoxy-6-O-sulfonato-D-erythro-hexitol disodium salt (33).

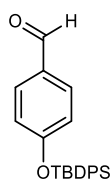


A solution of **66** (20.0 mg, 0.028 mmol) in 0.1 M aq. NaOH (1 mL) was stirred at rt for 16 h. Then, it was acidified to pH 5 with Amberlyst-15 and concentrated under reduced pressure to afford **33** (14.2 mg, 93%) as a white solid. $[\alpha]_D^{20} + 24.3$ (c 1, H_2O); 1H NMR (400 MHz, D_2O): δ = 1.37 (q, J = 11.8 Hz, 1H, H-4a), 1.60 (m, 1H, H-2a), 1.67 (t, J = 12.2 Hz, 1H, H-3'a), 1.89 (m, 1H, H-4e), 2.04 (m, 1H, H-2e), 2.05 (s, 3H, NHAc), 2.76 (dd, J = 4.7, 12.4 Hz, 1H, H-3'e), 3.53 (td, J = 1.9, 12.5 Hz, 1H, H-1a), 3.61 (dd, J = 1.8, 8.9 Hz, 1H, H-6'), 3.63-3.70 (m, 2H, H-4', H-9'), 3.76 (m, 1H, H-5), 3.79-3.90 (m, 3H, H-7', H-8', H-9'b), 3.96-4.03 (m, 2H, H-1e, H-6a), 4.09 (dd, J = 2.7, 11.0 Hz, 1H, H-6b), 4.15 (ddd, J = 4.1, 10.4, 14.5 Hz, 1H, H-3); ^{13}C NMR (100 MHz, D_2O): δ = 22.6 (NHAc), 34.7 (C-4), 34.8 (C-2), 41.6 (C-3'), 52.4 (C-5'), 63.1 (C-9'), 66.4 (C-1), 68.6 (C-6'), 68.9 (C-8'), 71.2 (C-6), 71.8 (C-3), 72.6 (C-7'), 73.4 (C-4'), 75.0 (C-5), 101.7 (C-2'), 174.3, 175.7 (2C, C=O); HR-MS: m/z : Calcd for $C_{17}H_{27}NO_{14}S^{2-}$ $[M]^{2-}$: 250.5582, found: 250.5582; HPLC purity: 77.4%.



Scheme 6. a) TBDPSCl, imidazole, DMF, rt, 16 h, 48%; b) NaBH₄, EtOH/Et₂O, rt, 2 h, quant.; c) i. NIS, TFOH, MeCN/DCM, -40 °C, 16 h, 80%; d) HF·pyr, pyr, 0 °C to rt, 5 h, 85%; e) i. SO₃pyr, DMF, 0 °C to rt, 2 h; ii. NaOH (H₂O/dioxane, 0.1 M), rt, 16 h, 3% over two steps.

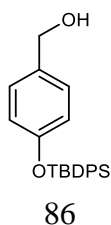
4-((*tert*-Butyldiphenylsilyloxy)benzaldehyde (68).



To a solution of 4-hydroxybenzaldehyde (1.00 g, 8.00 mmol) in dry DMF (20 mL) were added imidazole (1.20 g, 18.0 mmol) and TBDPSCl (2.34 mL, 9.00 mmol). The reaction was stirred under argon for 16 h. Then, it was diluted with Et₂O (20 mL) and washed with H₂O (3 × 30 mL) and aq. sat. NH₄Cl (3 × 30 mL), dried over Na₂SO₄, filtered and concentrated under reduced pressure. The crude was purified by flash chromatography (hexane/EtOAc, 1:0 → 7:3) to afford **68** (1.37 g, 48%) as a white solid. ¹H NMR (400 MHz, CDCl₃): δ = 1.11 (s, 9H, (C(CH₃)₃)), 6.86 (m, 2H, Ar-H), 7.36-7.40 (m, 4H, Ar-H), 7.43-7.47 (m, 2H, Ar-H), 7.63-7.66 (m, 2H, Ar-H), 7.68-7.72 (m, 4H, Ar-H), 9.81 (s, 1H, CHO); ESI-MS: *m/z*: Calcd for C₂₃H₂₄O₂Si [M+H]⁺: 361.2, found: 361.2.

The analytical data of **68** were in accordance with reported values.⁷⁴

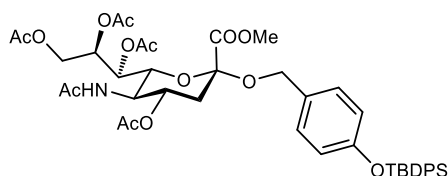
(4-((*tert*-Butyldiphenylsilyloxy)phenyl)methanol (69).



To a mixture of **68** (1.37 g, 3.80 mmol) in EtOH/Et₂O (1:1, 20 mL), NaBH₄ (288 mg, 7.60 mmol) was added at 0 °C. The reaction was then stirred at rt for 2 h. It was quenched with H₂O (20 mL) and extracted with EtOAc (3 × 20 mL), dried over Na₂SO₄, filtered and concentrated under reduced pressure to afford **69** (1.38 g, quant.) as colorless oil. ¹H NMR (400 MHz, CDCl₃): δ = 1.02 (s, 1H, (C(CH₃)₃), 4.43 (s, 2H, CH₂OH), 6.65-6.69 (m, 2H, Ar-H), 6.98-7.01 (m, 2H, Ar-H), 7.26-7.36 (m, 6H, Ar-H), 7.62-7.65 (m, 4H, Ar-H); ¹³C NMR (100 MHz, CDCl₃): δ = 19.6 (C(CH₃)₃), 26.6 (C(CH₃)₃), 65.2 (CH₂OH), 119.7, 127.8, 128.5, 129.9, 133.0, 133.5, 135.7 (14C, Ar-C); ESI-MS: *m/z*: Calcd for C₂₃H₂₆O₂Si [M+Na]⁺: 385.2, found: 385.2.

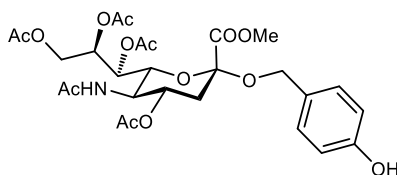
The analytical data of **69** were in accordance with reported values.⁷⁵

4-((*tert*-Butyldiphenylsilyl)oxy)benzyl (methyl 5-acetamido-4,7,8,9-tetra-*O*-acetyl-3,5-dideoxy-*D*-glycero- α -*D*-galacto-2-nonulopyranosylonate) (70**).**



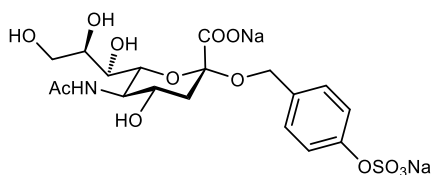
Compounds **69** (0.500 g, 1.38 mmol) and **8** (1.31 g, 2.76 mmol) were dissolved in a solution of dry MeCN/DCM (5:3, 30 mL) with 3Å molecular sieves (6.00 g) and the mixture was stirred under argon for 30 min. Then, the mixture was cooled down to -40 °C and NIS (1.24 g, 5.52 mmol) and TfOH (48.8 μL, 0.550 mmol) were added. The reaction was stirred at -40 °C under argon for 16 h. Then, it was neutralized with NEt₃, filtered over celite and evaporated under reduced pressure. The residue was dissolved in DCM (40 mL) and washed with 1 M aq. Na₂S₂O₃ (3 × 30 mL) and H₂O (3 × 30 mL), dried over Na₂SO₄ and concentrated under reduced pressure. The crude product was purified by flash chromatography (toluene/acetone, 1:0 → 7:3) to afford **70** (925 mg, 80%, α:β 2:1) as a brown solid. ¹H NMR (400 MHz, CDCl₃): δ = 1.08 (s, 9H, (C(CH₃)₃), 1.87 (s, 3H, NHAc), 1.97 (m, 1H, H-3a), 2.01, 2.03, 2.12, 2.14 (4 s, 12H, OAc), 2.59 (dd, *J* = 4.6, 12.8 Hz, 1H, H-3b), 3.58 (s, 3H, OMe), 4.01-4.16 (m, 3H, H-5, H-5, H-9a), 4.27 (d, *J* = 11.6 Hz, 1H, OCH₂Ar), 4.31 (dd, *J* = 2.8, 12.5 Hz, 1H, H-9b), 4.67 (d, *J* = 11.6 Hz, 1H, OCH₂Ar), 4.82 (m, 1H, H-4), 5.33 (dd, *J* = 2.0, 8.5 Hz, 1H, H-7), 5.44 (ddd, *J* = 2.7, 5.6, 8.4 Hz, 1H, H-8), 6.68-6.74 (m, 2H, Ar-H), 7.02-7.07 (m, 2H, Ar-H), 7.32-7.46 (m, 6H, Ar-H), 7.70 (m, 4H, Ar-H); ¹³C NMR (100 MHz, CDCl₃): δ = 19.5 (C(CH₃)₃), 20.91, 20.97, 21.0, 21.3 (4C, OAc), 23.3 (NHAc), 26.6 (C(CH₃)₃), 38.3 (C-3), 49.6 (C-5), 52.7 (OMe), 62.5 (C-9), 66.7 (OCH₂Ar), 67.4 (C-7), 68.6 (C-8), 69.2 (C-4), 72.6 (C-6), 98.5 (C-2), 119.5, 127.9, 129.4, 130.0, 135.6, 155.4 (15C, Ar-C), 168.5, 170.2, 170.3, 170.3, 170.8, 171.2 (6C, C=O); ESI-MS: *m/z*: Calcd for C₄₃H₅₃NO₁₄Si [M+Na]⁺: 858.3, found: 858.3.

4-Hydroxybenzyl (methyl 5-acetamido-4,7,8,9-tetra-*O*-acetyl-3,5-dideoxy-D-glycero- α -D-galacto-2-nonulopyranosylonate) (71).



To a solution of **70** (925 mg, 1.10 mmol) in pyridine (35.0 mL) in a Teflon container was added HF_{pyr} (4.60 mL) at 0 °C. The reaction was stirred at rt for 5 h and then neutralized with aq. sat. NaHCO₃ and Na₂CO₃. The aqueous phase was extracted with DCM (3 × 50 mL) and the organic layer was dried with Na₂SO₄, filtered and concentrated under reduced pressure. The crude product was purified by flash chromatography (DCM/MeOH, 30:1) to afford **71** (560 mg, 85%, α : β 5:1) as a white solid. ¹H NMR (400 MHz, CDCl₃): δ = 1.88 (s, 3H, NHAc), 1.99 (m, 1H, H-3a), 2.00, 2.03, 2.13, 2.16 (4 s, 12H, OAc), 2.61 (dd, J = 4.6, 12.8 Hz, 1H, H-3b), 3.68 (s, 3H, OMe), 4.03-4.17 (m, 3H, H-5, H-6, H-9a), 4.28 (d, J = 11.3 Hz, 1H, OCH₂Ar), 4.36 (dd, J = 2.8, 12.5 Hz, 1H, H-9b), 4.69 (d, J = 11.3 Hz, 1H, OCH₂Ar), 4.86 (m, 1H, H-4), 5.34 (dd, J = 2.1, 8.2 Hz, 1H, H-7), 5.45 (m, 1H, H-8), 6.76-6.81 (m, 2H, Ar-H), 7.13-7.17 (m, 2H, Ar-H); ¹³C NMR (100 MHz, CDCl₃): δ = 20.89, 20.94, 21.0, 21.3 (4C, OAc), 23.2 (NHAc), 38.2 (C-3), 49.6 (C-5), 52.8 (OMe), 62.6 (C-9), 66.9 (OCH₂Ar), 67.5 (C-7), 69.0 (C-8), 69.3 (C-4), 72.5 (C-6), 98.6 (C-2), 115.3, 128.7, 129.9, 156.2 (6C, Ar-C), 168.6, 170.5, 170.6, 171.0, 171.3 (5C, C=O); ESI-MS: m/z : Calcd for C₂₇H₃₅NO₁₄ [M+Na]⁺: 597.2, found: 597.2.

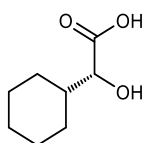
4-((Sulfonato)oxy)benzyl 5-acetamido-3,5-dideoxy-D-glycero- α -D-galacto-2-nonulopyranosylonate (36).



To a solution of **71** (225 mg, 0.380 mmol) in dry DMF (20 mL) was added SO₃·pyr (605 mg, 3.80 mmol) at 0 °C. The reaction was then stirred at rt for 2 h. Then, NaHCO₃ (2.00 g) was added and stirring continued for 1 h. After that, the mixture was filtered and concentrated. The residue was purified by reversed phase chromatography (C₁₈, H₂O/MeCN 1:0 → 7:3) and the fractions containing the product were collected and used in the next step. The crude product was dissolved in 0.1 M aq. NaOH (9 mL) and stirred at rt for 16 h. Then, it was acidified to pH 5 with Amberlyst-15, concentrated under reduced pressure and purified by size exclusion column chromatography (P-2 gel, H₂O) to afford **36** (6.0 mg, 3% over two steps) as a white solid. $[\alpha]_D^{20}$ -2.5 (c 1, MeOH); ¹H NMR (500 MHz,

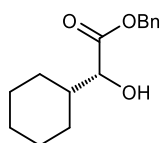
D₂O): δ = 1.71 (t, J = 12.1 Hz, 1H, H-3a), 2.06 (s, 3H, NHAc), 2.80 (dd, J = 4.7, 12.4 Hz, 1H, H-3e), 3.62 (dd, J = 1.9, 9.1 Hz, 1H, H-7), 3.66 (dd, J = 6.0, 11.9 Hz, 1H, H-9a), 3.72 (ddd, J = 4.7, 9.8, 11.9 Hz, 1H, H-4), 3.76 (dd, J = 1.9, 10.4 Hz, 1H, H-6), 3.81-3.86 (m, 2H, H-5, H-8), 3.89 (dd, J = 2.4, 12.0 Hz, 1H, H-9b), 4.54 (d, J = 11.0 Hz, 1H, OCH₂Ar), 4.79 (d, J = 11.0 Hz, 1H, OCH₂Ar), 7.31-7.34 (m, 2H, Ar-H), 7.45-7.49 (m, 2H, Ar-H); ¹³C NMR (126 MHz, D₂O): δ = 22.1 (NHAc), 40.6 (C-3), 52.0 (C-5), 62.7 (C-9), 66.5 (OCH₂Ar), 68.3 (C-7), 68.4 (C-4), 71.8 (C-8), 72.8 (C-9), 101.1 (C-2), 121.6, 130.2, 135.1, 151.0 (6C, Ar-C), 173.6, 175.2 (2C, C=O); HR-MS: m/z : Calcd for C₁₈H₂₃NNa₂O₁₃S [M+Na]⁺: 562.0583, found: 562.0583; HPLC purity: > 95%.

(R)-2-Cyclohexyl-2-hydroxyacetic acid (41).



To a solution of (*R*)-2-amino-2-cyclohexylacetic acid (3.50 g, 0.022 mol) in 0.5 M aq. H₂SO₄ (89 mL) a solution of NaNO₂ in H₂O (4.5 M, 30 mL) was added slowly at 0 °C. The mixture was stirred at 0 °C for 3 h, then warmed up to rt and stirred for another 24 h. The reaction mixture was extracted with Et₂O (3 × 30 mL), washed with brine (3 × 30 mL), dried over Na₂SO₄, filtered and concentrated under reduced pressure to afford **41** (2.98 g, 86%) as a white solid. $[\alpha]_D^{20}$ -5.9 (*c* 1.2, MeOH); ¹H NMR (400 MHz, CD₃OD): δ = 1.13-1.33 (m, 5H, H-cy), 1.57-1.73 (m, 4H, H-cy), 1.75-1.79 (m, 2H, H-cy), 3.91 (d, J = 4.3 Hz, 1H, H-2); ESI-MS: m/z : Calcd for C₈H₁₄O₃ [M-H]⁻: 157.1, found: 157.1. The analytical data of **41** were in accordance with reported values.⁷⁶

Benzyl (R)-2-cyclohexyl-2-hydroxyacetate (42).

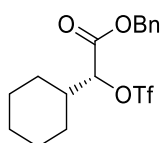


To a solution of **41** (0.882 g, 5.58 mmol) in anhydrous DMF (6 mL) was added Cs₂CO₃ (1.99 g, 6.13 mmol) at 0 °C and the resulting suspension was stirred at rt for 40 min. After that, benzyl bromide (0.664 mL, 5.58 mmol) was also added at 0 °C and the reaction mixture was stirred for 1 h at 0 °C and then for 16 h at rt. The suspension was then diluted with EtOAc (20 mL) and washed with aq. satd. NaHCO₃ (20 mL), water (20 mL) and brine (20 mL). The organic extract was dried over Na₂SO₄, filtered and concentrated under reduced pressure. The crude residue was purified by flash chromatography (hexane/EtOAc, 50:1 → 9:1) to afford **41** (0.996 g, 72%) as yellow oil. $[\alpha]_D^{20}$ +4.7 (*c* 1.0, CHCl₃); ¹H NMR (400 MHz, CDCl₃): δ = 1.16-1.30 (m, 5H, H-cy), 1.39 (m, 1H, H-cy), 1.62-

1.67 (m, 2H, H-cy), 1.70-1.77 (m, 3H, H-cy), 2.67 (d, $J = 6.3$ Hz, 1H, OH-2), 4.06 (dd, $J = 3.6, 6.1$ Hz, 1H, H-2), 5.20 (d, $J = 12.3$ Hz, 1H, OCH₂Ph), 5.24 (d, $J = 12.3$ Hz, 1H, OCH₂Ph), 7.33-7.40 (m, 5H, Ar-H); ¹³C NMR (100 MHz, CDCl₃): $\delta = 26.06, 26.12, 26.36, 26.39, 29.2$ (5C, CH₂-cy), 42.2 (CH-cy), 67.4 (OCH₂Ph), 75.0 (C-2), 128.5, 128.7, 128.8, 135.4 (6C, Ar-C), 174.9 (C=O); ESI-MS: m/z : Calcd for C₁₅H₂₀O₃ [M+Na]⁺: 271.1, found: 271.1.

The analytical data of **42** were in accordance with reported values.⁷⁷

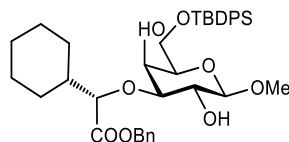
Benzyl (*R*)-2-cyclohexyl-2-(trifluoromethylsulfonyloxy)acetate (**43**).



Compound **42** (1 eq) was dissolved in dry DCM (10 mL) under argon. Then, 2,6-lutidine (0.915 mL, 7.86 mmol) was added, the mixture was cooled to -15 °C and triflic anhydride (0.992 mL, 5.90 mmol) was added. The reaction was stirred at -20 °C for 4 h. Then, it was diluted with DCM (20 mL), washed with cold water (2 × 20 mL) and brine (3 × 20 mL), dried over Na₂SO₄ and concentrated under reduced pressure. The crude product was purified by flash chromatography (hexane/EtOAc, 20:1 → 9:1) to afford **43** (1.16 g, 77%) as yellow oil. $[\alpha]_D^{20} +18.5$ (c 1.0, CHCl₃); ¹H NMR (400 MHz, CDCl₃): $\delta = 1.07$ -1.32 (m, 6H, H-cy), 1.66-1.70 (m, 2H, H-cy), 1.74-1.81 (m, 2H, H-cy), 2.02 (m, 1H, H-cy), 4.96 (d, $J = 4.4$ Hz, 1H, H-2), 5.24 (d, $J = 12.1$ Hz, 1H, OCH₂Ph), 5.28 (d, $J = 12.1$ Hz, 1H, OCH₂Ph), 7.33-7.41 (m, 5H, Ar-H); ¹³C NMR (100 MHz, CDCl₃): $\delta = 25.6, 25.7, 25.8, 26.8, 28.7$ (5C, CH₂-cy), 40.4 (CH-cy), 68.2 (OCH₂Ph), 87.7 (C-2), 118.6 (q, $J = 319.6$ Hz, CF₃), 128.7, 128.8, 129.0, 134.6 (6C, Ar-C), 166.8 (C=O).

The analytical data of **43** were in accordance with reported values.⁷⁷

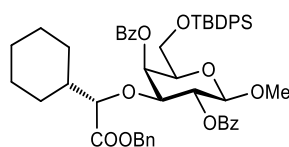
Methyl 3-*O*-[(*S*)-1-benzyloxycarbonyl-1-cyclohexyl-methyl]-6-*O*-(*tert*-butyldiphenylsilyl)- β -D-galactopyranoside (**49a**).



To a solution of **4** (1.50 g, 3.47 mmol) in dry MeOH (60.0 mL) was added Bu₂SnO (950 mg, 3.81 mmol) at rt under argon atmosphere. The reaction mixture was heated to reflux for 3 h, then the solvent was evaporated and the residue dried under vacuum for 4 h. The crude product was dissolved in dry DME (10 mL) and stirred at rt under argon atmosphere. A solution of **43** (2.02 g, 5.20 mmol) in dry DME (10 mL) was added dropwise, followed by CsF (682 mg, 4.50 mmol) at once, after being

dried at 70 °C under vacuum for 30 min. The reaction mixture was stirred for 16 h. Then, EtOAc (20 mL) and H₂O (20 mL) were added and the aqueous phase was extracted with EtOAc (3 × 20 mL). The organic phase was dried over Na₂SO₄, filtered and evaporated. The crude material was purified by flash column chromatography (petroleum ether/acetone, 9:1 → 8:2) to afford **49a** (864 mg, 38%) as a white solid. $[\alpha]_D^{20}$ -21.1 (*c* 1.0, CHCl₃); ¹H NMR (400 MHz, CDCl₃): δ = 1.06 (s, 9H, C(CH₃)₃), 1.09-1.32 (m, 7H, H-cy), 1.62 (m, 1H, H-cy), 1.67-1.74 (m, 2H, H-cy), 1.84 (m, 1H, H-cy), 2.27 (m, 1H, OH-2), 3.22-3.25 (m, 2H, H-3, OH-4), 3.47 (t, *J* = 6.2 Hz, 1H, H-5), 3.51 (s, 3H, OMe), 3.80 (d, *J* = 8.3 Hz, 1H, H-2), 3.84 (m, 1H, OH-4), 3.87-3.93 (m, 2H, 2 H-6), 3.96 (d, *J* = 4.8 Hz, 1H, H-1'), 4.11 (d, *J* = 7.8 Hz, 1H, H-1), 5.10 (d, *J* = 12.1 Hz, 1H, OCH₂Ph), 5.20 (d, *J* = 12.1 Hz, 1H, OCH₂Ph), 7.27-7.32 (m, 5H, Ar-H), 7.36-7.42 (m, 6H, Ar-H), 7.64-7.70 (m, 4H, Ar-H); ¹³C NMR (100 MHz, CDCl₃): δ = 19.4 (C(CH₃)₃), 26.05, 26.13, 26.2 (3C, CH₂-cy), 27.0 (C(CH₃)₃), 27.7, 29.3 (2C, CH₂-cy), 41.9 (CH-cy), 56.9 (OMe), 62.9 (C-6), 66.4 (C-4), 67.2 (OCH₂Ph), 71.3 (C-2), 74.9 (C-5), 83.8 (C-1'), 84.0 (C-3), 104.0 (C-1), 127.8, 128.67, 128.72, 128.8, 129.81, 129.83, 133.6, 133.7, 135.3, 135.7, 135.8 (24C, Ar-C), 173.8 (C=O); ESI-MS: *m/z*: Calcd for C₃₈H₅₀O₈Si [M+Na]⁺: 685.3, found: 685.5.

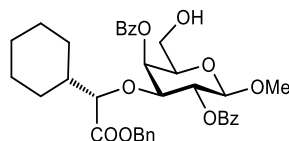
Methyl 2,4-di-*O*-benzoyl-3-*O*-[(*S*)-1-benzyloxycarbonyl-1-cyclohexyl-methyl]-6-*O*-*tert*-butyldiphenylsilyl- β -D-galactopyranoside (50a**).**



To a solution of **49a** (0.864 g, 1.30 mmol) in pyridine (16.9 mL) were added DMAP (0.096 g, 0.78 mmol) at once and Bz₂O (3.80 g, 16.9 mmol) portionwise at 0 °C. The mixture was warmed up to rt and stirred for 16 h and then the solvent was removed via co-evaporation with toluene. The crude product was dissolved in EtOAc (50 mL), washed with H₂O (3 × 30 mL), aq. satd. CuSO₄ (3 × 30 mL), H₂O (30 mL) and brine (30 mL). The organic phase was dried over Na₂SO₄, filtered and evaporated. The crude product was purified by flash column chromatography (petroleum ether/acetone, 9:1). It was not possible to completely remove the excess of benzoate from the mixture, so the compound was used for the next steps without further purification. ¹H NMR (500 MHz CDCl₃): δ = 0.72-0.92 (m, 4H, H-cy), 1.06 (s, 9H, C(CH₃)₃), 1.12-1.22 (m, 5H, H-cy), 1.32 (m, 1H, H-cy), 1.55 (m, 1H, H-cy), 3.49 (s, 3H, OMe), 3.74-3.83 (m, 3H, H-5, 2 H-6), 3.85 (dd, *J* = 3.4, 9.9 Hz, 1H, H-3), 3.93 (d, *J* = 4.5 Hz, 1H, H-1'), 4.46 (d, *J* = 8.0 Hz, 1H, H-1), 5.15 (d, *J* = 12.2 Hz, 1H, OCH₂Ph), 5.19 (d, *J* = 12.2 Hz, 1H, OCH₂Ph), 5.59 (dd, *J* = 8.1, 9.9 Hz, 1H, H-2), 5.94 (d, *J* = 3.0 Hz, 1H, H-4), 7.25-7.35 (m, 5H, Ar-H), 7.36-7.45 (m, 10H, Ar-H), 7.49-7.45 (m, 4H, Ar-H), 7.71-7.74 (m, 2H,

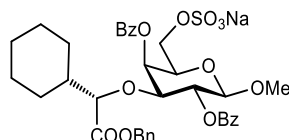
Ar-H), 8.13-8.15 (m, 2H, Ar-H), 8.04-8.08 (m, 2H, Ar-H); ^{13}C -NMR (126 MHz, CDCl_3): δ = 19.3 ($\text{C}(\text{CH}_3)_3$), 25.76, 25.80, 26.0 (4C, $\text{CH}_2\text{-cy}$), 27.0 ($\text{C}(\text{CH}_3)_3$), 28.9 ($\text{CH}_2\text{-cy}$), 41.1 (CH-cy), 56.9 (OMe), 62.5 (C-6), 66.6 (OCH_2Ph), 69.7 (C-4), 72.9 (C-2), 74.8 (C-5), 77.9 (C-3), 84.4 (C-1'), 102.4 (C-1), 127.78, 127.81, 127.85, 128.4, 128.61, 128.64, 129.5, 129.79, 129.85, 130.10, 130.13, 130.3, 132.9, 133.2, 133.4, 135.67, 135.73 (30C, Ar-C), 171.8, 173.4 (3C, C=O); ESI-MS: m/z : Calcd for $\text{C}_{52}\text{H}_{58}\text{O}_{10}\text{Si}$ $[\text{M}+\text{Na}]^+$: 893.4, found: 893.2.

Methyl 2,4-di-*O*-benzoyl-3-*O*-[(*S*)-1-benzyloxycarbonyl-1-cyclohexyl-methyl]- β -D-galactopyranoside (51a).



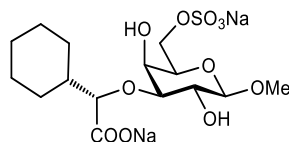
To a solution of **50a** (0.70 g, 0.80 mmol) in pyridine (18.0 mL) in a Teflon container was added HF \cdot pyr (6.0 mL) dropwise and the reaction mixture was stirred at rt for 2.5 h. The reaction was neutralized with aq. satd. NaHCO_3 and the aqueous phase was extracted with DCM (3×50 mL). Then, the organic phases were dried over Na_2SO_4 and concentrated under reduced pressure. The crude product was purified by flash chromatography (petroleum ether/acetone, 8:2 \rightarrow 7:3) to afford **51a** (465 mg, 57% yield over two steps) as a colorless oil. $[\alpha]_{\text{D}}^{20} +57.7$ (c 1.0, CHCl_3); ^1H NMR (500 MHz, CDCl_3): δ = 0.66-1.02 (m, 4H, H-cy), 1.13 (m, 1H, H-cy), 1.24-1.42 (m, 5H, H-cy), 1.54 (m, 1H, H-cy), 3.49 (s, 3H, OMe), 3.56 (dd, J = 5.7, 9.6 Hz, 1H, H-6a), 3.69-3.75 (m, 2H, H-5, H-6b), 3.80 (dd, J = 3.4, 10.0 Hz, 1H, H-3), 3.86 (d, J = 4.8 Hz, 1H, H-1'), 4.48 (d, J = 8.0 Hz, 1H, H-1), 5.07 (d, J = 12.1 Hz, 1H, OCH_2Ph), 5.11 (d, J = 12.1 Hz, 1H, OCH_2Ph), 5.65-5.69 (m, 2H, H-2, H-4), 7.28-7.35 (m, 5H, Ar-H), 7.45-7.49 (m, 4H, Ar-H), 7.57-7.61 (m, 2H, Ar-H), 8.06-8.07 (m, 2H, Ar-H), 8.13-8.15 (m, 2H, Ar-H); ^{13}C -NMR (126 MHz, CDCl_3): δ = 25.7, 25.8, 25.9, 27.1, 28.9 (5C, $\text{CH}_2\text{-cy}$), 41.2 (CH-cy), 57.1 (OMe), 60.4 (C-6), 66.8 (OCH_2Ph), 70.5 (C-4), 72.3 (C-2), 74.1 (C-5), 78.6 (C-3), 85.0 (C-1'), 102.5 (C-1), 128.56, 128.61, 128.65, 128.70, 129.3, 129.9, 130.0, 130.4, 133.4, 133.7, 135.5 (18C, Ar-C), 165.3, 168.1, 172.0 (3C, C=O); ESI-MS: m/z : Calcd for $\text{C}_{36}\text{H}_{40}\text{O}_{10}$ $[\text{M}+\text{Na}]^+$: 655.3, found: 655.3.

Methyl 2,4-di-*O*-benzoyl-3-*O*-[(*S*)-1-benzyloxycarbonyl-1-cyclohexyl-methyl]-6-*O*-sulfonato- β -D-galactopyranoside (52a).

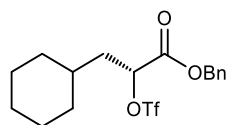


To a solution of **51a** (438 mg, 0.69 mmol) in dry DMF (20.0 mL) was added $\text{SO}_3\cdot\text{pyr}$ (760 mg, 6.90 mmol) at 0 °C under argon. The reaction mixture was warmed to rt and stirred for 2.5 h. Then NaHCO_3 (1.20 g, 13.8 mmol) was added and the suspension was stirred at rt for 2 h. The suspension was filtered over celite and the solvent removed via co-evaporation with toluene. The crude product was purified by flash column chromatography (DCM/MeOH, 20:1 \rightarrow 9:1) to afford **52a** (411 mg, 81%) as a white solid. $[\alpha]_{\text{D}}^{20} +48.5$ (c 1.0, MeOH); $^1\text{H NMR}$ (500 MHz, CD_3OD): δ = 0.57 (m, 1H, H-cy), 0.77-0.95 (m, 4H, H-cy), 1.16-1.35 (m, 5H, H-cy), 1.50 (m, 1H, H-cy), 3.54 (s, 3H, OMe), 4.01 (d, J = 4.2 Hz, 1H, H-1'), 4.05-4.12 (m, 2H, H-3, H-6a), 4.14-4.18 (m, 2H, H-5, H-6b), 4.66 (d, J = 8.0 Hz, 1H, H-1), 5.11 (d, J = 12.1 Hz, 1H, OCH_2Ph), 5.14 (d, J = 12.0 Hz, 1H, OCH_2Ph), 5.53 (m, 1H, H-2), 5.83 (d, J = 3.1 Hz, 1H, H-4), 7.31-7.37 (m, 5H, Ar-H), 7.51-7.56 (m, 4H, Ar-H), 7.64-7.67 (m, 2H, Ar-H), 8.08-8.14 (m, 4H, Ar-H); $^{13}\text{C-NMR}$ (126 MHz, CD_3OD): δ = 26.79, 26.82, 26.9, 28.2, 29.8 (5C, $\text{CH}_2\text{-cy}$), 42.5 (CH-cy), 57.3 (OMe), 67.6 (C-6), 67.7 (OCH_2Ph), 71.2 (C-4), 73.6 (C-5), 73.7 (C-2), 79.1 (C-3), 84.6 (C-1'), 103.3 (C-1), 129.4, 129.56, 129.59, 129.7, 130.8, 131.0, 131.2, 131.3, 134.4, 134.6, 137.2 (18C, Ar-C), 166.9, 167.3, 173.0 (3C, C=O); ESI-MS: m/z : Calcd for $\text{C}_{36}\text{H}_{39}\text{O}_{13}\text{S}$ $[\text{M}+\text{Na}]^+$: 757.2, found: 757.1.

Methyl 3-*O*-[(*S*)-1-carboxy-1-cyclohexyl-methyl]-6-*O*-sulfonato- β -D-galactopyranoside (**53**).

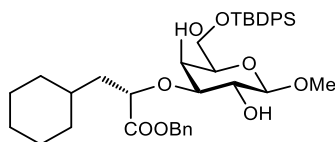


Compound **52a** (150 mg, 0.20 mmol) was dissolved in 0.1 M NaOH ($\text{H}_2\text{O}/\text{dioxane}$, 1:1, 20 mL) and the mixture was stirred at rt for 3 d. After that, it was neutralized with Amberlyst-15 resin, filtered and concentrated under reduced pressure. The residue was then purified by reversed-phase column chromatography (C_{18} , H_2O) and size-exclusion chromatography (P-2 gel, H_2O) to afford **53** (31.0 mg, 35%) as a white solid. $[\alpha]_{\text{D}}^{20} +39.4$ (c 1.5, H_2O); $^1\text{H NMR}$ (500 MHz, D_2O): δ = 1.13-1.36 (m, 5H, H-cy), 1.59-1.65 (m, 3H, H-cy), 1.71-1.79 (m, 3H, H-cy), 3.44 (dd, J = 3.2, 9.6 Hz, 1H, H-3), 3.59 (s, 3H, OMe), 3.65 (dd, J = 8.1, 9.6 Hz, 1H, H-2), 3.74 (d, J = 4.8 Hz, 1H, H-1'), 3.96 (m, 1H, H-5), 3.99 (d, J = 3.2 Hz, 1H, H-4), 4.20-4.27 (m, 2H, H-6), 4.36 (d, J = 8.1 Hz, 1H, H-1); $^{13}\text{C-NMR}$ (126 MHz, D_2O): δ = 25.95, 25.97, 26.1, 27.8, 29.0 (5C, $\text{CH}_2\text{-cy}$), 41.6 (CH-cy), 57.2 (OMe), 66.3 (C-4), 67.9 (C-6), 70.0 (C-2), 72.4 (C-5), 83.0 (C-3), 85.8 (C-1'), 103.6 (C-1), 181.4 (C=O); HR-MS: m/z : Calcd for $\text{C}_{15}\text{H}_{24}\text{O}_{11}\text{S}$ $[\text{M}]^{2-}$: 206.0525, found: 206.0520; HPLC purity: 93%.

Benzyl (*R*)-3-cyclohexyl-2-(trifluoromethylsulfonyloxy)-propanoate (45**).**

Benzyl (*R*)-3-cyclohexyl-2-hydroxypropanoate (2.00 g, 7.62 mmol) was dissolved in dry DCM (15 mL) under argon. Then, 2,6-lutidine (1.16 mL, 10.0 mmol) was added, the mixture was cooled down to -15 °C and triflic anhydride (1.26 mL, 8.00 mmol) was added. The reaction was stirred at -20 °C for 4 h. Then, it was diluted with DCM (20 mL), washed with cold water (2 × 20 mL) and brine (3 × 20 mL), dried over Na₂SO₄ and concentrated under reduced pressure. The residue was purified by flash chromatography (hexane/EtOAc, 20:1 → 9:1) to afford **45** (1.78 g, 59%) as a colorless oil. $[\alpha]_{\text{D}}^{20} +38.6$ (*c* 1.0, CHCl₃); ¹H NMR (400 MHz, CDCl₃): δ = 0.85-1.00 (m, 2H, H-cy), 1.07-1.27 (m, 3H, H-cy), 1.41 (m, 1H, H-cy), 1.63-1.77 (m, 5H, H-cy), 1.82 (m, 1H, H-3a), 1.91 (ddd, *J* = 5.0, 9.0, 14.3 Hz, 1H, H-3b), 5.21 (dd, *J* = 4.3, 9.0 Hz, 1H, H-2), 5.24 (d, *J* = 12.1 Hz, 1H, OCH₂Ph), 5.27 (d, *J* = 12.1 Hz, 1H, OCH₂Ph), 7.34-7.43 (m, 5H, Ar-H); ¹³C NMR (100 MHz, CDCl₃): δ = 25.8, 26.1, 26.3, 32.1 (4C, CH₂-cy), 33.4 (CH-cy), 33.5 (CH₂-cy), 39.4 (C-3), 68.4 (OCH₂Ph), 82.0 (C-2), 118.6 (q, *J* = 319.6 Hz, CF₃), 128.8, 128.9, 129.1, 134.6 (6C, Ar-C), 167.7 (C=O).

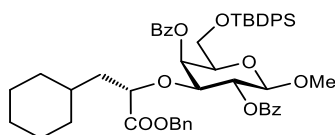
The analytical data of **45** were in accordance with reported values.⁷⁸

Methyl 3-*O*-[(1*S*)-1-benzoyloxycarbonyl-2-cyclohexyl-ethyl]-6-*O*-*tert*-butyldiphenylsilyl- β -D-galactopyranoside (49b**).**

To a solution of **4** (500 mg, 1.16 mmol) in dry MeOH (6.0 mL) was added Bu₂SnO (316 mg, 1.27 mmol) at rt under argon atm. The mixture was heated to reflux and stirred for 3 h. The solvent was then evaporated and the residue dried under vacuum for 4 h. The crude product was dissolved in THF (6 mL) and stirred under argon. A solution of **45** (686 mg, 1.74 mmol) in THF/DME (3:1, 5 mL) was added dropwise, followed by dried CsF (210 mg, 1.39 mmol) at once. The reaction mixture was stirred for 16 h at rt. Then, EtOAc (10 mL) and H₂O (10 mL) were added and the aqueous phase was extracted with EtOAc (3 × 10 mL). The combined organic phases were dried over Na₂SO₄, filtered and evaporated. The crude material was purified by flash column chromatography (petroleum ether/acetone, 1:0 → 7:3) to afford **49b** (425 mg, 54%) as a colorless oil. $[\alpha]_{\text{D}}^{20} -40.8$ (*c* 1.0, CHCl₃); ¹H NMR (400 MHz, CDCl₃): δ = 0.84-0.97 (m, 2H, H-cy), 1.06 (s, 9H, C(CH₃)₃), 1.10-1.22 (m, 3H, H-cy), 1.59-1.81 (m, 8H, 2 H-2', 6 H-cy), 2.28 (d, *J* = 2.2 Hz, 1H, OH-2), 3.24 (m, 1H, OH-4), 3.28

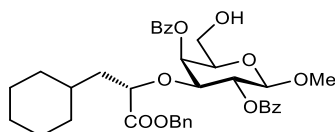
(dd, $J = 3.2, 9.3$ Hz, 1H, H-3), 3.50 (m, 1H, H-5), 3.52 (s, 3H, OMe), 3.81 (ddd, $J = 2.1, 7.8, 9.6$ Hz, 1H, H-2), 3.87-3.95 (m, 3H, H-4, 2 H-6), 4.13 (d, $J = 7.8$ Hz, 1H, H-1), 4.26 (dd, $J = 3.5, 9.7$ Hz, 1H, H-1'), 7.29-7.33 (m, 5H, Ar-H), 7.37-7.44 (m, 6H, Ar-H), 7.68-7.71 (m, 4H, Ar-H); ^{13}C NMR (100 MHz, CDCl_3): $\delta = 19.4$ ($\text{C}(\text{CH}_3)_3$), 26.2, 26.4, 26.5 (3C, $\text{CH}_2\text{-cy}$), 27.0 ($\text{C}(\text{CH}_3)_3$), 32.3 ($\text{CH}_2\text{-cy}$), 33.8 (CH-cy), 34.0 ($\text{CH}_2\text{-cy}$), 41.1 (C-2'), 56.9 (OMe), 62.9 (C-6), 66.6 (C-4), 67.2 (OCH_2Ph), 71.3 (C-2), 74.9 (C-5), 77.4 (C-1'), 83.7 (C-3), 104.0 (C-1), 127.9, 128.6, 128.7, 128.8, 129.83, 129.84, 133.5, 133.7, 135.3, 135.7, 135.8 (24C, Ar-C), 174.9 (C=O); ESI-MS: m/z : Calcd for $\text{C}_{39}\text{H}_{52}\text{O}_8\text{Si}$ $[\text{M}+\text{Na}]^+$: 699.3, found: 699.3.

Methyl 2,4,-*O*-benzoyl-3-*O*-[(1*S*)-1-benzyloxycarbonyl-2-cyclohexyl-ethyl]-6-*O*-*tert*-butyldiphenylsilyl- β -D-galactopyranoside (50b).



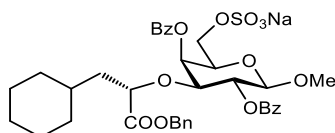
To a solution of **49b** (808 mg, 1.19 mmol) in pyridine (12.0 mL) was added DMAP (87.5 mg, 0.720 mmol) under argon. The solution was then cooled to 0 °C and Bz_2O (2.17 g, 11.9 mmol) was added. The reaction was stirred at rt for 16 h and then co-evaporated with toluene. The residue was dissolved in EtOAc (40 mL) and washed with H_2O (3×30 mL), 10% aq. CuSO_4 (3×30 mL), H_2O (30 mL) and brine (2×30 mL). The organic phase was dried over Na_2SO_4 , filtered and concentrated under reduced pressure. The crude product was then purified by flash chromatography (petroleum ether/acetone, 1:0 \rightarrow 4:1) to afford **50b** (661 mg, 63%) as a white solid. $[\alpha]_{\text{D}}^{20} +18.9$ (c 1.6, CHCl_3); ^1H NMR (500 MHz, CDCl_3): $\delta = 0.48\text{-}0.56$ (m, 2H, H-cy), 0.68 (qt, $J = 3.4, 12.6$ Hz, 1H, H-cy), 0.75-0.90 (m, 2H, H-cy), 1.10 (tdd, $J = 4.9, 7.9, 11.2$ Hz, 1H, H-cy), 1.20 (m, 1H, H-cy), 1.26-1.44 (m, 6H, 4 H-cy, 2 H-2'), 3.04 (m, 1H, OH-6), 3.48 (s, 3H, OMe), 3.55 (m, 1H, H-6a), 3.69-3.75 (m, 2H, H-5, H-6b), 3.83 (dd, $J = 3.4, 10.0$ Hz, 1H, H-3), 4.15 (dd, $J = 4.5, 8.1$ Hz, 1H, H-1'), 4.48 (d, $J = 8.0$ Hz, 1H, H-1), 5.10 (s, 2H, OCH_2Ph), 5.65 (dd, $J = 8.0, 10.0$ Hz, 1H, H-2), 5.69 (d, $J = 3.3$ Hz, 1H, H-4), 7.28-7.31 (m, 2H, Ar-H), 7.32-7.36 (m, 3H, Ar-H), 7.44-7.50 (m, 4H, Ar-H), 7.57-7.62 (m, 2H, Ar-H), 8.07-8.11 (m, 2H, Ar-H), 8.12-8.16 (m, 2H, Ar-H); ^{13}C NMR (126 MHz, CDCl_3): $\delta = 25.6, 25.9, 26.2, 32.8$ (4C, $\text{CH}_2\text{-cy}$), 33.5 (CH-cy), 33.6 ($\text{CH}_2\text{-cy}$), 40.8 (C-2'), 57.1 (OMe), 60.4 (C-6), 66.9 (OCH_2Ph), 70.6 (C-2), 72.5 (C-4), 74.1 (C-5), 78.3 (C-3), 78.9 (C-1'), 102.6 (C-1), 128.6, 128.6, 128.7, 128.8, 129.3, 129.9, 130.0, 130.5, 133.5, 133.7, 135.5 (30C, Ar-C), 165.2, 168.0, 172.8 (3C, C=O); ESI-MS: m/z : Calcd for $\text{C}_{53}\text{H}_{60}\text{O}_{10}\text{Si}$ $[\text{M}+\text{Na}]^+$: 907.4, found: 907.4.

Methyl 2,4,-O-benzoyl-3-O-[(1S)-1-benzyloxycarbonyl-2-cyclohexyl-ethyl]-β-D-galactopyranoside (51b).



To a solution of **50b** (226 mg, 0.260 mmol) in pyridine (10.0 mL) in a Teflon container was added HF·pyr (1.20 mL) at 0 °C. The reaction was stirred at rt for 3 h and then neutralized with aq. sat. NaHCO₃ and Na₂CO₃. The aqueous phase was extracted with DCM (3 × 30 mL) and the organic layer was dried with Na₂SO₄, filtered and concentrated under reduced pressure. The residue was purified by flash chromatography (petroleum ether/EtOAc, 1:0 → 7:3) to afford **51b** (114 mg, 69%) as a white solid. $[\alpha]_D^{20} +51.2$ (c 0.6, CHCl₃); ¹H NMR (500 MHz, CD₃OD): δ = 0.40-0.54 (m, 2H, H-cy), 0.63-0.89 (m, 3H, H-cy), 1.03 (m, 1H, H-cy), 1.15-1.39 (m, 7H, 5 H-cy, 2 H-2'), 3.50 (s, 3H, OMe), 3.66 (m, 1H), 4.03 (dd, *J* = 6.4, 9.4 Hz, 1H, H-6a), 4.08-4.17 (m, 3H, H-3, H-5, H-6b), 4.23 (dd, *J* = 4.9, 7.5 Hz, 1H, H-1'), 4.63 (d, *J* = 8.0 Hz, 1H, H-1), 5.10 (d, *J* = 12.0 Hz, 1H, OCH₂Ph), 5.14 (d, *J* = 11.6 Hz, 1H, OCH₂Ph), 5.49 (dd, *J* = 8.0, 9.9 Hz, 1H, H-2), 5.81 (dd, *J* = 0.9, 3.4 Hz, 1H, H-4), 7.28-7.38 (m, 5H, Ar-H), 7.46-7.55 (m, 4H, Ar-H), 7.59-7.67 (m, 2H, Ar-H), 8.09 (m, 4H, Ar-H); ¹³C NMR (126 MHz, CD₃OD): δ = 26.7, 26.9, 27.1, 34.0, 34.5 (5C, CH₂-cy), 34.6 (CH-cy), 41.6 (C-2'), 57.3 (OMe), 67.6 (C-6), 67.8 (OCH₂Ph), 71.5 (C-4), 73.6 (C-3), 73.9 (C-2), 78.7 (C-5), 79.1 (C-1'), 103.3 (C-1), 129.5, 129.6, 129.6, 129.7, 129.8, 130.8, 131.0, 131.1, 131.2, 134.4, 134.6, 137.1 (18C, Ar-C), 166.9, 167.3, 173.9 (3C, C=O); ESI-MS: *m/z*: Calcd for C₃₇H₄₂NaO₁₀ [M+Na]⁺: 669.3, found: 669.3.

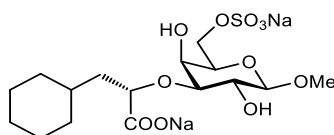
Methyl 2,4-di-O-benzoyl-3-O-[(1S)-1-benzyloxycarbonyl-2-cyclohexyl-ethyl]-6-O-sulfonato-β-D-galactopyranoside (52b).



To a solution of **51b** (114 mg, 0.176 mmol) in DMF (5 mL) was added SO₃·pyr (281 mg, 1.76 mmol) at 0 °C. The reaction was then stirred at rt under argon atmosphere. After 5 h, starting material was still present and another 5 eq of SO₃·pyr were added and stirring was continued for further 2 h. Then, NaHCO₃ (800 mg) was added and the mixture was stirred for 1 h. The mixture was filtrated over celite and concentrated under reduced pressure. The residue was purified by flash chromatography (DCM/MeOH, 1:0 → 9:1) to afford **52b** (79 mg, 60%) as a white solid. $[\alpha]_D^{20} +41.8$ (c 0.4, MeOH); ¹H NMR (500 MHz, CD₃OD): δ = 0.40-0.54 (m, 2H, H-cy), 0.63-0.89 (m, 3H, H-cy), 1.03 (m, 1H,

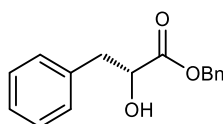
H-cy), 1.15-1.39 (m, 7H, 5 H-cy, 2 H-2'), 3.50 (s, 3H, OMe), 4.03 (dd, $J = 6.4, 9.4$ Hz, 1H, H-6a), 4.08-4.17 (m, 3H, H-3, H-5, H-6b), 4.23 (dd, $J = 4.9, 7.5$ Hz, 1H, H-1'), 4.63 (d, $J = 8.0$ Hz, 1H, H-1), 5.10 (d, $J = 12.0$ Hz, 1H, OCH₂Ph), 5.14 (d, $J = 11.6$ Hz, 1H, OCH₂Ph), 5.49 (dd, $J = 8.0, 9.9$ Hz, 1H, H-2), 5.81 (m, 1H, H-4), 7.28-7.38 (m, 5H, Ar-H), 7.48-7.53 (m, 4H, Ar-H), 7.61-7.65 (m, 2H, Ar-H), 8.07-8.11 (m, 4H, Ar-H); ¹³C NMR (126 MHz, CD₃OD): $\delta = 26.8, 26.9, 27.2, 34.0, 34.5$ (5C, CH₂-cy), 34.6 (CH-cy), 41.7 (C-2'), 57.3 (OMe), 67.7 (C-6), 67.8 (OCH₂Ph), 71.5 (C-4), 73.6 (C-3), 73.9 (C-2), 78.7 (C-5), 79.1 (C-1'), 103.3 (C-1), 129.5, 129.59, 129.63, 129.7, 129.8, 130.8, 131.0, 131.1, 131.2, 134.4, 134.7, 137.1 (18C, Ar-C), 166.9, 167.3, 173.9 (3C, C=O). ESI-MS: m/z : Calcd for C₃₇H₄₁NaO₁₃S [M+Na]⁺: 771.2, found: 771.2.

Methyl 3-*O*-[(1*S*)-1-carboxy-2-cyclohexyl-ethyl]-6-*O*-sulfonato- β -D-galactopyranoside (**39**).



Compound **52b** (62.0 mg, 0.083 mmol) was treated with 0.1 M aq. NaOH (8.0 mL) at rt for 24 h. Then it was neutralized with Amberlyst-15 and concentrated under reduced pressure. The residue was purified by reversed-phase column chromatography (C₁₈, H₂O) and size exclusion column chromatography (P-2 gel, H₂O) to afford **39** as a white solid (17.0 mg, 44%). $[\alpha]_D^{20} - 8.6$ (c 0.2, H₂O); ¹H NMR (500 MHz, D₂O): $\delta = 0.80-0.93$ (m, 2H, H-cy), 1.07-1.21 (m, 3H, H-cy), 1.43-1.67 (m, 7H, 5 H-cy, 2 H-2'), 1.73 (m, 1H, H-cy), 3.38 (dd, $J = 3.3, 9.6$ Hz, 1H, H-3), 3.51 (s, 3H, OMe), 3.53 (dd, $J = 8.1, 9.6$ Hz, 1H, H-2), 3.86-3.93 (m, 3H, H-1', H-4, H-5), 4.11-4.19 (m, 2H, H-6), 4.28 (d, $J = 8.1$ Hz, 1H, H-1); ¹³C NMR (126 MHz, D₂O): $\delta = 26.4, 26.6, 26.8, 32.5$ (4C, CH₂-cy), 33.9 (CH-cy), 34.3 (CH₂-cy), 41.8 (C-2'), 57.8 (OMe), 66.9 (C-4), 68.4 (C-6), 70.5 (C-2), 73.0 (C-1'), 79.9 (C-5), 83.1 (C-3), 104.2 (C-1), 183.2 (C=O); HR-MS: m/z : Calcd for C₁₆H₂₆Na₂O₁₁S [M+Na]⁺: 495.0889, found: 495.0889; HPLC purity: 93%.

Benzyl (*R*)-(+)-2-hydroxy-3-phenylpropanoate (**47**).

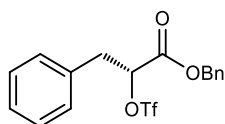


To a solution of D-phenyllactic acid (5.00 g, 0.033 mol) in anhydrous DMF (25 mL) was added Cs₂CO₃ (11.8 g, 0.036 mol) at 0 °C and the resulting suspension was stirred at rt for 40 min. After that, benzyl bromide (3.91 mL, 0.033 mol) was also added at 0 °C and the reaction mixture was stirred for 1 h at 0 °C and then for 16 h at rt. The suspension was then diluted with EtOAc (40 mL) and

washed with aq. satd. NaHCO₃ (30 mL), water (30 mL) and brine (30 mL). The organic extract was dried over Na₂SO₄, filtered and concentrated under reduced pressure. The crude residue was purified by flash chromatography (hexane/EtOAc 50:1 → 9:1) to afford **47** (2.82 g, 33%) as a yellow oil. $[\alpha]_D^{20} +5.6$ (*c* 1.2, CHCl₃); ¹H NMR (400 MHz, CDCl₃): δ = 2.75 (d, *J* = 6.1 Hz, 1H, OH-2), 2.98 (dd, *J* = 6.5, 13.9 Hz, 1H, H-3a), 3.13 (dd, *J* = 4.7, 13.9 Hz, 1H, H-3b), 4.50 (m, 1H, H-2), 5.17 (d, *J* = 12.1 Hz, 1H, OCH₂Ph), 5.20 (d, *J* = 12.1 Hz, 1H, OCH₂Ph), 7.13-7.16 (m, 2H, Ar-H), 7.21-7.26 (m, 3H, Ar-H), 7.32-7.34 (m, 2H, Ar-H), 7.36-7.40 (m, 3H, Ar-H); ¹³C NMR (100 MHz, CDCl₃): δ = 40.6 (C-3), 67.6 (OCH₂Ph), 71.4 (C-2), 127.0, 128.5, 128.75, 128.77, 128.80, 129.7, 135.1, 136.2 (12C, Ar-C), 174.1 (C=O); ESI-MS: *m/z*: Calcd for C₁₆H₁₆O₃ [M+Na]⁺: 279.1, found: 279.1.

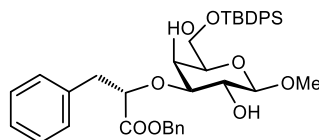
The analytical data of **47** were in accordance with reported values.⁷⁹

Benzyl (*R*)-(+)-3-phenyl-2-(trifluoromethylsulfonyloxy)-propanoate (**48**).



Compound **47** (2.81 g, 0.011 mol) was dissolved in dry DCM (43 mL) under argon. Then, 2,6-lutidine (2.55 mL, 0.022 mol) was added, the mixture was cooled down to -15 °C and triflic anhydride (2.76 mL, 0.016 mol) was added. The reaction was stirred at -20 °C for 4 h. Then, it was diluted with DCM (40 mL), washed with cold water (2 × 40 mL) and brine (3 × 40 mL), dried over Na₂SO₄ and concentrated under reduced pressure. The residue was purified by flash chromatography (hexane/EtOAc, 20:1 → 9:1) to afford **48** (3.56 g, 83%) as a yellow oil. $[\alpha]_D^{20} +1.2$ (*c* 1.0, CHCl₃); ¹H NMR (400 MHz, CDCl₃): δ = 3.18 (dd, *J* = 8.5, 14.6 Hz, 1H, H-3a), 3.32 (dd, *J* = 4.3, 14.6 Hz, 1H, H-3b), 5.22 (s, 2H, OCH₂Ph), 5.26 (dd, *J* = 4.3, 8.4 Hz, 1H, H-2), 7.13-7.17 (m, 2H, Ar-H), 7.22-7.38 (m, 8H, Ar-H); ¹³C NMR (100 MHz, CDCl₃): δ = 38.3 (C-3), 68.5 (OCH₂Ph), 83.9 (C-2), 118.3 (q, *J* = 319.7 Hz, CF₃), 128.0, 128.7, 128.86, 128.96, 129.01, 129.6, 133.3, 134.4 (12C, Ar-C), 166.6 (C=O).

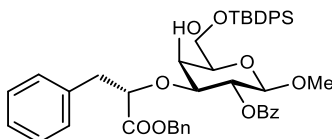
Methyl 3-*O*-[(1*S*)-1-benzyloxycarbonyl-2-phenyl-ethyl]-6-*O*-*tert*-butyldiphenylsilyl- β -D-galactopyranoside (**49c**).



To a solution of **4** (100 mg, 0.230 mmol) in dry MeOH (2 mL) was added Bu₂SnO (63.3 mg, 0.250 mmol) at rt under argon atmosphere. The reaction mixture was heated to reflux for 3 h, then the solvent was evaporated and the residue dried under vacuum for 4 h. The crude product was dissolved

in dry DME (2 mL) and stirred at rt under argon atmosphere. A solution of **48** (134 mg, 0.345 mmol) in dry DME (2 mL) was added dropwise, followed by CsF (42.0 mg, 0.276 mmol) at once, after being dried at 70°C under vacuum for 30 min. The reaction mixture was stirred for 16 h. Then, EtOAc (10 mL) and H₂O (10 mL) were added and the aqueous phase was extracted with EtOAc (3 × 10 mL). The organic phase was dried over Na₂SO₄, filtered and evaporated. The crude material was purified by flash column chromatography (petroleum ether/acetone, 9:1 → 8:2) to afford **49c** (36 mg, 24%) as a yellow oil. $[\alpha]_D^{20}$ -23.4 (*c* 1.0, CHCl₃); ¹H NMR (400 MHz, CDCl₃): δ = 1.04 (s, 9H, C(CH₃)₃), 2.96 (dd, *J* = 10.3, 13.9 Hz, 1H, H-2'a), 3.05 (dd, *J* = 3.3, 9.2 Hz, 1H, H-3), 3.20 (dd, *J* = 3.8, 13.9 Hz, 1H, H-2'b), 3.41 (m, 1H, H-5), 3.44 (s, 3H, OMe), 3.64 (dd, *J* = 7.8, 9.1 Hz, 1H, H-2), 3.84 (m, 1H, H-4), 3.86-3.93 (m, 2H, H-6), 4.01 (d, *J* = 7.8 Hz, 1H, H-1), 4.27 (dd, *J* = 3.7, 10.3 Hz, 1H, H-1'), 5.13 (d, *J* = 12.0 Hz, 1H, OCH₂Ph), 5.22 (d, *J* = 12.1 Hz, 1H, OCH₂Ph), 7.30-7.44 (m, 16H, Ar-H), 7.65-7.70 (m, 4H, Ar-H); ¹³C NMR (100 MHz, CDCl₃): δ = 19.4 (C(CH₃)₃), 26.9 (C(CH₃)₃), 39.8 (C-2'), 56.7 (OMe), 62.8 (C-6), 66.2 (C-4), 67.6 (OCH₂Ph), 70.7 (C-2), 74.7 (C-5), 80.6 (C-1'), 85.3 (C-3), 103.4 (C-1), 127.5, 127.8, 128.7, 128.86, 128.88, 129.0, 129.3, 129.82, 129.84, 133.5, 133.6, 135.0, 135.7, 135.8, 137.0 (24C, Ar-C), 173.4 (C=O); ESI-MS: *m/z*: Calcd for C₃₉H₄₆O₈Si [M+Na]⁺: 693.3, found: 693.3.

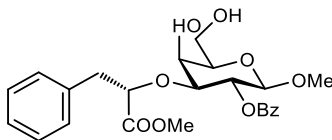
Methyl 2-O-benzoyl-3-O-[(1S)-1-benzyloxycarbonyl-2-phenyl-ethyl]-6-O-tert-butylidiphenylsilyl-β-D-galactopyranoside (50c).



To a solution of **49c** (0.346 g, 0.516 mmol) in pyridine (6.0 mL) were added DMAP (0.038 g, 0.309 mmol) at once and Bz₂O (1.50 g, 6.71 mmol) portionwise at 0 °C. The mixture was warmed to rt and stirred for 16 h and then the solvent was removed via co-evaporation with toluene. The crude product was dissolved in EtOAc (20 mL), washed with H₂O (3 × 10 mL), aq. satd. CuSO₄ (3 × 10 mL), H₂O (10 mL) and brine (10 mL). The organic phase was dried over Na₂SO₄, filtered and evaporated. The crude product was purified by flash column chromatography (petroleum ether/acetone, 9:1) to give impure **50c** which was used for the next step without further purification. ¹H NMR (400 MHz, CDCl₃): δ = 1.06 (s, 9H, C(CH₃)₃), 2.87 (dd, *J* = 7.3, 14.2 Hz, 1H, H-2'), 2.93 (dd, *J* = 5.1, 14.1 Hz, 1H, H-2'), 3.41 (s, 3H, OMe), 3.51-3.55 (m, 2H, H-3, H-5), 3.90-3.97 (m, 2H, H-6), 3.98 (m, 1H, H-4), 4.21 (dd, *J* = 5.0, 7.2 Hz, 1H, H-1'), 4.35 (d, *J* = 8.0 Hz, 1H, H-1), 5.03 (d, *J* = 12.0 Hz, 1H, OCH₂Ph), 5.12 (d, *J* = 12.0 Hz, 1H, OCH₂Ph), 5.48 (dd, *J* = 8.1, 9.6 Hz, 1H, H-2), 7.37-7.44 (m,

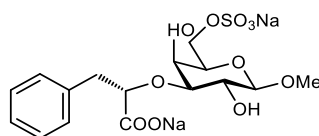
10H, Ar-H), 7.60-7.61 (m, 8H, Ar-H), 7.64-7.65 (m, 5H, Ar-H), 7.68-7.72 (m, 4H, Ar-H); ESI-MS: m/z : Calcd for $C_{46}H_{50}O_9Si$ $[M+K]^+$: 813.4, found: 813.3.

Methyl 2-O-benzoyl-3-O-[(1S)-1-methoxycarbonyl-2-phenyl-ethyl]- β -D-galactopyranoside (51c).



To a solution of crude **50c** (183 mg, 0.236 mmol) in pyridine (3.40 mL) in a Teflon container was added HF-pyr (2.40 mL) dropwise and the reaction mixture was stirred at rt for 2.5 h. The reaction was neutralized with aq. satd. $NaHCO_3$ and the aqueous phase was extracted with DCM (3×20 mL). Then, the solution was dried over Na_2SO_4 and concentrated under reduced pressure. The crude product was purified by flash chromatography (petroleum ether/acetone, 8:2 \rightarrow 7:3). During the reaction a *trans*-esterification occurred, leading to a mix of benzyl and methyl ester. The purification afforded the clean methyl ester **51c** (40 mg, 40%) as a white solid. $[\alpha]_D^{20} +4.8$ (c 0.4, $CHCl_3$); 1H NMR (400 MHz, $CDCl_3$): δ = 2.88 (dd, J = 7.4, 14.0 Hz, 1H, H-2'a), 2.95 (dd, J = 4.3, 14.0 Hz, 1H, H-2'b), 3.45 (s, 3H, OMe), 3.53-3.60 (m, 2H, H-3, H-5), 3.72 (s, 3H, COOMe), 3.86 (m, 1H, H-6a), 3.98 (m, 1H, H-4), 4.03 (dd, J = 6.6, 11.7 Hz, 1H, H-6b), 4.21 (dd, J = 4.4, 7.2 Hz, 1H, H-1'), 4.40 (d, J = 8.0 Hz, 1H, H-1), 5.48 (m, 1H, H-2), 6.89-7.02 (m, 6H, Ar-H), 7.21-7.33 (m, 4H, Ar-H), 7.43-7.46 (m, 2H, Ar-H), 7.59 (m, 1H, Ar-H), 7.97 (d, J = 7.4 Hz, 2H, Ar-H); ^{13}C NMR (126 MHz, $CDCl_3$): δ = 39.8 (C-2'), 52.6 (COOMe), 56.6 (OMe), 62.7 (C-6), 67.7 (C-4), 71.2 (C-2), 74.3 (C-5), 80.5 (C-1'), 82.0 (C-3), 102.2 (C-1), 126.8, 128.4, 128.5, 129.2, 130.0, 130.2, 133.2, 136.1 (12C, Ar-C), 165.3, 173.7 (2C, C=O); ESI-MS: m/z : Calcd for $C_{24}H_{28}O_9$ $[M+Na]^+$: 483.2, found: 483.1.

Methyl 3-O-[(1S)-1-carboxy-2-phenyl-ethyl]-6-O-sulfonato- β -D-galactopyranoside (54).



To a solution of **51c** (60 mg, 0.13 mmol) in DMF (4 mL) was added SO_3 pyr (207 mg, 1.30 mmol) at 0 °C. The reaction was then stirred at rt under argon atmosphere. After 5 h, $NaHCO_3$ (200 mg) was added and the reaction was stirred for another hour. The mixture was then filtrated over celite and concentrated under reduced pressure. Purification of the residue by flash chromatography (DCM/MeOH, 1:0 \rightarrow 9:1) did not afford a clean product, because the sulfate also attached in position 4, therefore the substance was dissolved in NaOH solution (0.1 M, H_2O /dioxane 1:1, 13 mL) and stirred

for 2 d. The conversion of the hydrolysis reaction was quantitative but the difficult purification, due to impurities from the previous steps, afforded **54** only with a low yield (2 mg, 3% over two steps). $[\alpha]_{\text{D}}^{20} -0.54$ (*c* 0.2, CHCl_3); $^1\text{H NMR}$ (400 MHz, D_2O): $\delta = 3.14$ (dd, $J = 7.0, 14.1$ Hz, 1H, H-2'a), 3.22 (dd, $J = 5.7, 14.0$ Hz, 1H, H-2'b), 3.54 (dd, $J = 3.1, 9.7$ Hz, 1H, H-3), 3.56 (s, 3H, OMe), 3.59 (dd, $J = 7.7, 9.7$ Hz, 1H, H-2), 3.89 (m, 1H, H-5), 4.12 (m, 1H, H-4), 4.18-4.21 (m, 2H, H-6), 4.31 (d, $J = 7.6$ Hz, 1H, H-1), 4.55 (dd, $J = 5.8, 6.9$ Hz, 1H, H-1'), 7.32-7.42 (m, 5H, Ar-H); $^{13}\text{C NMR}$ (126 MHz, D_2O): $\delta = 38.4$ (C-2'), 57.3 (OMe), 66.3 (C-4), 67.2 (C-6), 70.0 (C-2), 72.5 (C-5), 79.8 (C-1'), 81.7 (C-3), 103.6 (C-1), 127.2, 128.8, 129.7, 136.7 (6C, Ar-C), 178.5 (C=O); HR-MS: *m/z*: Calcd for $\text{C}_{16}\text{H}_{20}\text{Na}_2\text{O}_{11}\text{S}$ $[\text{M}+\text{Na}]^+$: 489.0419, found: 489.0419; HPLC purity: 88%.

Microscale thermophoresis. Microscale thermophoresis experiments were performed using a Monolith NT.115 instrument (Nanotemper, Munich, Germany) set to 25 °C, 50% LED power, and “medium” MST power. The Nanotemper MO. Affinity Analysis software suite was employed for analysis and nonlinear fitting of experimental data. In a typical experiment, a serial ligand dilution starting at 15 mM or 30 mM was incubated with an equal volume of 160 nM FITC-labeled Siglec-8-CRD and measured directly using the green channel of the instrument. Experiments were performed in triplicates.

Isothermal titration calorimetry. Isothermal titration calorimetric experiments were performed on an ITC200 instrument (MicroCal, Northampton, USA) at 25 °C using standard instrument settings (reference power 6 $\mu\text{cal s}^{-1}$, stirring speed 750 rpm, feedback mode high, filter period 2 s). Protein solutions were dialyzed against ITC buffer (20 mM HEPES, 150 mM NaCl, pH 7.4) prior to the experiments and all samples were prepared using the dialysate buffer to minimize dilution effects. Protein concentrations were determined spectrophotometrically with the specific absorbance at 280 nm employing an extinction coefficient of 33240 $\text{mol}^{-1} \text{cm}^{-1}$. Binding affinities of Siglec-8 ligands in the μM to mM range necessitated a low *c* titration setup. In a typical experiment, a 25 mM ligand solution was titrated to a solution containing 40 μM Siglec-8 to ensure >70% saturation. Baseline correction, peak integration, and non-linear regression analysis of experimental data was performed using the NITPIC (version 1.2.2.)⁸⁰ and SEDPHAT (version 12.1b)⁸¹ software packages. The stoichiometry parameter was manually constrained to a value of 1. Experiments were performed in duplicate and the 68% confidence intervals from global fitting of two experiments were calculated as an estimate of experimental error. For kinITC analysis, the AFFINImeter software suite (v2.1802.5, Software for Science Developments, Santiago de Compostela, Spain) was used. Raw ITC data was fit to a thermodynamic model assuming a stoichiometry of 1 to derive K_A . Dissociation rates were

then determined from a fit of the equilibration time curve to a 1:1 interaction model. Association rate constants were calculated from K_A and k_{off} according to the equation:

$$k_{on} = K_A \times k_{off} = \frac{k_{off}}{K_D}$$

Errors in rate constants are given as the 68% standard error of the fit for a single experiment.

Nano Differential Scan Fluorimetry. Differential scanning fluorimetry assays were performed using a Prometheus NT.48 (Nanotemper, Munich, Germany) instrument set to 50 % excitation power and 1.0 °C/min temperature slope. The Nanotemper Pr.ThermControl software suite was employed for analysis of experimental data. In a typical experiment, a 20 µM solution of Siglec-8-CRD was incubated alone or with 1 mM solution of ligand and measured over a temperature range from 20 to 80 °C.

2.5 References.

- (1) Kroezen, B. S.; Conti, G.; Girardi, B.; Cramer, J.; Jiang, X.; Rabbani, S.; Müller, J.; Kokot, M.; Luisoni, E.; Ricklin, D.; Schwardt, O.; Ernst, B. A Potent Mimetic of the Siglec-8 Ligand 6'-Sulfo-Sialyl Lewis^x. *ChemMedChem* **2020**, *15* (18), 1706–1719. <https://doi.org/10.1002/cmdc.202000417>.
- (2) Crocker, P. R.; Paulson, J. C.; Varki, A. Siglecs and Their Roles in the Immune System. *Nat. Rev. Immunol.* **2007**, *7* (4), 255–266. <https://doi.org/10.1038/nri2056>.
- (3) Varki, A.; Angata, T. Siglecs - the Major Subfamily of I-Type Lectins. *Glycobiology* **2006**, *16* (1), 1–27. <https://doi.org/10.1093/glycob/cwj008>.
- (4) Macauley, M. S.; Crocker, P. R.; Paulson, J. C. Siglec-Mediated Regulation of Immune Cell Function in Disease. *Nat. Rev. Immunol.* **2014**, *14* (10), 653–666. <https://doi.org/10.1038/nri3737>.
- (5) Ravetch, J. V.; Lanier, L. L. Immune Inhibitory Receptors. *Science* **2000**, *290* (5489), 84–89. <https://doi.org/10.1126/science.290.5489.84>.
- (6) Crocker, P. R.; Redelinghuys, P. Siglecs as Positive and Negative Regulators of the Immune System. *Biochem. Soc. Trans.* **2008**, *36* (Pt 6), 1467–1471. <https://doi.org/10.1042/BST0361467>.
- (7) Paulson, J. C.; MacAuley, M. S.; Kawasaki, N. Siglecs as Sensors of Self in Innate and Adaptive Immune Responses. *Ann. N. Y. Acad. Sci.* **2012**, *1253* (1), 36–48. <https://doi.org/10.1111/j.1749-6632.2011.06362.x>.
- (8) Collins, B. E.; Blixt, O.; DeSieno, A. R.; Bovin, N.; Marth, J. D.; Paulson, J. C. Masking of CD22 by Cis Ligands Does Not Prevent Redistribution of CD22 to Sites of Cell Contact. *Proc. Natl. Acad. Sci. U. S. A.* **2004**, *101* (16), 6104–6109. <https://doi.org/10.1073/pnas.0400851101>.
- (9) Collins, B. E.; Blixt, O.; Han, S.; Duong, B.; Li, H.; Nathan, J. K.; Bovin, N.; Paulson, J. C. High-Affinity Ligand Probes of CD22 Overcome the Threshold Set by Cis Ligands to Allow for Binding,

- Endocytosis, and Killing of B Cells. *J. Immunol.* **2006**, *177* (5), 2994–3003. <https://doi.org/10.4049/jimmunol.177.5.2994>.
- (10) Kikly, K. K.; Bochner, B. S.; Freeman, S. D.; Tan, K. B.; Gallagher, K. T.; D’Alessio, K. J.; Holmes, S. D.; Abrahamson, J. A.; Erickson-Miller, C. L.; Murdock, P. R.; Tachimoto, H.; Schleimer, R. P.; White, J. R. Identification of SAF-2, a Novel Siglec Expressed on Eosinophils, Mast Cells, and Basophils. *J. Allergy Clin. Immunol.* **2000**, *105* (6 Pt 1), 1093–1100. <https://doi.org/10.1067/mai.2000.107127>.
- (11) Floyd, H.; Ni, J.; Cornish, A. L.; Zeng, Z.; Liu, D.; Carter, K. C.; Steel, J.; Crocker, P. R. Siglec-8 - A Novel Eosinophil-Specific Member of the Immunoglobulin Superfamily. *J. Biol. Chem.* **2000**, *275* (2), 861–866. <https://doi.org/10.1074/jbc.275.2.861>.
- (12) Barnes, P. J. Immunology of Asthma and Chronic Obstructive Pulmonary Disease. *Nat. Rev. Immunol.* **2008**, *8* (3), 183–192. <https://doi.org/10.1038/nri2254>.
- (13) Fahy, J. V. Type 2 Inflammation in Asthma-Present in Most, Absent in Many. *Nat. Rev. Immunol.* **2015**, *15* (1), 57–65. <https://doi.org/10.1038/nri3786>.
- (14) Nutku, E.; Aizawa, H.; Hudson, S. A.; Bochner, B. S. Ligation of Siglec-8 : A Selective Mechanism for Induction of Human Eosinophil Apoptosis. *Blood* **2003**, *101* (12), 5014–5020. <https://doi.org/10.1182/blood-2002-10-3058>.
- (15) Yokoi, H.; Choi, O. H.; Hubbard, W.; Lee, H.; Canning, B. J.; Lee, H. H.; Ryu, S.; von Gunten, S.; Bickel, C. A.; Hudson, S. A.; Macglashan, D. W.; Bochner, B. S. Inhibition of FcεRI-Dependent Mediator Release and Calcium Flux from Human Mast Cells by Sialic Acid-Binding Immunoglobulin-like Lectin 8 Engagement. *J. Allergy Clin. Immunol.* **2008**, *121* (2), 499–506. <https://doi.org/10.1016/j.jaci.2007.10.004>.
- (16) Angata, T.; Nycholat, C. M.; Macauley, M. S. Therapeutic Targeting of Siglecs Using Antibody- and Glycan-Based Approaches. *Trends Pharmacol. Sci.* **2015**, *36* (10), 645–660. <https://doi.org/10.1016/j.tips.2015.06.008>.
- (17) Hudson, S. A.; Bovin, N. V.; Schnaar, R. L.; Crocker, P. R.; Bochner, B. S. Eosinophil-Selective Binding and Proapoptotic Effect in Vitro of a Synthetic Siglec-8 Ligand , Polymeric 6'-Sulfated Sialyl Lewis^x. *J. Pharmacol. Exp. Ther.* **2009**, *330* (2), 608–612. <https://doi.org/10.1124/jpet.109.152439.2007>.
- (18) Jia, Y.; Yu, H.; Fernandes, S. M.; Wei, Y.; Gonzalez-gil, A.; Bochner, B. S.; Kern, R. C.; Schleimer, R. P.; Schnaar, R. L. Expression of Ligands for Siglec-8 and Siglec-9 in Human Airways and Airway Cells. *J. Allergy Clin. Immunol.* **2015**, *135* (3), 799–810. <https://doi.org/10.1016/j.jaci.2015.01.004>.
- (19) von Gunten, S.; Vogel, M.; Schaub, A.; Stadler, B. M.; Miescher, S.; Crocker, P. R. Intravenous Immunoglobulin Preparations Contain Anti-Siglec-8 Autoantibodies. *J. Allergy Clin. Immunol.* **2007**, *119* (4), 1005–1011. <https://doi.org/10.1016/j.jaci.2007.01.023>.
- (20) Gao, P.; Shimizu, K.; Grant, A. V.; Rafaels, N.; Zhou, L.; Hudson, S. A.; Konno, S.; Zimmermann, N.; Araujo, M. I.; Ponte, E. V.; Cruz, A. A.; Nishimura, M.; Su, S.; Hizawa, N.; Beaty, T. H.; Mathias, R.

- A.; Rothenberg, M. E.; Barnes, K. C.; Bochner, B. S. Polymorphisms in the Sialic Acid-Binding Are Associated with Susceptibility to Asthma. *Eur. J. Hum. Genet.* **2010**, *18* (6), 713–719. <https://doi.org/10.1038/ejhg.2009.239>.
- (21) Kiwamoto, T.; Kawasaki, N.; Paulson, J. C.; Bochner, B. S. Siglec-8 as a Drugable Target to Treat Eosinophil and Mast Cell-Associated Conditions. *Pharmacol. Ther.* **2012**, *135* (3), 327–336. <https://doi.org/10.1016/j.pharmthera.2012.06.005>.
- (22) Farid, S. S.; Mirshafiey, A.; Razavi, A. Siglec-8 and Siglec-F, the New Therapeutic Targets in Asthma. **2012**, *34* (5), 721–726. <https://doi.org/10.3109/08923973.2011.589453>.
- (23) Legrand, F.; Cao, Y.; Wechsler, J.; Zhu, X.; Zimmermann, N.; Rampertaap, S.; Monsale, J.; Romito, K.; Youngblood, B. A.; Brock, E. C.; Makiya, M.; Tomasevic, N.; Bebbington, C.; Maric, I.; Metcalfe, D. D.; Bochner, B. S.; Klion, A. D. Siglec-8 in Eosinophilic Disorders: Receptor Expression and Targeting Using Chimeric Antibodies. *J. Allergy Clin. Immunol.* **2019**, *143* (6), 2227–2237. <https://doi.org/10.1016/j.jaci.2018.10.066>.
- (24) Simon, D.; Simon, H. U. Therapeutic Strategies for Eosinophilic Dermatoses. *Curr. Opin. Pharmacol.* **2019**, *46*, 29–33. <https://doi.org/10.1016/j.coph.2019.01.002>.
- (25) O’Sullivan, J. A.; Carroll, D. J.; Cao, Y.; Salicru, A. N.; Bochner, B. S. Leveraging Siglec-8 Endocytic Mechanisms to Kill Human Eosinophils and Malignant Mast Cells. *J. Allergy Clin. Immunol.* **2018**, *141* (5), 1774-1785.e7. <https://doi.org/10.1016/j.jaci.2017.06.028>.
- (26) Lee, R. T.; Lee, Y. C. Affinity Enhancement by Multivalent Lectin-Carbohydrate Interaction. *Glycoconj. J.* **2000**, *17* (7–9), 543–551. <https://doi.org/10.1023/a:1011070425430>.
- (27) Dam, T. K.; Gerken, T. A.; Brewer, C. F. Thermodynamics of Multivalent Carbohydrate-Lectin Cross-Linking Interactions: Importance of Entropy in the Bind and Jump Mechanism. *Biochemistry* **2009**, *48* (18), 3822–3827. <https://doi.org/10.1021/bi9002919>.
- (28) Zaccai, N. R.; Maenaka, K.; Maenaka, T.; Crocker, P. R.; Brossmer, R.; Kelm, S.; Jones, E. Y. Structure-Guided Design of Sialic Acid-Based Siglec Inhibitors and Crystallographic Analysis in Complex with Sialoadhesin. *Structure* **2003**, *11* (5), 557–567. [https://doi.org/10.1016/S0969-2126\(03\)00073-X](https://doi.org/10.1016/S0969-2126(03)00073-X).
- (29) Mesch, S.; Lemme, K.; Wittwer, M.; Koliwer-brandl, H. From a Library of MAG Antagonists to Nanomolar CD22. *ChemMedChem* **2012**, *7* (1), 134–143. <https://doi.org/10.1002/cmdc.201100407>.
- (30) Kelm, S.; Gerlach, J.; Brossmer, R.; Danzer, C.; Nitschke, L. The Ligand-Binding Domain of CD22 Is Needed for Inhibition of the B Cell Receptor Signal, as Demonstrated by a Novel Human CD22-Specific Inhibitor Compound. *J. Exp. Med.* **2002**, *195* (9), 1207–1213. <https://doi.org/10.1084/jem.20011783>.
- (31) Abdu-allah, H. H. M.; Watanabe, K.; Completo, G. C.; Sadagopan, M.; Hayashizaki, K.; Takaku, C.; Tamanaka, T.; Takematsu, H.; Kozutsumi, Y.; Paulson, J. C.; Tsubata, T.; Ando, H.; Ishida, H.; Kiso, M. CD22-Antagonists with Nanomolar Potency : The Synergistic Effect of Hydrophobic Groups at C-2 and C-9 of Sialic Acid Scaffold. *Bioorg. Med. Chem.* **2011**, *19* (6), 1966–1971.

- <https://doi.org/10.1016/j.bmc.2011.01.060>.
- (32) Mesch, S.; Moser, D.; Strasser, D. S.; Kelm, A.; Cutting, B.; Rossato, G.; Vedani, A.; Koliwer-brandl, H.; Wittwer, M.; Rabbani, S.; Schwarzt, O.; Kelm, S.; Ernst, B. Low Molecular Weight Antagonists of the Myelin-Associated Glycoprotein : Synthesis , Docking , and Biological Evaluation. *J. Med. Chem.* **2010**, *53*(4), 1597–1615. <https://doi.org/10.1021/jm901517k>.
- (33) Shelke, S. V.; Gao, G.; Mesch, S.; Ga, H. Synthesis of Sialic Acid Derivatives as Ligands for The Myelin-Associated glycoprotein (MAG). *Bioorg. Med. Chem.* **2007**, *15* (14), 4951–4965. <https://doi.org/10.1016/j.bmc.2007.04.038>.
- (34) Prescher, H.; Frank, M.; Gütgemann, S.; Kuhfeldt, E.; Schweizer, A.; Nitschke, L.; Watzl, C.; Brossmer, R. Design, Synthesis, and Biological Evaluation of Small, High-Affinity Siglec-7 Ligands: Toward Novel Inhibitors of Cancer Immune Evasion. *J. Med. Chem.* **2017**, *60* (3), 941–956. <https://doi.org/10.1021/acs.jmedchem.6b01111>.
- (35) Nycholat, C. M.; Duan, S.; Knuplez, E.; Worth, C.; Elich, M.; Yao, A.; O’Sullivan, J.; McBride, R.; Wei, Y.; Fernandes, S. M.; Zhu, Z.; Schnaar, R. L.; Bochner, B. S.; Paulson, J. C. A Sulfonamide Sialoside Analogue for Targeting Siglec-8 and-F on Immune Cells. *J. Am. Chem. Soc.* **2019**, *141* (36), 14032–14037. <https://doi.org/10.1021/jacs.9b05769>.
- (36) Bochner, B. S.; Alvarez, R. A.; Mehta, P.; Bovin, N. V.; Blixt, O.; White, J. R.; Schnaar, R. L. Glycan Array Screening Reveals a Candidate Ligand for Siglec-8. *J. Biol. Chem.* **2005**, *280* (6), 4307–4312. <https://doi.org/10.1074/jbc.M412378200>.
- (37) Tateno, H.; Crocker, P. R.; Paulson, J. C. Mouse Siglec-F and Human Siglec-8 Are Functionally Convergent Paralogs That Are Selectively Expressed on Eosinophils and Recognize 6'-Sulfo-Sialyl Lewis^x as a Preferred Glycan Ligand. *Glycobiology* **2005**, *15* (11), 1125–1135. <https://doi.org/10.1093/glycob/cwi097>.
- (38) Yu, H. F.; Gonzalez-Gil, A.; Wei, Y. D.; Fernandes, S. M.; Porell, R. N.; Vajn, K.; Paulson, J. C.; Nycholat, C. M.; Schnaar, R. L. Siglec-8 and Siglec-9 Binding Specificities and Endogenous Airway Ligand Distributions and Properties. *Glycobiology* **2017**, *27* (7), 657–668. <https://doi.org/10.1093/glycob/cwx026>.
- (39) Pröpster, J. M.; Yang, F.; Rabbani, S.; Ernst, B.; Allain, F. H.; Schubert, M. Structural Basis for Sulfation-Dependent Self-Glycan Recognition by the Human Immune-Inhibitory Receptor Siglec-8. *Proc. Natl. Acad. Sci.* **2016**, *113* (29), E4170–E4179. <https://doi.org/10.1073/pnas.1602214113>.
- (40) VIDA version 4.2.1. OpenEye Scientific Software, Santa Fe, NM. <http://www.eyesopen.com>.
- (41) Functional Glycomics Gateway, **2010**. Available at: http://www.functionalglycomics.org/glycomics/HServlet?operation=view&sideMenu=no&psId=primscreen_5605.
- (42) Chao, C. S.; Chen, M. C.; Lin, S. C.; Mong, K. K. T. Versatile Acetylation of Carbohydrate Substrates with Bench-Top Sulfonic Acids and Application to One-Pot Syntheses of Peracetylated Thioglycosides. *Carbohydr. Res.* **2008**, *343* (5), 957–964. <https://doi.org/10.1016/j.carres.2008.01.014>.
- (43) Dubey, R.; Reynolds, D.; Abbas, S.; Matta, K. Synthesis of O-Alpha-L-Fucopyranosyl-(1-3)-O-Beta-

- D-Galactopyranosyl-(1-4)-2-Acetamido-2-Deoxy-D-Glucopyranose (N-Acetyl-3'-O-Alpha-L-Fucopyranosyllactosamine). *Carbohydr. Res.* **1988**, *183* (2), 155–162. [https://doi.org/10.1016/0008-6215\(88\)84070-9](https://doi.org/10.1016/0008-6215(88)84070-9).
- (44) Rabbani, S.; Jiang, X.; Schwardt, O.; Ernst, B. Expression of the Carbohydrate Recognition Domain of FimH and Development of a Competitive Binding Assay. *Anal. Biochem.* **2010**, *407* (2), 188–195. <https://doi.org/10.1016/j.ab.2010.08.007>.
- (45) Carter, T. S.; Mooibroek, T. J.; Stewart, P. F. N.; Crump, M. P.; Galan, M. C.; Davis, A. P. Platform Synthetic Lectins for Divalent Carbohydrate Recognition in Water. *Angew. Chemie - Int. Ed. English* **2016**, *55* (32), 9311–9315. <https://doi.org/10.1002/anie.201603082>.
- (46) Hendlich, M.; Bergner, A.; Gunther, J.; Klebe, G. Relibase: Design and Development of a Database for Comprehensive Analysis of Protein-Ligand Interactions. *J. Mol. Biol.* **2003**, *326* (2), 607–620. [https://doi.org/10.1016/s0022-2836\(02\)01408-0](https://doi.org/10.1016/s0022-2836(02)01408-0).
- (47) Meanwell, N. A. Synopsis of Some Recent Tactical Application of Bioisosteres in Drug Design. *J. Med. Chem.* **2011**, *54* (8), 2529–2591. <https://doi.org/10.1021/jm1013693>.
- (48) Patani, G. A.; LaVoie, E. J. Bioisosterism: A Rational Approach in Drug Design. *Chem. Rev.* **1996**, *96* (8), 3147–3176. <https://doi.org/10.1021/cr950066q>.
- (49) Asmari, M.; Ratih, R.; Alhazmi, H. A.; El Deeb, S. Thermophoresis for Characterizing Biomolecular Interaction. *Methods* **2018**, *146*, 107–119. <https://doi.org/10.1016/j.ymeth.2018.02.003>.
- (50) Jerabek-Willemsen, M.; Wienken, C. J.; Braun, D.; Baaske, P.; Duhr, S. Molecular Interaction Studies Using Microscale Thermophoresis. *Assay Drug Dev. Technol.* **2011**, *9* (4), 342–353. <https://doi.org/10.1089/adt.2011.0380>.
- (51) Srivastava, V. K.; Yadav, R. Isothermal Titration Calorimetry. In *Data Processing Handbook for Complex Biological Data Sources*; Elsevier Inc., 2019.
- (52) Freyer, M. W.; Lewis, E. A. Isothermal Titration Calorimetry : Experimental Design , Data Analysis , and Probing Macromolecule / Ligand Binding and Kinetic Interactions. In *Methods in Cell Biology*; 2008.
- (53) Dam, T. K.; Brewer, C. F. Thermodynamic Studies of Lectin-Carbohydrate Interactions by Isothermal Titration Calorimetry. *Chem. Rev.* **2002**, *102* (2), 387–429. <https://doi.org/10.1021/cr000401x>.
- (54) Kelm, S.; Brossmer, R. Neuraminic Acid Derivatives for Use as Siglec Inhibitors. PCT Patent WO 03/000709A2, 2003.
- (55) Cramer, J.; Sager, C. P.; Ernst, B. Hydroxyl Groups in Synthetic and Natural-Product-Derived Therapeutics: A Perspective on a Common Functional Group. *J. Med. Chem.* **2019**, *62* (20), 8915–8930. <https://doi.org/10.1021/acs.jmedchem.9b00179>.
- (56) Copeland, R. A.; Pompliano, D. L.; Meek, T. D. Drug-Target Residence Time and Its Implications for Lead Optimization. *Nat. Rev. Drug Discov.* **2006**, *5* (9), 730–739. <https://doi.org/10.1038/nrd2082>.
- (57) Dumas, P.; Ennifar, E.; Da Veiga, C.; Bec, G.; Palau, W.; Di Primo, C.; Piñeiro, A.; Sabin, J.; Muñoz, E.; Rial, J. Extending ITC to Kinetics with KinITC. *Methods Enzymol.* **2016**, *567*, 157–180.

<https://doi.org/10.1016/bs.mie.2015.08.026>.

- (58) Zihlmann, P.; Silbermann, M.; Sharpe, T.; Jiang, X.; Mühlethaler, T.; Jakob, R. P.; Rabbani, S.; Sager, C. P.; Frei, P.; Pang, L.; Maier, T.; Ernst, B. KinITC-One Method Supports Both Thermodynamic and Kinetic SARs as Exemplified on FimH Antagonists. *Chem. Eur. J.* **2018**, *24* (49), 13049–13057. <https://doi.org/10.1002/chem.201802599>.
- (59) Hillisch, A.; Pineda, L. F.; Hilgenfeld, R. Utility of Homology Models in the Drug Discovery Process. *Drug Discov. Today* **2004**, *9* (15), 659–669. [https://doi.org/10.1016/S1359-6446\(04\)03196-4](https://doi.org/10.1016/S1359-6446(04)03196-4).
- (60) França, T. C. C. Homology Modeling: An Important Tool for the Drug Discovery. *J. Biomol. Struct. Dyn.* **2015**, *33* (8), 1780–1793. <https://doi.org/10.1080/07391102.2014.971429>.
- (61) Muhammed, M. T.; Aki-Yalcin, E. Homology Modeling in Drug Discovery: Overview, Current Applications, and Future Perspectives. *Chem. Biol. Drug Des.* **2019**, *93* (1), 12–20. <https://doi.org/10.1111/cbdd.13388>.
- (62) Alphey, M. S.; Attrill, H.; Crocker, P. R.; van Aalten, D. M. High Resolution Crystal Structures of Siglec-7. Insights into Ligand Specificity in the Siglec Family. *J. Biol. Chem.* **2003**, *278* (5), 3372–3377. <https://doi.org/10.1074/jbc.M210602200>.
- (63) Kroezen, B. Design, Synthesis and Biological Evaluation of Carbohydrate-Mimetics for Siglec-8: A Novel Target for Asthma, University of Basel, 2017.
- (64) Kolb, H. C.; Ernst, B. Development of Tools for the Design of Selectin Antagonists. *Chem. Eur. J.* **1997**, *3* (10), 1571–1578. <https://doi.org/10.1002/chem.19970031006>.
- (65) OEDocking version 3.0.2. OpenEye Scientific Software, Santa Fe, NM. <http://www.eyesopen.com>.
- (66) Guyon, H.; Boussonnière, A.; Castanet, A. S. Readily Accessible 1,2-Amino Ether Ligands for Enantioselective Intramolecular Carbolithiation. *J. Org. Chem.* **2017**, *82* (9), 4949–4957. <https://doi.org/10.1021/acs.joc.7b00423>.
- (67) Thoma, G.; Kinzy, W.; Bruns, C.; Patton, J. T.; Magnani, J. L.; Banteli, R. Synthesis and Biological Evaluation of a Potent E-Selectin Antagonist. *J. Med. Chem.* **1999**, *42* (23), 4909–4913. <https://doi.org/10.1021/jm990422n>.
- (68) Alexander, C. G.; Wanner, R.; Johnson, C. M.; Breitsprecher, D.; Winter, G.; Duhr, S.; Baaske, P.; Ferguson, N. Novel Microscale Approaches for Easy, Rapid Determination of Protein Stability in Academic and Commercial Settings. *Biochim. Biophys. Acta* **2014**, *1844* (12), 2241–2250. <https://doi.org/10.1016/j.bbapap.2014.09.016>.
- (69) Di Tommaso, P.; Moretti, S.; Xenarios, I.; Orobittg, M.; Montanyola, A.; Chang, J. M.; Taly, J. F.; Notredame, C. T-Coffee: A Web Server for the Multiple Sequence Alignment of Protein and RNA Sequences Using Structural Information and Homology Extension. *Nucleic Acids Res.* **2011**, *39* (Web Server issue), W13–W17. <https://doi.org/10.1093/nar/gkr245>.
- (70) Šali, A.; Blundell, T. L. Comparative Protein Modelling by Satisfaction of Spatial Restraints. *J. Mol. Biol.* **1993**, *234* (3), 779–815. <https://doi.org/10.1006/jmbi.1993.1626>.
- (71) Wiederstein, M.; Sippl, M. J. ProSA-Web: Interactive Web Service for the Recognition of Errors in

- Three-Dimensional Structures of Proteins. *Nucleic Acids Res.* **2007**, *35* (Web Server issue), 407–410. <https://doi.org/10.1093/nar/gkm290>.
- (72) The PyMOL Molecular Graphics System, Version 1.8 Schrödinger, LLC.
- (73) Schrödinger Release 2021-3: Maestro, Schrödinger, LLC, New York, NY, 2021.
- (74) Lee, K. C.; Moon, B. S.; Lee, J. H.; Chung, K. H.; Katzenellenbogen, J. A.; Chi, D. Y. Synthesis and Binding Affinities of Fluoroalkylated Raloxifenes. *Bioorganic Med. Chem.* **2003**, *11* (17), 3649–3658. [https://doi.org/10.1016/S0968-0896\(03\)00362-6](https://doi.org/10.1016/S0968-0896(03)00362-6).
- (75) Wei, P.; Xue, F.; Shi, Y.; Strand, R.; Chen, H.; Yi, T. A Fluoride Activated Methylene Blue Releasing Platform for Imaging and Antimicrobial Photodynamic Therapy of Human Dental Plaque. *Chem. Commun.* **2018**, *54* (93), 13115–13118. <https://doi.org/10.1039/c8cc07410k>.
- (76) Müller, J.; Feifel, S. C.; Schmiederer, T.; Zoicher, R.; Süßmuth, R. D. In Vitro Synthesis of New Cyclodepsipeptides of the PF1022-Type: Probing the α -D-Hydroxy Acid Tolerance of PF1022 Synthetase. *ChemBioChem* **2009**, *10* (2), 323–328. <https://doi.org/10.1002/cbic.200800539>.
- (77) Janssen, S.; Schmidt, R. R. Synthesis of Ganglioside Mimics for Binding Studies with Myelin-Associated Glycoprotein (MAG). *J. Carbohydr. Chem.* **2005**, *24* (4–6), 611–647. <https://doi.org/10.1080/07328300500176312>.
- (78) Thoma, G.; Kinzy, W.; Bruns, C.; Patton, J.; Magnani, J.; Banteli, R. Synthesis and Biological Evaluation of a Potent E-Selectin Antagonist. *J. Med. Chem.* **1999**, *42* (23), 4909–4913. <https://doi.org/10.1021/jm990422n>.
- (79) Kaur, H.; Harris, P.; Little, P.; Brimble, M. A. Total Synthesis of the Cyclic Depsipeptide YM-280193, a Platelet Aggregation Inhibitor. *Org. Lett.* **2015**, *17* (3), 492–495. <https://doi.org/10.1021/ol503507g>.
- (80) Scheuermann, T. H.; Brautigam, C. A. High-Precision, Automated Integration of Multiple Isothermal Titration Calorimetric Thermograms: New Features of NITPIC. *Methods* **2015**, *76*, 87–98. <https://doi.org/10.1016/j.ymeth.2014.11.024>.
- (81) Zhao, H.; Piszczek, G.; Schuck, P. SEDPHAT-A Platform for Global ITC Analysis and Global Multi-Method Analysis of Molecular Interactions. *Methods* **2015**, *76*, 137–148. <https://doi.org/10.1016/j.ymeth.2014.11.012>.

3. Virtual screening for the optimization of the Siglec-8 lead compound

This chapter presents two main virtual screening approaches to target Siglec-8. In the first case, we virtually combined fragments from commercially available libraries to position 5 of the lead compound **34** to explore the close binding pocket. The obtained molecules were docked to Siglec-8 and selected structures were synthesized and tested. Fragments chosen by rational design were also introduced via amide-linkage. In a second virtual screening approach, commercially available libraries were screened against Siglec-8, keeping constant the interactions with the main amino acids. Selected compounds were screened with different assays (MST, ITC & nanoDSF).

Contributions to the project

Benedetta Girardi synthesized and evaluated all the ligands presented in this chapter. She also performed the virtual screenings and homology modeling, with the help and guidance of Dr. Žan Toplak and Assoc. Prof. Dr. Tihomir Tomašič from the University of Ljubljana and PD Dr. Martin Smieško, who also suggested some fragments to be introduced at position 5 of sialic acid via amide-linkage. The protein was produced by Gabriele Conti with the help of PD Dr. Said Rabbani.

3.1 Introduction.

The process of drug development, from the first stages to the market, is extremely complex and requires a lot of time (15-20 years) and money. Combinatorial chemistry and high-throughput screening (HTS) allowed for having access to a large set of molecules that can be easily screened to an equally large number of targets.¹ Next to this, computer-aided drug design (CADD) techniques also contribute to speed up the first stages of drug discovery and help to reduce failures and costs by directing the focus on the most promising compounds. Principally, modeling is based on two separate approaches: ligand-based drug design (LBDD), where a pharmacophore model is built on different known ligands of the target, and structure-based drug design (SBDD) where, knowing the structure of the target, rational design and virtual screening may be useful tools for the identification of potential hits and leads (Figure 1).²⁻⁴

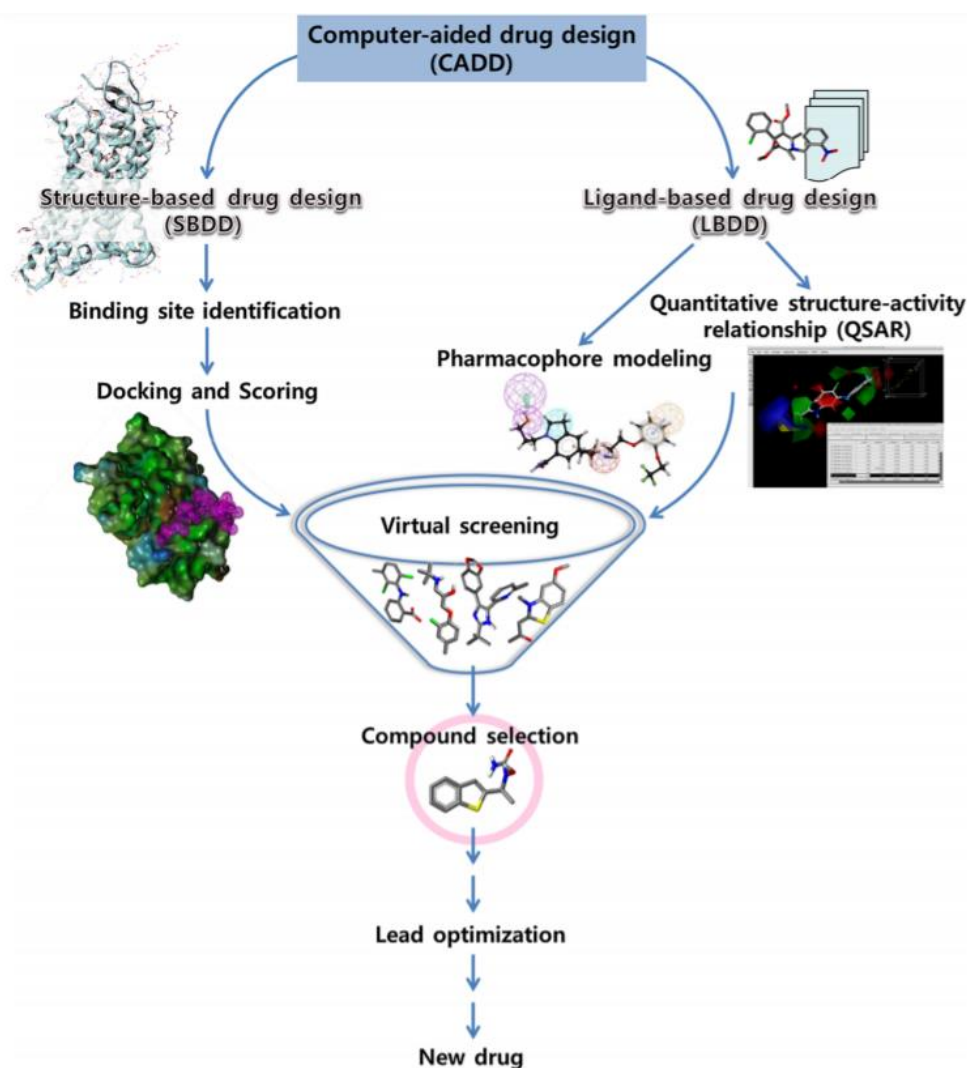


Figure 1. Workflow of computer aided drug design (CADD). Figure from Macalino *et al.*²

Fragment-based drug design (FBDD) is also part of structure-based methods. It consists of the identification of small molecules that can target a specific part of a protein.^{5,6} Virtual screening of sets of libraries allows preselecting the most promising candidates. Usually, fragment hits are characterized by low molecular weight, they can interact with the binding pocket and, being starting points for future optimization, they show high synthetical tractability.^{7,8} One of the rules traditionally used to select fragments is “the rule of three” (MW < 300 Da, clogP < 3 and H-bond acceptor or donor < 3).⁹ Once virtually selected, the fragments should be validated. They usually have low binding affinities, from micromolar to millimolar range, which can be measured by sensitive biophysical methods,¹⁰ such as MST,¹¹ Surface Plasmon Resonance (SPR),¹² DSF¹³ or ITC¹⁴. Different strategies can then be explored to transform hit fragments into a lead: fragment growing, merging (when two different fragments bind to different regions of a pocket they can be merged in one compound) or linking strategies (connecting two fragments binding to different adjacent sites at the same time).⁵

One of the primary methods used in SBDD to evaluate molecules or fragments is molecular docking.¹⁵ Molecular docking programs use different algorithms to predict the conformations adopted by a compound in a protein binding pocket and to evaluate the complementarity with surrounding amino acids. The quality of the so-called “poses” is calculated with different scoring functions.¹⁶ The ideal scoring functions should differentiate and classify ligands based on the lowest binding energies and on the prediction of their potency. However, in spite of the recent advances, more accuracy is needed for the correct correlation between the score and the actual more active ligands.¹⁷ Scoring functions are indeed based on a simplified model of the ligand-protein interactions. For example, proteins are treated as rigid structures, so different conformations of the target or induced-fit effects limit the precision of the docking score functions.^{18,19} The score function is anyway an important reference during the screening of large libraries but it cannot represent the only selection criteria itself.²⁰ For this reason, other methods such as Molecular Dynamics (MD) or visual inspection of the binding mode are crucial points for the most correct choice of a potential hit or in the hit-to-lead optimization process.²¹

In this chapter, we used virtual screening in two different ways: (i) by identifying fragments to explore the empty pocket close to position 5 of the Neu5Ac moiety of our lead compound **34** (Figure 2), and (ii) to screen and identify new potential non-carbohydrate hit molecules. In the first case, available libraries of fragments were first virtually linked to compound **34**, docked and evaluated, while in the second case molecules were directly docked to the Siglec-8 NMR solution structure, using as constraints the two important arginine residues (56 and 109). The fragments and compound **34** analogs were then validated with MST and nanoDSF screening.

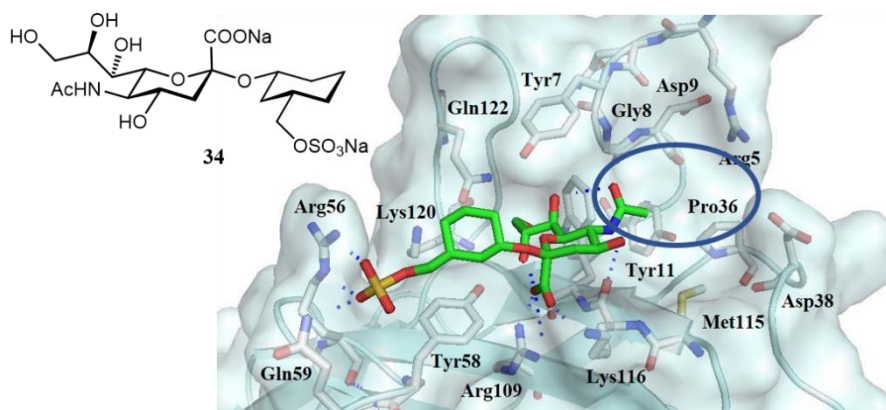


Figure 2. Docking pose of lead compound **34**. Blue circle: empty pocket close to position 5 of Neu5Ac to be explored by fragment screening. Only selected amino acids are presented as sticks. Docking was performed using the FRED algorithm of the OEDocking software (OEDOCKING 3.3.0.2: OpenEye Scientific Software). The figure was generated using the software Pymol.²² Color code: N: blue, O: red, S: yellow, protein backbone: grey, ligand C: green. Contacts with the protein are depicted as blue dashed lines.

3.2 Results and discussion.

Fragment screening for position 5 of lead compound 34. To perform a fragment screening for position 5 of the sialic acid, we applied different commercially available virtual libraries of fragments from different vendors (Chembridge, Enamine, Asinex, KeyOrganics, Pharmeks, Vitas) and, using the KNIME workflow,²³ we virtually combined them with the structure of compound **34**. To do so, we performed *in silico* reactions (reductive amination, coupling, click chemistry and alkylation) to connect the fragments via amide, amine, triazole and ester linkers. Then, the new molecules virtually obtained were docked to the Siglec-8 NMR solution structure.²⁴ Docking was performed using the FRED and HYBRYD algorithms of the OEDocking software.²⁵ At first, we evaluated both positions, 5 and 9, to find the best fragments but, as explained in the first chapter, the NMR solution structure hardly accommodates new fragments in position 9. Therefore, we focused only on position 5 (Figure 3).

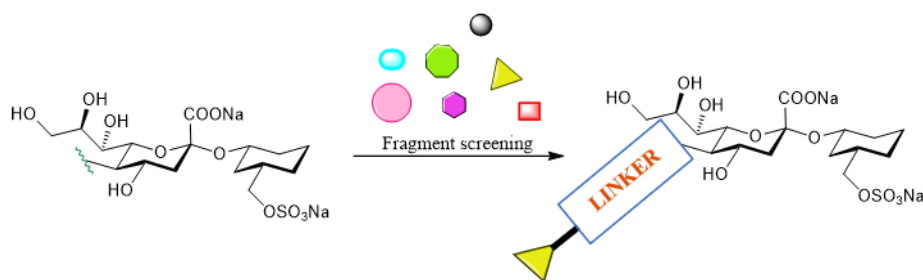


Figure 3. Virtual fragment screening for position 5 of compound **34** and *in silico* reactions.

As constraints, we used the two most important arginine residues that interact with Siglec-8 ligands by forming salt bridges, Arg109 with the carboxylic group of the sialic acid and Arg56 with the sulfate group.²⁴ Docking poses were evaluated with a scoring function and visual inspection, also considering the relative position to the native tetrasaccharide ligand 6'-sulfo-sLe^x (**1b**).

By visualizing the results, we observed that the fragments alone were not involved in many interactions within the binding site, except for a few exceptions (Figure 4).

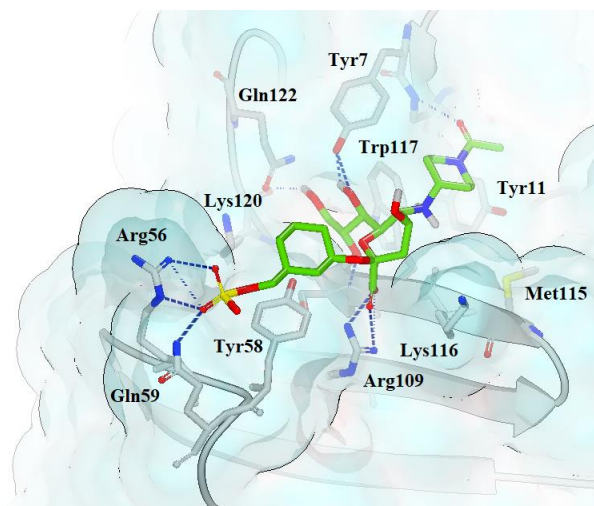


Figure 4. Representative docking pose of compound **34** with a fragment in position 5 identified from the virtual fragment screening. Only selected amino acids are presented as sticks. Docking was performed using the FRED algorithm of the OEDocking software (OEDOCKING 3.3.0.2: OpenEye Scientific Software). The figure was generated using the software VIDA.²⁶ Color code: N: blue, O: red, S: yellow, protein backbone: grey, ligand C: green. Contacts with the protein are depicted as blue dashed lines.

Therefore, we chose suited fragments based on their size and ability to not interfering with the correct pose of compound **34**'s core structure. The only linkers able to preserve the correct position of the core structure were triazole and amine. We therefore selected a few fragments per linker, synthetically linked them to lead compound **34** and evaluated the binding affinity of the resulting compounds to Siglec-8 by MST and nanoDSF.

Synthesis of analogs of compound 34 modified in position 5. The synthesis of the candidate compounds was envisaged starting from two building blocks, the sialic acid donor **73** and the cyclohexyl derivative **74** (Figure 5). As previously mentioned, fragments should be introduced in position 5 via triazole and amine linkers. Therefore, first an azide was introduced in the same position because it is a versatile group that could be directly used for click chemistry reactions and for reductive amination after reduction to amine.

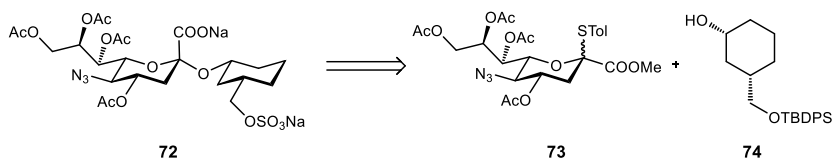
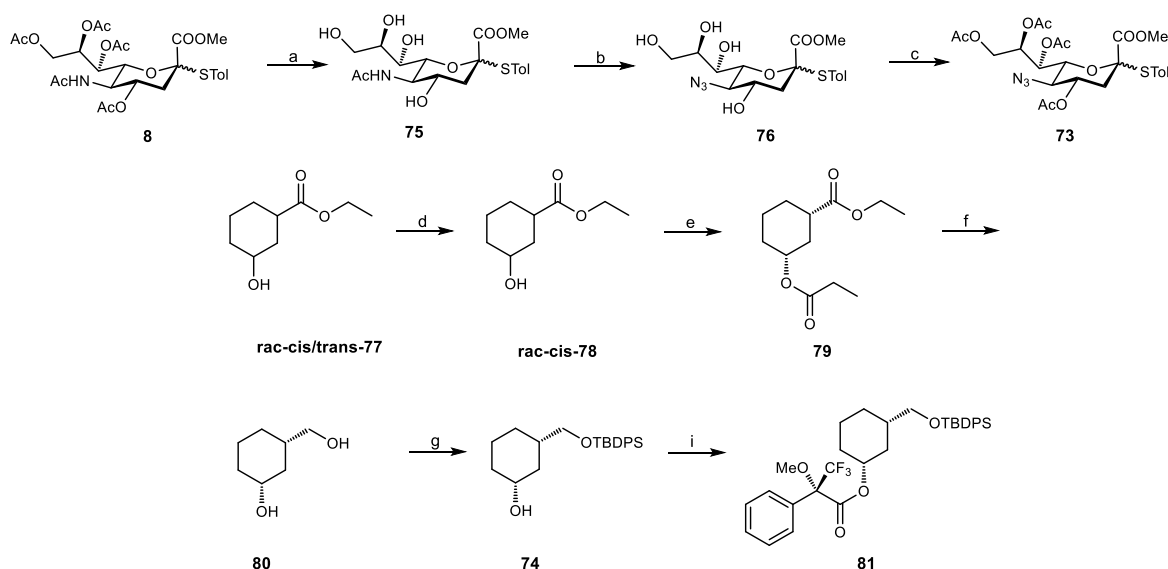


Figure 5. Retrosynthetic scheme for the synthesis of intermediate **72**.

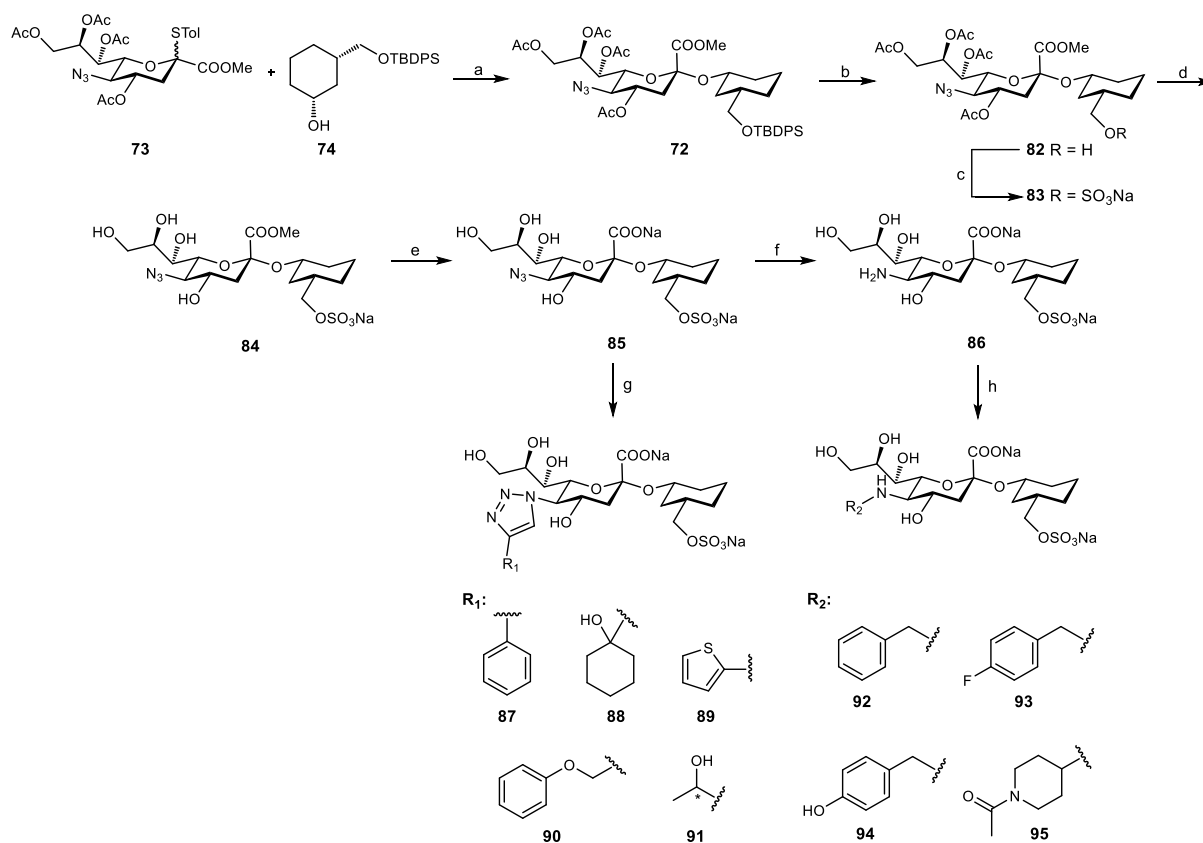
Intermediate **73** was synthesized starting from compound **8**, which first was completely deacetylated in a two-step procedure leaving a free amine in position 5. Reactions that involve azides are particularly dangerous. For this reason, a safer procedure, developed in a previous work in Prof. Ernst's group,²⁷ was followed. By replacing DCM with toluene, the diazotransfer from triflyl azide to a primary amine can be done avoiding the formation of hazardous byproducts, such as diazidomethane or azido-chloromethane, which can cause explosions. In this way, intermediate **76** was obtained, which was subsequently acetylated to afford donor **73** (Scheme 1).



Scheme 1. a) MeONa/MeOH, rt, 16 h, quant.; b) i. MsOH/MeOH, rt to reflux, 24 h; ii. NaHCO₃, CuSO₄, TfN₃, H₂O, MeOH, rt, 16 h; c) Ac₂O, pyr, rt, 16 h, 34% over 3 steps from **75**; d) chromatographic separation; e) vinyl butyrate, Novozyme 435, heptane, 25 °C, 3 h, 44%; f) DIBAL-*H*, THF, -15 °C, 1.5 h, quant.; g) TBDPSCl, DMAP, imidazole, rt, 16 h, 50%; h) (R)-(-)-MTPA-Cl, DMAP, DCM, 0 °C to rt.

For the enantioselective synthesis of cyclohexane derivative **74**, the same procedure used for the synthesis of lead compound **34** was followed (Appendix, p. 199).²⁸ A racemic mixture of *cis* and *trans* isomers of ethyl 3-hydroxycyclohexane-1-carboxylate (**77**) turned out to be a feasible starting material (Scheme 1). The racemic *cis*-isomer **78** was obtained by chromatographic separation of the commercial *cis/trans* mixture. The enzymatic separation of the enantiomeric mixture **rac-cis-78** using the lipase Novozyme 435 and vinyl butyrate yielded the butyrate **79** in 35% yield.^{29,30} The synthesis

of **74** was completed by reduction with DIBAL-H (\rightarrow **80**), followed by the regioselective protection of the primary hydroxyl group with TBDPSCl. The enantiomeric purity of the cyclohexanol derivative **74** (95% ee) was determined by conversion into the Mosher ester **81** and subsequent ^{19}F NMR analysis.



Scheme 2. a) NIS, TfOH, MS 3 Å, DCM/MeCN 5:3, -40 °C, 6 h, 41%; b) HF-pyr, pyridine, 0 °C to rt, 3 h, 98%; c) SO₃-pyr, DMF, 0 °C to rt, 3 h, 54%; d) MeONa/MeOH, rt, 16 h, 89% over two steps from **82**; e) NaOH (aq.), rt, 2 h, quant; f) H₂, Pd/C, MeOH, rt, 3 h, quant; g) CuI, DIPEA, R₁-alkyne, DMF, rt, 16 h, **87**: 37%, **88**: 30%, **89**: 55%, **90**: 24%, **91**: 32%; h) R₂CHO, CH₃COOH, NaCNBH₃, MeOH, rt, 16 h, **92**: 20%, **93**: 74%, **94**: 17%, **95**: 38%.

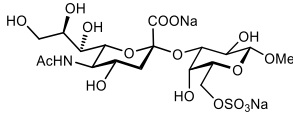
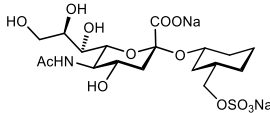
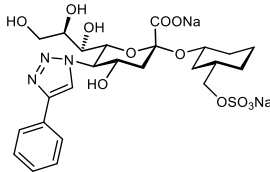
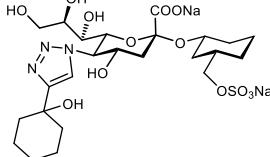
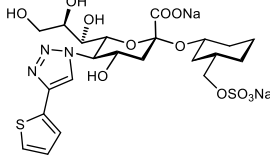
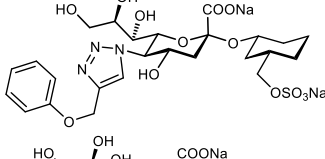
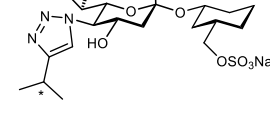
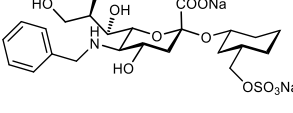
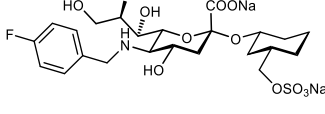
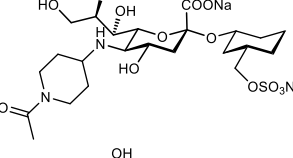
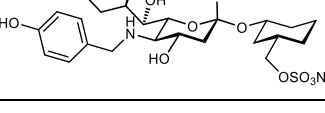
Sialylation of cyclohexanol **74** with sialic acid donor **73**, using the standard NIS/TfOH conditions presented in chapter 2, afforded intermediate **72** in 41% yield (Scheme 2). In this case, the yield was better compared to the glycosylation of the galactoside (34%, chapter 2) but worse compared to the one between **74** and **8** (81%, appendix). In fact, on one hand the yield was improved by a better solubility of **74** compared to the galactoside but on the other hand, an azido group in this position usually gives lower yields compared to an *N*-acetamido moiety.³¹ Subsequent removal of the TBDPSCl group (\rightarrow **82**) and introduction of a sulfate on the free primary alcohol afforded intermediate **83**. At first, it was intended to directly introduce modifications on position 5 of fully protected **83** to simplify purification. However, during column chromatography, acetates were partially cleaved creating a

mixture of various incompletely protected compounds. Therefore, the following reactions were performed with the fully unprotected compound **85**, which was obtained by complete deacetylation of the crude product of the sulfonation reaction (\rightarrow **84**) followed by hydrolyzation with aqueous NaOH. Fragments attached via triazole linkers were introduced by click chemistry with alkynes to afford the final compounds **87-91**. Click chemistry is the popular name of Cu(I)-catalyzed azide–alkyne 1,3-dipolar cycloaddition (CuAAC), a very common reaction in medicinal chemistry due to its broad application, even in complex molecules, mild reaction conditions and compatibility with different functionalities.³² Fragments via amine linkers were instead introduced by reductive amination after reducing the azide group to amine (\rightarrow **86**) to afford compounds **92-95**.

Binding affinities of compounds 87-95. To validate the affinity to Siglec-8 of compounds **87-95**, MST was used as a first screening method (Table 1). Unfortunately, the results were not as expected. All compounds with the triazole linker (**87-91**) showed none or only very weak affinities in mM range to Siglec-8. Besides, compound **88** showed a clear interaction with the dye. This was also the case for all compounds with the amine linker (**92-95**). Interactions with the dye may result in misleading K_D values, since it is not clear if they stem from direct interaction with the protein or just with the dye (Table 1). Therefore, another screening method is necessary. Like before (see Chapter 2), we chose nanoDSF, which allows checking the binding to the protein but without measuring the binding affinities. For this reason, we used ligands **2** and **34** as a reference: only compounds that show a higher shift of the so-called apparent melting temperature (T_m) of Siglec-8 than the one of the reference compounds will be considered as successful candidates. As can be seen from the ΔT values (Table 1), none of the compounds showed a higher shift, not even compared to the only moderately active disaccharide **2**. This probably confirms that the K_D values obtained with the MST were just the results of interactions with the dye and, therefore, might not be relevant. To overcome this problem, we tried to couple different dyes to the protein but with no success.

We can conclude that the fragment virtual screening did not lead to any remarkable candidates. A possible explanation could be that, looking at the docking pose, the absence of an H-bond acceptor in position 5, such as the carbonyl of the acetamide, destabilizes a sort of pre-organization due to intra-molecular interactions, in particular between the carbonyl group and the hydroxyl in position 7 of the sialic acid. Plus, a charged amine may also interfere with the correct binding mode. Hence, we decided to introduce further modifications keeping the amide in position 5.

Table 1. Biological evaluation of compounds **87-95** against human Siglec-8 with MST and nanoDSF assays. Compounds **2** and **34** are used as references. Average values of K_D were calculated from triplicate measurements. [a] Interactions with the dye. n.d. Not determined. n.a. Not active up to 15 mM.

Compound	Structure	K_D (MST, μM)	ΔT ($^{\circ}\text{C}$)
2		561	+ 1.3
34		256	+2.0
87		1800	n.d.
88		n.a. [a]	- 0.3
89		9400	- 0.1
90		7800	n.d.
91		12000	n.d.
92		391 [a]	- 1.0
93		4500 [a]	0
94		151 [a]	+ 0.5
95		n.d.	- 0.9

Modifications on the 5-acetamido group of lead compound 34. In our virtual fragment screening, fragments linked via amide linkers did not provide good binding poses. Therefore, we decided to rationally design the alternative modifications. In particular, we elongated the acetamido chain by a methylene unit, a phenyl ring or a methoxy propionate group. The idea was to better fill the cavity and possibly displace some water molecules, while a methoxy group can be engaged in hydrogen bond interactions with the Tyr11 at the bottom of the binding site. In the model, Tyr11 seems to only have a sulphur from Met115 as acceptor, so a methoxy group at the end of a newly introduced substituent may provide a more attractive acceptor (Figure 6). The docking pose also indicates that in this case the intra-molecular interaction between the carbonyl in position 5 and the hydroxyl in position 7 are maintained.

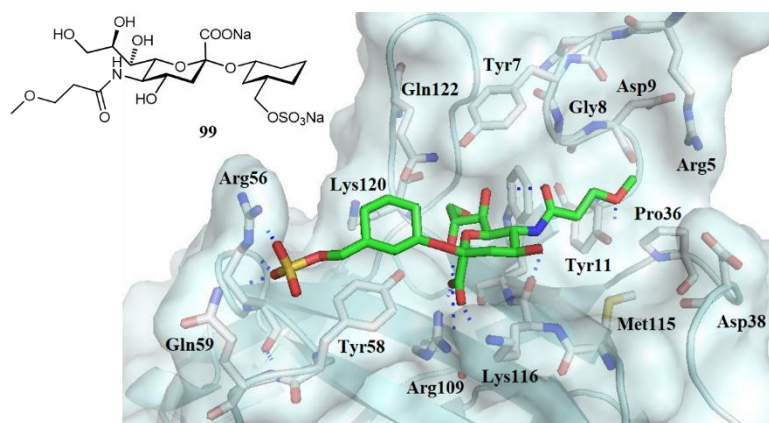
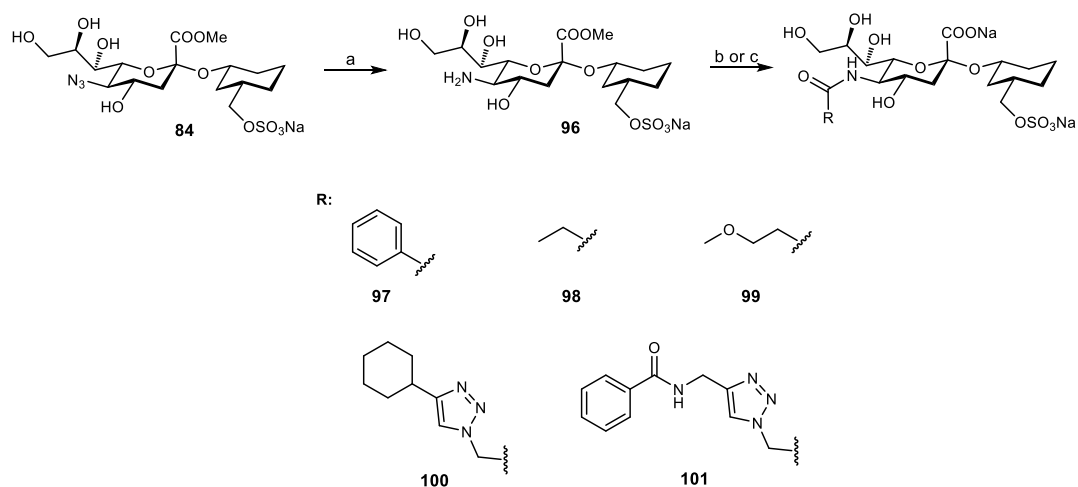


Figure 6. Docking pose of designed compound **99** modified in position 5. Only selected amino acids are presented as sticks. Docking was performed using the FRED algorithm of the OEDocking software (OEDOCKING 3.3.0.2: OpenEye Scientific Software). The figure was generated using the software Pymol.²² The figures were generated using the software Pymol.²² Color code: N: blue, O: red, S: yellow, protein backbone: grey, ligand C: green. Contacts with the protein are depicted as blue dashed lines.

Next to these three modifications, we also introduced two more fragments derived from previously reported ligands^{33,34} for CD33, a related Siglec-8 protein, and Siglec-F, the mouse paralog of Siglec-8, both consisting of a substituted triazole-methylene linker. When docked, these substituents were hosted within the binding pocket and might help to understand the effect of a larger substituent in this position.

Starting from intermediate **84**, the azide was first reduced to the amine (\rightarrow **96**) while keeping the carboxylate protected as a methyl ester to avoid possible cross-reactions in the following amidation reaction. The synthesis was performed by simple HATU-mediated coupling between intermediate **84** and the corresponding free carboxylic acid of the fragments. Only in the case of compound **100** *N*-

hydroxysuccinimide (NHS) was used as activating reagent for the carboxylic group.³⁴ Final deprotection of the methyl ester with aqueous NaOH afforded test compounds **97-101**.



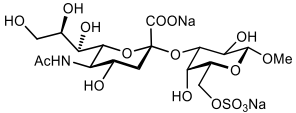
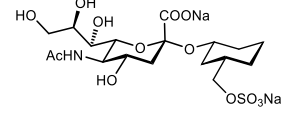
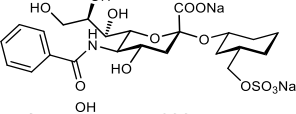
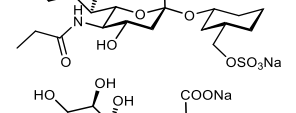
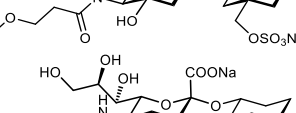
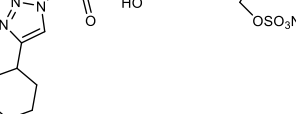
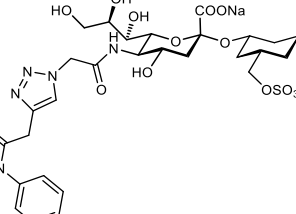
Scheme 3. a) H_2 , Pd/C, MeOH, rt, 3 h, 96%; b) i. RCOOH, HATU, DIPEA, R-NH₂, DMF, rt, 16 h; ii. NaOH (aq.), rt, 16 h, **97**: 37%, **98**: 40%, **99**: 41%, **101**: 32%; c) i. RCOOH, NHS, DCC, EtOAc, 0 °C to rt, 16 h; ii. NEt₃, DMF, rt, 16 h; iii. NaOH (aq.), rt, 16 h, **100**: 26%.

The binding affinities of compounds **97-101** were measured by MST and nanoDSF for a first screening (Table 2). Promising candidates then were also measured by ITC. Generally, the results of the ITC results were in good agreement with those from the MST assay, proving the robustness of the data. Overall, it can be definitely stated that amides in the 5-position are better linkers compared to amines and triazoles, so the possible intra-molecular interaction obviously plays a role for stabilizing the binding. While compound **97** bearing a bulky phenyl substituent on the carbonyl did not show any binding, indicating a steric clash within the binding pocket, the elongation of the acetamido group by just one methylene unit (\rightarrow **98**) had no relevant effect on the affinity compared to the lead compound **34**. Indeed, **98** showed only a slightly higher K_D compared to **34** on MST (266 vs 256 μM) and ITC (326 vs 259 μM), and nanoDSF also gave a slightly reduced T_m for **98** ($\Delta T = +1.6$ °C vs $\Delta T = +2.0$ °C for **34**).

However, as expected from the docking studies, the additional introduction of a methoxy group (\rightarrow **99**) improved the affinity by almost 2-fold compared to the parent compound **34** on MST (K_D 165 vs 256 μM) and ITC (K_D 166 vs 259 μM). Also in the nanoDSF assay, a marked positive shift of the T_m ($\Delta T = +3.6$ °C) was observed, confirming again that **99** is definitely more active than **34** ($\Delta T = +2.0$ °C) and making **99** the most active ligand of this series.

Finally, interesting results have been observed for the two literature-derived compounds bearing a substituted triazolyl-acetyl moiety (Table 2).

Table 2. Biological evaluation of compounds **97-101** against human Siglec-8 with MST, nanoDSF and ITC assays. Compounds **2** and **34** are used as references. Average values of K_D from MST were calculated from triplicate measurements. [a] Interactions with the dye. n.d. Not determined. n.a. Not active up to 15 mM.

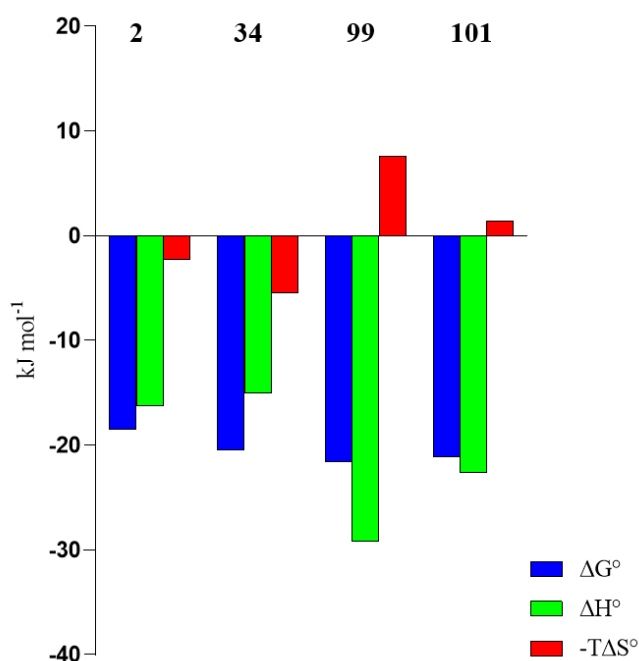
Compound	Structure	K_D (MST, μM)	ΔT ($^{\circ}\text{C}$)	K_D (ITC, μM)
2		561	+ 1.3	574
34		256	+2.0	259
97		n.a.	- 0.7	n.d.
98		266	+ 1.6	326
99		165	+ 3.6	166
100		n.a. [a]	+ 0.3	n.d.
101		201	+ 1.3	196

While the cyclohexyl substituent in **100** obviously is too bulky leading to an inactive compound, ligand **101** with a more flexible substituent showed slightly improved affinity compared to **34**, both on MST (K_D 201 vs 256 μM) and ITC (K_D 196 vs 259 μM), but, surprisingly, a lower ΔT on nanoDSF (**101**: + 1.3 $^{\circ}\text{C}$, **34**: + 2.0 $^{\circ}\text{C}$). However, considering that **101** was just derived from a published Siglec-F ligand, the assay results indicate that the triazolyl-acetyl moiety seems to be well tolerated in the cavity and the affinity might be further increased by adjusting and optimizing the substituent on the triazole.

To have a better insight into the binding mode, thermodynamic fingerprints of the interaction of the most active compounds **99** and **101** were compared to the ones of disaccharide **2** and lead compound **34** (Table 3, Figure 7).

Table 3. Thermodynamic parameters from ITC for selected Siglec-8 ligands **2**, **34**, **99** and **101**.

Compound	K_D [μM]	ΔG° [kJ mol^{-1}]	ΔH° [kJ mol^{-1}]	$-T\Delta S^\circ$ [kJ mol^{-1}]
2	574	-18.5	-16.3	-2.3
	(505 – 650)	(-18.8 – -18.2)	(-17.2 – -15.3)	(-3.5 – -1.0)
34	259	-20.5	-15.0	-5.5
	(222 – 303)	(-20.9 – -20.1)	(-16.2 – -13.9)	(-6.9 – -3.9)
99	166	-21.6	-29.2	+7.6
	(159 – 173)	(-21.7 – -21.5)	(-29.7 – -28.7)	(7.0 – 8.2)
101	196	-21.2	-22.7	+1.49
	(160 – 255)	(-21.7 – -20.5)	(-23.9 – -21.4)	(-0.25 – 3.42)

**Figure 7.** Thermodynamic signature (ΔG° , ΔH° and $-T\Delta S^\circ$) for compounds **2**, **34**, **99** & **101**.

The binding of compound **99** is definitely driven by a stronger enthalpic contribution ($\Delta H^\circ = -29.2 \text{ kJ mol}^{-1}$) compared to the ones of ligands **2** ($\Delta H^\circ = -16.3 \text{ kJ mol}^{-1}$) and **34** ($\Delta H^\circ = -15.0 \text{ kJ mol}^{-1}$), indicating additional beneficial interactions of the methoxyethyl substituent with the protein as, for example, a hydrogen bond with Tyr11 as assumed during the docking analysis. However, this enthalpy gain is in part compensated by a slightly unfavorable entropic term ($-T\Delta S^\circ = +7.6 \text{ kJ mol}^{-1}$) that might be due to a loss of flexibility of the rotatable bonds within the methoxyethyl substituent. Compound **101** showed a similar behavior, with a more favorable enthalpic contribution ($\Delta H^\circ = -22.7 \text{ kJ mol}^{-1}$) than parent compound **34** but slightly worse than **99** ($\Delta H^\circ = -29.2 \text{ kJ mol}^{-1}$). However, in this case the entropic term, even if minimally unfavorable ($-T\Delta S^\circ = +1.49 \text{ kJ mol}^{-1}$), was quite less pronounced than for the more active compound **99** ($-T\Delta S^\circ = +7.6 \text{ kJ mol}^{-1}$). The lower entropic penalty may be due to the higher pre-organization of the more rigid triazole moiety within the binding

cavity. These data confirm that the triazolyl-acetyl also presents a beneficial linker and that further optimization of the terminal substituents may lead to more potent ligands.

Virtual screening for the identification of non-sugar containing hit molecules. Up to date, there are no molecules known able to bind a Siglec that do not contain sugar moieties. Considering that standard small molecules with lower polarity than carbohydrates have better synthetical tractability and often improved pharmacokinetic properties, we decided to perform a virtual screening to identify possible new hits with affinities in micromolar range. The procedure was very similar to the one previously described: commercially available libraries were combined and docked to the Siglec-8 NMR solution structure with the OEDocking software.²⁵ As before, we kept Arg109 and Arg56 as constraints to identify molecules able to interact with these two important amino acids. Docking poses were evaluated based on scoring functions and visual inspection. The selected molecules, all commercially available, are shown in Figure 8.

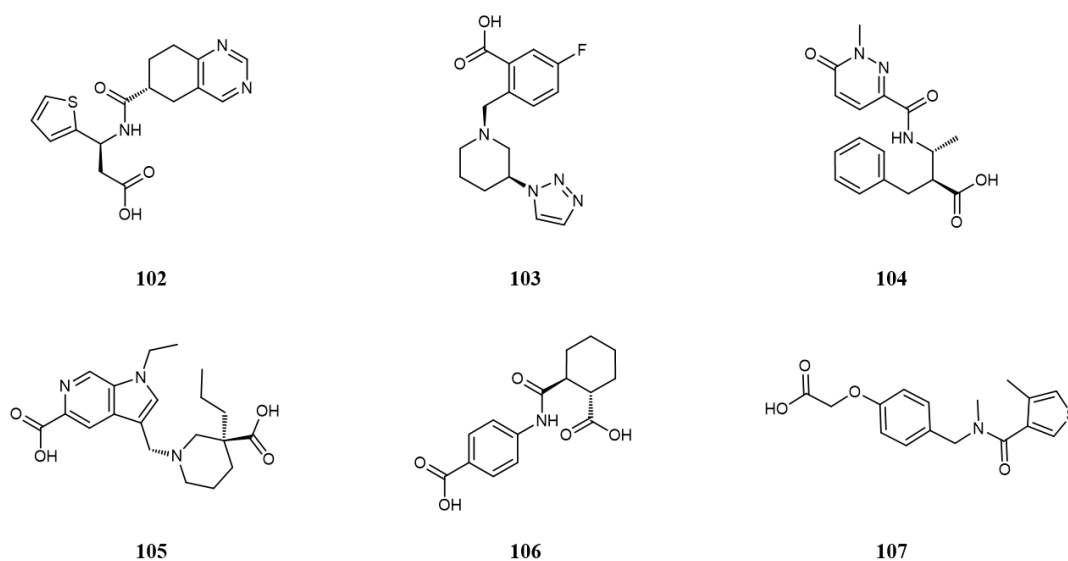


Figure 8. Selected non-carbohydrate containing molecules from virtual fragment screening.

As we can see, all the molecules contain groups able to interact by hydrogen bonds or salt bridges with the two selected arginines. To validate them, an MST assay was performed. In this case, the solubility was much lower compared to the one of our Siglec-8 ligands, therefore the assay was conducted by dissolving the molecules in the standard HEPES buffer (250 mM) but with the addition of 10% of DMSO. The stability of the protein under these conditions was checked repeating the assay with lead compound **34**. We obtained the same K_D value previously reported, therefore it could be confirmed that the protein was not denatured. The only insoluble compound was **102**, which could

not be tested. Unfortunately, none of the screened compounds showed any affinity in the assayed concentration (50 mM). Therefore, this side-project was discontinued.

3.3 Conclusions.

In this chapter, we presented virtual screening approaches. In one case, we virtually combined different fragments with the core structure of compound **34** and we docked them into the Siglec-8 solution structure. The most promising candidates, where fragments were attached via amine or triazole linkers, were synthesized and tested. However, none of them showed any affinity to our target protein. In the second case, we performed a virtual screening to identify new possible hits with no carbohydrate moiety. Also in this case, the compounds did not show any binding. We can therefore conclude that our virtual screening approach was not successful. We assume that the absence of an amide in position 5 of the sialic acid could be detrimental to the binding. In fact, modifications introduced by rational design via amide linkers were more successful. In particular, compound **99**, bearing a methoxypropionamide in position 5, showed an almost 2-fold affinity improvement compared to parent compound **34**, revealing that modifications in this position are beneficial to improve the binding. Further affinity improvement may be obtained by combining this modification with the favorable naphthyl-sulfonamide in position 9. Other substituents could also be introduced via triazolyl-acetyl moiety, since it seems to be well tolerated in this position. Nevertheless, a crystal or NMR solution structure would be definitely useful to provide better insight into the binding mode of our ligands and consequently make more reliable and accurate virtual predictions.

3.4 Experimental part.

Preparation of virtual libraries. We have prepared our fragment library consisting of 118570 fragments by merging libraries of various vendors (Chembridge, Enamine, Asinex, KeyOrganics, Pharmeks, Vitas) using the KNIME workflow.²³ Using the RdKit nodes³⁵ in KNIME we generated analogues of compound **34** which had amines extended with fragments from our fragment library in positions 5 and 9. To increase the possibility of successful synthesis of possible virtual screening hits we used four types of reactions: reductive amination, alkylation and formation of amides or esters. By performing *in silico* reactions with the KNIME workflow we obtained 65785 new molecules that had either of two amines, extended with the small fragments. For the purpose of the virtual screening of all compounds we also protonated at pH 7.4 using the OpenBabel KNIME node.³⁶ Prepared molecules were saved in SMILES format. For the virtual screening, different conformations for each

compound were calculated using the OpenEye Omega software.³⁷ For each compound a maximum of 200 conformations were generated using the OpenEye Omega2 (v2.5.1.4) algorithm with flipper setting turned on to prepare all stereoisomers if the stereogenic center was not defined.

Virtual screening. Docking was performed using OpenEye OEDocking with both algorithms, FRED and HYBRID (OEDOCKING 3.3.0.2: OpenEye Scientific Software, Santa Fe, NM, USA, <http://www.eyesopen.com>, accessed on 1 July 2021), at the Siglec-8 binding site (PDB entry: 2N7B).^{24,38,39} The binding site for docking experiments was created using MAKE RECEPTOR (Release 3.2.0.2, OpenEye Scientific Software, Inc., Santa Fe, NM, USA; www.eyesopen.com, accessed on 1 July 2021). The binding site was defined as a box in size 18.67 Å × 23.33 Å × 17.33 Å and a volume of 7549 Å³. We defined Arg109 and Arg56 as constraints. The best 5000 docking poses per algorithm were compared using the OpenEye's scoring function Chemgauss4 score and compounds with the best scoring by both methods were evaluated further for chemical synthesis. Docking poses were scored and ranked using Chemgauss4 scoring function. The results were visualized and analyzed with VIDA (version 4.3.0.4, OpenEye Scientific Software, Inc., Santa Fe, NM, USA, www.eyesopen.com, accessed on 1 July 2021).

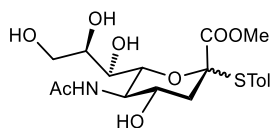
Synthesis. Unless otherwise stated, the starting materials, reagents, and solvents were purchased as high-grade commercial products from Sigma-Aldrich, Alfa-Aesar, Apollo Scientific and TCI, and used without further purification. MeCN and MeOH were dried over activated molecular sieves (4 Å and 3 Å, respectively) and stored under argon atmosphere. Dry DME was prepared by filtration through Al₂O₃ and stored over activated molecular sieves (4 Å) under argon atmosphere. Dry DCM, DMF, pyridine and THF were purchased from Sigma-Aldrich and TCI. Molecular sieves were activated under vacuum at 500 °C for 30 min immediately before use. Analytical TLC was performed on silica gel Merck 60 F254 plates (0.25 mm), using visualization with UV light and/or by charring with a phosphomolybdic acid solution (10 g in 100 mL of ethanol). Acidic ion-exchange resin (Amberlyst[®] IR-120 hydrogen form) was washed with MeOH prior to use. Column chromatography was carried out on silica gel 60 (particle size 240–400 mesh). Medium pressure chromatography (MPLC) separations were carried out on a CombiFlash R_f from Teledyne Isco equipped with RediSep normal phase or RP-18 reversed-phase flash columns. Reversed-phase chromatography was also performed on a Biotage Isolera[™] One using C-18 cartridges. Size exclusion chromatography was performed on Biogel P-2 media (Bio-Rad Laboratories, Inc.). ¹H and ¹³C NMR spectra were recorded at 400 MHz and 100 MHz, respectively, on an AVANCE III 400 spectrometer (Bruker Corporation, Billerica, MA, USA) or at 500 MHz and 126 MHz on a Bruker Avance DMX-500 spectrometer, in

chloroform-*d* (CDCl₃), methanol-*d*₄ (CD₃OD) or deuterium oxide (D₂O), with TMS as internal standard. Chemical shifts (δ) are expressed in parts per million (ppm) relative to the residual solvent peaks for the ¹H and ¹³C nuclei (CDCl₃: $\delta_{\text{H}} = 7.26$, $\delta_{\text{C}} = 77.16$; CD₃OD: $\delta_{\text{H}} = 3.31$, $\delta_{\text{C}} = 49.00$; D₂O: $\delta_{\text{H}} = 4.79$); coupling constants (*J*) are given in hertz (Hz). The following abbreviations are used to describe peak patterns when appropriate: s (singlet), d (doublet), dd (doublets of doublet), ddd (doublets of doublets of doublet), t (triplet), m (multiplet). 2D NMR experiments (COSY and HSQC) of representative compounds were carried out to assign protons and carbons of the new structures. Mass spectra were obtained using a single quadrupole mass spectrometer Advion Expression CMS^L coupled with an Agilent 1290 liquid chromatograph or on a Waters Micromass ZQ instrument. High resolution mass spectrometry (HRMS) was performed on a Q ExactiveTM Plus Hybrid Quadrupole-OrbitrapTM Mass Spectrometer (Thermo ScientificTM; ion source: Electrospray Ionization (ESI)). MS spectra were acquired in Fourier transform-mass spectrometry (FT-MS) scan mode with a target mass resolution of 100 000 at *m/z* 400. Recorded spectra were analyzed with Thermo Xcalibur Qual Browser (Xcalibur 4.2 SP1, Thermo Fisher Scientific Inc.). HRMS analysis was also performed on an Agilent 1100 LC, equipped with a photodiode array detector and a Micromass QTOF I, equipped with a 4 GHz digital-time converter. Optical rotations were measured with a PerkinElmer polarimeter 341. LCMS purifications were performed on Agilent Technologies 1260 Infinity II HPLC with Waters XSelect CSH Prep C18 5.0 μM OBD, 19 mm x 250 mm, used at a flow rate of 20 mL/min and a column temperature of 25 °C. The eluent consisted of H₂O + 0.1% trifluoroacetic acid (TFA) as solvent A and MeCN + 0.1% TFA as solvent B (Table 4, Method A). HPLC analysis was performed on a Thermo Scientific Dionex Ultimate 3000 Binary Rapid Separation LC System (Thermo Fisher Scientific, Waltham, MA, USA) equipped with an autosampler, a binary pump system and a photodiode array detector. A Waters Atlantis T3 dC18 column (3 μm , 2.1 x 100 mm) was used with a flow rate of 0.3 mL/min. The eluent consisted of H₂O + 0.1% trifluoroacetic acid (TFA) as solvent A and MeCN + 0.1% TFA as solvent B (Table 4, Method B and Method C (for compounds **97-101**)).

Method A		Method B		Method C	
T (min)	%B	T (min)	%B	T (min)	%B
2	5	2	5	2	5
15	50	16	95	10	20
16	95	18	95	16	80
17	5	20	5	18	80
-	-	21	5	20	5
-	-	-	-	21	5

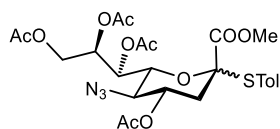
Table 4. Methods for LCMS purification and HPLC analysis.

Tolyl (methyl 5-acetamido-2,3,5-trideoxy-2-thio-D-glycero- α -D-galacto-2-nonulopyranosylonate) (75).



A solution of **8** (26.0 g, 0.044 mmol) in dry MeOH (300 mL) was treated with a freshly prepared solution of MeONa in MeOH (1 M, 15 mL) overnight at rt under argon atmosphere. Then, it was neutralized with Amberlyst-15 ion exchange resin and concentrated under reduced pressure to afford **75** (18.9 g, quant.) as a white solid. $[\alpha]_D^{20} -82.6$ (c 1.0, MeOH); $^1\text{H NMR}$ (500 MHz, CD_3OD): δ = 1.95 (dd, J = 11.6, 13.6 Hz, 1H, H-3a), 2.04 (s, 3H, NHAc), 2.33 (s, 3H, CH_3 -tol), 2.67 (dd, J = 4.7, 13.6 Hz, 1H, H-3e), 3.51 (s, 3H, OMe), 3.56 (d, J = 8.9 Hz, 1H, H-7), 3.67 (dd, J = 5.2, 11.1 Hz, 1H, H-9a), 3.76-3.84 (m, 2H, H-8, H-9b), 3.90 (td, J = 7.5, 10.1 Hz, 1H, H-5), 4.10 (td, J = 4.6, 10.9 Hz, 1H, H-4), 4.50 (d, J = 10.5 Hz, 1H, H-6), 7.16 (d, J = 7.9 Hz, 2H, Ar-H), 7.46 (d, J = 7.9 Hz, 2H, Ar-H); $^{13}\text{C NMR}$ (126 MHz, CD_3OD): δ = 21.3 (CH_3 -tol), 22.8 (NHAc), 42.1 (C-3), 52.9 (OMe), 54.1 (C-5), 65.1 (C-9), 68.1 (C-4), 70.7 (C-7), 71.3 (C-8), 73.4 (C-6), 91.4 (C-2), 127.8, 130.6, 137.4, 141.0 (6C, Ar-C), 170.8, 174.7 (2C, C=O); ESI-MS: m/z : Calcd for $\text{C}_{19}\text{H}_{27}\text{NO}_8$ $[\text{M}+\text{Na}]^+$: 452.1, found: 452.1.

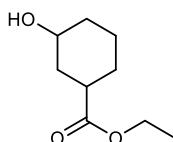
Tolyl (methyl 4,7,8,9-tetra-*O*-acetyl-5-azido-2,3,5-trideoxy-2-thio-D-glycero- α -D-galacto-2-nonulopyranosylonate) (73).



Compound **75** (19.9 g, 0.046 mol) was dissolved in dry MeOH (200 mL) and MsOH (5.97 mL, 0.092 mol) was added at rt. The reaction was heated to reflux for 24 h. After that, it was cooled down to rt and neutralized with NEt_3 . The solvents were co-evaporated with toluene and the crude material was used in the next step without further purification. A portion of the crude (3.87 g, 10.0 mmol) was dissolved in H_2O (13 mL). NaHCO_3 (3.36 g, 40.0 mmol) and CuSO_4 (0.10 g, 0.40 mmol) were added followed by the dropwise addition of 1 M solution of TfN_3 in toluene (20.0 mL). MeOH (87 mL) was added and the homogeneous mixture was stirred overnight at rt. The mixture was then concentrated under reduced pressure strictly below 25 °C. The crude material was dissolved in pyridine (25 mL) and Ac_2O (10 mL) and stirred at rt overnight. The solvents were evaporated via co-evaporation with toluene. The crude material was dissolved in EtOAc (50 mL) and washed with H_2O (30 mL), 10% aq. CuSO_4 (30 mL), H_2O (3 \times 30 mL), dried over Na_2SO_4 , filtered and evaporated. The crude product

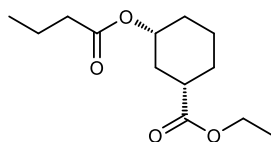
was purified by flash chromatography (petroleum ether/acetone, 10:1 → 8:2) to give **73** (1.88 g, 34% over 3 steps) as a glassy white solid. $[\alpha]_{\text{D}}^{20} - 91.2$ (c 4.7, CHCl_3); $^1\text{H NMR}$ (400 MHz, CDCl_3): $\delta = 1.90$ (dd, $J = 11.6, 13.8$ Hz, 1H, H-3a), 2.00, 2.07, 2.10, 2.15 (4 s, 12H, OAc), 2.33 (s, 3H, CH_3 -tol), 2.75 (dd, $J = 4.9, 13.8$ Hz, 1H, H-3e), 3.26 (t, $J = 10.1$ Hz, 1H, H-5), 3.58 (s, 3H, OMe), 4.13 (dd, $J = 6.9, 12.5$ Hz, 1H, H-9a), 4.36 (dd, $J = 2.0, 10.4$ Hz, 1H, H-6), 4.41 (dd, $J = 2.4, 12.5$ Hz, 1H, H-9b), 5.11 (ddd, $J = 2.4, 4.6, 6.9$ Hz, 1H, H-8), 5.39 (ddd, $J = 4.9, 9.7, 11.5$ Hz, 1H, H-4), 5.60 (dd, $J = 2.0, 4.6$ Hz, 1H, H-7), 7.07-7.16 (m, 2H, Ar-H), 7.29 (d, $J = 8.1$ Hz, 2H, Ar-H); $^{13}\text{C NMR}$ (100 MHz, CDCl_3): $\delta = 20.78, 20.84, 21.0, 21.1$ (4C, OAc), 21.4 (CH_3 -tol), 36.7 (C-3), 52.7 (OMe), 60.4 (C-5), 62.2 (C-9), 69.6 (C-7), 70.9 (C-4), 71.5 (C-8), 71.7 (C-6), 88.5 (C-2), 125.3, 130.0, 136.2, 140.3 (6C, Ar-C), 168.1, 169.7, 169.9, 170.3, 170.5 (5C, C=O); ESI-MS: m/z : Calcd for $\text{C}_{25}\text{H}_{31}\text{N}_3\text{O}_{11}\text{S}$ $[\text{M}+\text{Na}]^+$: 604.2; found: 604.2.

Ethyl *cis*-3-hydroxycyclohexane-1-carboxylate (*rac-cis*-**78**).



Racemic ethyl 3-hydroxycyclohexane-1-carboxylate (20.0 g, 116 mmol) was separated by flash column chromatography on silica (petroleum ether/EtOAc, 7:3 → 6:4). The lower fraction was collected to yield the racemic *cis* isomers *rac-cis*-**78** (9.34 g, 47%) as a colorless oil. The diastereomeric purity was confirmed by conversion to the racemic analogue of Mosher ester **81**. $^1\text{H NMR}$ (500 MHz, CDCl_3): $\delta = 1.18$ (m, 1H, H-6a), 1.22 (t, $J = 7.1$ Hz, 3H, OCH_2CH_3), 1.27-1.33 (m, 2H, H-4a, H-5a), 1.39 (m, 1H, H-2a), 1.78-1.89 (m, 2H, H-4e, H-5e), 1.93 (m, 1H, H-6e), 2.06 (s, 1H, OH), 2.17 (dt, $J = 1.8, 3.8, 12.2$ Hz, 1H, H-2e), 2.32 (tt, $J = 3.7, 11.7$ Hz, 1H, H-1), 3.59 (tt, $J = 4.2, 10.4$ Hz, 1H, H-3), 4.10 (q, $J = 7.1$ Hz, 2H, OCH_2CH_3).

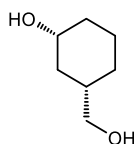
Ethyl (1*S*,3*R*)-3-(butyryloxy)cyclohexane-1-carboxylate (**79**).



To a solution of *rac-cis*-**78** (9.34 g, 0.054 mol) in heptane (50 mL) were added vinyl butyrate (13.7 mL, 0.108 mol) and lipase Novozyme 435 (0.192 g). The reaction was gently stirred at rt for 3 h. The suspension was filtered over celite, washed with petroleum ether and concentrated under reduced pressure. The crude was purified by flash chromatography (toluene/acetone, 1:0 → 6:4) to afford **79** (5.73 g, 44%) as a colorless oil. $[\alpha]_{\text{D}}^{20} + 44.0$ (c 1.0, CHCl_3); $^1\text{H NMR}$ (500 MHz, CDCl_3): $\delta = 0.93$

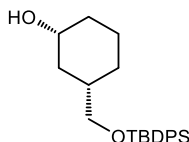
(t, $J = 7.4$ Hz, 3H, $\text{CH}_2\text{CH}_2\text{CH}_3$), 1.24 (t, $J = 7.1$ Hz, 3H, OCH_2CH_3), 1.27-1.40 (m, 3H, H-4a, H-5a, H-6a), 1.48 (q, $J = 12.3$ Hz, 1H, H-2a), 1.64 (sextet, $J = 7.4$ Hz, 2H, $\text{CH}_2\text{CH}_2\text{CH}_3$), 1.80-2.01 (m, 3H, H-4e, H-5e, H-6e), 2.20 (m, 1H, H-2e), 2.25 (t, $J = 7.4$ Hz, 2H, $\text{CH}_2\text{CH}_2\text{CH}_3$), 2.39 (tt, $J = 3.7, 12.0$ Hz, 1H, H-1), 4.11 (q, $J = 7.1$ Hz, 2H, OCH_2CH_3), 4.72 (tt, $J = 4.2, 11.0$ Hz, 1H, H-3); ^{13}C NMR (126 MHz, CDCl_3): $\delta = 13.8$ ($\text{CH}_2\text{CH}_2\text{CH}_3$), 14.3 (OCH_2CH_3), 18.7 ($\text{CH}_2\text{CH}_2\text{CH}_3$), 23.4 (C-5), 28.1 (C-6), 31.4 (C-4), 34.1 (C-2), 36.6 ($\text{CH}_2\text{CH}_2\text{CH}_3$), 41.8 (C-1), 60.6 (OCH_2CH_3), 71.9 (C-3), 173.2, 174.8 (2C, C=O); ESI-MS: m/z : Calcd for $\text{C}_{13}\text{H}_{22}\text{O}_4$ $[\text{M}+\text{Na}]^+$: 265.1, found: 265.0.

(1R,3S)-3-(Hydroxymethyl)cyclohexan-1-ol (80).



Compound **79** (5.73 g, 0.024 mol) was dissolved in THF (130 mL) and cooled to -15 °C. A 1 M solution of DIBAL-H in toluene (142 mL, 0.142 mol) was added dropwise and the solution was stirred at -15 °C for 1.5 h. Then, it was quenched by the addition of aq. sat. $\text{KNaC}_4\text{H}_4\text{O}_6$ (130 mL) and stirred for 30 min. The aqueous phase was extracted with Et_2O (3×80 mL), dried over Na_2SO_4 , filtered and concentrated under reduced pressure. The residue was purified by flash chromatography (toluene/acetone, 1:0 \rightarrow 1:1) to afford **80** (3.12 g, quant.) as a colorless oil. $[\alpha]_D^{20}$ 0.00 (c 0.6, MeOH); ^1H NMR (500 MHz, CDCl_3): $\delta = 0.86$ (qd, $J = 3.8, 12.7$ Hz, 1H, H-4a), 0.95 (m, 1H, H-2a), 1.16 (m, 1H, H-6a), 1.30 (qt, $J = 3.5, 13.2$ Hz, 1H, H-5a), 1.57 (m, 1H, H-3), 1.72 (m, 1H, H-4e), 1.82 (dp, $J = 3.5, 13.6$ Hz, 1H, H-5e), 1.98 (m, 1H, H-6e), 2.04 (dt, $J = 2.0, 3.9, 9.9$ Hz, 1H, H-2e), 3.49 (dt, $J = 3.2, 6.5$ Hz, 2H, CH_2OH), 3.61 (dq, $J = 4.3, 5.2, 10.8$ Hz, 1H, H-1); ^{13}C NMR (126 MHz, CDCl_3): $\delta = 23.8$ (C-5), 28.5 (C-4), 35.8 (C-6), 38.9 (C-2), 39.4 (C-3), 68.1 (CH_2OH), 70.6 (C-1).

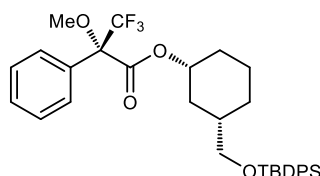
(1R,3S)-3-(tert-Butyldiphenylsilyloxymethyl)cyclohexan-1-ol (74).



To a solution of **80** (3.12 g, 24.0 mmol) in dry DCM (60 mL) were added DMAP (0.586 g, 5.00 mmol), imidazole (2.44 g, 36.0 mmol) and TBDPSCl (6.24 mL, 24.0 mmol) under argon. After 16 h, starting material was still present and another portion of TBDPSCl (2.50 mL, 9.60 mmol) was added. After further 16 h, TLC showed no starting material. The solution was diluted with DCM (50 mL) and washed with H_2O (3×100 mL), dried over Na_2SO_4 , concentrated under reduced pressure and purified by flash chromatography (DCM/MeOH, 100:0 \rightarrow 95:5) to afford **74** (4.46 g, 50%) as a

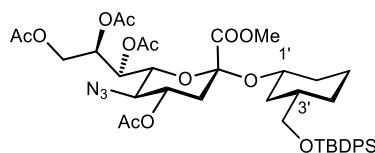
colorless oil. $[\alpha]_D^{20} + 1.30$ (c 1.0, CHCl_3); $^1\text{H NMR}$ (500 MHz, CDCl_3): $\delta = 0.89$ (m, 1H, H-4a), 0.98 (td, $J = 11.0, 12.0$ Hz, 1H, H-2a), 1.06 (s, 9H, $\text{C}(\text{CH}_3)_3$), 1.16 (m, 1H, H-6a), 1.29 (qt, $J = 3.5, 13.2$ Hz, 1H, H-5a), 1.46 (s, 1H, OH), 1.62 (tt, $J = 2.8, 6.1, 12.0$ Hz, 1H, H-3), 1.70 (m, 1H, H-4e), 1.80 (dp, $J = 3.5, 13.5$ Hz, 1H, H-5e), 1.98 (m, 1H, H-6e), 2.08 (m, 1H, H-2e), 3.51 (qd, $J = 6.0, 9.8$ Hz, 2H, CH_2OH), 3.61 (tt, $J = 4.3, 10.9$ Hz, 1H, H-1), 7.35-7.45 (m, 7H, Ar-H), 7.64-7.69 (m, 4H, Ar-H); $^{13}\text{C NMR}$ (126 MHz, CDCl_3): $\delta = 19.5$ ($\text{C}(\text{CH}_3)_3$), 23.9 (C-5), 27.0 ($\text{C}(\text{CH}_3)_3$), 28.6 (C-4), 36.0 (C-6), 39.2 (C-2), 39.5 (C-3), 68.9 (CH_2OH), 70.9 (C-1), 127.7, 129.7, 134.1, 135.7 (12C, Ar-C); ESI-MS: m/z : Calcd for $\text{C}_{23}\text{H}_{32}\text{O}_2\text{Si}$ $[\text{M}+\text{Na}]^+$: 391.2, found: 391.2.

(1*R*,3*S*)-3-(*tert*-Butyldiphenylsilyloxymethyl)cyclohexyl (*R*)-(-)- α -methoxy- α -(trifluoromethyl)phenylacetate (81).



To a solution of **74** (12.4 mg, 0.034 mmol) in dry DCM (0.2 mL) were added DMAP (9.53 mg, 0.078 mmol) and (*R*)-(-)-MTPA-Cl (9.50 μL , 0.051 mmol) at 0 °C. The reaction mixture was stirred at 0 °C for 15 min and then for 1 h at rt. The reaction mixture was diluted with Et_2O (5.0 mL), washed twice with 1 M aq. HCl (5.0 mL), satd aq. NaHCO_3 (5.0 mL) and water (5.0 mL), dried over Na_2SO_4 , filtered, and concentrated under reduced pressure. The residue was directly subjected to $^{19}\text{F NMR}$ investigation without further purification. $^{19}\text{F NMR}$ (565 MHz, CDCl_3): $\delta = -71.60$ ppm; enantiomeric purity: > 95 % ee.

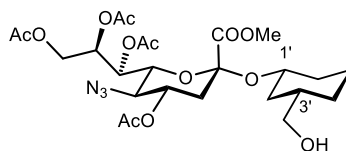
(1*S*,3*R*)-3-(*tert*-Butyldiphenylsilyloxymethyl)cyclohexyl (methyl 4,7,8,9-tetra-*O*-acetyl-5-azido-3,5-dideoxy-*D*-glycero- α -*D*-galacto-2-nonulopyranosylonate) (72).



A suspension of **74** (1.64 g, 4.45 mmol), **73** (5.18 g, 8.90 mmol) and 3 Å molecular sieves (13.0 g) in dry DCM/MeCN (5:3, 50 mL), was stirred at rt for 1 h under argon. Then, it was cooled to -40 °C and *N*-iodosuccinimide (3.75 g, 16.7 mmol) was added, followed by TfOH (148 μL , 1.67 mmol). The reaction mixture was stirred for 6 h at -40 °C under argon. After that, it was neutralized with NEt_3 , warmed to rt, filtered over celite and the solvents were evaporated. The crude product was dissolved in DCM (50 mL) and washed with aq. sat. $\text{Na}_2\text{S}_2\text{O}_3$ (3 \times 30 mL) and H_2O (2 \times 30 mL). The organic

layer was dried over Na₂SO₄, filtered and evaporated. The crude product was purified by repeated flash column chromatography (petroleum ether/acetone, 1:0 → 9:1) to separate the α:β mixture, finally affording **72** (1.50 g, 41%) as a brown solid. $[\alpha]_D^{20} - 10.6$ (*c* 1.0, CHCl₃); ¹H NMR (400 MHz, CDCl₃): δ = 0.86 (m, 1H, H-4'a), 0.98 (m, 1H, H-2'a), 1.03 (s, 9H, C(CH₃)₃), 1.20 (m, 1H, H-6'a), 1.38 (m, 1H, H-5'a), 1.57-1.62 (m, 2H, H-3', H-4'e), 1.72 (t, *J* = 12.5 Hz, 1H, H-3a), 1.73-1.80 (m, 2H, H-2'e, H-5'e), 2.02 (m, 1H, H-6'e), 2.07, 2.10, 2.17, 2.19 (4 s, 12H, OAc), 2.73 (dd, *J* = 4.7, 12.7 Hz, 1H, H-3e), 3.22 (t, *J* = 9.8 Hz, 1H, H-5), 3.40 (dd, *J* = 6.4, 9.8 Hz, 1H, CH₂OTBDPS), 3.47 (dd, *J* = 5.4, 9.7 Hz, 1H, CH₂OTBDPS), 3.65 (m, 1H, H-1'), 3.74 (s, 3H, OMe), 3.82 (dd, *J* = 1.6 Hz, 10.6 Hz, 1H, H-6), 4.21 (dd, *J* = 4.4, 12.6 Hz, 1H, H-9a), 4.31 (dd, *J* = 2.4, 12.6 Hz, 1H, H-9b), 4.79 (ddd, *J* = 4.6, 9.8, 12.3 Hz, 1H, H-4), 5.36 (ddd, *J* = 2.4, 4.4, 9.2 Hz, 1H, H-8), 5.51 (dd, *J* = 1.6, 9.2 Hz, 1H, H-7), 7.35-7.44 (m, 6H, Ar-H), 7.63-7.65 (m, 4H, Ar-H); ¹³C NMR (100 MHz, CDCl₃): δ = 20.9, 21.0, 21.2 (4C, OAc), 23.8 (C-5'), 27.0 (C(CH₃)₃), 28.4 (C-4'), 35.3 (C-6'), 36.6 (C-2'), 38.2 (C-3), 52.8 (OMe), 60.2 (C-5), 62.2 (C-9), 68.09 (C-8), 68.11 (C-7), 68.8 (CH₂OTBDPS), 71.2 (C-4), 71.6 (C-6), 75.0 (C-1'), 98.6 (C-2), 127.7, 129.7, 133.9, 134.0, 135.7 (12C, Ar-C), 168.6, 169.8, 169.98, 170.01, 170.9 (5C, C=O). ESI-MS: *m/z*: Calcd for C₄₁H₅₅N₃NaO₁₃Si [M+Na]⁺: 848.3, found: 848.3.

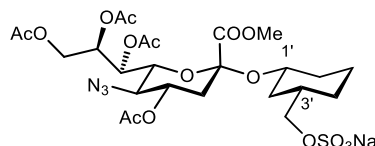
(1S,3R)-3-(Hydroxymethyl)cyclohexyl (methyl 4,7,8,9-tetra-*O*-acetyl-5-azido-3,5-dideoxy-*D*-glycero-*α*-*D*-galacto-2-nonulopyranosylonate) (82).



To a solution of **72** (400 mg, 0.490 mmol) in pyridine (20.0 mL) in a Teflon® container, was added HF·pyr (2.40 mL) dropwise at 0 °C under argon. The reaction mixture was stirred for 3 h at rt and then neutralized with aq. satd. NaHCO₃ and Na₂CO₃. The aqueous phase was extracted with DCM (3 × 50 mL) and the combined organic layers were dried over Na₂SO₄, filtered and evaporated. The crude product was purified by flash column chromatography (petroleum ether/acetone, 1:0 → 1:1) to afford **82** (280 mg, 98%) as a colorless oil. $[\alpha]_D^{20} - 16.9$ (*c* 1.0, CHCl₃); ¹H NMR (400 MHz, CDCl₃): δ = 0.81 (qd, *J* = 3.8, 12.6 Hz, 1H, H-4'a), 0.92 (q, *J* = 11.8 Hz, 1H, H-2'a), 1.15-1.29 (m, 1H, H-6'a), 1.38 (qt, *J* = 3.4, 13.1 Hz, 1H, H-5'a), 1.52 (m, 1H, H-3'), 1.65 (m, 1H, H-4'e), 1.68 (t, *J* = 12.7 Hz, 1H, H-3e), 1.72-1.81 (m, 2H, H-2'e, H-5'), 1.99 (m, 1H, H-6'e), 2.06, 2.08, 2.15, 2.18 (4 s, 12H, OAc), 2.70 (dd, *J* = 4.7, 12.7 Hz, 1H, H-3e), 3.20 (dd, *J* = 9.7, 10.6 Hz, 1H, H-5), 3.39 (m, 1H, CH₂OH), 3.47 (m, 1H, CH₂OH), 3.68 (tt, *J* = 4.3, 10.9 Hz, 1H, H-1'), 3.79 (s, 3H, OMe), 3.81 (dd, *J* = 1.7, 10.7 Hz, 1H, H-6), 4.19 (dd, *J* = 4.6, 12.6 Hz, 1H, H-9a), 4.31 (dd, *J* = 2.4, 12.5 Hz, 1H, H-9b), 4.79 (ddd, *J* = 4.7, 9.7, 12.3 Hz, 1H, H-4), 5.35 (ddd, *J* = 2.4, 4.6, 9.1 Hz, 1H, H-8), 5.50 (dd, *J*

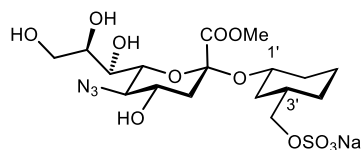
= 1.7, 9.1 Hz, 1H, H-7); ^{13}C NMR (100 MHz, CDCl_3): δ = 20.9, 21.0, 21.2 (4C, OAc), 23.7 (C-5'), 28.4 (C-4'), 35.0 (C-6'), 36.2 (C-2'), 38.1 (C-3), 39.5 (C-3'), 52.9 (OMe), 60.2 (C-5), 62.2 (C-9), 68.11 (C-7), 68.13 (CH_2OH), 68.2 (C-8), 71.2 (C-4), 71.6 (C-6), 74.5 (C-1'), 98.4 (C-2), 168.7, 169.8, 170.0, 170.2, 170.9 (5C, C=O); ESI-MS: m/z : Calcd for $\text{C}_{25}\text{H}_{37}\text{N}_3\text{O}_{13}$ $[\text{M}+\text{Na}]^+$: 610.2, found: 610.2.

(1S,3R)-3-(Sulfonatooxymethyl)cyclohexyl (methyl 4,7,8,9-tetra-*O*-acetyl-5-azido-3,5-dideoxy-D-glycero- α -D-galacto-2-nonulopyranosylonate) sodium salt (83).



To a solution of **82** (160 mg, 0.270 mmol) in dry DMF (15.0 mL) was added $\text{SO}_3\cdot\text{pyr}$ (434 mg, 2.73 mmol) at 0 °C and the reaction was stirred at rt for 3 h. Then, NaHCO_3 (2.00 g) was added and stirring continued for another 1 h. The mixture was filtered over celite and concentrated under reduced pressure. The residue was purified by flash column chromatography (DCM/MeOH, 1:0 → 9:1) to afford **83** (100 mg, 54%). ^1H NMR (500 MHz, CD_3OD): δ = 0.89 (qd, J = 3.4, 12.2, 12.8 Hz, 1H, H-4'a), 0.97 (q, J = 11.8 Hz, 1H, H-2'a), 1.18 (m, 1H, H-6'a), 1.42 (m, 1H, H-5'a), 1.63-1.69 (m, 2H, H-3', H-4'e), 1.70-1.79 (m, 2H, H-2'e, H-5'e), 1.75 (t, J = 12.5 Hz, 1H, H-3a), 2.00 (m, 1H, H-6'e), 2.04, 2.08, 2.15, 2.20 (4 s, 12H, OAc), 2.66 (dd, J = 4.6, 12.6 Hz, 1H, H-3e), 3.40 (dd, J = 9.7, 10.6 Hz, 1H, H-5), 3.70 (m, 1H, H-1'), 3.78 (dd, J = 1.6, 10.6 Hz, 1H, H-6), 3.73-3.84 (m, 2H, $\text{OCH}_2\text{SO}_3\text{Na}$), 3.82 (s, 3H, OMe), 4.17 (dd, J = 4.7, 12.5 Hz, 1H, H-9a), 4.34 (dd, J = 2.4, 12.5 Hz, 1H, H-9b), 4.76 (ddd, J = 4.6, 9.7, 12.3 Hz, 1H, H-4), 5.36 (ddd, J = 2.4, 4.7, 9.3 Hz, 1H, H-8), 5.47 (dd, J = 1.7, 9.3 Hz, 1H, H-7); ^{13}C NMR (126 MHz, CD_3OD): δ = 20.6, 20.7, 20.8, 21.2 (4C, OAc), 24.5 (C-5'), 29.4 (C-4'), 36.0 (C-6'), 37.4 (C-2'), 38.0 (C-3'), 38.8 (C-3), 53.3 (OMe), 61.2 (C-5), 63.1 (C-9), 69.1 (C-7), 69.4 (C-8), 72.5 (C-4), 72.8 (C-6), 73.5 ($\text{OCH}_2\text{SO}_3\text{Na}$), 75.4 (C-1'), 99.9 (C-2), 170.0, 171.3, 171.5, 171.7, 172.4 (5C, C=O); ESI-MS: m/z : Calcd for $\text{C}_{25}\text{H}_{36}\text{N}_3\text{NaO}_{16}\text{S}$ $[\text{M}+\text{Na}]^+$: 712.2, found: 712.2.

(1S,3R)-3-(Sulfonatooxymethyl)cyclohexyl (methyl 5-azido-3,5-dideoxy-D-glycero- α -D-galacto-2-nonulopyranosylonate) sodium salt (84).

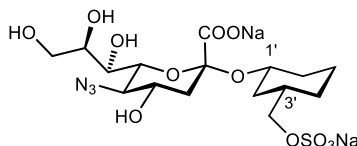


To a solution of **82** (207 mg, 0.350 mmol) in dry DMF (10.0 mL) was added $\text{SO}_3\cdot\text{pyr}$ (557 mg, 3.50 mmol). The reaction was stirred at rt for 2 h. Then, NaHCO_3 (2.50 g) was added and stirring continued

for another hour. After that, the mixture was concentrated under reduced pressure. The residue was dissolved in dry MeOH (3 mL) and a solution of NaOMe in MeOH (1 M, 150 μ L) was added. The reaction was stirred overnight at rt. The solution was then neutralized with AmberLite IR120, filtered and concentrated under reduced pressure. The crude product was purified by flash chromatography (DCM/(MeOH/H₂O 10:1), 1:0 \rightarrow 7:3) to afford **84** (155 mg, 89%) as a white solid. $[\alpha]_{\text{D}}^{20}$ -4.15 (c 1.0, MeOH); ^1H NMR (500 MHz, CD₃OD): δ = 0.89 (tt, J = 6.9, 12.6 Hz, 1H, H-4'a), 0.97 (q, J = 11.9 Hz, 1H, H-2'a), 1.22 (m, 1H, H-6'a), 1.31 (qt, J = 3.2, 12.6 Hz, 1H, H-5'a), 1.69-1.74 (m, 3H, H-3a, H-3', H-4'e), 1.76-1.85 (m, 2H, H-5'e, H-2'e), 2.05 (m, 1H, H-6'e), 2.62 (dd, J = 4.7, 12.9 Hz, 1H, H-3e), 3.43-3.49 (m, 2H, H-5, H-6), 3.56 (dddd, J = 1.3, 4.7, 8.0, 12.4 Hz, 1H, H-4), 3.66 (dd, J = 5.9, 11.3 Hz, 1H, H-9a), 3.71-3.77 (m, 2H, H-7, OCH₂SO₃Na), 3.79-3.84 (m, 6H, OMe, H-8, H-1', OCH₂SO₃Na), 3.86 (dd, J = 2.8, 11.3 Hz, 1H, H-9b); ^{13}C NMR (126 MHz, CD₃OD): δ = 24.8 (C-5'), 29.3 (C-4'), 35.7 (C-6'), 37.7 (C-2'), 38.0 (C-3'), 42.0 (C-3), 53.5 (OMe), 64.4 (C-5), 64.8 (C-9), 70.5 (C-7), 70.8 (C-4), 73.1 (C-8), 73.5 (OCH₂SO₃Na), 74.5 (C-6), 74.7 (C-1'), 100.3 (C-2), 171.4 (C=O); ESI-MS: m/z : Calcd for C₁₇H₂₈N₃NaO₁₂S [M+Na]⁺: 544.1, found: 544.1.

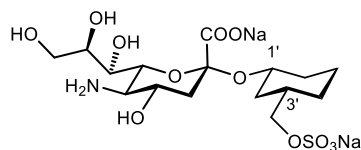
**(1S,3R)-3-(Sulfonatooxymethyl)cyclohexyl
nonulopyranosylonate disodium salt (85).**

**5-azido-3,5-dideoxy-D-glycero- α -D-galacto-2-
nonulopyranosylonate disodium salt (85).**



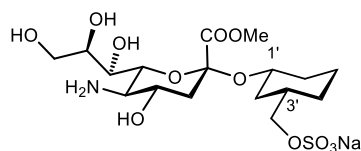
Compound **84** (145 mg, 0.320 mmol) was dissolved in 1 M aq. NaOH (9.60 mL) and stirred for 2 h. After that, it was neutralized with AmberLite IR120 and concentrated under reduced pressure to afford **85** (155 mg, quant.) as a white solid. $[\alpha]_{\text{D}}^{20}$ -5.66 (c 1.0, MeOH); ^1H NMR (500 MHz, D₂O): δ = 0.92 (qd, J = 3.8, 12.7 Hz, 1H, H-4'a), 1.04 (q, J = 11.9 Hz, 1H, H-2'a), 1.18-1.38 (m, 2H, H-5'a, H-6'a), 1.65 (t, J = 12.3 Hz, 1H, H-3a), 1.71 (m, 1H, H-4'e), 1.74-1.83 (m, 2H, H-3', H-5'e), 1.92 (m, 1H, H-2'e), 2.06 (m, 1H, H-6'e), 2.75 (dd, J = 4.8, 12.4 Hz, 1H, H-3e), 3.47 (dd, J = 9.5, 10.3 Hz, 1H, H-5), 3.59 (dd, J = 2.1, 10.3 Hz, 1H, H-6), 3.65-3.73 (m, 2H, H-4, H-9a), 3.84 (dd, J = 2.1, 9.0 Hz, 1H, H-7), 3.86-3.94 (m, 5H, H-1', H-8, H-9b, OCH₂OSO₃Na); ^{13}C NMR (126 MHz, D₂O): δ = 23.9 (C-5'), 28.2 (C-4'), 34.9 (C-6'), 36.3 (C-2'), 36.8 (C-3'), 41.5 (C-3), 63.1 (C-9), 63.3 (C-5), 69.0 (C-7), 70.2 (C-4), 72.9 (C-8), 73.3 (C-6), 74.2 (OCH₂OSO₃Na), 75.6 (C-1'), 101.8 (C-2), 174.3 (C=O); ESI-MS: m/z : Calcd for C₁₆H₂₅N₃Na₂O₁₂S [M+Na]⁺: 552.1, found: 552.1.

(1*S*,3*R*)-3-(Sulfonatooxymethyl)cyclohexyl 5-amino-3,5-dideoxy-D-glycero- α -D-galacto-2-nonulopyranosylonate disodium salt (86).



To a solution of **85** (106 mg, 0.220 mmol) in MeOH (3.0 mL), was added Pd/C (40.0 mg) under hydrogen atmosphere (1 atm). The reaction mixture was stirred at rt for 2 h. The suspension was filtered and concentrated under reduced pressure to afford **86** (101 mg, quant.) as a white solid. $[\alpha]_{\text{D}}^{20}$ -1.38 (c 1.0, MeOH); $^1\text{H NMR}$ (500 MHz, D_2O): δ = 0.92 (qd, J = 3.7, 12.6 Hz, 1H, H-4'a), 1.04 (q, J = 11.9 Hz, 1H, H-2'a), 1.19-1.38 (m, 2H, H-5'a, H-6'a), 1.58 (t, J = 12.1 Hz, 1H, H-3a), 1.69 (m, 1H, H-4'e), 1.79 (m, 2H, H-3', H-5'e), 1.92 (m, 1H, H-2'e), 2.07 (m, 1H, H-6'e), 2.71 (dd, J = 4.6, 12.3 Hz, 1H, H-3e), 2.76 (t, J = 9.7 Hz, 1H, H-5), 3.44 (ddd, J = 4.6, 9.5, 11.9 Hz, 1H, H-4), 3.53 (dd, J = 2.1, 9.9 Hz, 1H, H-6), 3.72 (dd, J = 5.6, 11.7 Hz, 1H, H-9a), 3.83 (dd, J = 2.1, 8.9 Hz, 1H, H-7), 3.86-3.95 (m, 5H, H-1', H-8, H-9b, $\text{OCH}_2\text{OSO}_3\text{Na}$); $^{13}\text{C NMR}$ (126 MHz, D_2O): δ = 23.2 (C-5'), 27.5 (C-4'), 34.3 (C-6'), 35.6 (C-2'), 36.2 (C-3'), 41.0 (C-3), 52.4 (C-5), 62.3 (C-9), 67.9 (C-7), 69.1 (C-4), 72.2 (C-8), 73.5 ($\text{OCH}_2\text{OSO}_3\text{Na}$), 74.8 (C-1'), 101.1 (C-2), 173.9 (C=O); ESI-MS: m/z : Calcd for $\text{C}_{16}\text{H}_{27}\text{NNa}_2\text{O}_{12}\text{S}$ $[\text{M}+\text{Na}]^+$: 526.1, found: 526.1.

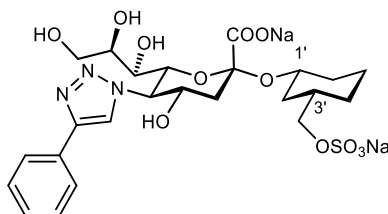
(1*S*,3*R*)-3-(Sulfonatooxymethyl)cyclohexyl (methyl 5-amino-3,5-dideoxy-D-glycero- α -D-galacto-2-nonulopyranosylonate) sodium salt (96).



To a solution of **84** (295 mg, 0.59 mmol) in MeOH (6.0 mL), was added Pd/C (111 mg) under hydrogen atmosphere (1 atm). The reaction mixture was stirred at rt for 3 h. The suspension was filtered and concentrated under reduced pressure to afford **96** (268 mg, 96%) as a white solid. $[\alpha]_{\text{D}}^{20}$ $+0.90$ (c 1.0, MeOH); $^1\text{H NMR}$ (500 MHz, CD_3OD): δ = 0.91 (m, 1H, H-4'a), 0.98 (q, J = 11.8 Hz, 1H, H-2'a), 1.15-1.40 (m, 2H, H-5'a, H-6'a), 1.64-1.72 (m, 3H, H-3a, H-3', H-4'e), 1.75-1.86 (m, 2H, H-2'e, H-5'e), 2.05 (m, 1H, H-6'e), 2.63 (dd, J = 4.6, 12.6 Hz, 1H, H-3e), 2.81 (t, J = 9.8 Hz, 1H, H-5), 3.35 (m, 1H, H-4), 3.50 (dd, J = 2.1, 9.9 Hz, 1H, H-9a), 3.68 (dd, J = 5.6, 11.1 Hz, 1H, H-6), 3.71-3.79 (m, 2H, H-7, H-8), 3.81-3.91 (m, 7H, H-1', H-9b, $\text{OCH}_2\text{OSO}_3\text{Na}$, OMe); $^{13}\text{C NMR}$ (126 MHz, CD_3OD): δ = 24.8 (C-5'), 29.3 (C-4'), 35.7 (C-6'), 37.7 (C-3'), 38.0 (C-2'), 41.9 (C-3), 53.5 (OMe), 54.3 (C-5), 64.8 (C-9), 70.1 (C-7), 70.9 (C-4), 73.4 (C-8), 73.5 ($\text{OCH}_2\text{OSO}_3\text{Na}$), 74.5 (C-1'),

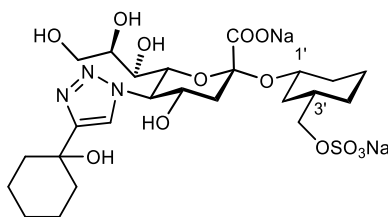
76.6 (C-6), 100.3 (C-2), 171.9 (C=O); ESI-MS: m/z : Calcd for $C_{17}H_{30}NO_{12}S$ $[M-H]^-$: 472.2, found: 472.3.

(1*S*,3*R*)-3-(Sulfonatoxymethyl)cyclohexyl 3,5-dideoxy-5-(4-phenyl-1*H*-1,2,3-triazol-1-yl)-D-glycero- α -D-galacto-2-nonulopyranosylonate disodium salt (87**).**



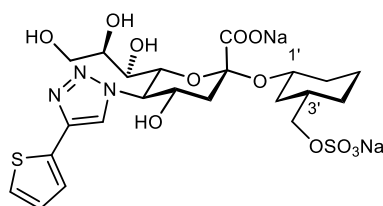
Compound **83** (31.0 mg, 0.045 mmol) and phenylacetylene (14.8 μ L, 0.135 mmol) were dissolved in dry DMF (3.0 mL) under argon. Then, CuI (1.0 mg, 0.005 mmol) and DIPEA (7.84 μ L, 0.045 mmol) were added and the mixture was stirred under argon at rt for 48 h. Then, it was diluted with EtOAc (10 mL) and washed with H₂O (10 mL) and brine (2 \times 10 mL), dried over Na₂SO₄, filtered and concentrated under reduced pressure. The crude product was purified by reversed-phase chromatography (C₁₈, H₂O/MeCN, 1:0 \rightarrow 7:3). The collected product was then treated with a 0.1 M solution of NaOH in H₂O/dioxane (1:1, 1.6 mL) overnight at rt. Then it was neutralized with AmberLite IR120, concentrated and further purified by reversed-phase chromatography (C₁₈, H₂O) to afford **87** (10 mg, 37% over two steps) as a white solid. $[\alpha]_D^{20} +4.0$ (c 1.0, MeOH); ¹H NMR (400 MHz, CD₃OD): δ = 0.91 (m, 1H, H-4'a), 1.02 (q, J = 12.0, 1H, H-2'a), 1.19-1.38 (m, 2H, H-5'a, H-6'a), 1.69-1.72 (m, 4H, H-3', H-3a, H-5'e, H-4'e), 2.06 (m, 1H, H-2'e), 2.21 (m, 1H, H-6'e), 2.95-3.01 (m, 2H, H-3e, H-7), 3.50 (dd, J = 5.8, 11.5 Hz, 1H, H-9a), 3.74 (dd, J = 2.6, 11.5 Hz, 1H, H-9b), 3.78-3.87 (m, 3H, H-8, OCH₂SO₃Na), 4.06 (td, J = 5.5, 10.8 Hz, 1H, H-1'), 4.35 (m, 1H, H-4), 4.45 (dd, J = 2.1, 10.3 Hz, 1H, H-6), 4.50 (m, 1H, H-5), 7.33 (m, 1H, Ar-H), 7.40-7.44 (m, 2H, Ar-H), 7.81-7.83 (m, 2H, Ar-H), 8.31 (s, 1H, H-triazole); ¹³C NMR (100 MHz, CD₃OD): δ = 25.0 (C-5'), 29.8 (C-4'), 36.0 (C-6'), 37.7 (C-2'), 38.2 (C-3'), 43.5 (C-3), 64.1 (C-9), 64.9 (C-5), 69.8 (C-7), 70.0 (C-4), 73.8 (OCH₂SO₃Na), 73.8 (C-8), 74.0 (C-6), 74.8 (C-1), 102.7 (C-2), 123.8 (CH-triazole), 126.7, 129.3, 129.9, 131.8, 148.1 (7C, Ar-C), 174.7 (C=O); HRMS (ESI): m/z : Calcd for $C_{24}H_{32}N_3Na_2O_{12}S$ $[M]^{2-}$: 292.5820, found: 292.5820; HPLC: Purity 96.0%.

(1*S*,3*R*)-3-(Sulfonatooxymethyl)cyclohexyl 3,5-dideoxy-5-(4-(1-hydroxycyclohexyl)-1*H*-1,2,3-triazol-1-yl)-*D*-glycero- α -*D*-galacto-2-nonulopyranosylonate disodium salt (88).



Compound **83** (60.0 mg, 0.087 mmol) and 1-ethynyl-1-cyclohexanol (34.0 μ L, 0.26 mmol) were dissolved in dry DMF (2 mL) under argon. Then, CuI (3.20 mg, 0.018 mmol) and DIPEA (15.0 μ L, 0.087 mmol) were added and the reaction was stirred under argon at rt for 24 h. Then, it was concentrated under reduced pressure and purified by reversed-phase chromatography (C₁₈, H₂O/MeCN, 1:0 \rightarrow 7:3). The collected product was treated with a 0.1 M solution of NaOH in H₂O/dioxane (1:1, 1.6 mL) overnight at rt. Then it was neutralized with AmberLite IR120, concentrated and further purified by reversed-phase chromatography (C₁₈, H₂O) to afford **88** (13 mg, 30% over two steps) as a white solid. $[\alpha]_D^{20} +2.9$ (*c* 1.0, MeOH); ¹H NMR (400 MHz, CD₃OD): δ = 0.89 (m, 1H, H-4'a), 1.01 (q, *J* = 12.0 Hz, 1H, H-2'a), 1.17-1.43 (m, 3H, H-5'a, H-6'a, H-cy), 1.43-1.54 (m, 2H, H-cy), 1.61 (m, 1H, H-cy), 1.69 (m, 1H, H-3a), 1.72-1.88 (m, 7H, H-3', H-4'e, H-5'e, 4 H-cy), 1.98-2.03 (m, 3H, H-2'e, H-cy), 2.19 (m, 1H, H-6'e), 2.89 (dd, *J* = 2.0, 9.1 Hz, 1H, H-7), 2.94 (dd, *J* = 4.9, 12.4 Hz, 1H, H-3e), 3.49 (dd, *J* = 6.0, 11.4 Hz, 1H, H-9a), 3.72-3.87 (m, 4H, H-8, H-9b, OCH₂SO₃Na), 4.03 (m, 1H, H-1'), 4.28 (ddd, *J* = 4.9, 9.4, 11.8 Hz, 1H, H-4), 4.37 (dd, *J* = 1.9, 9.9 Hz, 1H, H-6), 4.41 (m, 1H, H-5), 7.79 (s, 1H, H-triazole); ¹³C NMR (100 MHz, CD₃OD): δ = 23.0 (2C, C-cy), 24.9 (C-5'), 26.6 (C-cy), 29.8 (C-4'), 36.0 (C-6'), 37.7 (C-2'), 38.2 (C-3'), 38.7, 38.8 (2C, C-cy), 43.4 (C-3), 64.1 (C-9), 64.6 (C-5), 69.8 (C-7), 69.9 (C-4), 70.2 (C-cy), 73.8 (OCH₂SO₃Na), 73.9 (C-6), 74.8 (C-1'), 102.6 (C-2), 123.9 (CH-triazole), 156.0 (C-triazole), 174.6 (C=O); HRMS (ESI): *m/z*: Calcd for C₂₄H₃₇N₃Na₂O₁₃S [M]²⁻: 303.6029, found: 303.6029; HPLC: Purity > 99.5%.

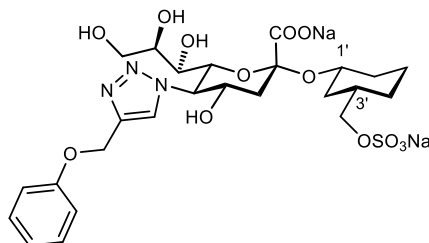
(1*S*,3*R*)-3-(Sulfonatooxymethyl)cyclohexyl 3,5-dideoxy-5-(4-(thiophen-2-yl)-1*H*-1,2,3-triazol-1-yl)-*D*-glycero- α -*D*-galacto-2-nonulopyranosylonate disodium salt (89).



Compound **85** (44.0 mg, 0.091 mmol) and 2-ethynylthiophene (27.2 μ L, 0.27 mmol) were dissolved in dry DMF (3 mL) under argon. Then, CuI (3.47 mg, 0.018 mmol) and DIPEA (15.9 μ L, 0.091

mmol) were added and the reaction was stirred under argon at rt for 24 h. Then, it was concentrated under reduced pressure and purified by reversed-phase chromatography (C₁₈, H₂O) and size-exclusion chromatography (P-2 gel, H₂O) to afford **89** (32 mg, 55%) as a white solid. $[\alpha]^{20}_{\text{D}} +2.83$ (*c* 1.0, MeOH); ¹H NMR (500 MHz, D₂O): δ = 0.86 (m, 1H, H-4'a), 1.01 (q, *J* = 11.9 Hz, 1H, H-2'a), 1.15-1.32 (m, 2H, H-5'a, H-6'a), 1.62 (m, 1H, H-4'e), 1.68-1.79 (m, 3H, H-3', H-3a, H-5'e), 1.89 (m, 1H, H-2'e), 2.04 (m, 1H, H-6'e), 2.85 (dd, *J* = 4.8, 12.6 Hz, 1H, H-3e), 2.95 (dd, *J* = 2.1, 9.0 Hz, 1H, H-7), 3.45 (dd, *J* = 6.3, 12.1 Hz, 1H, H-9a), 3.71 (dd, *J* = 2.4, 12.0 Hz, 1H, H-9b), 3.79-3.91 (m, 4H, H-8, OCH₂SO₃Na, H-1'), 4.24 (ddd, *J* = 4.7, 10.1, 11.8 Hz, 1H, H-4), 4.29 (dd, *J* = 2.1, 10.4 Hz, 1H, H-6), 4.57 (t, *J* = 10.3 Hz, 1H, H-5), 7.12 (dd, *J* = 3.6, 5.1 Hz, 1H, Ar-H), 7.44 (dd, *J* = 1.2, 5.1 Hz, 1H, Ar-H), 8.31 (s, 1H, H-triazole); ¹³C NMR (126 MHz, D₂O): δ = 24.9 (C-5'), 29.3 (C-4'), 36.0 (C-6'), 37.4 (C-2'), 37.9 (C-3'), 43.0 (C-3), 64.0 (C-9), 64.7 (C-5), 69.3 (C-7), 69.9 (C-4), 73.8 (C-8), 74.3 (C-6), 75.3 (OCH₂SO₃Na), 76.9 (C-1'), 103.1 (C-2), 123.3 (CH-triazole), 127.1, 128.0, 129.9, 133.0, 144.5 (5C, Ar-C), 175.2 (C=O); HRMS (ESI): *m/z*: Calcd for C₂₂H₂₉N₃Na₂O₁₂S₂ [M]²⁻: 295.5602, found: 295.5596; HPLC: Purity 95%.

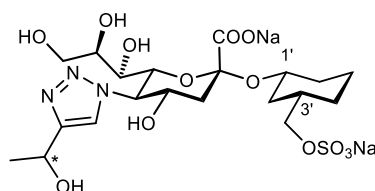
(1S,3R)-3-(Sulfonatooxymethyl)cyclohexyl 3,5-dideoxy-5-(4-(phenoxymethyl)-1H-1,2,3-triazol-1-yl)-D-glycero- α -D-galacto-2-nonulopyranosylonate disodium salt (90**).**



Compound **85** (46.0 mg, 0.095 mmol) and phenyl propargyl ether (37.5 mg, 0.284 mmol) were dissolved in dry DMF (3 mL) under argon. Then, CuI (14.0 mg, 0.076 mmol) and DIPEA (16.5 μ L, 0.095 mmol) were added and the reaction was stirred under argon at rt for 24 h. Then, it was concentrated under reduced pressure and purified by reversed-phase chromatography (C₁₈, H₂O) and size-exclusion chromatography (P-2 gel, H₂O) to afford **90** (15 mg, 24%) as a white solid. $[\alpha]^{20}_{\text{D}} +2.83$ (*c* 1.0, MeOH); ¹H NMR (500 MHz, CD₃OD): δ = 0.93 (m, 1H, H-4'a), 1.03 (q, *J* = 11.9 Hz, 1H, H-2'a), 1.26 (m, 2H, H-5'a, H-6'a), 1.67-1.78 (m, 4H, H-3', H-3, H-4'e, H-5'e), 2.02 (m, 1H, H-2'e), 2.21 (m, 1H, H-6'e), 2.90 (dd, *J* = 2.1, 9.0 Hz, 1H, H-7), 2.95 (dd, *J* = 4.9, 12.5 Hz, 1H, H-3e), 3.48 (dd, *J* = 5.9, 11.5 Hz, 1H, H-9a), 3.73 (dd, *J* = 2.7, 11.5 Hz, 1H, H-9b), 3.76-3.88 (m, 3H, H-8, OCH₂SO₃Na), 4.03 (ddt, *J* = 4.2, 8.2, 10.6 Hz, 1H, H-1'), 4.30 (ddd, *J* = 4.9, 9.6, 11.7 Hz, 1H, H-4), 4.39-4.50 (m, 2H, H-5, H-6), 5.15 (s, 1H, CH₂OPh), 6.94 (t, *J* = 7.4 Hz, 1H, Ar-H), 7.00 (d, *J* = 8.2 Hz, 2H, Ar-H), 7.18-7.35 (m, 2H, Ar-H), 8.04 (s, 1H, H-triazole); ¹³C NMR (126 MHz, CD₃OD): δ

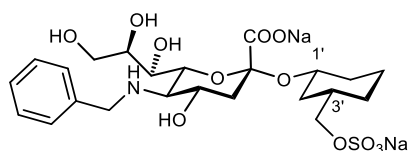
= 24.9 (C-5'), 29.9 (C-4'), 36.1 (C-6'), 37.7 (C-2'), 38.2 (C-3'), 43.5 (C-3), 62.4 (OCH₂Ph), 64.3 (C-9), 64.9 (C-5), 69.9 (C-4), 70.0 (C-7), 73.8 (OCH₂SO₃Na), 73.8 (C-8), 73.9 (C-6), 74.9 (C-1'), 102.8 (C-2), 115.8, 122.2 (3C, Ar-C), 126.7 (CH-triazole), 130.5, 144.3 (3C, Ar-C), 159.9 (C-triazole), 174.5 (C=O); HRMS (ESI): *m/z*: Calcd for C₂₅H₃₃N₃Na₂O₁₃S [*M*]²⁻: 307.5873, found: 307.5873; HPLC: Purity 81%.

(1S,3R)-3-(Sulfonatooxymethyl)cyclohexyl 3,5-dideoxy-5-(4-(1-hydroxyethyl)-1H-1,2,3-triazol-1-yl)-D-glycero- α -D-galacto-2-nonulopyranosylonate disodium salt (91).



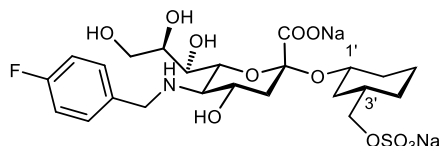
Compound **85** (40.0 mg, 0.083 mmol) and 3-butyn-2-ol (20 μ L, 0.247 mmol) were dissolved in dry DMF (3 mL) under argon. Then, CuI (3.00 mg, 0.016 mmol) and DIPEA (14.5 μ L, 0.083 mmol) were added and the reaction was stirred under argon at rt for 24 h. Then, it was concentrated under reduced pressure and purified by reversed-phase chromatography (C₁₈, H₂O) and size-exclusion chromatography (P-2 gel, H₂O) to afford **91** (16 mg, 32%) as a white solid. [α]_D²⁰ -0.67 (*c* 1.0, MeOH); ¹H NMR (500 MHz, D₂O): δ = 0.95 (m, 1H, H-4'a), 1.09 (q, *J* = 11.9 Hz, 1H, H-2'a), 1.23-1.39 (m, 2H, H-5'a, H-6'a), 1.58 (d, *J* = 6.7 Hz, 3H, CH₃), 1.71 (m, 1H, H-4'e), 1.77-1.86 (m, 3H, H-3a, H-3', H-5'e), 1.97 (m, 1H, H-2'e), 2.11 (m, 1H, H-6'e), 2.88-2.96 (m, 2H, H-3e, H-7), 3.53 (dd, *J* = 6.3, 12.1 Hz, 1H, H-9a), 3.79 (dd, *J* = 2.5, 12.0 Hz, 1H, H-9b), 3.88 (ddt, *J* = 3.0, 6.3, 8.9 Hz, 1H, H-8), 3.91-4.00 (m, 3H, H-1', OCH₂SO₃Na), 4.28 (m, 1H, H-4), 4.33 (dd, *J* = 2.1, 10.5 Hz, 1H, H-6), 4.60 (t, *J* = 10.3 Hz, 1H, H-5), 5.10 (q, *J* = 6.7 Hz, 1H, CH), 8.07 (s, 1H, H-triazole); ¹³C NMR (126 MHz, D₂O): δ = 22.08, 22.11 (2C, CH₃), 23.6 (C-4'), 28.0 (C-5'), 34.7 (C-6'), 36.1 (C-2'), 36.6 (C-3'), 41.7 (C-3), 62.4, 62.5 (CH), 62.7 (C-9), 63.2 (C-5), 68.0 (C-7), 68.6 (C-4), 72.5 (C-8), 73.0 (C-6), 74.0 (OCH₂SO₃Na), 75.6 (C-1'), 101.8 (C-2), 123.1 (CH-triazole), 152.1 (C-triazole), 173.9 (C=O); HRMS (ESI): *m/z*: Calcd for C₂₀H₃₁N₃Na₂O₁₃S [*M*]²⁻: 276.5794, found: 276.5793; HPLC: Purity 70.0%.

(1S,3R)-3-(Sulfonatooxymethyl)cyclohexyl 5-benzylamino-3,5-dideoxy-D-glycero- α -D-galacto-2-nonulopyranosylonate disodium salt (92).



To a solution of **86** (30.0 mg, 0.060 mmol) in dry MeOH (3 mL) were added benzaldehyde (4.10 μ L, 0.030 mmol), acetic acid (70.0 μ L, 1.20 mmol) and NaCNBH₃ (2.64 mg, 0.042 mmol). The reaction was stirred for 4 h at rt and under argon. Then, the solution was concentrated under reduced pressure and purified by LCMS. The clean product was hydrolyzed in 0.1 M NaOH (H₂O/dioxane, 1:1) at rt for 3 h. Then, the reaction was neutralized with AmberLite IR120, filtered and evaporated. The residue was purified again by LCMS and size exclusion column chromatography (P-2 gel, H₂O) to afford **92** as a white solid (3.56 mg, 20%). $[\alpha]_{\text{D}}^{20} +7.75$ (*c* 0.8, MeOH); ¹H NMR (500 MHz, D₂O): δ = 0.92 (qd, *J* = 3.7, 12.6 Hz, 1H, H-4'a), 1.05 (q, *J* = 11.9 Hz, 1H, H-2'a), 1.21-1.36 (m, 2H, H-5'a, H-6'a), 1.67-1.72 (m, 2H, H-3a, H-4'e), 1.75-1.84 (m, 2H, H-3', H-5'e), 1.93 (m, 1H, H-2'e), 2.02 (m, 1H, H-6'e), 2.77 (dd, *J* = 4.7, 12.6 Hz, 1H, H-3e), 3.31 (t, *J* = 10.4 Hz, 1H, H-5), 3.77 (dd, *J* = 5.6, 12.0 Hz, 1H, H-9a), 3.85-4.02 (m, 7H, H-4, H-7, H-8, H-9b, H-1', OCH₂SO₃Na), 4.19 (dd, *J* = 2.1, 10.4 Hz, 1H, H-6), 4.33 (d, *J* = 13.1 Hz, 1H, CH₂NH), 4.49 (d, *J* = 13.1 Hz, 1H, CH₂NH), 7.51-7.55 (m, 5H, Ar-H); ¹³C NMR (126 MHz, D₂O): δ = 24.1 (C-5'), 28.5 (C-4'), 35.1 (C-6'), 36.6 (C-2'), 37.1 (C-3'), 42.3 (C-3), 51.7 (CH₂NH), 58.9 (C-5), 63.1 (C-9), 67.1 (C-4), 69.1 (C-7), 72.1 (C-6), 73.2 (C-8), 74.4 (OCH₂SO₃Na), 76.0 (C-1'), 130.2, 131.0 (4C, Ar-C); HRMS (ESI): *m/z*: Calcd for C₂₃H₃₃NNa₂O₁₂S [M+Na]⁺: 616.1417, found: 616.1417; HPLC: Purity > 95.0%.

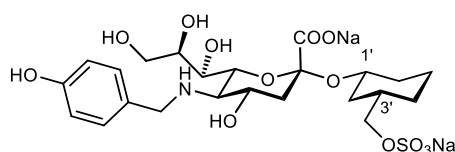
(1S,3R)-3-(Sulfonatooxymethyl)cyclohexyl 3,5-dideoxy-5-(4-fluorobenzyl)amino-D-glycero- α -D-galacto-2-nonulopyranosylonate disodium salt (93).



To a solution of **86** (30.0 mg, 0.065 mmol) in dry MeOH (2 mL) were added 4-fluoro-benzaldehyde (3.50 μ L, 0.033 mmol), acetic acid (75.0 μ L, 1.30 mmol) and NaCNBH₃ (2.90 mg, 0.046 mmol). The reaction was stirred for 4 h at rt under argon. Then, the solution was concentrated under reduced pressure and purified by LCMS. The residue was dissolved in H₂O, slightly basified with 0.1 M aq. NaOH solution and purified by size exclusion column chromatography (P-2 gel, H₂O) to afford **93** (14.9 mg, 74%) as a white solid. $[\alpha]_{\text{D}}^{20} +4.53$ (*c* 1, MeOH); ¹H NMR (500 MHz, D₂O): δ = 0.92 (qd, *J* = 4.2, 12.6, 13.1 Hz, 1H, H-4'a), 1.04 (q, *J* = 11.9 Hz, 1H, H-2'a), 1.17-1.37 (m, 2H, H-5'a, H-6'a), 1.62 (t, *J* = 12.1 Hz, 1H, H-3a), 1.69 (m, 1H, H-4'e), 1.71-1.85 (m, 2H, H-3', H-5'e), 1.92 (m, 1H, H-2'e), 2.04 (m, 1H, H-6'e), 2.78 (dd, *J* = 4.7, 12.4 Hz, 1H, H-3e), 3.22 (t, *J* = 10.3 Hz, 1H, H-5), 3.78 (dd, *J* = 5.4, 11.9 Hz, 1H, H-9a), 3.82-4.01 (m, 7H, H-4, H-7, H-8, H-9b, H-1', OCH₂SO₃Na), 4.11 (dd, *J* = 2.3, 10.4 Hz, 1H, H-6), 4.30 (d, *J* = 13.2 Hz, 1H, CH₂NH), 4.47 (d, *J* = 13.2 Hz, 1H, CH₂NH), 7.21-7.27 (m, 2H, Ar-H), 7.53-7.58 (m, 2H, Ar-H); ¹³C NMR (126 MHz, D₂O): δ = 23.8

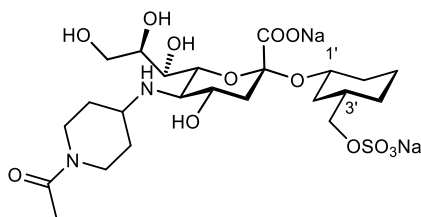
(C-5'), 28.1 (C-4'), 34.8 (C-6'), 36.2 (C-2'), 36.8 (C-3'), 41.9 (C-3), 50.6 (CH₂NH), 58.4 (C-5), 62.7 (C-9), 66.6 (C-4), 68.7 (C-7), 71.6 (C-6), 72.8 (C-8), 74.1 (OCH₂SO₃Na), 75.7 (C-1'), 101.6 (C-2), 116.6, 116.8, 127.3, 132.9, 133.0 (5C, Ar-C), 163.9 (d, $J_{CF} = 246.5$ Hz, Ar-C), 173.8 (C=O); HRMS (ESI): m/z : Calcd for C₂₃H₃₂FNNa₂O₁₂S [M+Na]⁺: 634.1322, found: 634.1322; HPLC: Purity > 95.0%.

(1S,3R)-3-(Sulfonatooxymethyl)cyclohexyl 3,5-dideoxy-5-(4-hydroxybenzyl)amino-D-glycero- α -D-galacto-2-nonulopyranosylonate disodium salt (94).



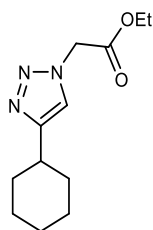
To a solution of **86** (36.0 mg, 0.078 mmol) in dry MeOH (2 mL) were added 4-hydroxybenzaldehyde (4.76 mg, 0.039 mmol), acetic acid (89.0 μ L, 1.56 mmol) and NaCNBH₃ (3.43 mg, 0.055 mmol). The reaction was stirred for 16 h at rt under argon. Then, the solution was concentrated under reduced pressure and purified by LCMS. The residue was dissolved in H₂O, slightly basified with 0.1 M aq. NaOH solution and purified by size exclusion column chromatography (P-2 gel, H₂O) to afford **94** (4.16 mg, 17%) as a white solid. $[\alpha]_D^{20} +6.93$ (c 0.95, MeOH); ¹H NMR (500 MHz, D₂O): δ = 0.92 (qd, $J = 3.7, 12.6$ Hz, 1H, H-4'a), 1.04 (q, $J = 11.9$ Hz, 1H, H-2'a), 1.17-1.38 (m, 2H, H-5'a, H-6'a), 1.62 (t, $J = 12.1$ Hz, 1H, H-3a), 1.69 (m, 1H, H-4'e), 1.73-1.83 (m, 2H, H-3', H-5'e), 1.91 (m, 1H, H-2'e), 2.04 (m, 1H, H-6'e), 2.78 (dd, $J = 4.7, 12.4$ Hz, 1H, H-3e), 3.22 (t, $J = 10.3$ Hz, 1H, H-5), 3.77 (dd, $J = 5.4, 11.8$ Hz, 1H, H-9a), 3.81-4.00 (m, 7H, H-4, H-7, H-8, H-9b, H-1', OCH₂SO₃Na), 4.10 (dd, $J = 2.2, 10.3$ Hz, 1H, H-6), 4.22 (d, $J = 13.1$ Hz, 1H, CH₂NH), 4.40 (d, $J = 13.1$ Hz, 1H, CH₂NH), 6.97 (d, $J = 8.6$ Hz, 2H, Ar-H), 7.41 (d, $J = 8.6$ Hz, 2H, Ar-H); ¹³C NMR (126 MHz, D₂O): δ = 23.8 (C-5'), 28.1 (C-4'), 34.8 (C-6'), 36.2 (C-2'), 36.8 (C-3'), 41.9 (C-3), 50.8 (CH₂NH), 58.2 (C-5), 62.8 (C-9), 66.6 (C-4), 68.7 (C-7), 71.6 (C-6), 72.8 (C-8), 74.1 (OCH₂SO₃Na), 75.7 (C-1'), 101.6 (C-2), 116.6, 132.6, 157.4 (6C, Ar-C), 173.8 (C=O); HRMS (ESI): m/z : Calcd for C₂₃H₃₃NNa₂O₁₃S [M+H]⁺: 610.1546, found: 610.1548; HPLC: Purity > 95.0%.

(1*S*,3*R*)-3-(Sulfonatooxymethyl)cyclohexyl 5-(1-acetylpiperidin-4-yl)amino-3,5-dideoxy-D-glycero- α -D-galacto-2-nonulopyranosylonate disodium salt (95).



To a solution of **86** (30.0 mg, 0.065 mmol) in dry MeOH (2 mL) were added 1-acetyl-4-piperidone (4.00 μ L, 0.033 mmol), acetic acid (75.0 μ L, 1.30 mmol) and NaCNBH₃ (2.90 mg, 0.046 mmol). The reaction was stirred for 16 h at rt under argon. After that, the solution was concentrated under reduced pressure and purified by LCMS. The compound was dissolved in H₂O, slightly basified with 0.1 M aq. NaOH solution and purified by size exclusion column chromatography (P-2 gel, H₂O) to afford **95** as a white solid (7.80 mg, 38%). $[\alpha]_{\text{D}}^{20} +1.59$ (*c* 1, MeOH); ¹H NMR (500 MHz, D₂O): δ = 0.84 (qd, *J* = 3.7, 12.5 Hz, 1H, H-4'a), 0.97 (q, *J* = 11.9 Hz, 1H, H-2'a), 1.10-1.30 (m, 2H, H-5'a, H-6'a), 1.39-1.76 (m, 6H, H-3a, H-3', H-4'e, H-5'e, CH₂-piperidine), 1.84 (m, 1H, H-2'e), 1.96 (m, 1H, H-6'e), 2.08 (s, 3H, NCOCH₃), 2.11-2.29 (m, 2H, CH₂-piperidine), 2.64-2.77 (m, 2H, H-3e, NCH₂-piperidine), 3.14 (m, 1H, NCH₂-piperidine), 3.21 (t, *J* = 10.2 Hz, 1H, H-5), 3.56 (m, 1H, CH-piperidine), 3.63-3.74 (m, 3H, H-4, H-7, H-9a), 3.78-3.90 (m, 5H, H-8, H-9b, H-1', OCH₂SO₃Na), 3.94-4.04 (m, 2H, H-6, NCH₂-piperidine), 4.42 (m, 1H, NCH₂-piperidine); ¹³C NMR (126 MHz, D₂O): δ = 21.0 (NCOCH₃), 23.8 (C-5'), 28.1 (C-4'), 28.7, 29.4 (2C, CH₂-piperidine), 34.8 (C-6'), 36.2 (C-2'), 36.8 (C-3'), 40.8 (NCH₂-piperidine), 42.0 (C-3), 45.4 (NCH₂-piperidine), 56.4 (CH-piperidine), 57.5 (C-5), 62.7 (C-9), 67.4 (C-4), 68.6 (C-7), 72.1 (C-6), 72.7 (C-8), 74.1 (OCH₂SO₃Na), 75.8 (C-1'), 101.6 (C-2), 173.0, 173.8 (2C, C=O); HRMS (ESI): *m/z*: Calcd for C₂₃H₃₈N₂Na₂O₁₃S [M+H]⁺: 628.1968, found: 629.1979; HPLC: Purity 95.0%.

Ethyl 2-(4-cyclohexyl-1*H*-1,2,3-triazol-1-yl)acetate (108).

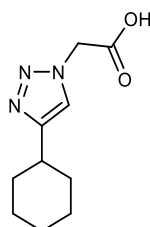


To a solution of ethynylcyclohexane (484 μ L, 3.68 mmol) and ethyl 2-azidoacetate (25% in toluene, 1.74 mL, 3.68 mmol) in DMF (12.0 mL) were added CuI (140 mg, 0.74 mmol) and DIPEA (640 μ L, 3.68 mmol). The solution was stirred overnight at rt under argon. Then, it was diluted with H₂O (10 mL) and extracted with DCM (3 \times 20 mL), dried over Na₂SO₄, filtered and concentrated under

reduced pressure. The crude product was then purified by flash column chromatography (petroleum ether/EtOAc, 1:0 → 8:2) to afford **108** (600 mg, 69%) as a white solid. ^1H NMR (500 MHz, CDCl_3): δ = 1.25 (m, 1H, $\text{CH}_2\text{-cy}$), 1.29 (t, J = 7.1 Hz, 3H, OCH_2CH_3), 1.34-1.48 (m, 4H, $\text{CH}_2\text{-cy}$), 1.72 (m, 1H, $\text{CH}_2\text{-cy}$), 1.77-1.84 (m, 2H, $\text{CH}_2\text{-cy}$), 2.01-2.12 (m, 2H, $\text{CH}_2\text{-cy}$), 2.79 (m, 1H, CH-cy), 4.26 (q, J = 7.2 Hz, 2H, OCH_2CH_3), 5.11 (s, 2H, CH_2), 7.37 (s, 1H, H-triazole); ^{13}C NMR (126 MHz, CDCl_3): δ = 14.2 (OCH_2CH_3), 26.2, 26.3, 33.1 (5C, $\text{CH}_2\text{-cy}$), 35.4 (CH-cy), 50.9 (CH_2), 62.4 (OCH_2CH_3), 120.8 (CH-triazole), 154.3 (C-triazole), 166.7 (C=O); ESI-MS: m/z : calcd for $\text{C}_{12}\text{H}_{19}\text{N}_3\text{O}_2$ [$\text{M}+\text{H}$] $^+$: 238.2, found: 238.0.

The analytical data of **108** were in accordance with reported values.³⁴

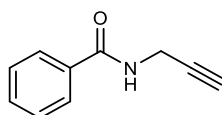
2-(4-Cyclohexyl-1H-1,2,3-triazol-1-yl)acetic acid (**109**).



Compound **108** (83.0 mg, 0.35 mmol) was dissolved in 0.1 M NaOH solution (H_2O /dioxane, 1:1, 6.0 mL) and stirred at rt for 4 h. Then, it was neutralized with AmberLite IR120 and concentrated under reduced pressure to afford **109** (73.0 mg, quant.) as a white solid. ^1H NMR (500 MHz, CDCl_3): δ = 1.25 (m, 1H, $\text{CH}_2\text{-cy}$), 1.33-1.46 (m, 4H, $\text{CH}_2\text{-cy}$), 1.72 (m, 1H, $\text{CH}_2\text{-cy}$), 1.76-1.85 (m, 2H, $\text{CH}_2\text{-cy}$), 1.96-2.10 (m, 2H, $\text{CH}_2\text{-cy}$), 2.77 (ddq, J = 3.4, 4.0, 6.7, 11.4 Hz, 1H, CH-cy), 5.15 (s, 2H, CH_2), 7.47 (s, 1H, H-triazole); ^{13}C NMR (126 MHz, CDCl_3): δ = 26.0, 26.1, 32.9 (5C, $\text{CH}_2\text{-cy}$), 35.0 (CH-cy), 51.3 (CH_2), 121.8 (CH-triazole), 153.6 (C-triazole), 168.5 (C=O); ESI-MS: m/z : Calcd for $\text{C}_{10}\text{H}_{15}\text{N}_3\text{O}_2$ [$\text{M}+\text{H}$] $^+$: 210.1, found: 210.1.

The analytical data of **109** were in accordance with reported values.³⁴

N-(Prop-2-yn-1-yl)benzamide (**110**).

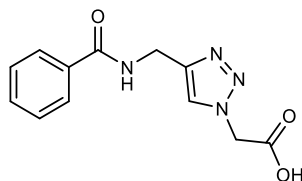


A solution of benzoic acid (0.364 g, 2.98 mmol) in dry DMF (10 mL) was stirred under argon with DIPEA (1.1 mL, 6.31 mmol) and HATU (1.70 g, 4.47 mmol) for 40 minutes. Then, propargylamine (572 μL , 8.94 mmol) was added and the reaction was stirred overnight at rt. After that, it was diluted with DCM (10 mL) and H_2O (10 mL) and the organic phase was washed with brine (10 mL), aq. satd. NaHCO_3 (10 mL) and H_2O (10 mL), dried over Na_2SO_4 , filtered and concentrated under reduced

pressure. The residue was purified by flash column chromatography (petroleum ether/EtOAc, 1:0 → 7:3) to afford **110** (0.364 g, 77%) as a white solid. ^1H NMR (500 MHz, CDCl_3): δ = 2.29 (t, J = 2.6 Hz, 1H, CH-alkyne), 4.27 (dd, J = 2.6, 5.2 Hz, 2H, CH_2), 6.26 (s, 1H, NH), 7.38-7.48 (m, 2H, Ar-H), 7.50-7.58 (m, 1H, Ar-H), 7.75-7.83 (m, 2H, Ar-H); ^{13}C NMR (126 MHz, CDCl_3): δ = 30.0 (CH_2), 72.1 (CH-alkyne), 127.1, 128.8, 132.0, 133.9 (6C, Ar-C); ESI-MS: m/z : Calcd for $\text{C}_{10}\text{H}_9\text{NO}$ $[\text{M}+\text{H}]^+$: 160.1, found: 160.0.

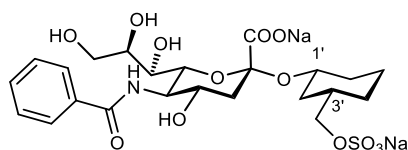
The analytical data of **110** were in accordance with reported values.⁴⁰

2-(4-Benzamidomethyl-1H-1,2,3-triazol-1-yl)acetic acid (**111**).



To a solution of **110** (354 mg, 2.22 mmol) and ethyl 2-azidoacetate (25% in toluene, 1.30 mL, 2.22 mmol) in DMF (10.0 mL) were added CuI (86.4 mg, 0.44 mmol) and DIPEA (387 μL , 2.22 mmol). The solution was stirred overnight at rt under argon. Then, it was diluted with H_2O (10 mL) and extracted with DCM (3 x 20 mL), dried over Na_2SO_4 , filtered and concentrated under reduced pressure. The residue was purified by flash column chromatography (petroleum ether/EtOAc, 1:0 → 6:4). The collected product was dissolved in 0.1 M NaOH solution (H_2O /dioxane, 1:1, 27 mL) and stirred at rt for 4 h. After that, it was neutralized with AmberLite IR120 and concentrated under reduced pressure to afford **111** (240 mg, 42% over two steps) as a white solid. ^1H NMR (500 MHz, CD_3OD): δ = 4.66 (s, 2H, CH_2NH), 5.26 (s, 2H, CH_2COOH), 7.45 (dd, J = 7.0, 8.3 Hz, 2H, Ar-H), 7.50-7.57 (m, 1H, Ar-H), 7.79-7.88 (m, 2H, Ar-H), 7.96 (s, 1H, H-triazole); ^{13}C NMR (126 MHz, CD_3OD): δ = 36.1 (CH_2NH), 51.7 (CH_2COOH), 125.9 (CH-triazole), 128.4, 129.6, 132.8, 135.3 (6C, Ar-C), 146.5 (C-triazole), 169.9, 170.2 (2C, C=O); ESI-MS: m/z : Calcd for $\text{C}_{12}\text{H}_{12}\text{N}_4\text{O}_3$ $[\text{M}+\text{H}]^+$: 261.1, found: 261.1.

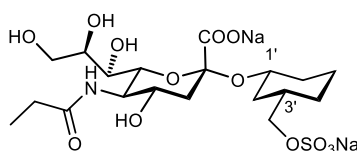
(1S,3R)-3-(Sulfonatooxymethyl)cyclohexyl 5-benzamido-3,5-dideoxy-D-glycero- α -D-galacto-2-nonulopyranosylonate disodium salt (**97**).



A solution of benzoic acid (14.7 mg, 0.120 mmol) in dry DMF (1 mL) was stirred under argon with DIPEA (26.0 μL , 0.15 mmol) and HATU (57.0 mg, 0.15 mmol) for 40 min. Then, **96** (30.0 mg, 0.06

mmol) was added and the reaction was stirred overnight at rt. The mixture was concentrated under reduced pressure and purified by flash column chromatography (DCM/(MeOH/H₂O 10:1), 1:0 → 7:3). A fraction of the collected product (13 mg, 0.02 mmol) was dissolved in 0.1 M NaOH solution (H₂O/dioxane, 1:1, 1 mL) and stirred for 48 h. After that, it was neutralized with AmberLite IR120, concentrated under reduced pressure and purified by size exclusion chromatography (P-2 gel, H₂O) to afford **97** (4.44 mg, 37% over two steps) as a white solid. $[\alpha]_{\text{D}}^{20} +4.80$ (*c* 1, MeOH); ¹H NMR (500 MHz, D₂O): δ = 0.94 (qd, *J* = 3.7, 12.6 Hz, 1H, H-4'a), 1.07 (q, *J* = 12.0 Hz, 1H, H-2'a), 1.22-1.41 (m, 2H, H-5'a, H-6'a), 1.66-1.87 (m, 4H, H-3a, H-3', H-4'e, H-5'e), 1.94 (m, 1H, H-2'e), 2.10 (m, 1H, H-6'e), 2.83 (dd, *J* = 4.7, 12.3 Hz, 1H, H-3e), 3.62-3.72 (m, 2H, H-7, H-9a), 3.81-3.99 (m, 7H, H-4, H-6, H-8, H-9b, H-1', OCH₂SO₃Na), 4.09 (t, *J* = 10.2 Hz, 1H, H-5), 7.53-7.56 (m, 2H, Ar-H), 7.64 (m, 1H, Ar-H), 7.80 (m, 2H, Ar-H); ¹³C NMR (126 MHz, D₂O): δ = 23.4 (C-5'), 27.8 (C-4'), 34.5 (C-6'), 35.8 (C-2'), 36.4 (C-3'), 41.5 (C-3), 52.6 (C-5), 62.7 (C-9), 68.5 (C-4, C-7), 72.3 (C-6), 72.9 (C-8), 73.6 (OCH₂SO₃Na), 75.0 (C-1'), 101.3 (C-2), 127.4, 128.9, 132.5, 133.5 (6C, Ar-C), 172.1, 174.0 (2C, C=O); HRMS (ESI): *m/z*: Calcd for C₂₃H₃₁NNa₂O₁₃S [M+Na]⁺: 630.1209, found: 630.1209; HPLC: Purity 93.0%.

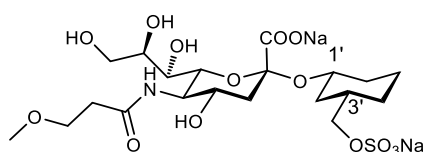
(1S,3R)-3-(Sulfonatooxymethyl)cyclohexyl 3,5-dideoxy-5-propionamido-D-glycero- α -D-galacto-2-nonulopyranosylonate disodium salt (98**).**



A solution of propionic acid (9.00 μ L, 0.126 mmol) in dry DMF (1 mL) was stirred under argon with DIPEA (27.0 μ L, 0.160 mmol) and HATU (60.0 mg, 0.160 mmol) for 40 min. Then, **96** (30.0 mg, 0.063 mmol) was added and the reaction was stirred overnight at rt for 16 h. After that, TLC still showed starting material, therefore another portion of DIPEA (0.160 mmol) and HATU (0.160 mmol) was added and stirring continued for further 16 h. Then, the mixture was concentrated under reduced pressure and the residue was purified by flash column chromatography (DCM/(MeOH/H₂O 10:1), 1:0 → 6:4). The collected product (21.8 mg, 0.029 mmol) was dissolved in 0.1 M NaOH solution (H₂O/dioxane, 1:1, 1 mL) and stirred for 24 h. Then, it was neutralized with AmberLite IR120, concentrated under reduced pressure and purified by size exclusion chromatography (P-2 gel, H₂O) to afford **98** (14.0 mg, 40% over two steps) as a white solid. $[\alpha]_{\text{D}}^{20} +8.65$ (*c* 1, MeOH); ¹H NMR (500 MHz, D₂O): δ = 0.92 (qd, *J* = 3.7, 12.6 Hz, 1H, H-4'a), 1.05 (q, *J* = 11.9 Hz, 1H, H-2'a), 1.13 (t, *J* = 7.7 Hz, 3H, NHCH₂CH₃), 1.20-1.37 (m, 2H, H-5'a, H-6'a), 1.65 (t, *J* = 12.2 Hz, 1H, H-3a), 1.71 (m, 1H, H-4'e), 1.80 (m, 2H, H-3', H-5'e), 1.92 (m, 1H, H-2'e), 2.08 (m, 1H, H-6'e), 2.32 (q, *J* = 7.6 Hz,

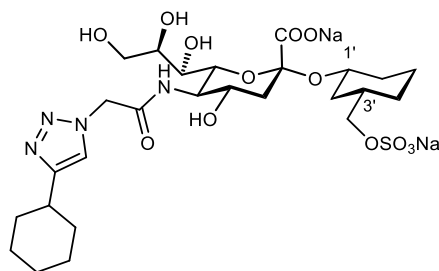
2H, NHCH_2CH_3), 2.77 (dd, $J = 4.6, 12.4$ Hz, 1H, H-3e), 3.60 (dd, $J = 2.0, 9.0$ Hz, 1H, H-7), 3.63-3.73 (m, 3H, H-4, H-6, H-9a), 3.81 (t, $J = 10.1$ Hz, 1H, H-5), 3.84-3.94 (m, 5H, H-8, H-9b, H-1', $\text{OCH}_2\text{SO}_3\text{Na}$); ^{13}C NMR (126 MHz, D_2O): $\delta = 10.1$ (NHCH_2CH_3), 23.8 (C-5'), 28.2 (C-4), 29.9 (NHCH_2CH_3), 34.9 (C-6'), 36.2 (C-2'), 36.8 (C-3'), 41.8 (C-3), 52.3 (C-5), 63.1 (C-9), 68.7 (C-7), 68.8 (C-4), 72.7 (C-8), 73.4 (C-4), 74.2 ($\text{OCH}_2\text{SO}_3\text{Na}$), 75.4 (C-1'), 101.6 (C-2), 174.5, 179.7 (2C, C=O); HRMS (ESI): m/z : Calcd for $\text{C}_{19}\text{H}_{31}\text{NNa}_2\text{O}_{13}\text{S}$ [$\text{M}+\text{Na}$] $^+$: 582.1209, found: 582.1209; HPLC: Purity 82.0%.

(1S,3R)-3-(Sulfonatooxymethyl)cyclohexyl 3,5-dideoxy-5-(3-methoxypropanamido)-D-glycero- α -D-galacto-2-nonulopyranosylonate disodium salt (99**).**



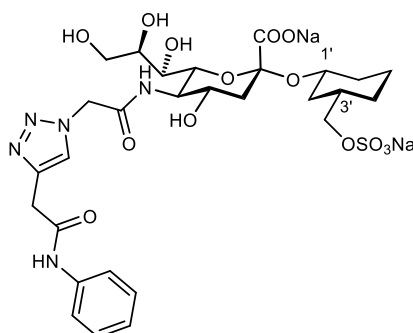
A solution of 3-methoxypropionic acid (8.30 μL , 0.088 mmol) in dry DMF (1 mL) was stirred under argon with DIPEA (19.0 μL , 0.110 mmol) and HATU (41.8 mg, 0.110 mmol) for 40 min. Then, **96** (20.0 mg, 0.044 mmol) was added and the reaction was stirred overnight at rt for 16 h. After that, TLC still showed starting material, therefore another portion of DIPEA (0.160 mmol) and HATU (0.160 mmol) was added and stirring continued for further 16 h. Then, the mixture was concentrated under reduced pressure and the residue was purified by flash column chromatography (DCM/(MeOH/ H_2O 10:1), 1:0 \rightarrow 6:4). The collected product (17.0 mg, 0.029 mmol) was dissolved in 0.1 M NaOH solution (H_2O /dioxane, 1:1, 1 mL) and stirred for 24 h. After that, it was neutralized with AmberLite IR120, concentrated under reduced pressure and purified by size exclusion chromatography (P-2 gel, H_2O) to afford **99** (10.6 mg, 41% over two steps) as a white solid. $[\alpha]_{\text{D}}^{20} +24.4$ (c 1, MeOH); ^1H NMR (500 MHz, D_2O): $\delta = 0.93$ (m, 1H, H-4'a), 1.05 (q, $J = 11.9$ Hz, 1H, H-2'a), 1.19-1.37 (m, 2H, H-5'a, H-6'a), 1.65 (t, $J = 12.2$ Hz, 1H, H-3a), 1.70 (m, 1H, H-4'e), 1.79 (m, 2H, H-3', H-5'e), 1.92 (m, 1H, H-2'e), 2.08 (m, 1H, H-6'e), 2.53-2.66 (m, 2H, CH_2CONH), 2.77 (dd, $J = 4.7, 12.4$ Hz, 1H, H-3e), 3.37 (s, 3H, OMe), 3.61 (dd, $J = 1.9, 8.9$ Hz, 1H, H-7), 3.64-3.79 (m, 5H, H-4, H-6, H-9a, CH_2OMe), 3.81-3.95 (m, 6H, H-5, H-8, H-9b, H-1', $\text{OCH}_2\text{SO}_3\text{Na}$); ^{13}C NMR (126 MHz, D_2O): $\delta = 23.9$ (C-5'), 28.2 (C-4'), 34.9 (C-6'), 36.3 (C-2'), 36.6 (CH_2CONH), 36.8 (C-3'), 41.8 (C-3), 52.5 (C-5), 58.6 (OMe), 63.2 (C-9), 68.8 (CH_2OMe), 68.78 (C-7), 68.81 (C-4), 72.8 (C-8), 73.4 (C-6), 74.2 ($\text{OCH}_2\text{SO}_3\text{Na}$), 75.5 (C-1'), 101.7 (C-2), 174.5, 175.7 (2C, C=O); HRMS (ESI): m/z : Calcd for $\text{C}_{20}\text{H}_{33}\text{NNa}_2\text{O}_{14}\text{S}$ [$\text{M}+\text{Na}$] $^+$: 612.1315, found: 612.1311; HPLC: Purity 87.0%.

(1*S*,3*R*)-3-(Sulfonatooxymethyl)cyclohexyl 5-(2-(4-cyclohexyl-1*H*-1,2,3-triazol-1-yl)acetamido)-3,5-dideoxy- α -D-galacto-2-nonulopyranosylonate disodium salt (100**).**



Compound **109** (67 mg, 0.32 mmol) and *N*-hydroxysuccinimide (46.0 mg, 0.40 mmol) were dissolved in EtOAc (4 mL) and cooled to 0 °C. DCC (82.5 mg, 0.40 mmol) was then added and the reaction stirred overnight at 0 °C. Then, the formed DCU by-product was filtered off and the solvents were evaporated. The crude intermediate was used in the next step without further purification. A part of the intermediate (40.0 mg, 0.13 mmol) was dissolved in DMF (1 mL) and added to a solution of **96** (15.0 mg, 0.032 mmol) in DMF (1 mL) with NEt₃ (7.0 μ L). The mixture was stirred overnight under argon at rt. The solvents were then evaporated and the residue was purified by flash chromatography (DCM/(MeOH/H₂O 10:1), 1:0 \rightarrow 6:4). The collected product (14 mg, 0.02 mmol) was dissolved in 0.1 M NaOH solution (H₂O/dioxane, 1:1, 1 mL) and stirred overnight. After that, it was neutralized with AmberLite IR120, concentrated under reduced pressure and purified by size exclusion chromatography (P-2 gel, H₂O) to afford **100** (5.50 mg, 26% over two steps) as a white solid. $[\alpha]_D^{20} +11.4$ (*c* 1, MeOH); ¹H NMR (500 MHz, D₂O): δ = 0.92 (qd, *J* = 3.7, 12.6 Hz, 1H, H-4'a), 1.04 (q, *J* = 11.9 Hz, 1H, H-2'a), 1.17-1.37 (m, 3H, H-5'a, H-6'a, CH₂-cy), 1.37-1.50 (m, 4H, CH₂-cy), 1.66 (t, *J* = 12.2 Hz, 1H, H-3a), 1.68-1.74 (m, 2H, H-4'e, H-5'e), 1.75-1.84 (m, 4H, H-3', CH₂-cy), 1.92 (m, 1H, H-2'e), 2.00 (m, 2H, CH₂-cy), 2.06 (m, 1H, H-6'e), 2.73-2.83 (m, 2H, H-3e, CH-cy), 3.62 (dd, *J* = 2.0, 9.1 Hz, 1H, H-7), 3.65-3.74 (m, 2H, H-4, H-9a), 3.77 (dd, *J* = 2.0, 10.5 Hz, 1H, H-6), 3.83-3.94 (m, 6H, H-5, H-8, H-9b, H-1', OCH₂SO₃Na), 5.26 (s, 2H, NHCOCH₂), 7.81 (s, 1H, H-triazole); ¹³C NMR (126 MHz, D₂O): δ = 23.3 (CH₂-cy), 25.6 (C-5'), 25.7 (2C, CH₂-cy), 27.7 (C-4'), 32.5 (2C, CH₂-cy), 34.4 (C-6'), 34.6 (CH-cy), 35.7 (C-2'), 36.3 (C-3'), 41.3 (C-3), 52.1 (NHCOCH₂), 52.2 (C-5), 62.6 (C-9), 68.2 (C-7), 68.5 (C-4), 72.3 (C-6), 72.5 (C-8), 73.7 (OCH₂SO₃Na), 75.0 (C-1'), 101.2 (C-2), 123.4 (CH-triazole), 154.4 (C-triazole), 168.8, 173.9 (2C, C=O); HRMS (ESI): *m/z*: Calcd for C₂₆H₄₀N₄Na₂O₁₃S [M+Na]⁺: 717.2006, found: 717.2006; HPLC: Purity 95.0%.

(1*S*,3*R*)-3-(Sulfonatooxymethyl)cyclohexyl 3,5-dideoxy-5-(2-(4-(2-oxo-2-(phenylamino)ethyl)-1*H*-1,2,3-triazol-1-yl)acetamido)-*D*-glycero- α -*D*-galacto-2-nonulopyranosylonate disodium salt (101).



A solution of **111** (33.0 mg, 0.126 mmol) in dry DMF (1 mL) was stirred under argon with DIPEA (27.0 μ L, 0.160 mmol) and HATU (60.0 mg, 0.160 mmol) for 40 min. Then, **96** (30.0 mg, 0.063 mmol) was added and the reaction was stirred overnight at rt for 16 h. After that, TLC still showed starting material, therefore another portion of DIPEA (0.160 mmol) and HATU (0.160 mmol) was added and stirring continued for further 16 h. Then, the mixture was concentrated under reduced pressure and the residue was purified by flash column chromatography (DCM/(MeOH/H₂O 10:1), 1:0 \rightarrow 6:4). The collected product (21.8 mg, 0.029 mmol) was dissolved in 0.1 M NaOH solution (H₂O/dioxane, 1:1, 1 mL) and stirred for 24 h. Then, it was neutralized with AmberLite IR120, concentrated under reduced pressure and purified by size exclusion chromatography (P-2 gel, H₂O) to afford **101** (15.0 mg, 32% over two steps) as a white solid. $[\alpha]_D^{20} +24.2$ (*c* 1, MeOH); ¹H NMR (500 MHz, D₂O): δ = 0.92 (qd, *J* = 3.7, 12.6 Hz, 1H, H-4'a), 1.04 (q, *J* = 11.9 Hz, 1H, H-2'a), 1.19-1.37 (m, 2H, H-5'a, H-6'a), 1.66 (t, *J* = 12.1 Hz, 1H, H-3a), 1.70 (m, 1H, H-4'e), 1.75-1.84 (m, 2H, H-3', H-5'e), 1.92 (m, 1H, H-2'e), 2.06 (m, 1H, H-6'e), 2.77 (dd, *J* = 4.7, 12.4 Hz, 1H, H-3e), 3.61-3.68 (m, 2H, H-7, H-9b), 3.71 (ddd, *J* = 4.7, 9.9, 12.0 Hz, 1H, H-4), 3.78 (dd, *J* = 2.0, 10.4 Hz, 1H, H-6), 3.82-3.94 (m, 6H, H-5, H-8, H-9b, H-1', OCH₂SO₃Na), 4.71 (s, 2H, CH₂CONHPh), 5.32 (s, 2H, CH₂CONH), 7.51-7.59 (m, 2H, Ar-H), 7.65 (m, 1H, Ar-H), 7.77-7.85 (m, 2H, Ar-H), 8.03 (s, 1H, H-triazole); ¹³C NMR (126 MHz, D₂O): δ = 23.9 (C-5'), 28.2 (C-4'), 34.9 (C-6'), 35.6 (CH₂CONHPh), 36.3 (C-2'), 36.8 (C-3'), 41.8 (C-3), 52.7 (CH₂CONH), 52.8 (C-5), 63.1 (C-9), 68.7 (C-7), 69.0 (C-4), 72.8 (C-8), 73.0 (C-6), 74.2 (OCH₂SO₃Na), 75.5 (C-1'), 101.7 (C-2), 126.0 (CH-triazole), 127.8, 129.5, 133.0, 133.9 (6C, Ar-C), 145.5 (C-triazole), 169.2, 171.5, 174.4 (3C, C=O); HRMS (ESI): *m/z*: Calcd for C₂₈H₃₇N₅Na₂O₁₄S [M+Na]⁺: 768.1751, found: 768.1752; HPLC: Purity 83.0%.

Microscale thermophoresis. Microscale thermophoresis experiments were performed using a Monolith NT.115 instrument (Nanotemper, Munich, Germany) set to 25 °C, 50% LED power, and

“medium” MST power. The Nanotemper MO. Affinity Analysis software suite was employed for analysis and nonlinear fitting of experimental data. In a typical experiment, a serial ligand dilution starting at 15 mM or 30 mM was incubated with an equal volume of 160 nM FITC-labeled Siglec-8-CRD and measured directly using the green channel of the instrument. Experiments were performed in triplicates.

Isothermal titration calorimetry. Isothermal titration calorimetric experiments were performed on an ITC200 instrument (MicroCal, Northampton, USA) at 25 °C using standard instrument settings (reference power 6 $\mu\text{cal s}^{-1}$, stirring speed 750 rpm, feedback mode high, filter period 2 s). Protein solutions were dialyzed against ITC buffer (20 mM HEPES, 150 mM NaCl, pH 7.4) prior to the experiments and all samples were prepared using the dialysate buffer to minimize dilution effects. Protein concentrations were determined spectrophotometrically with the specific absorbance at 280 nm employing an extinction coefficient of 33240 $\text{mol}^{-1} \text{cm}^{-1}$. Binding affinities of Siglec-8 ligands in the μM to mM range necessitated a low c titration setup. In a typical experiment, a 25 mM ligand solution was titrated to a solution containing 40 μM Siglec-8 to ensure > 70% saturation. Baseline correction, peak integration, and non-linear regression analysis of experimental data was performed using the NITPIC (version 1.2.2.)⁴¹ and SEDPHAT (version 12.1b)⁴² software packages. The stoichiometry parameter was manually constrained to a value of 1. Experiments were performed in duplicate and the 68% confidence intervals from global fitting of two experiments were calculated as an estimate of experimental error.

Differential scanning fluorimetry. Differential scanning fluorimetry assays were performed using a Prometheus NT.48 (Nanotemper, Munich, Germany) instrument set to 50 % excitation power and 1.0 °C/min temperature slope. The Nanotemper Pr.ThermControl software suite was employed for analysis of experimental data. In a typical experiment, a 20 μM solution of Siglec-8-CRD was incubated alone or with 1 mM solution of ligand and measured over a temperature range from 20 to 80 °C.

3.5 References.

- (1) Posner, B. A. High-Throughput Screening-Driven Lead Discovery: Meeting the Challenges of Finding New Therapeutics. *Curr. Opin. Drug Discov. Devel.* **2005**, 8 (4), 487–494.
- (2) Macalino, S. J. Y.; Gosu, V.; Hong, S.; Choi, S. Role of Computer-Aided Drug Design in Modern Drug Discovery. *Arch. Pharm. Res.* **2015**, 38 (9), 1686–1701. <https://doi.org/10.1007/s12272-015-0640-5>.

- (3) Lyu, J.; Wang, S.; Balius, T. E.; Singh, I.; Levit, A.; Moroz, Y. S.; O'Meara, M. J.; Che, T.; Alga, E.; Tolmachova, K.; Tolmachev, A. A.; Shoichet, B. K.; Roth, B. L.; Irwin, J. J. Ultra-Large Library Docking for Discovering New Chemotypes. *Nat. Biotechnol.* **2019**, *566* (7743), 224–229. <https://doi.org/10.1038/s41586-019-0917-9>.
- (4) Waszkowycz, B. Towards Improving Compound Selection in Structure-Based Virtual Screening. *Drug Discov. Today* **2008**, *13* (5–6), 219–226. <https://doi.org/10.1016/j.drudis.2007.12.002>.
- (5) Kirsch, P.; Hartman, A. M.; Hirsch, A. K. H.; Empting, M. Concepts and Core Principles of Fragment-Based Drug Design. *Molecules* **2019**, *24* (23), 4309. <https://doi.org/10.3390/molecules24234309>.
- (6) Erlanson, D. A. Introduction to Fragment-Based Drug Discovery. *Top. Curr. Chem.* **2012**, *317*, 1–32. https://doi.org/10.1007/128_2011_180.
- (7) Murray, C. W.; Rees, D. C. The Rise of Fragment-Based Drug Discovery. *Nat. Chem.* **2009**, *1* (3), 187–192. <https://doi.org/10.1038/nchem.217>.
- (8) Jhoti, H.; Williams, G.; Rees, D. C.; Murray, C. W. The “rule of Three” for Fragment-Based Drug Discovery: Where Are We Now? *Nat. Rev. Drug Discov.* **2013**, *12* (8), 644–645. <https://doi.org/10.1038/nrd3926-c1>.
- (9) Congreve, M.; Carr, R.; Murray, C.; Jhoti, H. A ‘Rule of Three’ for Fragment-Based Lead Discovery? *Drug Discov. Today* **2003**, *8* (19), 876–877. [https://doi.org/10.1016/S1359-6446\(03\)02831-9](https://doi.org/10.1016/S1359-6446(03)02831-9).
- (10) Li, Q. Application of Fragment-Based Drug Discovery to Versatile Targets. *Front. Mol. Biosci.* **2020**, *7*, 180. <https://doi.org/10.3389/fmolb.2020.00180>.
- (11) Jerabek-Willemsen, M.; André, T.; Wanner, R.; Roth, H. M.; Duhr, S.; Baaske, P.; Breitsprecher, D. MicroScale Thermophoresis: Interaction Analysis and Beyond. *J. Mol. Struct.* **2014**, *1077*, 101–113. <https://doi.org/10.1016/j.molstruc.2014.03.009>.
- (12) Navratilova, I.; Hopkins, A. L. Fragment Screening by Surface Plasmon Resonance. *ACS Med. Chem. Lett.* **2010**, *1* (1), 44–48. <https://doi.org/10.1021/ml900002k>.
- (13) Senisterra, G.; Chau, I.; Vedadi, M. Thermal Denaturation Assays in Chemical Biology. *Assay Drug Dev. Technol.* **2012**, *10* (2), 128–136. <https://doi.org/10.1089/adt.2011.0390>.
- (14) Leavitt, S.; Freire, E. Direct Measurement of Protein Binding Energetics by Isothermal Titration Calorimetry. *Curr. Opin. Struct. Biol.* **2001**, *11* (5), 560–566. [https://doi.org/10.1016/s0959-440x\(00\)00248-7](https://doi.org/10.1016/s0959-440x(00)00248-7).
- (15) Kuntz, I. D.; Blaney, J. M.; Oatley, S. J.; Langridge, R.; Ferrin, T. E. A Geometric Approach to Macromolecule-Ligand Interactions. *J. Mol. Biol.* **1982**, *161*, 269–288. [https://doi.org/10.1016/0022-2836\(82\)90153-x](https://doi.org/10.1016/0022-2836(82)90153-x).
- (16) Kroemer, R. T. Structure-Based Drug Design: Docking and Scoring. *Curr. Protein Pept. Sci.* **2007**, *8* (4), 312–328. <https://doi.org/10.2174/138920307781369382>.
- (17) Cheng, T.; Li, X.; Li, Y.; Liu, Z.; Wang, R. Comparative Assessment of Scoring Functions on a Diverse Test Set. *J. Chem. Inf. Model.* **2009**, *49* (4), 1079–1093. <https://doi.org/10.1021/ci9000053>.
- (18) Lexa, K. W.; Carlson, H. A. Protein Flexibility in Docking and Surface Mapping. *Q. Rev. Biophys.*

- 2012**, *45* (3), 301–343. <https://doi.org/10.1017/S0033583512000066>.
- (19) Schulz-Gasch, T.; Stahl, M. Scoring Functions for Protein-Ligand Interactions: A Critical Perspective. *Drug Discov. Today. Technol.* **2004**, *1* (3), 231–239. <https://doi.org/10.1016/j.ddtec.2004.08.004>.
- (20) Stanzione, F.; Giangreco, I.; Cole, J. C. Use of Molecular Docking Computational Tools in Drug Discovery, *Prog. Med. Chem.* **2021**; *60*, 273–343. <https://doi.org/10.1016/bs.pmch.2021.01.004>.
- (21) Fischer, A.; Smieško, M.; Sellner, M.; Lill, M. A. Decision Making in Structure-Based Drug Discovery: Visual Inspection of Docking Results. *J. Med. Chem.* **2021**, *64* (5), 2489–2500. <https://doi.org/10.1021/acs.jmedchem.0c02227>.
- (22) The PyMOL Molecular Graphics System, Version 1.8 Schrödinger, LLC.
- (23) Berthold, M. R.; Cebron, N.; Dill, F.; Di Fatta, G.; Gabriel, T. R.; Georg, F.; Meinl, T.; Ohl, P.; Sieb, C.; Wiswedel, B. KNIME: The Konstanz Information Miner. In *Studies in Classification, Data Analysis, and Knowledge Organization (GfKL 2007)*; Springer, 2007; Vol. 11, pp 58–61. <https://doi.org/10.1145/1656274.1656280>.
- (24) Pröpster, J. M.; Yang, F.; Rabbani, S.; Ernst, B.; Allain, F. H.; Schubert, M. Structural Basis for Sulfation-Dependent Self-Glycan Recognition by the Human Immune-Inhibitory Receptor Siglec-8. *Proc. Natl. Acad. Sci.* **2016**, *113* (29), E4170–E4179. <https://doi.org/10.1073/pnas.1602214113>.
- (25) OEDocking version 3.0.2. OpenEye Scientific Software, Santa Fe, NM. <http://www.eyesopen.com>.
- (26) VIDA version 4.2.1. OpenEye Scientific Software, Santa Fe, NM. <http://www.eyesopen.com>.
- (27) Titz, A.; Radic, Z.; Schwardt, O.; Ernst, B. A Safe and Convenient Method for the Preparation of Triflyl Azide, and Its Use in Diazo Transfer Reactions to Primary Amines. *Tetrahedron Lett.* **2006**, *47* (14), 2383–2385. <https://doi.org/10.1016/j.tetlet.2006.01.157>.
- (28) Kroezen, B. S.; Conti, G.; Girardi, B.; Cramer, J.; Jiang, X.; Rabbani, S.; Müller, J.; Kokot, M.; Luisoni, E.; Ricklin, D.; Schwardt, O.; Ernst, B. A Potent Mimetic of the Siglec-8 Ligand 6'-Sulfo-Sialyl Lewis^x. *ChemMedChem* **2020**, *15* (18), 1706–1719. <https://doi.org/10.1002/cmdc.202000417>.
- (29) ter Halle, R.; Bernet, Y.; Billard, S.; Bufferne, C.; Carlier, P.; Delaitre, C.; Flouzat, C.; Humblot, G.; Laigl, J. C.; Lombard, F.; Wilmouth, S. Development of a Practical Multikilogram Production of (R)-Seudenol by Enzymatic Resolution. *Org. Process Res. Dev.* **2004**, *8* (2), 283–286. <https://doi.org/10.1021/op034179k>.
- (30) Rotticci, D.; Norin, T.; Hult, K. Mass Transport Limitations Reduce the Effective Stereospecificity in Enzyme-Catalyzed Kinetic Resolution. *Org. Lett.* **2000**, *2* (10), 1373–1376. <https://doi.org/10.1021/ol005639m>.
- (31) Boons, G.-J.; Demchenko, A. V. Recent Advances in O-Sialylation. *Chem. Rev.* **2000**, *100* (12), 4539–4565. <https://doi.org/10.1021/cr990313g>.
- (32) Tiwari, V. K.; Mishra, B. B.; Mishra, K. B.; Mishra, N.; Singh, A. S.; Chen, X. Cu-Catalyzed Click Reaction in Carbohydrate Chemistry. *Chem. Rev.* **2016**, *116* (5), 3086–3240. <https://doi.org/10.1021/acs.chemrev.5b00408>.
- (33) Rillahan, C. D.; Schwartz, E.; McBride, R.; Fokin, V. V.; Paulson, J. C. Click and Pick: Identification

- of Sialoside Analogues for Siglec-Based Cell Targeting. *Angew. Chemie - Int. Ed. English* **2012**, *51* (44), 11014–11018. <https://doi.org/10.1002/anie.201205831>.
- (34) Rillahan, C. D.; Macauley, M. S.; Schwartz, E.; He, Y.; Arlian, B. M.; Rangarajan, J.; Fokin, V. V.; James, C. Disubstituted Sialic Acid Ligands Targeting Siglecs CD33 and CD22 Associated with Myeloid Leukaemias and B Cell Lymphomas. *Chem. Sci.* **2014**, *5* (6), 2398–2406. <https://doi.org/10.1039/C4SC00451E>.
- (35) Landrum, G. RDKit: Open-Source Cheminformatics Software.
- (36) O’Boyle, N. M.; Banck, M.; James, C. A.; Morley, C.; Vandermeersch, T.; Hutchison, G. R. Open Babel: An Open Chemical Toolbox. *J. Cheminform.* **2011**, *3*, 33. <https://doi.org/10.1186/1758-2946-3-33>.
- (37) Hawkins, P. C. D.; Skillman, A. G.; Warren, G. L.; Ellingson, B. A.; Stahl, M. T. Conformer Generation with OMEGA: Algorithm and Validation Using High Quality Structures from the Protein Databank and Cambridge Structural Database. *J. Chem. Inf. Model.* **2010**, *50* (4), 572–584. <https://doi.org/10.1021/ci100031x>.
- (38) McGann, M. FRED Pose Prediction and Virtual Screening Accuracy. *J. Chem. Inf. Model.* **2011**, *51* (3), 578–596. <https://doi.org/10.1021/ci100436p>.
- (39) McGann, M. FRED and HYBRID Docking Performance on Standardized Datasets. *J. Comput. Aided. Mol. Des.* **2012**, *26* (8), 897–906. <https://doi.org/10.1007/s10822-012-9584-8>.
- (40) Stefely, J. A.; Palchadhuri, R.; Miller, P. A.; Peterson, R. J.; Moraski, G. C.; Hergenrother, P. J.; Miller, M. J. N-((1-Benzyl-1H-1,2,3-Triazol-4-yl)Methyl)Arylamide as a New Scaffold That Provides Rapid Access to Antimicrotubule Agents: Synthesis and Evaluation of Antiproliferative Activity against Select Cancer Cell Lines. *J. Med. Chem.* **2010**, *53* (8), 3389–3395. <https://doi.org/10.1021/jm1000979>.
- (41) Scheuermann, T. H.; Brautigam, C. A. High-Precision, Automated Integration of Multiple Isothermal Titration Calorimetric Thermograms: New Features of NITPIC. *Methods* **2015**, *76*, 87–98. <https://doi.org/10.1016/j.ymeth.2014.11.024>.
- (42) Zhao, H.; Piszczek, G.; Schuck, P. SEDPHAT - A Platform for Global ITC Analysis and Global Multi-Method Analysis of Molecular Interactions. *Methods* **2015**, *76*, 137–148. <https://doi.org/10.1016/j.ymeth.2014.11.012>.

4. Development of an LC-MS method for the quantification of NEU2-mediated hydrolysis of Siglec-8 ligands

This chapter describes the development of an enzymatic assay to check the stability of our most important Siglec-8 ligands, presented in chapter 2, towards human neuraminidase 2 (NEU2). Structurally, they present a sialic acid connected by an α 2-3 linkage to galactose or mimics thereof and therefore may be subject to hydrolysis by neuraminidases present in our body. An LC-MS method has been developed to follow the potential hydrolysis and to quantify the consumption of the substrate.

Contribution to project

Benedetta Girardi performed the enzymatic assay and developed and optimized the LC-MS method. She also synthesized and characterized compound **2**, while compounds **34** and **38** were synthesized and characterized by Gabriele Conti. The enzyme NEU2 was kindly produced and provided by Prof. Christopher Cairo's group (University of Alberta, Canada).

4.1 Introduction.

The concept of pharmacokinetics (PK) can be simplified with the sentence “what the body does on a molecule”: once a compound is administered, it goes through a series of biological processes and chemical modifications that can be described by four main steps, **A**bsorption, **D**istribution, **M**etabolism and **E**xcretion (ADME). All these factors, together with the possible **T**oxicity of a drug as a fifth parameter (ADME-T), should be considered during the drug development process to make sure that the molecule reaches the target at the therapeutic concentration.¹⁻⁴ In the past, the first phases of drug discovery were quite focused on evaluating only the affinity and the selectivity of a compound on a target, without considering the general PK properties of the molecule, as for example metabolic soft spots, high clearance, plasma protein binding, etc. A study comprising seven pharma companies in UK showed how, until 1985, 39% of the molecules failed because of bad PK properties. Now, *in vitro* evaluation methods of these characteristics have become an important part of the preclinical development. The identification of possible limits of a molecule can guide the optimization process from the early phases, limiting failures and saving money and time.⁵⁻⁷ The failures of clinical trials due to pharmacokinetic reasons were reduced to less than 10% once physicochemical and biochemical properties were analyzed in the early phases of drug discovery.⁸

For these reasons, we decided to start evaluating some of these properties already at the first stages of our Siglec-8 project, or at least in parallel to our lead optimization process.

As described in the introduction of this thesis, sialic acids are abundantly expressed on the cell surface of our body, mediating many biological processes.⁹⁻¹² In mammals, two main classes of enzymes are involved in their chemical modifications: sialyltransferases, deputed to transfer Sia residues, and neuraminidases (NEU) able to remove them from glycoconjugates.¹³⁻¹⁵

Since our Siglec-8 ligands, extensively described in the previous chapters, contain sialic acid moieties, we were interested whether our molecules may be subject to NEU-mediated hydrolysis or if the modifications introduced on Neu5Ac could confer a sort of stability towards this class of enzymes.

To date, four human NEUs have been identified, which differ in subcellular and tissue localization as well as in substrate specificity.¹⁶ They are widely expressed in tissues, while regarding their subcellular localization, NEU1 can be found mainly on lysosomes but also on the plasma membrane, NEU2 in the cytosol, NEU3 in the plasma membrane and NEU4 in the endoplasmic reticulum (ER) membrane, mitochondria and lysosomes.¹⁷⁻²⁰ Concerning their main biological functions, NEU1 and NEU4 play a role in the lysosomal catabolism of glycoconjugates, while NEU1 and NEU3 are involved in desialylation of membrane receptors, thus being important regulators of cell signaling.

The biological role of NEU2 is still unclear but it is involved in myoblast differentiation and oncogenesis.²¹ Every enzyme also shows specificity for different substrates. A recent study analyzed the main differences towards the most abundant sialylated oligosaccharides. NEU1 has the broadest activity, which explains its ability to act on various receptors and glycoconjugates. NEU2 is more specific for α 2-3 linkages, while NEU3 and NEU4 are the most active. NEU4 has a reduced activity towards α 2-6 linkages compared to NEU3.²² In addition, NEU3 has a preference for aglycone moieties.²³ The presence of a branching 2-fucoside affected the binding to NEU2 and NEU4, but not to NEU1 and NEU3.²² Only NEU2 has been crystallized, both in apo form and in complex with the inhibitor DANA. Being the only structure available, it has been used for homology modeling to obtain 3D structures of the other NEUs.²⁴⁻²⁶

Considering that our ligands interact on the cell surface and are formed by sialic acid linked to galactose or mimics thereof by α 2-3 linkage, and looking at the expression and specificities of the different enzymes, NEU3 seems to be the preferred target enzyme for our stability assays. However, it was only possible to have access to NEU2. Since it is an enzyme active on α 2-3 linkages, our ligands might still be hydrolyzed. Therefore, we decided to use NEU2 as a proof of concept and to develop and validate a method which can be then also applied to the other enzymes.

We decided to test the three more significant Siglec-8 ligands described in the second chapter: first, the more natural disaccharide 6-sulfo-Sia-Gal (**2**), obtained by keeping the minimal binding epitope from parent tetrasaccharide 6-sulfo-sLe^x. Then, the first glycomimetic derivative (**34**), obtained by substituting the galactose with a cyclohexane moiety while keeping the sulfate in the same position and finally the most active Siglec-8 ligand, with an additional sulfonaphtyl moiety in position 9 of the sialic acid (**38**) (Figure 1).

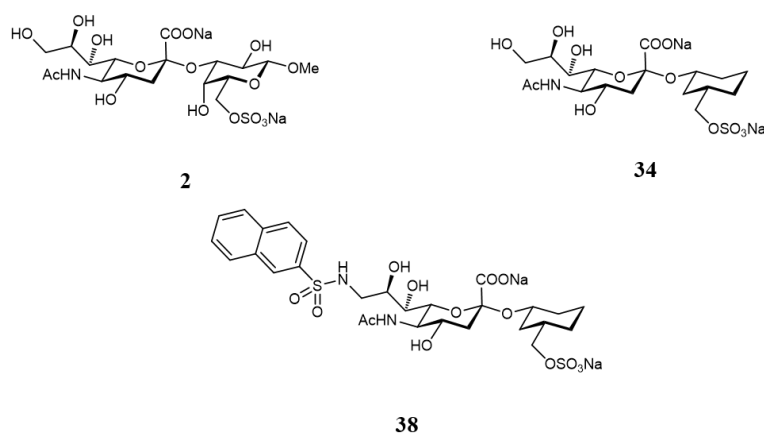


Figure 1. Siglec-8 ligands: from the natural substrate to a potent glycomimetic.

The stability of these compounds towards human NEU2 was assessed with an enzymatic assay and the possible hydrolysis was followed analyzing the consumption of the substrate with the development of a liquid chromatography-mass spectrometry (LC-MS) method.

4.2 Results and discussion.

hNEU2 calibration. The activity of the human NEU2 enzyme has to be calibrated against a bacterial neuraminidase before using it in experiments. In this case, the assay was performed using the bacterial *Clostridium prefrigens* neuraminidase and 4-methylumbelliferyl *N*-acetyl- α -D-neuraminic acid (4MU-NANA), a well-known substrate for this class of enzymes, bearing a sialic acid substituted with a fluorescent moiety (Figure 2A). Upon hydrolysis, the fluorescent moiety released can be detected and then quantified with a fluorimeter. Therefore, following an established protocol from Prof. Cairo's group, 4MU-NANA was incubated with serial dilutions of bacterial enzyme, and the produced fluorescence was plotted vs. the enzyme concentration. This calibration curve was then used to indirectly calculate the activity of human NEU2 (Figure 2B). Enzymatic assays were performed at 37 °C using sodium acetate buffer at the optimum enzyme pH (5.5 for NEU2), as previously published.²⁷

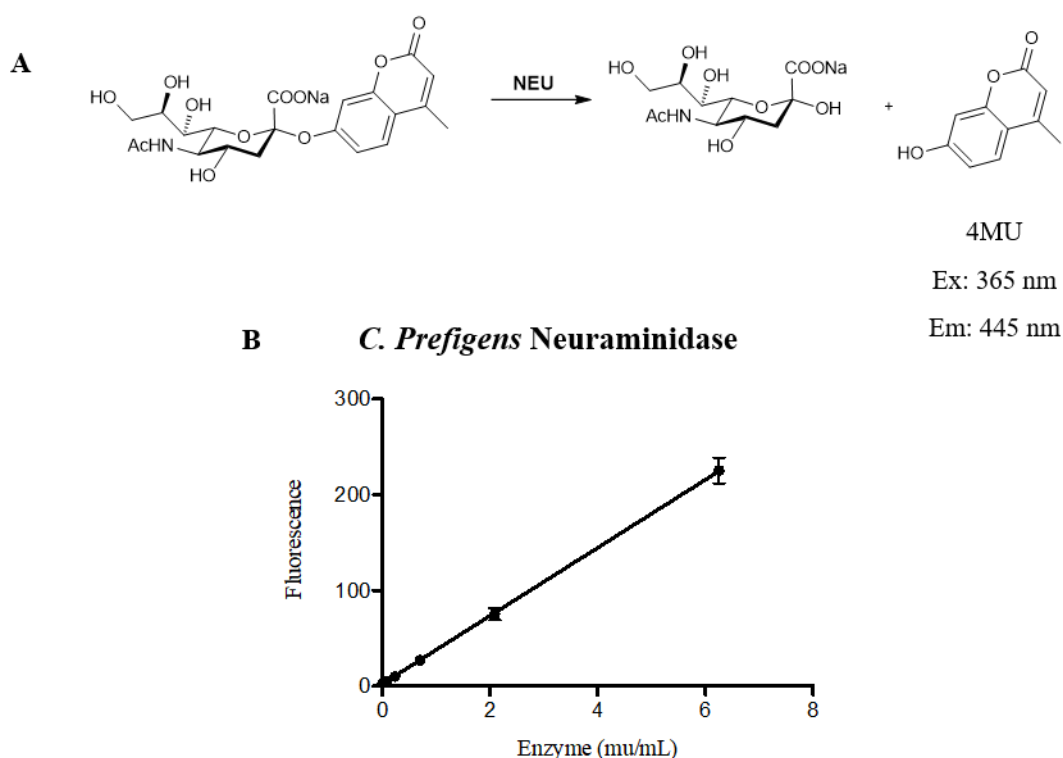


Figure 2. A: Neu-mediated hydrolysis of 4MU-NANA. The fluorescence of 4MU can be read at two values: Excitation (Ex) at 365 nm and emission (Em) at 445 nm. B: Calibration curve of produced fluorescence vs enzyme concentration.

Assay optimization and LC-MS. Considering that our compounds do not have a fluorophore group in the aglycone moiety, an LC-MS method was developed to quantify the consumption of the substrate or the released hydrolysis product. LC-MS is commonly used to study enzymatic reactions because it provides a fast and precise method to analyze and quantify a variety of substances in complex matrixes.²⁸ In our case, we used multiple reaction monitoring (MRM) on a triple quadrupole MS (QQQ-MS) which selects and observes the transition between a precursor ion and a product ion. This is advantageous because being so specific, it gives the possibility to distinguish even co-eluted compounds. Some optimization was required to find the best conditions. The buffer that gave the best ionization was 10 mM ammonium acetate (NH₄Ac), which was also used to dilute the samples before the injection. Due to the high polarity of our compounds, with two negative charges, a normal-phase column (HILIC) had to be used, because no retention was observed in a common reversed-phase column.

With the optimized LC-MS conditions, we incubated 4MU-NANA, as a positive control, with different NEU2 concentrations (2, 5 and 10 mU) to determine which concentration of enzyme should be used for our Siglec-8 ligands. Aliquots were collected at different timepoints over 24 hours and directly injected in the LC-MS. As can be seen from Figure 3A, 4MU-NANA was completely hydrolyzed within 24 hours when using 10 mU of NEU2. Starting from a certain area under the curve of the control without enzyme, the decrease of the area over time is attributed to the enzyme activity, also confirmed by the formation of the hydrolyzed product Neu5Ac, increasing proportionally over time (Figure 3B). Based on these results, 10 mU of hNEU2 were used to screen our Siglec-8 ligands.

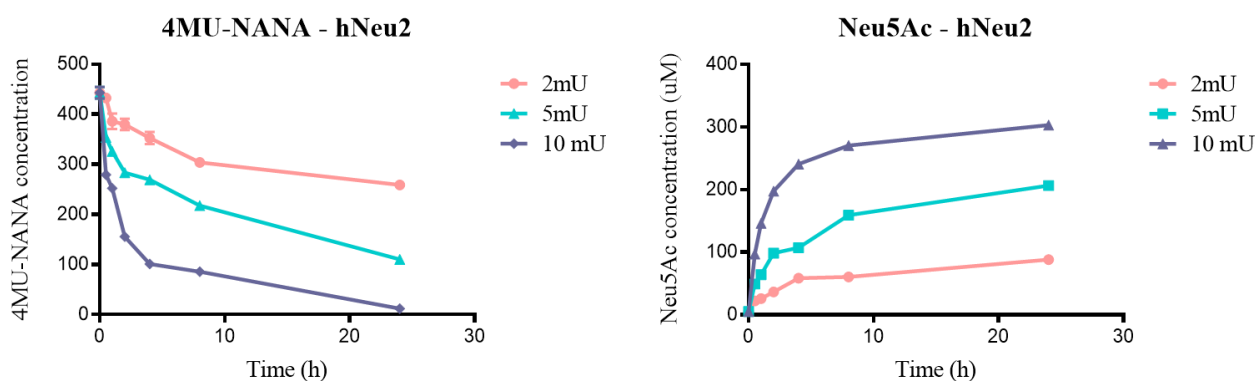


Figure 3. Hydrolysis of 4MU-NANA (A) and Neu5Ac product formation (B) over 24 h using different concentrations of enzyme.

Siglec-8 ligands assay. The same method was then applied to screen our compounds **2**, **34** and **38**. For every substance, a control reaction where the enzyme was replaced by an equal amount of buffer was run in parallel. Fragmentor and collision energy of the QQQ-MS were adjusted for every molecule to obtain optimal ionization. At seven timepoints over 24 h, the reaction was stopped and aliquots were injected in the LC-MS. A calibration curve with different substrate concentration was plotted and used to quantify substrate consumption in comparison to the control without enzyme. A plot of substrate concentration vs time is shown in Figure 4.

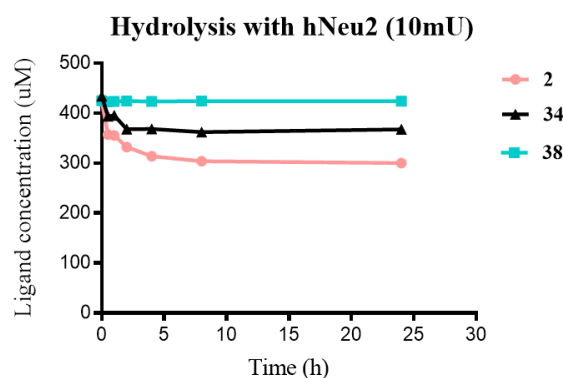


Figure 4. Hydrolysis of Siglec-8 ligands over 24 hours using 10 mU of NEU2.

A comparison of the measured concentrations at every timepoint with the initial concentration reveals that only disaccharide **2** is partially hydrolyzed (30%) over 24 h while mimics **34** and **38** are completely stable. The small decay for compound **34** represents only 7% of the initial concentration, which is a negligible amount that might be attributed to small variabilities in the LC-MS system. Furthermore, most of the hydrolysis obviously occurs in the first 4 h and then the concentration remains more or less stable. This may be explained by a possible partial inhibition of the enzyme with the aglycone reducing end. Since this effect was not observed with 4MU-NANA an inhibition by the sialic acid can be excluded.

4.3 Conclusions.

In this chapter, the stability of the main Siglec-8 ligands towards NEU2, a human enzyme able to hydrolyze sialic acid-containing molecules, has been presented. An LC-MS method has been developed to monitor the possible hydrolysis over time, checking the consumption of the substrate and the formation of the product. We observed that the glycomimetic derivatives were basically stable, while the more natural disaccharide **2** was partially hydrolyzed. Due to the findings that most

of the hydrolysis happened at the beginning, we hypothesize that the aglycone could be retained in the binding site, interfering with the hydrolysis of the remaining substrate. 4MU-NANA has been used as a positive control. However, even if definitively being a substrate, this compound is quite labile and NEU2 showed higher activity compared to other isoenzymes.^{19,29} Therefore, to definitively confirm the stability of our compounds, the additional use of another substrate, like the trisaccharide 3'-sialyllactose, should be considered. We can anyway conclude that the assay has been validated and can be easily be used for other compounds and enzymes.

4.4 Experimental part.

General information. HPLC grade solvents and reagents were purchased from Sigma-Aldrich, VWR or Roth). 4MU-NANA and neuraminidase from *Clostridium prefigens* were purchased from Sigma-Aldrich and stored at -20 °C. Experimental data regarding the synthesis and analysis of compounds **2**, **34** and **38** are reported in detail in chapter 2.

Enzymatic assay – Standardization protocol. Human NEU2 was expressed as fusion protein following previous reports.³⁰ Before use, it was standardized against bacterial neuraminidase from *C. prefigens* using 4-MU-NANA as substrate.³¹ Briefly, 20 µL of reaction mixture containing 5 µL of 4-MU-NANA (200 µM in H₂O) and 15 µL of serial dilutions of the standard enzyme in sodium acetate buffer (0.1 M NaOAc, 0.15 M NaCl, pH 5.5, optimum pH for NEU2²⁷), was incubated at 37 °C for 30 min. For blank samples, neuraminidase was replaced by an equal volume of buffer. Then, the reaction was stopped adding 100 µL of quenching buffer (0.2 M glycine/NaOH, pH 10.7), the mixture was transferred to a 96-well plate and the enzyme activity was determined by measuring fluorescence ($\lambda_{\text{ex}} = 365 \text{ nm}$; $\lambda_{\text{em}} = 445 \text{ nm}$) using a Varioskan Lux plate reader (Thermofisher) and SkanIt RE 4.1 as a program. This calibration curve was used to calculate indirectly the activity of hNEU2 samples with unknown concentration. The activity of hNEU2 was calculated with this protocol prior to every experiment.

Enzymatic assay with Siglec-8 ligands. The protocol described above was also used for the stability assay with Siglec-8 ligands with some small variants, using 15 µL of hNeu2 (10 mU) and 5 µL of substrate (400 µM in H₂O). Samples were incubated at 37 °C and aliquots were collected at 7 timepoints (0, 0.5, 1, 2, 4, 8, 24 h). The reaction was stopped using 160 µL of acetonitrile and 40 µL of ammonium acetate (100 mM in H₂O). The samples were centrifuged and 160 µL of the supernatant

were taken and used for LC-MS analysis. In each experiment, a reaction in which the enzyme had been substituted for buffer was run in parallel and used as a control.

Quantification method. Control samples at different concentrations were used to generate a concentration curve and quality control (QC) samples were used to check the precision of the curve. Analytes were then tested. In each reaction mixture, the initial substrate concentration was the same so any difference in signal between the control samples and the analyte was due to the formation of hydrolyzed product. The new concentrations were then quantified using the calibration curve prepared alongside the experiment. The concentration of the analytes was quantified by the Agilent Mass Hunter Quantitative Analysis software (version B.04.00).

LC-MS method. Analyses were performed using a 1100/1200 Series HPLC System coupled to a 6410 Triple Quadrupole mass detector (Agilent Technologies, Inc., Santa Clara, CA, USA) equipped with electrospray ionization. The system was controlled with the Agilent MassHunter Workstation Data Acquisition software (version B.03.01). The column used was a SeQuant® Zic®-pHILIC polymeric column (2.1 x 100 mm) with a 5 µm-particle size (Merck Millipore, Burlington, MA, USA). The mobile phase consisted of eluent A: 10 mM ammonium acetate, in H₂O; and eluent B: MeCN. The flow rate was maintained at 0.5 mL/min and isocratic elution (20% A/80% B) was run for a total duration of 8-10 min. The column temperature was kept at 30 °C, and 5 µL volume was injected into the column. Samples were ionized using negative electrospray ionization (ESI) and multiple reaction monitoring (MRM) in negative mode was used for analysis and mass scan. Fragmentor voltage and collision energy were optimized for the analysis of every compound (Table 1).

Compound	MRM transition Precursor ion → Product ion	Fragmentor	Collision energy
4MU-NANA	488.1 → 174.7	80	36
Neu5Ac	308.1 → 87	125	12
2	564.1 → 273	105	16
34	500.14 → 209	85	16
38	689.17 → 209	90	24

Table 1. MRM transitions and conditions for monitoring the hydrolysis reaction with NEU2.

Dwell time was 100 s. Regarding the source parameters, the capillary voltage was set to 4000 V, the gas temperature to 320 °C, the gas flow to 10 L/min and the nebulizer set to 50 psi.

4.5 References.

- (1) Hodgson, J. ADMET - Turning Chemicals into Drugs. *Nat. Biotechnol.* **2001**, *19* (8), 722–726. <https://doi.org/10.1038/90761>.
- (2) Li, Y.; Meng, Q.; Yang, M.; Liu, D.; Hou, X.; Tang, L.; Wang, X.; Lyu, Y.; Chen, X.; Liu, K.; Yu, A. M.; Zuo, Z.; Bi, H. Current Trends in Drug Metabolism and Pharmacokinetics. *Acta Pharm. Sin. B* **2019**, *9* (6), 1113–1144. <https://doi.org/10.1016/j.apsb.2019.10.001>.
- (3) Chung, T. D. Y.; Terry, D. B.; Smith, L. H. In Vitro and In Vivo Assessment of ADME and PK Properties During Lead Selection and Lead Optimization - Guidelines, Benchmarks and Rules of Thumb. In *Assay Guidance Manual*, 2015; Bethesda (MD): Eli Lilly & Company and the National Center for Advancing Translational Sciences; 2004–.
- (4) Rizk, M. L.; Zou, L.; Savic, R. M.; Dooley, K. E. Importance of Drug Pharmacokinetics at the Site of Action. *Clin. Transl. Sci.* **2017**, *10* (3), 133–142. <https://doi.org/10.1111/cts.12448>.
- (5) Prentis, R. A.; Lis, Y.; Walker, S. R. Pharmaceutical Innovation by the Seven UK-owned Pharmaceutical Companies (1964-1985). *Br. J. Clin. Pharmacol.* **1988**, *25* (3), 387–396. <https://doi.org/10.1111/j.1365-2125.1988.tb03318.x>.
- (6) Kola, I.; Landis, J. Can the Pharmaceutical Industry Reduce Attrition Rates? *Nat. Rev. Drug Discov.* **2004**, *3* (8), 711–715. <https://doi.org/10.1038/nrd1470>.
- (7) Walker, D. K. The Use of Pharmacokinetic and Pharmacodynamic Data in the Assessment of Drug Safety in Early Drug Development. *Br. J. Clin. Pharmacol.* **2004**, *58* (6), 601–608. <https://doi.org/10.1111/j.1365-2125.2004.02194.x>.
- (8) Hwang, T. J.; Carpenter, D.; Lauffenburger, J. C.; Wang, B.; Franklin, J. M.; Kesselheim, A. S. Failure of Investigational Drugs in Late-Stage Clinical Development and Publication of Trial Results. *JAMA Intern. Med.* **2016**, *176* (12), 1826–1833. <https://doi.org/10.1001/jamainternmed.2016.6008>.
- (9) Wang, B. Molecular Mechanism Underlying Sialic Acid as an Essential Nutrient for Brain Development and Cognition. *Adv. Nutr.* **2012**, *3* (3), 465-472S. <https://doi.org/10.3945/an.112.001875>.
- (10) Heida, R.; Bhide, Y.; Gasbarri, M.; Kocabiyik, Ö.; Stellacci, F.; Huckriede, A.; Hinrichs, W.; Frijlink, H. Advances in the Development of Entry Inhibitors for Sialic-Acid-Targeting Viruses. *Drug Discov. Today* **2021**, *26* (1), 122–137. <https://doi.org/10.1016/j.drudis.2020.10.009>.
- (11) Läubli, H.; Kawanishi, K.; George Vazhappilly, C.; Matar, R.; Merheb, M.; Sarwar Siddiqui, S. Tools to Study and Target the Siglec-Sialic Acid Axis in Cancer. *FEBS J.* **2020**. *Epub ahead of print*. <https://doi.org/10.1111/febs.15647>.
- (12) Giancchetti, E.; Arena, A.; Fierabracci, A. Sialic Acid-Siglec Axis in Human Immune Regulation, Involvement in Autoimmunity and Cancer and Potential Therapeutic Treatments. *Int. J. Mol. Sci.* **2021**,

- 22 (11), 5774. <https://doi.org/10.3390/ijms22115774>.
- (13) Lin, C. H.; Lin, C. C. Enzymatic and Chemical Approaches for the Synthesis of Sialyl Glycoconjugates. *Adv. Exp. Med. Biol.* **2001**, *491*, 215–230. https://doi.org/10.1007/978-1-4615-1267-7_16.
- (14) Li, Y.; Chen, X. Sialic Acid Metabolism and Sialyltransferases: Natural Functions and Applications. *Appl. Microbiol. Biotechnol.* **2012**, *94* (4), 887–905. <https://doi.org/10.1007/s00253-012-4040-1>.
- (15) Lipničánová, S.; Chmelová, D.; Ondrejovič, M.; Frečer, V.; Miertuš, S. Diversity of Sialidases Found in the Human Body - A Review. *Int. J. Biol. Macromol.* **2020**, *148*, 857–868. <https://doi.org/10.1016/j.ijbiomac.2020.01.123>.
- (16) Monti, E.; Miyagi, T. Structure and Function of Mammalian Sialidases. In *SialoGlyco Chemistry and Biology I. Topics in Current Chemistry*; Springer Berlin Heidelberg, 2012.
- (17) Bonten, E. J.; Campos, Y.; Zaitsev, V.; Nourse, A.; Waddell, B.; Lewis, W.; Taylor, G.; D’Azzo, A. Heterodimerization of the Sialidase NEU1 with the Chaperone Protective Protein/Cathepsin A Prevents Its Premature Oligomerization. *J. Biol. Chem.* **2009**, *284* (41), 28430–28441. <https://doi.org/10.1074/jbc.M109.031419>.
- (18) Comelli, E. M.; Amado, M.; Lustig, S. R.; Paulson, J. C. Identification and Expression of Neu4, a Novel Murine Sialidase. *Gene* **2003**, *321*, 155–161. <https://doi.org/10.1016/j.gene.2003.08.005>.
- (19) Tringali, C.; Papini, N.; Fusi, P.; Croci, G.; Borsani, G.; Preti, A.; Tortora, P.; Tettamanti, G.; Venerando, B.; Monti, E. Properties of Recombinant Human Cytosolic Sialidase HsNEU2. *J. Biol. Chem.* **2004**, *279* (5), 3169–3179. <https://doi.org/10.1074/jbc.M308381200>.
- (20) Zanchetti, G.; Colombi, P.; Manzoni, M.; Anastasia, L.; Caimi, L.; Borsani, G.; Venerando, B.; Tettamanti, G.; Preti, A.; Monti, E.; Bresciani, R. Sialidase NEU3 Is a Peripheral Membrane Protein Localized on the Cell Surface and in Endosomal Structures. *Biochem. J.* **2007**, *408* (2), 211–219. <https://doi.org/10.1042/BJ20070503>.
- (21) Miyagi, T.; Yamaguchi, K. Mammalian Sialidases: Physiological and Pathological Roles in Cellular Functions. *Glycobiology* **2012**, *22* (7), 880–896. <https://doi.org/10.1093/glycob/cws057>.
- (22) Smutova, V.; Albohy, A.; Pan, X.; Korchagina, E.; Miyagi, T.; Bovin, N.; Cairo, C. W.; Pshezhetsky, A. V. Structural Basis for Substrate Specificity of Mammalian Neuraminidases. *PLoS One* **2014**, *9* (9), e106320. <https://doi.org/10.1371/journal.pone.0106320>.
- (23) Sandbhor, M. S.; Soya, N.; Albohy, A.; Zheng, R. B.; Cartmell, J.; Bundle, D. R.; Klassen, J. S.; Cairo, C. W. Substrate Recognition of the Membrane-Associated Sialidase NEU3 Requires a Hydrophobic Aglycone. *Biochemistry* **2011**, *50* (32), 6753–6762. <https://doi.org/10.1021/bi200449j>.
- (24) Chavas, L. M. G.; Tringali, C.; Fusi, P.; Venerando, B.; Tettamanti, G.; Kato, R.; Monti, E.; Wakatsuki, S. Crystal Structure of the Human Cytosolic Sialidase Neu2. *J. Biol. Chem.* **2005**, *280* (1), 469–475. <https://doi.org/10.1074/jbc.M411506200>.
- (25) Magesh, S.; Suzuki, T.; Miyagi, T.; Ishida, H.; Kiso, M. Homology Modeling of Human Sialidase Enzymes NEU1, NEU3 and NEU4 Based on the Crystal Structure of NEU2: Hints for the Design of Selective NEU3 Inhibitors. *J. Mol. Graph. Model.* **2006**, *25* (2), 196–207.

<https://doi.org/10.1016/j.jmgm.2005.12.006>.

- (26) Mozzi, A.; Mazzacuva, P.; Zampella, G.; Forcella, M. E.; Fusi, P. A.; Monti, E. Molecular Insight into Substrate Recognition by Human Cytosolic Sialidase NEU2. *Proteins* **2012**, *80* (4), 1123–1132. <https://doi.org/10.1002/prot.24013>.
- (27) Zhang, Y.; Albohy, A.; Zou, Y.; Smutova, V.; Pshezhetsky, A. V.; Cairo, C. W. Identification of Selective Inhibitors for Human Neuraminidase Isoenzymes Using C4,C7-Modified 2-Deoxy-2,3-Didehydro-N-Acetylneuraminic Acid (DANA) Analogues. *J. Med. Chem.* **2013**, *56* (7), 2948–2958. <https://doi.org/10.1021/jm301892f>.
- (28) Liesener, A.; Karst, U. Monitoring Enzymatic Conversions by Mass Spectrometry: A Critical Review. *Anal. Bioanal. Chem.* **2005**, *382* (7), 1451–1464. <https://doi.org/10.1007/s00216-005-3305-2>.
- (29) Richards, M. R.; Guo, T.; Hunter, C. D.; Cairo, C. W. Molecular Dynamics Simulations of Viral Neuraminidase Inhibitors with the Human Neuraminidase Enzymes: Insights into Isoenzyme Selectivity. *Bioorg. Med. Chem.* **2018**, *26* (19), 5349–5358. <https://doi.org/10.1016/j.bmc.2018.05.035>.
- (30) Watson, D. C.; Leclerc, S.; Wakarchuk, W. W.; Martin, Y. N. Enzymatic Synthesis and Properties of Glycoconjugates with Legionaminic Acid as a Replacement for Neuraminic Acid. *Glycobiology* **2011**, *21* (1), 99–108. <https://doi.org/10.1093/glycob/cwq135>.
- (31) Potier, M.; Mameli, L.; Lisle, M. B.; Dallaire, L. Fluorometric Assay of Neuraminidase with a Sodium (4-Methylumbelliferyl- α -D-N-Acetylneuraminate) Substrate. *Anal. Biochem.* **1979**, *94* (2), 287–296. [https://doi.org/10.1016/0003-2697\(79\)90362-2](https://doi.org/10.1016/0003-2697(79)90362-2).

5. Selective monovalent Galectin-8 ligands based on 3-lactoylgalactoside

As small side project, in this chapter we aimed to improve the affinity and target selectivity of a recently published Galectin-8 ligand, 3-*O*-[1-carboxyethyl]- β -D-galactopyranoside. Considering that its structure is very similar to the lactic acid derivatives presented in chapter 2 as Siglec-8 ligands, we decided to test derivatives of these compounds without the sulfate at position 6 towards Galectin-8 and to further improve their affinity by introducing modifications at position 1 of the galactose. Affinity data measured by fluorescence polarization show that the most potent compound reached a K_D of 12 μ M. Furthermore, reasonable selectivity versus other galectins was achieved, making the highlighted compound a promising lead for the development of new selective and potent ligands for Galectin-8 as molecular probes to examine the protein's role in cell-based and *in vivo* studies.

Parts of this chapter have been published in *ChemMedChem*:

Girardi, B.; Manna, M.; Van Klaveren, S.; Tomašič, T.; Jakopin, Ž.; Leffler, H.; Nilsson, U. J.; Ricklin, D.; Mravljak, J.; Schwardt, O.; Anderluh, M. Selective Monovalent Galectin-8 Ligands Based on 3-Lactoylgalactoside, *ChemMedChem* **2022**, *17* (3), e202100514.

© 2021 Wiley-VCH GmbH

The entire article can be found in the appendix (p. 214).

Contributions to the project.

Benedetta Girardi designed all the ligands presented in this chapter, synthesized compounds **120** and **121** and contributed to the synthesis of compounds **109-112** and **114**. Synthesis of compound **109-112** and **114** was mostly carried out by Martina Manna as part of her master thesis project under supervision of Benedetta Girardi. Assoc. Prof. Dr. Tihomir Tomašič, from the University of Ljubljana, helped in the design and executed the MD analysis. Fluorescence polarization assay measurements were performed by Sjors Van Klaveren and Barbro Kahl Knutson at the University of Lund.

5.1 Introduction.

The galectin family.

Galectins are a family of small soluble proteins able to recognize glycans containing a β -D-galactopyranoside structural motif.¹⁻⁴ Since their discovery in 1970, 16 members of this family have been identified in mammals. They are small soluble proteins and they can be classified into three groups, according to their structural features and CRD organization: the prototype, containing one CRD (Galectins-1, 2, 5, 7, 10, 11, 13, 14, 15 and 16), the tandem-repeat type, consisting of two CRDs separated by a short linker polypeptide (Galectins-4, 6, 8, 9 and 12) and the chimera type, containing a single CRD and a N-terminal domain with proline-, glycine-, and tyrosine-rich repeats (Galectin-3) (Figure 1).⁵

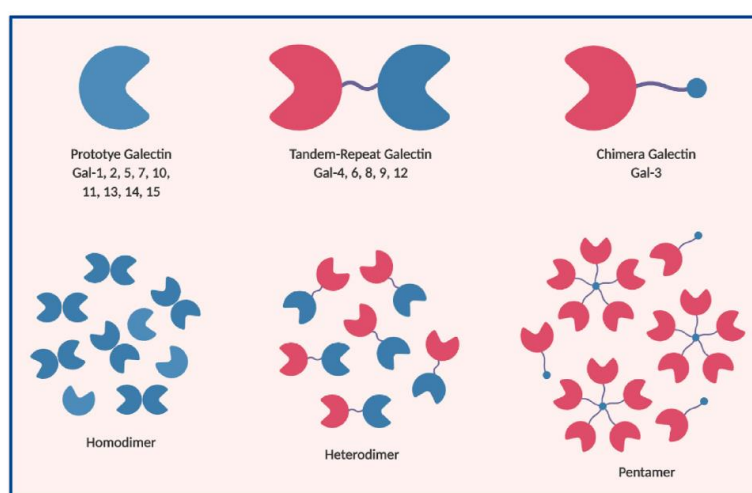


Figure 1. The galectin family. Figure from Sethi *et al.*⁶

Prototype galectins are in a dynamic equilibrium with a dimeric back to back form, which affects the ligand binding kinetics and affinity (Figure 1).⁷ The tandem-repeat galectins have a constant bivalency, which is the reason why they induce cell signaling at lower concentrations than the prototype ones, showing different potencies for triggering cellular response.^{8,9} Finally, Galectin-3 oligomerizes only upon ligand binding through its N-terminal domain, interacting then with surface receptors and inducing responses.¹⁰ Their CRD folds as a β -sandwich following an S-shaped groove where a sequence of seven conserved amino acids recognizes the galactose. Next to this, other close sites confer to each galectin the ability to recognize bigger ligands.^{11,12} Galectins also have non-carbohydrate binding sites, such as the C-terminus of Galectin-8.¹³

Galectins are synthesized as cytosolic proteins, where they stay for most of their lifetime before being secreted. They interact with and modulate the activity of glycoproteins expressed on the cell surface or in the lumen of intracellular compartments. All cells express Galectins, but the pattern changes depending on tissues and cell-types.¹⁴ The activity of a single galectin can vary considerably depending on the level of expression, self-association or interaction with other biomolecules *in situ*. For example, mitogenic activity of Galectin-1 on human fibroblasts is reduced at high concentrations, when dimerization is more probable, suggesting that this function belongs more to the monomeric form. However, at high concentration, it enhances the induction of fibroblasts and the growth of human epithelial (HEP) 2 carcinoma cells.¹⁵

Galectins are involved in several physiological functions such as cell migration, homeostasis, apoptosis, and pathological functions, as for example inflammation, host-pathogen interaction and antibacterial autophagy.^{4,16-18} Of particular interest is their role in cancer progression. Galectins can mediate the aggregation and adhesion of cancer cells, thus promoting metastasis, and when expressed on cancer cells, they can interact with normal cells inducing angiogenesis and immunosuppression.^{17,19,20} They can also be used as biomarkers for specific diseases when found in serum, as for example Galectin-3 has been connected to heart disease.²¹

Considering their important roles, it is clear why galectins have emerged as potential therapeutic targets for several diseases. High-affinity and selective ligands have been successfully designed, especially for Galectin-1 and Galectin-3, and some of them are already in clinical trials.²²

Among these lectins, in the next section we will focus more in detail on Galectin-8, which has recently gained attention as a potential new pharmacological target for the treatment of cancer, inflammation, and disorders associated with bone mass reduction.

Galectin-8.

Galectin-8 is a tandem-repeat type lectin that is widely expressed in tissues, both in normal and cancer cells. It mainly regulates cell-cell and cell-matrix interactions, thus playing a key role in many physiological and pathological processes.^{23,24}

It is an immunostimulatory lectin: evidences show how its interactions with glycans expressed on antigen-presenting cells (APCs) promote antigen uptake and processing. Galectin-8 activated APCs, in turn, stimulate T-cells more than when they are activated only by an antigen.^{25,26} Galectin-8 is also a pro-inflammatory molecule. Under stimulation, the endothelium secretes Galectin-8, which in turn increases the permeability of endothelial cells, thus promoting the release of other inflammatory molecules. Interacting with integrins on the cell surface of platelets and neutrophils, Galectin-8 also

mediates and enhances their adhesion and spreading. Activated DCs and B cells constitute another source of Galectin-8, which can in turn activate them to produce more pro-inflammatory cytokines (Figure 2).²⁶

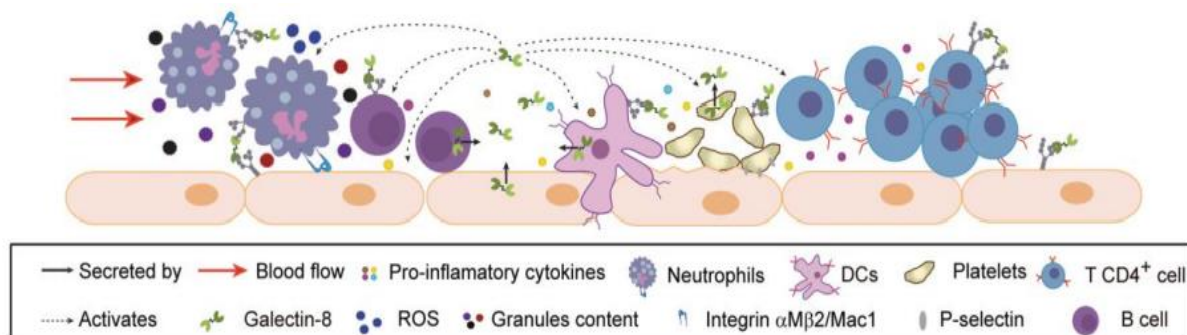


Figure 2. The role of Galectin-8 in the inflammatory process. Figure from Tribullati *et al.*²⁶

Higher levels of Galectin-8 have been found on the onset of autoimmune diseases such as multiple sclerosis or rheumatoid arthritis, where Galectin-8 can play a role in the stimulation of inflammation states connected to these diseases.^{27,28} By activating autophagy, the protein may contribute to host defense against bacteria.^{29,30} In fact, Galectin-8 senses and binds host glycans upon disruption of *Salmonella*-containing vesicles and through its C-terminal domain binds the autophagic receptor NDP52, promoting autophagy and bacterial clearance.³¹ Galectin-8 has also been reported to enhance the differentiation of osteoblasts into osteoclasts, and it is thus involved in bone turnover and remodeling.³² Ablation of the mammalian Galectin-8 in mice induces bone defect.³³

Of note, Galectin-8 stimulates, in a synergistic manner with the vascular endothelial growth factor (VEFG), lymphangiogenesis, which is involved in many pathological conditions, like tumor metastasis, organ graft rejection, corneal inflammation, and type 2 diabetes.³⁴ It also promotes the adhesion of tumor cells to vascular endothelium and their dissemination, thus promoting metastasis.^{35–38} For example, evidences show how it is involved in the metastatic evolution of prostatic cancer, and higher levels of Galectin-8 expression are also shown in lungs, bladder, kidney and breast cancerous tissues. The molecular mechanisms that explain its role in cancer growth and metastasis are still unclear, but evidences suggest a sort of Galectin-8-driven “vicious cycle,” whereby cancer cells that overexpress and secrete the lectin, benefit from its potential to promote their own growth.^{39,40} Considering the wide range of functions, Galectin-8 is a new interesting pharmacological target for the treatment of many diseases.

Galectin-8 contains two carbohydrate recognition domains (CRDs), one at the N- and the other at the C-terminus, with different binding specificities. They behave independently in the full length protein and the addition of a ligand specific for one CRD does not affect the binding to the other.^{41,42} Yet,

both Galectin-8 CRDs are required for its function so that blocking of either will hamper the functionality of the whole protein.^{9,43} Typically, the galectin CRD folds as a β -sandwich, formed from two β -sheets. The concave part comprises six β -strands, S1-S6, and the galactose recognition site consists of conserved amino acids on strands S4-S6. The Galectin-8 N-terminal CRD has an enhanced binding to anionic structures, such as 3'-sulfated lactose and 3'-*O*-sialylated lactose (3'-SiaLac). This is due to the presence of a long S3-S4 loop, bearing an arginine residue (Arg59), and a glutamine (Gln47) on strand S3, unique features among Galectins.^{44,45}

The development of high affinity ligands would represent an optimal research tool to further investigate the roles of this lectin and to design potential drug candidates for the treatment of many diseases. Up to date, galactomalonyl phenyl ester, a fused tricyclic galactose-benzene hybrid and benzimidazole galactoside have been successfully reported as Galectin-8 ligands in low micromolar range affinity.^{43,46,47}

Among the available crystal structures, the one with the preferred ligand, the trisaccharide 3'-SiaLac, has been solved (Figure 3A).⁴⁴ The investigation of the main interactions between this ligand and the protein revealed 3-lactoylgalactoside **108** as the minimal binding epitope, which was recently crystallized in its racemic form, in complex with Galectin-8N. It consists of a free galactose bearing a lactate residue attached by an ether linkage in position 3 (Figure 3B).⁴⁸

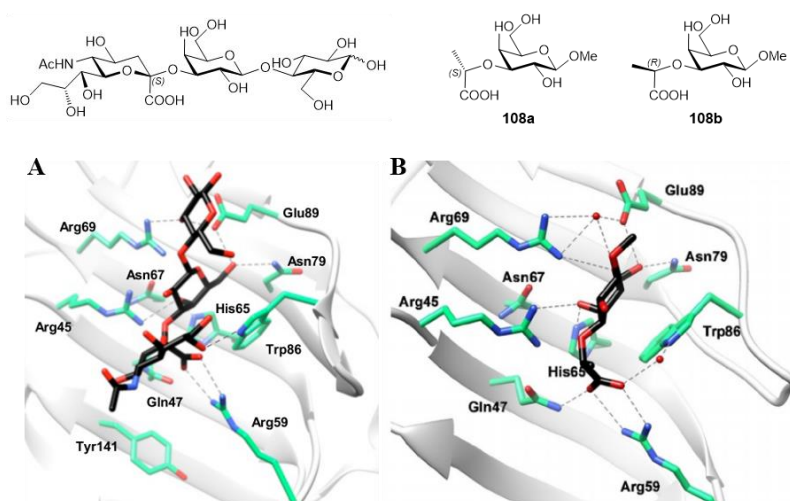


Figure 3. A: Galectin-8N in complex with 3'-SiaLac (PDB ID: 3AP7)⁴⁴; B: Galectin-8N in complex with racemic **108** (PDB ID: 5VWG).⁴⁸ Figure adapted from Bohari *et al.*⁴⁸

The crystal structure of the Galectin-8N/**108** complex revealed that all interactions of the previously reported ligand 3'-SiaLac were preserved. In particular, the carboxylic acid in **108** interacts with Arg59 and Gln47 forming a salt bridge and an H-bond; moreover, a complex network of H-bonds involves the galactose and Arg45, His65, Asn67, Asn79 and Glu89 (Figure 3).⁴⁸

Starting from this compound, we aimed to further explore the chemical space around it, in particular via (i) modification of the lactic acid moiety and (ii) by introducing an α -thiophenyl aglycone at position 1 of D-galactose. These modifications improved the affinity for Galectin-8N by 200-fold compared to the affinity of compound **108**. Besides, the affinity for other galectins was also evaluated. We focused on the N-terminal domain since the C-terminal in our hands showed weaker affinities for galactoside ligands.^{43,49}

5.2 Results and discussion.

Design. Starting from the lead compound 3-*O*-[1-carboxyethyl]- β -D-galactopyranoside (**108**),⁴⁸ we set out to derivatize the methyl group of the lactic acid side chain with cyclohexane and phenyl moieties; we focused on the *S*-configuration as with the *R*-configuration the added group would point away from the protein into solution (see Fig. 4B).

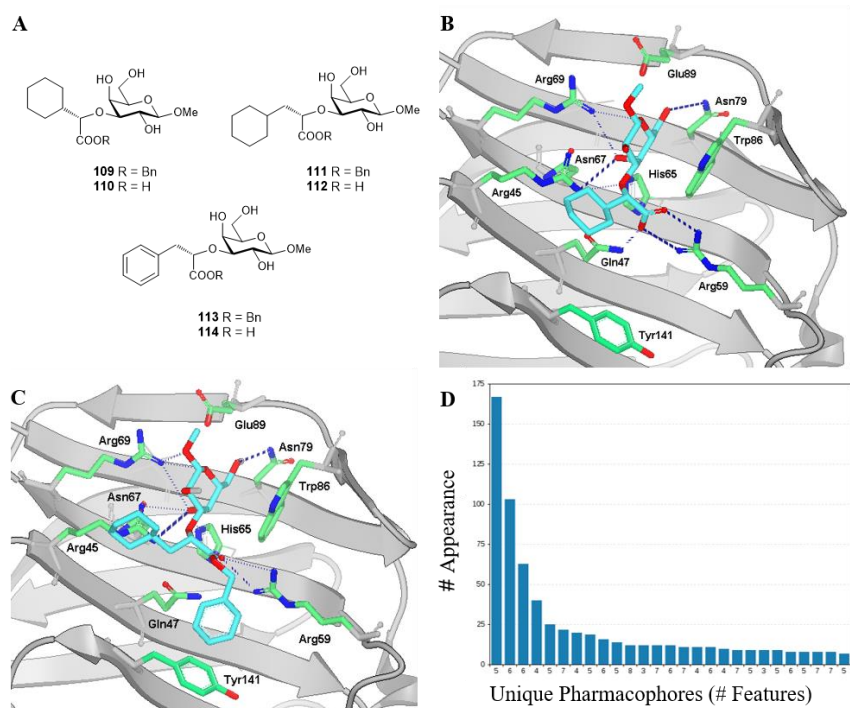
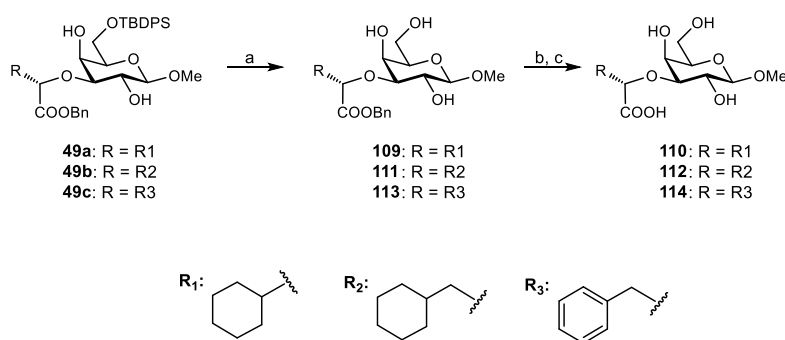


Figure 4. A: Designed Galectin-8 ligands **109-114**. B-C: Representative docking binding modes of compounds **110** (B) and **111** (C) in the Galectin-8N binding site (PDB ID: 3VKO).⁵⁰ Only selected amino acids are presented as sticks. Docking was performed using the FRED algorithm of the OEDocking software (OEDOCKING 3.3.0.2: OpenEye Scientific Software). D: Plot of the most frequently appearing unique structure-based pharmacophore models derived from MD simulations of Galectin-8N in complex with **111**. The x-axis shows unique models and the number of interaction features observed during the MD simulation. The numbers below the bar indicate the number of interaction features in the pharmacophore models. The y-axis shows the frequency of appearance of the models.

In addition, to determine the importance of the free carboxylic group for binding, we replaced it with an ester moiety (Figure 4A); a benzyl ester was chosen in order to gain possible hydrophobic contacts with the proximal Tyr141 in the binding site (Figure 4C). We did not consider modifications at positions 4 and 6 because they would probably clash with the protein, while substituents in position 2 would point towards the solvent, which would most likely bring little or no gain in affinity (Figures 4B and 4C). In our docking studies, as expected, the compounds maintained the position of the galactose and carboxylic acid of the reference compound's **108** pose including their interactions with the surrounding amino acids (Figure 3, Figure 4B and C). To assess the stability of the binding mode predicted by docking, interactions of compound **111** in the Galectin-8N binding site were further studied by a 200 ns molecular dynamics (MD) simulation using the MD analysis tool in LigandScout 4.4 Expert.⁵¹ A plot of the most frequently appearing unique structure-based pharmacophore models is shown in Figure 4D. The most frequently occurring model (166 times) contains 6 interaction features, including H-bonds of the galactose moiety with Arg45, His65 and Asn79, a H-bond between the ester carbonyl group and Gln47, and hydrophobic interactions of the benzyl moiety with Met56 and Tyr141. In pharmacophore models containing more features (Figure 4D), additional H-bonds are formed with the galactose moiety, as in the case of the crystal structure (Figure 3).

Synthesis. The synthesis of candidate compounds predicted by our *in silico* studies was accomplished as shown in Scheme 1, starting from intermediates **49a-c** shown in Chapter 2.



Scheme 1. a) HF·pyr, pyr, rt, 4 h, **109**: 62%, **111**: 75%; b) H₂, Pd/C, MeOH, 2 h, **110**: 86%, **112**: quant.; c) NaOH (H₂O/dioxane, 0.1 M), rt, 24 h, **7**: 10% over two steps from **49c**.

Removal of the TBDPS group on the galactose moiety with HF-pyridine yielded the benzylated test compounds **109** and **111**. Transesterification occurred during the reaction with the aromatic intermediate **49c**, making the purification of the benzylated product **113** extremely cumbersome. Therefore, the mixture was directly hydrolyzed to afford the final compound **114**. Hydrogenation was

instead carried out on compounds **109** and **111** thus affording the corresponding acids **110** and **112** (Scheme 1).

Fluorescence polarization assay. The binding affinities of the synthesized compounds **109-112** and **114** to the main target galectin-8N, and to galectin-1 and -3 as related members of the protein family, were evaluated in a competitive protein-binding assay based on fluorescence anisotropy (Table 1).^{41,52,53} Both enantiomers of the lead compound **112**⁴⁸ and methyl β -D-galactopyranoside (**3**)⁵⁴ were tested and used as references.

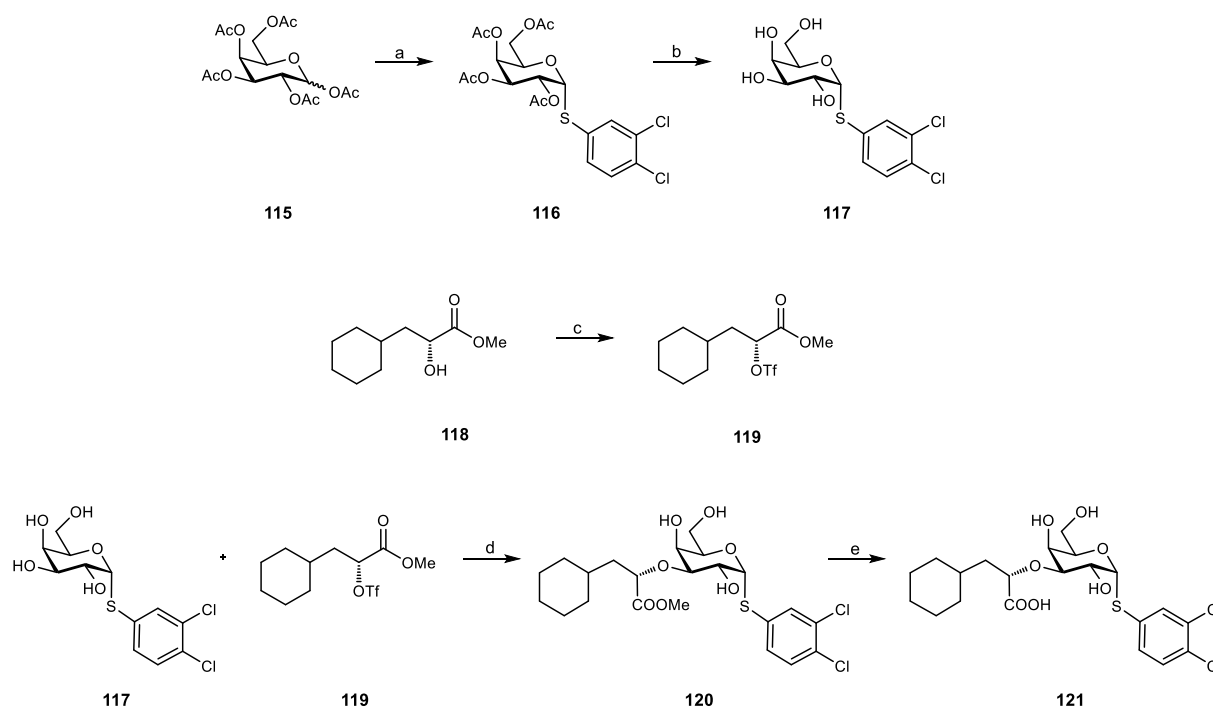
Table 1. K_D values of compounds **108-112**, **114** and **3** against human Galectin-8N, -1 and -3 measured by fluorescence polarization assay. The average values of K_D and SEM were calculated from 4 to 8 duplicate measurements. n.a.: not active.

Compound	Structure	Galectin-8N ($K_D \pm$ SEM, μ M)	Galectin-1 ($K_D \pm$ SEM, μ M)	Galectin-3 ($K_D \pm$ SEM, μ M)
3 ⁵⁴		5300	1000	4400
108a ⁵⁵		n.a.	2700 \pm 110	n.a.
108b ⁵⁵		\approx 2700	2800 \pm 69	2800 \pm 490
109		270 \pm 33	\approx 2500	n.a.
110		430 \pm 26	520 \pm 110	n.a.
111		210 \pm 18	\approx 2600	n.a.
112		470 \pm 39	n.a.	n.a.
114		550 \pm 66	1600 \pm 130	2100 \pm 600

With the fluorescence polarization assay, we were not able to reproduce the previously reported affinity of the reference compound **108** (K_D : 32 μ M).⁴⁸ Both enantiomers **108a** and **108b** bound very

weakly, or not at all, to Galectin-8N, Galectin-1 and Galectin-3. In contrast, several of our predicted compounds showed favorable binding and/or selectivity profiles. Overall, the addition of cyclohexane to the methyl increased affinity by about 5-fold (**110** and **112**), and the benzyl ester derivatives **109** and **111** showed an almost 2-fold further affinity increase for Galectin-8N when compared to the corresponding acids, despite carboxylates being stronger H-bond acceptors. In this case, the affinity gain of the ester could probably be explained by a lower desolvation penalty or by possible hydrophobic interactions of the benzyl residue with the Tyr141 side chain in the binding site. Compound **114**, carrying a phenyl ring on the lactic acid moiety, showed slightly poorer affinity to Galectin-8N when compared to the non-aromatic counterparts. To assess their target selectivity, all predicted Galectin-8 ligands were also tested on Galectins-1 and -3, which are known to feature overlaps in glycan specificities (Table 1). With the exception of **114**, which showed weak affinities, none of the compounds notably bound to Galectin-3. Compound **110** had similar affinity for both, Galectin-8 and Galectin-1, while **109**, **111** and **112** were moderately selective for Galectin-8N. Based on this, we concentrated on further optimization of compound **112**. This may sound irrational since **111** was an even more potent binder, but **112** was chosen because the intended optimisation described in the next chapter would involve addition of another aromatic group at the anomeric position. Based on previous experience, we assumed that molecules with 3 lipophilic rings around the galactose core would render the final compound(s) rather insoluble in aqueous media, so we decided to leave the free carboxylate.

Modification at the anomeric position of galactose. To improve the affinity of **112** for Galectin-8, we introduced a 3,4-dichlorophenyl ring in position 1 of the D-galactose moiety via an α -S-glycosidic bond since this group has been demonstrated to strongly enhance binding to many galectins.^{49,56} The desired compound **121** was synthesized from pentaacetylated galactose (**115**, Scheme 2), which was first transformed into the 3,4-dichlorophenyl- α -thioderivative **116**, and then deacetylated under Zemplén conditions (\rightarrow **117**). Donor **119** was synthesized from methyl (*R*)-3-cyclohexyl-2-hydroxypropanoate **118**⁵⁷ by triflation as shown above. The subsequent stannylidene-mediated regioselective alkylation gave **120**, which was further hydrolyzed to give final compound **121**.



Scheme 2. a) i. PCl_5 , $\text{BF}_3\cdot\text{Et}_2\text{O}$, DCM, rt, 1 h; ii. 3,4-dichlorothiophenol, NaH, DMF, rt, 50 °C, 16 h, 36%; b) MeONa/MeOH , rt, 16 h, 90%; c) Tf_2O , 2,6-lutidine, DCM, rt, 16 h, 70%; d) i. Bu_2SnO , dry MeOH, reflux, 3 h; ii. CsF, DME, rt, 16 h, 31%; e) NaOH ($\text{H}_2\text{O}/\text{dioxane}$, 0.1 M), rt, 16 h, 90%.

Compounds **120** and **121** were tested for their binding potency to Galectin-8N and other galectins using the established fluorescence polarization assay (Table 2).

Table 2. K_D values for compounds **120** and **121** against a panel of human galectins as measured by fluorescence polarization. The average values of K_D and SEM were calculated from 4 to 8 duplicate measurements. n.a.: not active.

Compound	Galectin ($K_D \pm \text{SEM}$, μM)					
	8N	8C	1	3	9C	9N
120	140 ± 27	2100 ± 27	780 ± 140	170 ± 16	110 ± 17	59 ± 14
121	12 ± 0.9	N.B.	580 ± 16	82 ± 7.5	360 ± 25	53 ± 16

The introduction of the 3,4-dichlorophenyl group increased the affinity by almost 40-fold ($12 \mu\text{M}$ for **121** vs $470 \mu\text{M}$ for **112**), confirming its beneficial effect for enhancing the binding to Galectin-8N. The methyl ester **120** showed a higher K_D value ($140 \mu\text{M}$) in this case and thus 10-fold weaker affinity compared to its free acid counterpart **121**, pointing that the free carboxylate most likely forms a salt bridge, which is disrupted in **120** where only H-bonding is possible. The binding mode of **121** in the

Galectin-8N binding site was predicted by docking and then studied further by a 200 ns MD simulation. Analysis of the binding mode in the most frequently appearing models (Figure 5B) showed an expected hydrogen bonding network of the galactose moiety with Arg45, His65, Asn79 and Glu89, while the carboxylate of **121** formed a salt bridge with the Arg59 side chain, as expected.

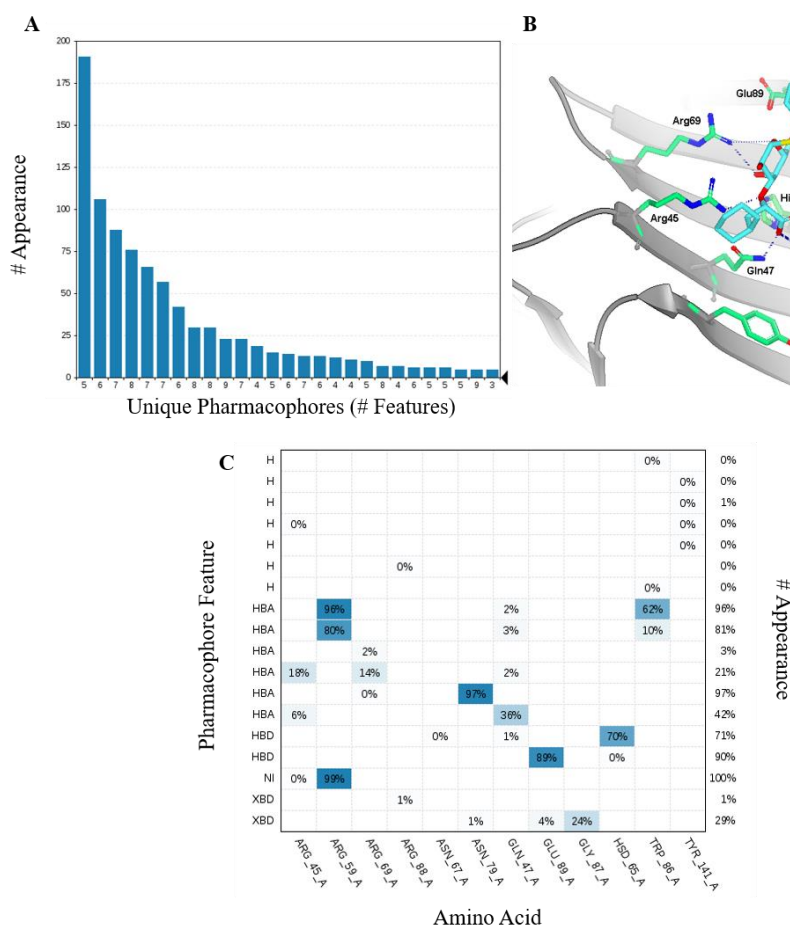


Figure 5. A: Plot of the most frequently appearing unique structure-based pharmacophore models derived from MD simulations of Galectin-8N in complex with **121**. The x-axis shows unique models and the number of interaction features observed during the MD simulation. The numbers below the bar indicate the number of interaction features in the pharmacophore models. The y-axis shows the frequency of appearance of the models. B: Docking binding mode of compound **121** in the Galectin-8N binding site (PDB ID: 3VKO).⁵⁰ Only selected amino acids are presented as sticks. Docking was performed using the FRED algorithm of the OEDocking software (OEDOCKING 3.3.0.2: OpenEye Scientific Software).⁵⁸ C: Interaction plot obtained by analyzing interactions of **121** with Galectin-8N binding site residues in the 200 ns MD simulation trajectory. Amino acid name and numbering are shown on the x-axis, pharmacophore feature type on the left y-axis (H – hydrophobic, HBA – hydrogen bond acceptor, HBD – hydrogen bond donor, NI – negative ionizable, XBD – halogen bond), % appearance on the right y-axis.

An important gain in binding affinity of 3,4-dichlorothiophenyl-based **121** in comparison with the methyl glycosides (Table 1) can be attributed to the formation of a halogen bond of 3-Cl with the

Gly87 backbone carbonyl.⁵⁶ This interaction was present for more than 24% of the simulation time (Figure 5C). The affinity for Galectin-8C was weak. Considering their strong affinities for the primary target, **120** and **121** were also tested towards a panel of other human galectins. The binding towards Galectin-3 and Galectin-9N was found to be considerable, which is in line with existing Galectin-8N ligands⁴⁹ that showed comparable affinity to these galectins. Still, **121** showed reasonable selectivity, especially versus Galectin-1, which is an important highlight of this series.

5.3 Conclusions.

In this study, we synthesized a focused library of 3-*O*-[1-carboxyethyl]- β -D-galactopyranoside (**108**) derivatives and measured their affinity for Galectin-8N using a fluorescence polarization assay. We first introduced modifications to the lactic acid moiety; the benzyl esters unexpectedly were more active than their acid counterparts. Moreover, the compounds showed good selectivity towards Galectin-8N when compared to Galectin-1 and, in particular, to Galectin-3. Interestingly, our assessment of reference compound **108** indicated a substantially weaker affinity to Galectin-8N than originally reported.⁴⁸ Thus, fluorescence polarization data should be interpreted relatively to the reference compound. The direct comparison to **108** shows that our design strategy based on *in silico* analyses was successful in predicting derivatives with affinity improvements by 2 orders of magnitude (from K_D about 2700 μ M to 12 μ M). The most suitable moiety at position 3 of galactose increased affinity about 5-fold, and adding a 3,4-dichlorophenyl ring in position 1, increased the potency a further 40-fold. With a K_D of 12 μ M, compound **121** is among the most potent Galectin-8 ligands reported thus far. Importantly, it also shows reasonable selectivity for Galectin-8. STD-NMR experiments of **121** binding to Galectin-8 may be considered in the future to further study the binding characteristics of **121**, an approach that has been already used in the past on lactic acid-containing molecules.^{59,60} Our results represent an ideal starting point for the development of Galectin-8 ligands with improved affinity and selectivity profiles, thereby providing new perspectives for targeting cancer or diseases associated with bone loss and inflammation.

5.4 Experimental part.

Ligand preparation. The structures of molecules were built with ChemDraw Professional 16.0 (PerkinElmer Informatics, Inc.). Conformers for each ligand, required by the docking software FRED, were generated with OMEGA (OMEGA version 2.5.1.4. OpenEye Scientific Software, Santa Fe, NM. <http://www.eyesopen.com>), with a maximum number of 200 conformations set as default.

Receptor preparation & docking protocol. The docking was performed using the Galectin-8 crystal structure in complex with sialyllactosamine (PDB code: 3VKO). Docking was done inside a grid box surrounding the ligand with the volume of 8350 \AA^3 , dimensions: $25.67 \text{ \AA} \times 16.00 \text{ \AA} \times 20.33 \text{ \AA}$, and outer contour of 2766 \AA^2 using Make Receptor 3.0.1.

The docking software FRED (OEDocking version 3.0.1. OpenEye Scientific Software, Santa Fe, NM. <http://www.eyesopen.com>) was used for docking studies with the default settings, and number of poses, which was set to 10. The proposed ten binding poses with the highest rank of the docked ligands were evaluated using final score and relative position to the native ligand. The graphical representations of the calculated binding poses were obtained using VIDA (VIDA version 4.2.1. OpenEye Scientific Software, Santa Fe, NM. <http://www.eyesopen.com>).

Molecular dynamics simulations. The molecular dynamics software NAMD (version 2.9)⁶¹ and the CHARMM22 force field^{62,63} were used for MD simulations using the Galectin-8N-**111** and Galectin-8N-**121** complexes, as obtained by docking, as input structures. Molecular mechanics parameters for compounds **111** and **121** were estimated using the ParamChem tool.^{64–66} Steepest descent (10000 steps) and adopted basis Newton–Raphson (10000 steps) energy minimizations were first performed to remove atomic clashes and to optimize the atomic coordinates of the Galectin-8N-**111** and Galectin-8N-**121** docking complexes. The structure of the energy minimized complex for MD simulation was prepared using psfgen in VMD (version 1.9.1.).⁶⁷ The complex was embedded in a box of TIP3P water molecules. The system was neutralized by addition of NaCl. The MD simulation was carried out in the NPT ensemble employing periodic boundary conditions. Langevin dynamics and Langevin piston methods were used for temperature (300 K) and pressure (1 atm) control, respectively. Short- and long-range forces were calculated every 1 and 2 time steps, respectively, with a time step of 2.0 ps. The smooth particle mesh Ewald method⁶⁸ was used to calculate electrostatic interactions. The short-range interactions were cut off at 12 \AA . All chemical bonds between hydrogen and heavy atoms were held fixed using the SHAKE algorithm.⁶⁹ The simulation consisted of three consecutive steps: (i) solvent equilibration for 0.5 ns with ligand and protein constrained harmonically around the initial structure, (ii) equilibration of the complete system for 0.5 ns with ligand and protein released, and (iii) an unconstrained 200 ns production run. For structure-based pharmacophore modeling 1000 frames from the production run were saved separately and used for interaction analysis.

Structure-based pharmacophore modeling. The MD trajectory of Galectin-8N in complex with compound **111** or **121** was used for chemical feature interaction analysis using LigandScout 4.4

Expert.⁷⁰ The first frame of the trajectory (in PDB format) and the MD trajectory files (DCD format) are needed as input for the creation of an ensemble of structure-based pharmacophore models. LigandScout 4.4 Expert was used to generate 1000 structure-based pharmacophore models from the 200 ns MD simulation.

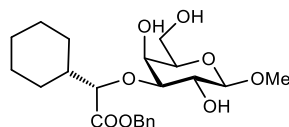
Synthesis. Unless otherwise stated, the starting materials, reagents, and solvents were purchased as high-grade commercial products from Sigma-Aldrich, Alfa-Aesar, Apollo Scientific and TCI, and used without further purification. MeCN and MeOH were dried over activated molecular sieves (4 Å and 3 Å, respectively) and stored under argon atmosphere. Dry DME was prepared by filtration through Al₂O₃ and stored over activated molecular sieves (4 Å) under argon atmosphere. Dry DCM, DMF, pyridine and THF were purchased from Sigma-Aldrich and TCI. Molecular sieves were activated under vacuum at 500 °C for 30 min immediately before use. Analytical TLC was performed on silica gel Merck 60 F254 plates (0.25 mm), using visualization with UV light and/or by charring with a phosphomolybdic acid solution (10 g in 100 mL of ethanol). Acidic ion-exchange resin (Amberlyst[®] IR-120 hydrogen form) was washed with MeOH prior to use. Column chromatography was carried out on silica gel 60 (particle size 240–400 mesh). Reversed-phase chromatography was performed on Biotage Isolera[™] One using C-18 cartridges. ¹H and ¹³C NMR spectra were recorded at 400 MHz and 100 MHz, respectively, on an AVANCE III 400 spectrometer (Bruker Corporation, Billerica, MA, USA) or at 500 MHz and 126 MHz on a Bruker Avance DMX-500 (500 MHz) spectrometer, in chloroform-*d* (CDCl₃), methanol-*d*₄ (CD₃OD) or deuterium oxide (D₂O), with TMS as internal standard. Chemical shifts (δ) are expressed in parts per million (ppm) relative to the residual solvent peaks for the ¹H and ¹³C nuclei (CDCl₃: δ_H = 7.26, δ_C = 77.16; CD₃O: δ_H = 3.31, δ_C = 49.00; D₂O: δ_H = 4.79); coupling constants (*J*) are given in hertz (Hz). The following abbreviations are used to describe peak patterns when appropriate: s (singlet), d (doublet), dd (doublets of doublet), ddd (doublets of doublets of doublet), t (triplet), m (multiplet). 2D NMR experiments (COSY and HSQC) of representative compounds were carried out to assign protons and carbons of the new structures. Mass spectra were obtained using a single quadrupole mass spectrometer Advion Expression CMS^L coupled with an Agilent 1290 liquid chromatograph or on a Waters Micromass ZQ instrument. High resolution mass spectrometry (HRMS) was performed on a Q Exactive[™] Plus Hybrid Quadrupole-Orbitrap[™] Mass Spectrometer (Thermo Scientific[™]; ion source: Electrospray Ionization (ESI)). MS spectra were acquired in Fourier transform-mass spectrometry (FT-MS) scan mode with a target mass resolution of 100 000 at *m/z* 400. Recorded spectra were analyzed with Thermo Xcalibur Qual Browser (Xcalibur 4.2 SP1, Thermo Fisher Scientific Inc.). HRMS analysis was also performed on an Agilent 1100 LC, equipped with a photodiode array detector and a

Micromass QTOF I, equipped with a 4 GHz digital-time converter. Optical rotations were measured with a PerkinElmer polarimeter 341. HPLC analyses for compounds **109** and **111** were performed on a UHPLC Thermo Scientific UltiMate™ 3000 Liquid Chromatography. An Acquity Beh C18 column (1.8 μm , 2.1 \times 50 mm) was used with a flow rate of 0.4 mL/min. The eluent consisted of H₂O as solvent A and MeCN as solvent B (Table 1: Method A). HPLC analysis for all the other compounds was performed on a Thermo Scientific Dionex Ultimate 3000 Binary Rapid Separation LC System (Thermo Fisher Scientific, Waltham, MA, USA) equipped with an autosampler, a binary pump system and a photodiode array detector. A Waters Atlantis T3 dC18 column (3 μm , 2.1 \times 100 mm) was used with a flow rate of 0.3 mL/min. The eluent consisted of H₂O + 0.1% trifluoroacetic acid (TFA) as solvent A and MeCN + 0.1% TFA as solvent B (Table 1: Method B).

Method A		Method B	
T (min)	%B	T (min)	%B
0	5	0	5
2	5	2	5
7	80	10	20
9	80	16	80
9.5	0	18	0
-	-	21	0

Table 3. Methods for HPLC analysis.

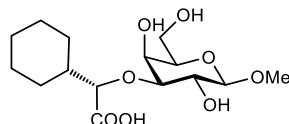
Methyl 3-*O*-[(*S*)-1-benzoyloxycarbonyl-1-cyclohexyl-methyl]- β -D-galactopyranoside (**109**).



To a solution of **49a** (150 mg, 0.23 mmol) in pyridine (3.0 mL) in a Teflon container was added HF_{pyr} (1.50 mL) dropwise and the reaction mixture was stirred at rt for 2.5 h. The reaction was neutralized with aq. satd. NaHCO₃ and the aqueous phase was extracted with DCM (3 \times 10 mL). Then, the organic phases were dried over Na₂SO₄ and concentrated under reduced pressure. The crude product was purified by flash chromatography (petroleum ether/acetone, 8:2 \rightarrow 7:3) to afford **109** (61 mg, 62%) as a white solid. $[\alpha]_{\text{D}}^{20}$ -22.7 (c 1.0, MeOH); ¹H NMR (400 MHz, CD₃OD): δ = 1.12-1.40 (m, 5H, H-cy), 1.51-1.65 (m, 3H, H-cy), 1.66-1.76 (m, 2H, H-cy), 1.80 (m, 1H, H-cy), 3.21 (dd, J = 3.3, 9.5 Hz, 1H, H-3), 3.40 (t, J = 6.1 Hz, 1H, H-5), 3.51 (s, 3H, OMe), 3.59-3.67 (m, 2H, H-2, H-6a), 3.73 (dd, J = 7.0, 11.3 Hz, 1H, H-6b), 3.82 (d, J = 3.0 Hz, 1H, H-4), 4.08 (d, J = 7.8 Hz, 1H, H-1), 4.18 (d, J = 4.8 Hz, 1H, H-1'), 5.15 (d, J = 12.0 Hz, 1H, OCH₂Ph), 5.25 (d, J = 12.1 Hz, 1H, OCH₂Ph), 7.32-7.40 (m, 5H, Ar-H); ¹³C NMR (100 MHz, CD₃OD): δ = 27.18, 27.20, 27.3, 28.7, 30.0 (5C, CH₂-cy), 43.1 (CH-cy), 57.3 (OMe), 62.5 (C-6), 67.8 (OCH₂Ph), 68.6 (C-4), 72.3 (C-2),

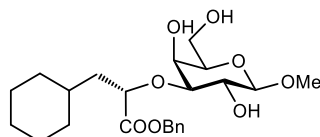
76.2 (C-5), 84.0 (C-3), 85.0 (C-1'), 105.9 (C-1), 129.5, 129.6, 129.8, 137.2 (6C, Ar-C), 175.4 (C=O); HR-MS: m/z : Calcd for $C_{22}H_{32}O_8$: 447.1995 $[M+Na]^+$, found: 447.1984; HPLC: Purity 98%.

Methyl 3-*O*-[(*S*)-1-carboxy-1-cyclohexyl-methyl]- β -D-galactopyranoside (110**).**



To a solution of compound **109** (22 mg, 0.052 mmol) in MeOH (2.2 mL), was added Pd/C (2.2 mg) under hydrogen atmosphere (1 atm). The reaction mixture was stirred at rt for 2 h. The suspension was filtered over celite and concentrated under reduced pressure to give **110** (14.9 mg, 86%) as a white solid. $[\alpha]_D^{20}$ -9.4 (c 1.0, MeOH); 1H NMR (400 MHz, CD_3OD): δ = 1.19-1.34 (m, 4H, H-cy), 1.49 (m, 1H, H-cy), 1.66-1.83 (m, 6H, H-cy), 3.23 (dd, J = 2.6, 9.4 Hz, 1H, H-3), 3.49 (t, J = 6.0 Hz, 1H, H-5), 3.52 (s, 3H, OMe), 3.63 (dd, J = 8.0, 9.2 Hz, 1H, H-2), 3.69-3.79 (m, 2H, 2 H-6), 3.86 (d, J = 4.1 Hz, 1H, H-4), 3.90 (d, J = 2.5 Hz, 1H, H-1'), 4.13 (d, J = 7.8 Hz, 1H, H-1); ^{13}C NMR (100 MHz, CD_3OD): δ = 27.3, 27.4, 27.5, 28.6, 30.4 (5C, CH_2 -cy), 43.2 (CH-cy), 57.2 (OMe), 62.6 (C-6), 67.9 (C-4), 71.7 (C-2), 76.1 (C-5), 85.2 (C-3), 85.8 (C-1'), 105.9 (C-1), 179.6 (C=O); HR-MS: m/z : Calcd for $C_{15}H_{26}O_8$: 333.1555 $[M-H]^-$, found: 333.1556; HPLC: Purity > 99.5%.

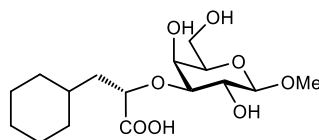
Methyl 3-*O*-[(1*S*)-1-benzyloxycarbonyl-2-cyclohexyl-ethyl]- β -D-galactopyranoside (111**).**



To a solution of **49b** (100 mg, 0.148 mmol) in pyridine (2.5 mL) in a Teflon container was added HF \cdot pyr (0.6 mL) dropwise and the reaction mixture was stirred at rt for 2.5 h. The reaction was neutralized with aq. satd. $NaHCO_3$ and the aqueous phase was extracted with DCM (3×10 mL). Then, the organic phases were dried over Na_2SO_4 and concentrated under reduced pressure. The crude product was purified by flash chromatography (petroleum ether/acetone, 8:2 \rightarrow 7:3) to afford **111** (48 mg, 75%) as a white solid. $[\alpha]_D^{20}$ -26.3 (c 1.0, MeOH); 1H NMR (400 MHz, $CDCl_3$): δ = 0.73-0.87 (m, 2H, H-cy), 0.95-1.15 (m, 3H, H-cy), 1.45-1.64 (m, 8H, 2 H-2', 6 H-cy), 2.27-2.41 (m, 2H, OH-2, OH-4), 3.26 (dd, J = 3.3, 9.3 Hz, 1H, H-3), 3.41-3.45 (m, 2H, H-5, OH-6), 3.55 (s, 3H, OMe), 3.72-3.82 (m, 3H, H-2, H-4, H-6a), 3.94 (dd, J = 6.5, 11.8 Hz, 1H, H-6b), 4.15 (d, J = 7.8 Hz, 1H, H-1), 4.24 (dd, J = 9.6, 3.5 Hz, 1H, H-1'), 5.15 (d, J = 12.1 Hz, 1H, OCH_2Ph), 5.21 (d, J = 12.1 Hz, 1H, OCH_2Ph), 7.33-7.40 (m, 5H, Ar-H); ^{13}C NMR (100 MHz, $CDCl_3$): δ = 26.2, 26.4, 26.5, 32.3 (4C, CH_2 -cy), 33.7 (CH-cy), 34.0 (CH_2 -cy), 41.1 (C-2'), 57.2 (OMe), 62.8 (C-6), 67.3 (OCH_2Ph), 67.8

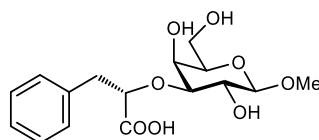
(C-4), 71.1 (C-2), 74.2 (C-5), 77.5 (C-1'), 83.2 (C-3), 104.0 (C-1), 128.7, 128.8, 135.3 (6C, Ar-C), 174.9 (C=O); HR-MS: m/z : Calcd for $C_{23}H_{34}O_8$: 439.2332 $[M+H]^+$, found: 439.2318; HPLC: Purity 95%.

Methyl 3-*O*-[(1*S*)-1-carboxy-2-cyclohexyl-ethyl]- β -D-galactopyranoside (112**).**



To a solution of **111** (35 mg, 0.080 mmol) in MeOH (4.0 mL), was added Pd/C (3.5 mg) under hydrogen atmosphere (1 atm). The reaction mixture was stirred at rt for 2 h. The suspension was filtered over celite and concentrated under reduced pressure to afford **112** (27.8 mg, quant) as a yellow solid. $[\alpha]_D^{20}$ -30.2 (c 1.0, MeOH); 1H NMR (400 MHz, CD_3OD): δ = 0.85-1.01 (m, 2H, H-cy), 1.16-1.34 (m, 3H, H-cy), 1.59-1.72 (m, 7H, 5 H-cy, 2 H-2'), 1.92 (m, 1H, H-cy), 3.27 (dd, J = 3.1, 9.4 Hz, 1H, H-3), 3.49 (m, 1H, H-5), 3.52 (s, 3H, OMe), 3.61 (dd, J = 8.0, 9.3 Hz, 1H, H-2), 3.70-3.78 (m, 2H, H-6), 3.94 (d, J = 2.5 Hz, 1H, H-4), 4.13 (d, J = 7.8 Hz, 1H, H-1), 4.22 (dd, J = 3.9, 9.2 Hz, 1H, H-1'); ^{13}C NMR (100 MHz, CD_3OD): δ = 27.2, 27.5, 27.7, 33.5 (4C, CH_2 -cy), 34.6 (CH-cy), 35.2 (CH₂-cy), 42.6 (C-2'), 57.2 (OMe), 62.5 (C-6), 68.2 (C-4), 71.9 (C-2), 76.1 (C-5), 78.9 (C-1'), 84.6 (C-3), 105.9 (C-1), 179.8 (C=O); HR-MS: m/z : Calcd for $C_{16}H_{28}O_8$: 347.1711 $[M-H]^-$, found: 347.1713; HPLC: Purity > 99.5%.

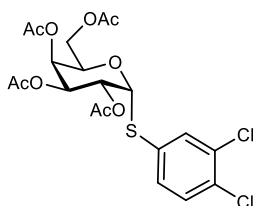
Methyl 3-*O*-[(1*S*)-1-carboxy-2-phenyl-ethyl]- β -D-galactopyranoside (114**).**



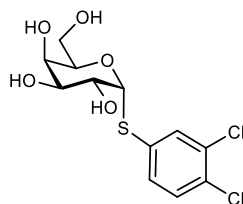
To a solution of **49c** (242 mg, 0.447 mmol) in pyridine (7.8 mL) in a Teflon container was added HF·pyr (2.25 mL) dropwise and the reaction mixture was stirred at rt for 2.5 h. The reaction was neutralized with aq. satd. $NaHCO_3$ and the aqueous phase was extracted with DCM (3×15 mL). Then, the organic phases were dried over Na_2SO_4 and concentrated under reduced pressure. The crude product was purified by flash chromatography (petroleum ether/acetone, 8:2 \rightarrow 7:3) to afford the desilylated product as a mix of methyl and benzyl esters (42 mg). The mixture was treated with a 1 M solution of NaOH in H_2O /dioxane (1:1, 10 mL) at rt for 24 h. Then it was neutralized with 1 M aq. HCl and concentrated under reduced pressure. The residue was purified by reversed-phase chromatography (C_{18} , H_2O /MeCN, 1:0 \rightarrow 7:3) to give **114** (15 mg, 10%, two steps) as a white solid. $[\alpha]_D^{20}$ -6.6 (c 0.5, MeOH); 1H NMR (500 MHz, D_2O): δ = 2.99 (dd, J = 8.6, 14.0 Hz, 1H, H-2'a),

3.16 (dd, $J = 4.7, 14.0$ Hz, 1H, H-2'b), 3.31 (dd, $J = 3.2, 9.6$ Hz, 1H, H-3), 3.52-3.56 (m, 4H, H-5, OMe), 3.64 (m, 1H, H-2), 3.75 (dd, $J = 4.4, 11.8$ Hz, 1H, H-6a), 3.79 (dd, $J = 7.7, 11.8$ Hz, 1H, H-6b), 3.94 (m, 1H, H-4), 4.17 (dd, $J = 4.7, 8.6$ Hz, 1H, H-1'), 4.24 (d, $J = 7.3$ Hz, 1H, H-1), 7.32 (m, 1H, Ar-H), 7.37-7.41 (m, 4H, Ar-H); ^{13}C NMR (126 MHz, D_2O): $\delta = 41.3$ (C-2'), 59.0 (OMe), 63.1 (C-6), 68.0 (C-4), 71.8 (C-2), 76.6 (C-5), 84.0 (C-1'), 84.6 (C-3), 105.3 (C-1), 128.7, 130.5, 131.5, 140.3 (6C, Ar-C), 182.7 (C=O); HR-MS: m/z : Calcd for $\text{C}_{16}\text{H}_{21}\text{O}_8$: 341.1242 $[\text{M}-\text{H}]^-$, found: 341.1242; HPLC: Purity > 99.5%.

3,4-Dichlorophenyl 2,3,4,6-tetra-*O*-acetyl-1-thio- α -D-galactopyranoside (**116**).

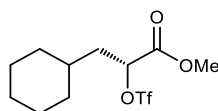


To a suspension of β -D-galactose pentaacetate (1.00 g, 2.60 mmol) and PCl_5 (0.587 g, 2.82 mmol) in dry DCM (10 mL) was added $\text{BF}_3 \cdot \text{Et}_2\text{O}$ (16.0 μL , 0.13 mmol). The mixture was stirred for 1 h. Then, it was diluted with DCM (30 mL) and subsequently washed with cold H_2O (50 mL), cold aq. satd. NaHCO_3 (2×50 mL), and cold H_2O (2×50 mL), dried over Na_2SO_4 and concentrated under reduced pressure. The crude galactopyranosyl chloride intermediate was used for the next step without further purification. NaH (0.022 g, 0.92 mmol) and 3,4-dichlorothiophenol (130 μL , 1.0 mmol) were dissolved in dry DMF (2 mL) and stirred at rt for 30 min. Then, a solution of the galactopyranosyl chloride in DMF (7 mL) was added to the reaction mixture. The mixture was stirred overnight at 50 $^\circ\text{C}$ and then diluted with DCM (50 mL) and H_2O (50 mL). The organic phase was washed with water (3×30 mL), dried over Na_2SO_4 and concentrated under reduced pressure. The residue was purified by flash chromatography (petroleum ether/EtOAc, 10:0 \rightarrow 7:3) to afford **116** (480 mg, 36%) as a white solid. $[\alpha]_{\text{D}}^{20} +22.6$ (c 1.0, MeOH); ^1H NMR (500 MHz, CDCl_3): $\delta = 1.98, 2.01, 2.11, 2.14$ (4 s, 12H, OAc), 4.06-4.10 (m, 2H, H-6), 4.65 (t, $J = 6.5$ Hz, 1H, H-5), 5.24 (dd, $J = 3.3, 11.0$ Hz, 1H, H-3), 5.33 (dd, $J = 5.6, 10.9$ Hz, 1H, H-2), 5.48 (dd, $J = 1.3, 3.4$ Hz, 1H, H-4), 5.98 (d, $J = 5.6$ Hz, 1H, H-1), 7.27 (dd, $J = 2.2, 8.4$ Hz, 1H, Ar-H), 7.36 (d, $J = 8.4$ Hz, 1H, Ar-H), 7.56 (d, $J = 2.2$ Hz, 1H, Ar-H); ^{13}C NMR (126 MHz, CDCl_3): $\delta = 20.70, 20.72, 20.9$ (4C, OAc), 62.0 (C-6), 67.7 (C-5), 67.9 (C-4), 68.0 (C-2), 68.1 (C-3), 85.5 (C-1), 130.8, 131.1, 132.3, 132.9, 133.1, 133.3 (6C, Ar-C), 170.0, 170.2, 170.5 (4C, C=O); ESI-MS: m/z : Calcd for $\text{C}_{20}\text{H}_{22}\text{Cl}_2\text{O}_9\text{S}$: 532.3 $[\text{M}+\text{Na}]^+$, found: 532.1. The analytical data of **116** were in accordance with reported values.⁴⁹

3,4-Dichlorophenyl 1-thio- α -D-galactopyranoside (117).

A solution of **116** (480 mg, 0.94 mmol) in MeOH (7 mL) was treated with 1 M MeONa/MeOH (1.5 mL) overnight at rt. Then, the mixture was neutralized with Amberlyst-15 ion-exchange resin and concentrated under reduced pressure to give **117** (289 mg, 90%) as a white solid. $[\alpha]_{\text{D}}^{20} +174$ (c 1.0, MeOH); ^1H NMR (500 MHz, CD_3OD): δ = 3.64 (dd, J = 3.3, 10.2 Hz, 1H, H-3), 3.69 (dd, J = 6.8, 11.5 Hz, 1H, H-6a), 3.73 (dd, J = 5.3, 11.5 Hz, 1H, H-6b), 3.95 (dd, J = 1.3, 3.3 Hz, 1H, H-4), 4.18 (dd, J = 5.5, 10.2 Hz, 1H, H-2), 4.27 (ddd, J = 1.3, 5.2, 6.7 Hz, 1H, H-5), 5.65 (d, J = 5.5 Hz, 1H, H-1), 7.43 (d, J = 8.4 Hz, 1H, Ar-H), 7.47 (dd, J = 2.1, 8.4 Hz, 1H, Ar-H), 7.73 (d, J = 2.0 Hz, 1H, Ar-H); ^{13}C NMR (126 MHz, CD_3OD): δ = 62.4 (C-6), 69.8 (C-2), 70.7 (C-4), 72.2 (C-3), 73.7 (C-5), 91.3 (C-1), 131.6, 132.0, 132.6, 133.5, 134.3, 137.2 (6C, C-Ar); ESI-MS: m/z : Calcd for $\text{C}_{12}\text{H}_{14}\text{Cl}_2\text{O}_5\text{S}$: 363.0 $[\text{M}+\text{Na}]^+$, found: 363.0.

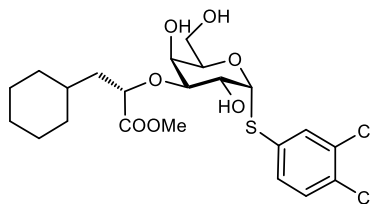
The analytical data of **117** were in accordance with reported values.⁴⁹

Methyl (*R*)-3-cyclohexyl-2-(trifluoromethylsulfonyloxy)-propanoate (119).

Methyl (*R*)-3-cyclohexyl-2-hydroxypropanoate **118** (222 mg, 1.19 mmol) was dissolved in dry DCM (5 mL) under argon. Then, 2,6-lutidine (277 μL , 2.38 mmol) was added, the mixture was cooled down to -15 $^{\circ}\text{C}$ and Tf_2O (301 μL , 1.79 mmol) was added. The reaction was stirred at -20 $^{\circ}\text{C}$ for 4 h. Then, it was diluted with DCM (15 mL), washed with cold water (2×20 mL) and brine (3×20 mL), dried over Na_2SO_4 and concentrated under reduced pressure. The residue was purified by flash chromatography (hexane/EtOAc, 20:1 \rightarrow 9:1) to afford **119** (265 mg, 70%) as a colorless oil. $[\alpha]_{\text{D}}^{20} +37.5$ (c 1.0, CHCl_3); ^1H NMR (500 MHz, CD_3OD): δ = 0.89-1.03 (m, 2H, H-cy), 1.12-1.32 (m, 3H, H-cy), 1.46 (m, 1H, H-cy), 1.64-1.76 (m, 4H, H-cy), 1.79-1.84 (m, 2H, H-3a, 2 H-cy), 1.92 (ddd, J = 4.9, 9.3, 14.4 Hz, 1H, H-3b), 3.84 (s, 3H, OMe), 5.19 (dd, J = 4.0, 9.3 Hz, 1H, H-2); ^{13}C NMR (126 MHz, CD_3OD): δ = 25.9, 26.1, 26.3, 32.1 (4C, CH_2 -cy), 33.4 (CH-cy), 33.6 (CH_2 -cy), 39.4 (C-3), 53.3 (OMe), 81.9 (C-2), 118.6 (q, J = 319.7 Hz, CF_3), 168.3 (C=O).

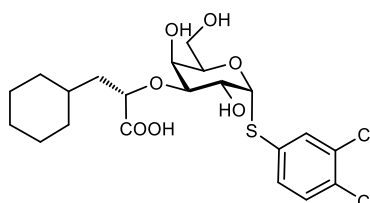
The analytical data of **119** were in accordance with reported values.⁵⁷

3,4-Dichlorophenyl

3-*O*-[(1*S*)-1-methoxycarbonyl-2-cyclohexyl-ethyl]-1-thio- α -D-galactopyranoside (**120**).

To a solution of **117** (34.0 mg, 0.10 mmol) in dry MeOH (3.0 mL) was added Bu₂SnO (27.3 mg, 0.13 mmol) at rt under argon. The mixture was heated to reflux and stirred for 3 h. The solvent was then evaporated and the residue dried under vacuum for 4 h. The crude product was dissolved in DME (1 mL) and stirred under argon. A solution of **119** (686 mg, 1.74 mmol) in DME (2 mL) was added dropwise, followed by dried CsF (18.2 mg, 0.12 mmol) at once. The reaction mixture was stirred for 16 h at rt. Then, EtOAc (10 mL) and H₂O (10 mL) were added and the aqueous phase was extracted with EtOAc (3 × 10 mL). The combined organic phases were dried over Na₂SO₄, filtered and evaporated. The crude material was purified by flash column chromatography (petroleum ether/acetone, 1:0 → 6:4) to afford **120** (15.8 mg, 31%) as a white solid. $[\alpha]_D^{20} +172.2$ (*c* 1.0, MeOH); ¹H NMR (500 MHz, CD₃OD): δ = 0.83-1.01 (m, 2H, H-cy), 1.16-1.35 (m, 3H, H-cy), 1.58 (m, 1H, H-cy), 1.65-1.73 (m, 6H, 2 H-2', 4 H-cy), 1.93 (m, 1H, H-cy), 3.41 (dd, *J* = 3.2, 10.0 Hz, 1H, H-3), 3.66 (dd, *J* = 6.8, 11.5 Hz, 1H, H-6a), 3.72 (dd, *J* = 5.3, 11.5 Hz, 1H, H-6b), 3.75 (s, 3H, OMe), 4.10 (dd, *J* = 1.3, 3.3 Hz, 1H, H-4), 4.23 (ddd, *J* = 1.4, 5.2, 6.8 Hz, 1H, H-5), 4.31 (dd, *J* = 5.6, 10.0 Hz, 1H, H-2), 4.45 (dd, *J* = 4.1, 8.8 Hz, 1H, H-1'), 5.63 (d, *J* = 5.6 Hz, 1H, H-1), 7.43 (d, *J* = 8.4 Hz, 1H, Ar-H), 7.46 (dd, *J* = 2.1, 8.4 Hz, 1H, Ar-H), 7.72 (d, *J* = 2.0 Hz, 1H, Ar-H); ¹³C NMR (126 MHz, CD₃OD): δ = 27.2, 27.4, 27.7, 33.6 (4C, CH₂-cy), 34.7 (CH-cy), 35.0 (CH₂-cy), 42.2 (C-2'), 52.6 (OMe), 62.3 (C-6), 69.1 (C-4), 69.6 (C-2), 73.4 (C-5), 78.5 (C-1'), 81.0 (C-3), 91.3 (C-1), 131.6, 132.0, 132.6, 133.5, 134.3, 137.0 (6C, Ar-C); HR-MS: *m/z*: Calcd for C₂₂H₃₀Cl₂O₇S: 531.0987 [M+Na]⁺, found: 531.0987; HPLC: Purity 99.5%.

3,4-Dichlorophenyl

3-*O*-[(1*S*)-1-carboxy-2-cyclohexyl-ethyl]-1-thio- α -D-galactopyranoside**(121)**.

Compound **120** (12 mg, 0.02 mmol) was treated with a 0.1 M solution of NaOH in H₂O/dioxane (1:1, 2 mL) overnight at rt. Then, the mixture was neutralized and concentrated under reduced pressure to

afford **121** (8.90 mg, 90%) as a white solid. $[\alpha]_D^{20} +80.0$ (c 1.0, MeOH); ^1H NMR (500 MHz, CD_3OD): δ = 0.88-1.03 (m, 2H, H-cy), 1.20 (m, 1H, H-cy), 1.27-1.35 (m, 2H, H-cy), 1.58-1.75 (m, 7H, 2 H-2', 5 H-cy), 1.94 (m, 1H, H-cy), 3.43 (dd, J = 3.0, 10.1 Hz, 1H, H-3), 3.67 (dd, J = 6.8, 11.6 Hz, 1H, H-6a), 3.72 (dd, J = 5.3, 11.6 Hz, 1H, H-6b), 4.10 (m, 1H, H-4), 4.26 (t, J = 6.2 Hz, 1H, H-5), 4.30 (m, 2H, H-2, H-1'), 5.63 (d, J = 5.4 Hz, 1H, H-1), 7.43 (d, J = 8.4 Hz, 1H, Ar-H), 7.47 (dd, J = 2.1, 8.4 Hz, 1H, Ar-H), 7.73 (d, J = 2.1 Hz, 1H, Ar-H); ^{13}C NMR (126 MHz, CD_3OD): δ = 27.2, 27.5, 27.7, 33.6 (4C, CH_2 -cy), 34.7 (CH-cy), 35.2 (CH_2 -cy), 42.4 (C-2'), 62.3 (C-6), 68.7 (C-4), 69.3 (C-2), 73.4 (C-5), 78.4 (C-1'), 81.5 (C-3), 91.2 (C-1), 131.6, 132.0, 132.6, 134.30, 134.31, 137.1 (6C, C-Ar); HR-MS: m/z : Calcd for $\text{C}_{21}\text{H}_{28}\text{Cl}_2\text{O}_7\text{S}$: 517.0830 $[\text{M}+\text{Na}]^+$, found: 517.0828; HPLC: Purity 99.1%.

Competitive fluorescence polarization experiments. Human Galectins-1, -3, -8N, -8C, -9N, and -9C were expressed and purified as previously described.^{41,52} Fluorescence polarization experiments were performed using the PHERAstar FS plate reader (software version 2.10 R3), and the fluorescence anisotropy of fluorescein tagged probes was measured by excitation at 485 nm and emission at 520 nm. The specific conditions for Galectins-1, -3, -8C, -8N, -9N, and -9C were kept as reported.^{52,53} The synthesized compounds were dissolved in pure DMSO at 20 mM concentration and diluted in PBS to 3-6 different concentrations, and each concentration was tested in duplicate. The highest inhibitor concentrations tested were 1.5 mM. The average values of K_D and SEM were calculated from 4 to 8 duplicate measurements, showing 10-90% inhibition.

5.5 References.

- (1) Yang, R. Y.; Rabinovich, G. A.; Liu, F. T. Galectins: Structure, Function and Therapeutic Potential. *Expert Rev. Mol. Med.* **2008**, *10*, e17. <https://doi.org/10.1017/S1462399408000719>.
- (2) Dings, R. P. M.; Miller, M. C.; Griffin, R. J.; Mayo, K. H. Galectins as Molecular Targets for Therapeutic Intervention. *Int. J. Mol. Sci.* **2018**, *19* (3), 905. <https://doi.org/10.3390/ijms19030905>.
- (3) Lella, S.; Sundblad, V.; Cerliani, J.; Guardia, C.; Estrin, D.; Vasta, G.; Rabinovich, G. When Galectins Recognize Glycans: From Biochemistry to Physiology and Back Again. *Biochemistry* **2011**, *50* (37), 7842–7857. <https://doi.org/10.1021/bi201121m>.
- (4) Johannes, L.; Jacob, R.; Leffler, H. Galectins at a Glance. *J. Cell Sci.* **2018**, *131* (9), jcs208884. <https://doi.org/10.1242/jcs.208884>.
- (5) Vasta, G. R. Galectins as Pattern Recognition Receptors: Structure, Function, and Evolution. In *Current Topics in Innate Immunity II. Advances in Experimental Medicine and Biology*; Springer, New York, NY, 2012.

- (6) Sethi, A.; Sanam, S.; Alvala, M. Non-Carbohydrate Strategies to Inhibit Lectin Proteins with Special Emphasis on Galectins. *Eur. J. Med. Chem.* **2021**, *222* (3), 113561. <https://doi.org/10.1016/j.ejmech.2021.113561>.
- (7) Di Lella, S.; Martí, M. A.; Croci, D. O.; Guardia, C. M.; Díaz-Ricci, J. C.; Rabinovich, G. A.; Caramelo, J. J.; Estrin, D. A. Linking the Structure and Thermal Stability of Beta-Galactoside-Binding Protein Galectin-1 to Ligand Binding and Dimerization Equilibria. *Biochemistry* **2010**, *49* (35), 7652–7658. <https://doi.org/10.1021/bi100356g>.
- (8) Stowell, S. R.; Karmakar, S.; Stowell, C. J.; Dias-Baruffi, M.; McEver, R. P.; Cummings, R. D. Human Galectin-1, -2, and -4 Induce Surface Exposure of Phosphatidylserine in Activated Human Neutrophils but Not in Activated T Cells. *Blood* **2007**, *109* (1), 219–227. <https://doi.org/10.1182/blood-2006-03-007153>.
- (9) Levy, Y.; Auslender, S.; Eisenstein, M.; Vidavski, R. R.; Ronen, D.; Bershadsky, A. D.; Zick, Y. It Depends on the Hinge: A Structure-Functional Analysis of Galectin-8, a Tandem-Repeat Type Lectin. *Glycobiology* **2006**, *16* (6), 463–476. <https://doi.org/10.1093/glycob/cwj097>.
- (10) Ahmad, N.; Gabius, H. J.; André, S.; Kaltner, H.; Sabesan, S.; Roy, R.; Liu, B.; Macaluso, F.; Brewer, C. F. Galectin-3 Precipitates as a Pentamer with Synthetic Multivalent Carbohydrates and Forms Heterogeneous Cross-Linked Complexes. *J. Biol. Chem.* **2004**, *279* (12), 10841–10847. <https://doi.org/10.1074/jbc.M312834200>.
- (11) Di Lella, S.; Sundblad, V.; Cerliani, J. P.; Guardia, C. M.; Estrin, D. A.; Vasta, G. R.; Rabinovich, G. A. When Galectins Recognize Glycans: From Biochemistry to Physiology and Back Again. *Biochemistry* **2011**, *50* (37), 7842–7857. <https://doi.org/10.1021/bi201121m>.
- (12) Leffler, H.; Carlsson, S.; Hedlund, M.; Qian, Y.; Poirier, F. Introduction to Galectins. *Glycoconj. J.* **2002**, *19* (7–9), 433–440. <https://doi.org/10.1023/B:GLYC.0000014072.34840.04>.
- (13) Li, S.; Wandel, M. P.; Li, F.; Liu, Z.; He, C.; Wu, J.; Shi, Y.; Randow, F. Sterical Hindrance Promotes Selectivity of the Autophagy Cargo Receptor NDP52 for the Danger Receptor Galectin-8 in Antibacterial Autophagy. *Sci. Signal.* **2013**, *6* (261), ra9. <https://doi.org/10.1126/scisignal.2003730>.
- (14) Cummings, R. D.; Liu, F. T.; Vasta, G. R. Galectins. In *Essentials of Glycobiology*; Cold Spring Harbor, NY: Cold Spring Harbor Laboratory Press., 2015.
- (15) Adams, L.; Scott, G. K.; Weinberg, C. S. Biphasic Modulation of Cell Growth by Recombinant Human Galectin-1. *Biochim. Biophys. Acta - Mol. Cell Res.* **1996**, *1312* (2), 137–144. [https://doi.org/10.1016/0167-4889\(96\)00031-6](https://doi.org/10.1016/0167-4889(96)00031-6).
- (16) Brinchmann, M. F.; Patel, D. M.; Iversen, M. H. The Role of Galectins as Modulators of Metabolism and Inflammation. *Mediators Inflamm.* **2018**, 9186940. <https://doi.org/10.1155/2018/9186940>.
- (17) Girotti, M. R.; Salatino, M.; Dalotto-Moreno, T.; Rabinovich, G. A. Sweetening the Hallmarks of Cancer: Galectins as Multifunctional Mediators of Tumor Progression. *J. Exp. Med.* **2020**, *217* (2), e20182041. https://doi.org/10.1084/jem_20182041.
- (18) Ayona, D.; Fournier, P. E.; Henrissat, B.; Desnues, B. Utilization of Galectins by Pathogens for

- Infection. *Front. Immunol.* **2020**, *51* (5), 473–484. <https://doi.org/10.3389/fimmu.2020.01877>.
- (19) Jin, Q. Y.; Li, Y. S.; Qiao, X. H.; Yang, J. W.; Guo, X. L. Targeting Galectins in T Cell-Based Immunotherapy within Tumor Microenvironment. *Life Sci.* **2021**, *277*, 119426. <https://doi.org/10.1016/j.lfs.2021.119426>.
- (20) Méndez-Huergo, S. P.; Blidner, A. G.; Rabinovich, G. A. Galectins: Emerging Regulatory Checkpoints Linking Tumor Immunity and Angiogenesis. *Curr. Opin. Immunol.* **2017**, *45*, 8–15. <https://doi.org/10.1016/j.coi.2016.12.003>.
- (21) Gehlken, C.; Suthahar, N.; Meijers, W. C.; de Boer, R. A. Galectin-3 in Heart Failure: An Update of the Last 3 Years. *Heart Fail. Clin.* **2018**, *14* (1), 75–92. <https://doi.org/10.1016/j.hfc.2017.08.009>.
- (22) Bertuzzi, S.; Quintana, J. I.; Ardá, A.; Gimeno, A.; Jiménez-Barbero, J. Targeting Galectins With Glycomimetics. *Front. Chem.* **2020**, *8*, 593. <https://doi.org/10.3389/fchem.2020.00593>.
- (23) Tazhitdinova, R.; Timoshenko, A. V. The Emerging Role of Galectins and O-GlcNAc Homeostasis in Processes of Cellular Differentiation. *Cells* **2020**, *9* (8), 1792. <https://doi.org/10.3390/cells9081792>.
- (24) Zick, Y.; Eisenstein, M.; Goren, R. A.; Hadari, Y. R.; Levy, Y.; Ronen, D. Role of Galectin-8 as a Modulator of Cell Adhesion and Cell Growth. *Glycoconj. J.* **2002**, *19* (7–9), 517–526. <https://doi.org/10.1023/B:GLYC.0000014081.55445.af>.
- (25) Prato, C. A.; Carabelli, J.; Campetella, O.; Tribulatti, M. V. Galectin-8 Enhances T Cell Response by Promotion of Antigen Internalization and Processing. *iScience* **2020**, *23* (7), 101278. <https://doi.org/10.1016/j.isci.2020.101278>.
- (26) Tribulatti, M.; Carabelli, J.; Prato, C.; Campetella, O. Galectin-8 in the Onset of the Immune Response and Inflammation. *Glycobiology* **2020**, *30* (3), 134–142. <https://doi.org/10.1093/glycob/cwz077>.
- (27) Stancic, M.; van Horssen, J.; Thijssen, V. L.; Gabius, H. J.; van der Valk, P.; Hoekstra, D.; Baron, W. Increased Expression of Distinct Galectins in Multiple Sclerosis Lesions. *Neuropathol. Appl. Neurobiol.* **2011**, *37* (6), 654–671. <https://doi.org/10.1111/j.1365-2990.2011.01184.x>.
- (28) Cattaneo, V.; Tribulatti, M. V.; Carabelli, J.; Carestia, A.; Schattner, M.; Campetella, O. Galectin-8 Elicits pro-Inflammatory Activities in the Endothelium. *Glycobiology* **2014**, *24* (10), 966–973. <https://doi.org/10.1093/glycob/cwu060>.
- (29) Hong, M. H.; Lin, W. H.; Weng, I. C.; Hung, Y. W.; Chen, H. L.; Chen, H. Y.; Chen, P.; Lin, C. H.; Yang, W. Y.; Liu, F. T. Intracellular Galectins Control Cellular Responses Commensurate with Cell Surface Carbohydrate Composition. *Glycobiology* **2019**, *30* (1), 49–57. <https://doi.org/10.1093/glycob/cwz075>.
- (30) Kim, B. W.; Hong, S. B.; Kim, J. H.; Kwon, D. H.; Song, H. K. Structural Basis for Recognition of Autophagic Receptor NDP52 by the Sugar Receptor Galectin-8. *Nat. Commun.* **2013**, *4*, 4–11. <https://doi.org/10.1038/ncomms2606>.
- (31) Thurston, T. L. M.; Wandel, M. P.; von Muhlinen, N.; Foeglein, Á.; Randow, F. Galectin 8 Targets Damaged Vesicles for Autophagy to Defend Cells against Bacterial Invasion. *Nature* **2012**, *482* (7385), 414–418. <https://doi.org/10.1038/nature10744>.

- (32) Vinik, Y.; Shatz-Azoulay, H.; Vivanti, A.; Hever, N.; Levy, Y.; Karmona, R.; Brumfeld, V.; Baraghithy, S.; Attar-Lamdar, M.; Boura-Halfon, S.; Bab, I.; Zick, Y. The Mammalian Lectin Galectin-8 Induces RANKL Expression, Osteoclastogenesis, and Bone Mass Reduction in Mice. *Elife* **2015**, *4*, e05914. <https://doi.org/10.7554/eLife.05914>.
- (33) Vinik, Y.; Shatz-Azoulay, H.; Hiram-Bab, S.; Kandel, L.; Gabet, Y.; Rivkin, G.; Zick, Y. Ablation of the Mammalian Lectin Galectin-8 Induces Bone Defects in Mice. *FASEB J.* **2018**, *32* (5), 2366–2380. <https://doi.org/10.1096/fj.201700716R>.
- (34) Chen, W. S.; Cao, Z.; Sugaya, S.; Lopez, M. J.; Sendra, V. G.; Laver, N.; Leffler, H.; Nilsson, U. J.; Fu, J.; Song, J.; Xia, L.; Hamrah, P.; Panjwani, N. Pathological Lymphangiogenesis Is Modulated by Galectin-8-Dependent Crosstalk between Podoplanin and Integrin-Associated VEGFR-3. *Nat. Commun.* **2016**, *7*, 11302. <https://doi.org/10.1038/ncomms11302>.
- (35) Shatz-Azoulay, H.; Vinik, Y.; Isaac, R.; Kohler, U.; Lev, S.; Zick, Y. The Animal Lectin Galectin-8 Promotes Cytokine Expression and Metastatic Tumor Growth in Mice. *Sci. Rep.* **2020**, *10* (1), 7375. <https://doi.org/10.1038/s41598-020-64371-z>.
- (36) Chen, W. S.; Cao, Z.; Sugaya, S.; Lopez, M. J.; Sendra, V. G.; Laver, N.; Leffler, H.; Nilsson, U. J.; Fu, J.; Song, J.; Xia, L.; Hamrah, P.; Panjwani, N. Pathological Lymphangiogenesis Is Modulated by Galectin-8-Dependent Crosstalk between Podoplanin and Integrin-Associated VEGFR-3. *Nat. Commun.* **2016**, *7*, 11302. <https://doi.org/10.1038/ncomms11302>.
- (37) Troncoso, M. F.; Ferragut, F.; Bacigalupo, M. L.; Delgado, V. M. C.; Nugnes, L. G.; Gentilini, L.; Laderach, D.; Wolfenstein-Todel, C.; Compagno, D.; Rabinovich, G. A.; Elola, M. T. Galectin-8: A Matricellular Lectin with Key Roles in Angiogenesis. *Glycobiology* **2014**, *24* (10), 907–914. <https://doi.org/10.1093/glycob/cwu054>.
- (38) Varinská, L.; Fáber, L.; Petrovová, E.; Balážová, L.; Ivančová, E.; Kolář, M.; Gál, P. Galectin-8 Favors VEGF-Induced Angiogenesis: In Vitro Study in Human Umbilical Vein Endothelial Cells and In Vivo Study in Chick Chorioallantoic Membrane. *Anticancer Res.* **2020**, *40* (6), 3191–3201. <https://doi.org/10.21873/anticancerres.14300>.
- (39) Gentilini, L. D.; Jaworski, F. M.; Tiraboschi, C.; Pérez, I. G.; Kotler, M. L.; Chauchereau, A.; Laderach, D. J.; Compagno, D. Stable and High Expression of Galectin-8 Tightly Controls Metastatic Progression of Prostate Cancer. *Oncotarget* **2017**, *8* (27), 44654–44668. <https://doi.org/10.18632/oncotarget.17963>.
- (40) Vinik, Y.; Shatz-Azoulay, H.; Zick, Y. Molecular Mechanisms Underlying the Role of Galectin-8 as a Regulator of Cancer Growth and Metastasis. *Trends Glycosci. Glycotechnol.* **2018**, *30* (172), SE119–SE128. <https://doi.org/10.4052/tigg.1742.1SE>.
- (41) Carlsson, S.; Öberg, C. T.; Carlsson, M. C.; Sundin, A.; Nilsson, U. J.; Smith, D.; Cummings, R. D.; Almkvist, J.; Karlsson, A.; Leffler, H. Affinity of Galectin-8 and Its Carbohydrate Recognition Domains for Ligands in Solution and at the Cell Surface. *Glycobiology* **2007**, *17* (6), 663–676. <https://doi.org/10.1093/glycob/cwm026>.
- (42) Gómez-Redondo, M.; Delgado, S.; Núñez-Franco, R.; Jiménez-Osés, G.; Ardá, A.; Jiménez-Barbero,

- J.; Gimeno, A. The Two Domains of Human Galectin-8 Bind Sialyl-and Fucose-Containing Oligosaccharides in an Independent Manner. A 3D View by Using NMR. *RSC Chem. Biol.* **2021**, *2* (3), 932–941. <https://doi.org/10.1039/d1cb00051a>.
- (43) Hassan, M.; van Klaveren, S.; Håkansson, M.; Diehl, C.; Kovačič, R.; Baussière, F.; Sundin, A. P.; Dernovšek, J.; Walse, B.; Zetterberg, F.; Leffler, H.; Anderluh, M.; Tomašič, T.; Jakopin, Ž.; Nilsson, U. J. Benzimidazole e Galactosides Bind Selectively to the Galectin-8 N- Terminal Domain : Structure-Based Design and Optimisation. *Eur. J. Med. Chem.* **2021**, *223*, 113664. <https://doi.org/10.1016/j.ejmech.2021.113664>.
- (44) Ideo, H.; Matsuzaka, T.; Nonaka, T.; Seko, A.; Yamashita, K. Galectin-8-N-Domain Recognition Mechanism for Sialylated and Sulfated Glycans. *J. Biol. Chem.* **2011**, *286* (13), 11346–11355. <https://doi.org/10.1074/jbc.M110.195925>.
- (45) Ideo, H.; Seko, A.; Ishizuka, I.; Yamashita, K. The N-Terminal Carbohydrate Recognition Domain of Galectin-8 Recognizes Specific Glycosphingolipids with High Affinity. *Glycobiology* **2003**, *13* (10), 713–723. <https://doi.org/10.1093/glycob/cwg094>.
- (46) Patel, B.; Kishor, C.; Houston, T. A.; Shatz-Azoulay, H.; Zick, Y.; Vinik, Y.; Blanchard, H. Rational Design and Synthesis of Methyl-β-D-Galactomalonyl Phenyl Esters as Potent Galectin-8N Antagonists. *J. Med. Chem.* **2020**, *63* (20), 11573–11584. <https://doi.org/10.1021/acs.jmedchem.0c00602>.
- (47) Wu, C.; Yong, C.; Zhong, Q.; Wang, Z.; Nilsson, U. J.; Zhang, Y. Synthesis of Tricyclic Carbohydrate-Benzene Hybrids as Selective Inhibitors of Galectin-1 and Galectin-8 N-Terminal Domains. *RSC Adv.* **2020**, *10* (33), 19636–19642. <https://doi.org/10.1039/d0ra03144e>.
- (48) Bohari, M. H.; Yu, X.; Kishor, C.; Patel, B.; Go, R. M.; Eslampanah Seyedi, H. A.; Vinik, Y.; Grice, I. D.; Zick, Y.; Blanchard, H. Structure-Based Design of a Monosaccharide Ligand Targeting Galectin-8. *ChemMedChem* **2018**, *13* (16), 1664–1672. <https://doi.org/10.1002/cmdc.201800224>.
- (49) Pal, K. B.; Mahanti, M.; Huang, X.; Persson, S.; Sundin, A. P.; Zetterberg, F. R.; Oredsson, S.; Leffler, H.; Nilsson, U. J. Quinolines. Quinoline-Galactose Hybrids Bind Selectively with High Affinity to Galectin-8 N-Terminal Domain. *Org. Biomol. Chem.* **2018**, *16* (34), 6295–6305. <https://doi.org/10.1039/x0xx00000x>.
- (50) Yoshida, H.; Yamashita, S.; Teraoka, M.; Itoh, A.; Nakakita, S.; Nishi, N.; Kamitori, S. X-Ray Structure of a Protease-Resistant Mutant Form of Human Galectin-8 with Two Carbohydrate Recognition Domains. *FEBS J.* **2012**, *279* (20), 3937–3951. <https://doi.org/10.1111/j.1742-4658.2012.08753.x>.
- (51) LigandScout v.4.4 available from Inte:Ligand. <https://www.inteligand.com/ligandscout>.
- (52) Delaine, T.; Collins, P.; MacKinnon, A.; Sharma, G.; Stegmayr, J.; Rajput, V. K.; Mandal, S.; Cumpstey, I.; Larumbe, A.; Salameh, B. A.; Kahl-Knutsson, B.; van Hattum, H.; van Scherpenzeel, M.; Pieters, R. J.; Sethi, T.; Schambye, H.; Oredsson, S.; Leffler, H.; Blanchard, H.; Nilsson, U. J. Galectin-3-Binding Glycomimetics That Strongly Reduce Bleomycin-Induced Lung Fibrosis and

- Modulate Intracellular Glycan Recognition. *ChemBioChem* **2016**, *17* (18), 1759–1770. <https://doi.org/10.1002/cbic.201600285>.
- (53) Pal, K. B.; Mahanti, M.; Leffler, H.; Nilsson, U. J. A Galactoside-Binding Protein Tricked into Binding Unnatural Pyranose Derivatives: 3-Deoxy-3-Methyl-Gulosides Selectively Inhibit Galectin-1. *Int. J. Mol. Sci.* **2019**, *20* (15), 3786. <https://doi.org/10.3390/ijms20153786>.
- (54) Cumpstey, I.; Carlsson, S.; Leffler, H.; Nilsson, U. J. Synthesis of a Phenyl Thio-Beta-D-Galactopyranoside Library from 1,5-Difluoro-2,4-Dinitrobenzene: Discovery of Efficient and Selective Monosaccharide Inhibitors of Galectin-7. *Org. Biomol. Chem.* **2005**, *3* (10), 1922–1932. <https://doi.org/10.1039/b502354h>.
- (55) Andersson, L.; Kenne, L. Synthesis and NMR Studies of Methyl 3-O-[(R)- and (S)-1-Carboxyethyl]- α -D-Gluc-, Galacto- and Manno- Pyranosides. *Carbohydr. Res.* **1998**, *313* (3–4), 157–164. [https://doi.org/10.1016/s0008-6215\(98\)00272-9](https://doi.org/10.1016/s0008-6215(98)00272-9).
- (56) Zetterberg, F.; Peterson, K.; Johnsson, R.; Brimert, T.; Håkansson, M.; Logan, D.; Leffler, H.; Nilsson, U. J. Monosaccharide Derivatives with Low-Nanomolar Lectin Affinity and High Selectivity Based on Combined Fluorine-Amide, Phenyl-Arginine, Sulfur- π , and Halogen Bond Interactions. *ChemMedChem* **2018**, *13* (2), 133–137. <https://doi.org/10.1002/cmdc>.
- (57) Scheidt, F.; Schäfer, M.; Sarie, J.; Daniliuc, C.; Molloy, J.; Gilmour, R. Enantioselective, Catalytic Vicinal Difluorination of Alkenes. *Angew. Chemie - Int. Ed.* **2018**, *57* (50), 16431–16435. <https://doi.org/10.1002/anie.201810328>.
- (58) OEDocking version 3.0.2. OpenEye Scientific Software, Santa Fe, NM. <http://www.eyesopen.com>.
- (59) Bernardi, A.; Potenza, D.; Capelli, A. M.; García-Herrero, A.; Cañada, F. J.; Jiménez-Barbero, J. Second-Generation Mimics of Ganglioside GM1 Oligosaccharide: A Three-Dimensional View of Their Interactions with Bacterial Enterotoxins by NMR and Computational Methods. *Chem. - A Eur. J.* **2002**, *8* (20), 4597–4612. [https://doi.org/10.1002/1521-3765\(20021018\)8:20<4597::AID-CHEM4597>3.0.CO;2-U](https://doi.org/10.1002/1521-3765(20021018)8:20<4597::AID-CHEM4597>3.0.CO;2-U).
- (60) Bernardi, A.; Arosio, D.; Potenza, D.; Sánchez-Medina, I.; Mari, S.; Cañada, F. J.; Jiménez-Barbero, J. Intramolecular Carbohydrate-Aromatic Interaction and Intermolecular van Der Waals Interactions Enhance the Molecular Recognition Ability of GM1 Glycomimetics for Cholera Toxin. *Chem. Eur. J.* **2004**, *10* (18), 4395–4406. <https://doi.org/10.1002/chem.200400084>.
- (61) Phillips, J. C.; Braun, R.; Wang, W.; Gumbart, J.; Tajkhorshid, E.; Villa, E.; Chipot, C.; Skeel, R. D.; Kalé, L.; Schulten, K. Scalable Molecular Dynamics with NAMD. *J. Comput. Chem.* **2005**, *26* (16), 1781–1802. <https://doi.org/10.1002/jcc.20289>.
- (62) Mackerell Jr, A.; Feig, M.; Brooks, C. Extending the Treatment of Backbone Energetics in Protein Force Fields: Limitations of Gas-Phase Quantum Mechanics in Reproducing Protein Conformational Distributions in Molecular Dynamics Simulations. *J. Comput. Chem.* **2004**, *25* (11), 1400–1415. <https://doi.org/10.1002/jcc.20065>.
- (63) MacKerell, A. D.; Bashford, D.; Bellott, M.; Dunbrack, R. L.; Evanseck, J. D.; Field, M. J.; Fischer,

- S.; Gao, J.; Guo, H.; Ha, S.; Joseph-McCarthy, D.; Kuchnir, L.; Kuczera, K.; Lau, F. T. K.; Mattos, C.; Michnick, S.; Ngo, T.; Nguyen, D. T.; Prodhom, B.; Reiher, W. E.; Roux, B.; Schlenkrich, M.; Smith, J. C.; Stote, R.; Straub, J.; Watanabe, M.; Wiórkiewicz-Kuczera, J.; Yin, D.; Karplus, M. All-Atom Empirical Potential for Molecular Modeling and Dynamics Studies of Proteins. *J. Phys. Chem. B* **1998**, *102* (18), 3586–3616. <https://doi.org/10.1021/jp973084fang>.
- (64) Vanommeslaeghe, K.; Hatcher, E.; Acharya, C.; Kundu, S.; Zhong, S.; Shim, J.; Darian, E.; Guvench, O.; Lopes, P.; Vorobyov, I.; MacKerell Jr, A. D. CHARMM General Force Field: A Force Field for Drug-like Molecules Compatible with the CHARMM All-Atom Additive Biological Force Fields. *J. Comput. Chem.* **2010**, *31* (4), 671–690. <https://doi.org/10.1002/jcc.21367>.
- (65) Vanommeslaeghe, K.; Raman, E.; MacKerell, A. J. Automation of the CHARMM General Force Field (CGenFF) II: Assignment of Bonded Parameters and Partial Atomic Charges. *J. Chem. Inf. Model.* **2012**, *52* (12), 3155–3168. <https://doi.org/10.1021/ci3003649>.
- (66) Vanommeslaeghe, K.; MacKerell Jr., A. J. Automation of the CHARMM General Force Field (CGenFF) I: Bond Perception and Atom Typing. *J. Chem. Inf. Model.* **2012**, *52* (12), 3144–3154. <https://doi.org/10.1021/ci300363c>.
- (67) Humphrey, W.; Dalke, A.; Schulten, K. VMD: Visual Molecular Dynamics. *J. Mol. Graph.* **1996**, *14* (1), 33–38, 27–28. [https://doi.org/10.1016/0263-7855\(96\)00018-5](https://doi.org/10.1016/0263-7855(96)00018-5).
- (68) Essmann, U.; Perera, L.; Berkowitz, M. L.; Darden, T.; Lee, H.; Pedersen, L. G. A Smooth Particle Mesh Ewald Method. *J. Chem. Phys.* **1995**, *103*, 8577–8593. <https://doi.org/10.1063/1.470117>.
- (69) Ryckaert, J.; Ciccotti, G.; Berendsen, H. Numerical Integration of the Cartesian Equations of Motion of a System with Constraints: Molecular Dynamics of n-Alkanes. *J. Comput. Phys.* **1977**, *23*, 327–341. [https://doi.org/10.1016/0021-9991\(77\)90098-5](https://doi.org/10.1016/0021-9991(77)90098-5).
- (70) Wolber, G.; Langer, T. LigandScout: 3-D Pharmacophores Derived from Protein-Bound Ligands and Their Use as Virtual Screening Filters. *J. Chem. Inf. Model.* **2005**, *45* (1), 160–169. <https://doi.org/10.1021/ci049885e>.

6. Discussion of the hypotheses

As previously mentioned, the work of this thesis has been condensed in six hypotheses.

Hypothesis 1. Low molecular weight and monovalent glycomimetic ligands with high affinity for Siglec-8 can be designed and synthesized by replacing galactose in 6-sulfo-Sia-Gal with a sulfo-substituted cyclohexane or aromatic ring.

Hypothesis confirmed (Chapter 2). The work addressing this hypothesis has been published in *ChemMedChem* (Appendix, p. 199).

The work related to this hypothesis has been described in Chapter 2. A deoxygenation strategy was followed by successively removing the polar groups on the galactose moiety to investigate the significance of the substituents on the ring. The compounds were then tested against Siglec-8 using MST and ITC. The most potent compound identified was the one bearing a hydroxymethyl-cyclohexane, with the sulfate held in the same position as in the replaced galactose: compound **34** showed a 6-fold higher affinity compared to the minimal binding epitope **2**, mainly due to the reduced desolvation cost due to the increased lipophilicity. Unexpectedly, the aromatic derivatives did not show affinity at the measured concentration for Siglec-8. We speculate that the directionality of the salt bridge formed by the sulfate is disturbed. In conclusion, by replacing the galactose moiety with a sulfo-substituted hydroxymethyl-cyclohexane, we have obtained a new optimal starting point for the development of high affinity ligands for Siglec-8.

Hypothesis 2. The sialic acid moiety is not essential for the binding to Siglec-8.

Hypothesis confirmed (Chapter 2).

In a previous unpublished work in B. Ernst's group, compound **39**, containing a 6-sulfo-galactose with a lactic acid derivative in position 3, showed good affinity for Siglec-8 (IC_{50} 249 μ M) in a competitive binding assay. Since the obtained affinity value was not reliable, we decided to repeat the synthesis along with the evaluation of a small library of similar compounds. The synthesized compounds were then tested against Siglec-8 using MST. Unfortunately, the affinity data of the reference compound **39** could not be confirmed but, on the other hand, controversial results were obtained for compound **53**, bearing a cyclohexyl ring on the side chain of the lactic acid. By MST, we measured a K_D of 265 μ M, but we also observed interactions with the dye of the protein. To rule out possible interference, we decided to test it using ITC and nanoDSF but questionable results were

also obtained with these assays. We think that the compound probably interacts with Siglec-8, but with different site(s) of the protein, therefore confirming the hypothesis that the sialic acid is not essential for the binding. ^1H - ^{15}N HSQC NMR analysis could probably be useful in the future to determine and definitely confirm the possibility of binding.

Hypothesis 3. Precise and reliable insights into the binding mode of our high affinity ligands can be provided by using homology modelling of Siglec-8.

Hypothesis not confirmed (Chapter 2).

Currently, only the NMR solution structure of the Siglec-8 lectin domain together with its preferred natural ligand 6'-sulfo-sLe^x is available. Since this model does not fit the binding mode of our most potent ligand **38**, with a naphthyl sulfonamide substituent in position 9 of the sialic acid, we assumed that a homology model of Siglec-8 could be useful for this purpose and for potential virtual screening. We created a homology model for Siglec-8 based on the Siglec-7 crystal structure since the proteins share 71% sequence similarity. In this model, the Arg46 loop region has a very different conformation, allowing a very good accommodation of the sulfate in a small positively charged pocket, while the naphthalene moiety binds to a second aromatic cluster near the loop region. This region is not accessible in the NMR structure because it is blocked by the N-terminus. Unfortunately, when we aligned the two proteins, we saw that much information was missing from the N-terminus of Siglec-7. Consequently, our model lacks the N-terminus, which should be instead included in a future work. In fact, it is important to determine its position because, being quite close to the binding site, it could affect the correct binding.

Hypothesis 4. New fragments and virtual hit molecules that fit into the binding pocket of Siglec-8 can be predicted and their binding affinity can be scored by using fragment-based and structure-based virtual screening.

Hypothesis not confirmed (Chapter 3).

Using the Siglec-8 NMR solution structure, we performed two types of virtual screening. First, we combined several commercially available libraries and docked them to Siglec-8, using the two major arginine residues (Arg109 and Arg56) as constraints. We evaluated the results checking the final scores and the relative position to the native ligand. We then selected 6 commercially available compounds, among which none contained a sugar moiety. They were screened against Siglec-8 by MST but, unfortunately, none of them showed any affinity in the assayed concentration (50 mM).

The second screening was performed to explore an empty pocket close to the position 5 of the sialic acid of the lead compound **34**. We virtually combined different commercially available fragments with position 5 of our ligand through different type of linkers using the KNIME workflow. Then, we docked the obtained molecules to Siglec-8 and we evaluated their poses based on final scores and relative position to the native ligand. The promising molecules, where fragments were attached via amine or triazole linkers, were synthesized and tested, but none of them showed significant affinity in the assayed concentration (15 μ M). We assume that the absence of an amide in position 5 could be detrimental for the binding because it could be involved in an intramolecular H-bond with the hydroxyl in position 7 of the sialic acid, which may preorganize the molecule. In fact, the introduction of substituents via amide linkers led to active compounds. In particular, the methoxypropionamide derivative **99** showed almost 2-fold affinity improvement compared to lead compound **34**.

Hypothesis 5. Siglec-8 ligands are stable to hydrolysis by neuraminidase-2.

Hypothesis confirmed (Chapter 4).

Pharmacokinetic studies are an important step in drug development and they are usually underestimated in the early stages. Since our ligands contain sialic acid, they may be subject to hydrolysis by neuraminidases *in vivo*. Human neuraminidases (hNEU) are 4 types of enzymes expressed both intracellularly and in the plasma membrane. They are glycosyl hydrolases that cleave the glycosidic bond of sialosides. Therefore, we decided to test the stability of our most interesting Siglec-8 ligands against hNeu2. We performed an enzymatic assay and developed an LCMS method to analyze and quantify the possible hydrolysis products. Our results show that glycomimetic ligands **34** and **38** were completely stable to hydrolysis, while the more natural 6-sulfo-Sia-Gal **2** was partially hydrolyzed (30%). 4MU-NANA, a well-known NEU-substrate, has been used as a positive control. However, considering that it is a very labile molecule, the use of a second positive control will be considered in the future to definitely confirm our findings.

Hypothesis 6. High affinity and selective ligands towards Galectin-8 can be obtained by introducing modifications in position 1 and 3 of the 3-*O*-[1-carboxyethyl]- β -D-galactopyranoside.

Hypothesis confirmed (Chapter 5). The work addressing this hypothesis has been published in *ChemMedChem* (Appendix, p. 214).

Galectin-8 has gained attention as a potential new pharmacological target for the treatment of various diseases such as cancer, inflammation and diseases associated with bone mass reduction. To this end,

new molecular probes are needed to better understand its role and functions. In this project, we tried to improve the affinity and selectivity of a recently published Galectin-8 ligand, 3-*O*-[1-carboxyethyl]- β -D-galactopyranoside, by introducing modifications at positions 1 and 3 of galactose. Affinity data, measured by fluorescence polarization, show that the most potent compound reached a K_D of 12 μ M. Moreover, reasonable selectivity towards other galectins was achieved, making the highlighted compound a promising starting point for the development of new selective and potent ligands for Galectin-8 as molecular probes to study the role of the protein in cell lines and *in vivo*.

7. Summary and outlook

Siglec-8 is an immunoreceptor exclusively expressed on eosinophils and mast cells. Upon ligation with antibodies or glycopolymers, it initiates an intracellular cascade that leads to apoptosis of the eosinophils and inhibition of degranulation of mast cells. Therefore, it is a new interesting pharmacological target for the treatment of diseases associated with these cells.

The main purpose of this thesis was to improve the affinity and the drug-like properties of the known Siglec-8 ligand, the sulfated tetrasaccharide 6'-sulfo-sLe^x. To achieve these goals, a common strategy in the carbohydrate field is the use of glycomimetics, more drug-like compounds which mimic the structure and the function of the natural sugars.

Applying some of the more common, classical medicinal chemistry approaches, we first identified the minimal binding epitope, the disaccharide 6-sulfo-Sia-Gal (**2**), which showed an only 2-fold lower affinity than the parent tetrasaccharide, but a reduced size, polarity, and by far easier synthetic accessibility (Chapter 2). Then, following a deoxygenation strategy replacing the galactose with a sulfo-substituted hydroxymethyl-cyclohexane, we obtained the new lead compound **34** which completely restored the affinity of the original tetrasaccharide while having a significantly simplified and more drug-like structure. Finally, the additional introduction of a naphthyl sulfonamide substituent in position 9 of the sialic acid, led to the identification of **38**, the most potent monovalent Siglec-8 ligand known to date with a 15 μ M affinity.

To further explore the chemical space around the lead compound **34**, we also performed a virtual screening approach to identify suitable fragments for the binding cavity close to position 5 of the sialic acid (Chapter 3). The fragments were virtually combined with the core structure of the lead compound and docked into the known Siglec-8 NMR solution structure. Docking poses were mainly evaluated by scoring functions and relative position to the native ligand. The most promising candidates, where fragments were attached via amine or triazole linkers, were synthesized and tested. However, none of them showed any affinity to the target protein. We assumed that the absence of an amide in position 5 of the sialic acid could be detrimental for binding. In fact, an intramolecular hydrogen bond between the carbonyl of the amide group in position 5 and the hydroxyl in position 7 of the sialic acid can stabilize a sort of pre-organization that would not be possible otherwise. These observations confirm that visual inspection of binding modes is crucial in the decision-making process, considering the inaccuracies of molecular docking and its scoring functions.

As a matter of fact, modifications introduced via amide linkers in the same position by rational design to adapt the ligands in the binding cavity, were more successful. In particular, the introduction of a methoxypropionamide in compound **99** showed an almost 2-fold affinity improvement compared to

the parent compound **34**, indicating that modifications in this position indeed are beneficial to improve binding. A future combination of the methoxypropionamide in position 5 with the favorable naphthyl-sulfonamide in position 9 should lead to a high-affinity ligand for Siglec-8.

Our results confirm how glycomimetics can enhance the affinity of the parent natural ligands and, at the same time, improve the drug-like properties. Thermodynamic analysis reveals how many factors could influence the binding besides gaining new interactions in the binding sites. For example, in our case, we obtained a more active compound by just decreasing its polarity, which only causes a minor desolvation penalty.

Considering the improved activity, the most active ligands presented may also be used to obtain a Siglec-8 crystal structure more easily. As we saw, the NMR solution structure does not accommodate our most active ligand and a homology model based on Siglec-7 had its limitations since the N-terminus, close to the binding site, could not be modeled. A resolved crystal structure definitely will contribute to better understand the binding mode of our ligands and, consequently, to allow for more reliable and accurate virtual predictions.

Our compounds not only represent important starting points for the development of potential drugs, but they may also serve as molecular probes to further study the function of Siglec-8. It would be very interesting to see whether monovalent high-affinity ligands could be sufficient to determine a response, or if a multimeric presentation is necessary. In fact, it's not clear yet if protein clustering is essential to initiate a response. Preliminary results from ongoing studies showed that the glycomimetic lead compound **34**, presented on a multimeric form on a polymer, was able to bind Siglec-8 expressed on Jurkat NFAT (Luc2) cells and to trigger a response, while the monovalent sulfonamide **38**, although with higher affinity, only bound weakly. Further studies on eosinophils or mast cells naturally expressing Siglec-8 will give more insights into the mechanism of activation of Siglec-8 and will guide future drug optimization.

Considering the positive results obtained with glycomimetics and the advantages that a non-carbohydrate structure would present, two more strategies were attempted. In the first case, we performed a second virtual screening for the identification of potential new hits with no carbohydrate moieties (Chapter 3). Promising compounds, all commercially available and able to virtually interact with the most important arginine residues in the binding site, were screened with the MST assay. Unfortunately, none of them showed any affinity to Siglec-8, suggesting that the presence of sugar moieties or at least mimics thereof are necessary for binding.

In the second case, as part of the successful deoxygenation strategy and on the basis of previous unpublished positive results, we synthesized and tested a small library of compounds where the sialic acid has been replaced by lactic acid derivatives (Chapter 2). If active, these molecules would be the

first example of Siglec-binding compounds that do not contain sialic acid. However, when tested with MST, we were not able to confirm the activity of the reference compound **39**, which has shown a good affinity in a previous competitive binding assay. However, one of our derivatives (**53**) showed controversial results, both in ITC and nanoDSF. From our observations, we assume that the compound is interacting with Siglec-8 but most probably in a different binding site. Further studies on the sialic acid-free ligands, such as ^1H - ^{15}N HSQC NMR, might reveal additional binding sites of the protein that could be used for allosteric modulation.

Interestingly, the structure of these ligands was very similar to a recently published Galectin-8 ligand, the 3-*O*-[1-carboxyethyl]- β -D-galactopyranoside, a galactose bearing a lactic acid in position 3. Galectin-8 is a new potential pharmacological target for the treatment of various diseases, including cancer, inflammation, and disorders associated with bone mass reduction. Therefore, we decided to test the corresponding non-sulfated derivatives of these compounds to Galectin-8 and to further improve their affinity by introducing modifications at position 1 of galactose (Chapter 5). With compound **121** we have obtained one of the most potent and selective Galectin-8 ligands known to date, with reasonable selectivity towards other galectins, showing another successful application of glycomimetics. Our results represent an optimal starting point for the development of high-affinity and selective ligands for Galectin-8, paving the way for new perspectives to combat diseases associated with this protein.

Finally, pharmacokinetic properties are an important factor to be considered during drug development. Related studies in the early stages can guide the optimization process and prevent failures. For this reason, we decided to test the stability of our most important Siglec-8 ligands towards neuraminidases (NEUs), human enzymes able to hydrolyze terminal sialic acids (Chapter 4). As proof of concept, we used NEU2 due to its easy availability, even if NEU3 would be more suitable considering its expression on the cell surface. We developed an LCMS method to follow the potential hydrolysis, using NANA, a known NEU2 substrate, as a positive control. The results indicated that our glycomimetic ligands have higher stability towards hydrolysis compared to more natural compounds. This represents an incredible advantage, since the glycomimetic modification introduced not only improved the affinity but also conferred higher pharmacokinetic stability. However, considering that NANA is quite labile, the use of another positive control should be considered to definitively confirm our results. The LCMS method has been validated and can be easily be used for other compounds and more appropriate enzymes, such as NEU3. The evaluation and improvement of other pharmacokinetic properties will definitely be performed in future studies, aimed at the development of potential therapeutic drugs for the treatment of eosinophil and mast-cell related disorders.

8. Appendix

Kroezen, B. S.; Conti, G.; Girardi, B.; Cramer, J.; Jiang, X.; Rabbani, S.; Müller, J.; Kokot, M.; Luisoni, E.; Ricklin, D.; Schwardt, O.; Ernst, E. A Potent Mimetic of the Siglec-8 Ligand 6'-Sulfo-Sialyl Lewis^x, *ChemMedChem* **2020**, *15* (18), 1706-1719.

© 2020 Wiley-VCH GmbH



A Potent Mimetic of the Siglec-8 Ligand 6'-Sulfo-Sialyl Lewis^x

Blijke S. Kroezen,^[a] Gabriele Conti,^[a] Benedetta Girardi,^[a] Jonathan Cramer,^[a] Xiaohua Jiang,^[a] Said Rabbani,^[a] Jennifer Müller,^[a] Maja Kokot,^[a] Enrico Luisoni,^[a] Daniel Ricklin,^[a] Oliver Schwardt,^[a] and Beat Ernst^{*[a]}

Siglecs are members of the immunoglobulin gene family containing sialic acid binding N-terminal domains. Among them, Siglec-8 is expressed on various cell types of the immune system such as eosinophils, mast cells and weakly on basophils. Cross-linking of Siglec-8 with monoclonal antibodies triggers apoptosis in eosinophils and inhibits degranulation of mast cells, making Siglec-8 a promising target for the treatment of eosinophil- and mast cell-associated diseases such as asthma. The tetrasaccharide 6'-sulfo-sialyl Lewis^x has been identified as a

specific Siglec-8 ligand in glycan array screening. Here, we describe an extended study enlightening the pharmacophores of 6'-sulfo-sialyl Lewis^x and the successful development of a high-affinity mimetic. Retaining the neuraminic acid core, the introduction of a carbocyclic mimetic of the Gal moiety and a sulfonamide substituent in the 9-position gave a 20-fold improved binding affinity. Finally, the residence time, which usually is the Achilles tendon of carbohydrate/lectin interactions, could be improved.

Introduction

Siglecs (sialic acid-binding immunoglobulin-type lectins) are cell surface proteins representing a subset of the I-type lectins located primarily on the surface of immune cells. They exhibit a sialic acid binding N-terminal domain, one or more C2-set immunoglobulin domains and a cytoplasmic tail.^[1–3] The cytoplasmic tail of most siglecs contains an immunoreceptor tyrosine-based inhibitory motif (ITIM), which participates in immunosuppressive cell signaling. Thus, ligand-binding induces phosphorylation of the tyrosine motif by an Src family kinase, resulting in the recruitment of the SH2 domain-containing phosphatases SH1, SH2 or SHIP-1.^[4] These phosphatases inhibit cellular processes through inactivation of essential kinases. Therefore, siglecs are inhibitory receptors, which can modulate crucial immune responses.^[5,6] In their resting state, most siglecs are engaged in *cis*-interactions with sialylated glycans expressed on the surface of the same cell.^[7] As a result, siglecs are essentially masked and can only interact with *trans*-ligands that display sufficient affinity or avidity to outcompete the *cis*-interactions.^[8]

Siglec-8 is a member of the CD33-related siglec family and is predominantly expressed on the cell-surface of eosinophils and mast cells and weakly on basophils.^[9,10] These cell types play a crucial role in the pathophysiology of asthma, a chronic

inflammatory disease characterized by a massive infiltration of eosinophils into the airways followed by degranulation of mast cells and the release of bronchoconstrictors.^[11,12] When Siglec-8 was cross-linked with antibodies, apoptosis of eosinophils^[13] and inhibition of the release of mediators from mast cells was observed.^[14] A promising alternative to target Siglec-8 with antibodies involves the multivalent display of siglec ligands on polymers and nanoparticles.^[15] Thus, it was shown that apoptosis can be initiated by treating eosinophils with a synthetic polyvalent Siglec-8 ligand^[16] and immunohistochemical analyses exhibited an up-regulation of Siglec-8 ligands in inflamed compared to healthy tissue.^[17] In addition, isolated eosinophils from the airways of allergen-challenged patients showed elevated susceptibility to Siglec-8-mediated apoptosis.^[18] Finally, variants in the Siglec-8 gene were associated with an increased susceptibility for asthma.^[19] In summary, Siglec-8 has been identified as a therapeutic target for the treatment of eosinophil and mast cell disorders.^[20–24]

Natural sialylated glycans generally exhibit only low monovalent affinities (0.5 to 3 mM), which, however, can be substantially improved by a multivalent presentation.^[25,26] The development of potent monovalent siglec ligands started from natural glycan ligands and successfully yielded high-affinity ligands for numerous siglecs: thus, high-affinity ligands for Siglec-1,^[27] Siglec-2,^[8,28–30] Siglec-4,^[31,32] Siglec-7^[33] and Siglec-8^[34] have been reported. The trisaccharide Neu5Ac α 2-3(6-*O*-sulfo)Gal β 1-4GlcNAc and the tetrasaccharide Neu5Ac α 2-3(6-*O*-sulfo)Gal β 1-4[Fuc α 1-3]GlcNAc [6'-sulfo-sLe^x (**1a**)] were identified in a glycan array screening as Siglec-8 ligands (Figure 1A).^[35–37] In this work, we describe the development of high-affinity Siglec-8 mimetics based on 6'-sulfo-sLe^x (**1a**).

[a] Dr. B. S. Kroezen, G. Conti, B. Girardi, Dr. J. Cramer, Dr. X. Jiang, Dr. S. Rabbani, J. Müller, M. Kokot, E. Luisoni, Prof. D. Ricklin, Dr. O. Schwardt, Prof. B. Ernst
 Molecular Pharmacy Group
 Department of Pharmaceutical Sciences
 University of Basel
 Klingelbergstrasse 50
 4056 Basel (Switzerland)
 E-mail: beat.ernst@unibas.ch

Supporting information for this article is available on the WWW under <https://doi.org/10.1002/cmdc.202000417>

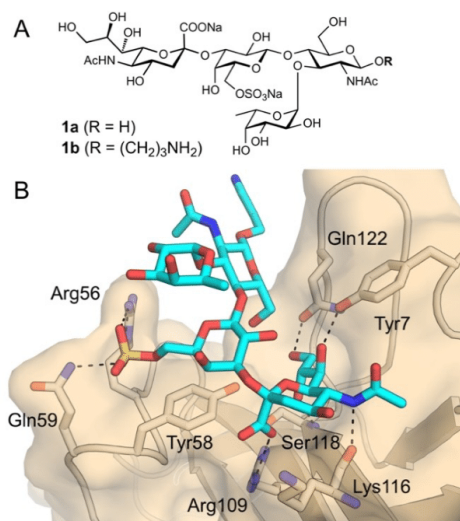


Figure 1. (A) 6'-sulfo-sLe^x (**1a**) and 3-aminopropyl 6'-sulfo-sLe^x (**1b**); (B) Binding mode of 3-aminopropyl 6'-sulfo-sLe^x (**1b**) in the carbohydrate-recognition domain (CRD) of Siglec-8 (PDB ID: 2N7B).^[38] The figure was generated using the software PyMOL.^[39] Color code: N: blue, O: red, S: yellow, protein backbone: beige, ligand C: light blue. Hydrogen bonds are depicted as dashed lines.

Results and Discussion

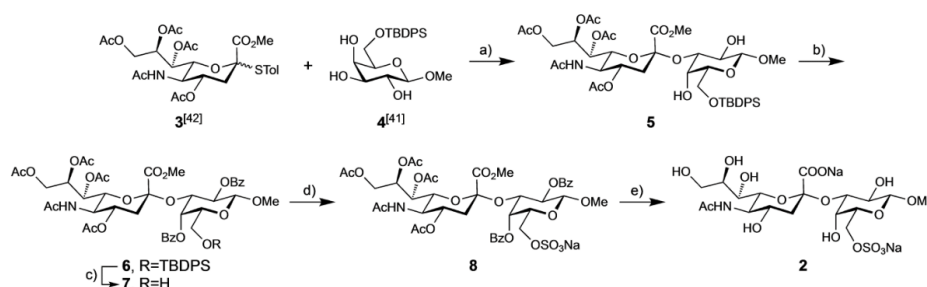
We recently published the NMR solution structures of the Siglec-8 lectin domain (PDB code: 2N7A) and its complex with 3-aminopropyl 6'-sulfo-sLe^x (**1b**) (PDB code: 2N7B).^[38] Using ¹H-¹⁵N HSQC titration and NOE experiments, both the affinity (295 μM), and the binding mode of Siglec-8 with tetrasaccharide **1b** (Figure 1B) have been determined.

Arg109, which is conserved in most siglecs,^[38] forms an essential salt bridge with the carboxylate of Neu5Ac. Moreover, the sulfate group in the 6'-position of the Gal moiety is engaged in another salt bridge with Arg56 and Gln59. This interaction proved to be crucial, as the binding affinity was drastically

reduced when the sulfate group in 3-aminopropyl 6'-sulfo-sLe^x (**1b**) was removed (28-fold loss of affinity) or moved to the D-GlcNAc moiety (9-fold loss in affinity).^[38] Essential hydrogen bonds are formed by the three hydroxyls of the glycerol side chain with Tyr7, Ser118 and Gln122, as well as by the *N*-acetyl group with the backbone of Lys116. Furthermore, various hydrophobic interactions, including *van der Waals* and sigma- π interactions with Tyr58 contribute to the binding affinity of tetrasaccharide **1b**. Surprisingly, the L-Fuc and D-GlcNAc moieties do not engage any interactions with the protein surface. Glycan arrays additionally showed that the fucose moiety does not significantly contribute to affinity.^[40] We therefore assumed that the disaccharide Neu5Ac α 2-3(6-*O*-sulfo)Gal (**2**, Scheme 1) represents the minimal binding epitope.

Synthesis and affinity of the minimal binding epitope. Sialylation of the galactose acceptor **4**^[41] with sialic acid donor **3**^[42] yielded disaccharide **5**. The highest yield and the best α -selectivity were obtained using NIS/TFOH as promoter, and MeCN/DCM as solvent. To avoid acetyl migration, the 2- and 4-OH of the Gal moiety were benzoylated (\rightarrow **6**) before the silyl protection was selectively cleaved using HF-pyridine to afford disaccharide **7**. Next, the sulfate group was introduced using an excess of SO₃pyr in DMF (\rightarrow **8**). Finally, acylate deprotection under Zemplén conditions and hydrolysis of the methyl ester with aq. NaOH yielded the test compound Neu5Ac α 2-3(6-*O*-sulfo)Gal (**2**, Scheme 1).

3-Aminopropyl 6'-sulfo-sLe^x (**1b**) has an affinity of 295 μM \pm 26 μM (*K_D* by NMR) or 303 μM \pm 11 μM (*IC*₅₀ in a competitive binding assay).^[38] Surprisingly, the *IC*₅₀ of the disaccharide Neu5Ac α 2-3(6-*O*-sulfo)Gal (**2**) is only by a factor 2 lower (733 μM, Table 1) than the *IC*₅₀ of lead tetrasaccharide **1b**. This result was quite encouraging, as the complexity of the epitope and the number of synthetic steps were significantly reduced, whilst the affinity was only modestly affected. For the determination of the *IC*₅₀'s, we applied a competitive binding assay^[43] with Siglec-8-CRD and streptavidin-peroxidase coupled to the biotinylated polyacrylamide glycopolymer 6'-sulfo-sLe^x-PAA as competitor. After incubation of the protein and the glycopolymer with a serial dilution of the tested ligand, the colorimetric reaction with the horseradish peroxidase substrate ABTS was measured to determine *IC*₅₀ values. We also applied



Scheme 1. a) NIS, TFOH, MeCN/DCM, -40°C , 16 h (34%); b) Bz₂O, DMAP, pyridine, rt, 16 h (92%); c) HFpyr, pyridine, rt, 4 h (93%); d) SO₃pyr, DMF, 0 $^{\circ}\text{C}$ to rt, 4 h (93%); e) i. MeONa/MeOH, rt to 50 $^{\circ}\text{C}$, 24 h; ii. NaOH (aq), rt, 1 h (81% over two steps).

Table 1. Binding affinity of 3-aminopropyl 6'-sulfo-sLe^x (**1b**)^[38] and derivatives thereof. IC₅₀ values were determined in a competitive binding assay.^[43] For the synthesis of monosaccharide **9** and disaccharides **11–13** with modified glycerol side chain see Supporting Information.

Compd.	Structure	IC ₅₀ [μM]	rIC ₅₀
1b ^[38]		303 ± 11	1
2		733 ± 163 ^[a]	2.2
9		n.a. ^[b]	–
10 ^[44]		n.a.	–
11		n.a.	–
12		n.a.	–
13		n.a.	–

[a] Average value over six measurements. [b] n.a.: not active up to 10 mM.

microscale thermophoresis (MST) for the determination of the K_D of binding.

The individual fragments, the galactose derivative **9** and the neuraminic acid derivative **10**,^[44] as well as the disaccharides **11–13** with modified glycerol side chains (for the synthesis see Supporting Information) did not show any affinity. The hydrogen bond network, the glycerol side chain is involved in (Figure 1B), obviously plays an important role in the binding process. Moreover, a ReLiBase^[45] search shows that the 8-OH stabilizes the bioactive conformation of sialic acid in the bound conformation via an intramolecular hydrogen bond with the carboxylate. Overall, these results confirmed that the sulfated disaccharide **2** indeed represents the minimal carbohydrate epitope necessary for Siglec-8 binding.

Bioisosteres of the carboxylate and the sulfate group. To further improve the PK/PD profile of disaccharide **2**, the possibility of bioisosteric replacements of the carboxylate and the sulfate were explored, not only to improve affinity, but also to enhance selectivity and alter physical properties.^[46,47] The IC₅₀ measurements for the derivatives **14–24** (for their synthesis see Supporting Information) were conducted in the competitive binding assay (Table 2). For the reference compound **2**, an additional K_D value of 561 μM was obtained in the microscale thermophoresis (MST) assay, which is in good agreement with the competitive binding assay (733 μM) (entry 1). When the sulfate was modified while the carboxylate substituent was maintained (entries 2–8), reduced affinity was observed in four cases (entries 2, 3, 4 & 8) while all other modifications resulted

Table 2. Binding affinities for derivatives of lead structure **2**, bearing replacements for the sulfate and carboxylic acid functional groups. IC₅₀ values were determined in a competitive binding assay,^[43] while dissociation constants (K_D) were measured with MST. For the synthesis of the disaccharides **14–24** see Supporting Information.

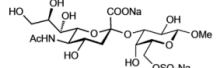
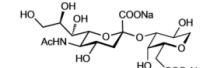
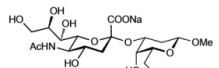
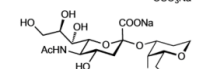
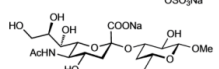
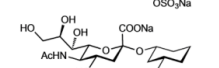
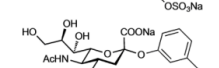
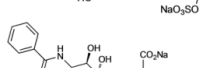
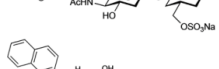
Entry	Compd.	R ¹	R ²	IC ₅₀ [μM]	K_D [μM]
Reference compound					
1	2	COONa	CH ₂ OSO ₃ Na	733 ^[a]	561
Sulfate bioisosteres					
2	14	COONa	COONa	1026	n.d. ^[b]
3	15	COONa	CH ₂ CH ₂ COONa	2199	n.d.
4	16	COONa	CH ₂ NH ₂	1393	n.d.
5	17	COONa	CH ₂ CH ₂ Ph	n.a. ^[c]	n.d.
6	18	COONa	CH ₂ N ₃	n.a.	n.d.
7	19	COONa	CH ₂ NHAc	n.a.	n.d.
8	20	COONa	CH ₂ OPO ₃ Na ₂	n.d.	2830
Carboxylic acid bioisosteres					
9	21	CONH ₂	CH ₂ OSO ₃ Na	1613	1011
10	22	CONHMe	CH ₂ OSO ₃ Na	n.d.	2850
11	23	CONHOH	CH ₂ OSO ₃ Na	n.d.	n.a.
12	24		CH ₂ OSO ₃ Na	n.d.	2836

[a] Average value over six measurements. [b] n.d.: not determined. [c] n.a.: not active up to 10 mM.

in inactive compounds. The carboxylate turned out to be the best replacement of the sulfate leading only to a moderate loss of affinity (1026 μM vs. 733 μM). Replacement of the carboxylate (entries 9–12) led to inactive or only moderately active ligands.

Modification of the galactose moiety. According to the structure of the complex of 3-aminopropyl 6'-sulfo-sLe^x (**1b**)/Siglec-8 obtained by NMR (Figure 1B) the 2- and the 4-OH of the galactose moiety do not significantly contribute to binding. In addition, the anomeric substituent points away from the protein surface and, when substituted with an OMe aglycone, cannot establish a contact with the protein surface. Therefore, a set of derivatives **25–30** where these three substituents were consecutively removed, was synthesized and evaluated regarding their binding to Siglec-8 with the competitive binding assay (Table 3). The syntheses of the test compounds **25–28** & **30** are available in the Supporting Information. For the enantioselective synthesis of disaccharide mimetic **29**, a racemic mixture of *cis* and *trans* isomers of ethyl 3-hydroxycyclohexane-1-carboxylate (**31**) turned out to be a feasible starting material (Scheme 2). The racemic *cis*-isomer **31** was obtained by chromatographic separation of the commercial *cis/trans* mixture. The enzymatic separation of the enantiomeric mixture *rac-cis*-**31** using the lipase Novozyme 435 and vinyl butyrate yielded the butyrate **32** in 35% yield.^[48,49] To determine its absolute configuration, ester **32** was hydrolyzed to acid **33**. Its optical rotation was in agreement with a literature value of the desired (1*S*,3*R*)-(+)-3-hydroxycyclohexane-1-carboxylate (**33**, $[\alpha]_D^{20} +10.3$ vs. $+10.7$ ^[50]). The synthesis of acceptor **35** was completed by reduction with DIBAL-*H* (**→34**), followed by the regioselective protection of the primary hydroxyl group with

Table 3. Biological evaluation of deoxygenated derivatives of lead structure **2**. IC₅₀ values were determined in a competitive binding assay,^[43] while dissociation constants (K_D) were measured with ITC. For the synthesis of the test compounds **25–28** & **30** with modified galactose moiety see Supporting Information.

Entry	Compd.	Structure	IC ₅₀ [μM]	K _D [μM]
1	2		733 ^[a]	574
2	25		381	n.d. ^[b]
3	26		674	n.d.
4	27		204	n.d.
5	28		271	n.d.
6	29		117	259
7	30		1246	n.d.
8	49		n.a. ^[c]	n.a.
9	50		n.d.	15

[a] Average value over six measurements. [b] n.d.: not determined. [c] n.a.: not active up to 10 mM.

TBDPSCI (\rightarrow **35**). The enantiomeric purity of the cyclohexanol derivative **35** (95% ee) was determined by conversion into the Mosher ester **36** and subsequent ¹⁹F NMR analysis (for details see Supporting Information). Then, acceptor **35** was glycosylated with donor **3** to yield the disaccharide mimic **37** in 81%. Finally, after removal of the silyl group with HF-pyr (\rightarrow **38**), the sulfate moiety was introduced using SO₃pyr in DMF to give sulfate **39**. Final deprotection with aqueous NaOH afforded the test compound **29**.

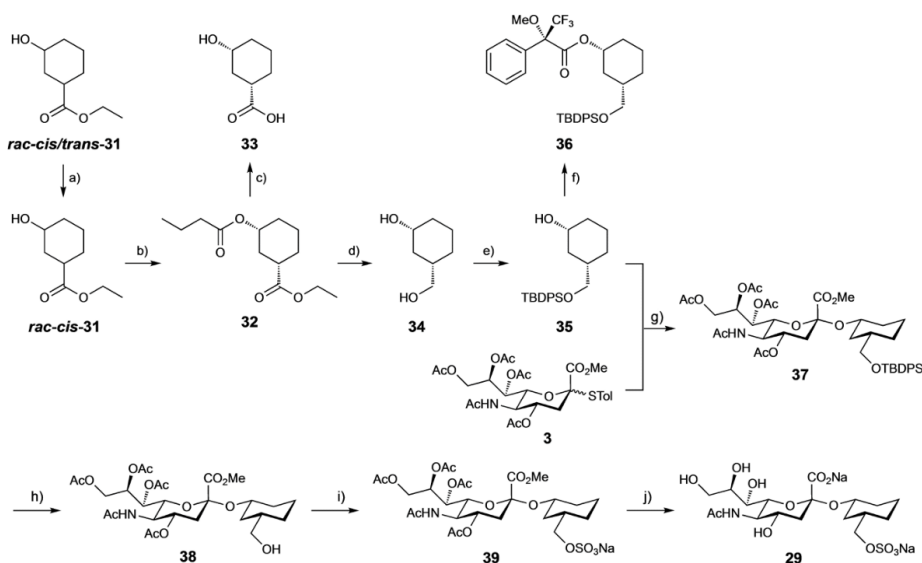
Almost the entire 2-fold affinity gain originated from deoxygenation at the anomeric center (\rightarrow **25**, Table 3, entry 2), rather than removal of the 2-OH group (\rightarrow **26**, entry 3). Noteworthy, these two modifications, i.e. removal of 1-OMe and 2-OH (\rightarrow **27**, entry 4), are positively cooperative, since the affinity for mimetic **27** (IC₅₀=204 μM) is more increased compared to the two individually deoxygenated compounds **25** (IC₅₀=381 μM) and **26** (IC₅₀=674 μM). Furthermore, deoxygenation in

the 4-position of the galactose moiety (\rightarrow **28**, entry 5) resulted in a three-fold improvement of affinity compared to the parent compound **2** (entry 1). Furthermore, with the cyclohexane derivative **29**, bearing only the CH₂OSO₃Na at the 5-position of the former galactose moiety, a further affinity enhancement could be realized, resulting in a six-fold higher potency for the cyclohexane derivative **29** (IC₅₀=117 μM) compared to disaccharide **2**. Finally, when the cyclohexane moiety of mimetic **29** was replaced by an aromatic aglycone (\rightarrow **30**, entry 7), the binding affinity was substantially reduced, probably because the directionality of the salt bridge formed by the sulfate is disturbed.

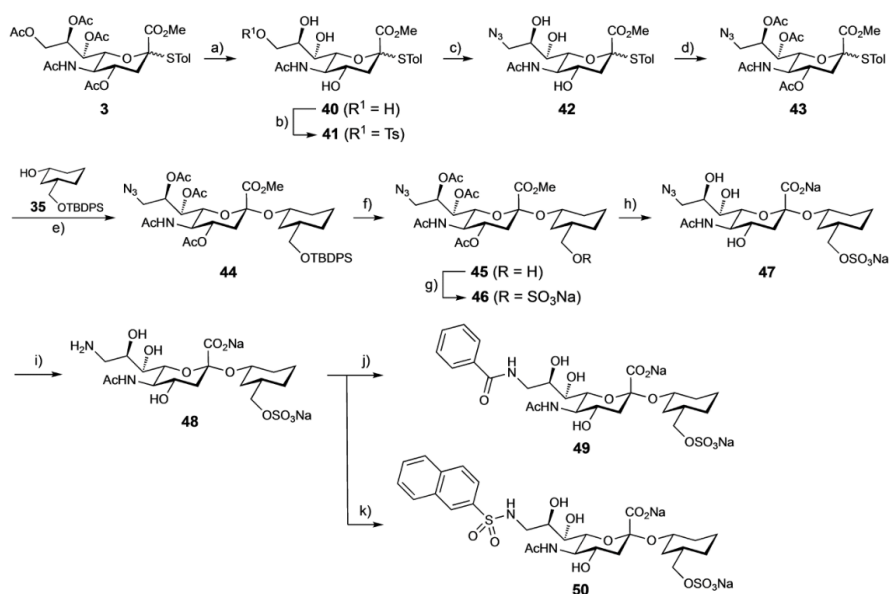
Modification of the 9-position of the Neu5Ac moiety. Amide formation in the 9-position of neuraminic acid is generally a successful approach to increase the affinity of siglec antagonists.^[8,27–33,51] Starting from the readily available Neu5Ac derivative **43** (Scheme 3) the cyclohexanol derivative **35** was sialidated to give intermediate **44**, but only in 25% yield. By desilylation (\rightarrow **45**), 6-O-sulfation (\rightarrow **46**) and hydrolysis of the ester function, azide **47** was obtained in an overall yield of 75%. After reduction of the 9'-azido group by catalytic hydrogenation (\rightarrow **48**), acylation yielded amide **49** and sulfonamide **50**. In accordance with a recent publication of Paulson *et al.*^[34] emphasizing that amide linked substituents at C-9 of the neuraminic acid moiety do not yield hits, benzamide **49** did not show any activity neither in the competitive binding assay nor in ITC experiments (Table 3, entry 8). When we, based on Paulson's findings, formed sulfonamide **50**, a Siglec-8 ligand with a K_D of 15 μM affinity was obtained (entry 9).

Thermodynamics of Siglec-8 antagonist/Siglec-8 interaction. Based on the thermodynamic fingerprints of the interaction of compounds **1b**, **2**, **29** and **50** with Siglec-8, a deeper insight into the binding process was intended. For this purpose, ITC data of the mimetics **2**, **29** and **50** were compared with the previous data for the parent tetrasaccharide 3-aminopropyl 6'-sulfo-sLe^x (**1b**).^[38] The K_D values determined by ITC (Table 4, Figure 2) correspond well with the data obtained from the competitive binding assay and by MST (Tables 1–3). Since the inventory of protonatable functional groups is constant throughout the compound series, we do not expect any superimposed effects from changes in protonation states upon binding.

The binding of 3-aminopropyl 6'-sulfo-sLe^x (**1b**) to Siglec-8 is driven by a strong binding enthalpy ($\Delta H^\circ = -32.6$ kJ mol⁻¹), which is partly offset by a large unfavorable entropic term ($-\Delta\Delta S^\circ = +12.4$ kJ mol⁻¹). Because the protein structure of apo-Siglec-8 and the complex of 6'-sulfo-sLe^x (**1b**) with Siglec-8 are identical to a large extent,^[38] a large entropy penalty resulting from induced fit can be excluded (Figure 3A & B). A potential reason for the entropy penalty could be related to a loss of conformational flexibility, especially of the Fuc and GlcNAc moiety as well as of the glycerol side chain. On the other hand, an extended network of perfect hydrogen bonds is the main reason for the large beneficial enthalpy term.^[52] For disaccharide **2** the enthalpic contribution is much less pronounced ($\Delta\Delta H^\circ_{2-1b} = 16.3$ kJ mol⁻¹), probably as a result of a slightly modified binding mode, aggravating a perfect alignment of the hydro-



Scheme 2. a) Chromatographic separation; b) vinyl butyrate, Novozyme 435, heptane, 23 °C, 2.5 h (35%); c) 2 M NaOH (aq), MeOH, 6 h (31%); d) DIBAL-*H*, THF, –15 °C, 1.5 h (94%); e) TBDPSCl, DMAP, imidazole, rt, 16 h (62%); f) (*R*)-(-)-MTPA-Cl, DMAP, DCM, 0 °C to rt; g) NIS, TfOH, MS 3 Å, DCM, MeCN, –40 °C, 6 h (81%); h) HF-pyr, pyridine, 0 °C, 5 h (88%); i) SO₃-pyr, DMF, 2 h (85%); j) NaOH (aq), overnight (83%).



Scheme 3. a) NaOMe, MeOH, rt, 16 h (83%); b) TsCl, pyridine, 0 °C to rt, 16 h (35%); c) NaN₃, 15-crown-5, DMF, 60 °C, 16 h (96%); d) Ac₂O, pyridine, rt, 6 h (93%); e) NIS, TfOH, MS 3 Å, DCM, MeCN, –40 °C, 4 h (25%); f) HF-pyr, pyridine, 0 °C to rt, 5 h (91%); g) SO₃-pyr, DMF, 2 h (99%); h) NaOH (aq), rt, 6 h (82%); i) Pd(OH)₂/C, H₂ (1 atm), H₂O, rt, 16 h (85%); j) PhCO₂H, HATU, DIPEA, DMF, 6 h (72%); k) 2-naphthalenesulfonyl chloride, DMF/H₂O (2:1), rt, 5 h (42%).

phobic α -face of the Gal moiety and Tyr58. As a second consequence of the modified binding mode, the geometry of

the hydrogen bond interactions is slightly altered, further reducing the enthalpy term. Overall, the complex exhibits

Table 4. Thermodynamic parameters from ITC for selected Siglec-8 ligands. Error estimates for thermodynamic data correspond to the 68% confidence interval from global fitting of two independent experiments. Errors in binding kinetic data represent the standard error of a single measurement.

Compound	K_D [μM]	ΔG° [$\text{kJ}\cdot\text{mol}^{-1}$]	ΔH° [$\text{kJ}\cdot\text{mol}^{-1}$]	$-\text{T}\Delta S^\circ$ [$\text{kJ}\cdot\text{mol}^{-1}$]	k_{on} [$\text{M}^{-1}\cdot\text{s}^{-1}$]	k_{off} [s^{-1}]	Residence time τ [s]
1b ^[a]	279 (273–285)	−20.3 (−20.3–−20.2)	−32.6 (−33.5–−31.8)	12.4 (11.5–13.2)	N/A	N/A	N/A
2	574 (505–650)	−18.5 (−18.8–−18.2)	−16.3 (−17.2–−15.3)	−2.3 (−3.5–−1.0)	$1.2\cdot 10^3$ ($\pm 5.1\cdot 10^2$)	$8.2\cdot 10^{-1}$ ($\pm 3.5\cdot 10^{-1}$)	1.2
29	259 (222–303)	−20.5 (−20.9–−20.1)	−15.0 (−16.2–−13.9)	−5.5 (−6.9–−3.9)	$6.6\cdot 10^2$ ($\pm 7.5\cdot 10^1$)	$1.6\cdot 10^{-1}$ ($\pm 1.8\cdot 10^{-2}$)	6.2
50	15 (13–18)	−27.5 (−27.1–−27.9)	−11.6 (−11.0–−12.2)	−16.0 (−15.0–−16.9)	$4.7\cdot 10^3$ ($\pm 7.1\cdot 10^2$)	$8.7\cdot 10^{-2}$ ($\pm 1.2\cdot 10^{-2}$)	11.5

[a] Data reproduced from Ref. [38] [b] N/A: Kinetic rate constants for **1b** have not been published in the cited reference.^[38]

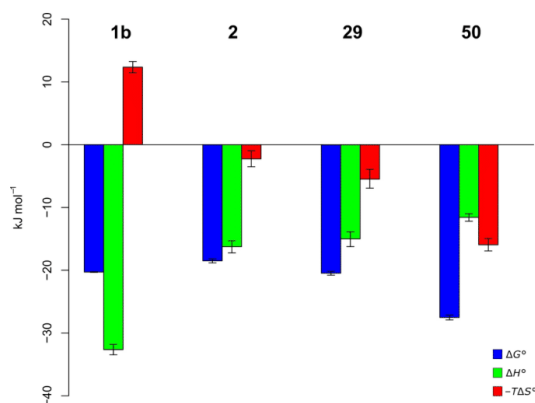


Figure 2. Thermodynamic signature (ΔG° , ΔH° and $-\text{T}\Delta S^\circ$) for 3-aminopropyl 6'-sulfo-sLe^x (**1b**) and the disaccharides **2**, **29** & **50**. Error estimates for thermodynamic data correspond to the 68% confidence interval from global fitting of two independent experiments.

higher flexibility, leading to a substantial improvement of the entropy term ($-\text{T}\Delta\Delta S^\circ_{2-1b} = -14.7 \text{ kJ mol}^{-1}$). Cyclohexane derivative **29** shows a slightly reduced binding enthalpy ($\Delta\Delta H^\circ_{29-2} = 1.3 \text{ kJ mol}^{-1}$) compared to disaccharide **2**, which is overcompensated by a beneficial entropy term ($-\text{T}\Delta\Delta S^\circ_{29-2} = -3.2 \text{ kJ mol}^{-1}$), resulting in a 2-fold higher binding affinity. Finally, the introduction of a benzamide in the 9-position of the Neu5Ac moiety (\rightarrow **49**, Table 3) yielded an inactive compound in the competitive binding assay as well as in ITC experiments. This was initially surprising because in a number of other siglecs a substantial improvement of affinity could be realized by the introduction of aromatic amides.^[8,27–33,51] It is, however, in accordance with a recent publication of Paulson *et al.* emphasizing that amide linked substituents at C-9 of the Neu5Ac moiety did not yield Siglec-8 hits.^[34] Possible reasons could be the exit vector of the amide bond, causing the aromatic substituent to point into the water environment. In contrast, the exit vector of a sulfonamide substituent positions an aromatic group much closer to the protein surface. However, an inspection of the binding site in the apo-Siglec-8 structure obtained by NMR,^[38] (Figure 3A) revealed that Lys120 blocks the area for possible

aromatic contacts (Figure 3B). For docking purposes, we performed an *in silico* mutation of Lys120 to Ala and used this mutant for docking (for details see experimental part). After visual inspection of the generated docking poses, Ala120 was mutated back to Lys and minimized (Figure 3C). In the docking solution of **50**, the salt bridges of the Neu5Ac carboxylic acid to Arg105 and of the sulfate group to Arg56 and Glu59 are conserved, as are the hydrogen bonds to Tyr7 and the Lys115 backbone oxygen. The naphthyl substituent of sulfonamide **50** binds to a hydrophobic pocket generated by the displacement of Lys120. This additional hydrophobic interaction likely drives the high-affinity interaction to Siglec-8. Presumably, the angular geometry of the sulfonamide bond is required for access to this region. Whereas benzamide **49** was inactive, sulfonamide **50** proved to be the best Siglec-8 antagonist in the series with a K_D of 15 μM . Surprisingly, this became possible by a substantial improvement of the entropy term ($-\text{T}\Delta\Delta S^\circ_{50-29} = -10.5 \text{ kJ/mol}$) compared to benzamide **29**, which overcompensates a marked enthalpy penalty ($\Delta\Delta H^\circ_{50-29} = 3.4 \text{ kJ/mol}$).

The residence times $\tau = 1/k_{\text{off}}$ ^[53] for carbohydrate/lectin interactions are regularly very short and represent one of the challenges to be addressed for therapeutic applications. We determined binding kinetic data for the interactions of the disaccharide mimetics **2**, **29**, and **50** with Siglec-8 from ITC data using the kinITC technology.^[54,55] This method analyses the equilibration time of each injection during a titration and fits this information to a kinetic model to derive rate constants. The binding kinetics of disaccharide **2** are characterized by a very short residence time of 1.2 s. For the mimetic **29**, the residence time is increased by a factor of 5, probably mainly based on the reduced polarity. The residence time of the complex with sulfonamide derivative **50** is even longer, *i.e.* 10-fold increased. Thus, structural modifications leading to improved affinities go in parallel with prolonged lifetimes of the protein–ligand complex, which is often correlated with beneficial pharmacological properties. In the association rate, the simplification of the carbohydrate core from disaccharide **2** to cyclohexane derivative **29** is associated with a reduction of the rate constant by a factor of 2. However, through the introduction of the sulfonamide substituent in mimetic **50**, an improvement of the association rate by a factor of 4 compared to disaccharide **2** was observed.

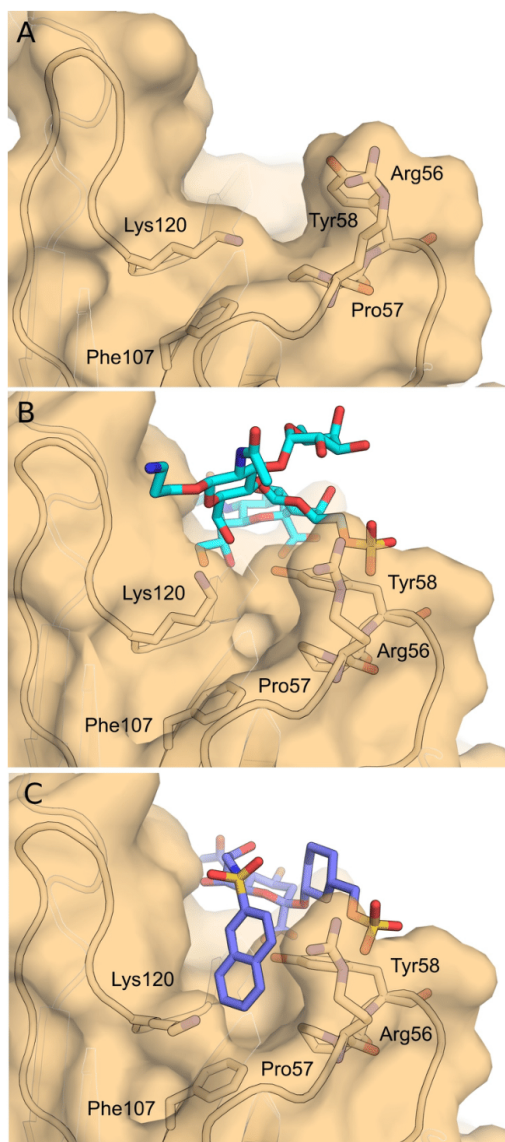


Figure 3. A) NMR structure of apo-Siglec-8 (PDB 2N7A) and B) the 3-aminopropyl 6'-sulfo-sLe^x (1b)/Siglec-8 complex (PDB 2N7B); C) Docking pose of antagonist 50/Siglec-8 (for details see experimental section).

Thus, the additional interactions of the hydrophobic naphthyl substituent influence both association and dissociation kinetics towards a higher binding affinity of sulfonamide 50. The discussion about the impact of receptor binding kinetics in early stage drug discovery is currently not fully settled. However, carbohydrates are often characterized by extremely short-lived interaction with their receptors. It, there-

fore, seems appropriate that dissociation kinetics represent an important optimization parameter when carbohydrate-based therapeutics are considered. The prolonged residence time of the high-affinity binder 50 is an indication that glycomimetic ligands have the potential to overcome one of the main drawbacks of carbohydrate ligands in the context of medicinal chemistry.

Conclusion

Siglec-8 is a CD33-related protein exclusively expressed on eosinophils, mast cells, and to some extent on basophils, cells playing a key role in the pathophysiology of asthma. However, the lack of a small molecule binding to Siglec-8 with high affinity and drug-like residence time τ limits therapeutic applications to monoclonal antibodies and polymeric displays of physiological ligands and derivatives thereof.^[15,20–24,34]

Here, in an extended study, we identified the pharmacophores of 6'-sulfo-Lewis^x (1a) and successfully developed the high-affinity mimetic 50. Its core is still neuraminic acid, however bearing a carbocyclic mimetic of the Gal moiety in the 2-position and a sulfonamide substituent in the 9-position. Compared to the lead structure 3-aminopropyl 6'-sulfo-Lewis^x (1b), the affinity could be improved 20-fold. We postulate a hypothetical binding mode that necessitates the formation of a hydrophobic pocket to accommodate the bulky aromatic substituent of sulfonamide 50. In addition, the residence time, which usually is the Achilles tendon of carbohydrate/lectin interactions could be substantially improved as well. Future activities will focus on further improvement of the pharmacokinetic profile, besides the exploration of the 4- and 5-position of the neuraminic acid core. Finally, a comparison of the best antagonists in their mono- and polyvalent presentation will give insight into possible therapeutic applications.

Experimental Section

General Methods. NMR spectra were recorded on a Bruker Avance DMX-500 (500 MHz) spectrometer. Assignment of ¹H and ¹³C NMR spectra was achieved using 2D methods (COSY, HSQC, HMBC). Chemical shifts are expressed in ppm using residual solvent signals (CHCl₃, CHD₂OD, HDO) as reference. Optical rotations were measured with a PerkinElmer polarimeter 341. Electrospray ionization mass spectrometry (ESI-MS) data were obtained on a Waters Micromass ZQ instrument. High resolution mass (HR-MS) analyses were carried out using an Agilent 1100 LC, equipped with a photodiode array detector and a Micromass QTOF I, equipped with a 4 GHz digital-time converter. Reactions were monitored by TLC using glass plates coated with silica gel 60 F254 (Merck) and visualized by using UV light and/or by charring with a molybdate solution (a 0.02 M solution of ammonium cerium sulfate dihydrate and ammonium molybdate tetrahydrate in 10% aq. H₂SO₄). Medium pressure chromatography (MPLC) separations were carried out on a CombiFlash Companion or R_f from Teledyne Isco equipped with RediSep normal phase or RP-18 reversed-phase flash columns. Size exclusion chromatography was performed on Biogel P-2 media (Bio-Rad Laboratories, Inc.). Reagents were purchased as reagent grade from Fluka, Aldrich, and Acros and used without further

purification. Solvents were purchased from Sigma-Aldrich (Buchs, Switzerland) or Acros Organics (Geel, Belgium) and were dried prior to use where indicated. MeOH was dried by reflux with sodium methoxide and distilled and stored under argon atmosphere. Dichloromethane (DCM), acetonitrile (MeCN) and toluene were dried by filtration over Al_2O_3 (Fluka, type 5016 A basic) and stored over activated molecular sieves (3 Å, 4 Å). Pyridine was distilled over KOH under argon atmosphere and stored over KOH pellets. Dry DMF was purchased from Acros Organics. Molecular sieves (3 Å, 4 Å) were activated under vacuum at 500 °C for 0.5 h immediately before use.

Methyl (methyl 5-acetamido-4,7,8,9-tetra-O-acetyl-3,5-dideoxy-D-glycero- α -D-galacto-2-nonulopyranosylonate)-(2 \rightarrow 3)-6-O-tert-butylidiphenylsilyl- β -D-galactopyranoside (5). To a suspension of **3**^{42f} (3.65 g, 6.10 mmol), **4**^{41f} (1.20 g, 2.77 mmol) and 3 Å molecular sieves in MeCN/DCM (5:3, 70 mL) at -40 °C, was added *N*-iodosuccinimide (2.74 g, 12.1 mmol), followed by dropwise addition of TfOH (98 μ L, 1.1 mmol). The reaction mixture was stirred at -40 °C for 16 h under argon and then was neutralized with NEt_3 . The suspension was warmed up to rt, filtered over celite and the solvents were evaporated. The residue was dissolved in DCM (60 mL), washed with 1 M $\text{Na}_2\text{S}_2\text{O}_5$ (30 mL) and H_2O (3 \times 30 mL), dried over Na_2SO_4 , filtered and evaporated. The crude product was purified by flash column chromatography (toluene/acetone, 1:0 to 1:1) to afford **5** (853 mg, 34%). $[\alpha]_D^{20} = -11.8$ ($c = 1.0$, CHCl_3); ^1H NMR (500 MHz, CDCl_3): $\delta = 7.79$ – 7.75 (m, 4H, Ar-H), 7.53–7.44 (m, 6H, Ar-H), 5.45 (ddd, $J = 2.7, 4.9, 9.3$ Hz, 1H, H-8'), 5.43 (dd, $J = 2.0, 9.2$ Hz, 1H, H-7'), 5.30 (d, $J = 9.8$ Hz, 1H, NH), 5.04 (ddd, $J = 4.6, 10.2, 12.2$ Hz, 1H, H-4'), 4.44 (d, $J = 7.7$ Hz, 1H, H-1), 4.36 (dd, $J = 2.8, 12.6$ Hz, 1H, H-9'a), 4.22–4.16 (m, 3H, H-3, H-6', H-9'b), 4.08 (q, $J = 10.2$ Hz, 1H, H-5'), 4.03 (dd, $J = 7.1, 10.1$ Hz, 1H, H-6a), 3.91 (dd, $J = 5.0, 10.2$ Hz, 1H, H-6b), 3.88 (d, $J = 3.6$ Hz, 1H, H-4), 3.85 (s, 3H, COOMe), 3.78 (ddd, $J = 1.1, 7.7, 9.2$ Hz, 1H, H-2), 3.68 (m, 1H, H-5), 3.63 (s, 3H, OMe), 2.89 (s, 1H, OH-4), 2.86 (dd, $J = 4.6, 12.9$ Hz, 1H, H-3'e), 2.59 (d, $J = 4.0$ Hz, 1H, OH-2), 2.24, 2.20, 2.13 (3 s, 9H, 3 OAc), 2.13 (m, 1H, H-3'a), 2.12 (s, 3H, OAc), 1.98 (s, 3H, NHAc), 1.13 ppm (s, 9H, $\text{C}(\text{CH}_3)_3$); ^{13}C NMR (126 MHz, CDCl_3): $\delta = 171.0, 170.7, 170.4, 170.2, 168.4$ (6 C, 6 C=O), 135.73, 135.67, 133.2, 133.1, 129.99, 129.95, 127.92, 127.88 (12 C, Ar-C), 104.0 (C-1), 97.4 (C-2'), 77.4 (C-3), 73.7 (C-5), 72.7 (C-6'), 69.5 (C-2), 68.6 (C-4'), 68.0 (C-8'), 67.9 (C-4), 66.9 (C-7'), 62.6 (C-6), 62.4 (C-9'), 56.8 (OMe), 53.2 (COOMe), 49.8 (C-5'), 38.2 (C-3'), 26.9 (3 C, $\text{C}(\text{CH}_3)_3$), 23.3 (NHAc), 21.4, 21.0, 20.91, 20.90 (4 OAc), 19.4 ppm ($\text{C}(\text{CH}_3)_3$); MS (ESI): m/z calcd for $\text{C}_{43}\text{H}_{59}\text{NO}_{18}\text{Si}$: 928.4 $[M + \text{Na}]^+$; found: 928.4.

Methyl (methyl 5-acetamido-4,7,8,9-tetra-O-acetyl-3,5-dideoxy-D-glycero- α -D-galacto-2-nonulopyranosylonate)-(2 \rightarrow 3)-2,4-di-O-benzoyl-6-O-tert-butylidiphenylsilyl- β -D-galactopyranoside (6). To a solution of **5** (974 mg, 1.08 mmol) in pyridine (30 mL) was added DMAP (47 mg, 0.38 mmol) followed by portion-wise addition of Bz_2O (3.18 g, 14.0 mmol) at 0 °C. The mixture was warmed up to rt and stirred for 16 h. Then, the solvent was removed by co-evaporation with toluene. The residue was dissolved in EtOAc (30 mL), washed with H_2O (3 \times 10 mL), satd aq. CuSO_4 (3 \times 10 mL), H_2O (10 mL) and brine (10 mL), dried over Na_2SO_4 , filtered and evaporated. The crude product was purified by flash column chromatography (petroleum ether/acetone, 1:0 to 1:1) to afford **6** (1.10 g, 92%) as a brown vitreous solid. $[\alpha]_D^{20} = +61.7$ ($c = 1.00$, CHCl_3); ^1H NMR (500 MHz, CDCl_3): $\delta = 8.23$ – 8.14 (m, 2H, Ar-H), 8.13–8.02 (m, 2H, Ar-H), 7.70–7.62 (m, 6H, Ar-H), 7.62–7.52 (m, 2H, Ar-H), 7.52–7.34 (m, 4H, Ar-H), 7.29–7.24 (m, 3H, Ar-H), 7.12 (t, $J = 7.6$ Hz, 1H, Ar-H), 5.66 (ddd, $J = 2.4, 5.4, 9.5$ Hz, 1H, H-8'), 5.62 (d, $J = 3.2$ Hz, 1H, H-4), 5.36 (dd, $J = 7.9, 10.1$ Hz, 1H, H-2), 5.25 (dd, $J = 2.8, 9.7$ Hz, 1H, H-7), 5.00 (d, $J = 10.2$ Hz, 1H, NH), 4.96–4.86 (m, 2H, H-3, H-4'), 4.73 (d, $J = 7.9$ Hz, 1H, H-1), 4.36 (dd, $J = 2.3, 12.5$ Hz, 1H, H-9'a), 3.97 (s, 3H, COOMe), 4.02–3.93 (m, 2H, H-5, H-9'b), 3.81 (q, $J =$

10.4 Hz, 1H, H-5'), 3.74–3.64 (m, 2H, H-6), 3.58 (dd, $J = 2.8, 10.7$ Hz, 1H, H-6'), 3.47 (s, 3H, OMe), 2.51 (dd, $J = 4.7, 12.6$ Hz, 1H, H-3'e), 2.24, 2.10, 1.93, 1.79 (4 s, 12H, 4 OAc), 1.67 (t, $J = 12.4$ Hz, 1H, H-3'a), 1.46 (s, 3H, NHAc), 1.03 ppm (s, 9H, $\text{C}(\text{CH}_3)_3$); ^{13}C NMR (126 MHz, CDCl_3): $\delta = 170.8, 170.7, 170.6, 170.2, 170.1, 168.1, 165.5, 165.4$ (8 C=O), 135.6, 135.4, 132.91, 132.89, 130.4, 130.2, 130.0, 129.9, 129.7, 129.6, 128.3, 127.7, 127.5 (24 C, Ar-C), 102.4 (C-1), 96.9 (C-2'), 73.2 (C-5), 71.9 (C-3), 71.6 (C-6'), 71.4 (C-2), 69.6 (C-4'), 67.9 (C-4), 67.5 (C-8'), 66.4 (C-7'), 62.3 (C-9'), 60.9 (C-6), 57.1 (OMe), 53.2 (COOMe), 48.9 (C-5'), 37.3 (C-3'), 26.6 (3 C, $\text{C}(\text{CH}_3)_3$), 23.1 (NHAc), 21.5, 20.8, 20.7, 20.3 (4 OAc), 19.0 ppm ($\text{C}(\text{CH}_3)_3$); MS (ESI): m/z calcd for $\text{C}_{57}\text{H}_{67}\text{NO}_{26}\text{Si}$: 1136.4 $[M + \text{Na}]^+$; found: 1136.4.

Methyl (methyl 5-acetamido-4,7,8,9-tetra-O-acetyl-3,5-dideoxy-D-glycero- α -D-galacto-2-nonulopyranosylonate)-(2 \rightarrow 3)-2,4-di-O-benzoyl- β -D-galactopyranoside (7). To a solution of **6** (485 mg, 0.44 mmol) in pyridine (10 mL) in a Teflon container was added HF-pyr (3.0 mL) dropwise and the reaction mixture was stirred at rt for 2.5 h. The reaction was neutralized with satd aq. NaHCO_3 and the aqueous phase was extracted with DCM. The crude product was purified by flash chromatography (DCM/MeOH, 1:0 to 19:1) to afford **7** (360 mg, 93%) as a white solid. $[\alpha]_D^{20} = +58.2$ ($c = 0.8$, MeOH); ^1H NMR (500 MHz, CDCl_3): $\delta = 8.24$ – 8.15 (m, 2H, Ar-H), 8.14–8.04 (m, 2H, Ar-H), 7.63–7.56 (m, 2H, Ar-H), 7.50–7.47 (m, 4H, Ar-H), 5.65 (m, 1H, H-8'), 5.47 (dd, $J = 8.0, 10.1$ Hz, 1H, H-2), 5.21 (dd, $J = 2.6, 9.6$ Hz, 1H, H-7'), 5.13 (d, $J = 3.3$ Hz, 1H, H-4), 4.90 (d, $J = 10.1$ Hz, 1H, NH), 4.82–4.66 (m, 3H, H-1, H-3, H-4'), 4.33 (dd, $J = 2.4, 12.4$ Hz, 1H, H-9'a), 3.98 (dd, $J = 5.8, 12.4$ Hz, 1H, H-9'b), 3.88 (m, 1H, H-5), 3.84 (m, 1H, H-5'), 3.80 (s, 3H, COOMe), 3.76–3.70 (m, 2H, H-6a, H-6'), 3.53 (s, 3H, OMe), 3.52 (m, 1H, H-6b), 2.77 (dd, $J = 6.5, 8.4$ Hz, 1H, OH-6), 2.45 (dd, $J = 4.5, 12.7, 1H, H-3'e$), 2.24, 2.09, 1.91, 1.79 (4 s, 12H, 4 OAc), 1.72 (t, 1H, $J = 12.5$ Hz, H-3'a), 1.51 ppm (s, 3H, NHAc); ^{13}C NMR (126 MHz, CDCl_3): $\delta = 170.72, 170.70, 170.6, 170.2, 170.0, 168.3, 167.7, 165.4$ (8 C=O), 133.7, 133.0, 130.21, 130.18, 130.1, 128.8, 128.6, 128.4 (12 C, Ar-C), 102.4 (C-1), 96.8 (C-2'), 73.2 (C-5'), 72.0 (C-6'), 71.4 (C-3), 71.0 (C-2), 69.1 (2 C, C-4, C-4'), 69.1 (C-8'), 67.5 (C-7'), 62.4 (C-9'), 60.3 (C-6), 57.2 (OMe), 53.2 (COOMe), 48.8 (C-5'), 37.5 (C-3'), 23.1 (NHAc), 21.5, 20.8, 20.7, 20.3 ppm (4 OAc); MS (ESI): m/z calcd for $\text{C}_{41}\text{H}_{49}\text{NO}_{20}$: 898.3 $[M + \text{Na}]^+$; found: 898.5.

Methyl (methyl 5-acetamido-4,7,8,9-tetra-O-acetyl-3,5-dideoxy-D-glycero- α -D-galacto-2-nonulopyranosylonate)-(2 \rightarrow 3)-2,4-di-O-benzoyl-6-O-sulfonato- β -D-galactopyranoside (8). To a solution of **7** (280 mg, 0.32 mmol) in dry DMF (7 mL) was added SO_3pyr (508 mg, 3.20 mmol) at 0 °C under argon atmosphere. The reaction mixture was warmed up to rt and stirred for 2.5 h. Then, powdered NaHCO_3 was added and the suspension was stirred for 2 h. The suspension was filtered over celite, and the solvent removed by co-evaporation with xylenes. The crude product was purified by flash column chromatography (DCM/MeOH, 1:0 to 8:2) to afford **8** (290 mg, 93%) as a white solid. $[\alpha]_D^{20} = +48.2$ ($c = 1.1$, MeOH); ^1H NMR (500 MHz, CD_3OD): $\delta = 8.21$ – 8.15 (m, 2H, Ar-H), 8.14–8.05 (m, 2H, Ar-H), 7.65 (m, 2H, Ar-H), 7.57–7.51 (m, 4H, Ar-H), 5.66 (ddd, $J = 2.5, 5.9, 9.7$ Hz, 1H, H-8'), 5.40 (m, 1H, H-4), 5.32 (dd, $J = 7.9, 10.1$ Hz, 1H, H-2), 5.19 (dd, 1H, $J = 2.7, 9.7$ Hz, H-7'), 4.93 (dd, $J = 3.3, 10.1$ Hz, 1H, H-3), 4.85–4.79 (m, 2H, H-1, H-4'), 4.34 (dd, $J = 2.5, 12.4$ Hz, 1H, H-9'a), 4.21 (m, 1H, H-5), 4.06–4.05 (m, 2H, H-6), 3.95 (s, 3H, COOMe), 3.94 (m, 1H, H-9'b), 3.74 (dd, $J = 2.6, 10.7$ Hz, 1H, H-6'), 3.67 (m, 1H, H-5'), 3.55 (s, 3H, OMe), 2.42 (dd, $J = 4.7, 12.5$ Hz, 1H, H-3'e), 2.24, 2.05, 1.88, 1.73 (4 s, 12H, 4 OAc), 1.48 (m, 1H, H-3'a), 1.45 ppm (s, 3H, NHAc); ^{13}C NMR (126 MHz, CD_3OD): $\delta = 172.42, 172.38, 171.7, 171.4, 169.4, 167.2, 167.0$ (8 C, 8 C=O), 131.5, 131.2, 130.9, 129.8, 129.7, 124.6 (12 C, Ar-C), 103.4 (C-1), 98.3 (C-2'), 73.1 (C-5), 72.8 (2 C, C-6', C-3), 72.7 (C-2), 71.0 (C-4'), 70.5 (C-4), 68.8 (C-8'), 68.7 (C-7'), 67.3 (C-6), 63.6 (C-9'), 57.5 (OMe), 53.9 (COOMe), 49.3 (C-5'), 38.4 (C-3'), 22.7 (NHAc), 21.7, 20.6 ppm (4 C, 4 OAc); MS (ESI): m/z calcd for $\text{C}_{41}\text{H}_{48}\text{NNaO}_{23}\text{S}$: 1000.2 $[M + \text{Na}]^+$; found: 1000.3.

Methyl (sodium 5-acetamido-3,5-dideoxy-D-glycero- α -D-galacto-2-nonulopyranosylonate)-(2 \rightarrow 3)-6-O-sulfonato- β -D-galactopyranoside sodium salt (2). To a solution of **8** (70 mg, 0.07 mmol) in dry MeOH (2 mL) was added a freshly prepared solution of MeONa in MeOH (1.5 M, to pH 10). The reaction mixture was stirred for 5 h at 50 °C and then neutralized with Dowex 50X8 (H⁺ form) to pH 5. The suspension was filtered, concentrated and the crude product dissolved in 0.1 M NaOH. The reaction mixture was stirred for 1 h, then neutralized and concentrated. The crude product was purified by reversed-phase column chromatography (RP-18, H₂O) and size-exclusion column chromatography (P-2 gel, H₂O) to afford **2** (40 mg, 84%) as a white solid. $[\alpha]_D^{20} = +5.8$ ($c = 0.7$, H₂O); ¹H NMR (500 MHz, D₂O): $\delta = 4.44$ (d, $J = 8.0$ Hz, 1H, H-1), 4.22–4.20 (m, 2H, H-6), 4.13 (dd, $J = 3.2, 9.8$ Hz, 1H, H-3), 4.02 (m, 1H, H-4), 3.95 (m, 1H, H-5), 3.91–3.85 (m, 3H, H-5', H-8', H-9'a), 3.74–3.64 (m, 3H, H-4', H-6', H-9'b), 3.62 (dd, $J = 1.8, 8.9$ Hz, 1H, H-7'), 3.60 (s, 3H, OMe), 3.57 (dd, $J = 8.0, 9.8$ Hz, 1H, H-2), 2.78 (dd, $J = 4.6, 12.4$ Hz, 1H, H-3'e), 2.06 (s, 3H, NHAc), 1.83 ppm (m, 1H, H-3'a); ¹³C NMR (126 MHz, D₂O): $\delta = 175.7, 174.5$ (2 C=O), 104.1 (C-1), 100.6 (C-2'), 76.3 (C-3), 73.5 (C-6'), 73.2 (C-5), 72.4 (C-8'), 69.7 (C-2), 69.0 (C-4), 68.8 (C-7'), 68.1 (C-4'), 68.0 (C-6), 63.2 (C-9'), 57.8 (OMe), 52.3 (C-5'), 40.2 (C-3'), 22.7 ppm (NHAc); HRMS (ESI): m/z calcd for C₁₈H₂₉NNa₂O₁₇S: 632.0849 [M + Na]⁺; found: 632.0849.

Ethyl *cis*-3-hydroxycyclohexane-1-carboxylate (*rac-cis*-31). Racemic ethyl 3-hydroxycyclohexane-1-carboxylate (**31**, 4.00 g, 23.2 mmol) was separated by flash column chromatography on silica (petroleum ether/EtOAc, 7:3 to 6:4). The lower fraction was collected to yield the racemic *cis* isomers *rac-cis*-**31** (1.50 g, 38%) as a colorless oil. The diastereomeric purity was confirmed by conversion to the racemic analogue of Mosher ester **36** (for details see Supporting Information).

Ethyl (1*S*,3*R*)-3-(butyryloxy)cyclohexane-1-carboxylate (32). Racemic *rac-cis*-**31** (3.01 g, 17.5 mmol) was dissolved in heptane (18 mL). Vinyl butyrate (4.40 mL, 34.7 mmol) and lipase Novozyme 435 (61.5 mg) were added and the mixture was shaken in an incubator at 23 °C and 140 rpm for 3.5 h. The suspension was filtered over celite, washed with petroleum ether, and the solvent was removed under reduced pressure. The crude product was purified by flash column chromatography on silica (toluene/acetone, 1:0 to 6:4) to afford **32** (1.48 g, 35%) as a colorless oil. $[\alpha]_D^{20} = +44.0$ ($c = 1.00$, CHCl₃); ¹H NMR (500 MHz, CDCl₃): $\delta = 4.73$ (tt, $J = 4.3, 11.0$ Hz, 1H, H-3), 4.13 (q, $J = 7.1$ Hz, 2H, OCH₂CH₃), 2.40 (tt, $J = 3.5, 11.9$ Hz, 1H, H-1), 2.25 (t, $J = 7.3$ Hz, 2H, CH₂CH₂CH₃), 2.21 (m, 1H, H-2e), 1.99–1.85 (m, 3H, H-4e, H-5e, H-6e), 1.65 (sextet, $J = 7.4$ Hz, 2H, CH₂CH₂CH₃), 1.49 (q, $J = 12.2$ Hz, 1H, H-2a), 1.43–1.28 (m, 3H, H-4a, H-5a, H-6a), 1.25 (t, $J = 7.1$ Hz, 3H, OCH₂CH₃), 0.95 ppm (t, $J = 7.4$ Hz, 3H, CH₂CH₂CH₃); ¹³C NMR (126 MHz, CDCl₃): $\delta = 174.0, 172.5$ (2 C=O), 71.3 (C-3), 60.0 (OCH₂CH₃), 41.3 (C-1), 36.1 (CH₂CH₂CH₃), 33.7 (C-2), 30.9 (C-4), 27.7 (C-6), 22.9 (C-5), 18.2 (CH₂CH₂CH₃), 13.8 (OCH₂CH₃), 13.2 ppm (CH₂CH₂CH₃); MS (ESI): m/z calcd for C₁₃H₂₂O₄: 265.1 [M + Na]⁺; found: 265.0.

(1*S*,3*R*)-(+)-3-Hydroxycyclohexane-1-carboxylate (33). To a solution of **32** (31.1 mg, 0.128 mmol) in MeOH (0.5 mL) was added 2 M aq. NaOH (0.32 mL, 0.64 mmol) dropwise at 0 °C and the solution was stirred at 0 °C for 6 h. The reaction mixture was neutralized with HOAc and then concentrated at reduced pressure. The residue was purified by flash column chromatography on silica (DCM/MeOH, 9:1 to 4:1) to give **33** (5.7 mg, 31%) as white solid. $[\alpha]_D^{20} = +10.3$ ($c = 0.64$, MeOH), [Ref.:⁵⁰] $[\alpha]_D^{20} = +10.7$ ($c = 1.77$, MeOH); ¹H NMR (500 MHz, CD₃OD): $\delta = 3.54$ (tt, $J = 4.2, 11.0$ Hz, 1H), 2.33 (tt, $J = 3.5, 12.2$ Hz, 1H), 2.17 (dt, $J = 2.0, 3.9, 12.1$ Hz, 1H), 1.98–1.76 (m, 3H), 1.47–1.03 ppm (m, 4H).

(1*R*,3*S*)-3-(Hydroxymethyl)cyclohexane-1-ol (34). Compound **32** (701 mg, 2.89 mmol) was dissolved in dry THF (28 mL) and cooled

to –15 °C. Then, DIBAL-*H* (1 M in toluene, 17.0 mL, 17.0 mmol) was added dropwise under argon and the mixture was stirred at –15 °C for 1.5 h. The reaction was quenched by the addition of satd aq. KNaC₄H₄O₆ (20 mL) and vigorously stirred for 30 min. The aqueous phase was extracted with Et₂O (4 × 20 mL) and the combined organic fractions were dried over Na₂SO₄, filtered and concentrated. The crude product was purified by flash column chromatography on silica (toluene/acetone, 1:0 to 1:1) to give **34** (352 mg, 94%). $[\alpha]_D^{20} = 0.0$ ($c = 0.4$, CHCl₃); ¹H NMR (500 MHz, CDCl₃): $\delta = 3.61$ (m, 1H, H-3), 3.48 (m, 2H, CH₂OH), 2.03 (m, 1H, H-2e), 1.98 (m, 1H, H-4e), 1.81 (dq, $J = 3.5, 13.5$ Hz, 1H, H-5e), 1.71 (m, 1H, H-6e), 1.62 (m, 1H, H-1), 1.30 (tq, $J = 3.5, 13.2$ Hz, 1H, H-5a), 1.18 (m, 1H, H-4a), 0.94 (q, $J = 11.5$ Hz, 1H, H-2a), 0.86 ppm (dq, $J = 3.8, 12.7$ Hz, 1H, H-6a); ¹³C NMR (126 MHz, CDCl₃): $\delta = 71.2$ (C-3), 68.3 (CH₂OH), 40.7 (C-1), 39.8 (C-2), 36.5 (C-4), 29.8 (C-6), 24.9 ppm (C-5).

(1*R*,3*S*)-3-(*tert*-Butyldiphenylsilyloxymethyl)cyclohexane-1-ol (35). To a solution of **34** (608 mg, 4.67 mmol) in dry DCM (14 mL) were consecutively added imidazole (471 mg, 6.92 mmol), DMAP (113 mg, 0.92 mmol) and TBDPSCI (1.32 mL, 5.08 mmol) and the mixture was stirred at rt under argon. After 16 h, additional TBDPSCI (0.24 mL, 0.92 mmol) was added, and after further 2 h another portion of TBDPSCI (0.24 mL, 0.92 mmol) was added. After additional 4 h, the mixture was diluted with DCM (40 mL) and washed with H₂O. The organic fraction was dried over Na₂SO₄, filtered and concentrated in vacuo. The crude product was purified by flash column chromatography on silica (DCM/MeOH, 1:0 to 95:5) to yield **35** (1.07 g, 62%). $[\alpha]_D^{20} = +1.3$ ($c = 1.0$, CHCl₃); ¹H NMR (500 MHz, CDCl₃): $\delta = 7.68$ –7.64 (m, 4H, Ar–H), 7.45–7.36 (m, 6H, Ar–H), 3.61 (m, 1H, H-3), 3.50 (dq, $J = 6.1, 9.8$ Hz, 2H, CH₂O), 2.08 (m, 1H, H-2e), 1.98 (m, 1H, H-4e), 1.80 (dq, $J = 3.4, 13.5$ Hz, 1H, H-5e), 1.70 (m, 1H, H-6e), 1.61 (m, 1H, H-1), 1.42 (d, $J = 4.4$ Hz, 1H, OH), 1.29 (tq, $J = 3.5, 13.2$ Hz, 1H, H-5a), 1.15 (m, 1H, H-4a), 1.05 (s, 9H, C(CH₃)₃), 0.98 (q, $J = 11.5$ Hz, 1H, H-2a), 0.88 ppm (dq, $J = 3.6, 12.1$ Hz, 1H, H-6a); ¹³C NMR (126 MHz, CDCl₃): $\delta = 135.6, 134.0, 129.6, 127.7, 12.7$ (12 C, Ar–C), 70.7 (C-3), 68.8 (CH₂O), 39.4 (C-1), 39.0 (C-2), 35.9 (C-4), 28.5 (C-6), 26.9 (3 C, C(CH₃)₃), 23.8 (C-5), 19.4 ppm (C(CH₃)₃); MS (ESI): m/z calcd for C₂₃H₃₂O₂Si: 391.2 [M + Na]⁺; found: 391.1.

(1*R*,3*S*)-3-(*tert*-Butyldiphenylsilyloxymethyl)cyclohexyl (*R*)-(-)- α -methoxy- α -(trifluoromethyl)phenylacetate (36). To a solution of **35** (9.5 mg, 0.026 mmol) in dry DCM (0.2 mL) were added DMAP (72 mg, 0.061 mmol) and (*R*)-(-)-MTPA-Cl (9.2 μ L, 0.038 mmol) at 0 °C. The reaction mixture was stirred at 0 °C for 15 min and then for 1 h at rt. The reaction mixture was diluted with Et₂O (5.0 mL), washed twice with 1 M aq. HCl, satd aq. NaHCO₃ and water, dried over Na₂SO₄, filtered, and concentrated under reduced pressure. The crude **36** was directly subjected to ¹⁹F NMR investigation without further purification. ¹⁹F NMR (470 MHz, CDCl₃): $\delta = -71.60$ ppm; Enantiomeric purity: 95% ee (for ¹⁹F NMR see Supporting Information).

(1*S*,3*R*)-3-(*tert*-Butyldiphenylsilyloxymethyl)cyclohexyl (methyl 5-acetamido-4,7,8,9-tetra-O-acetyl-3,5-dideoxy-D-glycero- α -D-galacto-2-nonulopyranosylonate) (37). A suspension of **35** (1.99 g, 5.40 mmol), **3**²² (6.49 g, 10.8 mmol) and MS 3 Å (11.4 g) in dry MeCN (39 mL) was cooled to –40 °C under argon. Then, *N*-iodosuccinimide (4.89 g, 21.7 mmol) was added, followed by dropwise addition of TfOH (195 μ L, 2.2 mmol). After stirring at –40 °C for 6 h, the mixture was neutralized with Et₃N, warmed to rt, filtered over celite and concentrated under reduced pressure. The residue was dissolved in DCM (40 mL) and washed with 1 M aq. Na₂S₂O₃ (2 × 30 mL) and H₂O (3 × 30 mL). The organic layer was dried over Na₂SO₄, filtered and concentrated in vacuo. The crude product was purified by flash column chromatography on silica (toluene/acetone, 3:1 to 1:3) to afford **37** (3.69 g, 81%) as a pale brown solid. $[\alpha]_D^{20} = -5.6$ ($c = 1.6$, CHCl₃); ¹H NMR (500 MHz, CDCl₃): $\delta = 7.66$ –7.62 (m, 4H, Ar–H), 7.44–7.35 (m, 6H, Ar–H), 5.38 (dd, $J = 2.6,$

5.5, 8.2 Hz, 1H, H-8'), 5.32 (dd, $J=1.8, 8.4$ Hz, 1H, H-7'), 5.07 (d, $J=9.4$ Hz, 1H, NH), 4.82 (ddd, $J=4.6, 9.7, 12.4$ Hz, 1H, H-4'), 4.30 (dd, $J=2.6, 12.4$ Hz, 1H, H-9'a), 4.14–4.04 (m, 3H, H-5', H-6', H-9'b), 3.73 (s, 3H, OMe), 3.69 (m, 1H, H-3), 3.48 (dd, $J=5.5, 9.8$ Hz, 1H, CH₂O), 3.41 (dd, $J=6.4, 9.8$ Hz, 1H, CH₂O), 2.60 (dd, $J=4.6, 12.7$ Hz, 1H, H-3'e), 2.17, 2.14 (2 s, 6H, 2 OAc), 2.07–2.00 (m, 7H, H-4e, 2 OAc), 1.94 (t, $J=12.5$ Hz, 1H, H-3'a), 1.88 (s, 3H, NHAc), 1.82–1.73 (m, 2H, H-2e, H-5e), 1.61 (m, 2H, H-1, H-6e), 1.39 (tq, $J=2.6, 13.3$ Hz, 1H, H-5a), 1.23 (m, 1H, H-4a), 1.04 (s, 9H, C(CH₃)₃), 0.99 (m, 1H, H-2a), 0.82 ppm (dq, $J=3.2, 12.7$ Hz, 1H, H-6a); ¹³C NMR (126 MHz, CDCl₃): $\delta=171.2, 170.8, 170.4, 170.3, 170.1, 169.2$ (6 C=O), 135.7, 133.98, 133.95, 129.6, 127.7 (12 C, Ar-C), 98.8 (C-2'), 74.7 (C-3), 72.6 (C-6'), 69.4 (C-4'), 68.9 (C-8'), 68.8 (CH₂O), 67.6 (C-7'), 62.6 (C-9'), 52.6 (OMe), 49.5 (C-5'), 39.6 (C-1), 38.7 (C-3'), 36.6 (C-2), 35.2 (C-4), 28.4 (C-6), 27.0 (3 C, C(CH₃)₃), 23.7 (C-5), 23.3 (NHAc), 21.2, 20.97, 20.95, 20.88 (4 OAc), 19.4 ppm (C(CH₃)₃); MS (ESI): m/z calcd for C₄₃H₅₉NO₁₄S: 864.4 [M + Na]⁺; found: 864.2.

(15,3R)-3-(Hydroxymethyl)cyclohexyl (methyl 5-acetamido-4,7,8,9-tetra-O-acetyl-3,5-dideoxy-D-glycero- α -D-galacto-2-nonulopyranosylonate) (38). Compound **37** (201 mg, 0.239 mmol) was dissolved in pyridine (6.5 mL) in a Teflon container under argon at 0 °C. Then, HF-pyr (1.20 mL, 13.3 mmol) was added dropwise and the mixture was stirred at 0 °C for 5 h. The reaction mixture was neutralized with satd aq. NaHCO₃ and the aqueous phase was extracted with DCM (3 × 30 mL). The combined organic layers were dried over Na₂SO₄, filtered and concentrated in vacuo. The residue was purified by flash column chromatography on silica (toluene/acetone, 3:1 to 1:3) to give **38** (127 mg, 88%) as a pale brown solid. [α]_D²⁰ = -9.5 ($c=1.0$, CHCl₃); ¹H NMR (500 MHz, CDCl₃): $\delta=5.37$ (ddd, $J=2.6, 5.9, 8.4$ Hz, 1H, H-8'), 5.31 (m, 1H, H-7'), 5.12 (br d, $J=9.5$ Hz, 1H, NH), 4.83 (ddd, $J=4.6, 9.9, 12.3$ Hz, 1H, H-4'), 4.33 (dd, $J=2.5, 12.4$ Hz, 1H, H-9'a), 4.12–4.01 (m, 3H, H-5', H-6', H-9'b), 3.79 (s, 3H, OMe), 3.75 (m, 1H, H-3), 3.49 (m, 1H, CH₂O), 3.40 (m, 1H, CH₂O), 2.58 (dd, $J=4.6, 12.8$ Hz, 1H, H-3'e), 2.15, 2.14, 2.04, 2.02 (4 s, 12H, 4 OAc), 2.03 (m, 1H, H-4e), 1.95 (t, $J=12.5$ Hz, 1H, H-3'a), 1.88 (s, 3H, NHAc), 1.82–1.76 (m, 2H, H-2e, H-5e), 1.64 (br d, $J=12.4$ Hz, 1H, H-6e), 1.55 (t, $J=5.9$ Hz, 1H, H-1), 1.40 (tq, $J=3.6, 13.4$ Hz, 1H, H-5a), 1.25 (dq, $J=3.8, 12.7$ Hz, 1H, H-4a), 0.94 (q, $J=11.8$ Hz, 1H, H-2a), 0.82 ppm (dq, $J=3.8, 12.6$ Hz, 1H, H-6a); ¹³C NMR (126 MHz, CDCl₃): $\delta=171.0, 170.8, 170.3, 170.22, 170.17, 169.0$ (6 C=O), 98.5 (C-2'), 74.0 (C-3), 72.5 (C-6'), 69.2 (C-4'), 68.8 (C-8'), 68.0 (CH₂O), 67.4 (C-7'), 62.5 (C-9'), 52.7 (OMe), 49.5 (C-5'), 39.5 (C-1), 38.3 (C-3'), 36.2 (C-2), 34.8 (C-4), 28.3 (C-6), 23.5 (C-5), 23.2 (NHAc), 21.2, 20.88, 20.86, 20.8 ppm (4 OAc); MS (ESI): m/z calcd for C₂₇H₄₁NO₁₄: 626.2 [M + Na]⁺; found: 626.3.

(15,3R)-3-(Sulfonatooxymethyl)cyclohexyl (methyl 5-acetamido-4,7,8,9-tetra-O-acetyl-3,5-dideoxy-D-glycero- α -D-galacto-2-nonulopyranosylonate) sodium salt (39). To a solution of **38** (148 mg, 0.246 mmol) in dry DMF (12 mL) was added SO₃·pyr (391 mg, 2.46 mmol) under argon and the mixture was stirred at rt for 2 h. Solid NaHCO₃ was added to the solution, which was stirred vigorously for 10 min. Then, the suspension was filtered, and the solvents were removed via co-evaporation with toluene. The residue was purified by flash column chromatography on silica (DCM/MeOH, 1:0 to 7:3) to yield **39** (147 mg, 85%) as a pale white solid. [α]_D²⁰ = 0.0 ($c=1.0$, MeOH); ¹H NMR (500 MHz, CD₃OD): $\delta=5.39$ (ddd, $J=2.6, 5.4, 8.3$ Hz, 1H, H-8'), 5.32 (dd, $J=2.2, 9.1$ Hz, H-7'), 4.77 (ddd, $J=4.5, 10.5, 12.1$ Hz, 1H, H-4'), 4.30 (dd, $J=2.5, 12.4$ Hz, 1H, H-9'a), 4.12 (dd, $J=2.1, 10.8$ Hz, 1H, H-6'), 4.04 (dd, $J=5.5, 12.4$ Hz, 1H, H-9'b), 3.94 (t, $J=10.5$ Hz, 1H, H-5'), 3.86–3.71 (m, 3H, H-3, CH₂O), 3.82 (s, 3H, OMe), 2.62 (dd, $J=4.6, 12.6$ Hz, 1H, H-3'e), 2.15, 2.11 (2 s, 6H, 2 OAc), 2.03 (m, 1H, H-4e), 2.00, 1.97 (2 s, 6H, 2 OAc), 1.83 (s, 3H, NHAc), 1.75 (m, 3H, H-3'a, H-5e, H-2e), 1.67 (m, 2H, H-1, H-6e), 1.46 (qt, $J=3.0, 13.0$ Hz, 1H, H-5a), 1.20 (m, 1H, H-4a), 1.02–0.81 ppm (m, 2H, H-2a, H-6a); ¹³C NMR (126 MHz, CD₃OD): $\delta=173.5,$

172.4, 171.8, 171.64, 171.58, 170.1 (6 C=O), 99.9 (C-2'), 75.9 (C-3), 73.5 (CH₂O), 73.1 (C-6'), 70.8 (C-4'), 69.4 (C-8'), 68.7 (C-7'), 63.5 (C-9'), 53.2 (OMe), 50.1 (C-5'), 39.6 (C-3'), 38.0 (C-1), 37.4 (C-2), 36.1 (C-4), 29.4 (C-6), 24.5 (C-5), 22.7 (NHAc), 21.3, 20.8, 20.70, 20.65 ppm (4 OAc); MS (ESI): m/z calcd for C₂₇H₄₀NNaO₁₇S: 682.2 [M-Na]⁺; found: 682.3.

(15,3R)-3-(Sulfonatooxymethyl)cyclohexyl (sodium 5-acetamido-3,5-dideoxy-D-glycero- α -D-galacto-2-nonulopyranosylonate) sodium salt (29). Compound **39** (416 mg, 0.590 mmol) was dissolved in 0.1 M NaOH (19 mL) and the mixture was stirred at rt overnight. The solution was neutralized with 1 M HCl and concentrated in vacuo. The residue was purified by size-exclusion chromatography (P-2 gel, H₂O) to afford **29** (266 mg, 83%) as a white solid. [α]_D²⁰ = +18.3 ($c=0.2$, H₂O); ¹H NMR (500 MHz, D₂O): $\delta=3.96$ –3.78 (m, 6H, H-3, H-5', H-7', H-9'a, CH₂O), 3.71–3.59 (m, 4H, H-4', H-6', H-8', H-9'b), 2.77 (dd, $J=4.7, 12.4$ Hz, 1H, H-3'e), 2.07 (m, 1H, H-4e), 2.05 (s, 3H, NHAc), 1.92 (m, 1H, H-2e), 1.85–1.72 (m, 2H, H-1, H-5e), 1.70 (m, 1H, H-6e), 1.65 (t, $J=12.1$ Hz, 1H, H-3'a), 1.39–1.19 (m, 2H, H-4a, H-5a), 1.05 (q, $J=11.9$ Hz, 1H, H-2a), 0.92 ppm (dq, $J=3.7, 12.6$ Hz, 1H, H-6a); ¹³C NMR (126 MHz, D₂O): $\delta=176.0, 174.8$ (2 C=O), 102.0 (C-2'), 75.8 (C-3), 74.5 (CH₂O), 73.7, 73.0, 69.3 (C-4', C-6', C-7'), 69.0 (C-8'), 63.4 (C-9'), 52.8 (C-5'), 42.1 (C-3'), 37.1 (C-1), 36.6 (C-2), 35.2 (C-4), 28.5 (C-6), 24.2 (C-5), 23.0 ppm (NHAc); HRMS (ESI): m/z calcd for C₁₈H₂₉NNaO₁₃S: 568.1053 [M + Na]⁺; found: 568.1048.

p-Tolyl (methyl 5-acetamido-2,3,5-trideoxy-2-thio-D-glycero- β -D-galacto-2-nonulopyranosylonate) (40). To a solution of **3**^[42] (2.00 g, 3.35 mmol) in dry MeOH (60 mL) was added NaOMe (25% w/v, 70 μ L, 0.33 mmol) under argon and the solution was stirred at rt for 16 h. The mixture was neutralized with Amberlyst-15 and filtered over a pad of celite. The celite was washed with MeOH and the solvent was evaporated. The crude product was purified by flash column chromatography on silica (DCM/MeOH, 1:0 to 85:15) to give **40** (1.20 g, 83%) as an orange oil. [α]_D²⁰ = -27.7 ($c=0.13$, MeOH); ¹H NMR (500 MHz, CD₃OD): $\delta=7.46$ (d, $J=8.1$ Hz, 2H, Ar-H), 7.17 (d, $J=8.0$ Hz, 2H, Ar-H), 4.50 (dd, $J=0.8, 10.5$ Hz, 1H, H-6), 4.10 (m, 1H, H-4), 3.89 (t, $J=10.3$ Hz, 1H, H-5), 3.82 (m, 1H, H-9a), 3.78 (m, 1H, H-8), 3.66 (m, 1H, H-9b), 3.55 (m, 1H, H-7), 3.52 (s, 3H, OMe), 2.67 (dd, $J=4.7, 13.6$ Hz, 1H, H-3e), 2.33 (s, 3H, CH₃), 2.03 (s, 3H, NHAc), 1.94 ppm (dd, $J=11.7, 13.6$ Hz, 1H, H-3a); ¹³C NMR (126 MHz, CD₃OD): $\delta=173.5, 171.4$ (2 C=O), 141.1, 137.4, 130.7, 127.8 (6 C, Ar-C), 94.5 (C-2), 73.3 (C-6), 71.2 (C-8), 70.6 (C-7), 68.1 (C-4), 65.1 (C-9), 54.0 (C-5), 53.0 (OMe), 42.1 (C-3), 22.8 (NHAc), 21.4 ppm (CH₃); MS (ESI): m/z calcd for C₁₉H₂₇NO₈S: 452.2 [M + Na]⁺; found: 452.2.

p-Tolyl (methyl 5-acetamido-2,3,5-trideoxy-2-thio-9-O-tosyl-D-glycero- β -D-galacto-2-nonulopyranosylonate) (41). To a solution of **40** (1.90 g, 4.42 mmol) in dry pyridine was added tosyl chloride (1.01 g, 5.31 mmol) at 0 °C under argon. The reaction mixture was stirred at rt for 16 h. Then, MeOH was added and the mixture was stirred for 30 min. The solvents were evaporated under reduced pressure and the crude product was purified by flash column chromatography on silica (DCM/MeOH, 1:0 to 9:1) to give **41** (0.904 g, 35%). [α]_D²⁰ = -6.4 ($c=0.08$, CHCl₃); ¹H NMR (500 MHz, CDCl₃): $\delta=7.77$ (d, $J=8.3$ Hz, 2H, Ar-H), 7.34–7.31 (m, 4H, Ar-H), 7.11 (d, $J=8.0$ Hz, 2H, Ar-H), 4.62 (d, $J=7.1$ Hz, 1H, NH), 4.33–4.28 (m, 2H, H-6, H-9a), 4.14 (m, 1H, H-4), 4.09 (m, 1H, H-9b), 3.95 (m, 1H, H-8), 3.85 (m, 1H, H-5), 3.55 (m, 1H, H-7), 3.50 (s, 3H, OMe), 2.72 (dd, $J=4.6, 13.8$ Hz, 1H, H-3e), 2.34, 2.33 (2 s, 6H, 2 CH₃), 2.07 (s, 3H, NHAc), 1.98 ppm (m, 1H, H-3a); ¹³C NMR (126 MHz, CDCl₃): $\delta=173.6, 168.9$ (2 C=O), 145.2, 140.2, 135.7, 132.6, 130.1, 130.0, 128.2, 126.1 (12 C, Ar-C), 89.6 (C-2), 72.7 (C-9), 72.4 (C-6), 69.1 (C-7), 68.7 (C-8), 67.8 (C-4), 53.7 (C-5), 52.7 (OMe), 41.1 (C-3), 23.4 (NHAc), 21.8, 21.4 ppm (2 CH₃); MS (ESI): m/z calcd for C₂₆H₃₃NO₁₅S₂: 606.2 [M + Na]⁺; found: 606.0.

p-Tolyl (methyl 5-acetamido-9-azido-2,3,5,9-tetraoxy-2-thio-D-glycero-β-D-galacto-2-nonulopyranosylonate) (42). To a solution of **41** (570 mg, 0.98 mmol) in dry DMF (15 mL) were added Na₂S₂O₃ (313 mg, 4.82 mmol) and 15-crown-5 (0.1 mL, 0.49 mmol). The reaction mixture was stirred under argon at 60 °C for 16 h. The suspension was filtered through a pad of celite and the celite was washed with MeOH. The solvents were removed by co-evaporation with *n*-heptane and the crude product was purified by flash column chromatography on silica (DCM/MeOH, 1:0 to 9:1) to afford **42** (422 mg, 96%) as a white solid. [α]_D²⁰ = -141 (*c* = 0.33, MeOH); ¹H NMR (500 MHz, CD₃OD): δ = 7.42 (d, *J* = 8.1 Hz, 2H, Ar-H), 7.18 (d, *J* = 7.9 Hz, 2H, Ar-H), 4.44 (d, *J* = 10.5, 1H, H-6), 4.11 (m, 1H, H-4), 3.91–3.84 (m, 2H, H-5, H-8), 3.61–3.56 (m, 2H, H-7, H-9a), 3.54 (s, 3H, OMe), 3.41 (m, 1H, H-9b), 2.66 (dd, *J* = 4.7, 13.6 Hz, 1H, H-3e), 2.34 (s, 3H, CH₃), 2.04 (s, 3H, NHAc), 1.93 ppm (dd, *J* = 11.6, 13.7 Hz, 1H, H-3a); ¹³C NMR (126 MHz, CD₃OD): δ = 174.8, 170.8 (2 C=O), 141.2, 137.4, 130.8, 127.7 (6 C, Ar-C), 91.3 (C-2), 73.3 (C-6), 71.3 (C-7), 70.6 (C-8), 68.0 (C-4), 55.7 (C-9), 54.1 (C-5), 53.0 (OMe), 42.0 (C-3), 22.8 (NHAc), 21.3 ppm (CH₃); MS (ESI): *m/z* calcd for C₁₉H₂₆N₄O₅S: 477.2 [*M* + Na]⁺; found: 477.2.

p-Tolyl (methyl 5-acetamido-4,7,8-tri-O-acetyl-9-azido-2,3,5,9-tetraoxy-2-thio-D-glycero-β-D-galacto-2-nonulopyranosylonate) (43). A solution of **42** (330 mg, 0.73 mmol) in dry pyridine (3.2 mL) was cooled to 0 °C. Then, DMAP (15.4 mg, 0.13 mmol) and Ac₂O (1.6 mL, 16.7 mmol) were added. The reaction mixture was stirred at rt for 6 h under argon. The volatiles were co-evaporated with toluene and the crude product was purified by flash column chromatography on silica (DCM/MeOH, 1:0 to 96:4) to yield **43** (392 mg, 93%) as a white solid. [α]_D²⁰ = -89.4 (*c* = 0.23, CHCl₃); ¹H NMR (500 MHz, CDCl₃): δ = 7.30 (d, *J* = 8.1 Hz, 2H, Ar-H), 7.19 (d, *J* = 7.9 Hz, 2H, Ar-H), 5.49 (d, *J* = 10.2 Hz, 1H, NH), 5.43 (m, 1H, H-7), 5.37 (m, 1H, H-4), 4.76 (m, 1H, H-8), 4.58 (dd, *J* = 2.4, 10.5 Hz, 1H, H-6), 4.12 (m, 1H, H-5), 3.68 (s, 3H, OMe), 3.63 (dd, *J* = 2.4, 13.4 Hz, 1H, H-9a), 3.31 (dd, *J* = 9.4, 13.4 Hz, 1H, H-9b), 2.67 (dd, *J* = 4.8, 13.8 Hz, 1H, H-3e), 2.35 (s, 3H, CH₃), 2.15–2.10 (m, 4H, H-3a, OAc), 2.09, 2.04 (2 s, 6H, 2 OAc), 1.90 ppm (s, 3H, NHAc); ¹³C NMR (126 MHz, CDCl₃): δ = 171.5, 171.3, 170.7, 170.6, 168.6 (5 C=O), 141.2, 136.3, 130.5, 124.8 (6 C, Ar-C), 88.8 (C-2), 74.9 (C-8), 73.3 (C-6), 69.2 (C-4), 69.1 (C-7), 53.1 (OMe), 50.0 (C-9), 49.6 (C-5), 37.5 (H-3), 23.5 (NHAc), 21.6 (CH₃), 21.4, 21.2, 21.1 ppm (3 OAc); MS (ESI): *m/z* calcd for C₂₅H₃₂N₄O₁₀S: 603.2 [*M* + Na]⁺; found: 603.0.

(1S,3R)-3-(tert-Butyldiphenylsilyloxymethyl)cyclohexyl (methyl 5-acetamido-4,7,8-tri-O-acetyl-9-azido-3,5,9-trideoxy-D-glycero-α-D-galacto-2-nonulopyranosylonate) (44). A suspension of **43** (340 mg, 0.57 mmol), **35** (320 mg, 0.88 mmol) and MS 3 Å (620 mg) in dry MeCN (6 mL) was cooled to -40 °C under argon. Then, *N*-iodosuccinimide (1.53 g, 6.79 mmol) was added, followed by dropwise addition of TfOH (60 μL, 0.68 mmol). After stirring at -40 °C for 4 h, the mixture was neutralized with Et₃N, warmed to rt, filtered over celite and concentrated under reduced pressure. The residue was dissolved in DCM (20 mL) and washed with 1 M Na₂S₂O₃ (4 × 10 mL) and H₂O (2 × 10 mL). The organic layer was dried over Na₂SO₄, filtered and concentrated in vacuo. The crude product was purified by flash column chromatography on silica (toluene/acetone, 1:0 to 6:4) to afford **44** (110 mg, 25%). [α]_D²⁰ = -1.2 (*c* = 0.29, CHCl₃); ¹H NMR (500 MHz, CDCl₃): δ = 7.66–7.60 (m, 4H, Ar-H), 7.42–7.35 (m, 6H, Ar-H), 5.33–5.26 (m, 2H, H-6', H-8'), 5.21 (d, *J* = 10.1 Hz, 1H, NH), 4.81 (m, 1H, H-4'), 4.11 (m, 1H, H-5'), 4.01 (m, 1H, H-7'), 3.75 (s, 3H, OMe), 3.71 (m, 1H, H-3), 3.61 (dd, *J* = 2.9, 13.5 Hz, 1H, H-9'a), 3.45–3.39 (m, 2H, OCH₂), 3.28 (dd, *J* = 6.4, 13.5 Hz, 1H, H-9'b), 2.62 (dd, *J* = 4.6, 12.7 Hz, 1H, H-3'e), 2.18, 2.16, 2.02 (3 OAc), 2.00 (m, 1H, H-4e), 1.93 (t, *J* = 12.5 Hz, 1H, H-3'a), 1.87 (s, 3H, NHAc), 1.81–1.74 (m, 2H, H-2e, H-5e), 1.62–1.56 (m, 2H, H-1, H-6e), 1.40 (m, 1H, H-5a), 1.25 (m, 1H, H-4a), 1.04 (s, 9H, C(CH₃)₃), 0.99 (m, 1H, H-2a), 0.82 ppm (m, 1H, H-6a); ¹³C NMR (126 MHz, CDCl₃): δ = 171.5,

170.67, 170.66, 170.5 (5 C, 5 C=O), 135.8, 134.0, 129.8, 127.9 (12 C, Ar-C), 98.9 (C-2'), 74.7 (C-3'), 73.1 (C-7'), 70.5 (C-6'), 69.3 (C-4'), 68.8 (CH₂O), 68.3 (C-8'), 53.0 (OMe), 51.0 (C-9'), 49.5 (C-5'), 39.7 (C-1), 38.7 (C-3'), 36.7 (C-2'), 35.4 (C-4), 28.5 (C-6), 27.1 (3 C, C(CH₃)₃), 23.5 (C-5), 23.5 (NHAc), 21.4, 21.24, 21.22 (3 OAc), 19.6 ppm (C(CH₃)₃); MS (ESI): *m/z* calcd for C₄₁H₅₆N₄O₁₂Si: 847.4 [*M* + Na]⁺; found: 847.2.

(1S,3R)-3-(Hydroxymethyl)cyclohexyl (methyl 5-acetamido-4,7,8-tri-O-acetyl-9-azido-3,5,9-trideoxy-D-glycero-α-D-galacto-2-nonulopyranosylonate) (45). To a solution of **44** (110 mg, 0.13 mmol) in dry pyridine (3.8 mL) was added HF-pyr (0.75 mL) dropwise at 0 °C under argon and the reaction mixture was stirred at rt for 5 h. The reaction mixture was neutralized with satd aq. NaHCO₃. The aqueous phase was extracted with DCM (3 × 20 mL), and the combined organic layers were dried over Na₂SO₄, filtered and evaporated. The crude product was purified by flash column chromatography on silica (toluene/acetone, 1:0 to 1:1) to afford **45** (71.4 mg, 91%). [α]_D²⁰ = -35.6 (*c* = 0.73, CHCl₃); ¹H NMR (500 MHz, CDCl₃): δ = 5.32–5.26 (m, 2H, H-6', H-8'), 5.12 (d, *J* = 10.0 Hz, 1H, NH), 4.82 (m, 1H, H-4'), 4.09 (m, 1H, H-5'), 4.02 (m, 1H, H-7'), 3.81 (s, 3H, OMe), 3.75 (m, 1H, H-3), 3.58 (dd, *J* = 2.9, 13.5 Hz, 1H, H-9'a), 3.51–3.38 (m, 2H, CH₂O), 3.28 (m, 1H, H-9'b), 2.60 (dd, *J* = 4.6, 12.7 Hz, 1H, H-3'b), 2.18, 2.17 (2 s, 6H, 2 OAc), 2.03–2.01 (m, 4H, H-4, OAc), 1.94 (t, *J* = 12.6 Hz, 1H, H-3'a), 1.88 (s, 3H, NHAc), 1.80 (m, 1H, H-5e), 1.75 (m, 1H, H-2e), 1.66 (m, 1H, H-6e), 1.42 (m, 1H, H-1), 1.37 (m, 1H, H-5a), 1.29 (m, 1H, H-4a), 0.95 (m, 1H, H-2a), 0.88 ppm (m, 1H, H-6a); ¹³C NMR (126 MHz, CDCl₃): δ = 170.8, 170.52, 170.51, 170.46, 170.3 (5 C=O), 98.5 (C-2'), 74.1 (C-3'), 72.9 (C-7'), 70.1 (C-6'), 69.1 (C-4'), 68.0 (CH₂O), 67.9 (C-8'), 52.9 (OMe), 50.9 (C-9'), 49.4 (C-5'), 39.5 (C-1), 38.5 (C-3'), 36.1 (C-2), 34.9 (C-4), 28.3 (C-6), 23.6 (C-5), 23.4 (NHAc), 21.3, 21.2, 21.1 ppm (3 OAc); MS (ESI): *m/z* calcd for C₂₅H₃₈N₄O₁₂: 609.3 [*M* + Na]⁺; found: 609.0.

(1S,3R)-3-(Sulfonatooxymethyl)cyclohexyl (methyl 5-acetamido-4,7,8-tri-O-acetyl-9-azido-3,5,9-trideoxy-D-glycero-α-D-galacto-2-nonulopyranosylonate) sodium salt (46). To a solution of **45** (65.0 mg, 0.11 mmol) in dry DMF (7 mL) was added SO₃pyr (176 mg, 1.11 mmol) and the reaction mixture was stirred under argon for 2 h at rt. Then, the reaction was quenched by the addition of solid NaHCO₃ and stirred vigorously for 10 min. The suspension was filtered, and the filtrate was co-evaporated with toluene. The crude product was purified by flash column chromatography on silica (DCM/MeOH, 1:0 to 4:1) to give **46** (75.6 mg, 99%). [α]_D²⁰ = +10.3 (*c* = 0.47, MeOH); ¹H NMR (500 MHz, CD₃OD): δ = 5.19 (s, 2H, H-7', H-8'), 4.64 (m, 1H, H-4'), 3.98 (d, *J* = 10.8 Hz, 1H, H-6'), 3.80 (t, *J* = 10.5 Hz, 1H, H-5'), 3.70 (s, 3H, OMe), 3.70–3.60 (m, 3H, H-3, CH₂O), 3.47 (d, *J* = 13.3 Hz, 1H, H-9'a), 3.14 (m, 1H, H-9'b), 2.50 (dd, *J* = 4.4, 12.6 Hz, 1H, H-3'e), 2.05, 1.99 (2 s, 6H, 2 OAc), 1.88 (m, 1H, H-4e), 1.85 (s, 3H, OAc), 1.70 (s, 3H, NHAc), 1.64–1.59 (m, 3H, H-2e, H-5e, H-3'a), 1.56–1.51 (m, 2H, H-1, H-6e), 1.37 (m, 1H, H-5a), 1.08 (m, 1H, H-4a), 0.83 (m, 1H, H-2a), 0.75 ppm (m, 1H, H-6a); ¹³C NMR (126 MHz, CD₃OD): δ = 173.6, 171.7, 171.5, 170.1 (5 C, 5 C=O), 99.9 (C-2'), 74.9 (C-3'), 73.5 (C-6'), 73.3 (CH₂O), 70.7 (C-4'), 70.5 (C-7'), 69.3 (C-8'), 53.3 (OMe), 52.0 (C-9'), 50.0 (C-5'), 39.5 (C-3'), 38.0 (C-1), 37.4 (C-2), 36.1 (C-4), 29.4 (C-6), 24.5 (C-5), 22.7 (NHAc), 21.3, 21.0, 20.8 ppm (3 OAc); MS (ESI): *m/z* calcd for C₂₅H₃₇N₄NaO₁₅S: 711.2 [*M* + Na]⁺; found: 711.1.

(1S,3R)-3-(Sulfonatooxymethyl)cyclohexyl (sodium 5-acetamido-9-azido-3,5,9-trideoxy-D-glycero-α-D-galacto-2-nonulopyranosylonate) sodium salt (47). Compound **46** (79.2 mg, 0.12 mmol) was treated with 0.1 M NaOH (11.5 mL, 1.15 mmol) at rt for 6 h. Then, the reaction mixture was neutralized with Amberlyst-15 (to pH 7), the suspension was filtered, and the solvent was evaporated. The crude product was purified by flash column chromatography on silica (DCM/MeOH, 1:0 to 1:1) and size-exclusion chromatography (P-2 gel, H₂O) to afford **47** (54.1 mg, 82%) as a white solid. [α]_D²⁰ = +25.4 (*c* = 1.00, H₂O); ¹H NMR (500 MHz, D₂O): δ = 3.97–3.79 (m, 4H,

H-3, CH₂O, H-8'), 3.75–3.58 (m, 4H, H-4', H-5', H-6', H-9'a), 3.54 (m, 1H, H-7'), 3.45 (m, 1H, H-9'b), 2.73 (m, 1H, H-3'e), 2.10–1.96 (m, 4H, H-4, NHAc), 1.89 (m, 1H, H-2e), 1.83–1.69 (m, 2H, H-1, H-5e), 1.69–1.54 (m, 2H, H-6, H-3'a), 1.36–1.14 (m, 2H, H-4a, H-5a), 1.02 (m, 1H, H-2a), 0.89 ppm (m, 1H, H-6a); ¹³C NMR (126 MHz, D₂O): δ = 176.1, 174.7 (2 C=O), 102.2 (C-2'), 75.9 (C-3), 74.5 (CH₂O), 73.7 (C-4'), 71.8 (C-8'), 70.0 (C-7'), 69.5 (C-6'), 54.1 (C-9'), 53.0 (C-5'), 42.4 (C-3'), 37.4 (C-1), 36.8 (C-2), 35.5 (C-4), 28.8 (C-6), 24.4 (C-5), 23.1 ppm (NHAc); MS (ESI): *m/z* calcd for C₁₈H₂₈N₄Na₂O₁₂S: 593.1 [M+Na]⁺; found: 593.2.

(15,3R)-3-(Sulfonatoxyethyl)cyclohexyl (sodium 5-acetamido-9-amino-3,5,9-trideoxy-D-glycero-α-D-galacto-2-nonulopyranosylonate) sodium salt (48). To a solution of **47** (38.3 mg, 0.07 mmol) in water (1.7 mL) was added Pd(OH)₂C (10% Pd, 20.8 mg). The reaction mixture was hydrogenated at rt for 16 h (1 atm H₂). Then, the suspension was filtered over a pad of celite and the celite was washed with water. The solvent was evaporated, and the crude product was purified by size-exclusion chromatography (P-2 gel, H₂O) to afford **48** (31.1 mg, 85%) as a white solid. [α]_D²⁰ = +13.4 (c = 0.50, H₂O); ¹H NMR (500 MHz, D₂O): δ = 3.86 (m, 1H, H-8'), 3.76–3.66 (m, 3H, H-3, CH₂O), 3.61 (m, 1H, H-5'), 3.53–3.41 (m, 2H, H-4', H-6'), 3.36 (m, 1H, H-7'), 3.22 (m, 1H, H-9'a), 2.81 (m, 1H, H-9'b), 2.57 (dd, *J* = 4.5, 12.4 Hz, 1H, H-3'e), 1.89–1.82 (m, 4H, H-4e, NHAc), 1.75 (m, 1H, H-2e), 1.66–1.54 (m, 2H, H-1, H-5e), 1.53–1.44 (m, 2H, H-6e, H-3'a), 1.18–1.01 (m, 2H, H-4a, H-5a), 0.85 (m, 1H, H-2a), 0.73 ppm (m, 1H, H-6a); ¹³C NMR (126 MHz, D₂O): δ = 176.1, 174.9 (2 C=O), 102.0 (C-2'), 75.6 (C-3), 74.5 (CH₂O), 73.4 (C-4'), 71.1 (C-7'), 69.2 (2 C, C-6', C-8'), 52.7 (C-5'), 43.1 (C-9'), 41.8 (C-3'), 37.2 (C-1), 36.7 (C-2), 35.2 (C-4), 29.5 (C-6), 24.3 (C-5), 23.0 ppm (NHAc); MS (ESI): *m/z* calcd for C₁₈H₃₀N₄Na₂O₁₂S: 567.1 [M+Na]⁺; found: 567.3.

(15,3R)-3-(Sulfonatoxyethyl)cyclohexyl (sodium 5-acetamido-9-benzamido-3,5,9-trideoxy-D-glycero-α-D-galacto-2-nonulopyranosylonate) sodium salt (49). A solution of benzoic acid (10.3 mg, 0.084 mmol), HATU (23.3 mg, 0.061 mmol) and DIPEA (20 μL, 0.115 mmol) in dry DMF (0.5 mL) was stirred for 10 min and then added to a solution of **48** (21.0 mg, 0.039 mmol) in dry DMF (0.5 mL) under argon. The resulting mixture was stirred at rt for 6 h. The solvent was removed in vacuo and the residue was purified by flash chromatography on silica [DCM/(MeOH/H₂O, 10:1), 1:0 to 1:1] and size-exclusion chromatography (P-2 gel, H₂O) to give **49** (18.0 mg, 72%). [α]_D²⁰ = +39.6 (c = 1.00, H₂O); ¹H NMR (500 MHz, D₂O): δ = 7.80–7.76 (m, 2H, Ar-H), 7.63 (m, 1H, Ar-H), 7.57–7.52 (m, 2H, Ar-H), 4.03 (ddd, *J* = 3.0, 7.6, 8.9 Hz, 1H, H-8'), 3.93–3.85 (m, 3H, H-3, CH₂O), 3.85–3.77 (m, 2H, H-5', H-9'a), 3.73 (dd, *J* = 2.0, 10.4 Hz, 1H, H-6'), 3.66 (ddd, *J* = 4.6, 9.8, 11.9 Hz, 1H, H-4'), 3.57 (m, 2H, H-7', H-9'b), 2.75 (dd, *J* = 4.7, 12.4 Hz, 1H, H-3'e), 2.07 (m, 1H, H-4e), 2.01 (s, 3H, NHAc), 1.90 (m, 1H, H-2e), 1.79–1.68 (m, 2H, H-1, H-5e), 1.68–1.60 (m, 2H, H-6e, H-3'a), 1.29–1.17 (m, 2H, H-4a, H-5a), 1.03 (q, *J* = 12.1 Hz, 1H, H-2a), 0.88 ppm (qd, *J* = 3.8, 12.7 Hz, 1H, H-6a); ¹³C NMR (126 MHz, D₂O): δ = 176.0, 174.8, 172.2 (3 C=O), 134.7, 133.0, 129.7, 128.0 (6 C, Ar-C), 102.0 (C-2'), 75.8 (C-3), 74.4 (CH₂O), 73.6 (C-6'), 71.6 (C-8'), 70.8 (C-7'), 69.2 (C-4'), 52.8 (C-5'), 43.5 (C-9'), 42.0 (C-3'), 37.1 (C-1), 36.5 (C-2), 35.3 (C-4), 28.5 (C-6), 24.2 (C-5), 22.9 ppm (NHAc); HRMS (ESI): *m/z* calcd for C₂₅H₃₄N₄Na₂O₁₃S: 671.1469 [M+Na]⁺; found: 671.1468.

(15,3R)-3-(Sulfonatoxyethyl)cyclohexyl (sodium 5-acetamido-3,5,9-trideoxy-9-(naphthalene-2-sulfonamido)-D-glycero-α-D-galacto-2-nonulopyranosylonate) sodium salt (50). Compound **48** (20.6 mg, 0.038 mmol), NaHCO₃ (15.1 mg, 0.180 mmol) and 2-naphthalenesulfonyl chloride (10.1 mg, 0.045 mmol) were dissolved in DMF/H₂O (2:1, 1.8 mL) and the solution was stirred at rt for 5 h. The solution was neutralized with aq. HCl and evaporated to dryness. The residue was purified by flash chromatography on silica [DCM/(MeOH/H₂O, 10:1), 8:2 to 6:4] and size-exclusion chromatography (P-2 gel, H₂O) to afford **50** (11.7 mg, 42%). [α]_D²⁰ = +21.5 (c =

0.50, H₂O); ¹H NMR (600 MHz, D₂O): δ = 8.52 (d, *J* = 1.9 Hz, 1H, Ar-H), 8.12 (d, *J* = 8.8 Hz, 1H, Ar-H), 8.09 (d, *J* = 8.1 Hz, 1H, Ar-H), 8.03 (d, *J* = 8.1 Hz, 1H, Ar-H), 7.85 (dd, *J* = 2.0, 8.7 Hz, 1H, Ar-H), 7.73 (m, 1H, Ar-H), 7.69 (m, 1H, Ar-H), 3.77–3.72 (m, 2H, CH₂O), 3.72–3.66 (m, 2H, H-5', H-8'), 3.63–3.53 (m, 3H, H-3, H-4', H-6'), 3.47–3.42 (m, 2H, H-7', H-9'a), 3.09 (dd, *J* = 8.0, 14.2 Hz, 1H, H-9'b), 2.64 (dd, *J* = 4.6, 12.4 Hz, 1H, H-3'e), 1.97 (s, 3H, NHAc), 1.75–1.69 (m, 2H, H-2e, H-4e), 1.52 (t, *J* = 12.1 Hz, 1H, H-3'a), 1.41–1.35 (m, 2H, H-5e, H-6e), 1.32 (m, 1H, H-1), 0.90 (dq, *J* = 3.8, 12.4 Hz, 1H, H-4a), 0.83 (q, *J* = 11.9 Hz, 1H, H-5a), 0.74 (tq, *J* = 3.3, 13.2 Hz, 1H, H-2a), 0.65 ppm (dq, *J* = 3.6, 12.5 Hz, 1H, H-6a); ¹³C NMR (126 MHz, D₂O): δ = 176.0, 174.5 (2 C=O), 137.1, 135.7, 132.9, 130.9, 130.3, 130.2, 128.93, 128.91, 128.89, 122.5 (10 C, Ar-C), 101.9 (C-2'), 75.6 (C-3), 74.3 (CH₂O), 73.5 (C-6'), 71.9 (C-8'), 70.4 (C-7'), 69.2 (C-4'), 52.8 (C-5'), 46.3 (C-9'), 42.1 (C-3'), 36.8 (C-1), 36.4 (C-2), 35.0 (C-4), 28.3 (C-6), 23.9 (C-5), 22.9 ppm (NHAc); HRMS (ESI): *m/z* calcd for C₂₈H₃₆N₂Na₂O₁₄S₂: 757.1296 [M+Na]⁺; found: 757.1296.

Cloning of 6His-tagged Siglec-8-CRD. The Siglec-8 encoding sequence was amplified by PCR from cDNA clone MN_014442 (OriGene, Rockville, USA) and applied to site-directed mutagenesis to replace proline 173 and cysteine 23 by serines. The fragment was inserted into the NdeI and XhoI cloning site of the expression vector pET22b (Novagen). The resulting construct encoding a 6His tag at the C-terminus was amplified in chemo-competent *E. coli* DH5 and the correctness of the DNA sequence was confirmed by double-strand sequencing (Microsynth, Balgach, Switzerland).

Expression and purification of 6His-tagged Siglec-8-CRD. Protein expression was performed in *Escherichia coli* strain Rosetta-gami B (DE3). Bacterial culture was grown in LB medium (Luria-Bertani broth) containing 100 μg/mL of ampicillin at 30 °C and 300 rpm to reach an OD₆₀₀ of 0.7–1. The temperature was lowered gradually to reach 18 °C and isopropyl-β-D-1-thiogalactoside (IPTG) was added to a final concentration of 1 mM. The bacteria were further cultivated at 18 °C and 300 rpm for 36 h after induction and collected by centrifugation at 5000 rpm for 20 min at 4 °C. The bacterial lysis was performed in binding buffer (50 mM NaH₂PO₄, 300 mM NaCl, 10 mM imidazole, pH 8) containing 1 mg/mL lysozyme followed by sonication. After centrifugation at 11000 rpm for 20 min at 4 °C, the supernatant (cytoplasmic extract) was dialyzed overnight against binding buffer and applied to a Ni-NTA column (Sigma, Buchs, Switzerland) attached to a BioLogic fast protein liquid chromatography system (BioRad, Reinach BL, Switzerland). The column was washed with binding buffer and afterwards eluted with elution buffer (50 mM NaH₂PO₄, 300 mM NaCl and 250 mM imidazole, pH 8). The fractions containing 6His-Siglec-8-CRD were pooled and dialyzed against assay buffer (20 mM HEPES, 150 mM NaCl, 1 mM CaCl₂, pH 7.4). The purity of the protein was verified by non-reducing SDS-PAGE.

Competitive binding assay. The polyacrylamide-based competitive binding assay^[43] was used to evaluate the binding of Siglec-8 ligands. Microtiter plates (F96 MaxiSorp, Nunc) were coated with 100 μL/well of a 10 μg/mL solution of Siglec-8-CRD in 20 mM HEPES, 150 mM NaCl, and 1 mM CaCl₂, pH 7.4 (assay buffer), overnight at 4 °C. The coating solution was discarded, and the wells were blocked with 150 μL/well of 3% BSA in assay buffer for 2 h at 4 °C. After three washing steps with assay buffer (150 μL/well), a 3-fold serial dilution of the test compound (50 μL/well) in assay buffer and streptavidin-peroxidase coupled biotinylated polyacrylamide (PAA) glycopolymers (6'-sulfo-sLe^x-PAA, 50 μL/well of a 0.3 μg/mL solution) were added. The plate was incubated for 3 h at 25 °C and 350 rpm and then carefully washed four times with 150 μL/well assay buffer. After the addition of 100 μL/well of the horseradish peroxidase substrate (2,2'-azino-di(3-ethylbenzthiazoline-6-sulfonic acid), ABTS), the colorimetric reaction was allowed to develop for 3 min, then stopped by the addition of 2% aqueous oxalic acid

before the optical density (OD) was measured at 415 nm on a microplate-reader (Spectramax 190, Molecular Devices, CA). The IC_{50} values of the compounds were calculated with the prism software (GraphPad Software, Inc., La Jolla, CA). The IC_{50} defines the molar concentration of the test compound that reduces the maximal specific binding of 6'-sulfo-sLe^x-PAA polymer to Siglec-8-CRD by 50%.

Microscale thermophoresis. Microscale thermophoresis experiments were performed using a Monolith NT.115 (Nanotemper, Munich, Germany) instrument set to 25 °C, 50% LED power, and "medium" MST power. The Nanotemper MO.Affinity Analysis software suite was employed for analysis and nonlinear fitting of experimental data. In a typical experiment, a serial ligand dilution starting at 50 mM or 100 mM was incubated with an equal volume of 200 nM FITC labeled Siglec-8-CRD and measured directly using the green channel of the instrument.

Isothermal titration calorimetry. Isothermal titration calorimetric experiments were performed on an ITC200 instrument (MicroCal, Northampton, USA) at 25 °C using standard instrument settings (reference power 6 μ cal s^{-1} , stirring speed 750 rpm, feedback mode high, filter period 2 s). Protein solutions were dialyzed against ITC buffer (20 mM HEPES, 150 mM NaCl, pH 7.4) prior to the experiments and all samples were prepared using the dialysate buffer to minimize dilution effects. Protein concentrations were determined spectrophotometrically with the specific absorbance at 280 nm employing an extinction coefficient of 33240 $mol^{-1} cm^{-1}$. Binding affinities of Siglec-8 ligands in the μ M to mM range necessitated a low c titration setup. In a typical experiment, a 5–25 mM ligand solution was titrated to a solution containing 30–50 μ M Siglec-8-CRD to ensure > 70% saturation. Baseline correction, peak integration, and non-linear regression analysis of experimental data was performed using the NITPIC (version 1.2.2.)^[56] and SEDPHAT (version 12.1b)^[57] software packages. The stoichiometry parameter was manually constrained to a value of 1. Experiments were performed in duplicate and the 68% confidence intervals from global fitting of two experiments were calculated as an estimate of experimental error. For kinITC analysis, the AFFINImeter software suite (v2.1802.5, Software for Science Developments, Santiago de Compostela, Spain) was used. Raw ITC data was fit to a thermodynamic model assuming a stoichiometry of 1 to derive K_A . Dissociation rates were then determined from a fit of the equilibration time curve to a 1:1 interaction model. Association rate constants were calculated from K_A and k_{off} according to the equation:

$$k_{on} = K_A \times k_{off} = \frac{k_{off}}{K_D}$$

Errors in rate constants are given as the 68% standard error of the fit for a single experiment.

Generation of pseudo induced-fit docking pose for 50. Structure preparation and docking studies were carried out using programs from the Maestro suite version 2016-4.^[58] The ligand bound Siglec-8-CRD NMR solution structure 2N7B was retrieved from the PDB and frame 1 was chosen for the docking procedure. After *in silico* mutation of Lys120 to Ala, the protein was prepared for docking by protonation, bond order and hydrogen bond assignment, and subsequent restrained minimization using the OPLS3 force field.^[59,60] The LigPrep module employing the OPLS3 force field was used for the preparation of low energy conformations and charge assignment of 50. Receptor grid generation and ligand docking was carried out with Glide in standard precision mode using the ligand bound in 2N7B as the centroid of the bounding box.^[61] After visual inspection of the generated docking poses, Ala120 was mutated to Lys and minimized.

Acknowledgements

This project has received funding from the European Union's Horizon 2020 research and innovation programme under the Marie Skłodowska-Curie grant agreement No 765581.

Conflict of Interest

The authors declare no conflict of interest.

Keywords: Siglec-8 · asthma · 6'-sulfo-sialyl Lewis^x · glycosides · calorimetry

- [1] P. R. Crocker, J. C. Paulson, A. Varki, *Nat. Rev. Immunol.* **2007**, *7*, 255–266.
- [2] A. Varki, T. Angata, *Glycobiology* **2005**, *16*, 1R-27R.
- [3] M. S. Macauley, P. R. Crocker, J. C. Paulson, *Nat. Rev. Immunol.* **2014**, *14*, 653–666.
- [4] J. V. Ravetch, L. L. Lanier, *Science* **2000**, *290*, 84–89.
- [5] P. R. Crocker, P. Redelinghuys, *Biochem. Soc. Trans.* **2008**, *36*, 1467–1471.
- [6] J. C. Paulson, M. S. MacAuley, N. Kawasaki, *Ann. N. Y. Acad. Sci.* **2012**, *1253*, 37–48.
- [7] B. E. Collins, O. Blixt, A. R. DeSieno, N. Bovin, J. D. Marth, J. C. Paulson, *Proc. Natl. Acad. Sci. USA* **2004**, *101*, 6104–6109.
- [8] B. E. Collins, O. Blixt, S. Han, B. Duong, H. Li, J. K. Nathan, N. Bovin, J. C. Paulson, *J. Immunol.* **2006**, *177*, 2994–3003.
- [9] K. K. Kikly, B. S. Bochner, S. D. Freeman, K. B. Tan, K. T. Gallagher, K. J. D. Alessio, S. D. Holmes, J. A. Abrahamson, C. L. Erickson-Miller, P. R. Murdock, H. Tachimoto, P. Robert, J. R. White, *Clin. Exp. Allergy* **2009**, *39*, 1093–1100.
- [10] H. Floyd, J. Ni, A. L. Cornish, Z. Zeng, D. Liu, K. C. Carter, J. Steel, P. R. Crocker, *J. Biol. Chem.* **2000**, *275*, 861–866.
- [11] P. J. Barnes, *Nat. Rev. Immunol.* **2008**, *8*, 183–192.
- [12] J. V. Fahy, *Nat. Rev. Immunol.* **2015**, *15*, 57–65.
- [13] E. Nutku, H. Aizawa, S. A. Hudson, B. S. Bochner, *Blood* **2003**, *101*, 5014–5020.
- [14] H. Yokoi, O. H. Choi, W. Hubbard, H.-S. Lee, B. J. Canning, H. H. Lee, S.-D. Ryu, S. von Gunten, C. A. Bickel, S. A. Hudson, D. W. MacGlashan, B. S. Bochner, *J. Allergy Clin. Immunol.* **2008**, *121*, 499–505.
- [15] T. Angata, C. M. Nycholat, M. S. Macauley, *Trends Pharmacol. Sci.* **2015**, *36*, 645–660.
- [16] S. A. Hudson, N. V. Bovin, R. L. Schnaar, P. R. Crocker, B. S. Bochner, *J. Pharmacol. Exp. Ther.* **2009**, *330*, 608–612.
- [17] Y. Jia, H. Yu, S. M. Fernandes, Y. Wei, A. Gonzalez-Gil, B. S. Bochner, R. C. Kern, R. P. Schleimer, R. L. Schnaar, *J. Allergy Clin. Immunol.* **2015**, *135*, 799–810.
- [18] S. V. Gunten, M. Vogel, A. Schaub, B. M. Stadler, S. Miescher, P. R. Crocker, *J. Allergy Clin. Immunol.* **2007**, *119*, 1005–1011.
- [19] P.-S. Gao, K. Shimizu, A. V. Grant, N. Rafaels, L.-F. Zhou, S. A. Hudson, S. Konno, N. Zimmermann, M. I. Araujo, E. V. Ponte, A. A. Cruz, M. Nishimura, S.-N. Su, N. Hizawa, T. H. Beaty, R. A. Mathias, M. E. Rothenberg, K. C. Barnes, B. S. Bochner, *Eur. J. Hum. Genet.* **2010**, *18*, 713–719.
- [20] T. Kiwamoto, N. Kawasaki, J. C. Paulson, B. S. Bochner, *Pharmacol. Ther.* **2012**, *135*, 327–336.
- [21] S. Farid, A. Mirshafiey, A. Razavi, *Immunopharmacol. Immunotoxicol.* **2012**, *34*, 721–726.
- [22] F. Legrand, Y. Cao, J. B. Wechsler, X. Zhu, N. Zimmermann, S. Rampertaap, J. Monsale, K. Romito, B. A. Youngblood, E. C. Brock, M. A. Makiya, N. Tomasevic, C. Bebbington, I. Maric, D. D. Metcalfe, B. S. Bochner, A. D. Klion, *J. Allergy Clin. Immunol.* **2019**, *143*, 2227–2237.
- [23] D. Simon, H. U. Simon, *Curr. Opin. Pharmacol.* **2019**, *46*, 29–33.
- [24] J. A. O'Sullivan, D. J. Carroll, Y. Cao, A. N. Salicru, B. S. Bochner, *J. Allergy Clin. Immunol.* **2018**, *141*, 1774–1785.
- [25] R. T. Lee, Y. C. Lee, *Glycoconjugate J.* **2000**, *17*, 543–551.
- [26] T. K. Dam, T. A. Gerken, C. F. Brewer, *Biochemistry* **2009**, *48*, 3822–3827.
- [27] N. R. Zaccai, K. Maenaka, T. Maenaka, P. R. Crocker, R. Brossmer, S. Kelm, E. Y. Jones, *Structure* **2003**, *11*, 557–567.

- [28] S. Mesch, K. Lemme, M. Wittwer, H. Koliwer-Brandl, O. Schwardt, S. Kelm, B. Ernst, *ChemMedChem* **2012**, *7*, 134–143.
- [29] S. Kelm, J. Gerlach, R. Brossmer, C. P. Danzer, L. Nitschke, *J. Exp. Med.* **2002**, *195*, 1207–1213.
- [30] H. H. M. Abdu-Allah, K. Watanabe, G. C. Completo, M. Sadagopan, K. Hayashizaki, C. Takaku, T. Tamanaka, H. Takematsu, Y. Kozutsumi, J. C. Paulson, T. Tsubata, H. Ando, H. Ishida, M. Kiso, *Bioorg. Med. Chem.* **2011**, *19*, 1966–1971.
- [31] S. Mesch, D. Moser, D. S. Strasser, A. Kelm, B. Cutting, G. Rossato, A. Vedani, H. Koliwer-Brandl, M. Wittwer, S. Rabbani, O. Schwardt, S. Kelm, B. Ernst, *J. Med. Chem.* **2010**, *53*, 1597–1615.
- [32] S. V. Shelke, G.-P. Gao, S. Mesch, H. Gächje, S. Kelm, O. Schwardt, B. Ernst, *Bioorg. Med. Chem.* **2007**, *15*, 4951–4965.
- [33] H. Prescher, M. Frank, S. Gütgemann, E. Kuhfeldt, A. Schweizer, L. Nitschke, C. Watzl, R. Brossmer, *J. Med. Chem.* **2017**, *60*, 941–956.
- [34] C. M. Nycholat, S. Duan, E. Knuplez, C. Worth, M. Elich, A. Yao, J. O'Sullivan, R. McBride, Y. Wei, S. M. Fernandes, Z. Zhu, R. L. Schnaar, B. S. Bochner, J. C. Paulson, *J. Am. Chem. Soc.* **2019**, *141*, 14032–14037.
- [35] B. S. Bochner, R. A. Alvarez, P. Mehta, N. V. Bovin, O. Blixt, J. R. White, R. L. Schnaar, *J. Biol. Chem.* **2005**, *280*, 4307–4312.
- [36] H. F. Yu, A. Gonzalez-Gil, Y. D. Wei, S. M. Fernandes, R. N. Porell, K. Vajn, J. C. Paulson, C. M. Nycholat, R. L. Schnaar, *Glycobiology* **2017**, *27*, 657–668.
- [37] H. Tateno, P. R. Crocker, J. C. Paulson, *Glycobiology* **2005**, *15*, 1125–1135.
- [38] J. M. Pröpster, F. Yang, S. Rabbani, B. Ernst, F. H. T. Allain, M. Schubert, *Proceed. Natl. Acad. Sci. U. S. A.* **2016**, *113*, E4170–E4179.
- [39] The PyMOL Molecular Graphics System, Version 1.8 Schrödinger, LLC.
- [40] Functional Glycomics Gateway, **2010**. Available at: http://www.functionalglycomics.org/glycomics/H5Servlet?operation=view&sideMenu=no&psi d=primscreen_5605. Accessed: January 2017.
- [41] R. Dubey, D. Reynolds, S. A. Awas, K. L. Matta, *Carbohydr. Res.* **1988**, *183*, 155–162.
- [42] C.-S. Chao, M.-C. Chen, S.-C. Lin, K.-K. T. Mong, *Carbohydr. Res.* **2008**, *343*, 957–964.
- [43] S. Rabbani, X. Jiang, O. Schwardt, B. Ernst, *Anal. Biochem.* **2010**, *407*, 188–195.
- [44] T. S. Carter, T. J. Mooibroek, P. F. N. Stewart, M. P. Crump, M. C. Galan, A. P. Davis, *Angew. Chem. Int. Ed.* **2016**, *55*, 9311–9315; *Angew. Chem.* **2016**, *128*, 9457–9461.
- [45] M. Hendlich, A. Bergner, J. Gunther, G. Klebe, *J. Mol. Biol.* **2003**, *326*, 607–620.
- [46] G. A. Patani, E. J. LaVoie, *Chem. Rev.* **1996**, *96*, 3147–3176.
- [47] N. A. Meanwell, *J. Med. Chem.* **2011**, *54*, 2529–2591.
- [48] D. Rotticci, T. Norin, K. Hult, *Org. Lett.* **2000**, *2*, 1373–1376.
- [49] R. ter Halle, Y. Bernet, S. Billard, C. Bufferre, P. Carlier, C. Delaitre, C. Flouzat, G. Humblot, J. C. Laigle, F. Lombard, S. Wilmouth, *Org. Process Res. Dev.* **2004**, *8*, 283–286.
- [50] A. Numata, T. Suzuki, K. Ohno, S. Uyeo, *Yakugaku Zasshi* **1968**, *88*, 1298–1305.
- [51] S. Kelm, R. Brossmer, PCT patent WO 03/000709A2, **2003**.
- [52] J. Cramer, C. P. Sager, B. Ernst, *J. Med. Chem.* **2019**, *62*, 8915–8930.
- [53] R. A. Copeland, D. L. Pompliano, T. D. Meek, *Nat. Rev. Drug Discovery* **2006**, *5*, 730–739.
- [54] P. Dumas, E. Ennifar, C. Da Veiga, G. Bec, W. Palau, C. Di Primo, A. Piñeiro, J. Sabin, E. Muñoz, J. Rial, *Methods Enzymol.* **2016**, *567*, 157–180.
- [55] P. Zihlmann, M. Silbermann, T. Sharpe, X. Jiang, T. Mühlethaler, R. P. Jakob, S. Rabbani, C. P. Sager, P. Frei, L. Pang, T. Maier, B. Ernst, *Chem. Eur. J.* **2018**, *24*, 13049–13057.
- [56] T. H. Scheuermann, C. A. Brautigam, *Methods* **2015**, *76*, 87–98.
- [57] G. Piszczek, *Methods* **2015**, *76*, 137–148.
- [58] Schrödinger Release 2016–4: Maestro Schrödinger LLC. New York, NY (USA), **2016**.
- [59] G. Madhavi Sastry, M. Adzhigirey, T. Day, R. Annabhimoju, W. Sherman, *J. Comput.-Aided Mol. Des.* **2013**, *27*, 221–234.
- [60] E. Harder, W. Damm, J. Maple, C. Wu, M. Reboul, J. Y. Xiang, L. Wang, D. Lupyan, M. K. Dahlgren, J. L. Knight, J. W. Kaus, D. S. Cerutti, G. Krilov, W. L. Jorgensen, R. Abel, R. A. Friesner, *J. Chem. Theory Comput.* **2016**, *12*, 281–296.
- [61] R. A. Friesner, J. L. Banks, R. B. Murphy, T. A. Halgren, J. J. Klicic, D. T. Mainz, M. P. Repasky, E. H. Knoll, M. Shelley, J. K. Perry, D. E. Shaw, P. Francis, P. S. Shenkin, *J. Med. Chem.* **2004**, *47*, 1739–1749.

Manuscript received: June 10, 2020

Accepted manuscript online: August 3, 2020

Version of record online: August 31, 2020

Girardi, B.; Manna, M.; Van Klaveren, S.; Tomašič, T.; Jakopin, Ž.; Leffler, H.; Nilsson, U. J.; Ricklin, D.; Mravljak, J.; Schwardt, O.; Anderluh, M. Selective Monovalent Galectin-8 Ligands Based on 3-Lactoylgalactoside, *ChemMedChem* **2022**, *17* (3), e202100514.

© 2021 Wiley-VCH GmbH


 Very Important Paper


Selective Monovalent Galectin-8 Ligands Based on 3-Lactoylgalactoside

Benedetta Girardi,^[a, b] Martina Manna,^[a] Sjors Van Klaveren,^[a, c] Tihomir Tomašič,^[a] Žiga Jakopin,^[a] Hakon Leffler,^[c] Ulf J. Nilsson,^[c] Daniel Ricklin,^[b] Janez Mravljak,^[a] Oliver Schwardt,^{*[b]} and Marko Anderluh^{*[a]}

Galectin-8 has gained attention as a potential new pharmacological target for the treatment of various diseases, including cancer, inflammation, and disorders associated with bone mass reduction. To that end, new molecular probes are needed in order to better understand its role and its functions. Herein we aimed to improve the affinity and target selectivity of a recently published galectin-8 ligand, 3-O-[1-carboxyethyl]-β-D-galactopyranoside, by introducing modifications at positions 1 and 3 of the galactose. Affinity data measured by fluorescence polarization show that the most potent compound reached a K_D of 12 μM. Furthermore, reasonable selectivity versus other galectins was achieved, making the highlighted compound a promising lead for the development of new selective and potent ligands for galectin-8 as molecular probes to examine the protein's role in cell-based and *in vivo* studies.

cells.^[11,12] By activating autophagy, the protein may contribute to host defence against bacteria.^[13,14] Galectin-8 has also been reported to enhance differentiation of osteoblasts in osteoclasts, and it is thus involved in bone turnover and remodelling.^[15] Of note, galectin-8 has an important role in cancer, as it was shown to stimulate lymphangiogenesis and the adhesion and dissemination of tumour cells.^[16–18] Therefore, galectin-8 is a new interesting pharmacological target for the treatment of many diseases.

Galectin-8 contains two carbohydrate recognition domains (CRDs), one at the N- and the other at the C-terminus, with different binding specificities. They behave independently in the full length protein and the addition of a ligand specific for one CRD does not affect the binding to the other.^[19,20] Yet, both galectin-8 CRDs are required for its function so that blocking of either will hamper the functionality of the whole protein.^[21,22] The N-terminal CRD has an enhanced binding to structures containing 3-O-sialylated galactose, unique among galectins, and the crystal structure with such a preferred ligand, the trisaccharide 3-SiaLac, has been solved (Figure 1A).^[23] The investigation of the main interactions between this ligand and the protein revealed 3-lactoylgalactoside **1** as the minimal binding epitope, which was recently crystallized, in its racemic form, in complex with galectin-8N. It consists of a free galactose bearing a lactate residue attached by an ether linkage in position 3 (Figure 1B).^[24]

The crystal structure of the galectin-8N/1 complex revealed that all interactions of the previously reported ligand 3-SiaLac were preserved. In particular, the carboxylic acid in **1** interacts with Arg59 and Gln47 forming a salt bridge and an H-bond; moreover, a complex network of H-bonds involves the galactose and Arg45, His65, Asn67, Asn79 and Glu89 (Figure 1).^[24] Starting from this compound, we aimed to further explore the chemical space around it, in particular via (i) modification of the lactic acid moiety and (ii) by introducing an α-thiophenyl aglycone at position 1 of D-galactose. These modifications improved the affinity for galectin-8N by 200-fold compared to the affinity of compound **1**. Besides, the affinity for other galectins was also evaluated. We focused on the N-terminal domain since the C-terminal in our hands showed weaker affinities for galactoside ligands.^[21,25]

Introduction


Galectins are a family of small soluble proteins able to recognize glycans containing a β-D-galactopyranoside structural motif.^[1–4] They are found both intracellularly and extracellularly, where they are involved in many physiological and pathological functions, such as metabolism, immunity, inflammation and cancer progression.^[4–8]

Galectin-8 is a tandem-repeat type lectin that is widely expressed in tissues, both in normal and cancer cells. It mainly regulates cell-cell and cell-matrix interactions, thus playing a key role in many physiological and pathological processes.^[9,10] It can act as a pro-inflammatory and immunostimulatory lectin in different resting cells of the immune system and, at the same time, downregulate inflammation upon activation of these

[a] B. Girardi, M. Manna, S. Van Klaveren, Prof. T. Tomašič, Prof. Ž. Jakopin, Prof. J. Mravljak, Prof. M. Anderluh
Faculty of Pharmacy, University of Ljubljana
Askerčeva cesta, 7 – 1000 Ljubljana (Slovenia)
E-mail: marko.anderluh@ffa.uni-lj.si

[b] B. Girardi, Prof. D. Ricklin, Dr. O. Schwardt
Department of Pharmaceutical Sciences
University of Basel
Klingelbergstrasse 50 - 4056 Basel (Switzerland)
E-mail: oliver.schwardt@unibas.ch

[c] S. Van Klaveren, Prof. H. Leffler, Prof. U. J. Nilsson
Centre for Analysis and Synthesis – Department of Chemistry
Lund University, Box 124-221 00 Lund (Sweden)

 Supporting information for this article is available on the WWW under <https://doi.org/10.1002/cmdc.202100514>

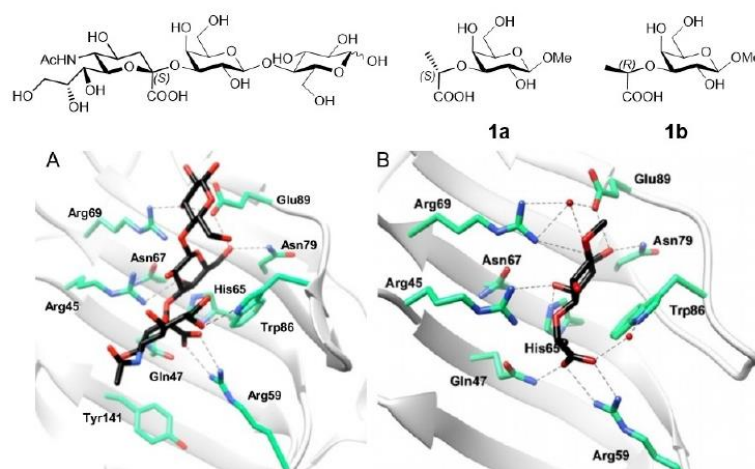


Figure 1. A: Galectin-8N in complex with 3-SiaLac (PDB ID: 3AP7)^[23]; B: Galectin-8N in complex with racemic 1 (PDB ID: 5VWG).^[24] Figure adapted from Bohari *et al.*^[24]

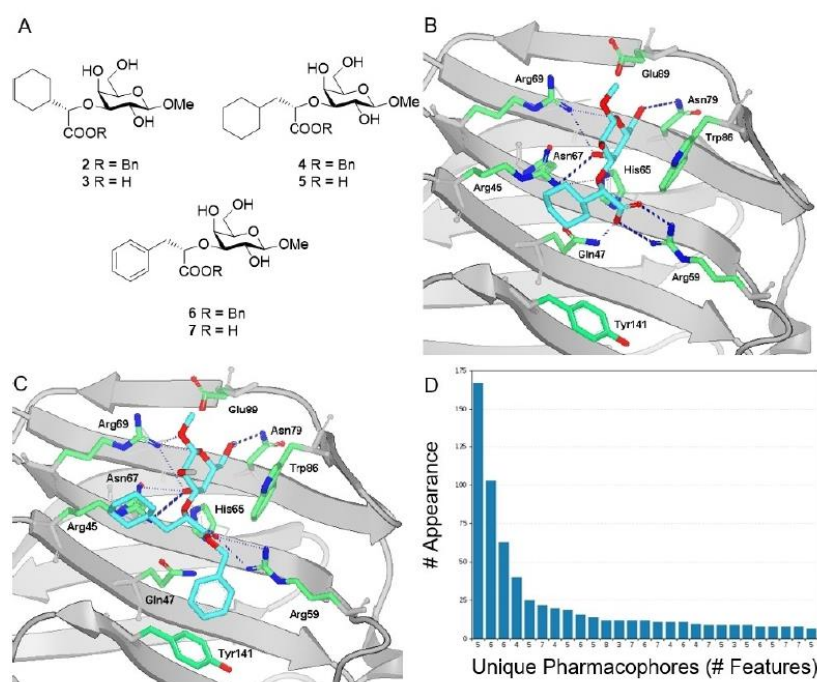


Figure 2. A: Designed galectin-8 ligands 2-7. B-C: Representative docking binding modes of compounds 3 (B) and 4 (C) in the galectin-8N binding site (PDB ID: 3VKO).^[26] Only selected amino acids are presented as sticks. Docking was performed using the FRED algorithm of the OEDocking software (OEDOCKING 3.3.0.2; OpenEye Scientific Software). D: Plot of the most frequently appearing unique structure-based pharmacophore models derived from MD simulations of galectin-8N in complex with 4. The x-axis shows unique models and the number of interaction features observed during the MD simulation. The numbers below the bar indicate the number of interaction features in the pharmacophore models. The y-axis shows the frequency of appearance of the models.

Results and Discussion

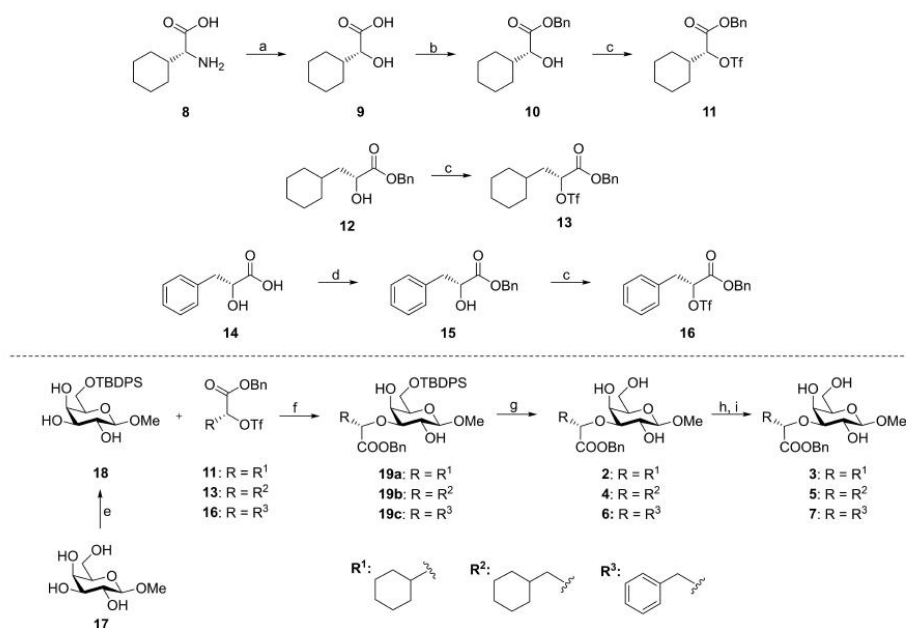
Design

Starting from the lead compound 3-O-[1-carboxyethyl]- β -D-galactopyranoside (**1**),^[24] we set out to derivatize the methyl group of the lactic acid side chain with cyclohexane and phenyl moieties; we focused on the *S*-configuration as with the *R*-configuration the added group would point away from the protein into solution (see Figure 1B). In addition, to determine the importance of the free carboxylic group for binding, we replaced it with an ester moiety (Figure 2A); a benzyl ester was chosen in order to gain possible hydrophobic contacts with the proximal Tyr141 in the binding site (Figure 2C). We did not consider modifications at positions 4 and 6 because they would probably clash with the protein, while substituents in position 2 would point towards the solvent, which would most likely bring little or no gain in affinity (Figures 2B and 2C). In our docking studies, as expected, the compounds maintained the position of the galactose and carboxylic acid of the reference compound's **1** pose including their interactions with the surrounding amino acids (Figure 1, Figure 2B and C). To assess the stability of the binding mode predicted by docking, interactions of compound **4** in the galectin-8N binding site were further studied by a 200 ns molecular dynamics (MD) simulation using the MD analysis tool in LigandScout 4.4 Expert.^[27] A plot of the most frequently appearing unique structure-based pharmaco-

phore models is shown in Figure 2D. The most frequently occurring model (166 times) contains 6 interaction features, including H-bonds of the galactose moiety with Arg45, His65 and Asn79, a H-bond between the ester carbonyl group and Gln47, and hydrophobic interactions of the benzyl moiety with Met56 and Tyr141. In pharmacophore models containing more features (Figure 2D), additional H-bonds are formed with the galactose moiety, as in the case of the crystal structure (Figure 1).

Synthesis

The synthesis of candidate compounds predicted by our *in silico* studies was accomplished as shown in Scheme 1. Intermediate **11** was obtained starting from α -D-cyclohexylglycine (**8**), via a diazotization–hydrolysis reaction^[28] (\rightarrow **9**) and subsequent esterification of the carboxylic group with benzyl bromide (\rightarrow **10**). The hydroxyl group of **10** was transformed into a good leaving group by reacting it with triflic anhydride to give donor **11**. The same sequence was employed to prepare intermediates **13** and **16**, starting from benzyl ester **12**,^[29] available in-house, and commercially available D-(*R*)-3-phenyllactic acid **14**, respectively. The reaction steps involving the phenyllactic acid derivatives were characterized by low yields, due to the preferential formation of the elimination product, affording a conjugate system between the aromatic ring and the carbonyl



Scheme 1. Reagents and conditions: a) NaNO₂, H₂SO₄, H₂O, 0 °C to rt, 24 h, 86%; b) BnBr, Cs₂CO₃, DMF, rt, 16 h, 72%; c) Tf₂O, 2,6-lutidine, DCM, rt, 16 h, **11**: 77%, **13**: 59%, **16**: 83%; d) BnBr, Cs₂CO₃, DMF, rt, 16 h, 33%; e) TBDPSCl, imidazole, DMF, rt, 16 h, 80%; f) i. Bu₃SnO, dry MeOH, reflux, 3 h; ii. CsF, DME, rt, 16 h, **19a**: 38%, **19b**: 44%, **19c**: 24%; g) HF-pyr, pyr, rt, 4 h, **2**: 62%, **4**: 75%; h) H₂, Pd/C, MeOH, rt, 2 h, **3**: 86%, **5**: quant; i) NaOH (H₂O/dioxane, 0.1 M), rt, 24 h, **7**: 10% over two steps from **19c**.

group. The galactoside acceptor **18**,^[30] protected in position 6 with a *tert*-butyldiphenylsilyl group (TBDPS), was subsequently alkylated with the triflates **11**, **13** and **16**. The alkylation reactions were performed by first activating the galactose with dibutyltin oxide (Bu_2SnO), followed by the treatment of the resulting stannylidene acetal with triflates **11**, **13**, and **16**, employing CsF, to afford intermediates **19a–c**.

Removal of the TBDPS group on the galactose moiety with HF-pyridine yielded the benzylated test compounds **2** and **4**. Transesterification occurred during the reaction with the aromatic intermediate **19c**, making the purification of the benzylated product **6** extremely cumbersome. Therefore, the mixture was directly hydrolysed to afford the final compound **7**. Hydrogenation was instead carried out on compounds **2** and **4** thus affording the corresponding acids **3** and **5** (Scheme 1).

Fluorescence polarization assay

The binding affinities of the synthesized compounds **2–5** and **7** to the main target galectin-8N, and to galectin-1 and –3 as related members of the protein family, were evaluated in a

competitive protein-binding assay based on fluorescence anisotropy (Table 1).^[19,31,32] Both enantiomers of the lead compound **1**^[24] and methyl β -D-galactopyranoside (**17**)^[33] were tested and used as references.

With the fluorescence polarization assay, we were not able to reproduce the previously reported affinity of the reference compound **1** (K_D : 32 μM).^[24] Both enantiomers **1a** and **1b** bound very weakly, or not at all, to galectin-8N, galectin-1 and galectin-3. In contrast, several of our predicted compounds showed favourable binding and/or selectivity profiles. Overall, the addition of cyclohexane to the methyl increased affinity by about 5-fold (**3** and **5**), and the benzyl ester derivatives **2** and **4** showed an almost 2-fold further affinity increase for galectin-8N when compared to the corresponding acids, despite carboxylates being stronger H-bond acceptors. In this case, the affinity gain of the ester could probably be explained by a lower desolvation penalty or by possible hydrophobic interactions of the benzyl residue with the Tyr141 side chain in the binding site. Compound **7**, carrying a phenyl ring on the lactic acid moiety, showed slightly poorer affinity to galectin-8N when compared to the non-aromatic counterparts.

Table 1. K_D values of compounds **1–5**, **7** and **17** against human galectin-8N, –1 and –3 measured by fluorescence polarization assay.

Compound	Structure	Galectin-8N [$K_D \pm \text{SEM}$, μM] ^[a]	Galectin-1 [$K_D \pm \text{SEM}$, μM] ^[a]	Galectin-3 [$K_D \pm \text{SEM}$, μM] ^[a]
17 ^[33]		5300	1000	4400
1a ^[34]		N.B.	2700 \pm 110	N.B.
1b ^[34]		\approx 2700	2800 \pm 69	2800 \pm 490
2		270 \pm 33	\approx 2500	N.B.
3		430 \pm 26	520 \pm 110	N.B.
4		210 \pm 18	\approx 2600	N.B.
5		470 \pm 39	N.B.	N.B.
7		550 \pm 66	1600 \pm 130	2100 \pm 600

[a] The average values of K_D and SEM were calculated from 4 to 8 duplicate measurements. N.B.: not binding.

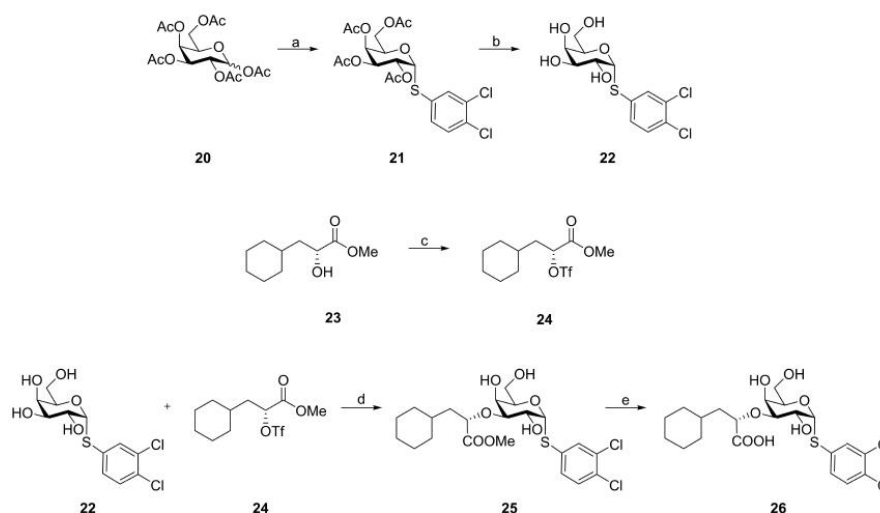
To assess their target selectivity, all predicted galectin-8 ligands were also tested on galectin-1 and galectin-3, which are known to feature overlaps in glycan specificities (Table 1). With the exception of **7**, which showed weak affinities, none of the compounds notably bound to galectin-3. Compound **3** had similar affinity for both galectin-8 and galectin-1, while **2**, **4** and **5** were moderately selective for galectin-8N. Based on this, we concentrated on further optimization of compound **5**. This may sound irrational since **4** was an even more potent binder, but **5** was chosen because intended optimisation described in the next chapter would involve addition of another aromatic group at the anomeric position. Based on previous experience, we assumed that molecules with 3 lipophilic rings around the galactose core would render the final compound(s) rather insoluble in aqueous media, so we decided to leave the free carboxylate.

Modification at the anomeric position of galactose

To improve the affinity of **5** for galectin-8, we introduced a 3,4-dichlorophenyl ring in position 1 of the D-galactose moiety via an α -S-glycosidic bond since this group has been demonstrated to strongly enhance binding to many galectins.^[25,35] The desired

compound **26** was synthesized from pentaacetylated galactose (**20**, Scheme 2), which was first transformed into the 3,4-dichlorophenyl- α -thio derivative **21**, and then deacetylated under Zemplén conditions (\rightarrow **22**). Donor **24** was synthesized from methyl-(*R*)-3-cyclohexyl-2-hydroxypropanoate **23**^[36] by triflation as shown above. The subsequent stannylidene-mediated regioselective alkylation gave **25**, which was further hydrolysed to give final compound **26**. Compounds **25** and **26** were tested for their binding potency to galectin-8N and other galectins using the established fluorescence polarization assay (Table 2).

The introduction of the 3,4-dichlorophenyl group increased the affinity by almost 40-fold (12 μ M for **26** vs 470 μ M for **5**), confirming its beneficial effect for enhancing the binding to galectin-8N. The methyl ester **25** showed a higher K_D value (140 μ M) in this case and thus 10-fold weaker affinity compared to its free acid counterpart **26**, pointing that the free carboxylate most likely forms a salt bridge, which is disrupted in **25** where only H-bonding is possible. The binding mode of **26** in the galectin-8N binding site was predicted by docking and then studied further by a 200 ns MD simulation. Analysis of the binding mode in the most frequently appearing models (Figure 3B) showed an expected hydrogen bonding network of the galactose moiety with Arg45, His65, Asn79 and Glu89, while the carboxylate of **26** formed a salt bridge with the Arg59 side



Scheme 2. Reagents and conditions: a) i. PCl_5 , $\text{BF}_3 \cdot \text{Et}_2\text{O}$, DCM, rt, 1 h; ii. 3,4-dichlorothiophenol, NaH, DMF, rt, 50 °C, 16 h, 36%; b) MeONa/MeOH , rt, 16 h, 90%; c) Tf_2O , 2,6-lutidine, DCM, rt, 16 h, 70%; d) i. Bu_3SnO , dry MeOH, reflux, 3 h; ii. CsF, DME, rt, 16 h, 31%; e) NaOH ($\text{H}_2\text{O}/\text{dioxane}$, 0.1 M), rt, 16 h, 90%.

Compound	Galectin [$K_D \pm \text{SEM}$, μM] ^[a]	8N	8C	1	3	9C	9N
25	140 ± 27	2100 ± 140		780 ± 140	170 ± 16	110 ± 17	59 ± 14
26	12 ± 0.9	N.B.		580 ± 16	82 ± 7.5	360 ± 25	53 ± 16

[a] The average values of K_D and SEM were calculated from 4 to 8 duplicate measurements. N.B.: not binding

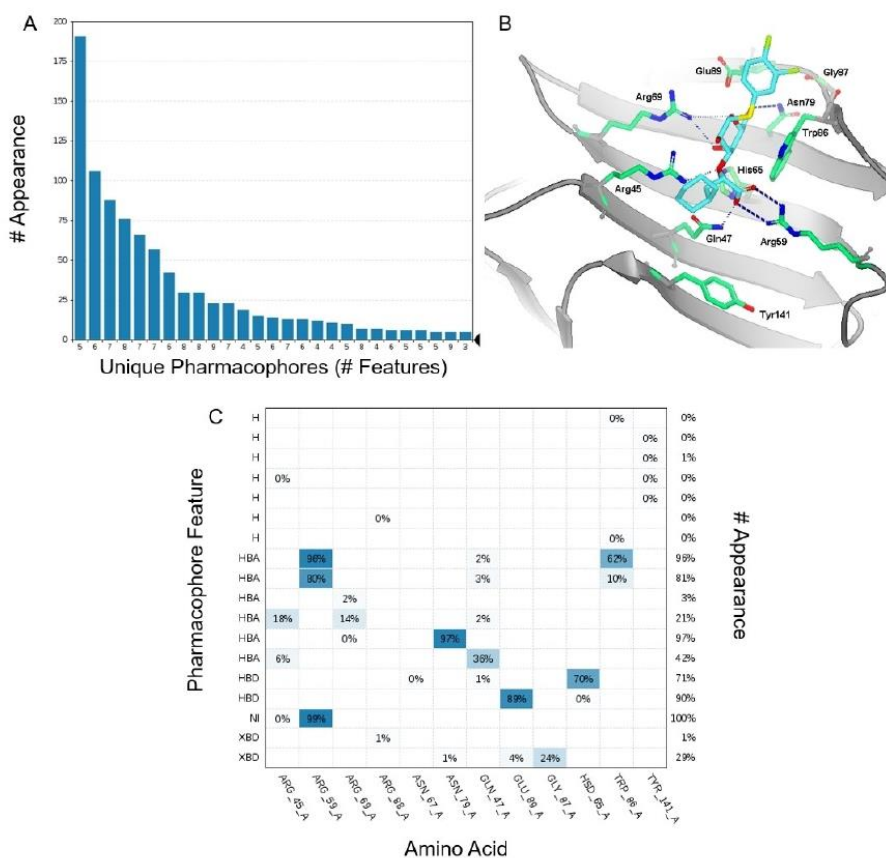


Figure 3. A: Plot of the most frequently appearing unique structure-based pharmacophore models derived from MD simulations of galectin-8N in complex with **26**. The x-axis shows unique models and the number of interaction features observed during the MD simulation. The numbers below the bar indicate the number of interaction features in the pharmacophore models. The y-axis shows the frequency of appearance of the models. B: Docking binding mode of compound **26** in the galectin-8N binding site (PDB ID: 3VKO).^[26] Only selected amino acids are presented as sticks. Docking was performed using the FRED algorithm of the OEDocking software (OEDOCKING 3.3.0.2; OpenEye Scientific Software).^[37] C: Interaction plot obtained by analysing interactions of **26** with galectin-8N binding site residues in the 200 ns MD simulation trajectory. Amino acid name and numbering are shown on the x-axis, pharmacophore feature type on the left y-axis (H – hydrophobic, HBA – hydrogen bond acceptor, HBD – hydrogen bond donor, NI – negative ionisable, XBD – halogen bond), % appearance on the right y-axis.

chain, as expected. An important gain in binding affinity of 3,4-dichlorothiophenyl-based **26** in comparison with the methyl glycosides (Table 1) can be attributed to the formation of a halogen bond of 3-Cl with the Gly87 backbone carbonyl.^[35] This interaction was present for more than 24% of the simulation time (Figure 3C). The affinity for galectin-8C was weak. Considering their strong affinities for the primary target, **25** and **26** were also tested towards a panel of other human galectins. The binding towards galectin-3 and galectin-9N was found to be considerable, which is in line with existing galectin-8N ligands^[25] that showed comparable affinity to these galectins. Still, **26** showed reasonable selectivity, especially versus galectin-1, which is an important highlight of this series.

Conclusions

In this study, we synthesized a focused library of 3-O-[1-carboxyethyl]- β -D-galactopyranoside (**1**) derivatives and measured their affinity for galectin-8N using a fluorescence polarization assay. We first introduced modifications to the lactic acid moiety; the benzyl esters unexpectedly were more active than their acid counterparts. Moreover, the compounds showed good selectivity towards galectin-8N when compared to galectin-1 and, in particular, to galectin-3. Interestingly, our assessment of reference compound **1** indicated a substantially weaker affinity to galectin-8 than originally reported.^[24] Thus, fluorescence polarization data should be interpreted relatively to the reference compound. The direct comparison to **1** shows

that our design strategy based on *in silico* analyses was successful in predicting derivatives with affinity improvements by 2 orders of magnitude (from K_D about 2700 μM to 12 μM). The most suitable moiety at position 3 of galactose increased affinity about 5-fold, and adding a 3,4-dichlorophenyl ring in position 1, increased the potency a further 40-fold. With a K_D of 12 μM , compound **26** is among the most potent galectin-8 ligands reported thus far. Importantly, it also shows reasonable selectivity for galectin-8. STD-NMR experiments of **26** binding to galectin-8 may be considered in the future to further study the binding characteristics of **26**, an approach that has been already used in the past on lactic acid-containing molecules.^[38,39] Our results represent an ideal starting point for the development of galectin-8 ligands with improved affinity and selectivity profiles, thereby providing new perspectives for targeting cancer or diseases associated with bone loss and inflammation.

Acknowledgements

This project has received funding from the European Union's Horizon 2020 research and innovation programme under the Marie Skłodowska-Curie grant agreement No 765581, from Slovenian Research Agency (Grant P1-0208) and from Galecto Biotech Inc.. We thank OpenEye Scientific Software, Santa Fe, NM (USA), for free academic licenses for the use of their software. The authors kindly thank Barbro Kahl Knutson for performing fluorescence polarization measurements.

Conflict of Interest

H.L. and U.J.N. are shareholders in Galecto Biotech Inc., a company developing galectin inhibitors. The other authors declare no conflict of interest.

Keywords: galectins · galectin-8 · carbohydrates · fluorescence polarization · molecular probes

- [1] R. Y. Yang, G. A. Rabinovich, F. T. Liu, *Expert Rev. Mol. Med.* **2008**, *10*, e17.
- [2] R. P. M. Dings, M. C. Miller, R. J. Griffin, K. H. Mayo, *Int. J. Mol. Sci.* **2018**, *19*, 905.
- [3] S. Di Lella, V. Sundblad, J. P. Cerliani, C. M. Guardia, D. A. Estrin, G. R. Vasta, G. A. Rabinovich, *Biochemistry* **2011**, *50*, 7842–7857.
- [4] L. Johannes, R. Jacob, H. Leffler, *J. Cell Sci.* **2018**, *131*, jcs208884.
- [5] M. F. Brinckmann, D. M. Patel, M. H. Iversen, *Mediators Inflammation* **2018**, 9186940.
- [6] M. R. Girotti, M. Salatino, T. Dalotto-Moreno, G. A. Rabinovich, *J. Exp. Med.* **2020**, *217*, e20182041.
- [7] D. Ayona, P. E. Fournier, B. Henrissat, B. Desnues, *Front. Immunol.* **2020**, *11*, 1877.
- [8] Q. Y. Jin, Y. S. Li, X. H. Qiao, J. W. Yang, X. L. Guo, *Life Sci.* **2021**, *277*, 119426.
- [9] R. Tazhitdinova, A. V. Timoshenko, *Cells* **2020**, *9*, 1792.
- [10] Y. Zick, M. Eisenstein, R. A. Goren, Y. R. Hadari, Y. Levy, D. Ronen, *Glycoconjugate J.* **2002**, *19*, 517–526.
- [11] M. V. Tribulatti, J. Carabelli, C. A. Prato, O. Campetella, *Glycobiology* **2020**, *30*, 134–142.
- [12] C. A. Prato, J. Carabelli, O. Campetella, M. V. Tribulatti, *iScience* **2020**, *23*, 101278.
- [13] M. H. Hong, W. H. Lin, I. C. Weng, Y. H. Hung, H. L. Chen, H. Y. Chen, P. Chen, C. H. Lin, W. Y. Yang, F. T. Liu, *Glycobiology* **2019**, *30*, 49–57.
- [14] B. W. Kim, S. B. Hong, J. H. Kim, D. H. Kwon, H. K. Song, *Nat. Commun.* **2013**, *4*, 1613.
- [15] Y. Vinik, H. Shatz-Azoulay, A. Vivanti, N. Hever, Y. Levy, R. Karmona, V. Brumfeld, S. Baraghithy, M. Attar-Lamdar, S. Boura-Halfon, I. Bab, Y. Zick, *eLife* **2015**, *4*, e05914.
- [16] H. Shatz-Azoulay, Y. Vinik, R. Isaac, U. Kohler, S. Lev, Y. Zick, *Sci. Rep.* **2020**, *10*, 7375.
- [17] W. S. Chen, Z. Cao, S. Sugaya, M. J. Lopez, V. G. Sendra, N. Laver, H. Leffler, U. J. Nilsson, J. Fu, J. Song, L. Xia, P. Hamrah, N. Panjwani, *Nat. Commun.* **2016**, *7*, 11302.
- [18] M. F. Troncoso, F. Ferragut, M. L. Bacigalupo, V. M. Cárdenas Delgado, L. G. Nugnes, L. Gentilini, D. Laderach, C. Wolfenstein-Todel, D. Compagno, G. A. Rabinovich, M. T. Eola, *Glycobiology* **2014**, *24*, 907–914.
- [19] S. Carlsson, C. T. Öberg, M. C. Carlsson, A. Sundin, U. J. Nilsson, D. Smith, R. D. Cummings, J. Almkvist, A. Carlsson, H. Leffler, *Glycobiology* **2007**, *17*, 663–676.
- [20] M. Gómez-Redondo, S. Delgado, R. Núñez-Franco, G. Jiménez-Osés, A. Ardá, J. Jiménez-Barbero, A. Gimeno, *RSC Chem. Biol.* **2021**, *2*, 932–941.
- [21] M. Hassan, S. Van Klaveren, M. Håkansson, C. Diehl, R. Kovačič, F. Baussière, A. P. Sundin, J. Dermovšek, B. Walse, F. Zetterberg, H. Leffler, M. Anderlüh, T. Tomašič, Ž. Jakopin, U. J. Nilsson, *Eur. J. Med. Chem.* **2021**, *223*, 113664.
- [22] Y. Levy, S. Auslender, M. Eisenstein, R. R. Vidavsky, D. Ronen, A. D. Bershadsky, Y. Zick, *Glycobiology* **2006**, *16*, 463–476.
- [23] H. Ideo, T. Matsuzaka, T. Nonaka, A. Seko, K. Yamashita, *J. Biol. Chem.* **2011**, *286*, 11346–11355.
- [24] M. H. Bohari, X. Yu, C. Kishor, B. Patel, R. M. Go, H. A. Eslampanah Seyedi, Y. Vinik, I. D. Grice, Y. Zick, H. Blanchard, *ChemMedChem* **2018**, *13*, 1664–1672.
- [25] K. B. Pal, M. Mahanti, X. Huang, S. Persson, A. P. Sundin, F. R. Zetterberg, S. Oredsson, H. Leffler, U. J. Nilsson, *Org. Biomol. Chem.* **2018**, *16*, 6295–6305.
- [26] H. Yoshida, S. Yamashita, M. Teraoka, A. Itoh, S. Nakakita, N. Nishi, S. Kamitori, *FEBS J.* **2012**, *279*, 3937–3951.
- [27] "LigandScout v.4.4 available from Inte:Ligand. <https://www.inteligand.com/ligandscout>."
- [28] H. Guyon, A. Boussonnière, A. S. Castanet, *J. Org. Chem.* **2017**, *82*, 4949–4957.
- [29] G. Thoma, W. Kinzy, C. Bruns, J. T. Patton, J. L. Magnani, R. Banteli, *J. Med. Chem.* **1999**, *42*, 4909–4913.
- [30] R. Dubey, D. Reynolds, S. A. Abbas, K. L. Matta, *Carbohydr. Res.* **1988**, *183*, 155–162.
- [31] T. Delaine, P. Collins, A. MacKinnon, G. Sharma, J. Stegmayr, V. K. Rajput, S. Mandal, I. Cumpstey, A. Larumbe, B. A. Salameh, B. Kahl-Knutson, H. van Hattum, M. van Scherpenzeel, R. J. Pieters, T. Sethi, H. Schambye, S. Oredsson, H. Leffler, H. Blanchard, U. J. Nilsson, *ChemBioChem* **2016**, *17*, 1759–1770.
- [32] K. B. Pal, M. Mahanti, H. Leffler, U. J. Nilsson, *Int. J. Mol. Sci.* **2019**, *20*, 3786.
- [33] I. Cumpstey, S. Carlsson, H. Leffler, U. J. Nilsson, *Org. Biomol. Chem.* **2005**, *3*, 1922–1932.
- [34] L. Andersson, L. Kenne, *Carbohydr. Res.* **1998**, *313*, 157–164.
- [35] F. K. Zetterberg, K. Peterson, R. E. Johnsson, T. Brimert, M. Håkansson, D. T. Logan, H. Leffler, U. J. Nilsson, *ChemMedChem* **2018**, *13*, 133–137.
- [36] T. Storz, P. Dittmar, P. F. Fauquex, P. Marschal, W. U. Lottenbach, H. Steiner, *Org. Proc. Res. Dev.* **2003**, *7*, 559–570.
- [37] "OEDocking version 3.0.2. OpenEye Scientific Software, Santa Fe, NM. <http://www.eyesopen.com>."
- [38] A. Bernardi, D. Potenza, A. M. Capelli, A. Garcia-Herrero, F. J. Cañada, J. Jiménez-Barbero, *Chem. Eur. J.* **2002**, *8*, 4597–4612.
- [39] A. Bernardi, D. Arosio, D. Potenza, I. Sánchez-Medina, S. Mari, F. J. Cañada, J. Jiménez-Barbero, *Chem. Eur. J.* **2004**, *10*, 4395.

Manuscript received: July 28, 2021
Version of record online: October 6, 2021

Curriculum vitae – Benedetta Girardi

After the PhD in pharmaceutical sciences, I transitioned to consulting in market access, thrilled by the idea of applying my scientific background and passion for medical innovation in a new field that is closer to patients' needs. I support pharmaceutical companies in developing clinical strategies and evidence-generation plans, assessing products' values from scientific, clinical, and market potential perspectives. Additionally, I am involved in pricing and reimbursement strategies for different European countries, with specific expertise in market access in Italy.

Professional experience

Research Associate Market Access & Pricing

July 2022 - on going

LatticePoint Consulting
Geneva, Switzerland

Supporting pharmaceutical companies for: evaluation and prioritization of drugs' indications, tailored pricing and reimbursement strategies, evidence generation plans, clinical development strategies, launch sequence planning and optimization.

Research Assistant – PhD

March 2018 - December 2021

University of Basel and University of Ljubljana
Basel, Switzerland – Ljubljana, Slovenia

Besides planning the PhD project in collaboration with my supervisors and colleagues, I performed the experimental work, wrote two academic articles, mentored a master student for her thesis project, and received specific training to improve my scientific communication and project management skills.

Internship in Computer-Aided Drug Design (CADD) at Idorsia

June 2021

Internship for PhD studies
Basel, Switzerland

Master thesis (Erasmus fellowship)

February 2017 - July 2017

MedChemLab, Universidad Complutense de Madrid
Madrid, Spain

Medicinal chemistry work to develop inhibitors of FtsZ, a protein involved in bacterial division and proliferation

Academic internship at “All’università” pharmacy

August 2016 - January 2017

Trieste, Italy

Education

PhD in Pharmaceutical Sciences

March 2018 - December 2021

Marie Curie fellowship – PhD4Glycodrug consortium

University of Basel – Basel, Switzerland

Cotutelle de these between the University of Basel and University of Ljubljana

The project was focused on the design, synthesis and biological evaluation of glycomimetic ligands for Siglec-8, a protein involved in inflammatory diseases associated with eosinophils and mast cells.

M. Sci. in Pharmaceutical Chemistry and Technology (CTF)

October 2012 - October 2017

Università degli studi di Trieste – Trieste, Italy

Publications and presentations

- **Girardi B, Perez S. The fascinating world of Siglec Proteins: A primer.** Glycopedia, 2022.
- **Girardi B, Manna M, Van Klaveren S, Tomašič T, Jakopin Ž, Leffler H, Nilsson U J, Ricklin D, Mravljak J, Schwardt O, Anderluh M. Selective Monovalent Galectin-8 Ligands Based on 3-Lactoylgalactoside.** ChemMedChem. 2022, 17 (3): e202100514. Selected as a Very Important Paper.
- **Kroezen B S, Conti G, Girardi B, Cramer J, Jiang X, Rabbani S, Müller J, Kokot M, Luisoni E, Ricklin D, Schwardt O, Ernst B. A Potent Mimetic of the Siglec-8 Ligand 6'-Sulfo-Sialyl Lewis^x.** ChemMedChem. 2020, 15 (18):1706-1719. Selected as a Very Important Paper.
- **Virtual poster presentation – EFMC conference**
29.08.2021– 02.09.2021
- **Virtual poster presentation – SCS fall meeting conference**
25.08.2020
- **Poster presentation – Eurocarb XX conference**
Poster selected for flash presentation
Leiden, The Netherlands
30.06.2019 – 04.07.2019
- **Poster presentation – Annual Research meeting at University of Basel**
University of Basel, Switzerland
08.02.2018

Certificates

Good Clinical Practice (GCP)
Swiss TPH
February 2021
Pharmacist license
November 2017 - Italy

Languages

- Italian – native speaker
- English – C1 level
- Spanish – C1 level
- German – A1 level
- French – A1 level

Software and web-tools

- Microsoft Office
(Word, Excel, PowerPoint)
- Microsoft Windows/Mac
- Pubmed and Mendeley

Hobbies

I love **nature** and **outdoor activities** like **hiking** or **skiing**, and I especially enjoy **traveling**: I feel deeply enriched after exploring new countries, discovering local culture and meeting new people with completely different backgrounds. I also like playing **guitar** and **dancing forrò**, a Brazilian partner dance.